A mechanistic evaluation and design of tunnel support systems for deep level South African mines

Andrew Thurlo Haile

1999

Johannesburg South Africa

Submitted in fulfilment of the academic requirements for the degree of Doctor of Philosophy in the Department of Mechanical Engineering, University of Natal.

Abstract

The design of support systems, comprising rock bolt reinforcement and fabric containment components for tunnels in deep level mining environments does not currently cater well for adverse rock mass conditions. This often results in periodic failure of the support system, particularly under dynamic (rockburst) conditions with the potential for total collapse of the excavation. The design of support systems is currently based either on empirical design guidelines often not applicable to this environment or simple mechanistic models.

This thesis details a methodology for the rational design of tunnel support systems based on a mechanistic evaluation of the interaction between the components of a support system and a highly discontinuous rock mass structure. This analysis is conducted under both static and dynamic loading conditions. Due to the highly complex and variable nature of the rock mass structure and the dynamic loading environment, a large component of the practical work on the evaluation of the mechanisms of rock mass deformation and support interaction is based on rockburst case studies. The understanding gained from these investigations is further evaluated by means of laboratory testing of the performance of the components of the support systems and numerical modelling of the interaction of the components of the support system with the rock mass.

Due to the complex nature of this design environment the methodology developed in this thesis is but a step towards our greater understanding of the behaviour of the rock mass, and the interaction of support systems in the stabilisation of tunnel excavations. However, in comparison to the current design, this methodology now allows the design engineer to make better estimations of the anticipated demand on the different components of the support systems, under a defined rock mass environment on engineering principles. This understanding will give the design engineer greater flexibility, and confidence to design the appropriate tunnel support system for a specific rock mass and loading condition based on the often limited availability of different support units in the underground mining environment.

Preface

The work detailed in this thesis represents the thoughts and concepts of the author and has not been submitted in part, or in whole to any other University. The research was carried out at the Rock Engineering Programme of the CSIR Division of Mining Technology, under the supervision of Professors Viktor Verijenko and Sarp Adali of the University of Natal and guidance of Mr. Tony Jager. This work forms part of the research strategy of the Safety in Mines Research Advisory Committee. It addresses the identified need for an improved understanding of the stability and support requirements of tunnel excavations in adverse rock mass environments in the South African mining industry, and, the development of a rational design methodology for tunnel support systems.

In order to address the defined limitations in the current support system design, and, thus, the needs of the South African mining industry, it was considered appropriate to examine the interaction of the support systems with the rock mass on a mechanistic basis. This would enable the development of a rational design methodology based on an understanding of the interaction between the components of the support system and the rock mass environment.

Acknowledgements

The author would like to thank the following people for their invaluable assistance and guidance in the aspects of the work that are encompassed in this thesis.

Professor Viktor Verijenko and Professor Sarp Adali, who, as supervisors have shown great enthusiasm for the work and for continual guidance and encouragement in the compilation of this thesis. Also thanks to their team at the Applied Mechanics Group of the Department of Mechanical Engineering at the University of Natal for their assistance in aspects of this work.

Tony Jager and Dr. Guner Gutunca for initiating my involvement in the research of support design considerations for tunnel excavations in the South African mines and providing the opportunity and resources to continue with the research over the years. Particular thanks to Tony for his continued support and guidance over the whole period of this investigation, and to Mike Roberts more recently for encouragement and resources to complete the thesis.

The other members of the Rock Burst Task Force, Dr. Ray Durrheim, Mike Roberts, Tony Jager, Dave Ortlepp, Dr. Terry Hagan, Dr. Steve Spottiswoode and Dr. Mathew Handley for their contributions during the investigations of the rock burst case studies. Particular thanks to Dave and Ray for many of the photographs of the damage observed on these visits.

Mark Grave, Dr. Leszek Wojno and Dave Roberts for their work on the testing of the support systems in the laboratory and in situ which laid the foundation for the analysis of these components of the support system and incorporation in the design process.

The mining companies on which rockburst investigations and in situ support testing were conducted, Buffelsfontein gold mining company, East Driefontein division of Driefontein consolidated, Vaal Reefs Mining and Exploration, Hartebeestfontein gold mining company. The place of my previous employment, Kloof gold mining company, for the experience gained and initial investigations into tunnel support design.

The Safety in Mines Research Advisory Committee (SIMRAC) for funding the research into tunnel support design, under which much of this work was conducted, and to the GAPREAG (Gold and Platinum Rock Engineering Advisory Group) committee for their constructive comments and guidance of the research work in this area over the past few years.

Thanks to Tony Jager (again) and Dr. John Napier for technical comments on this thesis and Cheryl Langbridge for editing.

Finally, and most importantly, thanks to my wife Sylvia, daughter Julia and son Aidan for their encouragement and giving me the opportunity and time to finish this work at home over the last couple of months.

Table of Contents

Tables

Figures

Photographs

List of Symbols

R	Rand
km	kilometre
m	metre
cm	centimetre
mm	millimetre
MPa	Mega Pascal
Pa	Pascal
σ_c	Uniaxial compressive strength
σ_1	Maximum principal stress
σ_2	Intermediate principle stress
σ_3	Minor principal stress
szz	vertical stress component
syy	dip parallel horizontal stress component
sxx	strike parallel horizontal stress component
ρ	density of rock mass
g	gravitational acceleration constant (10 m/s^2)
E	energy
m	mass
v	velocity
M	magnitude of seismic event (M=)

List of Abbreviations

RCF	Rockwall Condition Factor (Anon., 1988)
UCS	Uniaxial Compressive Strength
RMR	Rock Mass Rating (Bieniawski 1973, 1979)
Q	Rock Quality - rock mass classification (Barton, 1974)
UDEC	Universal Distinct Element Code
FLAC	Fast Lagrangian Analysis of Continua

Glossary of Terms

Because of the specialised nature of the mining industry and the local terms often associated with a certain sector of the mining industry, it is considered useful to review some of the common terminology associated with the deep level South African mines which may be encountered within this thesis.

Figure I illustrates a typical South African deep level mining layout.

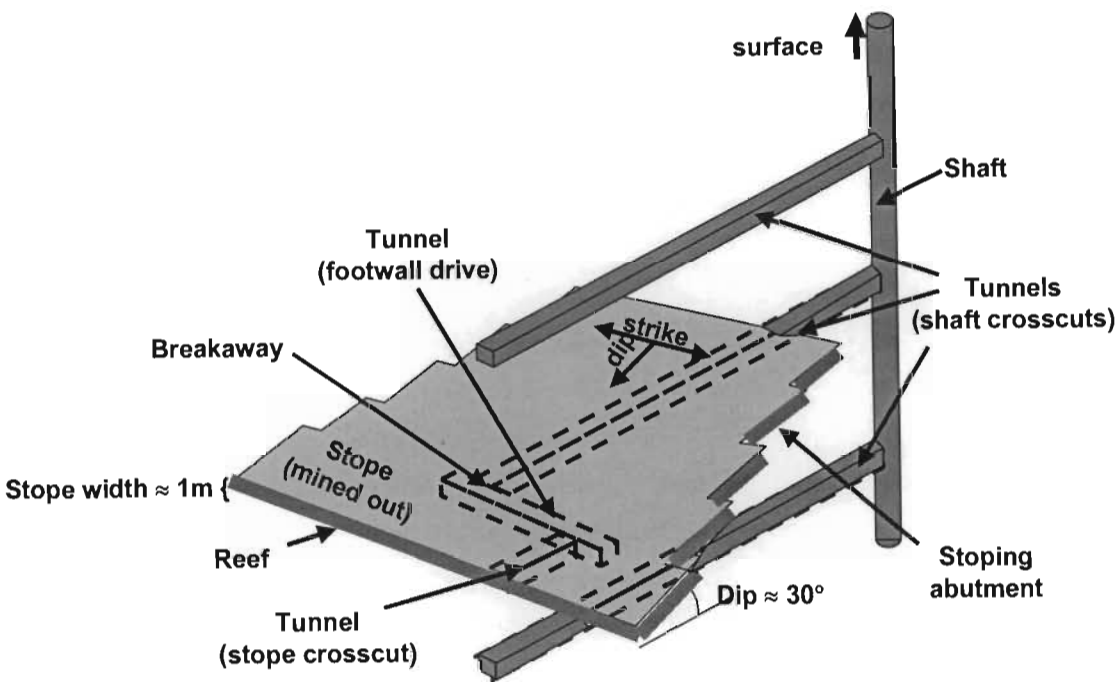

Figure I. Schematic of principal features of a typical deep level South African gold mine. (not to scale)

The following gives a brief description of the terminology shown in Figure 3, and additional terminology applied to the large scale mine layout and rock mass behaviour typical of the South African deep level mines.

Rock mass - This refers to the large-scale rock volume that encompasses the intact rock material and the natural, or mining induced, ubiquitous discontinuities such as joints and fractures. The presence of large scale geological structures, such as faults and dykes, are generally referred to specifically but may cause a change in the local rock mass characteristics. The structure within the rock mass is orientated with regard to its dip direction (steepest inclination of the plane) and strike direction, 90° to dip, and defines a horizontal line at any point on the plane surface. The rock mass structure within the South African gold mines generally conforms to the structure of the **reef** horizon with the principal natural structure within the rock

mass being the reef parallel bedding planes. The spacing of the bedding planes may vary from 10cm to 1m.

Reef - (orebody, reef horizon) The mineralised rock from which the mining product is derived. In the South African context this is usually a very thin structure (1 cm – 1 m) with large lateral extent and relatively low dip, typically referred to as a tabular deposit.

Shaft - The excavation giving the primary means of access to the reef from surface. Typically these are vertical with diameters of the order of 10 m, in which conveyances run to transport the men, material and the extracted reef to and from surface. These excavations may also be inclined (>30°). For deep level mining a shaft system will consist of a series of shafts to access depths between 2000 m and 4000 m below surface.

Tunnel - (haulage, crosscut, footwall drive) A horizontal (or very low inclination) excavation, typically 3.5 m x 3.5 m, which provides the access infrastructure for men and material from the main shaft access to the working places on the reef horizon. The tunnels usually contain pipe work for the supply of water and compressed air to the workings and rail tracks for locomotives and rail cars for the transport of men, material and broken rock. The local terms of crosscut and footwall drive refer to the orientation of the tunnel relative to the reef horizon and local rock mass structure. Thus a crosscut will cut across the general rock mass structure and is perpendicular to the strike of the reef horizon, whereas a footwall drive is generally orientated parallel to the strike of the reef and rock mass structure.

Breakaway - The junction between two tunnels is often referred to as the breakaway position. This area of the excavation results in increased excavation dimension and thus reduced stability.

Stope - The stope excavation is the mined out area of the orebody (reef) with dimensions defined by the strike and dip spans and the **stoping width** (typically slightly greater than the reef width). The large lateral extent of this excavation results in large stress concentrations in the rock mass at the boundary of the excavation (stope face). These large stress concentrations are often referred to as **stoping abutments**.

Seismic event - (seismicity) Due to the large stress changes and concentrations in the rock mass due to extensive mining operations (stope excavations), this results in large strain energy within the rock mass, the violent release of which is termed a seismic event (singular) or seismicity (plural). The mechanism of energy release is due to either the creation of a fracture within previously intact rock or slip on an existing discontinuity within the rock mass.

Rockburst - A rockburst is the manifestation of damage within an excavation due to the radiation of energy from a seismic event. The radiation of energy from a seismic event is in the form of transient stress waves in the rock mass which may result in violent failure of the rock mass around an excavation and/or expulsion of discontinuous rock mass in the boundary of an excavation. The intensity of damage is a function of the proximity of the excavation to the source of the seismic event, the magnitude (M) of the event and the attenuation of the energy within the rock mass.

Terminology specific to tunnel excavations is indicated below in Figure II.

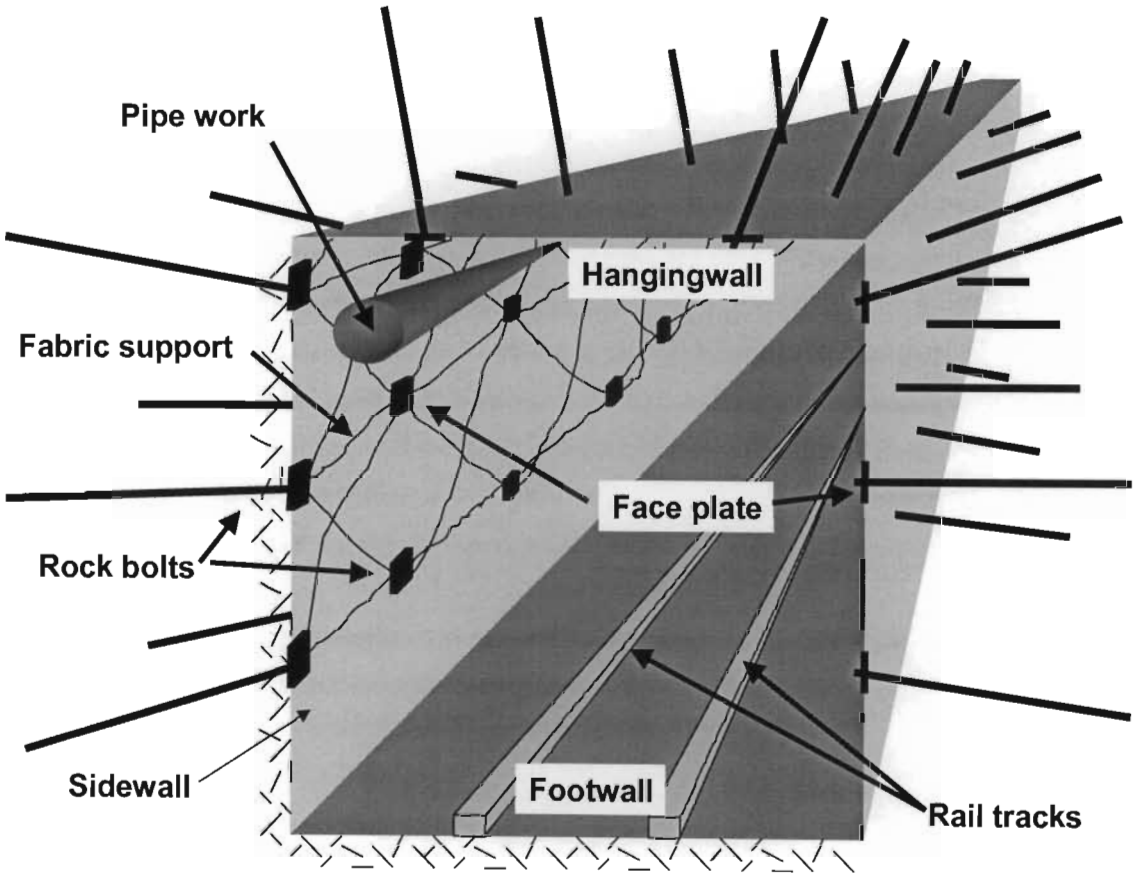

FigureII. Illustration of typical components of a tunnel and its reinforcement / support system.

The following gives a brief description of the terminology shown in Figure 33 and terminology applied to tunnel excavations and local rock mass behaviour.

Hangingwall, Footwall and Sidewall - (roof, floor and side respectively) These terms describe the relative position of the exposed rockwall on the boundary of the typically square tunnel profile. These terms are often used to also reference sections of the tunnel support system. Within the tunnel excavation service infrastructure such as **pipe work** and **rail tracks** are often installed.

Rock bolts - (rock anchors, tendons, cables, reinforcement unit) These are the primary rock mass reinforcement units used in the stabilisation of the rock mass around tunnel excavations. A rock bolt is installed in a hole drilled into the rock mass generally perpendicular to the excavation boundary. The rock bolt is anchored within the rock mass either by means of mechanical end anchorage and / or bonding over the length of the bolt by cementitous or resin based grouts. The use of end anchorage may also allow pre-tensioning of the rock bolt between the end anchorage and a **Face plate** on the boundary of the tunnel. The characteristic of the rock bolt unit, surface profile or shape, may also be used to describe this component of the support system, such as smooth bar, rebar, or shepherd crook, Split Set etc. The arrangement of a series of rock bolts within a unit length of the excavation is referred to as the rock bolt pattern. This pattern is then repeated on a regular basis along the length of the excavation. The term cables refers to reinforcement elements constructed of wire rope.

Fabric support - The fabric component of the support system spans between the rock bolt reinforcement on the surface of the excavation. It is generally a high areal coverage support system but may vary from single lacing (cable rope) strands between rock bolts, through the incorporation of wire mesh's, to 100 per cent coverage membrane or shotcrete (gunite) support. The role of the fabric is to provide support, or even reinforcement, to the potentially unstable rock mass between the rock bolt units.

Sets - Sets are the construction of an internal framework type support within the tunnel excavation. It will generally consist of either simple vertical concrete filled pipes, embedding in the footwall with rail beams across the hangingwall, or more sophisticated use of specialised '3' beam units to construct the framework. The framework is not in direct contact with the rock mass surrounding the tunnel and thus use is made of 'cribbing' to fill the space between the set framework and the rock mass surface. This cribbing can again vary from simple timber packing to pumped foam grout systems.

Chapter 1

1. Introduction

1.1 Nature of problem and previous work

Tunnels at great depths, which are typical of the South African gold mines, are subjected to stresses (loading) which are sufficient to cause fracturing of the rock around the tunnel. The rock breaks up into discontinuous blocks and the rock mass dilates causing deformation of the rock wall into the tunnel. A seismic event may occur on a fault due to changes in the stress environment in close proximity to a stope. Tunnels that are accessing this section of the mine are subjected to violent shaking, which may be sufficient to result in the rapid deformation and potential expulsion of this fractured rock into the tunnel. If this movement cannot be controlled by the tunnel support system, then total failure of the tunnel may result. This can have serious implications with regard to safety of personnel and the operational status of the tunnel. This damage is known as rockburst damage. It is in this environment that the design of tunnel support systems is evaluated in this thesis.

Approximately 10000 km of tunnels are in use in South African gold and platinum mines that constitute the essential link between shafts and production stopes for men, materials, services and ventilation. The environments in which these tunnels are located vary from depths close to surface to approximately 3500 m below surface. They may be sited in rock types varying from sedimentary rock masses to igneous. This results in a significant variation in the rock mass condition of tunnels. In a low stress environment, control of potentially unstable key blocks defined by the geotechnical structure of the rock mass is of primary concern. In a high stress environment, stress fracturing of the rock mass for distances of one to three times the tunnel height into the sidewall may occur. As mining progresses to depths of 4 to 5 km, the ability to ensure the stability of tunnels becomes an even more critical issue. At current mining depths the support systems in use, and the way in which they are applied, makes it impossible to ensure the integrity of tunnels under adverse rock mass or loading conditions. This is demonstrated by the statistic that greater than 85 km of tunnel have to be rehabilitated to varying degrees annually (Jager and Wojno 1991). In addition, some tunnels have to be abandoned due to severe rockburst damage or because impossible conditions are encountered. The estimated cost of these losses, rehabilitation and associated disruption to mining operations is estimated at R 400 million per annum (Jager and Wojno, 1991).

Analysis of accident data shows that 12 % of rock related fatalities within the South African mining industry occur in tunnels and other service excavations. The majority of these fatalities occur within the first 10 m back from the development face where, usually, only primary support is installed. However, almost 30 % occur outside of this region where excavation stability should have been secured by the more robust secondary support. In the face area 77 % of the

fatalities are caused by rockfalls and 23 % by rockbursts. Significantly, this proportion of rockfall to rockburst accidents is reversed away from the tunnel face where 64 % are the result of rockbursts. This distribution of the cause of accidents suggests that the primary support systems and procedures are deficient in their ability to prevent simple rockfalls, while secondary support is successful in preventing rockfall accidents but is likely to fail under the severe loading conditions associated with rockbursts.

There is thus a strong incentive from both the safety and economic points of view to improve the design and support of tunnels subjected to these severe conditions.

Current support design philosophy as applied within the South African mining industry is generally empirically or semi-empirically based. Within the shallow mining environments, reference may be made to the rock mass classification systems of Bieniawski (1979) or Barton, Lien and Lunde (1974), based on the geotechnical structure of the rock mass. Within the deeper, high stress, rock mass environments reference is generally made to the empirical tables derived from the Chamber of Mines Research Organization (Anon 1988) and applied via the Rockwall Condition Factor (RCF) criterion. Alternatively, the design may be based on consideration of energy absorption criteria and support resistance determined from simple mechanistic analysis. The application of numerical models to excavation design has also increased in popularity. However, the complexity of establishing the models means that as a daily design tool these are not used on a routine basis within the mining industry.

These design methods, especially the ones based on in situ experience, have been developed over many years and have proved more than adequate within their general areas of application. The basis of their design methodology is either to create an integrated reinforced shell of rock around the excavation by interaction of the support units or the retainment / containment of the unstable rock mass by suitable anchorage. However, where rock mass conditions are abnormal to those under which the support system was generally developed, or there is a significant change in the loading conditions due to stress-induced failure or dynamic loading, then failure of the support system may occur. This is generally observed as large deformations and unravelling of the rock mass between the rock bolts, or as a total failure of the support system and subsequent collapse of the excavation. Under these conditions, it is presumed that the support interaction and load distribution was insufficient to control the associated dilation of the rock mass due to the imposed loading condition.

The mines generally have a limited variety of support units at their disposal, and, thus, "standard" support systems are designed to cater for the majority of rock mass conditions. These may well have to cater for the support of approximately 1500 - 2000 m of new development per month on a large gold mine. Unless the excavation is of a special nature or problematic ground conditions are foreseen well ahead, then the operator only has access to these standard support types to ensure excavation stability. The semi empirical basis of the

current design methodologies makes it difficult for the support design engineer to utilise a limited number of support unit types to cater for variations in the rock mass environment.

A survey of tunnel conditions and support practices (Haile, Jager and Wojno, 1995) for the South African mining industry indicated that a significant cause of problems, particularly in abnormal ground conditions, was the lack of a rational design methodology. This was found to be particularly true in the high stress, highly fractured environments of the gold mining industry. In addition, significant excavation damage was associated with dynamic loading due to seismicity.

1.2. Scope of research

The scope of this research is to improve the design considerations for tunnel support systems for excavations sited in a high stress environment and under the influence of high quasi static and dynamic deformations, based on a mechanistic analysis. Of fundamental importance to the investigation is an understanding of the interaction between a tunnel support system and the highly discontinuous (fractured) rock mass structure. The in situ interaction of the components of the support systems with the rock mass is extremely complex, as are the loading conditions; particularly those associated with seismic events.

Components of the support systems, such as the rock bolts and fabric, may be tested in the laboratory under conditions considered representative of the in situ environment. The interaction of the support system with the rock mass, and thus an understanding of the applicable loading conditions, is however a far more complex problem. Numerical models may provide a suitable means of evaluating the performance of the support system. These may give insight into the mechanistic interaction between the support components and the rock mass. It is however important to calibrate these models with in situ evaluation. Due to the highly variable nature of seismicity and associated rockburst damage, it is extremely difficult to implement detailed instrumentation at an underground site and to be guaranteed of capturing this behaviour. Detailed observations of numerous rockburst incidents could form a database of the in situ performance of different support systems within different rock mass environments, and, thus, the evaluation of the interaction between the support system and the rock mass.

Due to the inherent complexities of design within a highly variable medium such as the rock mass, this observational approach has formed the basis of the majority of practical support design guidelines within the civil tunnelling and mining industries.

Due to the breadth of the investigation, the interconnectivity between the different aspects of the proposed design methodology, and the areas of research and respective chapters within this document, are shown in Figure 1-1.

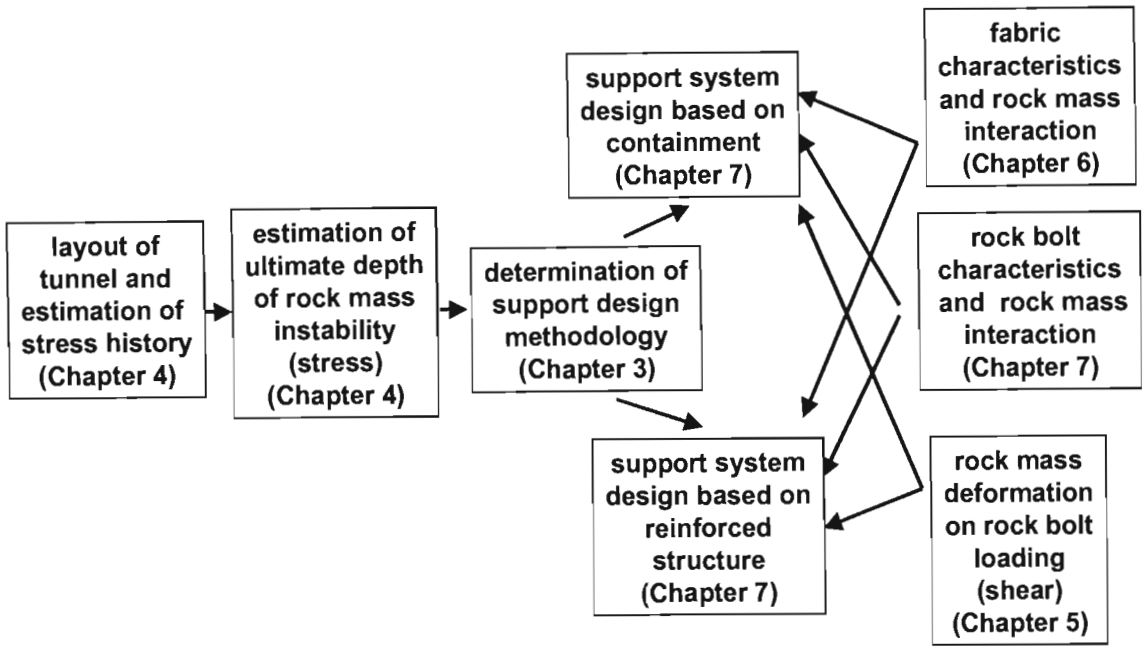

Figure 1-1. Aspects of investigation and respective chapters within this thesis for the proposed tunnel support design methodology.

Throughout this thesis reference will be made to this figure to assist the reader in understanding the relevance of the work within the respective chapter to the overall context of the proposed tunnel support design methodology.

1.3 Objectives

The objective of this research is to provided a better mechanistic understanding of the interaction between the components of a support system and the rock mass surrounding an excavation in a deep level mining environment. It is envisaged that this will allow:

- Site specific understanding of the influence of the rock mass structure on support system performance.
- An understanding of the relationship between the excavation geometry, rock mass environment and the mechanism of support system interaction
- Estimation of the mechanism of loading and demand on the individual components of the support system
- An ability to design the capacity of the components of the support system based on mechanistic analysis

- Flexibility of design, with a limited availability of support component types, with changing rock mass environment

- Practical guidelines for the design of support systems in a deep level rock mass environment

It is envisaged that this understanding will allow improved design of support systems, for tunnel type excavations, within this adverse underground environment, with consequent improvement in the safety of personnel as well as the operational viability of these excavations.

Chapter 2

2. A literature survey on the rock mass behaviour around highly stressed tunnel excavations and the design of support systems.

2.1 Introduction

This section reviews the rock mass characteristics which may be anticipated around tunnel excavations sited in high stress environments and the design of support systems under these conditions. The first aspect deals with the former area and thus sets the scene with regard to the rock mass environment in which the support design engineer must conduct the analysis. The latter aspect of the review examines support design concepts and methodologies that are currently used in mining.

2.2 Rock mass behaviour around highly stressed tunnel excavations

Due to the abnormally deep nature of gold mining in South Africa, the characteristic of the rock mass behaviour around tunnel excavations is fairly unique to this environment. It is in this environment that the majority of the fundamental work on the in situ fracturing around tunnel excavations has been conducted.

The early work conducted into the analysis of fracturing around a tunnel examined the phenomenon of vertical slabbing of the sidewall of the excavation in the direction parallel to the maximum principle stress (Fairhurst and Cook, 1965). This evaluation indicated that the intensity of fracturing was a function of a constant slenderness ratio, which led to the formation of more finely fractured rock at depth. This contrasted with subsequent observations by Ortlepp (1984) that indicated that fracturing was closely spaced at the surface of the excavation and that the spacing increased with depth into the rock wall.

Barrow (1966) investigated the development of failure around an unsupported square tunnel (3 m x 3 m), which is typical of the current excavation dimensions, that was sited in quartzite at a depth of approximately 1600 m below surface. The tunnel was originally in near virgin stress conditions and was subsequently destressed by the adjacent stoping operations (overstoping). The displacement history of the sidewall of the excavation indicated an initial linear increase, with respect to vertical stress increase, up to a point were rapid displacement occurred prior to a subsequent lower rate of deformation during significant overstoping. Almost all the sidewall movement was associated with the first 0.75 m during the period of stress increase, and deeper movement was only noted during overstoping. This displacement was directly associated with

the development of the fracture zone. However, within the upper corners of the tunnel, although intense fracturing was observed, displacement was only associated with overstoping. No movement was detected in the hangingwall or abutments of the tunnel until overstoping was in progress. Hangingwall displacements were measured to depths in excess of 7 m, and again these were associated primarily with overstoping. Barrow noted that the application of support is not practical to prevent failure, but must be designed to control the failed rock mass by the use of a yielding bolt.

Observations of the development of the fracture zone around a 5 m x 5.5 m excavation sited in quartzite indicated the presence of "bow wave" fractures up to 2 metres in advance of the face in a stress regime of approximately 100 MPa. (More O'Ferrall and Brinch, 1983). During this trial it was observed that fracturing of the sidewall had occurred to a depth of 3 m at a point 2 m back from the face, and this increased to 4.3 m at a distance of 20 m. This compared favourably with the work of Hepworth (1985) who noted that up to 60 % of sidewall convergence occurred in the first 3 m to 4.5 m of the sidewall. Jager, Wojno and Henderson (1990) estimated that deformation of the sidewall of a tunnel may occur up to three times the diameter behind the development face. It was noted that in the hangingwall, fracturing was to a depth of approximately half of that in the sidewall. It was observed that bedding planes had a limited influence on the development of fractures. This was attributed to the initial development of fractures in the confined environment in advance of the face. It was further noted that where irregularities in the profile of the excavation occurred, this was associated with excessive scaling. With regard to the support system (9 mm x 2.4 m rock studs), it was noted that there was little failure of the support elements in the sidewall of the excavation but noticeable failure of the support elements in the hangingwall. This was related to the rapid development of load within the hangingwall support units subsequent to installation due to the development of the hangingwall fracture zone, whereas the sidewall support units were placed in pre-fractured ground.

Analysis of the development of fracturing around a large excavation was conducted by Kersten, Piper and Greef (1983). The excavation had a cross-sectional dimension of 10 m x 10 m and was sited in argillaceous quartzite. The approximate depth of fracturing was indicated to be in the region of 7 m, with a fracture intensity of approximately 3 fractures per metre. This resulted in an approximate sidewall deformation of 90 mm. This deformation lead to the failure of the initial support system of 3 m rock studs integrated with 5 m cable anchors that were designed on the basis of standard support practices. The installation of the secondary, or remedial, support system resulted in the stabilisation of the excavation. It was proposed that the presence of bedding had allowed for increased movement of the rock mass, in excess of that anticipated, resulting in failure of the initial support system. The increase in the support resistance of the remedial support was considered to have stabilised this deformation.

A study was conducted of the performance of an experimental tunnel subjected to stresses ranging from 50 MPa to 230 MPa (Ortlepp and Gay, 1984). The tunnel was situated in massive siliceous quartzite of approximate uniaxial compressive strength (UCS) 350 MPa., at a depth of 3075 m below surface. It was noted that very limited fracturing occurred in this competent ground in the absence of significant geological features. In subsequently developed cubbies, the stress fracturing around the excavation was seen to be confined to approximately 200 mm from the side of the tunnel. This observation contrasts markedly with those described above (Barrow, 1966, More O'Ferrall and Brinch 1983, Hepworth 1985). Where a geologically weak zone was present in the sidewall of the tunnel, this area created a stress raising notch which initiated fracturing. The fracturing rapidly stabilised with the formation of an elliptical profile. This was considered to be due to the indicated increase in stress confinement deeper into the rock mass. In general it was noted that abrupt changes in fracturing occurred and this was caused by geological inhomogeneities. In such an environment there was limited influence on the stability of the tunnel by the support installation, and thus it was proposed that even the weakest support system was adequate. However, the application of a yielding type support system was proposed as essential to ensure long term stability.

Wagner (1983) indicated that the intensity of fracturing was a function of the brittleness of the rock type and the magnitude of the local stress regime. This was illustrated with reference to glassy quartzite having a fracture separation of approximately 10 mm, and argillaceous quartzite with a fracture separation of 50 mm; this was also noted by Wojno, Jager and Roberts (1987) and Jager, Wojno and Henderson (1990). Fractures were initiated at a compressive field stress level of approximately 40 % of the laboratory uniaxial compressive strength of the rock. It was also noted that the presence of bedding planes assisted in the slabbing of the sidewall of the excavation. However, Wagner (1979) concluded that there is still very little understanding of the mechanism of rock fracture for the design of excavations.

Empirically determined levels of excavation deterioration, due to the maximum principal stress, are indicated to be as follows (Wagner 1979): > 0.2 σ_c start of scaling, > 0.3 σ_c severe scaling, > 0.4 σ_c heavy scaling. Thus it was advised that, where the boundary stress exceeds the rock mass strength, excavation design should consider minimisation of the fracture zone. This will be a function of the distribution of the maximum principal stress (σ_1) and the minimum principal stress (σ_3), the stress gradient at the periphery of the excavation, and the radii of curvature of the sidewall (in a vertical stress regime). Support recommendations made by Wagner concern the control of deformation to improve the self supporting role of the rock mass, and, within a fracture zone, to provide confinement to further deformation. Support characteristics should include active loading and yield potential.

The influence of seismicity on the stability of the excavation must also be considered. The incidence of seismicity will result in a dynamic stress increase on the excavation periphery,

which would be a function of the size and proximity of the seismic event to the excavation (Kaiser, McCreath and Tannant, 1996).

Wiseman (1979) examined the significance of rock fracturing in the design and support of mine tunnels. He estimated that a tunnel will be influenced by an induced stress at a level > 0.5 σ_c. Wiseman had produced a relationship between the stress concentration on the sidewall of an excavation and tunnel deterioration, known as the Stress Concentration Factor:

$SCF = (3\sigma_1 - \sigma_3) / \sigma_c$.

Where SCF = Stress concentration factor

σ_1 = Major stress component

σ_3 = Minor stress component

σ_c = Uniaxial compressive strength

This was related to support recommendations based on the value of the stress concentration factor. It was estimated that if this were greater than 0.8, then deterioration of the excavation could be expected. It was indicated that the function of the support was to stabilise the fracture zone and provide confinement, rather than the prevention of failure.

Hoek and Brown (1982) developed the Rock Support Interaction Analysis to investigate the support pressure in relation to a ground reaction curve. However, this is based on circular tunnels in a hydrostatic stress field in a homogeneous rock mass with uniform support pressure and thus is generally more applicable to shallow, civil engineering type excavations.

The applicability of rock mass classification methods for the design of underground excavations at depth are generally limited as the majority of systems are based on structurally controlled environments, and thus are considered not applicable. Piper (1984) conducted an investigation into the effect of rock mass characteristics on fracturing around a large excavation at depth. The analysis was based on a comparison of the elastic stress field around an excavation based on the Mohr Coulomb strength criteria. The rock mass strength was derived by application of the RMR (Bieniawski 1973) and Q (Barton *et al*, 1974) rock mass classification systems. This still resulted in an under estimation of the extent of fracturing by approximately 50 %.

2.3 Design of tunnel support systems

The reinforcement of the rock mass in the immediate periphery of an excavation is in general still incompletely understood. This may be reflected by the lack of rational design methodologies for rock mass reinforcement, and the widespread use of empirical design methods and the experience of the design engineer (Stillborg 1986). The mechanical behaviour

and properties of the support units may be analysed in detail from a mechanical engineering perspective, but the rock mass - rock bolt interaction is very poorly understood. The interaction of the rock bolt system with the rock mass is a function of the qualitative differences in the immediate interaction of the rock bolt unit with the rock mass. Fully grouted or frictional support units interact with the rock mass along the full barrel of the borehole in which they are installed. These units primarily influence the blocks with which they make contact, and the stiff nature of the support unit interaction makes it generally applicable to the control of discrete structural blocks which require retainment to maintain excavation stability. The capacity requirement of the support unit is thus directly a function of the unstable volume to be supported. This forms the basis of the mechanistic design of support systems within the South African mining environment (Wojno and Jager 1987). The use of point anchored support systems, with subsequent tensioning, results in the development of confinement within the rock mass. This may result in the interaction of individual rock blocks to create a reinforced rock arch structure. The capacity and loading of the support units in this structure is small compared to the loads acting within the rock mass. The basic design principle is to create the most effective structure to allow the rock mass to be self-supporting. A review of methodologies for the design of tunnel support systems (Choquet and Hadjigeorgiou, 1993, Stillborg, 1986) characterises excavation design principles into three systems: analysis of structural stability, empirical design and numerical modelling.

Within a low stress environment the principle design methodologies are based on either the analysis of structural stability of discrete blocks or the application of empirical design criteria to more structurally complex rock masses. It is within this environment that most support design methodologies have been developed and refined. As the depth at which excavation takes place increases, so the understanding of the rock bolt - rock mass interaction and applicable design methodologies decreases. It is within the highly discontinuous and fractured rock mass structures of the South African gold and platinum mines that the lack of rational design criteria results in potentially unstable ground conditions (Haile *et al.*, 1995).

The design of tunnel support systems will be dependent primarily on the rock mass environment in which these excavations are sited. The design engineer must thus presently use either experience or a rock mass classification system in order to assess the potential excavation stability and determine the support system requirements. The rock bolt support system should be designed to minimise the instability of the excavation peripheral rock mass and thus excessive deformations of blocks within the rock mass. The philosophy of the design process is currently based on structural analysis, empirical design guidelines or support rules. It is useful to review all the current support design methodologies applicable to discontinuous rock mass structures. This will allow an evaluation of their applicability to the rock mass environments typical of the South African deep level gold mines.

2.3.1 Structural Analysis

Within low stress environments, and fairly competent rock mass structures, the principal excavation instability is due to the formation of blocks that are free to move, either by falling or sliding, into the excavation. These blocks may be defined by direct discontinuity mapping or probabilistic analysis of the potential for block formation, based on known discontinuity sets and excavation orientation. The support requirement is usually specific to individual blocks and the optimum support system is based on spot bolting as opposed to systematic bolting patterns. The simplest analysis considers the ability of a block to fall from the rock mass (Figure 2-1). The characteristics of the discontinuities, which define the block, are generally neglected in this analysis.

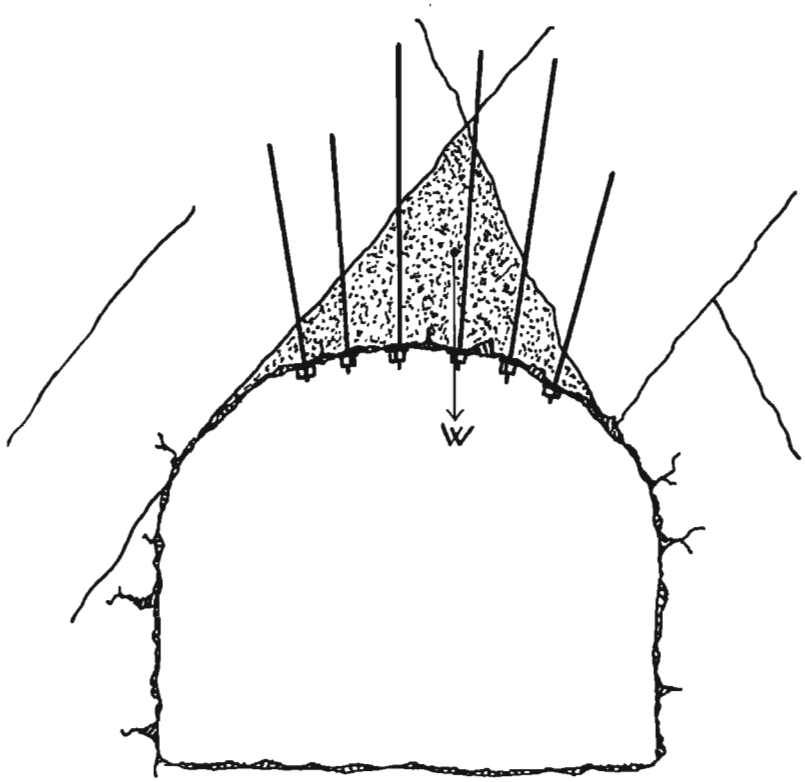

Figure 2-1: Support of key block structure (after Stillborg 1986)

Under these conditions, static design considerations are based on the load capacity and length of the rock bolt system in relation to the size and mass of the defined unstable block. This will allow the number of rock bolt units to be determined that will provide a suitable factor of safety. However, complex failure modes may still result in sequential loading of the rock bolt units, and failure of the support system in excess of its static capacity. Thus even with this simplest of support design analyses a suitable factor of safety is necessary.

Where sliding of the block may occur, then the influence of the discontinuity characteristics must be considered in addition to the factors discussed above (Figure 2-2). The development of

tension within the rock bolt units will increase the normal stress on the sliding plane and thus increase its frictional resistance. Resolving of the forces within this system allows the determination of the minimum rock bolt capacity to stabilise the block of weight W over area A. If the rock bolt reinforcement is of sufficient stiffness to limit any shear deformation on the discontinuity plane, then the cohesive strength (c) of the discontinuity may be considered in the analysis of stability.

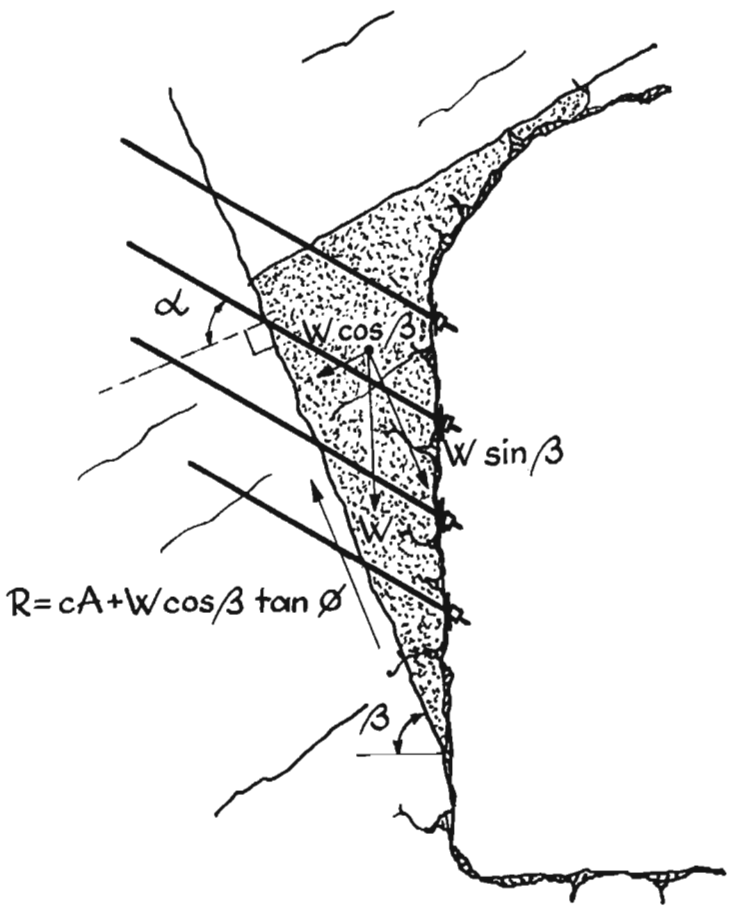

Figure 2-2: Support of sliding block (after Stillborg 1986).

However, generally the cohesive strength is ignored from the analysis as an additional factor of safety, but also due to the lack of confidence with regard to its in situ value. If significant deformation on the discontinuity plane is allowed to occur prior to the development of the support forces, then the influence of the cohesion will be lost due to a breakdown of the discontinuity infilling.

As the frequency of discontinuities within the rock mass increases so the rock bolting requirement changes from the stabilisation of individual, well defined blocks to more systematic rock bolt patterns in order to reinforce and/or support the potentially unstable rock mass volume.

Where the limits of rock mass instability can be defined, and are within a practical depth from the excavation boundary, then the rock bolt system is designed on the basis of suspension or

containment. This will be possible where a more competent horizon occurs immediately above the unstable strata (Figure 2-3).

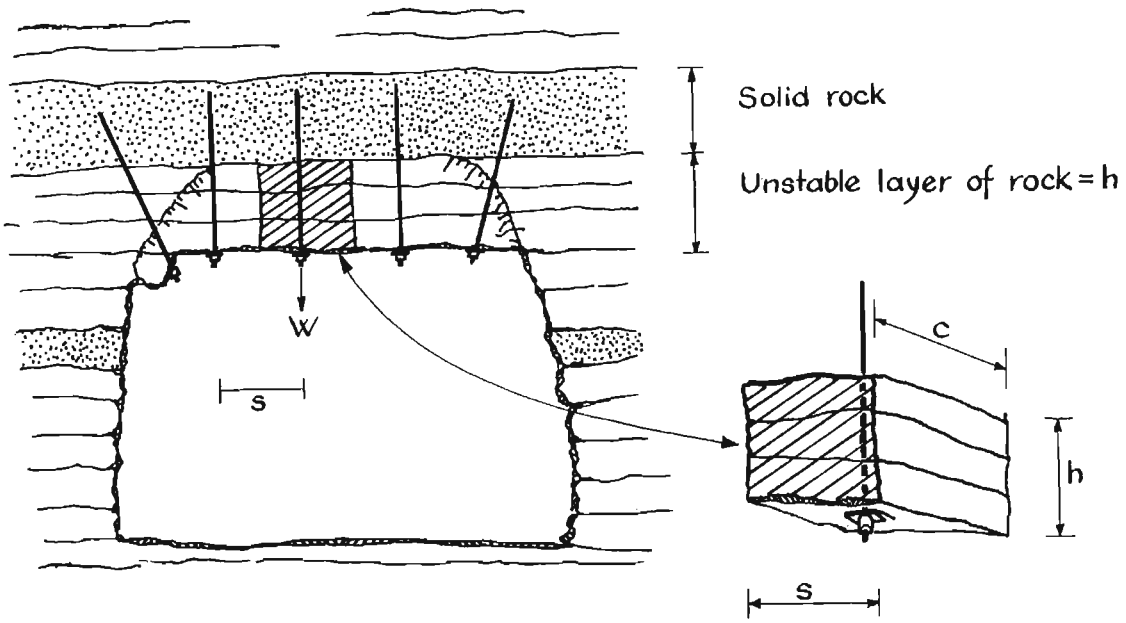

Figure 2-3: Suspension of laminated rock mass based on tributary area loading (after Stillborg 1986)

Under these conditions the length of the rock bolt unit must be sufficient to anchor beyond the limit of rock mass instability. The spacing of the rock bolts is based on the load capacity of the rock bolt unit in relation to the tributary area loading of the rock mass. In Figure 2-3 the tributary area loading is given by the density of the rock mass and the tributary area unstable volume (s x c x h)

Within a moderately jointed, discontinuous rock mass structure, the stabilisation of the excavation may be based on a similar analysis. The creation of an excavation results in the formation of an unstable tensile zone in the immediate roof, above which a natural arch is formed where the rock mass loading condition is primarily compressive (Figure 2-4). The extent of the unstable zone will be a function of the rock mass structure, loading environment, span of the excavation and stability of the sidewalls. The application of un-tensioned, grouted support units within this environment is to pin the unstable rock mass to the competent natural arch.

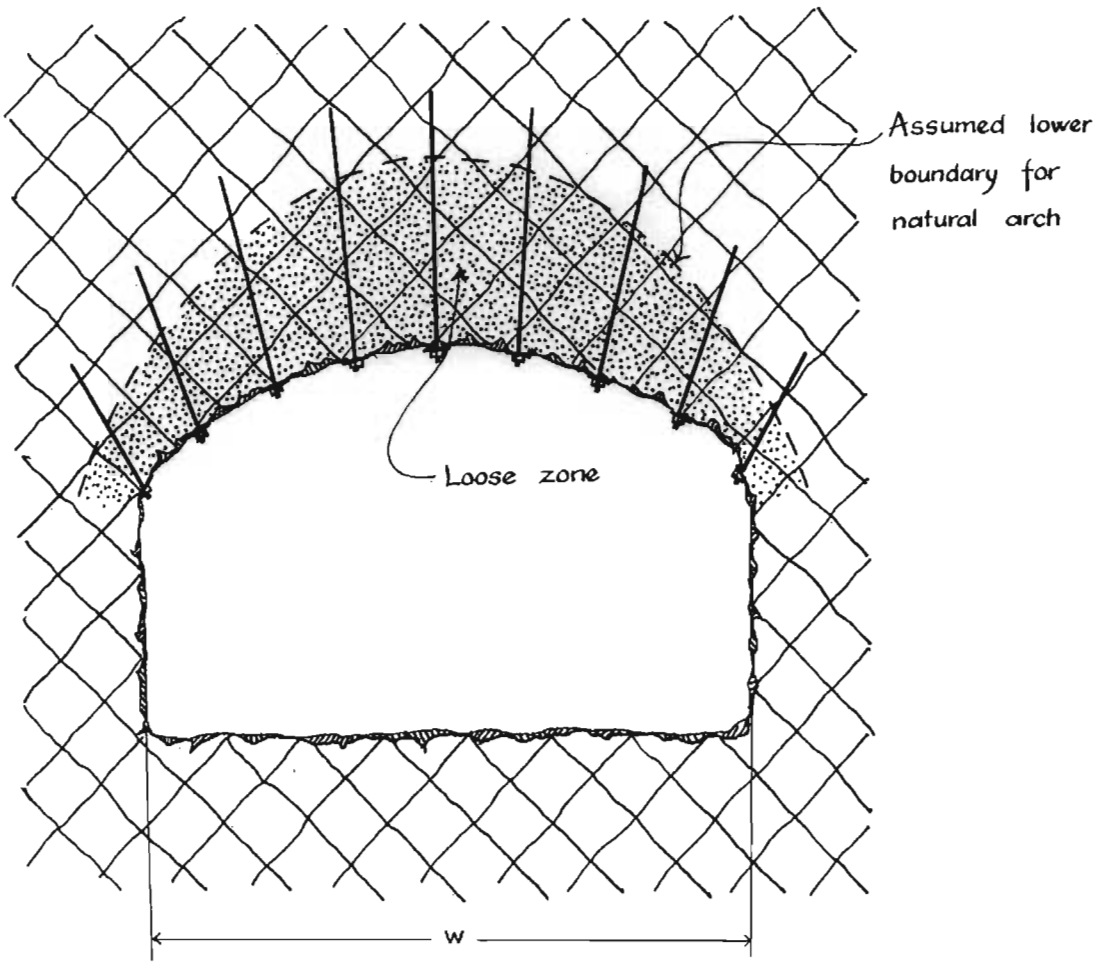

Figure 2-4: Formation of unstable zone and natural stable arch within moderately jointed rock mass structures (after Stillborg 1986).

The length of the rock bolts must be sufficient to anchor into this competent rock mass. An estimation of the required rock bolt length is given by:

$$L = 1.40 + 0.184w \qquad (2\text{-}1)$$

where w is the span of the excavation (metres) and L the required rock bolt length (Norwegian Institute for Rock Blasting Technique, after Stillborg, 1986). This technique, and the use of untensioned grouted rock bolts, is generally more applicable to competent, moderately jointed rock mass structures, that results in the lower boundary of the natural arch being closer to the boundary of the excavation.

This design philosophy currently forms the basis of the mechanistic methodology for the design of rock bolt support systems within the South African mining industry (Anon, 1996). It is recommended that the determination of the depth of instability is based on analysis of accident data within an applicable geotechnical environment, and may incorporate both gravity induced falls of ground and seismically induced rockbursts. It must be recognised that the use of such a

database implicitly incorporates all factors that may influence the stability of the rock mass. This would include the influence of the current support systems and excavation dimensions, in addition to the critical rock mass characteristics. As such this may not necessarily define the natural depth of instability of the rock mass. The spacing of the rock bolts is principally based on tributary area loading in relation to the load capacity of the rock bolt under the defined loading conditions. Thus, under gravitational loading, the minimum required capacity of the rock bolts, or maximum spacing of defined support units, will be given by:

$$W = \rho \times g \times (s \times c \times h) \qquad (2\text{-}2)$$

where W is the load on the bolt and thus the minimum capacity, ρ is the rock mass density, g is gravitational acceleration, and s, c and h (see Figure 2-3) are the tributary area dimensions of the rock mass volume to be supported by a rock bolt unit. The demand on the support system is often expressed per unit area of excavation rockwall and is termed the required minimum support resistance of the rock bolt system, expressed as kN/m^2. If highly friable ground conditions are anticipated then additional use of areal coverage support systems is made. These are utilised to try to maintain the rock mass integrity between the rock bolt units. The demand on the fabric support system is currently not considered in the support system design analysis.

Under dynamic loading conditions the same design philosophy is adopted. However, consideration is now given to the energy demand on, and absorption capability of, the rock bolt unit. Loading is again assumed to be under tributary area conditions, even within highly discontinuous rock mass environments. The depth of instability is again based on historical accident data for rockburst conditions within the typical geotechnical environment. The minimum energy absorption requirement, per unit area of rockwall, will be a function of the kinetic energy of the unstable rock mass volume and in the hangingwall the constant gravitational energy of the rock mass. This is defined for the hangingwall and sidewall of the excavation by:

Hangingwall $$E = {}^1/_2 \, m \, v^2 + m \, g \, h \qquad (2\text{-}3)$$

Sidewall $$E = {}^1/_2 \, m \, v^2 \qquad (2\text{-}4)$$

where: E = energy absorption requirement of the rock bolt system per unit area,
m = mass of ejected rock based on the defined unstable rock mass depth and density,
v = anticipated peak ground velocity,
h = yield capacity of the support system at a given point in time,
g = gravitational acceleration.

Within high stress environments, and particularly mining environments, where the stress state may change over the life of the excavation, consideration must also be given to the progressive deformation of the rock mass. This will determine the remaining yield capacity of the rock bolt units at a given time in the life of the excavation, and thus the support system energy absorption capacity.

In high stress environments, where significant fracturing of the rock mass may occur, or under low stress conditions but within more highly discontinuous rock mass structures, the depth of instability may exceed the practical depth of rock bolt anchorage. Under these conditions excavation stability may be achieved by the creation of reinforced beam (Figure 2-5) or arch (Figure 2-6) structures within the discontinuous rock mass.

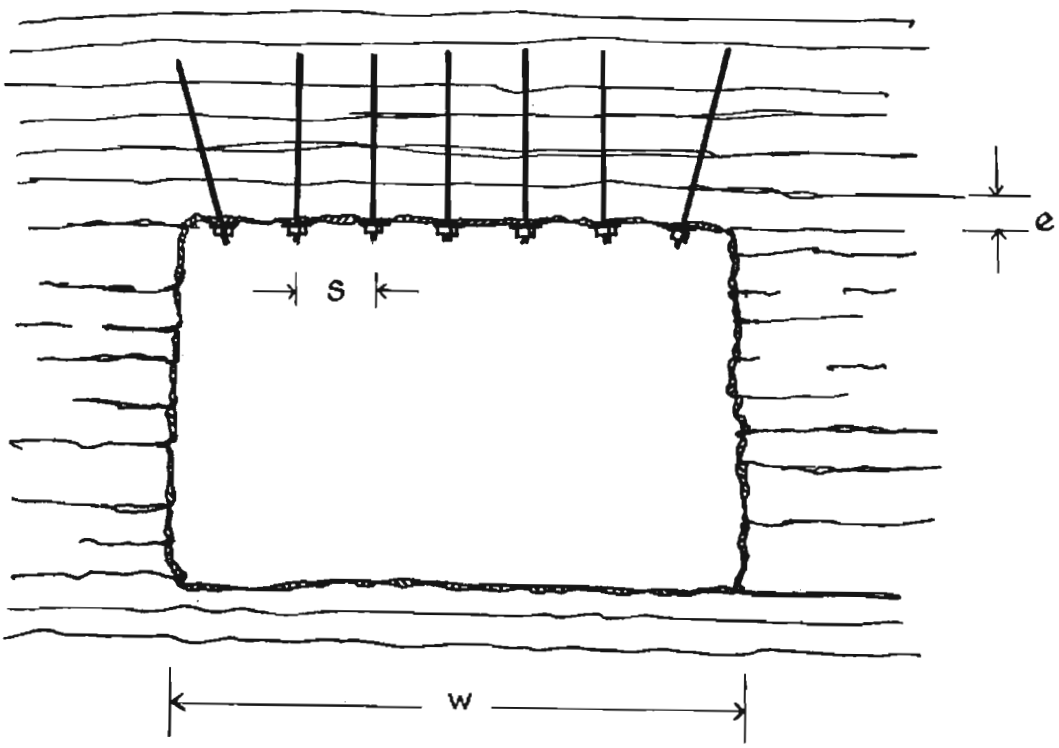

Figure 2-5: Creation of reinforced beam within stratified rock mass (after Stillborg 1986).

The basis of the design of the rock bolt system is the use of tensioned rock bolts to increase the friction between slabs or blocks within the defined arch. This will result in an enhancement of the resistance of the rock mass to shear and deformation. The design of a rock bolt system under these conditions is principally based on empirical rules and guidelines, which may be adapted into design charts or nomograms for specific geotechnical conditions.

Guidelines for the design of a rock bolt system to create a reinforced structure within a stratified rock mass (Figure 2-5) (Lang and Bischoff, 1982), based on the increase of shear resistance between layers within the rock mass are:

Bolt length = $w^{2/3}$ (2-5)

Bolt tension = $((a.\gamma.A.R)/((\tan\phi)k)).(1-c/(\gamma.R)).((1-\exp^{(-(\tan\phi).kD/r)})/(1-\exp^{(-(\tan\phi).kL/R)}))$ (2-6)

where: P = shear perimeter of reinforced rock unit (4 x s)

ϕ = angle of internal friction for the rock mass

k = ratio of average horizontal to average vertical stress

R = shear radius of the reinforced rock unit (A/P = s/4)

w = excavation span

A = area of roof carried by one bolt (s x s)

L = bolt length

s = bolt spacing

c = apparent cohesion of the rock mass

D = height of destressed zone

a = factor depending on time of installation of bolts

γ = unit weight of the rock

Notes: 1) If the rock reinforcement is installed prior to the occurrence of significant deformation, then it is considered to have an active contribution to the excavation stability (a=0.5)

2) If passive (more conservative) reinforcement is assumed, a=1.0

3) Cohesion should be taken as zero for initial design.

Guidelines for support system design in order to create a reinforced rock mass arch within a highly jointed rock mass (Figure 2-6) are:

Bolt length = $1.60 + \sqrt{(1.0 + 0.012.w^2)}$ (Schach et al. 1979) (2-8)

Bolt spacing = 3 x joint spacing (e) (Stillborg 1986) (2-9)

Bolt tension = 0.5 - 0.8 x capacity of bolt (Stillborg 1986) (2-10)

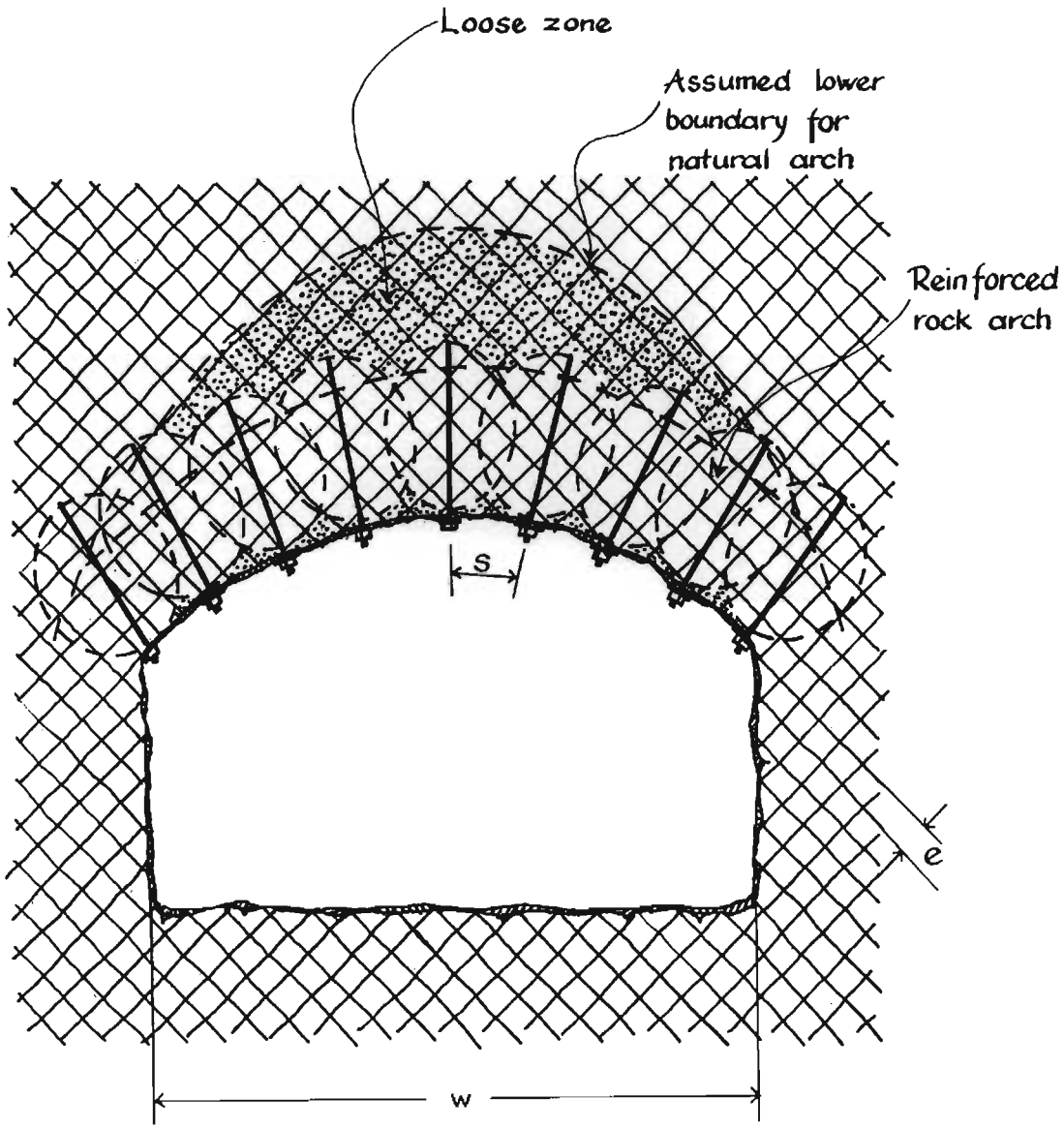

Figure 2-6: Creation of reinforced rock mass arch within highly discontinuous rock mass structures (after Stillborg 1986)

In addition, the requirement for areal coverage support systems such as mesh or shotcrete must be considered in order to maintain the integrity of the rock mass between the rockbolt reinforcement. These guidelines may find application within the South African mining environment although they are not commonly used. Consideration is also not given to specific characteristics of the rock mass and thus will tend to be conservative in nature.

It is considered (Stillborg 1986) that the concept of the creation of a structurally competent reinforced rock mass arch is the basis of most of the empirical rock bolt system design methods.

2.3.2 Empirical design methodologies

Due to the complexities within the rock mass structure, or the lack of detailed design parameters, the design of the rock bolt system based on specific structural analysis may not be possible. Under these conditions it is convenient to utilise empirical design methodologies based on analysis of the geotechnical environment. The analysis of the geotechnical environment, and thus design confidence, will be a function of the maturity of the design process and the availability of suitable geotechnical data.

The majority of empirical design methodologies are based on experience gained within shallow, low stress, civil engineering applications. They thus take limited consideration of an environment of stress change due to mining and the potential for rockbursting. As a result they find limited application within the general South African mining industry (Piper 1985). Exceptions can be found, particularly in the platinum and diamond mining industries that operate at shallower depths.

Table 2-1: Tunnel support guidelines after US Corps of Engineers.

Parameter	**Empirical Rule**
Minimum length	Greatest of:
	a) 2 x bolt spacing
	b) 3 x thickness of critical and potentially unstable rock blocks
	c) For elements above the springline*
	spans < 6 m : 0.5 x span
	spans between 18 m and 30 m ; 0.25 x span
	spans between 6 m and 18 m : interpolate 3 - 4.5 m
	d) For elements below the springline*
	height < 18 m : as c) above
	height > 18 m : 0.2 x height
Minimum spacing	Least of:
	a) 0.5 x bolt length
	b) 1.5 x width of critical and potentially unstable blocks
	c) 2.0 m (greater spacing difficult to attach fabric support)
Minimum spacing	0.9 to 1.2 m
Minimum average confining pressure	Greatest of
	a) Above springline
	either pressure = vertical rock load of 0.2 x opening width
	or 40 kN/m^2
	b) Below springline
	either pressure = vertical rock load of 0.1 x opening height
	or 40 kN/m^2
	c) Intersections: 2 x confining pressure determined above

* this is typically interpreted in South Africa as the point of deviation from vertical in the upper sidewall.

Simple design rules based on an evaluation of case studies were developed by the US Corps of Engineers. These rules have found widespread application, particularly as an initial estimate of support requirements, and are applied as the basis for rock bolt spacing in the design of rock bolt support systems within many South African mines. A summary of the recommendations is indicated in Table 2-1.

Other design rules for rock bolting within jointed rock mass structures, with tight joint conditions, were put forward by Farmer and Shelton (1980). These are similar to those given by the US Corps of Engineers, but consideration is also given to the number of joint sets and their orientation relative to the excavation and rock bolt installation (Table 2-2).

Table 2-2. Empirical guidelines for design of rock bolt system in excavations <15 m span (after Farmer and Shelton 1980)

Number of discontinuity sets	Rock bolt design	Comments
≤ 2 inclined at 0 - 45° to horizontal	L = 0.3 B s = 0.5.L (depending on thickness and strength of strata). Install bolts perpendicular to lamination where possible with wire mesh to prevent flaking	The purpose of bolting is to create a load carrying beam over the span. Fully bonded bolts create greater discontinuity shear stiffness. Tensioned bolts should be used in weak rock, sub-horizontal tensioned bolts where vertical discontinuities occur.
≤ 2 inclined at 45 - 90° to horizontal	For side bolts: L > h.sinψ (if installed perpendicular to discontinuity): L > h.tanψ (if installed horizontally). Where h is the distance of installation from the point of daylight of laminations in the sidewall that defines the largest unstable wedge, and ψ the inclination of laminations from vertical.	Roof bolting as above. Side bolts designed to prevent sliding along planar discontinuities. Spacing should be such that anchorage capacity is greater than sliding or toppling weight. Bolts should be tensioned to prevent sliding.
≤ 3 with clean, tight interfaces	L = 2s s = 3-4 x block dimension. Install bolts perpendicular to excavation periphery with wire mesh to prevent flaking.	Bolts should be installed quickly after excavation to prevent loosening and retain tangential stresses. Pre-stresses should be applied to create a zone of radial confinement. Sidewall bolting where toe of wedge daylights in sidewall.

Wojno, Jager and Roberts (1987) and Jager, Wojno and Henderson (1990) have conducted investigations into the design and support of tunnels under high stress conditions and the definition of support performance requirements. The support guidelines applicable to this rock mass environment indicate the need for yielding tendons. The proposed specification of the support system, based on the previously discussed mechanistic evaluation (section 2.3.1), is as follows:

Work Done	> 25 kJ
Static Yield	> 100 KN
Dynamic Yield	> 50 KN

Maximum Yield	< 500 mm
Tendon Strength	> 25 % static yield

These simple design rules allow initial estimations of support requirements but give limited or no consideration of the rock mass characteristics and as such will be very conservative in nature. A more detailed empirical design methodology can be based on a rock mass classification system to indicate the selection of a support system. The most widely used classification systems are the Q system (Barton, Lien and Lunde 1974) and the Geomechanics Classification, or Rock Mass Rating (RMR) system (Bieniawski 1973, 1979), which also forms the basis of the Modified (or Mining) Rock Mass Rating (MRMR) system (Laubscher, Taylor 1976),.

The Geomechanics Classification was based on case studies of civil constructions within South Africa. The basic RMR value is derived from a rating based on the consideration of critical rock mass parameters. These include the intact rock strength, discontinuity frequency, discontinuity condition and the presence of water within the rock mass (Table 2-3).

Table 2-3. Geomechanics Classification system (Bieniawski 1973)

Parameter			**Range of Values**						
1	Strength of intact rock material	Point-load strength index	> 10 MPa	4 - 10 MPa	2 - 4 MPa	1 - 2 MPa	For this low range - uniaxial compressive test is preferred		
		Uniaxial compressive strength	> 250 MPa	100 - 250 MPa	50 - 100 MPa	25 - 50 MPa	5 - 25	1 - 5	< 1
	Rating		15	12	7	4	2	1	0
2	Drill core quality RQD		90 % - 100 %	75 % - 90 %	50 % - 75 %	25 % - 50 %	< 25 %		
	Rating		20	17	13	8	3		
3	Spacing of discontinuities		> 2 m	0.6 - 2 m	200 - 600 mm	60 - 200 mm	< 60 mm		
	Rating		20	15	10	8	5		
4	Condition of discontinuities		Very rough surface. Not continuous. No separation. Un-weathered wall rock	Slightly rough surfaces. Separation < 1 mm. Slightly weathered walls	Slightly rough surfaces. Separation < 1 mm. Highly weathered walls	Slickensided surfaces. OR. Gouge < 5 mm thick. OR. Separation 1 - 5 mm continuous	Soft gouge > 5 mm thick. OR. Separation > 5 mm continuous		
	Rating		30	25	20	10	0		
5	Ground water	Inflow per 10 m tunnel	None	< 10 litres / min	10 - 25 litres / min	25 - 125 litres / min	> 125 litres / min		
		Ratio (joint water press. / major principle stress)	OR 0	OR 0.0 - 0.1	OR 0.1 - 0.2	OR 0.2 - 0.5	OR > 0.5		
		General conditions	OR Completely dry	OR Damp	OR Wet	OR Dripping	OR Flowing		
	Rating		15	10	7	4	0		

Further adjustments may also be made in relation to the orientation of the joints relative to the excavation orientation and type to obtain an overall rock mass description (Tables 2-4, 2-5 and 2-6).

Table 2-4. Adjustment to RMR for joint orientation

Strike and dip orientations of joints		Very favourable	Favourable	Fair	Unfavourable	Very unfavourable
Ratings	Tunnels	0	-2	-5	-10	-12
	Foundations	0	-2	-7	-15	-25
	Slopes	0	-5	-25	-50	-60

Table 2-5. Adjustment to RMR for joint orientations applicable to tunnels

Strike perpendicular to tunnel axis				Strike parallel to tunnel axis		Dip 0 - 20° irrespective of strike
Drive with dip		Drive against dip				
dip 45 - 90°	dip 20 - 45°	dip 45 - 90°	dip 20 - 45°	dip 45 - 90°	dip 20 - 45°	
Very favourable	Favourable	Fair	Unfavourable	Very unfavourable	Fair	Unfavourable

Table 2-6. Rock mass class and description as determined from RMR

Rating	100 ← 81	80 ← 61	60 ← 41	40 ← 21	< 20
Class No.	I	II	III	IV	V
Description	Very good rock	Good rock	Fair rock	Poor rock	Very poor rock

The description of the rock mass may be utilised to define overall rock mass parameters which may be used to analyse the large scale response of the rock mass (Table 2-7)

Table 2-7. Rock mass parameters based on RMR

Class No.	I	II	III	IV	V
Average stand up time	10 years for 15 m span	6 months for 8 m span	1 week for 5 m span	10 hours for 2,5 m span	30 minutes for 1 m span
Cohesion of the rock mass	> 400 kPa	300 - 400 kPa	200 - 300 kPa	100 - 200 kPa	< 100 kPa
Friction angle of the rock mass	> 45°	35 - 45°	25 - 35°	15 - 25°	< 15°

Based on the Geomechanics Classification system as proposed by Bieniawski, support recommendations were made for a specific civil construction as detailed in Table 2-8. Due to the empirical nature of the design methodology this is based on the experience and technology of the specific sites incorporated in the analysis.

Table 2-8. Excavation technique and support selection based on RMR.

Shape: horseshoe; width: 10 m; vertical stress: below 25 MPa; construction: drill and blast				
Rock mass class	Excavation	Support		
		Rock bolts (20 mm dia. fully bonded)	Shotcrete	Steel sets
Very good rock I RMR:81 - 100	Full face 3 m advance	Generally no support required except for occasional spot bolting		
Good rock II RMR: 61 - 80	Full face 1.0 - 1.5 m advance Complete support 20 m from face	Locally bolts in crown 3 m long, spaced 2.5 m with occasional wire mesh	50 mm in crown where required	None
Fair rock III RMR: 41 - 60	Top heading and bench 1.5 - 3 m advance in top heading. Commence support after each blast. Complete support 10 m from face	Systematic bolts 4 m long, spaced 1.5 m - 2 m in crown and walls with wire mesh in crown.	50 - 100 mm in crown and 30 mm in sides	None
Poor rock IV RMR: 21 - 40	Top heading and bench 1 - 1.5 m advance in top heading. Install support concurrently with excavation 10 m from face	Systematic bolts 4 - 5 m long, spaced 1 - 1.5 m in crown and walls with wire mesh	100 - 150 mm in crown and 100 mm in sides	Light to medium ribs spaced 1.5 m where required.
Very poor rock V RMR: < 20	Multiple drifts. 0.5 - 1.5 m advance in top heading. Install support concurrently with excavation, Shotcrete as soon as possible after blasting	Systematic bolts 5 - 6 m long, spaced 1 - 1.5 m in crown and walls with wire mesh. Bolt invert	150 - 200 mm in crown, 150 mm in sides and 50 mm on face	Medium to heavy ribs spaced 0.75 m with steel lagging and fore poling if required. Close invert.

Applications of the rock mass rating system have included a semi-empirical method for the estimation of the depth of instability around an excavation (Stimpson 1989). This system defines an elliptical boundary around the excavation within which the rock mass is considered to require reinforcement (Figure 2-7).

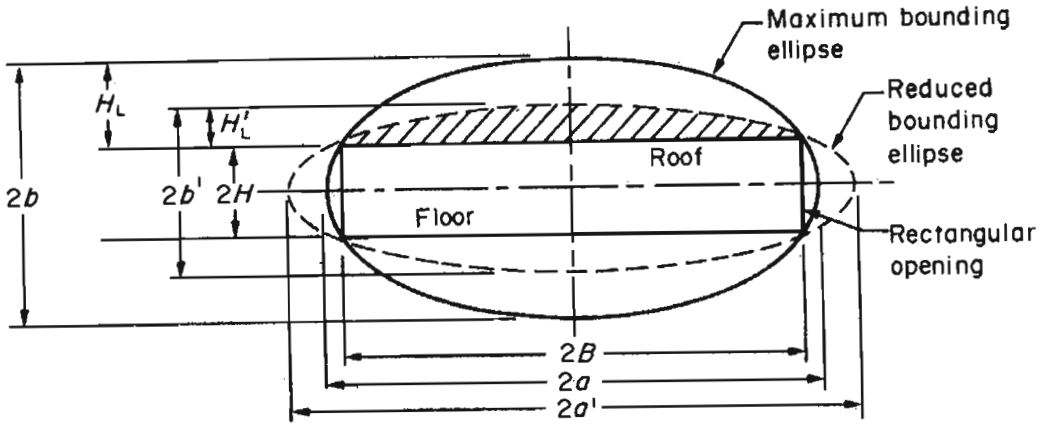

Maximum principal stress is horizontal	Maximum principal stress is vertical
$a = kb$	$a = (H^2 + k^2.B^2)^{0.5}$
$b = (B^2 + k^2.H^2)^{0.5}/k$	$b = a/k$
$a' = Bb'/(b'^2 - H^2)^{0.5}$	$a' = (1 - 0.01.RMR)a + H(0.01.RMR)$
$b' = (1 - 0.01.RMR)b + H(0.01.RMR)$	$b' = Ba'/(a'^2 - H^2)^{0.5}$
$H_L = b - H$	$H_L = a - H$
$H_L' = (1 - 0.01.RMR).H_L$	$H_L' = (1 - 0.01.RMR).H_L$

Figure 2-7. Semi-empirical design of the extent of instability around an excavation based on RMR (after Stimpson (1989))

where k = ratio of maximum to minimum stresses

2B = opening width

2H = height of opening

RMR = Rock Mass Rating

H_L = maximum height requiring support

H_L' = reduced height requiring support

a,a' = semi major axis of ellipse

b, b' = semi minor axis of ellipse

Laubscher and Taylor (1976) suggested modifications to the Geomechanics Classification system, and its associated support recommendations. These modifications are to cater for the differences in support requirements between the original civil environment and a mining environment. The modifications represent an alteration (percentage) of the individual parameters within the RMR as a function of weathering, stress environment, excavation orientation relative to the rock mass structure, and the excavation method.

The influence of weathering is applied to the intact rock strength (decrease down to 96 %), RQD (decrease down to 95 %) and condition of joints (decrease down to 82 %), dependent on the degree of weathering. The influence of the stress environment is a function of the initial field

stress level and any potential stress changes, and is considered to influence the relative joint condition. Where the stress environment is, or becomes, compressive, relative to the rock mass structure and excavation periphery, then this will be favourable to joint conditions (increase up to 120 %). Where shear deformation may be anticipated on the joints in the periphery of the excavation, or a low stress results in the opening of joints, then this will be unfavourable to rock mass stability (decrease down to 90 % or 76 % respectively). Where subsequent stress changes occur, this may also cause adverse shear movement or joint opening within the excavation peripheral rock mass (decrease down to 60 %).

Laubscher and Taylor considered the influence of the excavation orientation relative to the rock mass structure as accounted for by Bieniawski to be insufficient, and thus further adjustments may be required. These adjustments are made to the joint spacing rating and are based on the number of non-vertical rockwalls of the excavation and the number of joints as shown in Table 2-9.

Table 2-9. Percentage adjustment to joint spacing rating for joint number and number of non-vertical excavation rockwalls.

Number of joints	70 %	75 %	80 %	85 %	90 %
3	3		2		
4	4	3		2	
5	5	4	3	2	1
6	6		4	3	2 - 1

A further adjustment to the joint spacing rating is also considered necessary for the presence and orientation of shear zones (decrease dependent on angle of incidence down to 0 - 15° = 76 %, 15 - 45° = 84 % and 45 - 75° = 92 %). Finally an adjustment may be made to the RQD and condition of joints rating for the influence of the method of excavation. The degree of reduction of the parameters is based on the consideration of the adverse effects of blasting (boring – 100 %, smooth wall blasting – 97 %, good conventional blasting – 94 %, poor conventional blasting – 80 %) on the immediate excavation peripheral rock mass stability.

It was considered by Laubscher and Taylor that the application of these adjustments to the original parameters of the Geomechanics Classification, and in some cases several parameters for a specific site, should not reduce the modified RMR by more than 50 % of the original value. These modified Geomechanics Classifications were compared to typical mining support practices in order to define a relationship between the MRMR and support systems as indicated in Table 2-10.

Table 2-10. Support system guide based on Modified Geomechanics Classification after Laubscher and Taylor (1976).

Adjusted ratings	Original rock mass ratings, RMR									
	90 - 100	80 - 90	70 - 80	60 - 70	50 - 60	40 - 50	30 - 40	20 - 30	10 - 20	0 - 10
60 - 100										
50 - 60		a	a	a	a					
40 - 50			b	b	b	b				
30 - 40				c,d	c,d	c,d,e	d,e			
20 - 30					g	f,g	f,g,j	f,h,j		
10 - 20						i	i	h,i,j	h,j	
0 - 10							k	k	l	l

a) Generally no support but locally joint intersections might require bolting.

b) Patterned grouted bolts at 1 m collar spacing.

c) Patterned grouted bolts at 0.75 m collar spacing.

d) Patterned grouted bolts at 1 m collar spacing and shotcrete 100 mm thick.

e) Patterned grouted bolts at 1 m collar spacing and massive concrete 300 mm thick and only used if stress change is not excessive.

f) Patterned grouted bolts at 0.75 m collar spacing and shotcrete 100 mm thick.

g) Patterned grouted bolts at 0.75 m collar spacing with mesh reinforced shotcrete 100 mm thick.

h) Massive concrete 450 mm thick with patterned grouted bolts at 1 m spacing if stress changes are not excessive.

i) Grouted bolts at 0.75 m collar spacing if reinforcing potential is present, and 100 mm reinforced shotcrete, and then yielding steel arches as a repair technique if stress changes are excessive.

j) Stabilise with rope cover support and massive concrete 450 mm thick if stress changes not excessive.

k) Stabilise with rope cover support followed by shotcrete to and including face if necessary, and then closely spaced yielding arches as a repair technique where stress changes are excessive.

l) Avoid development in this ground otherwise use support systems j or k.

Supplementary notes:

I The original Geomechanics Classification as well as the adjusted ratings must be taken into account in assessing the support requirements.

II Bolts serve little purpose in highly jointed ground and should not be used as the sole support where the joint spacing rating is less than 6.

III The recommendations contained in the above table are applicable to mining operations with stress levels less than 30 MPa.

IV Large chambers should only be excavated in rock with adjusted total classification ratings of 50 or better.

These support design guidelines have found some application within the shallow mining environments, such as platinum and diamond, within the South African mining industry. Although comparable support systems are utilised at depth, the design is generally not based on these guidelines.

Applications of the MRMR have included the determination of the minimum rock bolt density derived from case studies of rock bolting in hard rock mines of Quebec (Choquet and Charette 1988). The minimum required support density (D= No. of bolts/m^2) is given by:

$$D = - 0.0214.MRMR + 1.68 \quad (\text{or } D = - 0.227.\ln Q + 0.839) \qquad (2\text{-}11)$$

thus

$$s = 1/D^{0.5} \qquad (2\text{-}12)$$

where: Q = rating based on the NGI Q system classification and s = bolt spacing on a square pattern.

The other widely utilised and internationally recognised rock mass classification system is the Q system (Barton, Lien and Lunde, 1974). This again is generally applicable to shallow tunnel excavations, as these form the majority of the empirical database. However, recent experience with dynamic failure of the immediate peripheral rock mass of excavations, known as "strain bursting", has been incorporated within this system (Barton 1997). The system utilises rock mass parameters to determine a Q value for which there is a recommended support system based on excavation dimensions and utilisation. The tables of the rock mass parameters, which are used to define the rock mass, and their relative weighting, are shown under Table 2-11.

Table 2-11. Tables for classification of the rock mass based on the Q system.

1. Rock Quality Designation		RQD
A	Very poor	0 - 25
B	Poor	25 - 50
C	Fair	50 - 75
D	Good	75 - 90
E	Excellent	90 - 100
Note i) Where RQD is reported or measured as ≤ 10 (including 0), a nominal value of 10 is used to evaluate Q. ii) RQD intervals of 5, i.e. 100, 95, 90 etc. are sufficiently accurate		

2. Joint Set Number		Jn
A	Massive, no or few joints	0.5 - 1.0
B	One joint set	2
C	One joint set plus random joints	3
D	Two joint sets	4
E	Two joint sets plus random joints	6
F	Three joint sets	9
G	Three joint sets plus random joints	12
H	Four or more joint sets, random, heavily jointed, "sugar cube", etc.	15
J	Crushed rock, earth like.	20
Note i) For intersections use, 3 x Jn. ii) For portals, use 2 x Jn.		

3. Joint Roughness Number		Jr
a) Rock wall contact, and b) rock wall contact before 10 cm shear		
A	Discontinuous joints	4
B	Rough or irregular, undulating	3
C	Smooth, undulating	2
D	Slickensided, undulating	1.5
E	Rough or irregular, planar	1.5
F	Smooth, planar	1.0
G	Slickensided, planar	0.5
Note: i) Descriptions refer to small scale features and intermediate scale features in that order		
c) No rock wall contact when sheared		
H	Zone containing clay minerals thick enough to prevent rock wall contact	1.0
J	Sandy, gravely or crushed zone thick enough to prevent rock wall contact.	1.0
Note: i) Add 1.0 if the mean spacing of the relevant joint set is greater than 3 m. ii) Jr = 0.5 can be used for planar slickensided joints having lineations, provided the lineations are orientated for minimum strength.		

4. Joint Alteration Number		φr approx.	Ja
a) Rock wall contact (no mineral filling, only coatings)			
A	Tightly healed, hard, non-softening, impermeable filling i.e. quartz or epidote.	-	0.75
B	Unaltered joint walls, surface staining only	25 - 35°	1.0
C	Slightly altered joint walls. Non-softening mineral coatings, sandy particles, clay free disintegrated rock, etc.	25 - 30°	2.0
D	Silty- or sandy-clay coatings, small clay fraction (non-softening)	20 - 25°	3.0
E	Softening or low friction clay mineral coatings i.e., kaolinite or mica. Also chlorite, talc, gypsum, graphite, etc. and small quantities of swelling clays	8 - 16°	4.0
b) Rock wall contact before 10 cm shear (thin mineral fillings)			
F	Sandy particles, clay free disintegrated rock, etc.	25 - 30°	4.0
G	Strongly over consolidated non-softening clay mineral fillings (continuous, but < 5 mm thickness)	16 - 24°	6.0
H	Medium or low over consolidation, softening, clay mineral fillings (continuous, but < 5 mm thickness)	12 - 16°	8.0
J	Swelling clay fillings, i.e. montmorillonite (continuous, but < 5 mm thickness). Value of Ja depends on percent of swelling clay-size particles, and access to water, etc.	6 - 12°	8 - 12
c) No rock wall contact when sheared (thick mineral fillings)			
K,L, M	Zones or bands of disintegrated or crushed rock and clay (see G, H, J for description of clay condition)	6 - 24°	6, 8, or 8 - 12
N	Zones or bands of silty- or sandy-clay, small clay fraction (non-softening)	-	5.0
O,P, R	Thick, continuous zones or bands of clay (see G, H, J for description of clay condition)	6 - 24°	10, 13, or 13 - 20

5. Joint Water Reduction Factor		approx. water pres. (kg/cm^2)	Jw
A	Dry excavations or minor inflow, i.e. < 5 l/min locally	<1	1.0
B	Medium inflow or pressure, occasional outwash of joint fillings	1 - 2.5	0.66
C	Large inflow or high pressure in competent rock with unfilled joints	2.5 - 10	0.5
D	Large inflow or high pressure, considerable outwash of joint fillings	2.5 - 10	0.33
E	Exceptionally high inflow or water pressure at blasting, decaying with time	> 10	0.2 - 0.1
F	Exceptionally high inflow or water pressure continuing without noticeable decay	> 10	0.1 - 0.05
Notes: i) Factors C to F are crude estimates, Increase Jw if drainage measures are installed. ii) Special problems caused by ice formation are not considered.			

6. Stress Reduction Factor		SRF
a) Weakness zones intersecting excavation, which may cause loosening of rock mass when tunnel is excavated		
A	Multiple occurrences of weakness zones containing clay or chemically disintegrated rock, very loose surrounding rock (any depth)	10
B	Single weakness zones containing clay or chemically disintegrated rock (depth of excavation ≤ 50 m)	5
C	Single weakness zones containing clay or chemically disintegrated rock (depth of excavation > 50 m)	2.5
D	Multiple shear zones in competent rock (clay free), loose surrounding rock (any depth)	7.5
E	Single shear zones in competent rock (clay free) (depth of excavation ≤ 50 m)	5.0
F	Single shear zones in competent rock (clay free) (depth of excavation > 50 m)	2.5
G	Loose, open joints, heavily jointed or "sugar cube", etc. (any depth)	5.0
Note: i) Reduce these values of SRF by 25 - 50 % if the relevant shear zones only influence but do not intersect the excavation.		

b) Competent rock, rock stress problems		σ_c / σ_1	σ_θ / σ_c	SRF
H	Low stress, near surface, open joints	> 200	< 0.01	2.5
J	Medium stress, favourable stress condition	200 - 10	0.01 - 0.3	1
K	High stress, very tight structure. Usually favourable to stability, may be unfavourable for wall stability	10 - 5	0.3 - 0.4	0.5 - 2
L	Moderate slabbing after > 1 hour in massive rock	5 - 3	0.5 - 0.65	5 - 50
M	Slabbing and rock burst after a few minutes in massive rock	3 - 2	0.65 - 1	50 - 200
N	Heavy rock burst (strain-burst) and immediate dynamic deformations in massive rock	< 2	> 1	200 - 400

Note: ii) For strongly anisotropic virgin stress field (if measured): when $5 \leq \sigma_1 / \sigma_3 \leq 10$, reduce σ_c to 0.75 σ_c. When $\sigma_1 / \sigma_3 > 10$, reduce σ_c to 0.5 σ_c. where σ_c = unconfined compression strength, σ_1 and σ_3 are the major and minor principle stresses, and σ_θ = maximum tangential stress (estimated from elastic theory).

iii) Few case records available where depth of crown below surface is less than span width. Suggest SRF increase from 2.5 to 5 for such cases (see H)

c) Squeezing rock: plastic flow of incompetent rock under the influence of high rock pressure.		σ_θ / σ_c	SRF
O	Mild squeezing rock pressure	1.5	5 - 10
P	Heavy squeezing rock pressure	> 5	10 - 20

Note: iv) Cases of squeezing rock may occur for depth $H > 350\ Q^{1/3}$ (Singh et al., 1992). Rock mass compression strength can be estimated from $q = 7\ \gamma\ Q^{1/3}$ (MPa) where γ = rock density in gm/cc (Singh 1993).

d) Swelling rock: chemical swelling activity depending on pressure of water		
R	Mild swelling rock pressure	5 - 10
S	Heavy swelling rock pressure	10 - 15

Note: Jr and Ja classification is applied to the joint set or discontinuity that is least favourable for stability both from the point of view of orientation and shear resistance (where $\tau = \sigma_n \tan (Jr/Ja)$

$$Q = \frac{RQD}{Jn} \times \frac{Jr}{Ja} \times \frac{Jw}{SRF} \qquad (2\text{-}13)$$

Thus by the determination of the applicable rock mass characteristic, within the defined parameter fields, and their associated rating, an overall classification of the rock mass is obtained. This may now be utilised to assess the stability of the proposed excavation and recommend suitable support systems based on case studies.

The assessment of the relative stability of an excavation from the classification of the rock mass, based on the Q system, will also be dependent on the size and utilisation of the excavation. An assessment of the relative safety of an excavation defines the Excavation Support Ratio (ESR) as shown in Table 2-12.

Table 2-12. Recommended ESR values for excavation safety level.

Type of Excavation		ESR
A	Temporary mine openings, etc.	2 - 5
B	Permanent mine openings, water tunnels for hydropower (excluding high pressure penstocks), pilot tunnels, drifts and headings for large openings, surge chambers.	1.6 - 2.0
C	Storage caverns, water treatment plants, minor road and railway tunnels, access tunnels.	1.2 - 1.3
D	Power stations, major road and railway tunnels, civil defence chambers, portals, intersections.	0.9 - 1.1
E	Underground nuclear power stations, railway stations, sports and public facilities, factories, major gas pipeline tunnels.	0.5 - 0.8

For unsupported stability the maximum span of an opening is given by:

$$\text{Span of opening} = 2 \times \text{ESR} \times Q^{0.4} \qquad (2\text{-}14)$$

The Q classification caters for rock mass structures that necessitate systematic support systems. For excavation spans that are indicated to be self supporting, consideration must still be given to the support of potentially unstable blocks defined by jointing.

At spans in excess of that as self supporting support recommendations are given as shown in Figure 2-8.

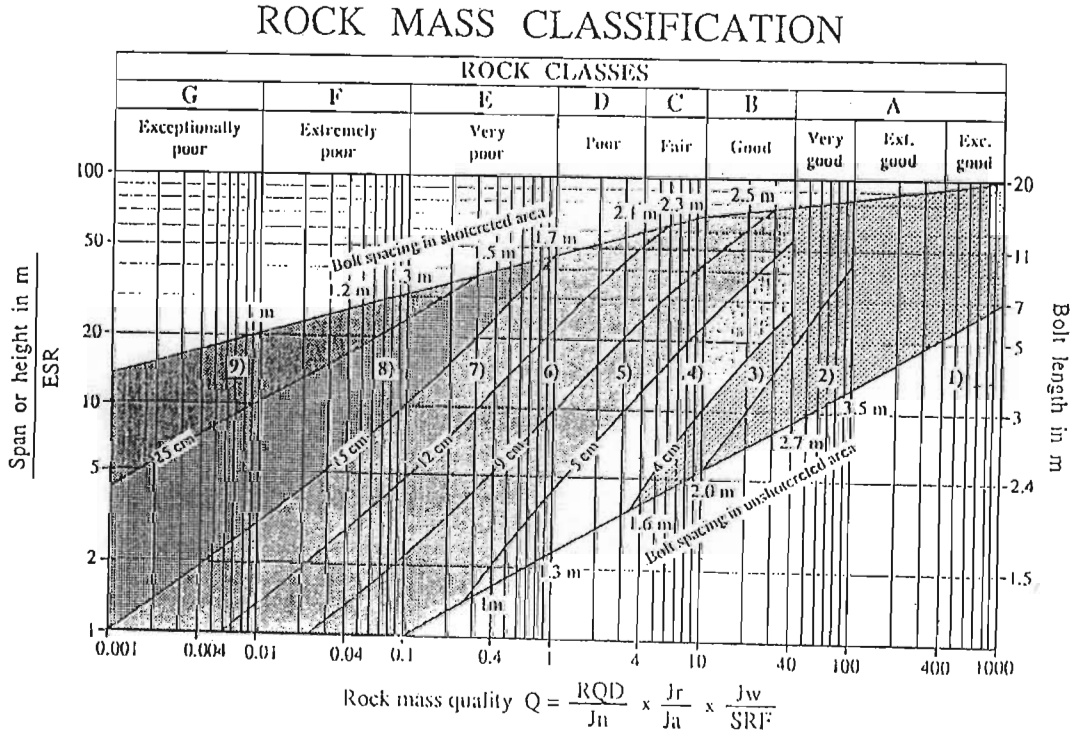

Figure 2-8. Support recommendations based on the Q system (Barton, 1997).

The Q system has found application in tunnel excavations of shallow mining orebodies within South Africa, but very limited application in deep level mining environments and usually associated with local adjustments.

Within the Q system the length of the rock bolts is purely a function of the relative size of the excavation, although the spacing of the rock bolts and the necessity for, and type of, fabric support is a function of the rock mass classification. The support pressure, or distributed rock bolt load, may also be defined as a function of the Q value and the roughness of the discontinuity which is likely to result in the potential instability (Figure 2-9).

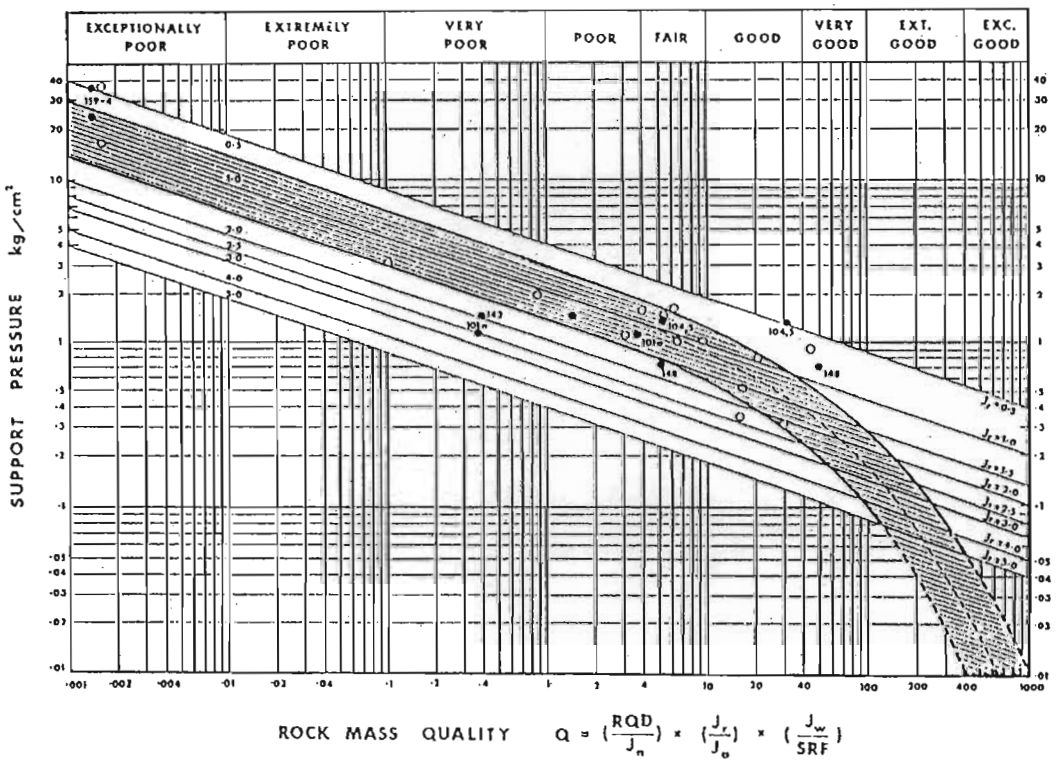

Figure 2-9. Determination of support pressure from Q value and joint roughness condition (Barton 1997).

Guidelines for the design of primary support systems were proposed by Barton, Lien and Lunde (1974) based on the Q system as shown in Table 2-13.

Table 2-13. Estimations of support pressure, length and spacing of primary support based on the Q system.

Rock mass jointing	Support pressure	Length and spacing of reinforcement
If the number of discontinuity sets > 2	$P_{roof} = (0.2Q^{-1/3}) / J_r$	Bolts $L_{roof} = (2 + 0.15B)/ESR$ Anchors $L_{roof} = (0.4B)/ESR$ $s = ((Cx10^{-3})/P_{roof})^{1/2}$
If the number of discontinuity sets ≤ 2	$P_{roof} = (0.2.J_n^{-1/2} Q^{-1/3}) / 3J_r$	
	P_{wall} : calculated with the same formulae as P_{roof}, by replacing Q with Q': $Q' = 5Q$ if $Q > 10$ $Q' = 2.5Q$ if $0.1 \leq Q \leq 10$ $Q' = Q$ if $Q < 0.1$	Bolts $L_{wall} = (2 + 0.15H)/ESR$ Anchors $L_{wall} = (0.35H)/ESR$ $s = ((Cx10^{-3})/P_{roof})^{1/2}$

Where Jr = joint roughness number; Jn = joint set number; P = support pressure (MPa); B = span of excavation (m); H = height of excavation (m); ESR = excavation support ratio; L = length of reinforcement (m); s = spacing of reinforcement (m); C = load exceeding yield strength of bolt (kN).

Tunnel support design guidelines applicable to tunnels developed under high, and often variable, stress environments, and with the potential for rockbursts, are limited in number, due to the unique nature of this environment. The recommended, and widely utilised, design guidelines within the South African mining industry are those based on the work of Wiseman (1979), and given in the Chamber of Mines research Organization industry design guidelines (Anon., 1988). The design criterion for the control of tunnel condition and the recommendation of suitable support systems is the Rockwall Condition Factor (RCF).

$$RCF = (3\sigma_1 - \sigma_3) / F.\sigma_c \qquad (2\text{-}15)$$

where σ_1 and σ_3 are the maximum and minimum principle stresses within the plane of the excavation cross section and F is a factor to represent the downgrading of σ_c, the uniaxial compressive strength, for the rock mass condition and excavation size. In a highly discontinuous rock mass it is recommended that F is approximately 0.5, and in large excavations (> 6 m x 6 m) F may be further downgraded by 10 %.

The formulation of the RCF represents a comparison of the maximum induced tangential stress of an assumed circular excavation to the estimated rock mass strength. Wiseman (1979) used this criterion to examine the implementation of support systems within South African Witwatersrand gold mine tunnels. This allowed the development of an empirical relationship between the support systems and typical (3 m x 3 m) mine tunnels within this specific geotechnical environment.

In general it was found that for RCF<0.7 good conditions prevailed with minimum support (Table 2-14); for 0.7< RCF < 1.4 average conditions prevailed with typical support systems (Table 2-

15); and for RCF > 1.4 poor ground conditions prevailed with specialist support requirements (Table 2-16).

Table 2-14. Support recommendation for good ground conditions (RCF < 0.7).

Case	Primary support (Typical requirements)	Secondary support (Typical requirements
Static stress conditions	"Spot" support where necessary (Split Sets, rock studs, etc.)	"Spot" support where necessary (rock studs, etc.)
Stress changes anticipated	"Spot" support where necessary (Split Sets, rock studs, etc.)	Fully grouted tendons > 1.5 m in length, installed on basic 2 m pattern. Support resistance: 30 - 50 kN/m^2. Rope lacing (sidewalls only)
Seismic activity anticipated	Split Sets or tendons > 1.2 m in length, installed as close to face as possible, on basic 2 m or 1.5 m pattern. Support resistance: 30 - 50 kN/m^2.	Fully grouted (pref. yield) tendons > 1.5 m in length, installed on basic 2 m pattern. Support resistance: 50 kN/m^2. Mesh and lace (hangingwall and sidewalls)

Table 2-15. Support recommendation for average ground conditions (0.7 < RCF < 1.4).

Case	Primary support (Typical requirements)	Secondary support (Typical requirements
Static stress conditions	Rock studs or tendons > 1.5 m in length, installed as close to face as possible on basic 2 m pattern. Support resistance: 30 - 50 kN/m^2.	Steel strapping or rope lacing integrated with primary support tendons; or gunite.
Stress changes anticipated	Fully grouted tendons or steel ropes > 1.8 m in length, installed as close to face as possible, on basic 2 m or 1.5 m pattern. Support resistance: 40 - 60 kN/m^2.	Rope lacing and wire mesh integrated with primary support tendons.
Seismic activity anticipated	Fully grouted (pref. yield) tendons or steel ropes > 1.8 m in length, installed as close to face as possible, on 1.5 m or double 2 m pattern. Support resistance: 80 - 110 kN/m^2.	Rope lacing and wire mesh integrated with primary support tendons, plus optional gunite.

Table 2-16. Support recommendation for poor ground conditions (RCF > 1.4).

Case	Primary support (Typical requirements)	Secondary support (Typical requirements)
Static stress conditions	(If necessary) gunite to face, then fully grouted tendons or steel ropes, length > 1.8 m on basic 1.5 m pattern, as close to face as possible. Support resistance: 80 - 110 kN/m^2.	Steel wire mesh integrated with primary support; optional gunite / shotcrete.
Stress changes anticipated	(If necessary) gunite to face, then fully grouted steel ropes or yielding tendons, length > 1.8 m on basic 1 m or double 2 m pattern, as close to face as possible. Support resistance: 120 - 230 kN/m^2.	Rope lacing and wire mesh integrated with primary support. Add integral gunite in long life tunnels. If necessary, additional hangingwall support comprising grouted steel ropes.
Seismic activity anticipated	(If necessary) gunite to face, then fully grouted steel ropes or yielding tendons, length > 2.3 m on basic 1 m pattern, as close to face as possible. Support resistance: 220 - 290 kN/m^2.	Rope lacing and wire mesh integrated with primary support. Add integral gunite in long life tunnels. If necessary, additional hangingwall support comprising grouted steel ropes.

The empirical relationship, as evaluated by Wiseman, thus primarily considered the influence of the stress environment on the excavation rock mass condition, in relation to the typical support systems utilised. In addition (Anon., 1988) consideration was also taken of the potential for seismicity and thus the rockburst hazard, and also for an environment of stress change. The empirical nature of the design is considered to cater well for bedded deep level rock mass environments, but may be less effective in environments outside of this empirical range.

The classification systems, as reviewed in this section, tend to result in a specific support category for a given rock mass condition. Thus, as the rock mass changes, due to a change in stratigraphy or stress environment, then the support recommendations may dramatically alter due to the transition to a different rock mass class. The coarser the classification system support categories, the greater this change is likely to be. Within a mining environment, with numerous areas of simultaneous tunnel excavation, the logistics of supply and control of the support system components make this potential scenario problematic. Thus there is a tendency towards standard support systems which will generally cater for the more adverse ground conditions. This results in inefficient, over supporting of the more favourable ground conditions.

Recent work based on experience in Canadian mines at depth (Kaiser, McCreath and Tannant, 1996) also examines the influence of seismicity on the design of tunnel support. The basis of the design recommendations is an evaluation of the potential for rockburst damage, and the mechanism of damage. This may vary from rockfall to violent ejection of the rock mass. An evaluation of this failure process allows the determination of the demand on a support unit, which thus allows an evaluation of the capacity of the support system.

The design methodology for support selection as detailed by Kaiser *et al.* (1996) is shown in Figure 2-10.

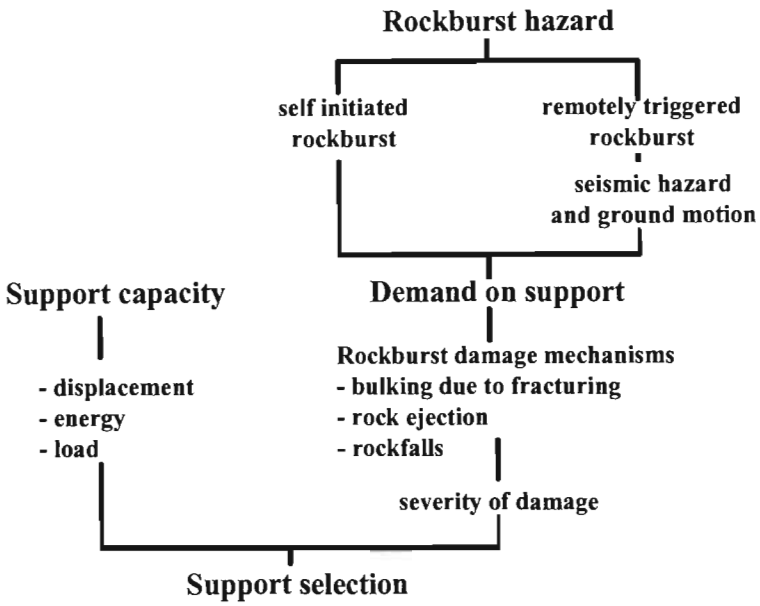

Figure 2-10. Approach for support design under rockburst conditions after Kaiser *et al.* (1996)

The demand on the support will be a function of the rock mass environment and the potential for seismic events, which will determine the mechanisms of rockburst damage as shown in Figure 2-11.

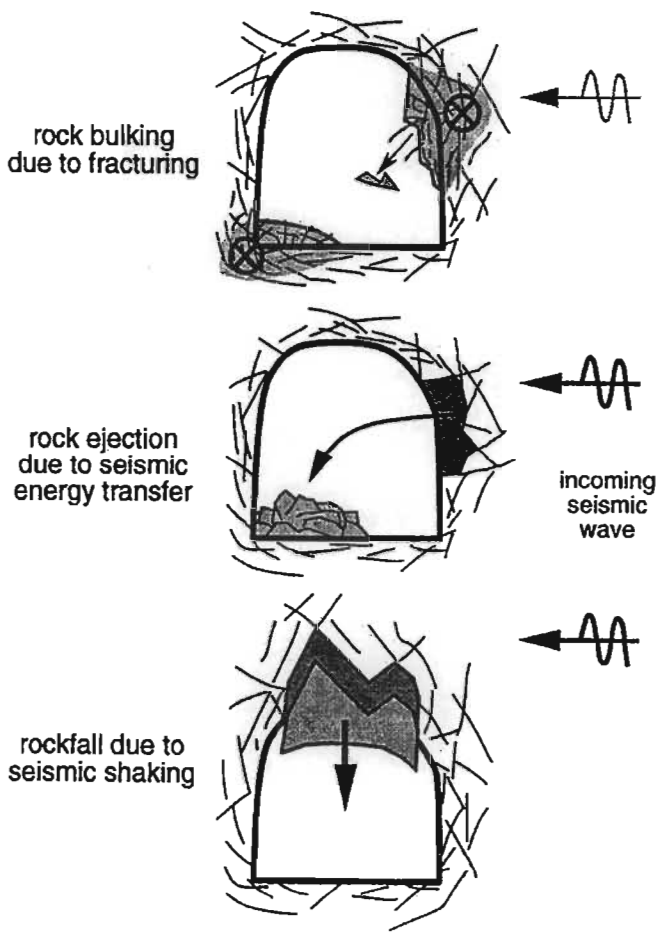

Figure 2-11. Rockburst damage mechanisms as defined by Kaiser *et al.* (1996)

The design requirements for the support system are indicated to be based on the envisaged damage mechanisms. From this, the support capacity and rock mass interaction can be defined as indicated in Figure 2-12.

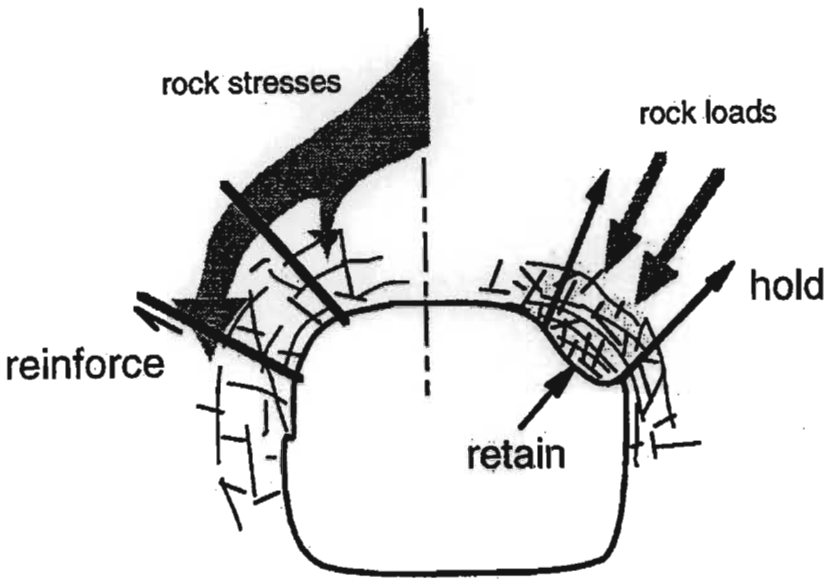

Figure 2-12. Primary functions of support elements.

The capacity of typical support systems (rock bolts, mesh and shotcrete) was evaluated by Kaiser *et al.* (1996) to determine the energy absorption capability of the systems compared to the envisaged demand. This knowledge can then be utilised to enable the design engineer to select suitable support systems based on the proposed methodology.

Aspects of this recent work are compatible with the study being conducted by the author, and these relevant sections are discussed in more detail under the appropriate aspects of research within this thesis. The work of Kaiser *et al.* (1996) gives good insight into the demands on the support systems, and consideration was also given to the loading of the support system. However, the assumption of this analysis is that the support is loaded as a system and thus tributary area loading and average support resistance of the support system is considered. This assumption is generally valid under the more massive rock mass conditions of the excavation periphery in the North American mining environment. However, this differs significantly from the current investigation where the interaction of the components of the support system within a highly discontinuous rock mass structure may result in significant differential loading.

2.4 Conclusions

The designs of tunnel support systems are principally based on either mechanistic evaluation or empirical design rules. Mechanistic evaluation allows the estimation of the demand and characteristics of the support system based on an understanding of the interaction between the

support and the rock mass. This allows an estimation of the load and deformation requirements of the specific components of the support system. However, these design considerations are currently based on relatively simple mechanisms and are generally only applicable to simple rock mass structures. As the complexity of the rock mass environment increases, design procedures tend to be based more on empirical design rules derived from experience in similar rock mass environments. This design procedure requires some form of assessment, or classification, of the rock mass in order to define the comparable rock mass environment. Most classification systems currently in use have been derived from civil engineering experience. They thus reflect a shallow, generally low, static stress environment and support systems that will ensure levels of excavation stability suitable for public use over long time frames. The applicability of these design procedures to the mining environment, and particularly deep level mining, is limited due to the significant differences in the dynamic rock mass environment and the required level of support. Empirical design procedures that have been developed specifically for the South African mining environment have proved successful in the majority of rock mass conditions encountered. However, in more adverse rock mass conditions, where significant failure of the rock mass around a tunnel excavation has occurred, and where the tunnel is subjected to dynamic loading, then failure of the support systems are encountered. The large variability in the rock mass environments within mining operations also leads to complex rock mass behaviour that is often not captured within the empirical design rules. Many of the failures of the support systems can be linked to the lack of a rational design procedure which encompasses an understanding of the mechanistic interaction between the rock mass and the support system. Recently legislation by the Department of Minerals and Energy (Anon., 1996) has recommended that support design should be based on mechanistic evaluation. The basis of this current procedure gives consideration to the support resistance or energy absorption capability of the rock bolt reinforcement system based on tributary area loading. This assumes that the rock mass between the rock bolts is inherently stable and there is thus no mechanistic consideration of the requirement for, or demand on, a fabric support system. However, these are often considered a necessity in many tunnels within the South African deep level mining environment, and, thus, the selection of these systems is still based on empirical guidelines.

There is thus an immediate need for a more rigorous method to determine, on an engineering basis, the interaction between the rock mass and all components of the support system to provide a practical and flexible support design alternative.

The focus of this research work is to improve the understanding of the mechanistic interaction of the components of the support system, both the rock bolt reinforcement and the fabric support systems, in an environment typical of that encountered in deep level mining. This understanding should allow improved estimation of the demand on the components of the support systems and thus enhanced design procedures for these mining environments.

Chapter 3

3. Rockburst case studies and mechanisms of tunnel deformation.

3.1 Introduction

Off reef excavations are not directly related to the initiation of large seismic events, however, they are often subjected to ground motions radiated from such events, which may result in severe, and sometimes quite erratic damage. This damage will be a function of the site response, which will be controlled by the current state of the support system and rock mass, in relation to the proximity to the seismic event.

In order to evaluate the current performance of support systems within this environment, a series of detailed case studies was conducted over a period of approximately three years. These visits concentrated on events that caused significant failure within the rock mass, and of the support system. In this way a detailed picture of the mechanisms of support interaction, and the relative performance of the support systems, could be constructed.

3.2 Case studies and observations

This chapter reviews the case studies chronologically, and pays particular attention to the mechanisms of the deformation of the rock mass in the vicinity of the tunnels. In this way it is considered that insight may be gained into the interaction between the rock mass and the support system.

The terms used in the description of the excavations and the support systems may be specific to the mining industry. Reference should be made to the glossary of terms if there is doubt concerning the meaning of a phrase. A brief description of a typical tunnel environment is however given in the following section.

Tunnel excavations are generally square in shape, although the blasting techniques used for excavation (the development process) often result in a very irregular profile. The tunnel will generally have rockwall dimensions of approximately 3 m to 4 m. A description of the rockwall, such as sidewall (sides), hangingwall (roof), and footwall (floor) is often used. At the development face, where the tunnel is blasted, primary support (initial support) consisting of rock bolts is installed in the freshly exposed sidewall and hangingwall rock. Rock bolts (tendons, anchors) are generally steel bars of circular cross-section, approximately 12 mm to 20 mm in diameter, which are installed in holes drilled into the rock mass perpendicular to the

excavation boundary. These may be anchored either mechanically by an expansion shell mechanism at the end of the hole, or by the encapsulation of cementitious or resin grouts, generally over the full length of the rock bolt. In the high stress environments of the deep level gold mines, failure of the rock around the tunnel excavation generally occurs during development. This results in a fractured and highly discontinuous medium in which the tunnel opening must be maintained. The rock bolts act within the rock mass to reinforce this highly discontinuous medium and are also referred to as reinforcement units. Under these conditions high areal coverage support systems are incorporated with the rock bolt reinforcement to maintain the integrity of the rock mass in the exposed skin of the excavation between the rock bolt units. Typical high areal coverage support systems consist of is a combination of steel mesh with an overlying pattern of 10 mm to 20 mm steel ropes, or shotcrete, which is a fine concrete mixture, often with reinforcing fibres, applied by spraying.

The condition of these tunnels will be influenced by the stress state in which they are developed and changes in the local field stress due to adjacent mining (extraction) of the orebody (mineral host rock). In addition, the most dramatic influence may be due to the occurrence of a seismic event (mining induced earth tremor) which results in the rapid dynamic loading of the rock mass surrounding the excavation. If the event occurs in close proximity to the tunnel, then this loading may result in violent deformations of the rock mass and loading of the support system. It is this environment in which the current support systems are often found to be inadequate, and the investigation of which will give insight into the mechanistic interaction between the components of the support system and the rock mass. This knowledge will allow improved evaluation of the support systems and thus identification of the factors relevant to the design of the support systems under these conditions.

3.2.1 Investigation into mechanisms of tunnel damage associated with seismicity at Buffelsfontein gold mine Orangia shaft pillar, December 1995.

During the initial phases of the extraction of the Orangia shaft pillar at Buffelsfontein gold mine in the Klerksdorp gold field, a series of large seismic events occurred over the past two year period. The most recent of these was a magnitude M=3.4 event on 4 July 1995, which resulted in significant damage to tunnel excavations within the immediate vicinity of the shaft pillar area. Extraction of the shaft pillar reef is a complex operation due to the presence of large normal faults, bedding plane parallel thrust faulting and dykes. This necessitated the design of complicated extraction sequences causing complex stress changes on tunnels in close proximity to the reef plane. Observations concentrated on tunnels on 24 level, at a depth of approximately 2221 m below surface, as shown in Figure 3-1.

Typical tunnel support systems used in this area comprised 3 m x 16 mm shepherd crook smooth bar on a 1.0 m x 1.0 m pattern with mesh (100 mm weld) and steel rope lacing (10 mm).

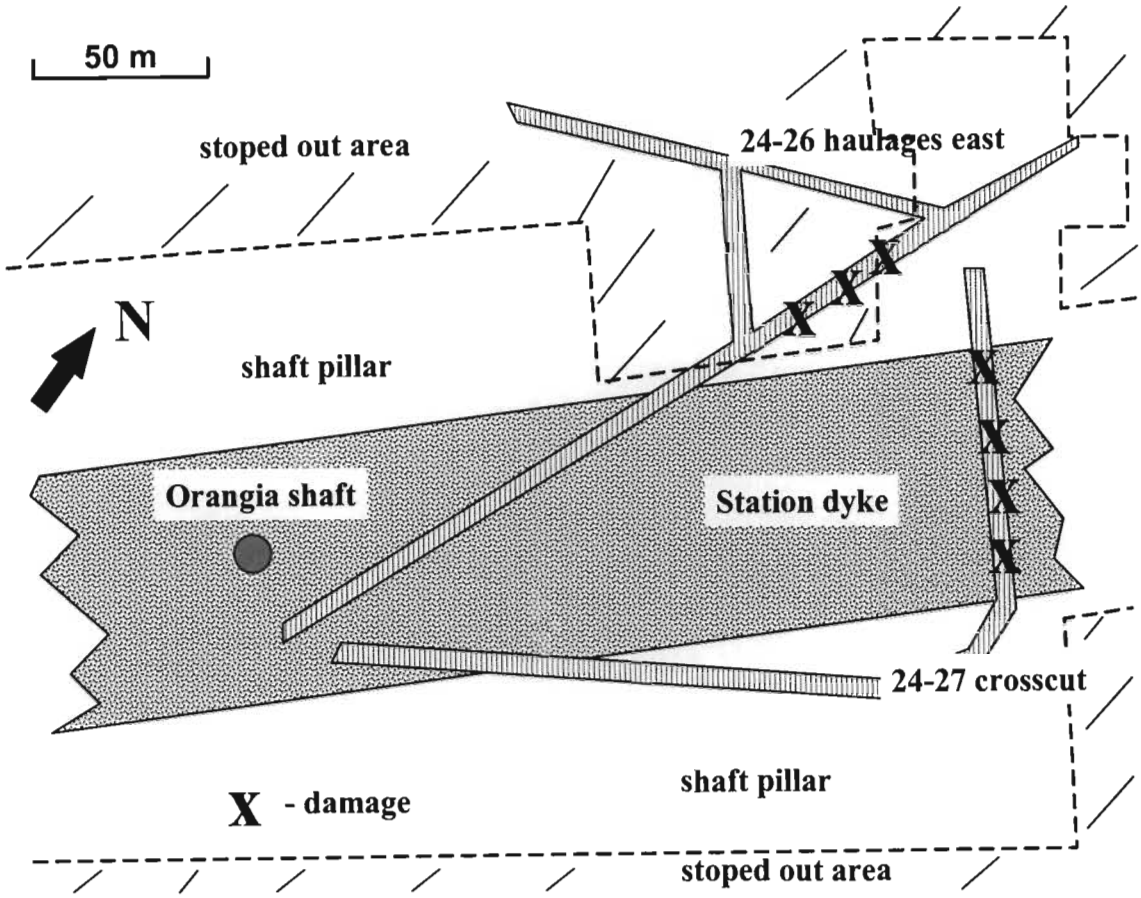

Figure 3-1. Schematic plan of 24 level tunnels where damage was observed.

In general, the highly fractured nature of the rock mass and the degree of deformation of the tunnel sidewalls and hangingwall indicated a history of high stress levels, either static or dynamic in the immediate shaft area. A significant amount of footwall heave, of the order of 1.0 - 1.5 m, was also observed in this area.

Observations of damage were made of the main 24-26 haulages east, close to the boundary of the shaft pillar and in close proximity to current shaft pillar stoping operations. Extensive damage to these excavations, sited in footwall quartzite close to the western contact of the Station dyke, was over a length of approximately 60 m. The tunnels were developed with typical square profiles with minimum design dimensions of 3.0 m x 3.0 m.

Observations of tunnel damage indicated large overall sidewall deformations, particularly on the east side of the excavation (Photograph 3-1).

Photograph 3-1. View north along 24-26 haulage east showing severe damage and deformation of the eastern sidewall of the tunnel. Note displacement of tracks (bottom right) and material rail car.

This large uniform deformation of the sidewall, particularly of with the lower portion, is indicative of either the loss of anchorage of the rock bolt reinforcement or that the depth of instability of the rock mass around the tunnel was in excess of the rock bolt length. An evaluation of the potential mechanism of loss of anchorage of the support system at this site could not be determined. However, the characteristic of uniform deformation of the sidewall rock mass structure is usually associated with the integrity of the support system and peripheral rock mass being retained. The greater deformation of the lower portion of the sidewall of the tunnel may be indicative of the weakness of the rock mass / support interaction in this area, and thus the increased degree of freedom for deformation to take place.

Immediately to the north of this damage site, deformation of the tunnel had resulted in its complete closure. At this location direct observations of the performance of the rock bolt reinforcement within the rock mass could be made.

Photograph 3-2. Shear deformation of smooth bar rock bolt in upper east sidewall of 24-26 haulage east.

In the highly fractured, and bedded rock mass, significant shear deformation of the smooth bar rock bolts was observed (Photograph 3-2). It was observed that shear deformation within the rock mass was more prevalent in the hangingwall than in the sidewall. Also, that where the rock mass was more massive, greater interaction between the rock bolt and the rock mass resulted in tensile failure of the rock bolt unit (Photograph 3-3), particularly under the dynamic loading conditions.

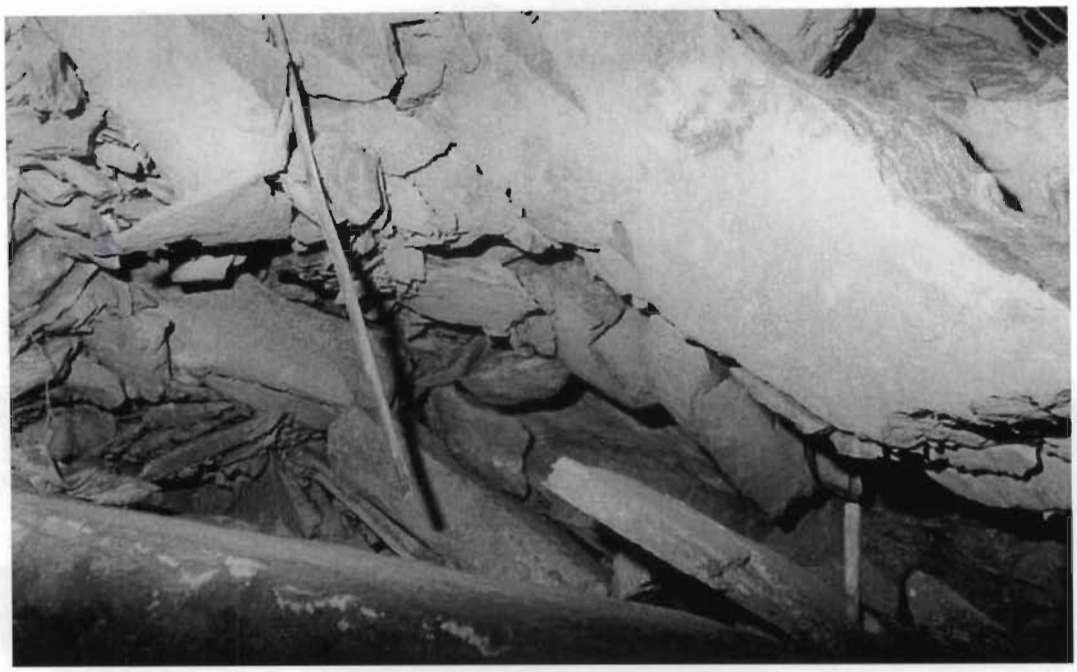

Photograph 3-3. Tensile failure of a smooth bar rock bolt in the immediate hangingwall of the 24-26 haulage east.

Photograph 3-3 indicates that significant debonding along the length of the rock bolt had occurred, but anchorage of the rock bolt within the stable rock mass was maintained. This was sufficient to generate tension in the rock bolt in excess of its yield strength and resulted in subsequent tensile failure.

Further observations of tunnel damage beyond this point were conducted from the north side of the fall of ground. In this area significant damage was associated with the hangingwall of the excavation, the extent of which resulted in total collapse. This enabled access above the fall of ground (Photograph 3-4).

Photograph 3-4. View south along 24-26 haulage east showing collapse of hangingwall to an estimated height of 1.5 m to 2.0 m.

The height of collapse, and most of the hangingwall instability, was of the order of 1.5 m to 2.0 m above the estimated previous hangingwall profile. The pattern of the remaining hangingwall rock bolt support as shown in Photograph 3-4 is low. From this it may be concluded that the current hangingwall profile is essentially self supporting. Thus the remaining rock bolt units are considered to be anchored within the stable rock mass. The failure of the support system in this area appears to be due to the failure of the mesh and lace fabric support between the rock bolts. This resulted in a subsequent general unravelling of the rock mass from between the rock bolt reinforcement (Photograph 3-5).

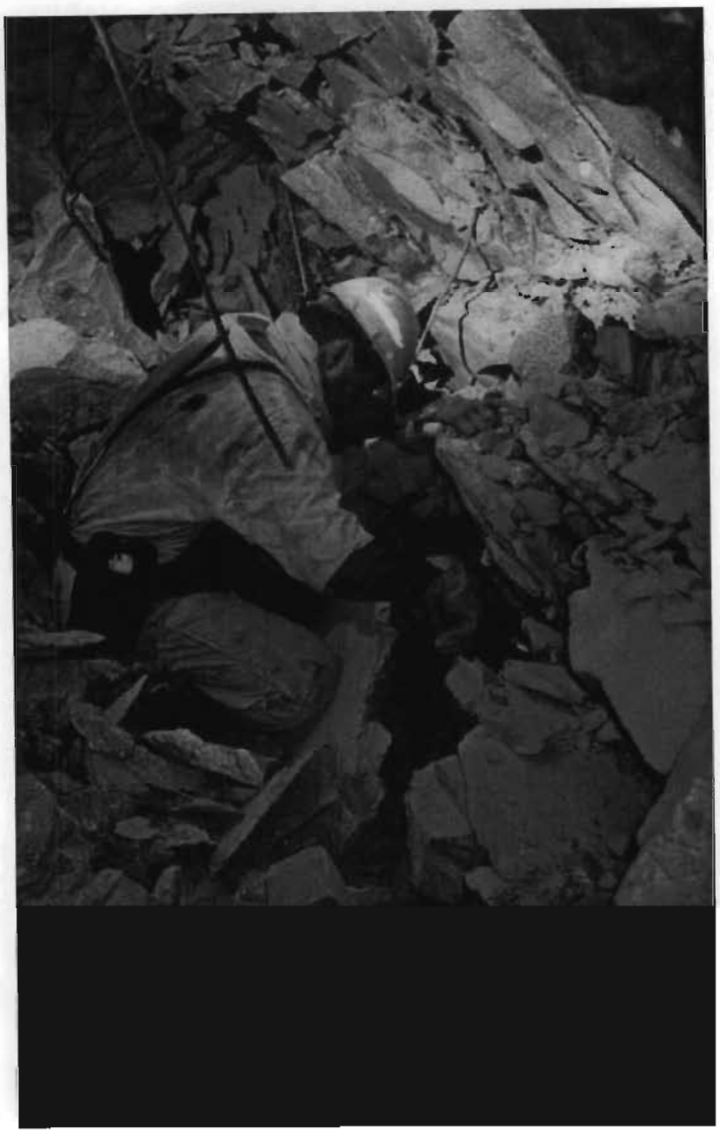

Photograph 3-5. View south along 24-26 haulage east at the end of the area of hangingwall collapse showing the highly fractured nature of the immediate hangingwall rock mass and remaining rock bolt reinforcement.

The highly fractured nature of the rock mass as shown in photograph 3-5 resulted in poor interaction of the rock bolt reinforcement in the immediate hangingwall rock mass.

Further observations were conducted in the 24-27 crosscut. This excavation traverses the Station dyke within the shaft pillar area and was developed for the purposes of accessing reef for stoping of the shaft pillar. Rockburst damage of this excavation resulted in large uniform deformation of the sidewalls of the excavation (Photograph 3-6).

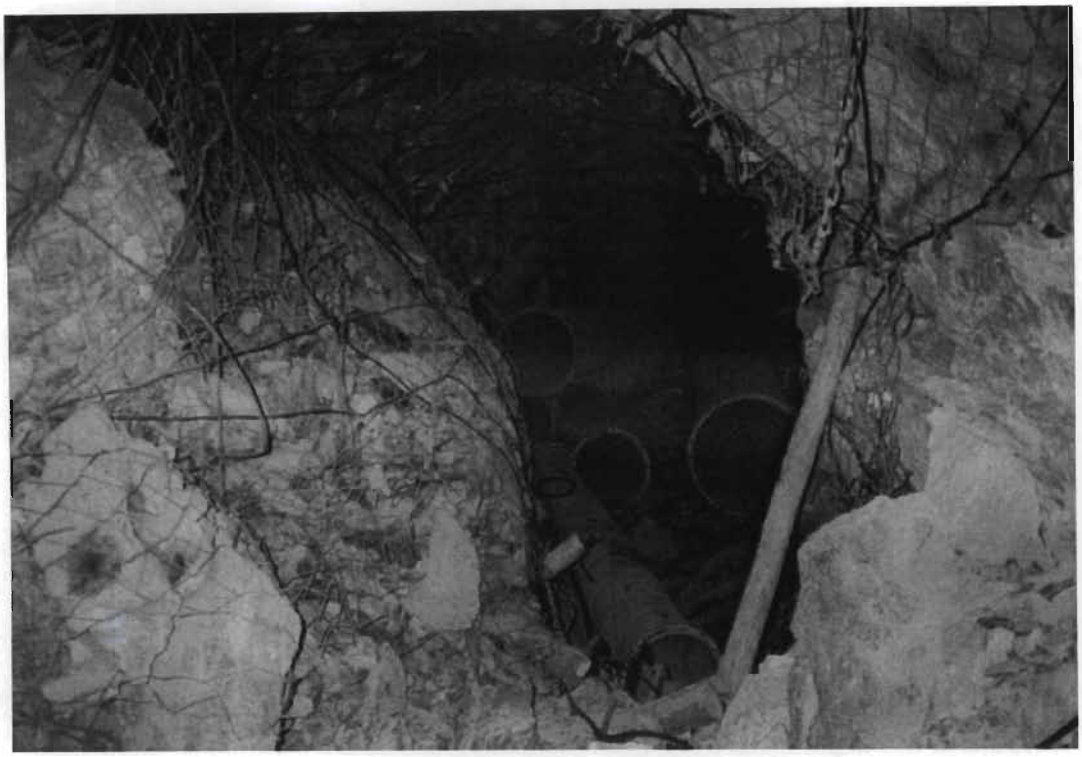

Photograph 3-6. View north west along 24-27 crosscut showing large deformation of south west sidewall of tunnel.

The sidewall again showed greater deformation of the lower portion. In this area the magnitude of the deformation caused some damage to the mesh and lacing fabric support as a result of differential deformation across the sidewall profile. However, integrity of the support system was maintained thus ensuring the safety of anyone in the excavation.

Conclusions

Damage to the sidewalls at this site was characterised by large uniform deformation. Whereas, damage in the hangingwall was due to unravelling of the rock mass between the rock bolts due to excess loading of the mesh and lace fabric support.

3.2.2 Investigation into mechanisms of tunnel damage associated with a seismic event of M=3.6 at East Driefontein Gold Mine No.4 shaft on 14 September 1995.

On 14 September 1995 a rockburst occurred at East Driefontein gold mine, causing extensive damage to haulages east of No. 4 Shaft between 31- and 36 Levels, about 2500 m below surface (Figure 3-2). A seismic event with magnitude M=3.6 was recorded by the seismic network based at West Driefontein gold mine at the same time.

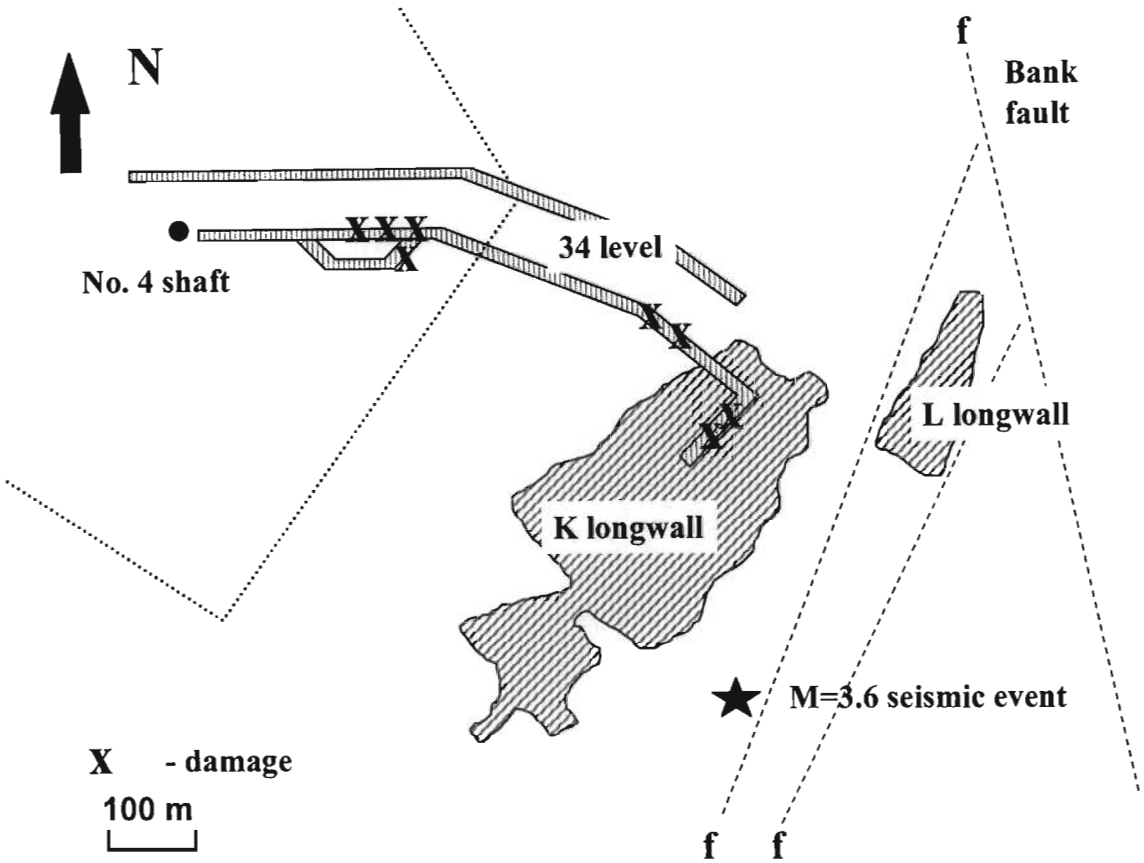

Figure 3-2. Schematic of stoping layout and tunnel damage for 34 level No.4 shaft East Driefontein gold mine.

The seismic event affected excavations from 31 to 36 Levels over a wide area east of No. 4 Shaft. The damage was confined mainly to crosscuts and haulages that provide access to the K- and L Longwalls situated to the south-east of 4 Shaft (Figure 3-2). This area has a history of large seismic events, many of which have caused damage to the access development.

The damage on 34 and 35 Levels mainly affected the north-eastern sidewall and the hangingwall of the excavations. These excavations were orientated in a south-easterly direction which corresponded to the general strike of the local stratigraphy. A key factor controlling the distribution of the damage was the type of support in place at the time of the rockburst. Sections which were supported by grouted rebar's, mesh, lacing and shotcrete, experienced little

damage, while other sections, where mesh and lacing had not yet been installed, sustained severe damage.

In the 34 level deep footwall drive East, the damage was concentrated in the north-eastern sidewall and hangingwall. An exception was in the area of the tunnel loop east of the shaft, where the southern sidewall was severely damaged for a short distance where the loop approached the main development (Photograph 3-7). Here the damage to the upper sidewall and hangingwall of the tunnel is clearly illustrated. The lack of a fabric (mesh and lace) support system in this area has resulted in the unravelling of the rock mass from between the rebar rock bolt reinforcement under the dynamic loading conditions associated with the seismic event.

Photograph 3-7. View east along 34 level deep footwall drive showing collapse of rock mass between rock bolt reinforcement.

It is of interest to note that in this area no failures of the rebar rock bolt support type were observed under these severe rockburst conditions. This observation was consistent with other areas at the same tunnel damage site (Photograph 3-8).

Photograph 3-8. View east along 34 level deep footwall drive indicating rockburst damage to the tunnel excavation. Note crushing of metal ventilation tubes on left hand side.

The generally highly fractured and slab like nature of the debris rock mass from the failure of the tunnel structure is also shown in Photographs 3-7 and 3-8. The highly discontinuous nature of the rock mass is considered to result in poorer interaction between the rock bolt reinforcement and the body of the rock mass. The absence of fabric support in this case resulted in collapse of the rock mass structure. The poor interaction between this unstable rock mass volume and the rock bolt reinforcement also results in low dynamic loading on the rock bolt, and survival under these conditions. The violent nature of the failure process is illustrated by the crushing of the ventilation pipe situated in the bottom left corner of Photograph 3-8.

The high intensity of failure of the tunnel peripheral rock mass in this area compared to other areas of 34 level, with similar support systems, may also have been a function of the interaction between the tunnel excavations in the loop. This would result in a generally higher induced stress state, with associated increased rock mass damage prior to the event, and thus the excavation being more prone to seismic induced rockburst damage.

Along most of the length of the 34 level deep footwall drive, the support system consisted of weld mesh and lacing attached to shepherd crook rebar rock bolt reinforcement. This support system in general maintained the stability of the excavation. However, significant deformation of the tunnel peripheral rock mass did occur. This resulted in bulking and bagging of the mesh and lace fabric, to such an extent that the excavation was no longer operational. The general nature of the sidewall of the tunnel is shown in Photograph 3-9. Differential bulking of the rock mass is clearly indicated, dependent on the relative interaction and resistance to deformation provided by the different components of the support system.

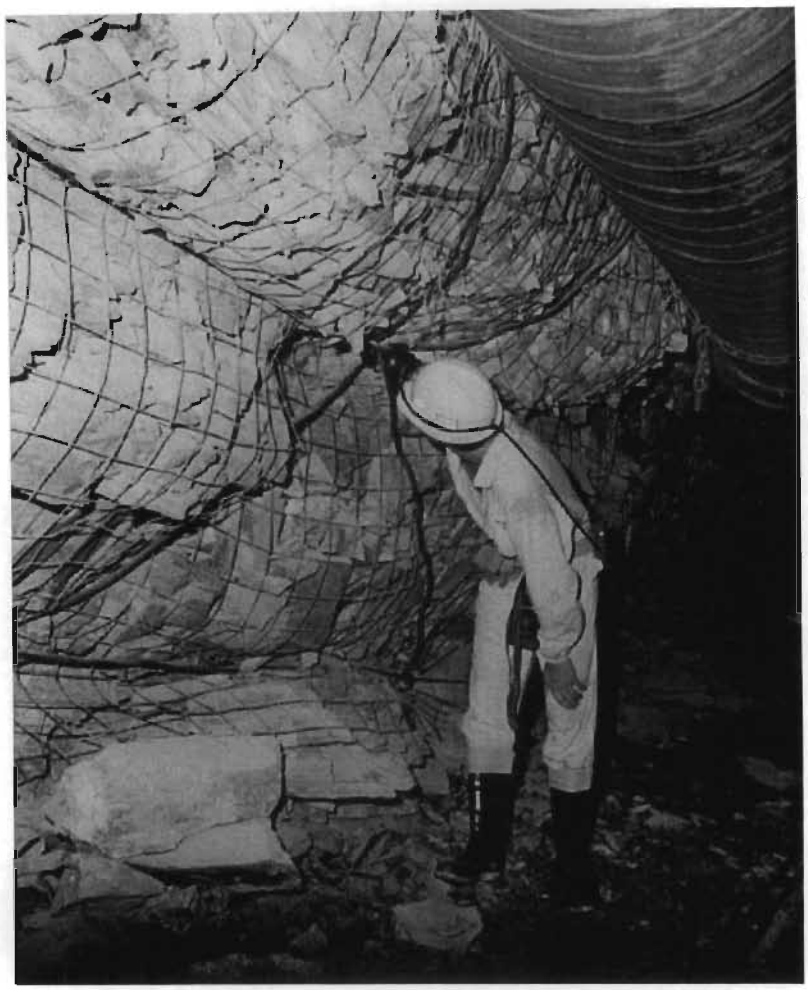

Photograph 3-9. View of general nature of sidewall deformation of 34 level deep footwall drive north.

The volume of rock mass bulking had at one site resulted in loading of the lacing fabric to the extent that failure of the rock bolt had resulted (Photograph 3-10). The failure appeared to be predominantly axial, as indicated by the rough nature of the failure plane, the limited degree of bending of the remaining rock bolt shaft, and the necking of the rockbolt shaft in the vicinity of the failure plane.

Photograph 3-10. View indicating mesh and lacing with loss of containment at point of lacing cross over. The cleanly failed (circular) surface of the rock bolt may be seen in the darker area of the rock near the centre of the photograph.

Further observations in a parallel excavation indicated similar mechanisms of rock mass deformation. However, of interest at this site, was the use of shotcrete in sections of the tunnel, and its influence on general rock mass deformations and tunnel condition (Photograph 3-11).

It was noted that, where shotcrete was utilised in conjunction with rock bolt reinforcement, minimal damage occurred. Some cracking of the shotcrete fabric was noted, but this did not appear to influence the overall integrity of the system. In an immediately adjacent section of the tunnel, where only rock bolt reinforcement was utilised, significant unravelling of the rock mass between the rock bolt units was again observed. Thus the relatively thin (10 mm – 20 mm) application of shotcrete as a full areal coverage support system had a significant effect on the stability of the excavation.

Photograph 3-11. View east in 34 level twin footwall drive comparing shotcreted and un-shotcreted sections of the tunnel.

The lack of deformation associated with the shotcrete section of the tunnel, in comparison to the adjacent bolted sections, would indicate that the primary mechanism of rock mass deformation was due to expulsion of previously fractured material. The relatively stiff nature of the shotcrete fabric will greatly limit deformation as a result of forces below its yield capacity. It is envisaged that, if initiation of fracturing within the rock mass had occurred as a result of the dynamic loading then more significant damage to the shotcrete fabric would have been observed.

An area of significant damage was associated with the plan position of the K longwall abutment. This area also coincided with a transition between full mesh and lace support and an area supported solely by rock bolt reinforcement. The area supported by only rock bolts had again experienced general unravelling of the rock mass and falls of ground as previously discussed. In the area supported by mesh and lacing, again in close proximity to the intersection of another tunnel excavation, significant failure of the support system had also occurred. An aspect of this failure was the isolated collapse of the hangingwall of the tunnel. The mode of support system failure was shear failure of the rock bolt reinforcement. This guillotining of a significant number of the rock bolts resulted in the overall failure of the support system. This shear movement appeared to have occurred along well defined bedding planes, sub-parallel to the hangingwall of the tunnel (Photograph 3-12).

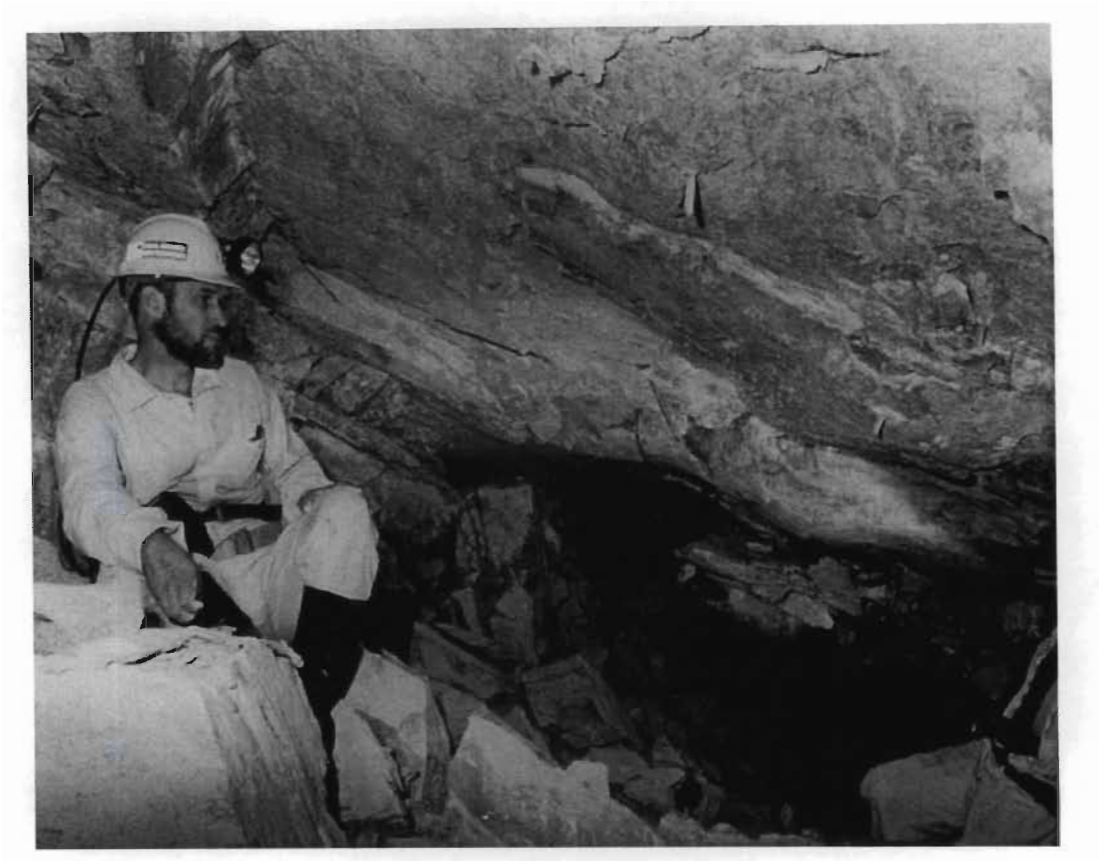

Photograph 3-12. View east along 34 level deep footwall drive showing shear failure of hangingwall rock bolt reinforcement on a dominant bedding plane, with subsequent collapse of the general hangingwall rock mass.

In the near vicinity to this failure, examination of the performance of identical rebar rock bolt reinforcement under shear deformation could be clearly observed (Photographs 3-13 and 3-14). At this site it is considered that the higher frequency of the bedding planes, and thus thinner layer thickness, has enabled the rock bolts to deform rather than to be guillotined at a localised shear. An estimated 25 mm of shear had occurred within the reinforced rock mass due to the dynamic loading conditions. It is interesting to observe the degree of deformation that these relatively stiff rock bolt units can accommodate within a fractured rock mass structure.

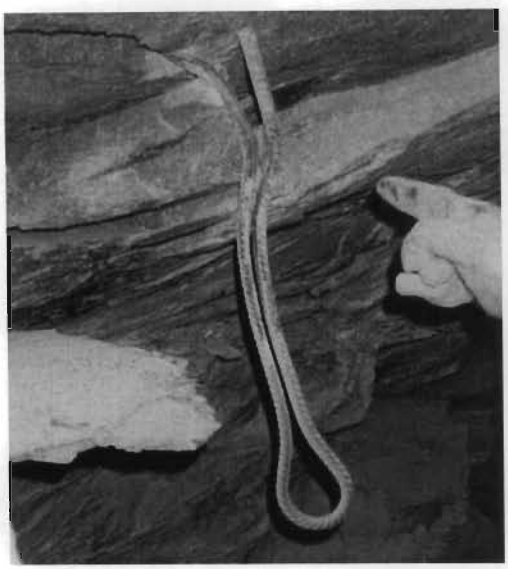


Photographs 3-13 and 3-14. Examples of shear deformation of shepherd crook rebar rock bolts installed in the hangingwall of 34 level deep footwall drive subsequent to dynamic loading

The high incidence of shear deformation and failure in the hangingwall of this section of the tunnel may be a function of the structure of the rock mass relative to the orientation of the excavation. The orientation of the excavation parallel to the strike of the stratigraphy, and the highly bedded nature of the rock mass, results in a higher degree of freedom of hangingwall blocks to shear across the excavation compared to crosscut orientated excavations.

The localised nature of excavation failure under rockburst conditions is also clearly illustrated in this vicinity (Photograph 3-15). Failure at this site is a function of the loss of anchorage of the rock bolt reinforcement system. This may be caused by the depth of instability of the rock mass being in excess of the rock bolt length, or failure (snapping) of the rock bolt at a point within the unstable rock mass. The mode of rock bolt failure could not be determined for this site. Failure of the mesh and lace fabric support was due to both the ripping of the mesh and tensile failure of lacing strands. This resulted in a relatively large scale unravelling of the rock mass.

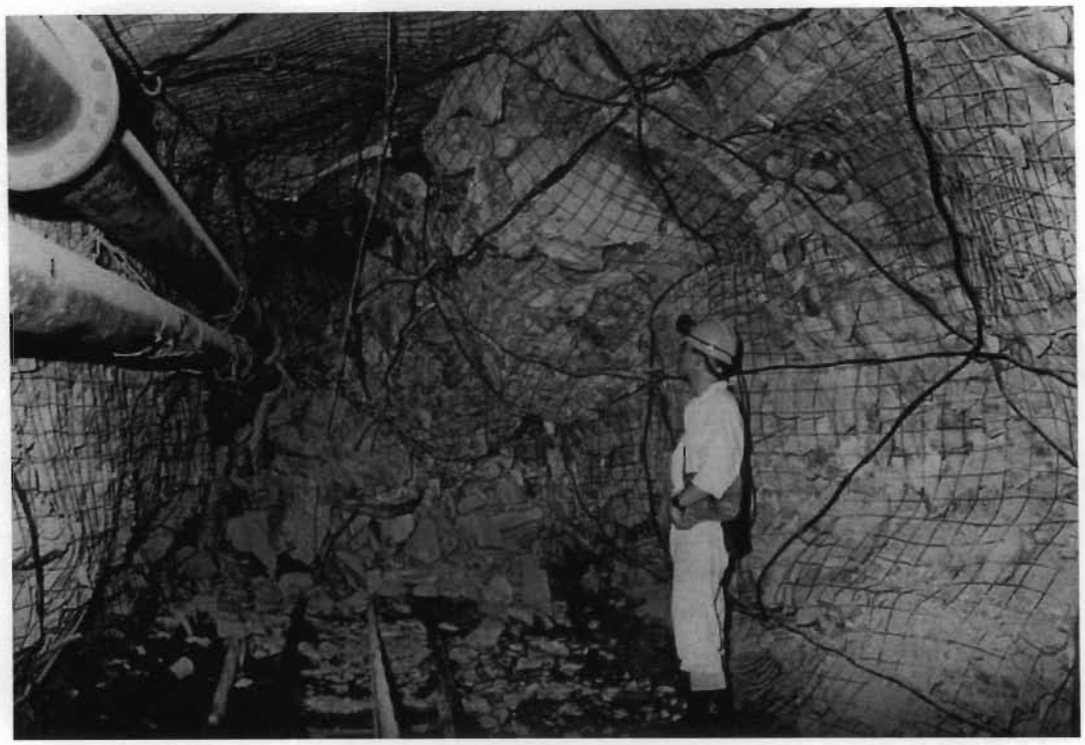

Photograph 3-15. View west along 34 level deep footwall drive showing localised failure of mesh and lacing support system and complete closure of the tunnel at this site.

A further failed section of tunnel, to the east of the last site, was only supported by rebar rock bolts. This also suffered a general unravelling of the rock mass between the rock bolt units (Photograph 3-16). It is estimated that at this site between 0.5 m and 1 m of the tunnel peripheral rock mass collapsed under dynamic loading associated with the seismic event. Of significant importance is the limited failure of the rock bolts under these conditions.

At this site a failed rebar rock bolt was observed, which, due to the variability in fracture intensity, had previously supported a well defined rock mass block (foreground of Photograph 3-16). The dynamic energy associated with this block had resulted in the recent failure of the rock bolt under tensile loading. This was characterised by the necking of the bar and cupped nature of the fresh failure surface.

An estimate could be made of the minimum peak particle velocity in the skin of the 34 level deep footwall drive at this site based on the above observation. The mass of the block, attached to the failed rebar, was estimated to be approximately 800 kg. Energy calculations can thus be used to estimate the minimum dynamic ground velocity to result in failure (Anon., 1988).

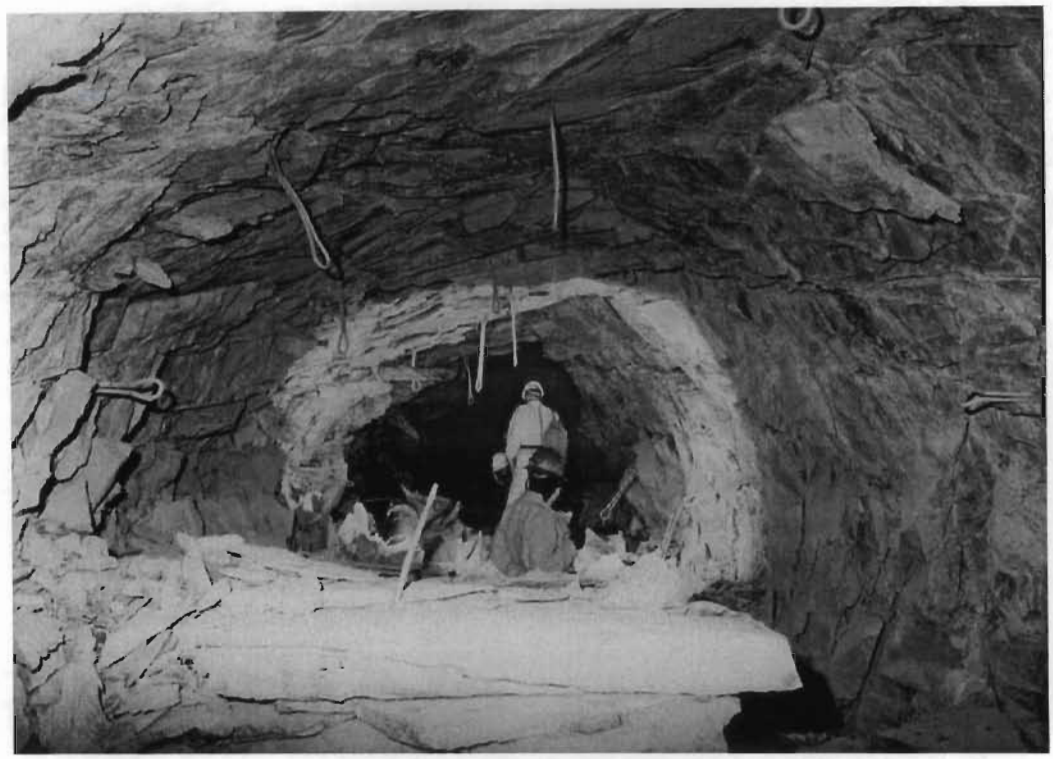

Photograph 3-16. View east along 34 level deep footwall drive showing general rock mass unravelling around shepherd crook rebar rock bolts and dynamic failure and necking of one rock bolt in the foreground.

The following procedure details the calculation of the minimum ground velocity of the excavation fractured peripheral rock mass.

Kinetic + Potential energy of block ≥ Elastic energy absorbed by bar up to failure

$$E = {}^1/_2.m.v^2 + m.g.h \qquad (3\text{-}1)$$

The bar protruding from the block exhibited necking for a distance of about 10 mm. It is assumed that similar necking occurred on the section of the bar still grouted in the roof. It is estimated that the bar was extended by about 10 mm before failure.

m = mass of block = 800 kg
h = extension of bar at failure = 0.01 m
g = gravitational acceleration = $10 m/s^2$
F = Tensile strength of ripple bar = 15 tons = 150 kN

Energy absorption capability of bar

$$E = {}^1/_2.F.h = {}^1/_2.150e3 \times 0.01$$
$$E = 750 \text{ J}$$

Therefore

$$E = 750 = {}^{1}/_{2} \times 800 \times v^2 + 800 \times 10 \times 0.01$$

Thus the minimum dynamic ground velocity is estimated as:

$$v = 1.3 \text{ m/s}$$

From the magnitude of the event, and the ground velocity on the skin of the excavation as indicated above, it is estimated that the source of the seismic event was relatively distant (Durrheim *et al*, 1996). Thus comparisons of the observed damage in the tunnels may be related to the site effects due to the indicated relatively large distance of the source in comparison to the extent of damage. This would result in a more uniform seismic radiation pattern and associated ground velocities.

Observations of tunnel deformation along the 34 level deep footwall drive closer to the K longwall revealed greater footwall heave and more sidewall deformation close to the floor. This was particularly the case with the up dip, north sidewall of the excavation (Photograph 3-17).

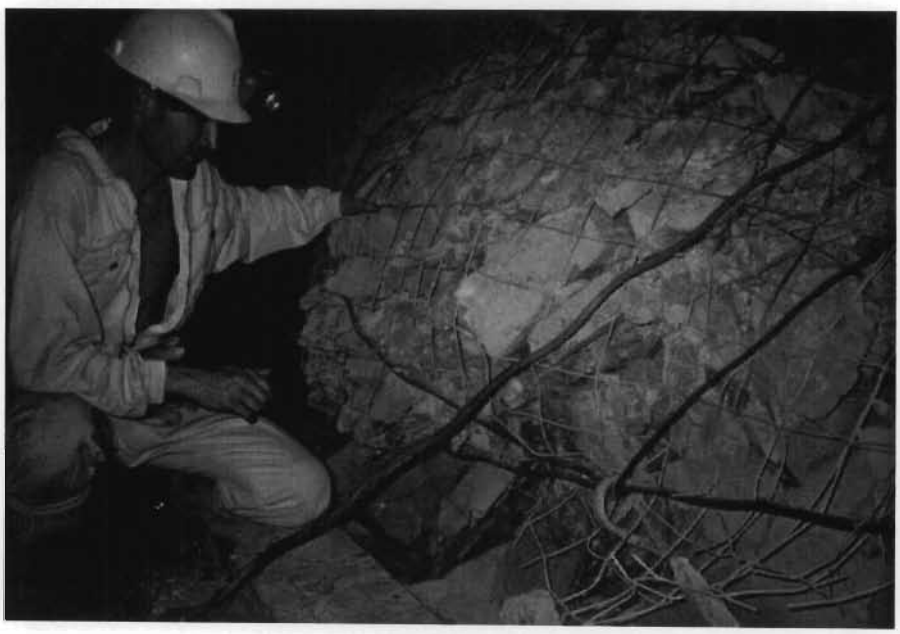

Photograph 3-17. View of the bottom corner of 34 level deep footwall drive tunnel showing large, contained deformations of the rock mass in this area.

The characteristic of this deformation is that it is considered to be a function of the structure of the rock mass relative to the excavation orientation. Footwall heave and deformation of the lower north sidewall is sympathetic with the general dip of the strata in this vicinity. This has resulted result in buckling and dilational deformation mechanisms. The differential bulking of the

rock mass (Photograph 3-17) indicates the relative interaction of the components of the support system and their influence on this deformation of the rock mass.

Conclusions

At this rockburst investigation the principal mechanisms of support system failure was the unravelling of the rock mass between the rock bolts, particularly in the sidewall of the tunnels. The shear failure of hangingwall rock bolts was a characteristic of this site. The observation of shotcrete indicated the significant support role which this stiff membrane can provide under the loading conditions experienced at this site.

3.2.3 Investigation into mechanisms of tunnel damage associated with a seismic event of M=4.4 at Vaal Reefs Gold Mine No.5 shaft on 10 February 1997

A rockburst occurred at Vaal Reefs Gold Mine on 10 February 1997, causing severe damage to haulages and crosscuts in the vicinity of No 5 Shaft Fault, about 1900 m below surface. A seismic event with a local magnitude M=4.4 was recorded by the mine seismic network. The focus of the event was near the intersection of the No 5 Shaft fault and the Clemcor dyke, about 1.2 km north of the No. 5 Shaft (Figure 3-3). Damage was sustained over two levels (60-50 and 62) and an area of about 1200 x 600 m. The damage to the haulages caused severe disruptions to production operations.

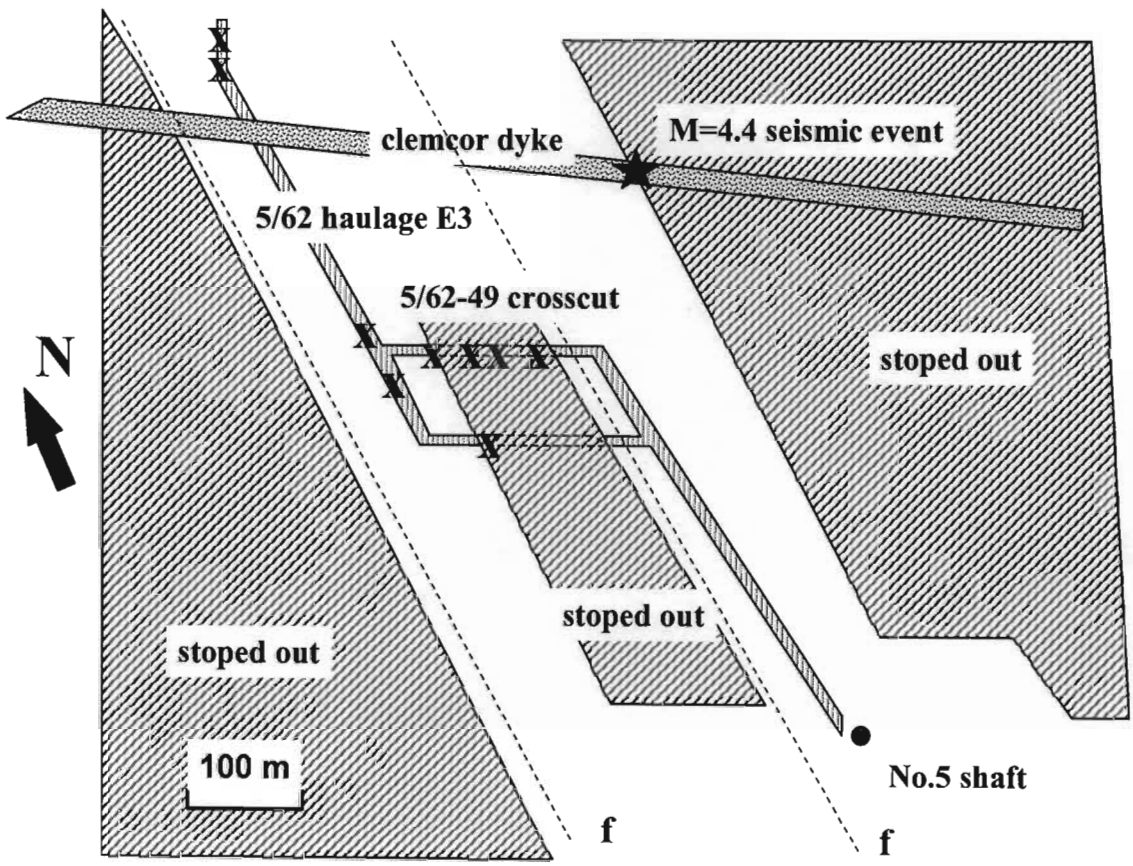

Figure 3-3. Schematic plan of 62 level tunnel damage Vaal Reefs No.5 shaft

The footwall and hangingwall strata in the vicinity of the Vaal Reef in which the tunnels were sited comprise a series of argillaceous to siliceous quartzites.

The main haulages on 60-50 and 62 level are developed within the plan projection of the fault losses associated with the No. 5 Shaft Fault and other faults. Tunnel support in the No. 5 Shaft Fault area is installed in three phases:

a) Primary support is installed during development and consists of 2.4 m Gewibar rock bolts.

b) Secondary support consists of a 1 m diamond pattern of 2.2 m grouted wire rope loops plus mesh and lacing, i.e. 5 loops/ring, rings spaced at 0.5 m.

c) Tertiary support may consist of 4.5 m or 6 m cable anchors, where considered necessary.

The location of the damage for 62 level may be found on Figure 3-3. The limited damage observed on 60-50 level was approximately in the same general plan location.

On 60-50 level most damage was found in crosscuts passing from solid to overstoped ground, especially in the vicinity of the dyke which was intruded close to the fault surface.

In the 60-50 50N crosscut both the hanging- and sidewalls experienced significant bulking. In places the support system had failed due to either breaking of the lacing, made of destranded hoist rope, or failure of the mesh panel (Photograph 3-18). This mode of failure indicates the localised nature of the interaction between the rock bolt reinforcement and the immediate sidewall rock mass. The energy associated with this large dynamic deformation was, in this case, in excess of the capacity of the mesh panel, as defined by the lacing configuration. The fractured, plate like nature of the rock mass in the immediate sidewall of the excavation is clearly shown in Photograph 3-18.

The crosscut beyond this point was completely blocked due to collapse of the hangingwall. This was as a result of the failure of the hangingwall grouted wire rope loops. The mechanism of failure was either the snapping of the cable, or the loop at the skin of the excavation having been pulled out of the hole. The collapse occurred about 20 m to the west of the fault plane.

Photograph 3-18. Failure of lower sidewall between rock bolt reinforcement in 60-50 50N crosscut.

On 62 level the most severe damage was sustained in the 62-49 northern haulage. The general damage was similar to that observed on 60 50 level. Damage commenced close to the fault contact, which also defined the limit of the over lying mining abutment. Significant closure of the sidewalls, hangingwall and footwall had occurred at this point. The integrity of the mesh and lacing support had generally been maintained. However, significant bagging had occurred and large overall deformations are indicative of the lack of rock bolt reinforcement anchorage. This loss of anchorage may be due either to failure of the rock bolt reinforcement system or that, due to the influence of the higher stresses associated with the mining abutment at this point, the depth of rock mass instability was in excess of the length of the reinforcement.

Immediately to the west of this area the mesh and lacing areal coverage support had failed on the north sidewall due to excess bulking of the rock mass between the rock bolt reinforcement. The grouted wire rope reinforcement had however generally maintained its anchorage, although a few units were observed to have failed.

The crosscut from this point to the down dip stope abutment is generally overstoped. Damage was still observed to the northern sidewall, hangingwall and footwall, but of lower magnitude to the damage close to the mining abutments. Unravelling of the rock mass between the rock bolt reinforcement resulted in severe bagging of the mesh and lacing fabric support in parts of the tunnel. Evidence of the severity of the dynamic ground motion experienced by the tunnel was the observation of a pipe, which was originally lying against the sidewall, now trapped below the rails of the haulage.

Close to the western stoping abutment complete closure of the tunnel had occurred. Viewed from the east, closure was due to the failure of the mesh and lacing fabric support and unravelling of the rock mass, while the reinforcement units remained intact and anchored in stable ground. To the west of the mining abutment, viewed from the opposite side of the fall of ground (Photograph 3-19), the mesh and lacing fabric support remained intact but failure of the reinforcement units resulted in collapse of the hangingwall rock mass.

Photograph 3-19. View west of total collapse of hangingwall of 62-49 crosscut close to a stoping abutment.

The mode of the hangingwall failure could not be determined from observation but is considered to be due to either the failure of the rock bolt reinforcement system or the depth of instability being in excess of the length of anchorage.

The 62-48 crosscut, parallel and approximately 100 m to the south of 62-49, had sustained relatively minor damage in comparison to the previously described tunnel damage. Close to the

western, down dip mining abutment, hangingwall collapse had occurred due to failure of the mesh and lacing fabric support and unravelling of the rock mass between the rock bolts (Photograph 3-20). This mechanism of failure again illustrates the limited direct interaction between the rock bolt reinforcement and the immediately peripheral, highly discontinuous rock mass. The use of mesh and lacing fabric support, of sufficient capacity, is necessary under these conditions.

Photograph 3-20. Unravelling of hangingwall between rock bolt reinforcement due to highly fractured nature of the hangingwall and failure of mesh fabric (bottom right) in 62-48 crosscut.

In the 62 level haulage north from the 62-49 crosscut, most deformation occurred in the hangingwall and footwall of the tunnel, although the support system had prevented collapse of the hangingwall strata. Subsequent rehabilitation work of the hangingwall consisted of removal of the bagged mesh and lacing fabric support. Observation of the stability of the rock mass subsequent to this removal of the mesh and lacing indicated an unstable rock mass thickness of approximately 1.5 m. Loss of the retaining function of the mesh and lacing caused significant unravelling of the hangingwall between reinforcement units in spite of large blocks being involved (Photograph 3-21). This again demonstrates the mechanism of limited interaction between the rock bolt reinforcement and the more highly fractured rock mass in the immediate hangingwall of the excavation. The bagging of the mesh and lacing fabric subsequent to the seismic event, and prior to the rehabilitation work, shows how the fabric can be directly loaded by the total volume of unstable rock mass.

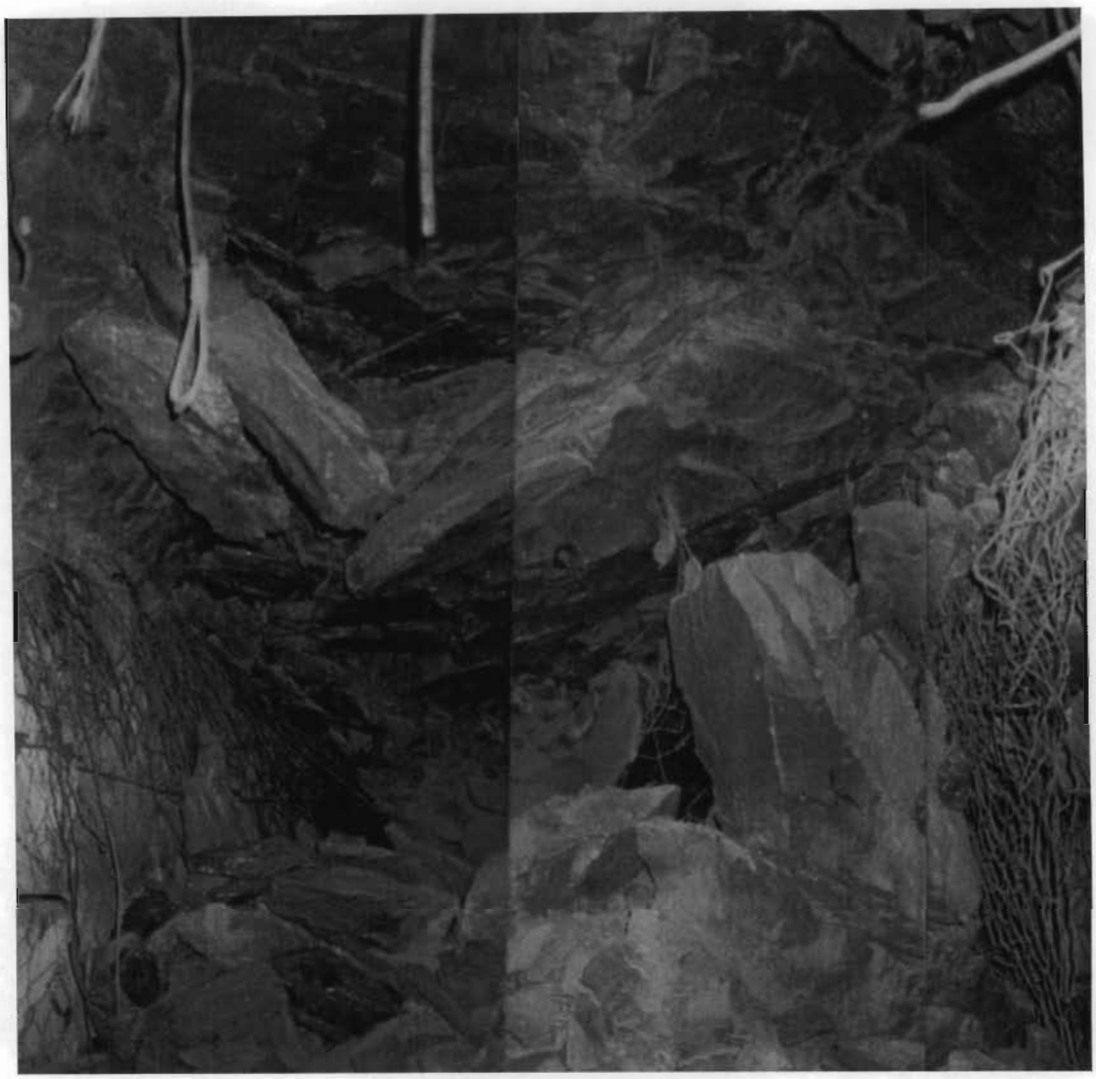

Photograph 3-21. View north along 62 haulage at site of hangingwall rehabilitation work indicating depth of hangingwall instability due to rock mass unravelling upon removal of the mesh and lace fabric support.

The unstable rock mass in the hangingwall of the tunnel consisted of some relatively large blocks, but in general the largest block dimension was estimated to be approximately 0.2 m.

A comment made by the rehabilitation crew was that the hangingwall of the tunnel unravelled rapidly when the central strand of the lacing system was cut. This is indicative of the sensitivity of the support system to the loss of a single.

The 62 haulage north between 62-52 and 62-52A crosscuts lies to the north of the Clemcor dyke (Figure 3-3). At this site catastrophic failure of the eastern sidewall and hangingwall of the haulage, occurred (Photograph 3-22).

Photograph 3-22. View north of the failure of the 62 haulage north sidewall showing the highly fractured nature of the rock mass and the damage to the mesh and lacing fabric support.

Failure of the sidewall of the tunnel was principally a result of the failure of the mesh and lacing fabric support and subsequent unravelling of the rock mass. Observation of rock bolt reinforcement in the upper sidewall of the excavation showed that these support units had not failed, and remained anchored to the deeper, stable rock mass. The loading of the fabric support was due to the dynamic deformation of the unstable rock mass between the rock bolt reinforcement.

In the hangingwall of the excavation the mode of failure of the support system was due to violent guillotining (Photograph 3-23), or tensile snapping (Photograph 3-24) of the reinforcement units under hangingwall shear. This resulted in subsequent collapse of the hangingwall rock mass. Failure of the relatively stiff, fully grouted Gewibar support system was characterised by minimal bending of the rock bolt shaft and more clearly defined guillotining, compared to the wire loop cable reinforcement.

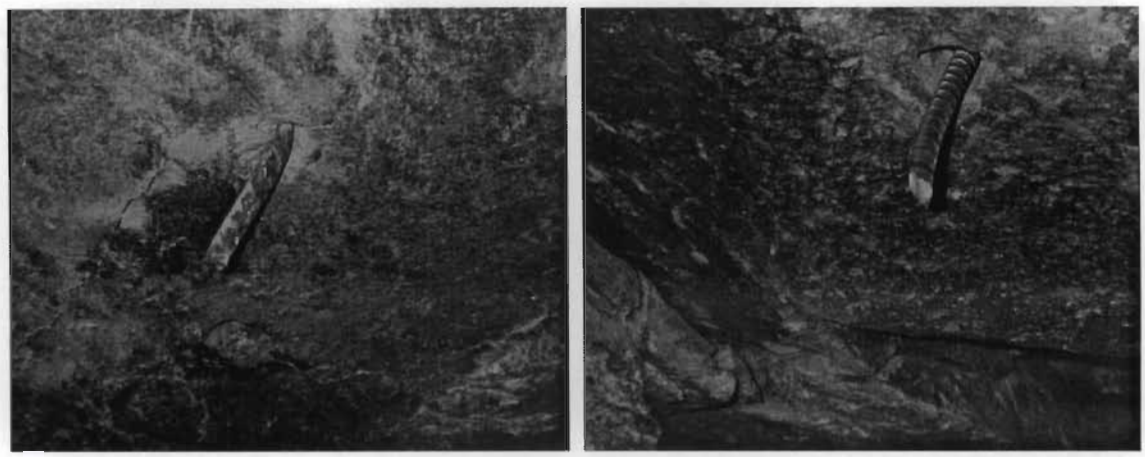

Photographs 3-23 and 3-24. Failure of hangingwall rock bolts due to shear deformation on well defined bedding planes within the rock mass sub-parallel to the excavation hangingwall.

Shear deformation in the hangingwall of the excavation occurred on well defined bedding planes in the quartzite rock mass. The dip of the strata relative to the profile and orientation of the hangingwall also enabled these blocks to move more freely into the excavation.

Conclusions

Rockburst damage at this site was characterised by the large deformation of the rock mass between the rock bolt reinforcement and the subsequent failure of the mesh and lace fabric support. In areas of high static stress levels failures were characterised by large, more uniform deformation of the support system. Shear failure of rock bolts was specific to the hangingwall at strike parallel rockburst sites.

3.2.4 Investigations into mechanisms of rockburst damage to tunnels associated with a seismic event of M=3.7 at Hartebeestfontein gold mine No.4 shaft on 21 July 1997.

An event of magnitude M=3.7 at Hartebeestfontein gold mine No.4 shaft resulted in damage to tunnels which extended from 31 level to 34 level, and was spread over a distance of approximately 1300 m. The intensity of the observed damage was very erratic over this area and was probably a function of its proximity to the seismic event and the relative criticality of the support system and rock mass state.

The support pattern, as generally implemented by Hartebeestfontein Gold Mine for high stress haulages and burst prone ground, consists of 11 x 2.2 m x 16 mm smooth bar per linear metre of tunnel with mesh and lacing. For a 3 m x 3 m square profile tunnel this would give a theoretical support resistance of approximately 122 kN/m^2 based on an average capacity of 100 kN per rock bolt.

Initial observations of tunnel damage were made in the vicinity of 33SE35 stope. Damage to the tunnels was observed from 31 level to 33 level in the main crosscuts accessing this stoping area. Severe tunnel damage occurred on with 31 and 32 levels in close proximity to the 33SE35 3N and 4N panels (Figure 3-4). Minor damage, which was considered to be "shake down", was also observed on 33 level, in close proximity to a small dyke structure. Support in the 33 level section of the tunnel comprised only mechanical end anchored bolts.

Figure 3-4 shows that this dyke structure is intersected in all three levels in this area and is closely associated with tunnel damage.

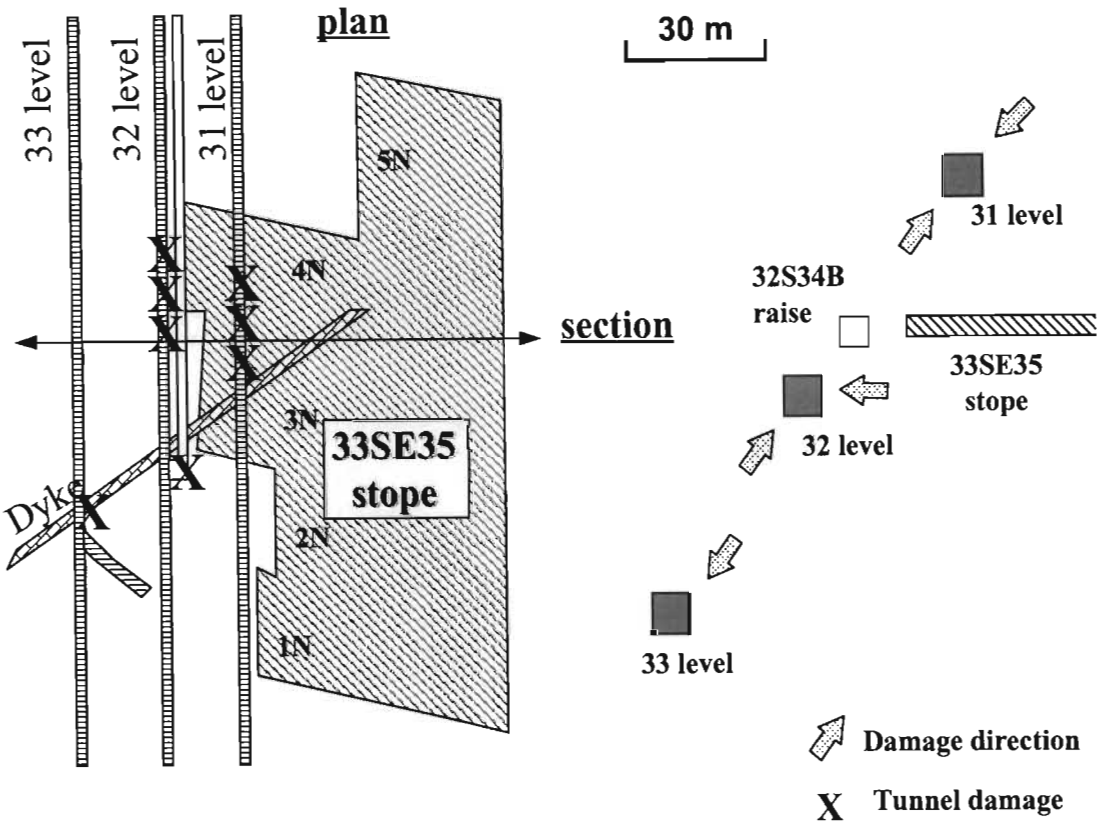

Figure 3-4. Plan and section of tunnel damage in the vicinity of 33SE35 stope.

31 and 32 level tunnels experienced severe localised damage in the indicated areas, with failure of the support systems and total collapse of the tunnel. The severity of this tunnel damage, and its proximity to the stope damage, in the vicinity to relatively minor damage in close proximity, may be indicative of a localised seismic event.

The large volume of failed rock, and the loss, or failure, of anchorage of the smooth bar tendon support in these areas is indicative of high ground velocities and dynamic stress concentrations on these portions of the excavations. It could not be ascertained if the close proximity of the stoping operations prior to the seismic event had influenced the effectiveness of the tunnel support system and the rock mass competency in this area. Induced dynamic stress concentrations, due to a seismic event, may result in a rapid increase in the extent of the fracture zone at certain quadrants of the excavation boundary, dependent on the orientation and magnitude of the incident wave and the stress history of the excavation. This potential rapid development of the fracture zone and dynamic ground velocity imparted to the fractured rock mass would result in extremely high rock mass displacement which resulted in the failure of the support system at this site.

Several modes of failure of the tunnel support system, or portions of this system, were observed at this site. The most severe damage was associated with the failure of the rock bolt reinforcement, and although the mesh and lace fabric support in this particular area did not fail,

the loss of anchorage, and limited rock mass reinforcement from the rock bolts, allowed large sidewall rock mass deformations.

However, failure of the mesh and lacing fabric support did occur at some sites. This may be considered as partial failure of the support system as minor spillage of sidewall rock mass occurred, but the overall integrity of the excavation was maintained.

Photograph 3-25 indicates the bulk rock mass movement into the tunnel excavation as observed on 31 level. This large sidewall deformation, relative to the hangingwall, is illustrated by the deformation of a smooth bar rock bolt along a bedding plane surface that defines the hangingwall contact. The presence of this well defined bedding plane in the immediate hangingwall of the tunnel excavation would also have contributed to the mechanism of bulk sidewall movement due to the limited end constraints of the sidewall rock mass structure. In addition this area experienced large differential deformations of the rock mass, resulting in failure of the mesh and lace fabric support between the rock bolt reinforcement units.

Photograph 3-25. View of south sidewall of 31SE35 showing large deformation of the fractured sidewall and failure of the mesh and lace fabric support.

Tunnel damage in the 33 level No.4^{A} shaft tramming loop area, approximately 1 km south of the previous site and closer to the main seismic event, was over a length of approximately 70 m.

Damage in this area varied from isolated collapse of the hangingwall, and minor deformation of the sidewall, to massive footwall heave and total closure of the excavation. The extent of damage is indicated in Figure 3-5.

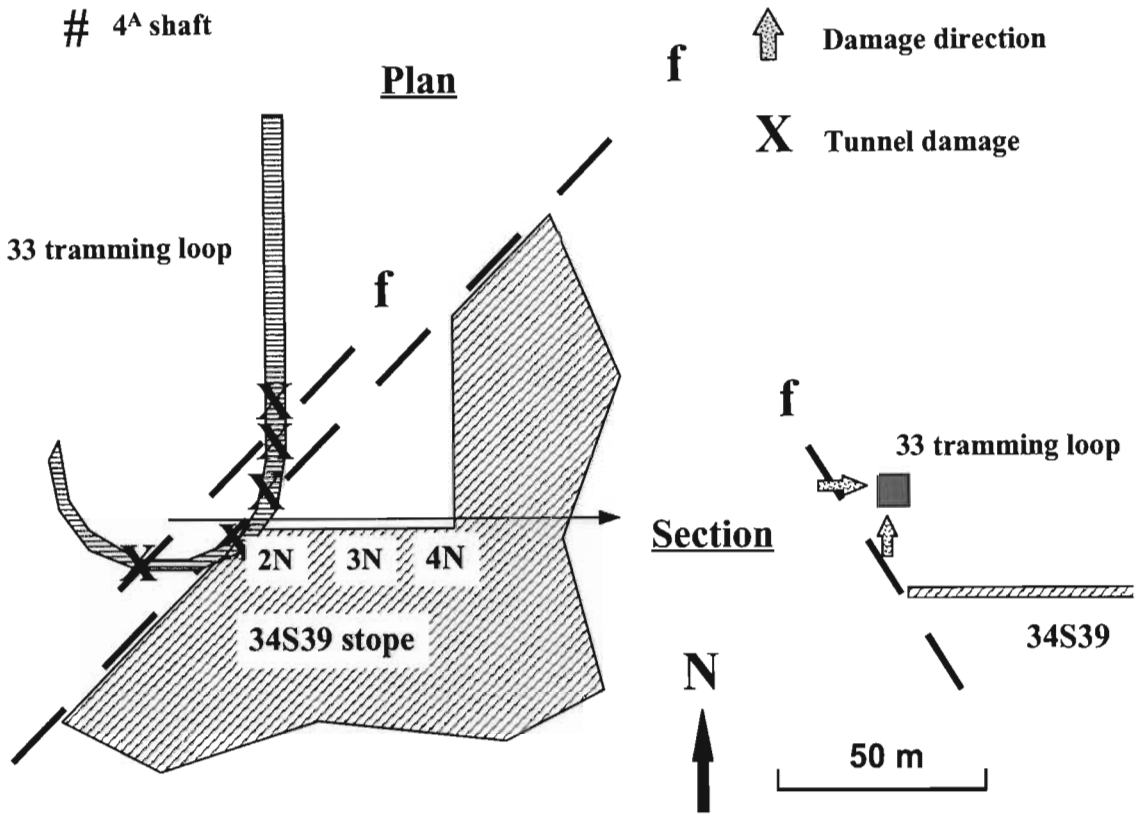

Figure 3-5. Plan and section of 4A shaft 33 level tramming loop damage

The damage in this area was associated very closely with the indicated intersection of the East fault split on which the main seismic event is thought to have occurred. Although damage was intense where failure occurred, the support systems utilised contained damage to within 10 m of the position of the indicated fault intersections. Support in this area comprised 2.2 m, 16 mm diameter mechanical end anchored rock bolts with face plates to contain the diamond mesh fabric support. Additional 16 mm smooth bar with lacing was installed to the west of the collapsed area.

Total closure of this excavation occurred in the area vertically above the indicated position of the 34S39 2N gully. Damage consisted of substantial footwall heave (Photograph 3-26), deformation of the lower portion of the west sidewall of tunnel (Photograph 3-27), and partial collapse of the hangingwall. Very little damage was experienced by the eastern sidewall of the excavation in this portion of the tunnel.

Photograph 3-26. View north east of 33 level No.4^{A} shaft tramming loop showing footwall heave and displacement of lower west (left) sidewall and associated movement of tracks (bottom right corner)

Photograph 3-27. View of west sidewall of 33 level No.4^{A} shaft tramming loop showing large deformation of lower sidewall and footwall heave.

Both of tension and shear failure (Photograph 3-28) of rock bolts in the hangingwall of the excavation at this site occurred. The large general deformation of the lower portion of the west sidewall is indicative of the loss of anchorage of the rock bolts or snapping within the rock mass.

Photograph 3-28. View into hangingwall of 33 level No.4^{A} shaft tramming loop showing shear deformation of smooth bar rock bolt shaft.

To the north of the collapsed area, damage to the support system comprised loading of the diamond mesh due to loosening and collapse of isolated blocks within the hangingwall and sidewall of the excavation. This resulted in the failure of the mesh fabric in some areas. This failure mechanism was considered to have initiated from the cutting of the mesh strands by the mechanical anchor face plates (Photograph 3-29).

Photograph 3-29. View of east sidewall of 33 level No.4^{A} shaft tramming loop showing highly fractured nature of the rock mass and failure of the mesh fabric.

The reduction in damage away from the fault plane and stope abutment position was very rapid. To the south west of the collapsed area, excavation damage due to footwall heave and large scale sidewall deformation also declined rapidly. An isolated failure of the hangingwall of the tunnel was observed at approximately the southern extremity of the tramming loop (Figure 3-5). This failure comprised tensile failure of a 16 mm rock stud by an isolated block (Photograph 3-30).

Photograph 3-30. View into hangingwall cavity of fall of ground within 33 level No.4^{A} shaft tramming loop showing necking of mechanical bolt shaft and tensile failure.

The surrounding tendons remained intact, and thus their contribution to the stability of the isolated block is assumed to have been negligible. The block had dimensions of 2.0 m x 1.9 m and an average thickness of 0.3 m. The portion of the tendon remaining in the hangingwall clearly indicated failure under tensile loading (Photograph 3-30). The loading history of the tendon may be complex, and thus it was assumed that the tendon was close to the limit of its elastic deformation prior to the seismic event. The energy absorption associated with the failure may thus be attributed solely to the necking and plastic deformation of the tendon. It is assumed that the in situ yield load of an M16 rock stud is approximately 100 kN over a plastic deformation of 20 mm (Anon., 1988). Thus the available energy would be given as:

$$E = \text{Force} \times \text{deformation} \qquad (3\text{-}2)$$

$$E = 100 \times 0.02 = 2 \text{ kJ}$$

The constant gravitational energy absorption requirement would be given as:

$$Eg = \text{mass} \times \text{gravitational acceleration} \times \text{distance} \qquad (3\text{-}3)$$

$$Eg = 2 \times 1.9 \times 0.3 \times 2750 \times 10 \times 0.02 = 0.63 \text{ kJ}$$

Thus the energy available for absorption of dynamic energy is:

$$Ed = E - Eg \qquad (3\text{-}4)$$

$$Ed = 2 - 0.63 = 1.37 \text{ kJ}$$

The estimated minimum ground velocity (v) is thus given by:

$$Ed = {}^{1}/_{2}.m.v^2 \qquad (3\text{-}5)$$

$$Ed = 1.37 \text{ kJ} = 0.5 \times (2 \times 1.9 \times 0.3 \times 2750) \times v^2$$

$$v = 0.94 \text{ m/s}$$

A minimum ground velocity, on the skin of the excavation, of approximately 1 m/s would indicate a relatively distant source of the seismic event, and thus a fairly uniform seismic deformation and stresses at the rockburst site. The isolated nature of the failure at this point may be attributed to the more fractured nature of the rock mass in the general area. This would result in loading of the fabric support in these areas as opposed to direct loading of the rock bolts by the full tributary area.

Minor damage was observed on 34 level in the vicinity of 34S39 stope. Support in these areas comprised mesh and lacing on 16 mm smooth bar, with mechanical anchor primary support. In general, bagging of the mesh was observed due to bulking of the rock mass between the tendons. At the western breakaway position of the 34S39 crosscut, failure of the support system and collapse of the west sidewall had occurred to a depth of approximately 0.5 m.

Conclusions

Rockburst damage at this site was characterised by the large uniform deformation of the sidewalls of the tunnel. A combination of shear and tensile failures of rock bolts in the hangingwall of tunnels was observed.

3.2.5 Investigation of rockburst damage, at Hartebeestfontein No.2^{A} shaft pillar due to a seismic event of magnitude M=3.5 on 11 October 1997.

Initial observations of damage were conducted on 29 level of the No.2^{A} shaft, NE, along the shaft access crosscut running parallel to, and approximately 10 m to the NE of the tip crosscut (Figure 3-6). The intensity of damage increased away from the shaft and towards the intersection of the shaft crosscut and the tip crosscut.

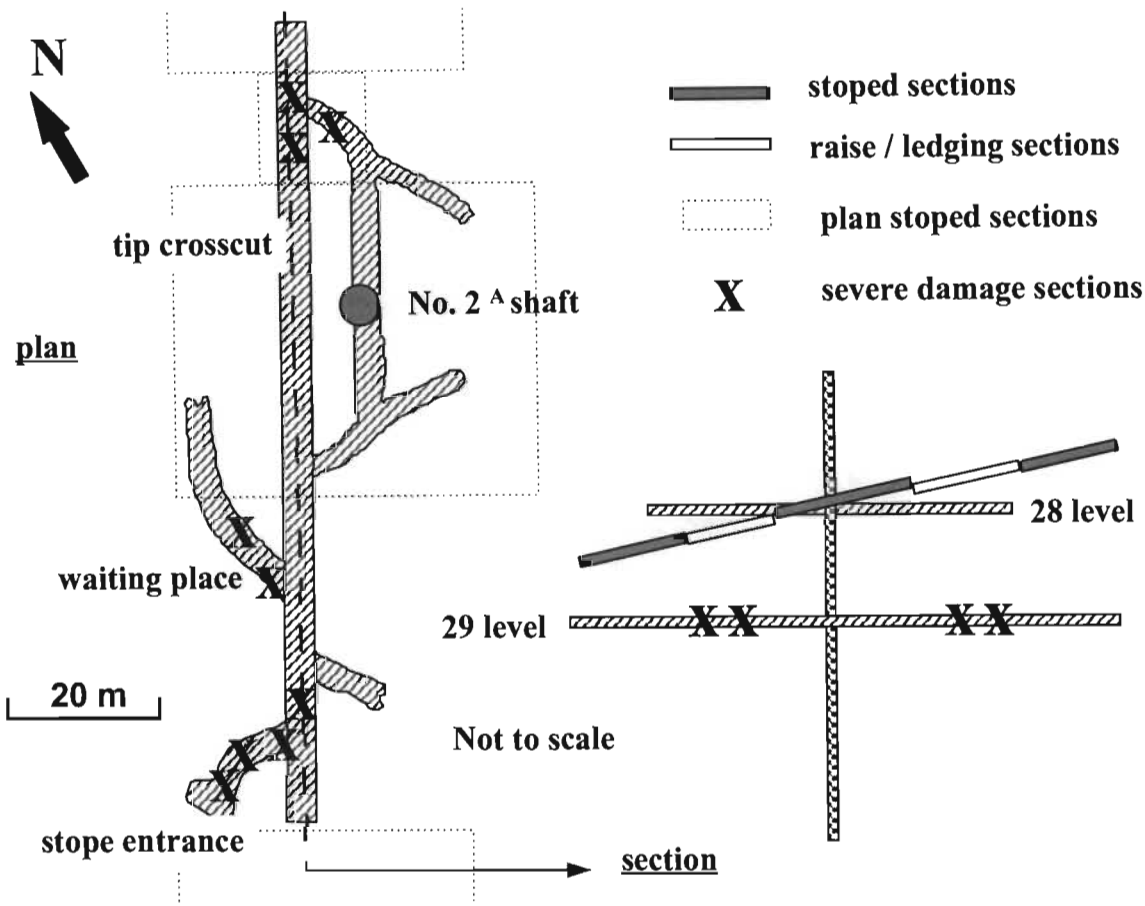

Figure 3-6. Schematic of 29 level tunnel layout and damage

Observations in the vicinity of this "bullnose" indicated a bedded, argillaceous quartzite rock mass structure, with an approximate bedding interval of 30 cm – 40 cm. The rock mass was also fractured, resulting in a highly discontinuous structure. The approximate size of the rock mass rubble from the fall of ground ranged from blocks of the order of centimetres to slabs of approximately a metre maximum dimension. Support in this area consisted of smooth bar rock bolts with mesh and lacing fabric support. Substantial concrete work had also been conducted on the sidewalls of the tunnels in the vicinity of the "bullnose". Deformation of the sidewalls of the tunnels was observed despite this concrete work (Photograph 3-31).

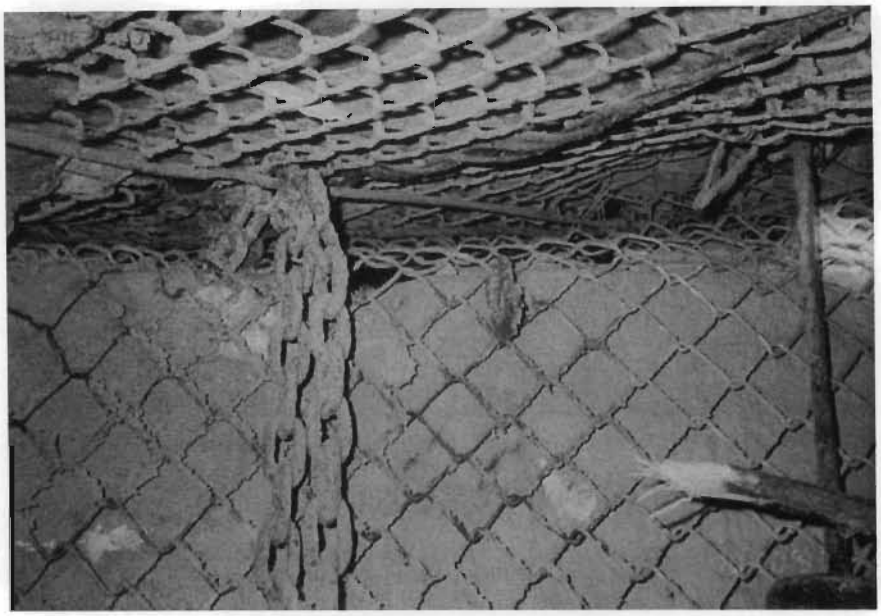

Photograph 3-31. View of east sidewall of 29 level station crosscut showing deformation of sidewall concrete wall relative to hangingwall.

Observations of the performance of the smooth bar rock bolts at this site indicated that these units had undergone shear deformations (Photograph 3-32). Failure of these rock bolts could be observed, but the mode of failure and estimation of "freshness" of the failure could not be determined due to the hazardous ground conditions in the vicinity.

Photograph 3-32. View of smooth bar rock bolt in hangingwall cavity at intersection of 29 level shaft crosscut and tip crosscut indicating severe shear deformation within the rock mass.

Observations of this rockburst site were also made in the tip crosscut excavation. These observations, in particular indicated the failure of the sidewall of the "bullnose" with associated failure of the mesh and lacing fabric support.

Examination of the stoping sequence in the vicinity of the 29 level tip and shaft crosscut NE shows that overstoping of this area was delayed relative to the excavations further to the NE and SW. This would have resulted in these excavations under examination being exposed to a generally higher stress field and associated increased extent of fracturing and progressive deformation. This would be particularly true of the pillar area created between the shaft crosscut and the tip crosscut in the immediate vicinity of the "bullnose". In addition, the close proximity of a second bullnose area approximately 10 m to the north east would also result in an increased induced stress field. This interaction of excavations would have caused a relative weakening of the rock mass structure in the immediate vicinity of the tunnels, resulting in these excavations being more susceptible to rockburst damage. In addition the potential subsequent stress reduction experienced by this excavation due to stoping operations would also have resulted in further deformation of the rock mass around the tunnel. This would compound the deterioration of the rock mass structure and progressive loading of the rock bolt supports.

Observations within the 29 level tip crosscut indicated large sidewall movement. It was considered that this had resulted in the observed footwall heave. Severe damage to the hangingwall of the excavation was limited to the vicinity of the 'bullnose' location at the NE end of the tip crosscut.

Support in this area again consisted of mesh and lacing on smooth bar rock bolts with substantial concrete work on the sidewall of the excavation. It was observed that, although these concrete walls maintained their overall integrity, sections of the concrete were displaced up to 50 cm into the tunnel (Photograph 3-33). This large, uniform displacement of the sidewalls resulted in the buckling of the loose footwall material, and represents the main mechanism of the observed footwall heave in this excavation.

Photograph 3-33. View of west sidewall of tip crosscut showing reinforcement and scouring (centre of photograph) within sidewall concrete work, indicating a relative differential displacement between the blocks of approximately 50 cm.

Collapse of the hangingwall was restricted to the NE end of the tip crosscut. The rock mass condition in this vicinity was considered to be less fractured than the previous site, with the main discontinuities being due to natural bedding within the rock mass. The remains of rock bolts could be observed in the hangingwall of the cavity left by the collapse of the previous hangingwall rock mass (Photograph 3-34). Although the surfaces of the planes of failure of the rock bolts appeared clean, indicating recent failure, the mode of failure could not be clearly determined due to the height of the excavation. Failure of these rock bolts would have resulted in additional loading of the hangingwall mesh and lacing system and the observed collapse of this fabric support and unravelling of the hangingwall. Observations of the remaining intact rock bolts in the hangingwall of the excavation indicated only minor shear deformation in this area. It is thus considered that the major component of rock bolt loading would have been tensile due to the more massive structure of the rock mass at this location.

Photograph 3-34. View of collapsed hangingwall area in the 29 level tip crosscut indicating the remains of the rock bolt reinforcement.

At the site of this collapse a large portion of the fall of ground material was removed prior to the visit. This therefore prevented detailed observation of the failed rock mass and support units.

Substantial footwall heave and lower sidewall deformation were also observed in the 29 level waiting place and stope entrance area. In general, damage to the hangingwall of the excavation in these areas appeared to be less significant than that previously discussed. The mode of excavation deformation is clearly illustrated by the inclination of machinery within these tunnels (Photograph 3-35). The lifting of a locomotive and the dynamic failure of tracks and fish plate joins illustrated the intensity of this deformation.

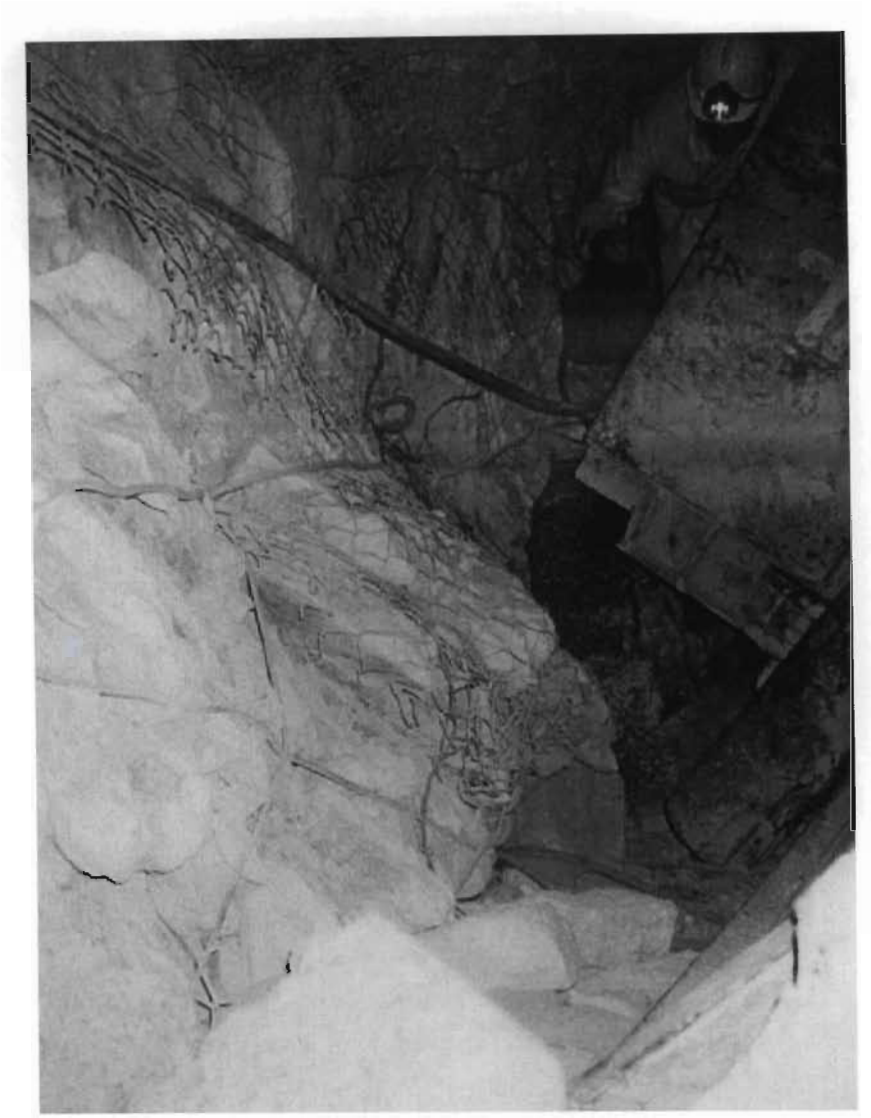

Photograph 3-35. View of west sidewall of stope entrance crosscut indicating relatively large displacement of lower sidewall and tipping of material rail car.

The relative intensity of damage appeared to increase towards the stope entrance. The stoping sequence in this area had resulted in these excavations being subjected to generally higher field stress levels. The increased stress environment in these areas would have probably resulted in increased susceptibility to rockburst damage.

Damage to tunnel excavations was also observed on 25 level. This damage was probably the result of an after shock of the main event, which had its source in close proximity to the 25 level station. Damage was observed in the main shaft crosscut and an adjacent material / tramming crosscut. This damage was associated with the indicated position of a dyke structure in both excavations (Figure 3-7).

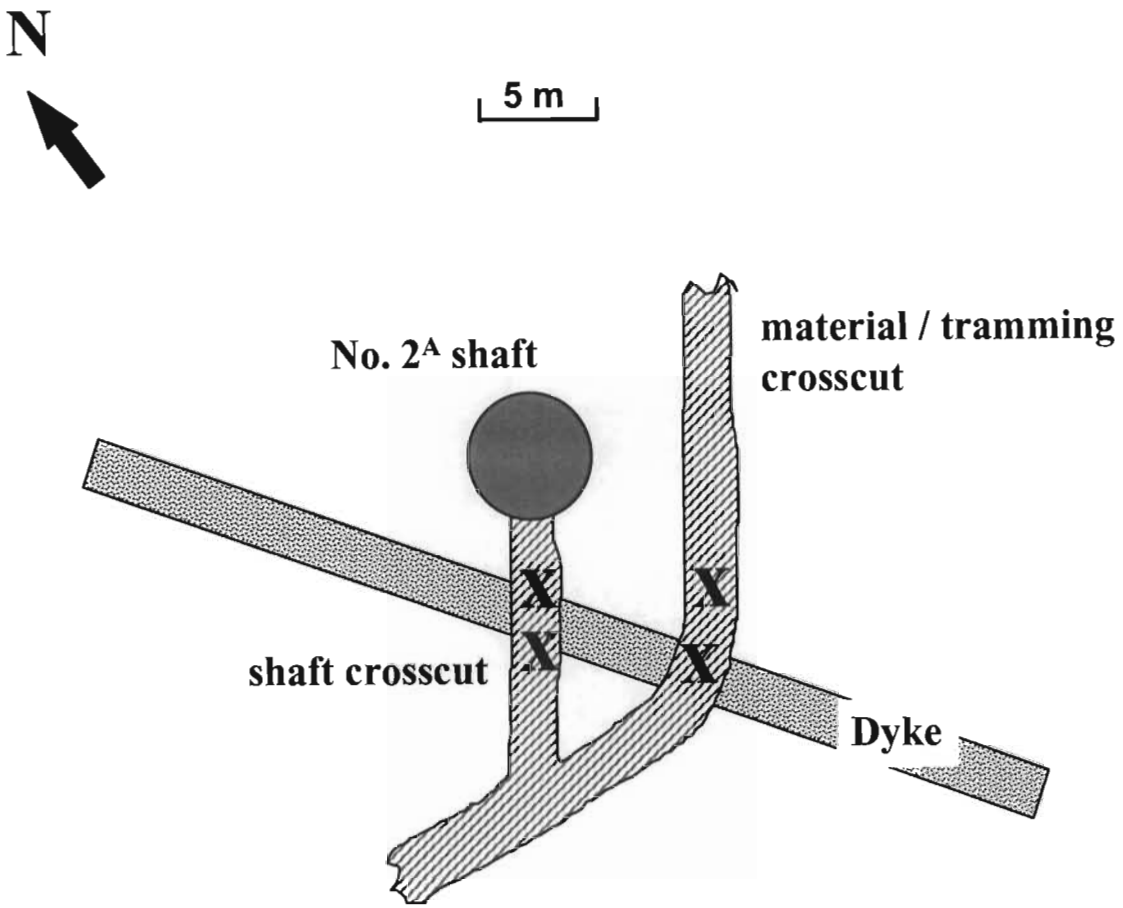

Figure 3-7. Schematic of 25 level tunnel layout and damage

Damage appeared to be far more "'violent" in nature, and also much more localised to the dyke structure than that on 29 level. This was probably due to the closer proximity of the seismic event, which resulted in the rockburst, to the excavations. Failure of the support system was clearly attributable to dynamic failure of rock bolts and associated failure of the mesh fabric support system pinned back by mechanical rock bolts.

Damage in the shaft crosscut was principally of the hangingwall of the excavation. At this site failure of a smooth bar rock bolt under tension (Photograph 3-36) was clearly observed. Failure of the mesh fabric attachment resulted in the subsequent unravelling of the unstable hangingwall rock mass. The rubble of the fall of ground comprised relatively large blocks (Photograph 3-37).

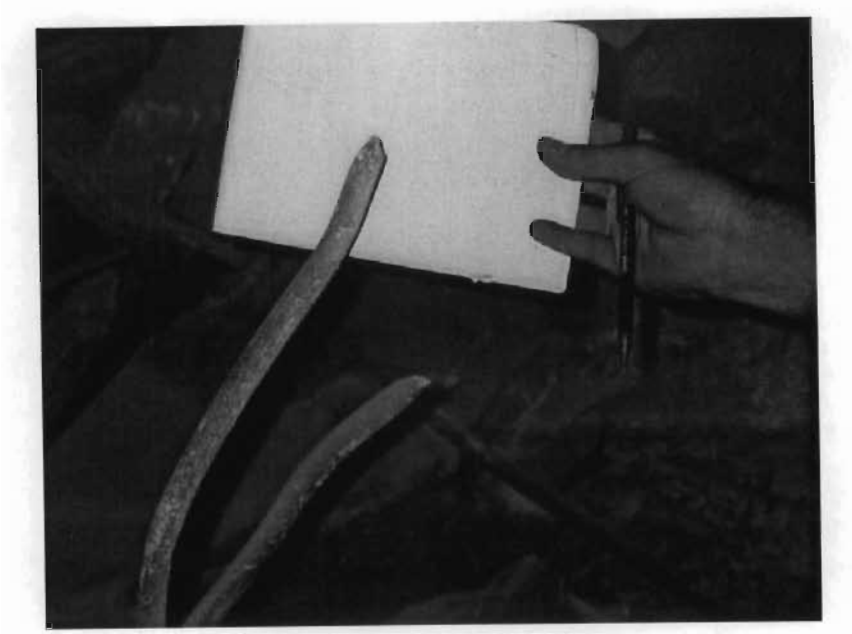

Photograph 3-36. Detailed view of tensile failure of smooth bar rock bolt from hangingwall of 25 level station crosscut.

Photograph 3-37. View of damage to hangingwall of 25 level station crosscut showing collapse of hangingwall and failure of mesh fabric support.

More severe damage was associated with the parallel material / tramming crosscut, where total failure of the sidewall and hangingwall support system had occurred (Photograph 3-38). Here the rock mass structure was far more highly fractured, resulting in potentially lower rock bolt interaction and thus the fabric support being more susceptible to loading under the rockburst conditions.

Photograph 3-38. View of total closure of 25 level tramming / material crosscut around material rail car indicating violent nature of failure and highly fractured rock mass conditions.

In the near vicinity to the "bullnose" between the shaft crosscut and the material crosscut, the dynamic failure of several mechanical anchors was observed. Tensile failures, as characterised by necking and cupped shaped failure surfaces, had (photograph 3-39). The general area exhibited significant "spitting" of fine rock fragments, although the overall rock mass and excavation stability was maintained.

Photograph 3-39. Detailed view of tensile failure of mechanical anchor rock bolt shaft in the near vicinity of the area of collapse in the 25 level material / tramming crosscut.

Conclusions

Rockburst damage at this site was characterised by large uniform deformation of the sidewalls of the tunnels. In areas of generally higher stress levels unravelling of the rock mass between rock bolts was observed with failure of the mesh and lacing fabric support system. Where the rock mass was more competent and massive, particularly in the hangingwall, tensile failure of the rock bolts was the primary mechanism of support system failure.

3.2.6 Investigations into mechanisms of tunnel damage associated with a seismic event of magnitude M=4.3 at East Driefontein gold mine No.4 shaft on 25 September 1997

The No.4 shaft area of East Driefontein has a history of large seismic events associated with very limited mining activity in the general area (section 3.2.2). The event that occurred on the 25 September 1997 resulted in widespread damage to the shaft area and haulages accessing the major production areas (Figure 3-8). Establishing the location of the event was based on information from adjacent mines due to loss of data at the East Driefontein site. This resulted in a low confidence in the location of the seismic event in relation to the widespread damage.

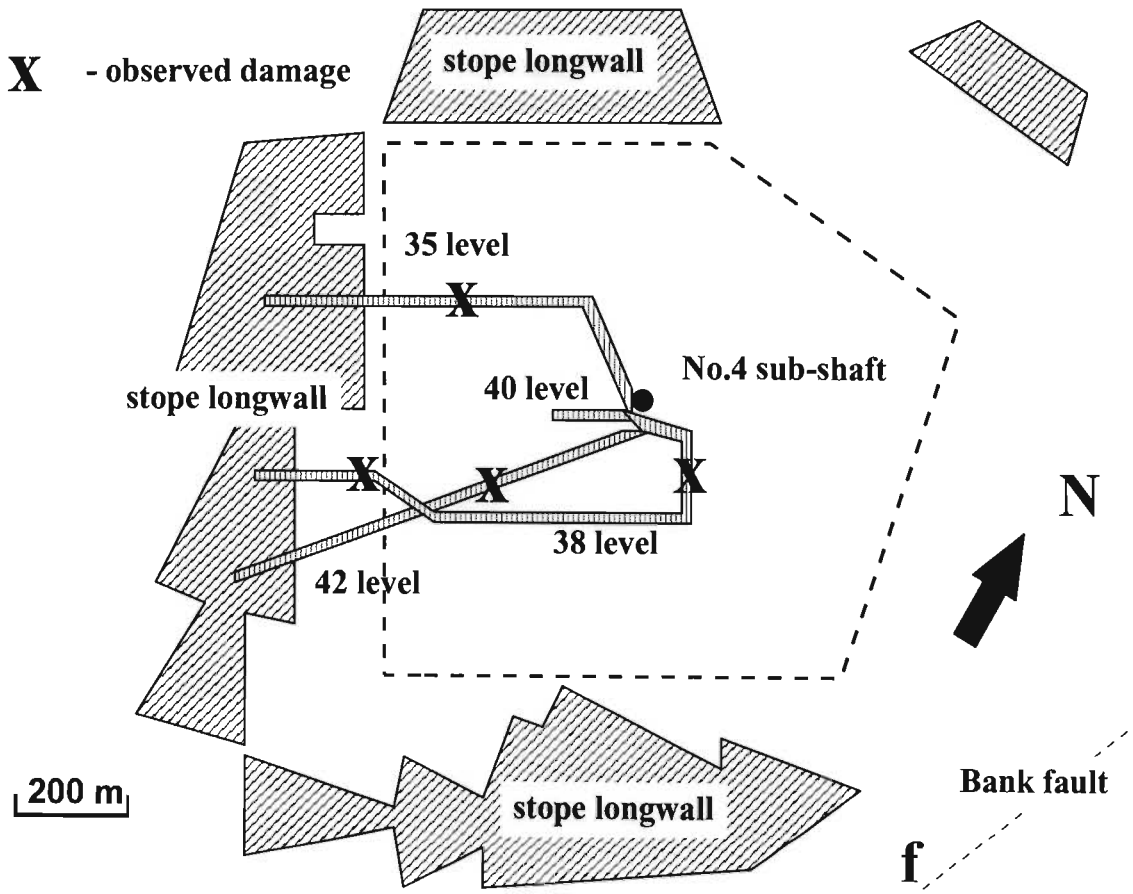

Figure 3-8. Schematic plan of tunnel and stoping layout and distribution of observed damage.

Observations of damage were conducted on 35, 38, 40 and 42 levels, over a period of several months. These excavations range in depth below surface from approximately 2400 m to 2800 m. Most of the observed damage occurred in excavations developed in quartzites in the footwall of the Venterdorp Contact Reef. The shaft area is in close proximity to the Bank fault, which is a major sub-vertical regional discontinuity. In association with this feature is the Master bedding plane fault, a major sub-horizontal plane which intersects the No.4 sub-shaft between 40 – 42 level and on 42 level approximately 200 m south west of the shaft axis (Figure 3-9). The seismic event is considered to be associated with these features.

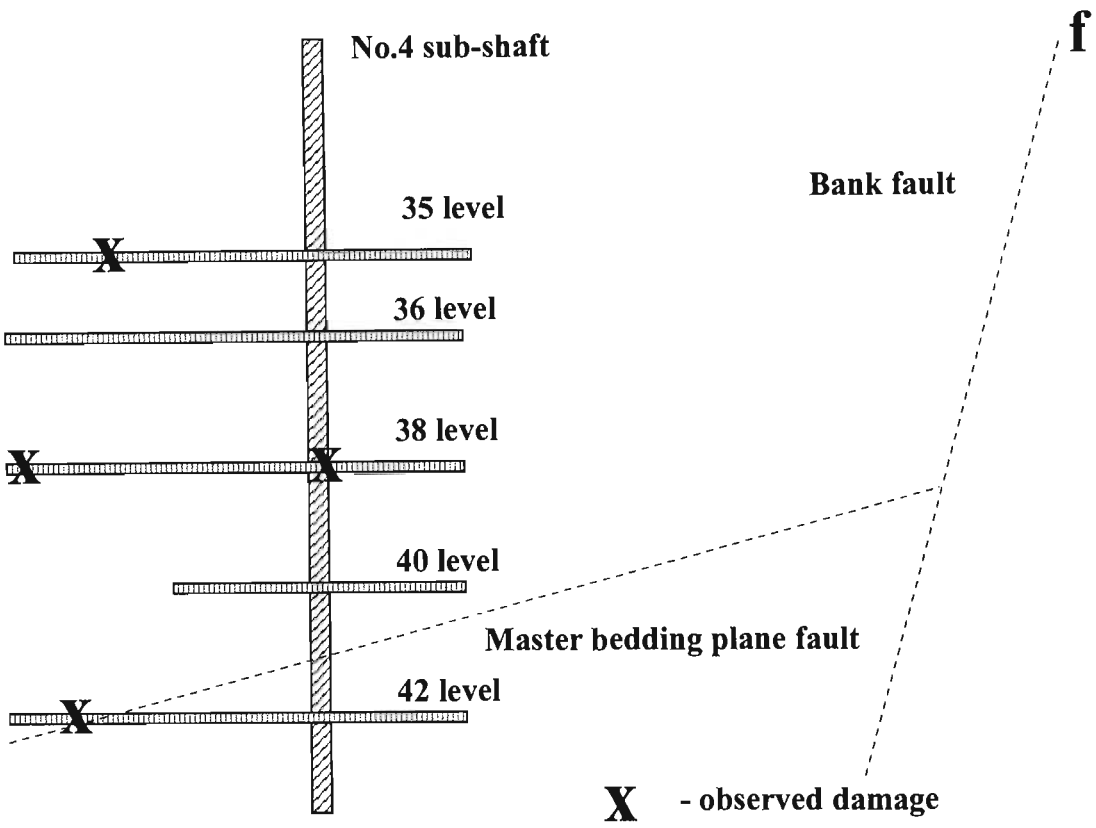

Figure 3-9. Schematic section of shaft layout and major fault planes with distribution of damage.

Damage on 35 level in the main haulage west was observed approximately two months after the main event, and subsequent to the completion of rehabilitation work. Rockburst damage consisted primarily of the failure of the south sidewall of the tunnel to a depth of approximately 1.5 m. The mechanism of failure of the support system was the failure of the mesh and lacing fabric support and the unravelling of the rock mass from around the rock bolt reinforcement. At a breakaway position further along the 35 level footwall drive, close to the stope longwall abutment, observations were made of rock bolt failure under shear deformation, failure of mesh and lacing, and significant closure of the crosscut. The rock mass in the immediate periphery of the excavation was highly fractured. This is considered to have contributed to the significant bulking of the sidewall mesh and lacing systems, and the implied limited direct interaction with the rock bolt reinforcement.

Significant damage of excavations in the immediate area of the 38 level shaft station was observed. Initial observations were conducted in the pump chamber. In the access incline and adjacent sub-parallel excavation, orientated approximately north / south, heave of the footwall concrete work and failure of shotcrete on the hangingwall and upper sidewalls were evident. The pump chamber, orientated approximately east / west, had limited excavation damage, but machinery in this excavation had been displaced along the axis as a result of the seismic event.

This information, in relation to that of the distribution of damage observed in the access incline and adjacent tunnel may be indicative of the incidence direction, and thus relative location of the seismic event and associated dynamic stress wave, being from the east. The best estimate of the location of the M=4.3 event was approximately 1000 m to the east of the No.4 sub-shaft position.

The rock mass condition in the immediate sidewall of the pump chamber is shown to be highly fractured, with fractures spaced 50 – 100 mm apart sub-parallel to the excavation sidewall (Photograph 3-40).

Photograph 3-40. View of south sidewall of 38 level pump chamber showing distribution of fracturing within the sidewall rock mass at the junction of the pump chamber and dam access excavations.

Greater damage to the sidewalls of the dam excavations, orientated perpendicular to the main pump chamber, was noted, and this was associated with some damage to the concrete dam

walls. This disruption to the rock mass due to dynamic loading was reported to have resulted in further progressive deformation subsequent to the main seismic event.

Damage of the 38 level tip crosscut, orientated approximately north / south, was associated with the hangingwall and footwall of the excavation. Hangingwall failures were of the order of 1.5 m to 2.0 m in height and consisted of failures of rock bolt reinforcement units and mesh and lace and shotcrete fabric support. This excavation is sited within a dyke, and the more competent rock mass structure associated with this feature is considered to have caused increased failure of the rock bolt reinforcement compared to observations of hangingwall damage at other rockburst sites. A characteristic of the rock mass in this area was the inflow of water. This resulted in rock bolt reinforcement being corroded up to a well defined plane within the rock mass on which significant water out flow could be observed. Failure generally occurred in the corroded position of the bolts. Water was also concentrated at the interface between the rock and shotcrete.

Damage to the 39 level deep footwall drive, close to the edge of the shaft pillar, was in the plan position of a major stoping abutment. Significant damage had been experienced by this excavation prior to the M=4.3 seismic event. This had necessitated the initiation of rehabilitation work. Damage was over a distance of approximately 50 m and comprised sidewall deformation and the collapse of the hangingwall at a breakaway position. Damage to the sidewall of the excavation had resulted in significant bulging of the rock mass, confined by mesh and lacing, between the points of rock bolt reinforcement anchorage (Photograph 3-41). This was particularly evident in the lower portion of the sidewall and on the north (up dip) side of the excavation.

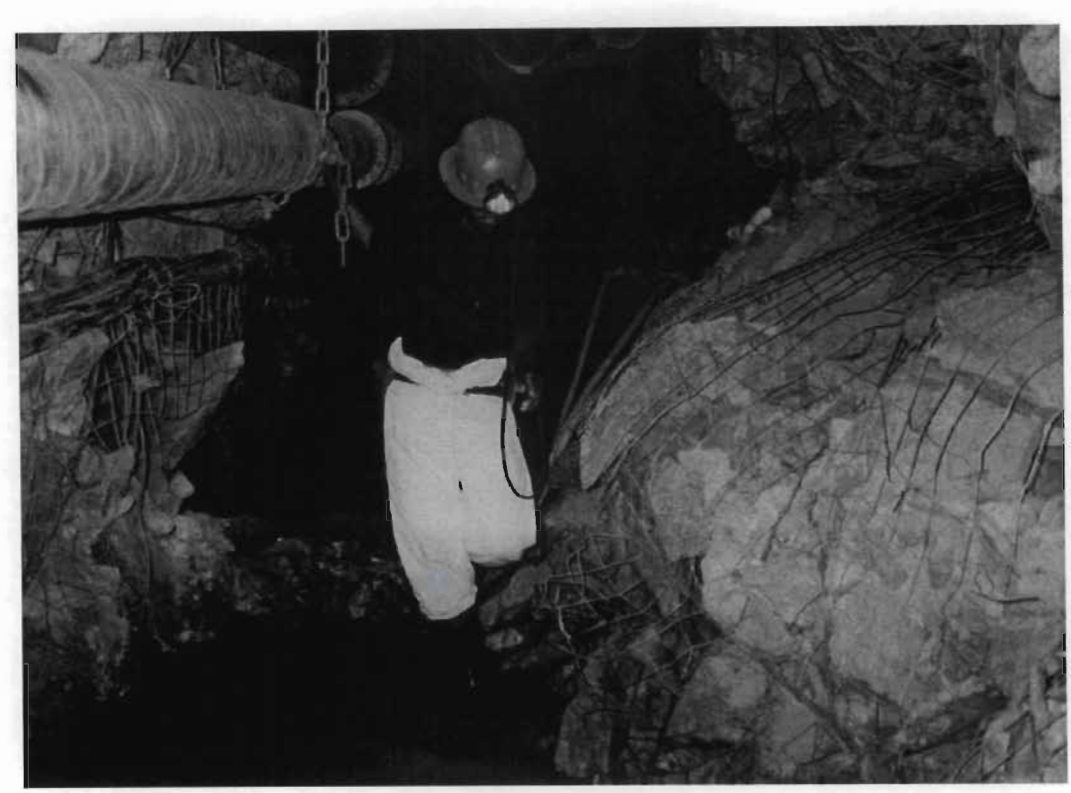

Photograph 3-41. View west along 38 level deep footwall drive showing large scale bulking of the rock mass, particularly of the lower north sidewall.

This damage is consistent with a highly fractured rock mass, with relatively stiff rock bolt reinforcement that is anchored at depth to a more competent rock mass structure. The highly fractured nature of the immediate sidewall rock mass is considered to result in very limited direct interaction between the rock bolt and the rock mass. This caused direct loading of the mesh and lacing fabric support. The larger deformation of the rock mass in the lower portion of the sidewall is considered to be due to the lower support system resistance in this area, particularly of the fabric support.

In areas of higher rock bolt reinforcement, and associated higher lacing density, improved control of sidewall deformations was obtained (Photograph 3-42). This is a function of the increased overall stiffness of the system and thus increased compatibility of loading between the rock bolt reinforcement and the mesh and lace fabric. However, the lower confinement of the rock mass between the rock bolt reinforcement was still evident, with associated localised bulking, and failure of the mesh fabric.

Photograph 3-42. View east along 38 level deep footwall drive of south sidewall showing more uniform containment and deformation of the sidewall rock mass with isolated areas of mesh failure.

Observations of damage at the breakaway location indicated a collapse of approximately 1.0 m to 1.5 m of hangingwall over the excavation. The rock mass in this area was again highly fractured, but the dominant mode of failure was of the rock bolt reinforcement, with subsequent collapse of the mesh and lacing fabric support system. Failure of the rock bolts was due to localised corrosion, usually associated with a major discontinuity within the rock mass structure, and tensile failure of the rock bolt at this point.

Observations of damage on 40 level included collapse of the hangingwall of the shaft crosscut at the location of a breakaway. Previous ground control problems had occurred in this area as indicated by the use of steel support sets in addition to mesh and lacing. Damage of a "shakedown" nature was also associated with the access tunnel to the 40 to 38 level travellingway. The depth of stress induced fracturing due to the main 3.5 m x 3.5 m tunnel, as

observed in the travellingway, was estimated to be approximately 2.5 m, of which approximately 1.0 m had collapsed around the rock bolt reinforcement due to the seismic event.

Very limited damage was observed in the 40 to 42 level travellingway. This excavation was developed through the Master bedding plane fault.

Damage on 42 level was in close proximity to the intersection of the Master bedding plane fault. This feature is associated with generally poorer ground conditions due to the disturbed nature of the rock mass. This is in contrast to the observation of this feature in the 40 to 42 level travellingway.

A large collapse had occurred at the intersection of the 42 level haulage south west and a workshop area. Support had been upgraded to include the use of long cables and shotcrete in addition to the standard mesh and lacing on rock bolts. Rehabilitation work had commenced and thus direct observation of the damage was not possible. Failure was indicated to be associated with infilled joints within the hangingwall to a height of approximately 2.0 m, and approximately 1.0 m of sidewall. This breakaway is within 10 m of a second breakaway excavation, and the higher induced stress levels associated with the interaction of these excavations, in addition to the general poor ground conditions, contributed to the area being more prone to rockburst damage.

South west of this collapse direct observations of damage to the support system could be made (Photograph 3-43). This damage consisted of a combination of mechanisms, either bulk sidewall deformation due to the failure, or loss of anchorage of the rock bolts and cables, or failure of the fabric support system with stable anchorage of the rock bolts. The large scale deformations of the overall sidewall were generally associated with the lower portion of the excavation. This resulted in significant footwall heave of the excavation.

Photograph 3-43. View south west along 42 level haulage showing the highly fractured nature of the rock mass, footwall heave of approximately 1.5 m, bulk sidewall deformation (bottom right) and failure of mesh and lacing in upper portions of excavation.

The extent of differential deformation within the rock mass, particularly where the rock bolt anchorage was maintained, caused damage to the mesh and lacing fabric support system. This again illustrates the low interaction between the rock bolt reinforcement and the rock mass, particularly in the highly fractured immediate skin of the excavation. The result of this is direct loading of the fabric support.

Further observations in this area showed failure of the rock bolt reinforcement with subsequent collapse of the mesh and lacing system (Photograph 3-44). The tensile failure of the rock bolts and cable anchors had occurred due to localised corrosion of these reinforcement units within the rock mass. The subsequent collapse was to a depth of approximately 1.5 m.

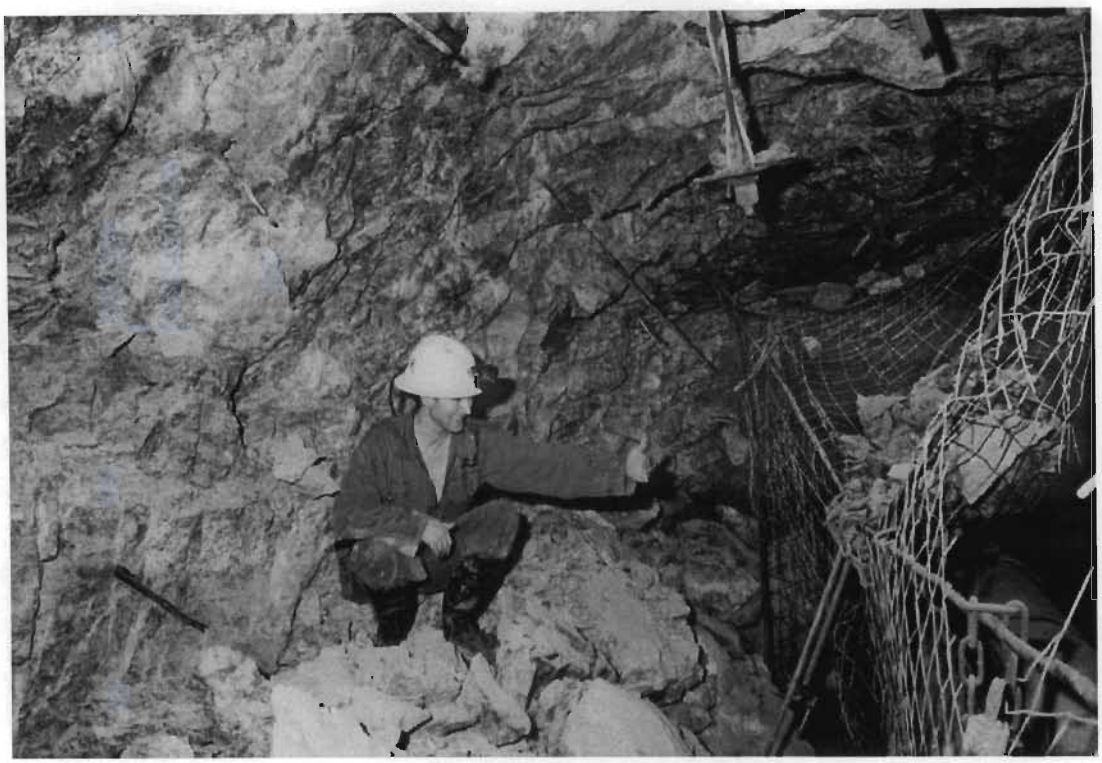

Photograph 3-44. View north east along 42 level haulage showing failure of rock bolt reinforcement (left), and thus loss of fabric anchorage (right), and collapse of approximately 1.5 m of fractured sidewall rock mass.

The rock at this location appeared highly weathered, commensurate with the occurrence of water within the rock mass, and an associated highly corrosive environment.

Overall stability was maintained in some sections of the tunnel, but again characteristic bulking of the rock mass between the rock bolts and the lacing is evident, with the associated loading of the mesh panels (Photograph 3-45).

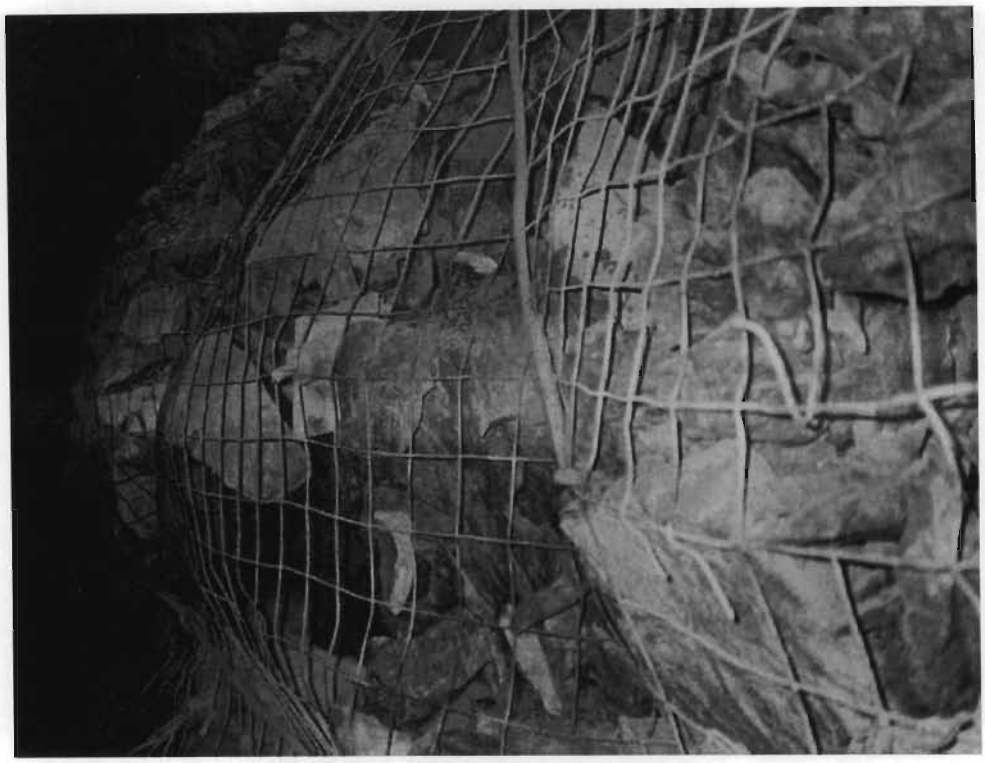

Photograph 3-45. Bulking of fractured sidewall rock mass between rock bolt reinforcement and lacing within 42 level haulage.

In areas of the 42 level haulage where shotcrete was applied, isolated failures indicated the highly corrosive nature of this environment which caused cable anchor failure at the shotcrete / rock mass boundary. Under these conditions the tunnel walls acted as a free surface within the rock mass, towards which groundwater would naturally drain. Shotcrete represented an impermeable skin on the upper boundary of the excavation along which groundwater would gather and drain to the base of the excavation. This may occur either along this interface or within the immediate fractured rock mass. Under these conditions the concentrated groundwater flow results in very localised corrosion of the steel reinforcement within the rock mass. This had occurred to the extent that the dynamic energy imparted to the shotcrete skin during the seismic event was sufficient to cause failure of these units.

Conclusions

Rockburst damage at this site was characterised by the corrosion of the rock bolt units in the presence of natural groundwater. The performance of the support system under these conditions was again characterised by the failure of rock bolts within more massive rock mass structure, particularly of the hangingwall, and failure of the fabric under more highly discontinuous rock mass conditions.

3.2.7 Investigation into mechanisms of tunnel damage due to a seismic event of magnitude M=3.5 at Hartebeestfontein gold mine on 5 March 1998.

Damage to tunnel excavations, associated with a magnitude M=3.5 seismic event on 5 March 1998, was concentrated in the vicinity of the 33SE39 crosscut in the No4 shaft area of Hartebeestfontein gold mine (Figure 3-10). Detailed observations of the performance of the tunnel support systems were made in this area.

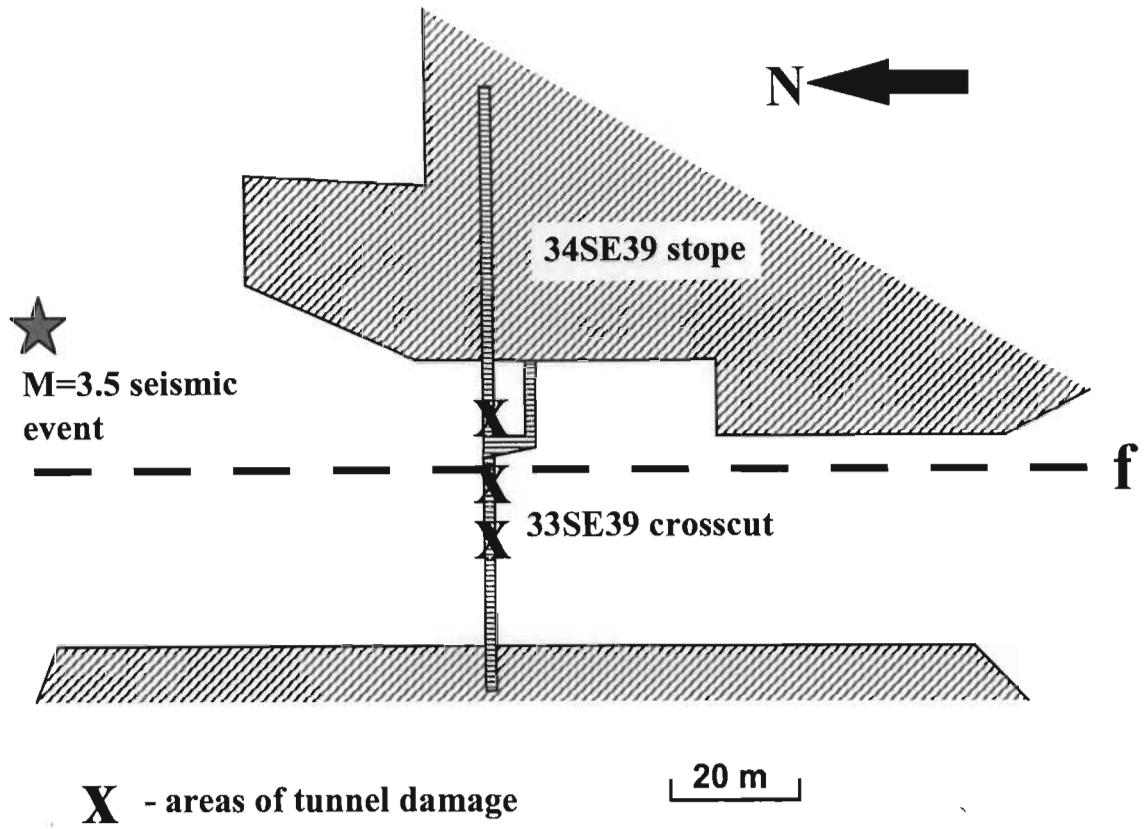

Figure 3-10.Schematic plan of the 33SE39 stope and tunnel layouts with areas of observed damage.

Damage, which could be associated with the seismic event, started approximately 50 m west of the stope entrance. The crosscut at this location was sited in a large fault loss of approximately 60 m width between reef blocks, and 90 m between the stoped out areas. This 'pillar' area resulted in higher stress levels on the haulages and associated increased fracturing of the wall rock. The area of significant haulage damage was also in the vicinity of the intersection between the excavation and the fault zone.

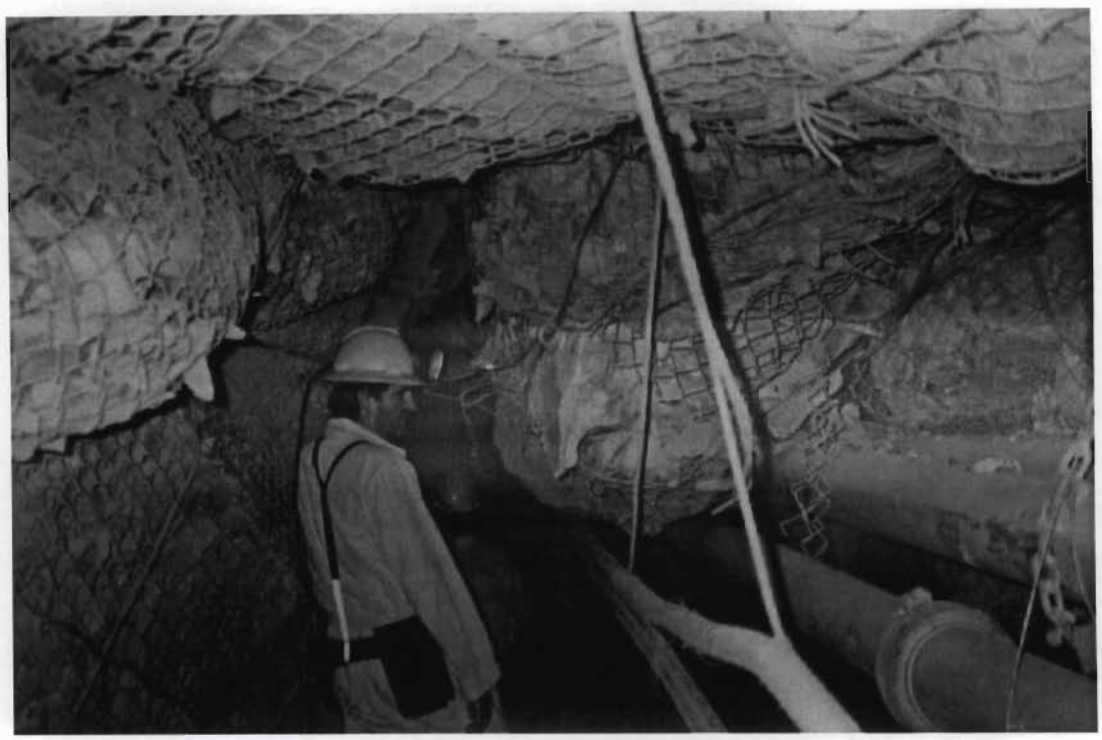

Photograph 3-46. View east along 33SE39 crosscut showing significant bulging of the rock mass between the rock bolt reinforcement. Failure was principally associated with the hangingwall and upper sidewall of the south side of the tunnel.

Damage to the 33SE39 crosscut consisted of significant bulking of the rock mass between the rock bolts (2.2 m smooth bar on a 1.0 m x 1.0 m square pattern) with loading of the mesh and lacing fabric support (Photograph 3-46). In some cases the loss of interaction between the rock bolt reinforcement and the rock mass was such that bulking of the order of 30 cm was observed within 10 cm of the rock bolt (Photograph 3-47).

Damage around the tunnel profile was most severe in the hangingwall and upper sidewall on the south side of the tunnel (Photograph 3-46), and also in the footwall and lower sidewall of the north side of the tunnel (Photograph 3-48).

Photograph 3-47. Detail of 30 cm bulking of the rock mass within 10 cm of a rock bolt reinforcement unit.

Photograph 3-48. View west along 33SE39 crosscut showing significant bulging of the rock mass between the rock bolt reinforcement, and increased failure of the footwall and lower northern sidewall of the tunnel.

The intensity of damage to the tunnel clearly increased as the stope was approached from the west, and was at a maximum in the vicinity of a ventilation door approximately 20 m from the

stope entrance. This area was also in close proximity to the edge of the fault loss area, and thus the main fault plane. It was also associated with the position of an inclined travellingway perpendicular to the tunnel axis and accessing a reef block approximately 5 m above the crosscut. The interaction between these excavations may also have resulted in increased stress induced damage to the surrounding rock mass, making it more prone to rockburst damage. Damage to the tunnel appeared to reduce from this point towards the stope entrance.

In the vicinity of the travellingway most of the deformation of the north sidewall was by shearing on a well defined bedding plane. This resulted in shear / tensile failure of rock bolt reinforcements crossing this plane.

Conclusions

Observations of the limited rockburst damage at this site was characterised by the highly discontinuous nature of the rock mass and the resultant direct loading and deformation of the mesh and lace fabric support.

3.2.8 Summary of tunnel damage observations

From the seven detailed rockburst case studies presented here the following points are highlighted with regard to the performance of the support systems and the mechanisms of failure of the rock mass.

- Bulking of the rock mass between the rock bolt reinforcement was observed at all the rockburst sites. At 70 % of the sites this was observed to have resulted in failure of the fabric support system over a significant area of investigation. At 30 % of the sites the integrity of the fabric support system was maintained and the unstable rock mass between the rock bolt reinforcement was contained.

- Large scale deformation over the whole height of the sidewall was observed at 60 % of the investigations. This was especially prevalent at investigations conducted in the Klerksdorp gold field. This may be a function of the different geotechnical environment and / or the more prolific use of smooth bar rock bolt reinforcement compared to the use of ripple bar on the West Rand gold field. Only isolated beam type failure was associated with the hangingwall of the tunnel.

- Shear failure of rock bolt reinforcement was observed at 70 % of the rockburst sites. In all cases this was in the hangingwall of the tunnel excavation.

- Tensile failure of rock bolt reinforcement was directly observed at 60 % of the rockburst sites. This was associated with both the hangingwall and sidewalls of the tunnels.

Of significance from this investigation is the large proportion of damage associated with the bulking and unravelling of the sidewall rock mass between the rock bolt reinforcement and the prevalence of shear deformation and failure of hangingwall rock bolt units. These mechanisms are not considered in the current design procedures. The purpose of this research to improve the mechanistic understanding of this interaction between the rock mass and the support system to improve the design considerations of support systems in these environments.

3.3 Mechanism of rock mass interaction with support systems and considerations for support design methodology

The erratic nature of the damage to tunnel excavations with respect to the source of the causative seismic event is indicative of the role that site response has in understanding the failure mechanisms. The main factors which influence the type and severity of damage are:

- the structure and competence of the rock mass prior to the seismic event.
- the previous history of deformation of the support system and thus its remaining capacity immediately prior to the seismic event.
- the orientation and proximity of the excavation relative to the source of the seismic event.

The containment of potential rockburst damage will involve the ability to define high risk excavations with a reasonable degree of certainty and also the implementation of effective excavation and support design strategies. These aspects of design will also require due consideration of the relative cost of these strategies compared to the identified level of risk and the limits of these design considerations.

For an anticipated level of rock mass instability of an excavation, the design engineer must be able to select a suitable support system for the given conditions. This will be based on the current and anticipated rock mass condition, anticipated loading conditions and allowable deformation, the availability of support elements and practicalities of installation, and the cost effectiveness of the support system on the basis of material and installation costs.

Of fundamental importance to the selection of the support design methodology is to ensure effective interaction between the support system and the rock mass in the periphery of the excavation. This will be a function of the competency of the rock mass under the anticipated loading conditions, which will influence the depth of instability and the interaction of the elements of the support system.

Within relatively competent rock mass structures, the role of the rock bolts is to pin potential key block structures by anchorage to stable ground in excess of the defined unstable block geometry. The purpose of this research is to develop support design methodologies for highly discontinuous rock mass structures where specific unstable block geometry's can not be identified and the dominant mode of rock mass instability is an unravelling of the rock mass structure.

3.3.1 Principal design considerations

It is considered that the principal design methods for support systems are either by containment or structural reinforcement. Containment of the rock mass may be achieved by ensuring anchorage outside of the limit of rock mass instability, with sufficient capacity within the support system to accommodate the full rock mass loading conditions. Alternatively the support system may act to reinforce the unstable rock mass and thus create a reinforced rock mass structure, again capable of withstanding the envisaged loading conditions. Within some support systems these support mechanisms may be combined to derive an optimum rock mass support system. Such a system may involve relatively short anchors and fabric support combined with long anchors. This would result in reinforcement of the immediate skin of the excavation with suitably anchorage to the deeper rock mass. The principal design considerations as discussed above are shown in Figure 3-11.

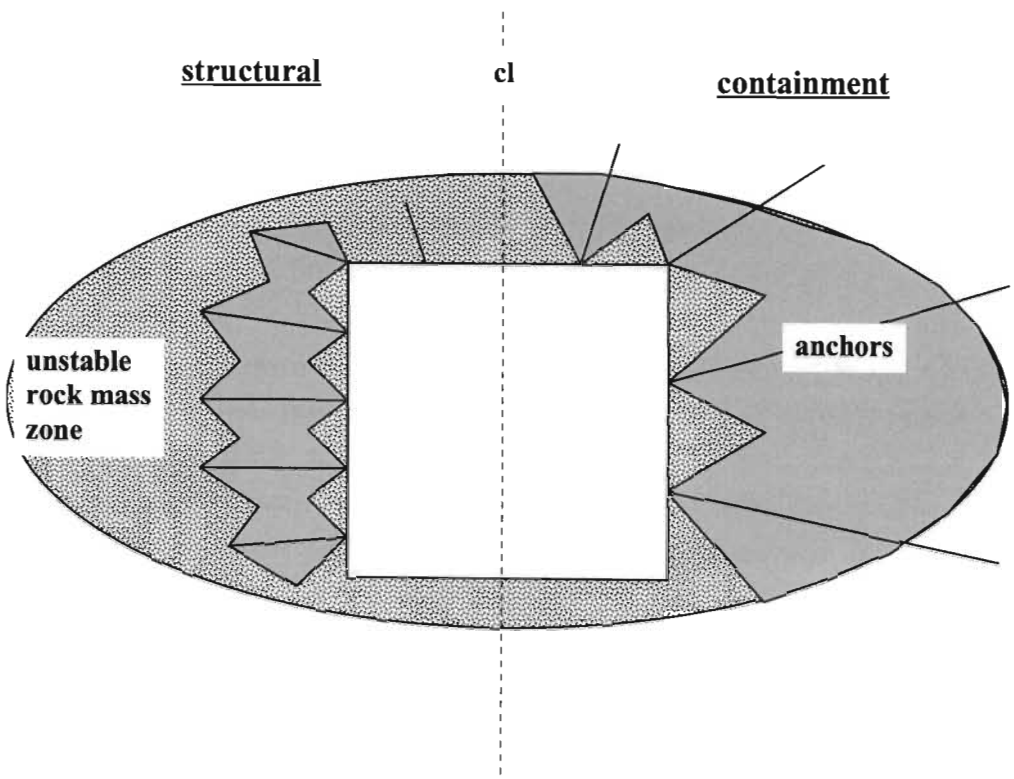

Figure 3-11. Definition of principle methodologies of excavation stabilisation

Of critical importance is an estimation of the depth of rock mass instability around the excavation, to enable the determination of a suitable anchor length. This may be based on data of anticipated depths of instability, empirical relationships, or numerical modelling analysis.

The importance of the influence of the mechanism of the support system interaction with the rock mass, on the deformation characteristics of the excavation, is illustrated in Figure 3-12.

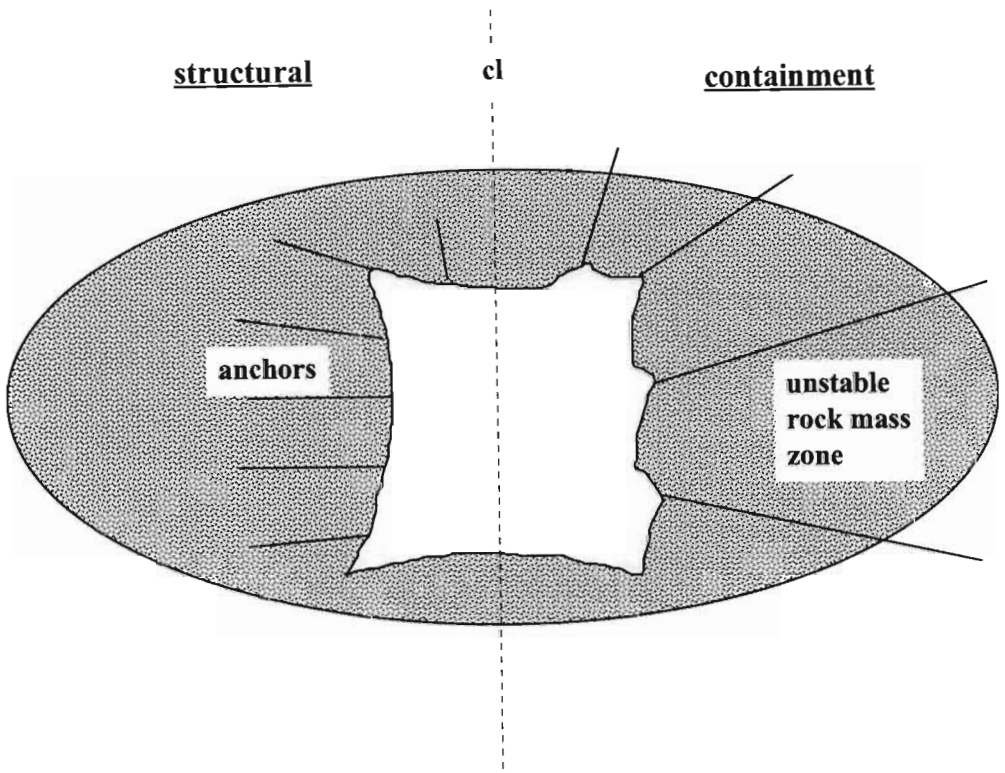

Figure 3-12. Generalised deformation characteristics for principal support methodologies under high loading conditions.

These deformation mechanisms are clearly illustrated by the rockburst case studies, where deformations often occurred to the extent that failure of components of the support system resulted. A review of the basis of these design methodologies is given below.

The methodology of the creation of a reinforced rock mass structure will be dependent on the interaction of the support system with the rock mass to create a reinforced structure of sufficient capacity to maintain the rock wall stability under the defined rock mass environment. The behaviour of the reinforced structure under loading will result in a more uniform sidewall deformation characteristic. If however the support is under designed, differential deformation within the structure will occur, causing a loss of capacity of the structure to withstand increased loading. The influence of the fabric support within this methodology will be to maintain the integrity of the discontinuous rock mass between the rock bolt reinforcement. The required load capacity of the fabric will thus be relatively low. However, it is important that relatively stiff fabric

systems be employed, such as shotcrete, in order to limit differential deformations within the structure, and thus maintain its overall integrity.

The methodology of excavation stabilisation based on retainment /containment is considered to be a more robust support design methodology, but it is critical that anchorage of the system within stable ground is achieved. Although the engineer should strive to design the support system in order to maximise the inherent strength of the rock mass structure, and thus minimise the support requirements, this methodology will allow consideration of loss of the inherent rock mass strength. This methodology therefore must carefully consider the interaction of the individual components of the support system with the rock mass, and the anticipated demand on these units. To maximise the inherent rock mass strength, for optimum design considerations, the yield capacity of the anchors should be compatible with the envisaged rock mass deformation characteristics. That is, yield of the anchors must be compatible with the dilation of the rock mass between anchor points in order to minimise differential deformations. Incompatibility will result in differential deformation, and thus loosening within the rock mass structure with resultant loss of rock mass strength. The incorporation of high quality, relatively stiff fabric support systems will result in a more even load distribution between the rock mass directly confined by the rock bolts and the potentially unstable rock mass between the rock bolt reinforcement. If the inherent strength of the rock mass is lost due to the degree of rock mass discontinuity, or deformation, then increased demand on the fabric component of the support system must be considered.

The combination of structural and retainment design principals may be the optimum design procedure under more adverse loading conditions, such as those associated with seismic events or large stress changes, in order to maintain reasonably practical support systems.

Within the hangingwall of the excavation, the general bedded nature of the rock mass structure tends to result in shear deformation of the rock bolt reinforcement. The degree of shear, and the propensity for damage, is also a function of the rock mass structure. In general, a significant amount of shear deformation is associated with the rock mass in the vicinity of a tunnel under dynamic loading conditions. Under these conditions the ability of the support system to accommodate shear is an important consideration. The use of relatively stiff rock bolt reinforcement within the hangingwall of an excavation may thus be prone to guillotining. The requirement for yield capacity under shear conditions would be an important consideration in the design of rock bolt reinforcement systems in order to maintain the overall hangingwall integrity.

3.3.2 Analysis of case studies

Analysis of the case studies clearly indicates the development of characteristic deformation mechanisms and also indicates the shortcomings of the current support systems. Major support system failure was due to loss of anchorage of rock bolts at approximately 60 % of the rockburst

sites. This may have resulted from the limited yield and debonding, or snapping of bolts and thus significant reduction in support resistance and rock mass reinforcement; or due to inadequate anchorage depth in relation to depth of rock mass instability, and limited containment of the unstable rock mass volume. Inadequate fabric support (mesh and lacing) capacity and stiffness also resulted in failures of the support system and reduced capacity of a potentially reinforced rock mass structure at all rockburst sites.

The design of the support system interaction with the rock mass is generally based on anchorage into stable ground (Anon., 1996). Where tunnels negotiate elevated stress fields due to major stoping abutments, the depth of rock mass fracturing may increase the extent of instability in excess of the length of these anchors. Under these conditions, the basis of support design should be the formation of a competent rock mass structure (beam, arch or shell). The large closures associated with the haulages at these sites may be indicative of low levels of rock mass reinforcement and thus weak structural competency. This may often be a result of the current design procedures not considering this mechanism of support interaction. Under these conditions it is important to ensure sufficient interaction between the reinforcement units as opposed to relying on the fabric support to provide sufficient structural strength to the rock mass. Therefore, rock bolt reinforcement spacing should be reduced to improve rock mass interaction.

The current design recommendations for tunnels in deep level mining indicate the necessity for yielding tendons, particularly under dynamic loading conditions associated with major seismic events, to ensure energy absorption capacity. However, throughout numerous case studies, it was observed that relatively stiff rebar rock bolts, with very limited yield capability and thus energy absorption, would survive the major dynamic deformations and damage. This is due to the poor interaction between the rock bolts and the rock mass in these environments. This causes the loading of the rock bolts at levels far lower than that anticipated by the design process. Under these conditions dynamic energy associated with the unstable rock mass is dissipated through the deformation of the rock mass contained by the relatively soft mesh and lace fabric support systems, resulting in the often observed bulking profile of the tunnel. This large bulking process between the rock bolt reinforcement, and thus large differential deformations, results in a further reduction of the rock bolt interaction with the rock mass. Thus this mechanism, although not catered for in the design process, results in the stability of the tunnel under these loading conditions. It must thus be appreciated that if the stiffness of the fabric support is increased, to try to limit the deformations of the rock mass to maintain the excavation in an operational condition subsequent to such events, then the distribution of loading between the fabric and the rock bolts will change. This will result in increased direct loading of the rock bolt reinforcement to the extent that failure may occur and the total support system unravels. The importance of the yield capacity within the rock bolt system to absorb the dynamic energy is thus heightened.

The design of the support system must therefore carefully evaluate the relative demand on the reinforcing rock bolts and the fabric support. In some areas, particularly where anchorage of the tendons was maintained or had relatively higher resistance than the general peripheral rock mass, excessive bulking of the rock mass between the reinforcing rock bolts was observed. This often resulted in failure of the fabric support. It is thus important to ensure compatibility between load deformation characteristics of the tendons and the fabric support based on an estimation of the relative demand due to rock mass loading. Incompatibility, such as the use of very stiff tendons and soft fabric, will result in large relative deformations within the tunnel peripheral rock mass and associated reduced structural competency. This will lead to subsequent higher loading of the fabric support, due to a further reduction in the interaction of the rock bolt reinforcement. Under dynamic loading conditions it was observed that in 70 % of the rockburst sites the kinetic energy associated with this unstable rock mass volume was in excess of the capacity of the typical mesh and lacing fabric support panels.

Within certain geotechnical areas, the occurrence of highly persistent, and mobile, bedding planes may result in a reduction in confinement provided by a reinforced rock mass structure. This is particularly evident if these bedding planes coincide with the hangingwall or footwall of an excavation and are of low inclination. This was often observed in the case studies conducted within the Klerksdorp gold field, where tunnels are sited in the MB Formation quartzites. These planes of weakness within a reinforced rock mass structure are orientated sub parallel to the typical orientation of the rock bolt reinforcement. This appears to result in low interaction between the rock bolt units and the bulk of the rock mass, and also poor interaction between the rock bolts within the reinforcing system.

The observed increased deformation of the lower sidewall than of the upper sidewall is considered to be a function of the presence of these dominant sub-horizontal bedding planes in addition to a lack of continuity of the lower sidewall support into the footwall. The presence of hangingwall support, and the general upward inclination of the upper sidewall rock bolt reinforcement, can create a more competent reinforced rock mass structure and thus greater end constraint to the sidewall reinforced rock mass structure (Figure 3-13).

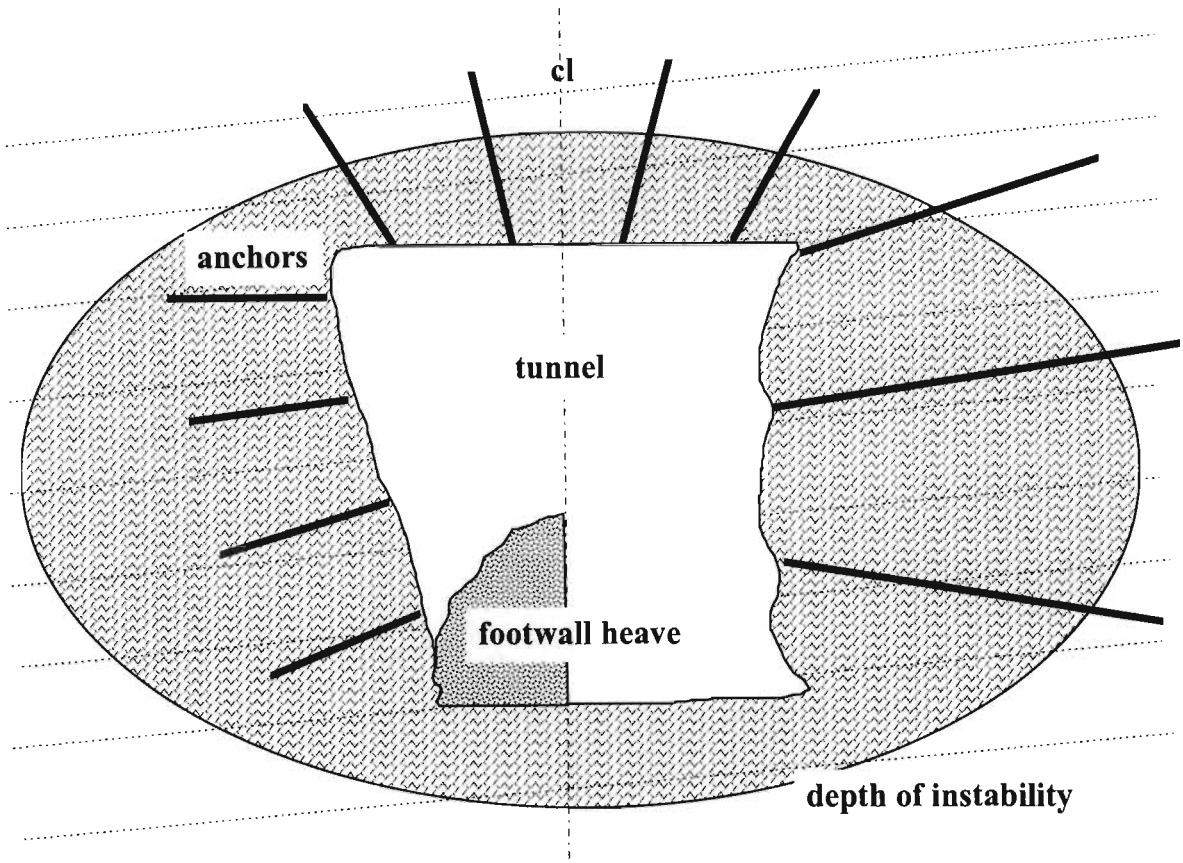

Figure 3-13. A conceptual model of design methodologies and potential rock mass deformations in the presence of weak bedding planes.

The weakness of these low inclination bedding planes, and their susceptibility to mobilisation under conditions of dynamic loading, was clearly illustrated in the Hartebeestfontein No.2 shaft investigation (section 3.2.5). Even in the presence of significant concrete structures, the sidewall deformed up to an estimated 50 cm during the seismic event (Figure 3-14).

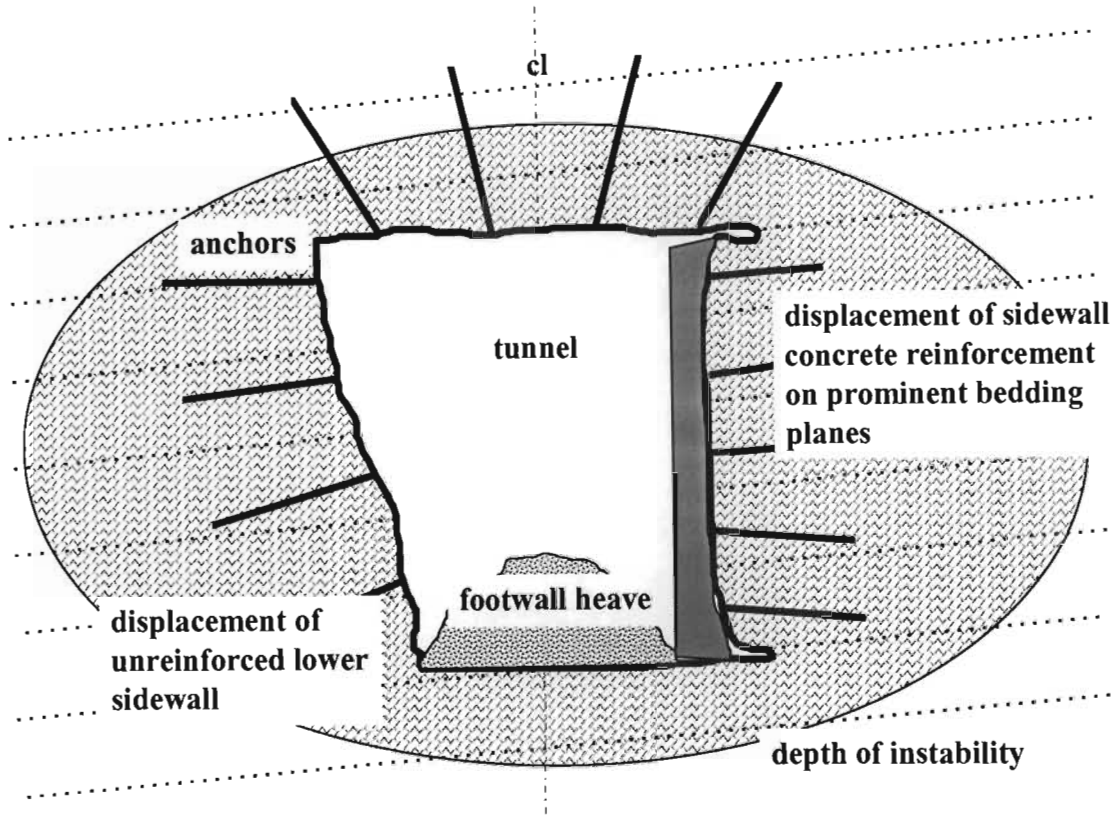

Figure 3-14. Conceptual model of rock mass deformations at Hartebeestfontein No.2 shaft 29 level tip crosscut.

Analysis of hangingwall stability often indicated shear failure of tendons in the hangingwall of the tunnel profile. Consideration of the shear capacity of tendons would not be catered for in standard support design practice, but this has been indicated to contribute to hangingwall failures at 70 % of the rockburst case studies. Consideration of the shear capacity of tendons and cables is suggested and that these reinforcing systems be utilised in areas where hangingwall shear, due to existence of prominent bedding and dynamic loading, is anticipated.

The relative intensity of the discontinuities within the hangingwall of an excavation had an influence on the potential of the support system to either accommodate or fail under shear loading. It is considered that in some cases rock bolts were able to accommodate relatively large shear deformations due to the highly discontinuous nature of the rock mass. This is thought to allow numerous incremental shear dislocations along the rock bolt length, each within the shear capacity of the rock bolt. This results in lower direct shear interaction between the rock mass and the rock bolt and thus reduced dynamic shear loading per shear plane.

The depth of instability within the hangingwall of the tunnel excavations (3.0 m x 3.0 m) has been estimated at 1.5 m to 2.0 m, based on these case studies. With typical support systems as used in the South African mining industry, this implies that hangingwall stabilisation is

primarily based on anchorage of the rock bolt reinforcement, and containment of the potentially unstable rock mass rather than structural reinforcement.

3.3.3 Conclusions

From the evaluation of the case studies, the importance of a procedure for the selection of a suitable support design methodology is indicated. This will form the first step in a more mechanistic evaluation of support requirements for these highly discontinuous and dynamic rock mass environments. The concept for an envisaged support design selection procedure is illustrated by means of a simple chart (Figure 3-15). This is primarily based on determination of the length of anchorage in relation to the depth of instability and an assessment of the rock mass competency. The length of reinforcement in relation to the depth of instability defines the mechanism of rock mass stabilisation. The assessment of the rock mass competency, as indicated in the rows of the selection chart, gives a very broad indication of the level of discontinuity within the tunnel peripheral rock mass. This may be assessed by means of a rock mass classification system such as the Q system (Barton *et al*, 1974) or more simply be an estimation of the frequency and persistence of discontinuity sets within the rock mass.

The calibration against the Q system as shown in Figure 3-15 is based on a suitable representation of the RQD and joint number set for the equivalent rock mass description. The other main rock mass characteristic is the joint condition parameter and, for the typical South African gold mining environment these are considered to be planer and rough with surface staining only. Within the South African gold mines, the rock mass is generally in dry condition but can be subjected to loading conditions from moderate compressive stresses to severe rockbursting conditions. This last parameter represents a significant downgrading in the Q system. By substitution of these conditions in the Q system, the approximate classification limits are established as 200, 0.4 and 0.01 for the increase in rock mass discontinuity as defined by the rock mass description.

Selection of support design methodology

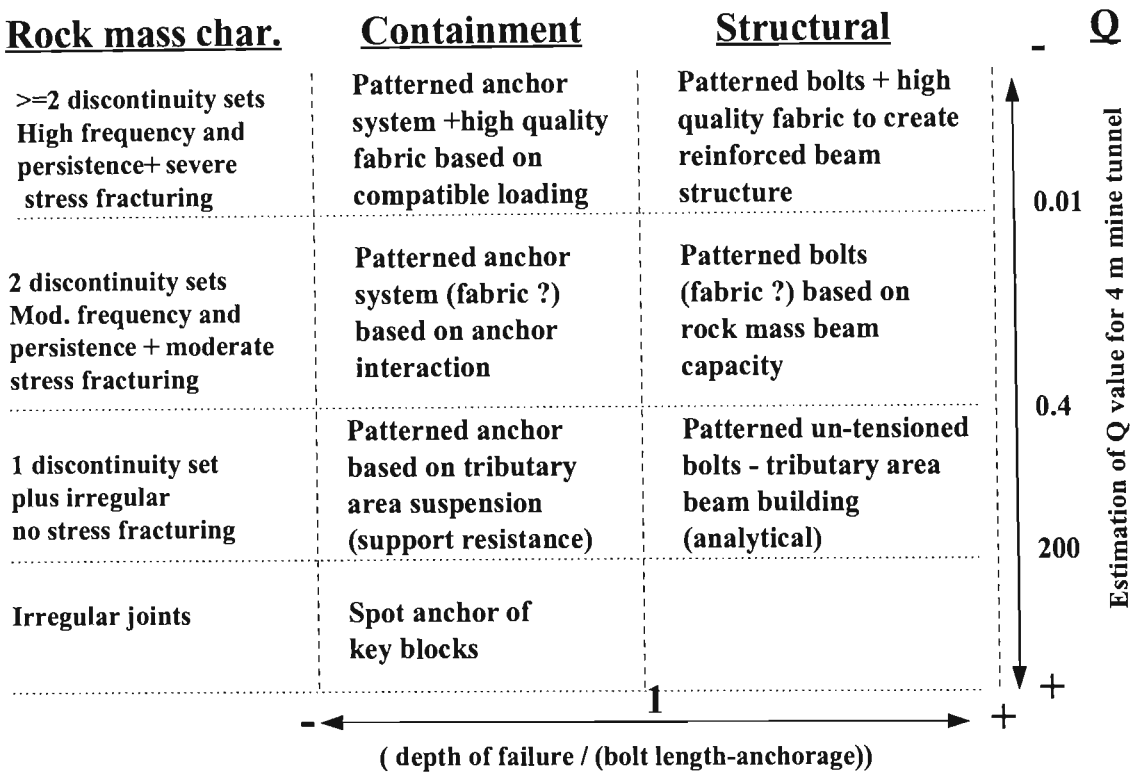

Figure 3-15. Estimated selection limits for support design considerations

A rock mass environment described by a high Q value (>100) would be characterised by isolated key blocks, the method of stabilisation of which is by means of specifically located rock bolts of sufficient stiffness and capacity to prevent movement. An increase in the level of discontinuity of the rock mass, where it may become more difficult to define individual blocks, will necessitate the use of more systematic bolting. Under these conditions the engineer will need to define the optimum mechanism of rock mass stabilisation of either containment or structural, or a combination of the systems. Usually for these rock mass environments, empirical design guidelines are available which generally cater well for the stabilisation of the excavation. As the level of rock mass discontinuity increases, the process of support methodology selection becomes more onerous due to the complex nature of the interaction between the support system and the rock mass. In this case support selection may be based on experience, if deemed suitable, or empirical design guidelines if they are being applied in appropriate rock mass environments. If the rock mass conditions are abnormal, due to a change in rock mass structure or loading conditions, then a more mechanistic based approach to the design process may again be more appropriate. It is this aspect of design that is considered in the following chapters of this document.

Chapter 4

4. In situ evaluation of tunnel stability and deformation mechanisms.

4.1 Introduction

Numerous authors have conducted detailed studies of the behaviour of tunnels and their support systems under high stress and changing stress conditions, particularly in the South African mining environment. With the understanding of deformation mechanisms gained from the rockburst investigations and case studies, as evaluated under Chapter 3, the available database was re-examined, rather than repeating these expensive experiments. This evaluation focuses on recent work conducted by Martin, McCreath and Stochmal (1997) and a fairly detailed investigation conducted by Hepworth (1984) at Buffelsfontein gold mine in the Klerksdorp gold field of South Africa.

The data of Martin *et al* (1997) is examined with regard to its applicability in determining the depth of anticipated rock mass instability around excavations in which stress induced fracturing is the dominant mode of failure. This understanding will allow a more rigorous estimation of the anticipated depth of instability, an important component of the selection process of a suitable support design methodology to ensure excavation stability.

The data of Hepworth (1984) has been re-evaluated with regard to deriving an understanding of the relationship between the three dimensional stress state history, in order to develop a better understanding of the deformation mechanisms. In addition, the influence of the different support systems, as installed in the experimental tunnel is also evaluated.

The definition of the rock mass environment around a tunnel excavation is the first step in the design process (Figure 4-1) and it is these design considerations which are investigated in this chapter.

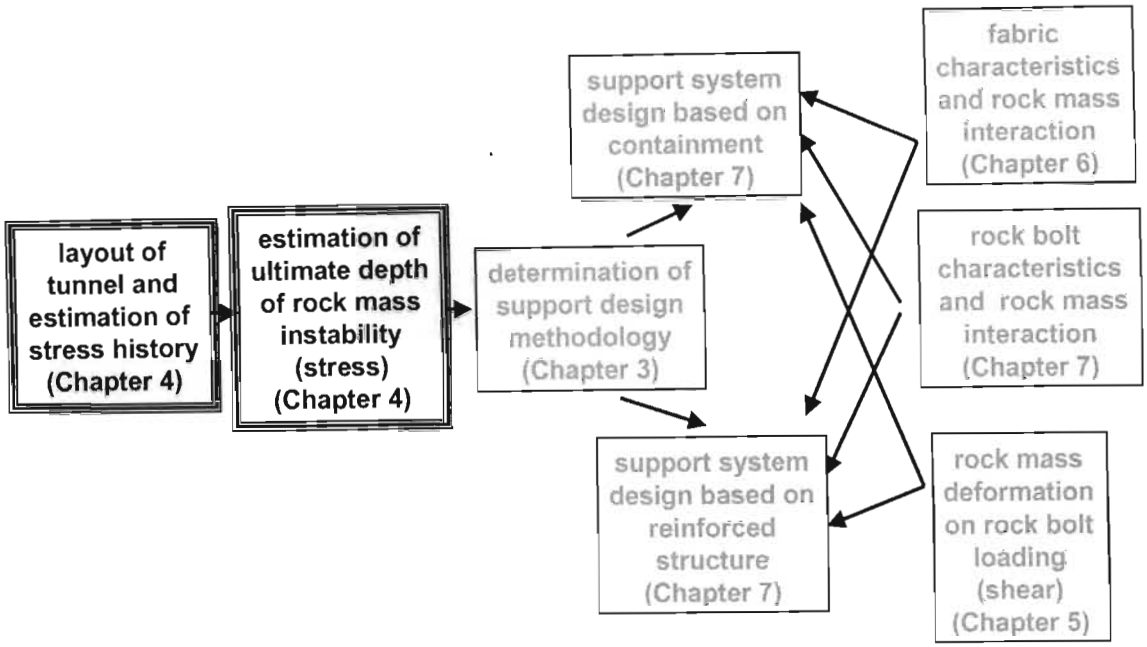

Figure 4-1. The relevance of research conducted in Chapter 4 on the overall tunnel support design methodology.

4.2 Evaluation of the anticipated depth of instability

4.2.1 Introduction

The depth of rock mass instability around an excavation will determine the required rock bolt capacity and length based on the mode of interaction between the support systems and the excavation peripheral rock mass.

The depth of instability will be a function of the competency of the rock mass in which the excavation is placed. The rock mass strength, in relation to the stress level, will control the potential for stress induced fracturing. Within the deep level mining environment, fracturing in the skin of the excavation will principally control the depth of instability of an excavation.

Empirical guidelines also exist for the determination of the length of reinforcement, however it is not be always clear whether the length of reinforcement is for the design of bolts to be anchored within stable ground, or to create a reinforced structure within the unstable zone. A guideline proposed by the Norwegian Institute for Rock Blasting Techniques (Stillborg, 1986), for stable anchorage in moderately jointed rock masses, estimates the length of bolts at the centreline of the excavation span to be:

$$L = 1.40 + 0.184a \qquad \text{(Stillborg 1986)} \qquad (4\text{-}1)$$

where L is the derived bolt length in metres and a is the span of the excavation in metres. Thus, for a typical mine tunnel of 3.5 m hangingwall span, the minimum bolt length to ensure stable anchorage would be 2.0 m, which is typical of the reinforcement lengths used in the South African mining environment.

Other general guidelines for more highly discontinuous rock mass structures indicate that the length of the bolts should be approximately twice their spacing, or that the spacing be less than or equal to three times the discontinuity spacing (Stillborg 1986). Other guidelines (Douglas and Arthur 1983) indicate that for typical tunnel excavations the length of bolts should be the greater of 2 x bolt spacing, 3 x discontinuity spacing or 0.5 x span of excavation. These guidelines are generally based on the design consideration of creating a reinforced, structurally competent rock mass, and thus may not represent the full depth of instability.

The depth of instability of the rock mass around an excavation may also be derived by data analysis of more site-specific case studies.

4.2.2 Analysis of accident data

The use of accident data from investigations in a relatively similar mining environment, can be utilised to analyse the depth of instability for a rock mass typical of that of the data set. Examples of the data sets, for rockfalls and rockbursts for the South African gold mining industry are shown in Figures 4-2 and 4-3. This data has been restricted to off reef excavations of dimensions of less than 3.5 m. The analysis on the graphs indicates the 95 % confidence limit of maximum unstable height. This is generally accepted as the minimum limit for support design purposes in South Africa.

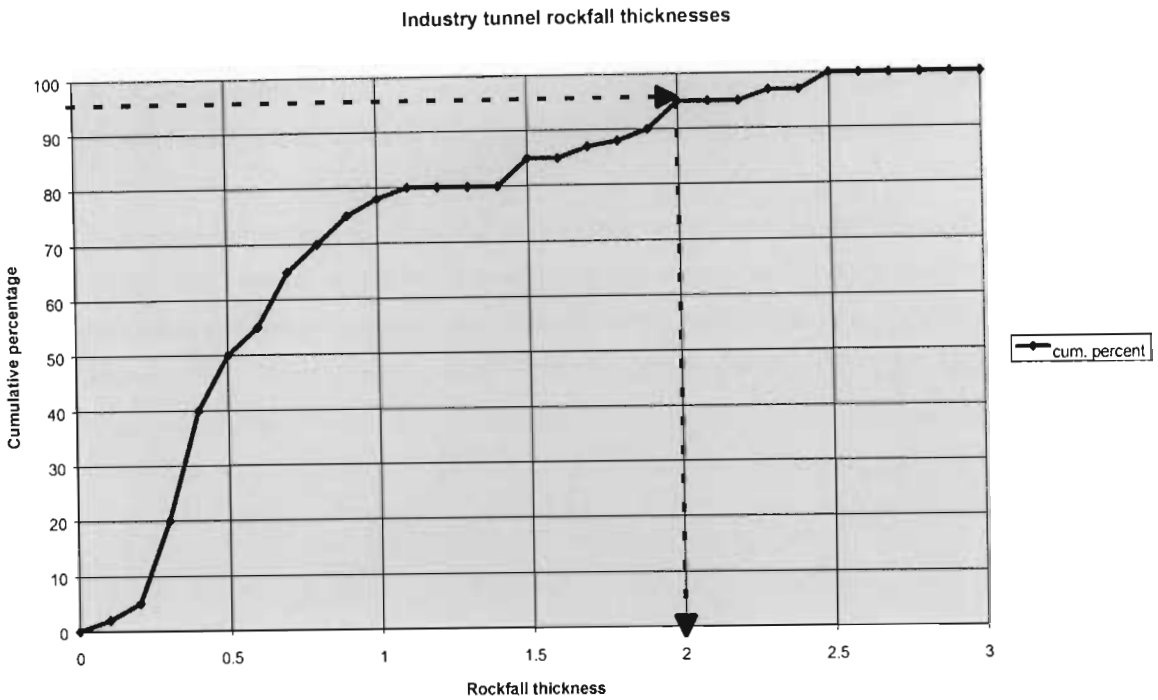

Figure 4-2. Analysis of tunnel fall of ground data for the South African gold mining industry

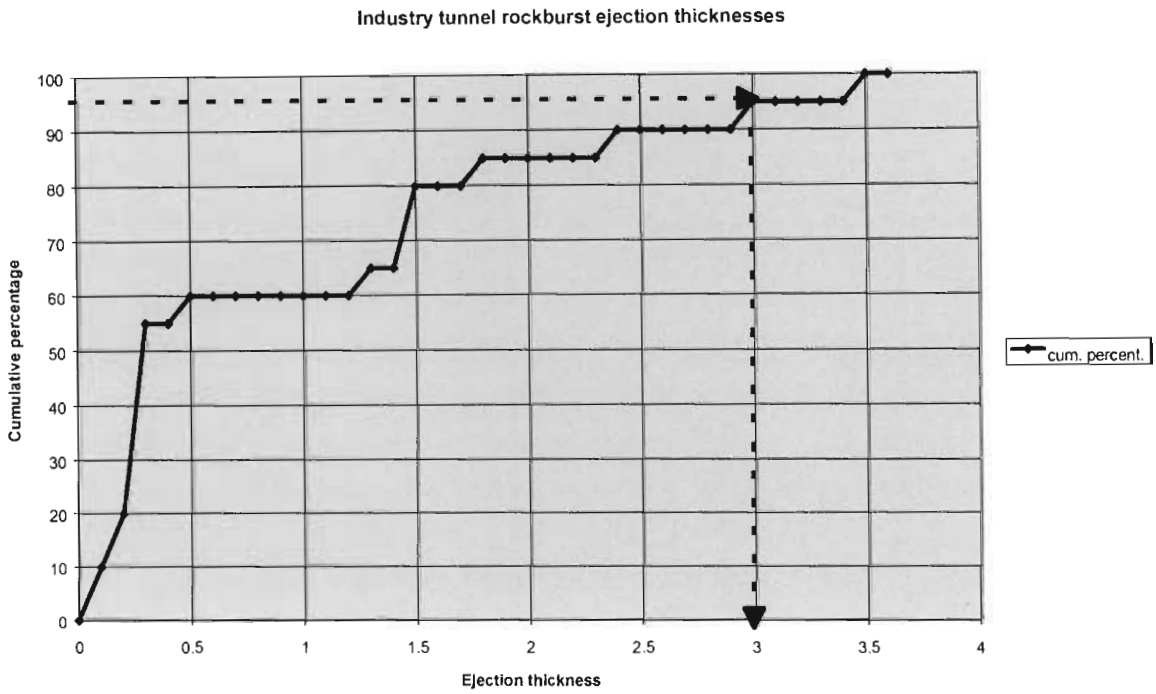

Figure 4-3. Analysis of tunnel rockburst ejection thickness data for the South African gold mining industry.

The design procedure utilising this data is to ensure that the length of anchor, excluding the required bond / anchorage length, is greater than the height of instability.

However, it must be remembered that the use of the data set implicitly includes all other factors that may influence the depth of failure. These will include the implemented support system, rock type, stress environment, magnitude of the seismic event, etc. If the data set is limited to the mine of application then some factors may be considered constant, such as rock mass type, and thus are valid for the data selected. However, the data will still be influenced by the presence of the support systems, unless the data is restricted to where the depth of failure is substantially greater than the reinforcement length. Thus, for the 95 % confidence limit indicated in Figures 4-2 and 4-3, for rockfall and rockburst accident data respectively, the average unstable depths for the South African gold mining industry are 1.8 m and 3 m respectively.

The length of tunnel reinforcement units, as typically used in the South African mining industry, is between 1.8 m and 3 m. Thus, most of the unstable height collapses are within the length of the typical reinforcement units. The assumption must therefore be that a substantial number of these may have fallen between the tendons, where the peripheral rock mass is more discontinuous. In these cases the reinforcement may still act to stabilise the deeper rock mass and thus, in the absence of any reinforcement, the depth of instability would have been substantially greater. Where collapse in excess of typical tendon lengths has occurred then it may be considered that this would represent the natural depth of instability for the given rock mass environment.

4.2.3 Depth of instability due to stress induced fracturing

Work conducted by Martin *et al* (1997) investigated the depth of breakout for tunnels where the mode of failure of the rock mass was stress induced fracturing, and the failure process was not constrained by rock mass reinforcement or support. A large proportion of the case studies utilised by Martin were based on South African mine tunnels.

Under high stress environments, typical of South African gold mining conditions, the mechanism of rock mass failure around an excavation is principally stress induced fracturing. In this environment it is considered that the original rock mass structure is of lesser importance in determining the ultimate extent of instability (Jager, Wojno and Henderson, 1990). The initiation and development of the fracture zone is thus a function of the ratio between the induced tangential stress at the excavation boundary and the rock strength. This formulation is consistent with that proposed by Wiseman (1979), and incorporated in the Rockwall Condition Factor criterion (Anon., 1988).

$$RCF = \frac{3.\sigma_1 - \sigma_3}{F.\sigma_c} \qquad (4\text{-}2)$$

where: σ_1 is the maximum principle stress in the plane of analysis

σ_3 is the minimum principle stress in the plane of analysis

F is a factor between 0.1 and 1, dependent on the rock mass characteristics and excavation size used to downgrade the intact rock strength

σ_c is the uniaxial compressive strength of the intact rock from laboratory testing.

The numerator of equation 4-2 represents an approximation of the stress concentration on the rockwall of the excavation and the denominator an estimation of the in situ rock mass strength.

The relationship as utilised by Kaiser *et al* (1996) also evaluates the influence of the induced excavation boundary stress in relation to the rock strength on the depth of failure as a function of the excavation size. For a comparison of excavations of different shapes, but of similar size, the dimension of the excavation is simplified to an equivalent excavation size. This is represented by the radius of an encompassing circle, and is considered valid for excavations of w/h<2. The equivalent excavation dimension (a) is given as

$$a = \frac{h \text{ (or } w)}{\sqrt{2}} \qquad (4\text{-}3)$$

This is represented in Figure 4-4.

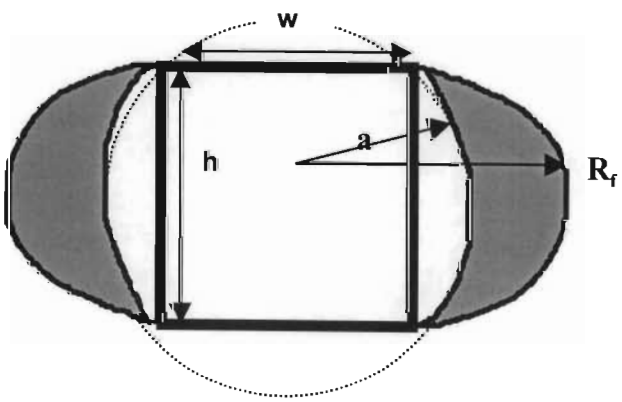

Figure 4-4. Definition of equivalent excavation dimension and depth of instability (Kaiser *et al*. 1996)

Figure 4-4. indicates the depth of instability R_f due to stress induced fracturing around an excavation.

The relationship between the stress level and depth of instability as derived by Martin is shown in Figure 4-5. This shows the data of case studies used to derive the relationship between the ratios of induced tangential stress to rock strength, and depth of instability to equivalent excavation dimension.

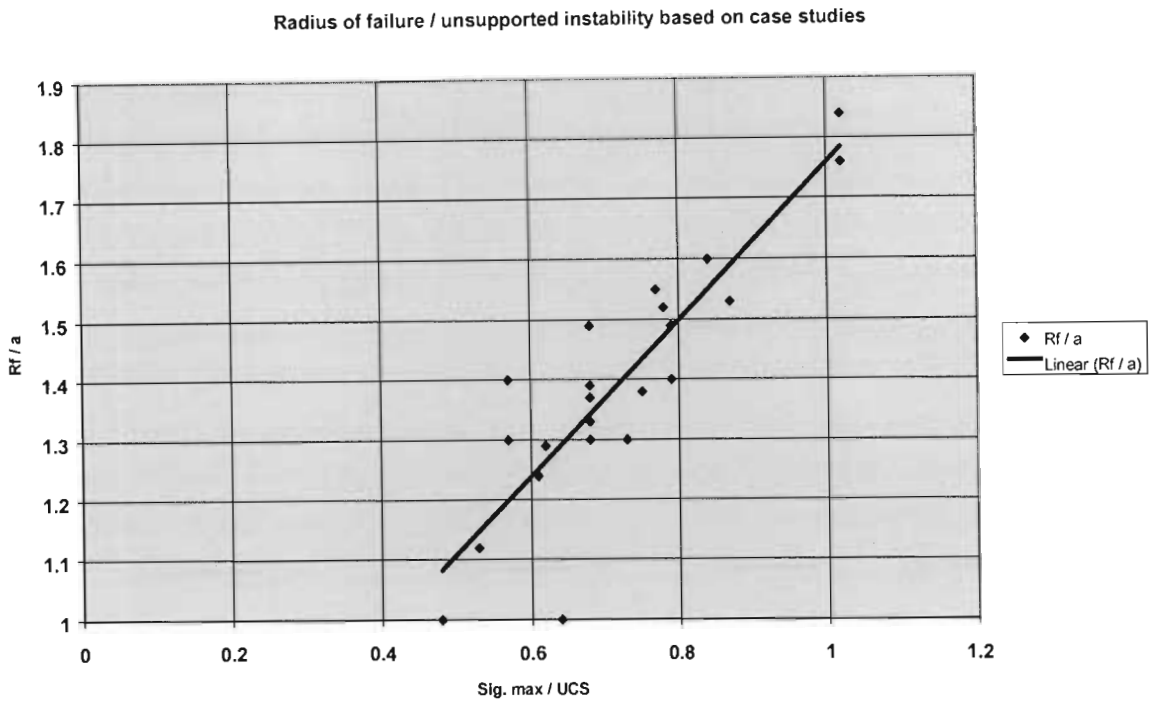

Figure 4-5. Relationship between induced stress and depth of instability after Martin *et al* (1997).

This relationship may be expressed as:

$$R_f/a = 1.34\ \sigma_{max} / \sigma_c + 0.43 \qquad (4\text{-}4)$$

where $\sigma_{max} = 3\sigma_1 - \sigma_3$ (4-5)

Analysis of Martin's data indicates the onset of significant fracturing to commence at a stress level of 43 % of the rock strength. This is consistent with other authors (Wagner, 1983).

Kaiser *et al* (1996) have also examined the theoretical influence of dynamic loading, as a function of seismic activity in the vicinity of the excavation, on the extent of rock mass damage and instability of the excavation. The incidence of a shear wave associated with a seismic event will result in a peak dynamic stress of:

$$\sigma^d = +/- c_s\ \rho\ ppv_s \qquad (4\text{-}6)$$

where: σ^d = the induced dynamic stress in the rock mass

c_s = the propagation speed of the shear wave

ρ = the rock mass density

ppv_s = the peak particle velocity of the shear wave at the point of analysis.

The waveform of a seismic event may be divided into a primary compressional wave (p-wave) and a secondary shear wave (s-wave) if the rock mass is assumed to be an isotropic elastic medium. Most of the seismic energy is associated with the s-wave component of an event. At the point of analysis the ground motion velocity of the shear wave is utilised as this is generally substantially greater than that of the p-wave. This dynamic stress is additive to the in situ stress state and thus alters the in situ stresses according to its magnitude and direction relative to the principle stress directions. This dynamic stress is also concentrated in the vicinity of an excavation as are the static field stresses. For an excavation of circular geometry, this stress concentration factor is given by:

$$n = 4\cos 2\theta \qquad \text{(Kaiser } et\ al\text{, 1996)} \qquad (4\text{-}7)$$

Where: n = dynamic stress concentration factor

θ = angle of incidence between the seismic wave and the maximum principal stress direction.

For design purposes it is considered that a value of n=4 should be taken. This would represent the worst case scenario when the angle of incidence between the dynamic shear wave and the maximum principal stress direction is 0°. Under these conditions the maximum dynamic stress concentration in the periphery of the excavation is given by:

$$\sigma_{max} = 3.\sigma 1 - \sigma 3 + 4\, c_s\, \rho\, ppv_s \qquad (4\text{-}8)$$

The value for c_s is a function of the rock mass density and elastic constants and may be taken as approximately 3650 m/s for intact hard rock mining environments. The shear wave peak particle velocity (ppv_s) will be a function of the magnitude of the seismic event and the distance from source. This may be estimated from charts such as that shown in Figure 4-6.

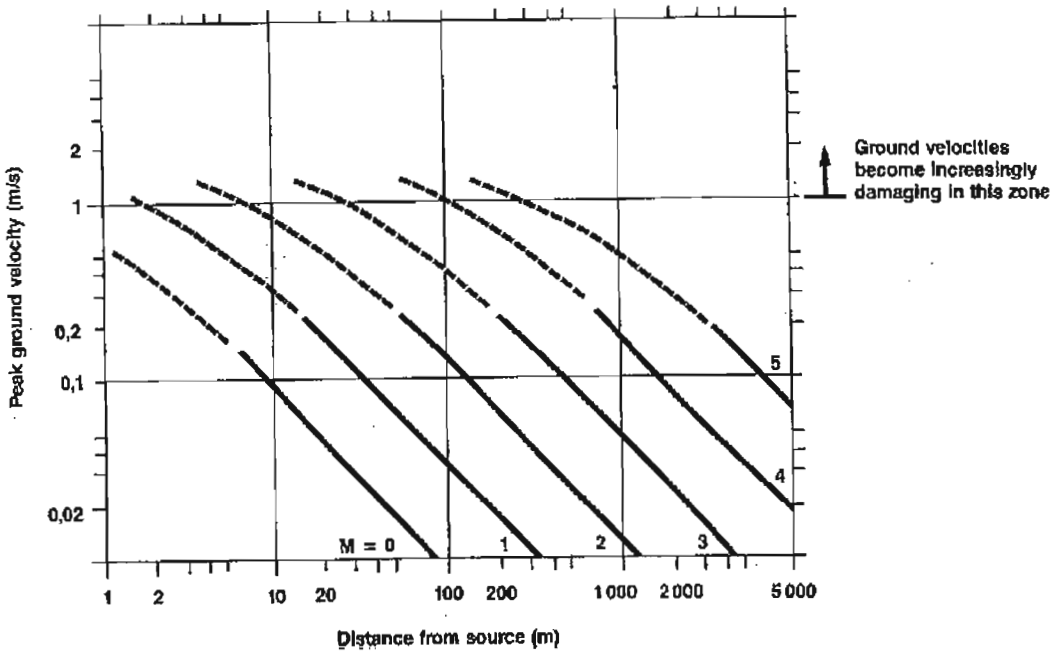

Figure 4-6. Ground velocity with distance from seismic event (Anon., 1988)

Substitution of data derived from Figure 4-6 into equation 4-8 yields a relationship between the parameters of a seismic event and the anticipated maximum induced dynamic stress on the boundary of an equivalent circular excavation (Figure 4-7).

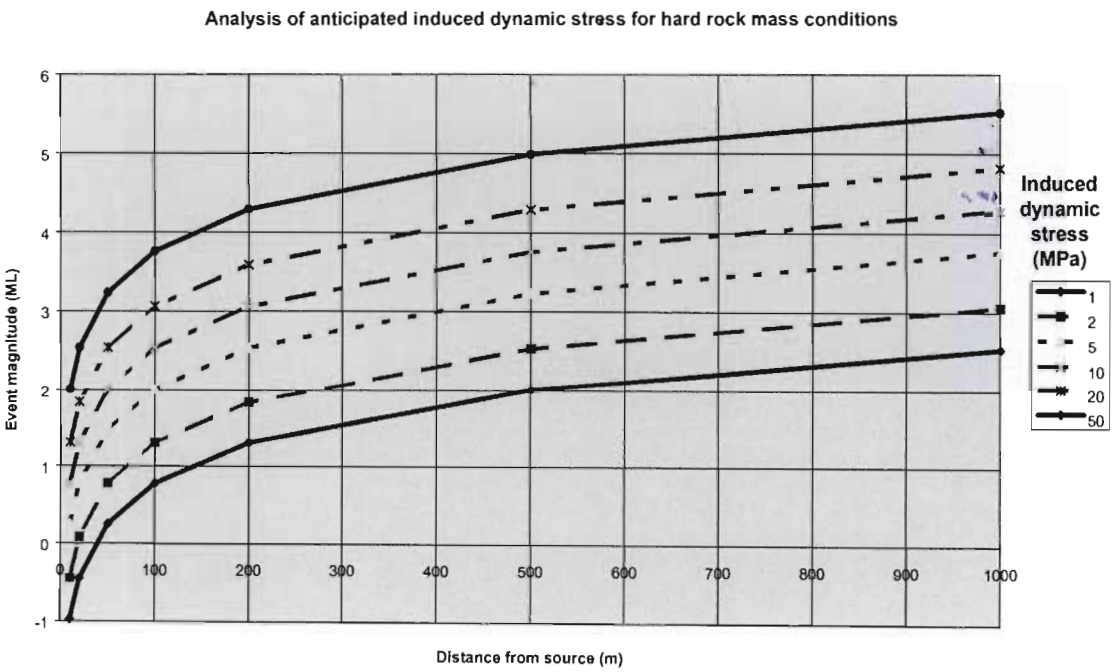

Figure 4-7. Determination of anticipated maximum induced dynamic stress due to a defined seismic event.

Data from Figure 4-7 is added to the static stress concentration to estimate the additional depth of instability as a function of the induced dynamic stress due to a seismic event. Although not

investigated here, the differences in the effect of loading rate on rock mass strength between the static and the dynamic environments is considered important. Some work in this area has been conducted by Martin (1993) and indicated that the long term strength of rock, as determined in the laboratory, is approximately 70 % of that determined under typical laboratory loading rates. Uniaxial compressive strength data used in the derivation of Figure 4-5 is based on typical laboratory samples (Kaiser *et al*,1996), and thus, although they may represent a higher strength than the in situ intact rock, the empirical relationship would be still be valid on this basis. However, the direct application of the induced dynamic stress to this relationship would give an over estimation of the extent of failure, due to the higher short term strength of the rock mass.

An additional consideration is that, in an area of high incidence of seismicity, the ultimate depth of failure is suggested by Kaiser *et al* (1996) to be a function of the largest magnitude event and not a cumulative process. However, this does not mean that rock mass dilation within the fracture zone is not cumulative, and thus deformation of the rock mass into the excavation may be a function of the cumulative incidence of seismicity.

For ease of application to the South African mining environment, the relationships discussed above have been adapted for typical South African tunnel rock mass environments. They are expressed in the form of the in situ field stress, to the total depth of failure for a square tunnel of dimension 3.5 m x 3.5 m, and for a range of typical uniaxial compressive rock strengths of 150 MPa to 200 MPa. These relationships are shown in Figure 4-8.

It is noted that with rock mass parameters of a tunnel environment typical for South African mining conditions, the empirical range, as defined by Martin's data set, and thus limit of applicability of the criterion, is for stress fields of up to only 90 MPa. The associated maximum depth of instability is 3 m from the sidewall of the tunnel. This would not be representative of the maximum stress field in which mine tunnels are developed.

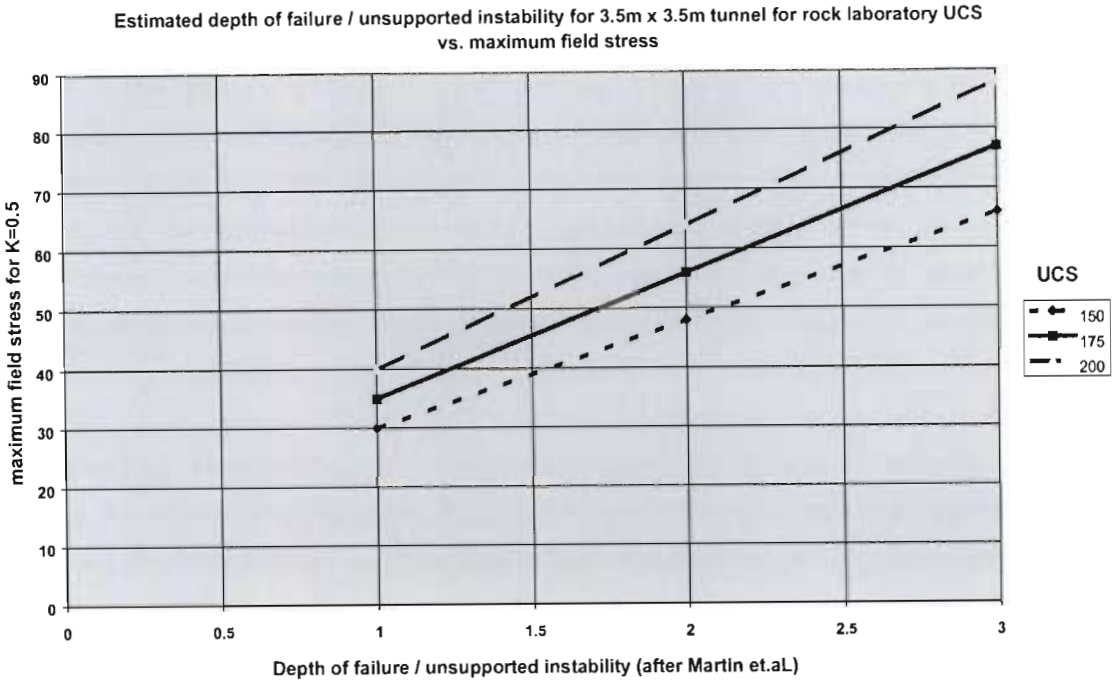

Figure 4-8. Adapted design chart for typical South African mine tunnel applications to determine depth of potential sidewall instability.

It is considered important to clarify that the criterion, and the basis of subsequent support design, is the definition of the potential depth of instability. This does not necessarily represent the depth of rock mass damage due to stress induced fracturing.

Tunnel excavations are often sited in relatively high stress fields, where the induced stresses are of the order of two to three times the rock mass strength. Even under these conditions the operational stability of the excavation may be maintained. Although this is well outside Martin's empirical range, and thus the application of the criterion, extrapolation would indicate a depth of instability of up to four times the effective radius of the excavation. Experience has shown that this extent of instability is generally not observed. It has been shown that as fracturing, and instability develops around an excavation, these zones tend to develop an elliptical profile that becomes increasingly self-supporting. Thus, it appears that the increase in the extent of instability, with increasing stress level, is limited.

A case study of a tunnel subjected to stresses ranging from 50 MPa to 230 MPa, conducted by Ortlepp and Gay (1984), was evaluated against the criteria of Martin *et al* (1997). The excavation was sited in high strength quartzites, with an average laboratory determined UCS of 350 MPa. One particularly highly stressed measuring station was selected for evaluation. The initial stress state for this section of the tunnel was σ_1 = 140 MPa and σ_3 = 60 MPa, giving an estimated induced tangential stress of 360 MPa (equation 4-5)

The equivalent dimension (radius) of the excavation, which was developed as a horseshoe profile approximately 1.5 m wide, would be approximately 1.05 m (equation 4-3). At this site the observed self mining of the excavation resulted in "over break" to an average width of 3.75 m, and the development of an elliptical profile. This "over break" would give an initial ratio of depth of instability of approximately 1.8.

The ratio of maximum induced stress as determined above to the UCS would be approximately 1.03.

This would plot at approximately the upper limit of Martin's empirical data range as indicated in Figure 4-9.

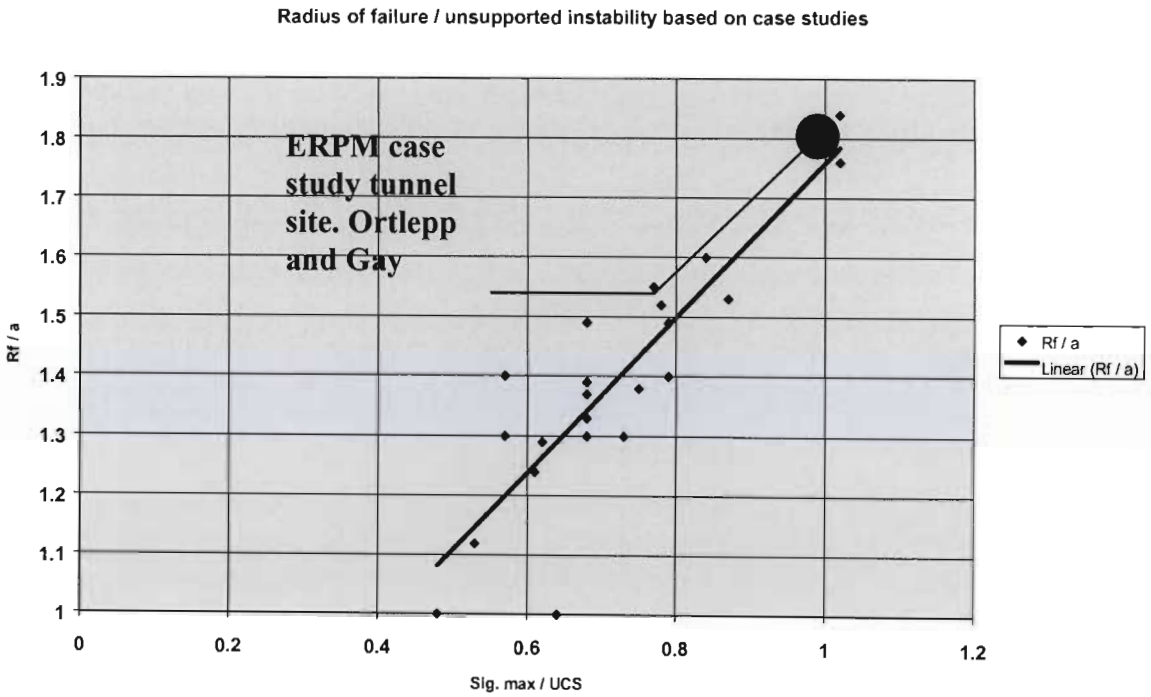

Figure 4-9. Location of ERPM case study tunnel based on Martin's criterion.

The data for the initial stress state acting on the excavation in this case study correlates very well with the empirical relationship. The tunnel site was however subjected to several large magnitude seismic events and a gradual increase in the field stress to a final level of approximately σ_1 = 230 MPa and σ_3 = 70 MPa. This would result in a maximum induced stress of 620 MPa (equation 4-5).

This would thus give a ratio to the rock UCS of 1.77. Over the period of subsequent stress increase, from 140 MPa to 230 MPa, a standard rock bolt reinforcement and mesh and lacing support system supported the tunnel. Although this may have influenced the potential for the development of the extent of instability, and as such would not be representative of Martin's criterion, it was felt by the authors (Ortlepp and Gay, 1984) that little further damage to the rock

mass and support system had occurred. This would indicate that at this stage the rock mass on the boundary of the tunnel was inherently stable. Therefore, although there was a substantial increase in the induced stress level, there was minimal further increase in the depth of instability. With regard to Martin's criterion, this would indicate a marked deviation from the linear relationship in excess of the current limit. This would, however, confirm observations of tunnel damage in high stress, and dynamic loading environments. The reviewed stress state in relation to the maximum considered depth of instability for this case study is shown in Figure 4-10.

From the South African gold mining industry accident database, an attempt was made to establish case histories with the depth of failure of the rock mass in excess of the rock bolt length.

The sparse nature of this data meant that only one additional case study could be established. This represented a site at a Far West Rand gold mine. The excavation was sited in a quartzite rock with an estimated UCS of 150 MPa, in a vertical stress field of 110 MPa. The recorded maximum depth of instability, over an average excavation dimension of 4.65 m, was 3.3 m. This would give an estimated maximum tangential stress of 290 MPa (equation 4-5). The equivalent excavation dimension would be 3.3 m (equation 4-3). The depth of instability is hence estimated to be 5.6 m and thus $\sigma_{max} / \sigma_c = 1.9$ and $R_f / a = 1.7$

This point is plotted on the revised chart as indicated in Figure 4-10.

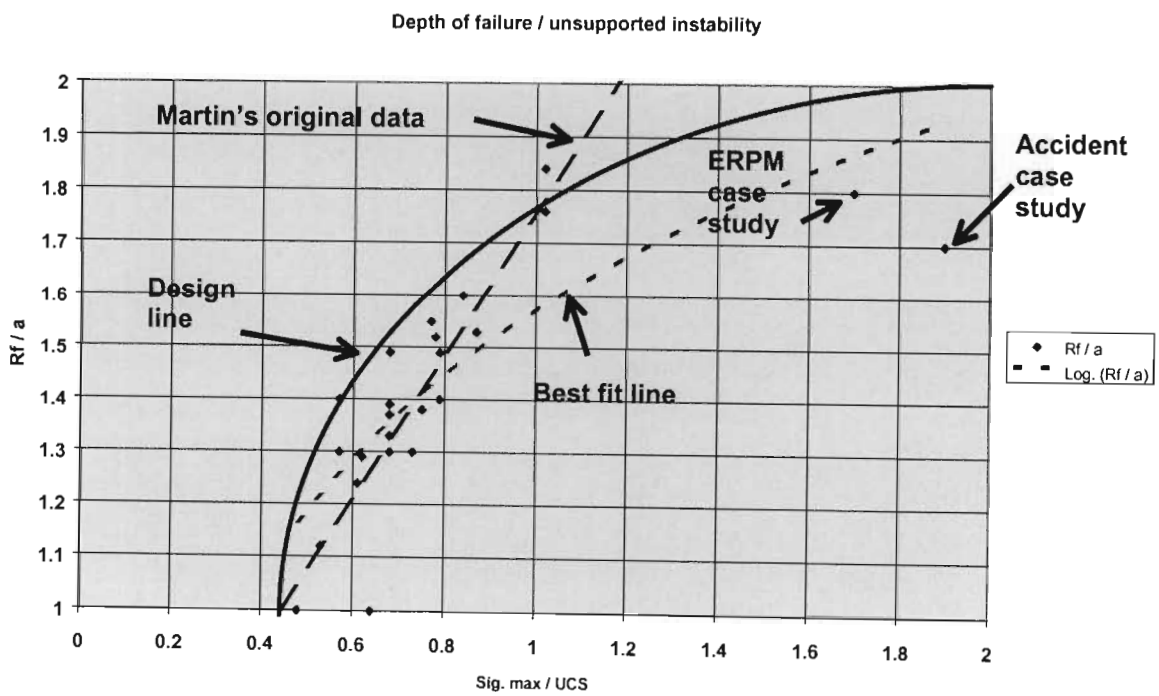

Figure 4-10. Revised relationship of depth of instability for additional South African case studies.

The tendency for a maximum upper limit of depth of instability is indicated in Figure 4-10 by the "design curve" which encompasses the majority of data points. This illustrates the observed tendency for an excavation to attain a stable profile. This may be as a function of the rock mass structure, or the gradual restriction in the area of maximum tangential stress and active rock mass fracturing. Data for excavation stability at these high stress levels is very limited and thus suitable regard must be given to the degree of confidence in the design relationship. However, it is considered that this relationship is more appropriate for the design of rock mass reinforcement systems in the high stress environments as experienced in many of the deep level South African gold mines.

4.3 Evaluation of Rock mass deformation mechanisms

4.3.1 Review of the Buffelsfontein site and Hepworth's analysis

A tunnel was developed approximately 30 m below the reef horizon between two crosscuts and on reef raises specifically for the purpose of the investigation (Hepworth, 1985) (Figure 4-11). The dimensions of the tunnel, as planned, were approximately 3.4 m high by 3 m wide, with an anticipated over break of less than 10 %. However, due to the local geology (bedding), hangingwall breakout occurred to a bedding plane resulting in a "lean to" profile of the tunnel such that the down dip sidewall is smaller than the up dip sidewall profile. The tunnel was subjected to a stress increase and subsequent stress decrease as a result of the mining between the raise lines (Figure 4-12). The support systems were evaluated by Hepworth with regard to the increase in the maximum principle stress (σ_1). The experimental tunnel consisted of 13 test sections as shown in Table 4-1

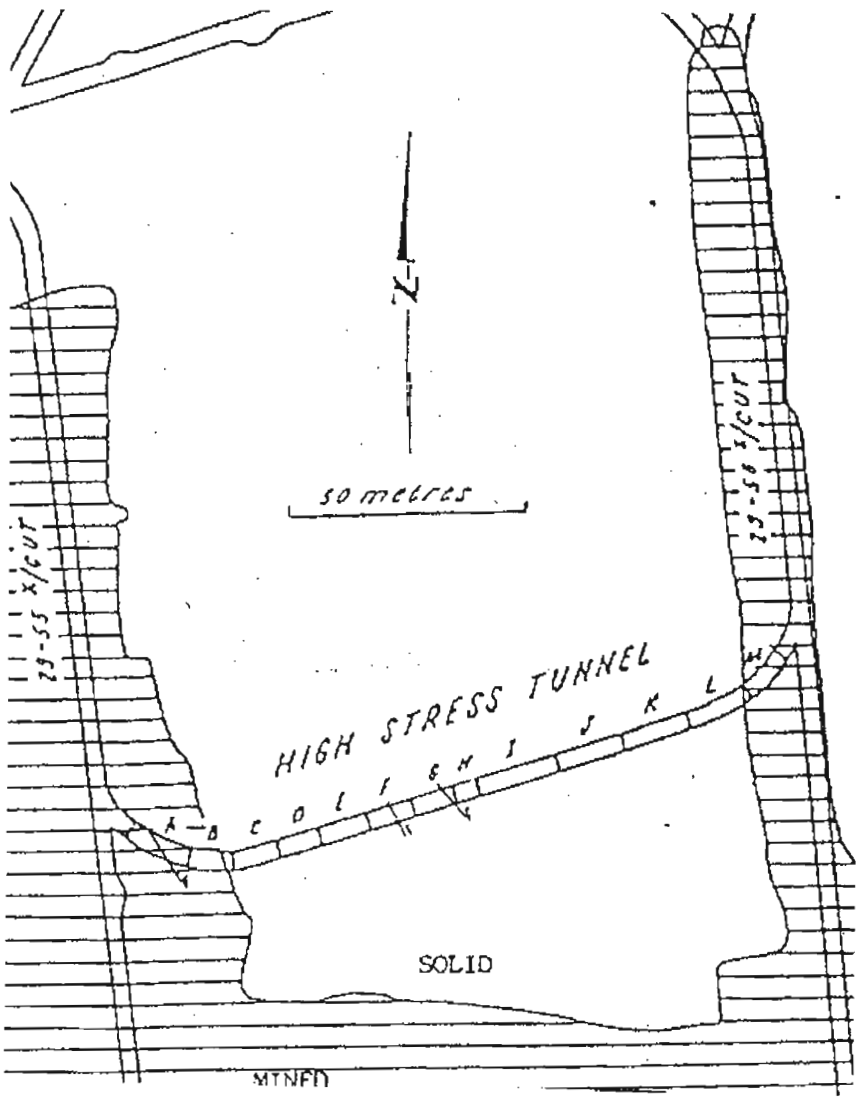

Figure 4-11. Detail of tunnel support sections (after Hepworth, 1985).

The primary support, installed under tunnel development consisted of 1.8 m split sets on a 2 m x 2 m pattern in the sidewalls and a 1 m x 1 m pattern in the hangingwall. These were installed to within 3 m of the face during the development cycle. The secondary support comprised of the support systems, as detailed in Table 4-1, installed approximately 30 m from the development face. The density of the support system is indicated in Table 4-2.

Table 4-1. Support installed in experimental tunnel (in addition to primary split sets) (Hepworth, 1985)

Section	Length	Description
A	11.5 m	3 m fully grouted, pre-tensioned, M20 rockstud in a 1.2 m x 1.5 m pattern in the tunnel roof. Mesh and lace attached to 2.2 m, 16 mm diameter fully grouted shepherds crook rebar.
B	14.1 m	As above but 1.8 m, pre-tensioned, M16 rockstuds in the roof.
C	9.7 m	Mesh and lace attached to 3 m fully grouted steel rope slings.
D	9.2 m	Mesh and lace attached to 2.2 m, 16 mm diameter fully grouted shepherd crook rebar and then shotcreted.
E	11.0 m	First shotcreted and then as above.
F	9.3 m	Shotcrete of approx. 50 mm thickness.
G	9.6 m	Shotcrete of approx. 30 mm thickness.
H	5.2 m	Shotcrete of approx. 30 mm thickness applied within 24 hours of excavation (not achieved).
I	17.8 m	Mesh and lace affixed to 2.2 m fully grouted M20 pig tail end threaded smooth bar which were integrated with primary split sets
J	14.7 m	Integrated split set support with mesh and lace affixed to pig tail end of 2.2 m fully grouted rebars.
K	14.9 m	Mesh and lace affixed to pig tail end of 2.2 m fully grouted rebar.
L	14.5 m	Mesh and lace affixed to pig tail end of 2.0 m grouted M20 smooth bar. No thread on bolt end. Bolt inside split set but not integrated.
M	8.2 m	3 m fully grouted, pre-tensioned, M20 rockstud in a 1.2 m x 1.5 m pattern in tunnel roof. Mesh and lace attached to 2.2 m, 16 mm diameter fully grouted shepherd crook rebar.

Table 4-2. Rock bolt density in experimental sections (Hepworth, 1985).

Section	Support	Tendon length (m)	Tendon density (unit/m^2)	Split set density (unit/m^2)	Total support density
A - roof	16 mm rebar	2.2	0.46	1.1	2.34 + m&l
	M20 rockstuds	3.0	0.78		
A - sidewall	16 mm rebar	2.2	0.81	0.55	1.36 + m&l
B - roof	16 mm rebar	2.2	0.35	1.1	2.02 + m&l
	M16 rockstuds	1.8	0.57		
B - sidewall	16 mm rebar	2.2	0.76	0.68	1.44 + m&l
C - roof	16 mm steel rope	3.0	0.34	1.0	1.34 + m&l
C - sidewall	16 mm steel rope	3.0	0.72	0.67	1.39 + m&l
D - roof	16 mm rebar	2.2	0.35	1.1	1.45 + s/c + m&l
D - sidewall	16 mm rebar	2.2	0.75	0.6	1.35 + s/c + m&l
E - roof	16 mm rebar	2.2	0.35	1.1	1.45 + s/c + m&l
E - sidewall	16 mm rebar	2.2	0.75	0.6	1.35 + s/c + m&l
F - roof				1.1	1.1 + s/c
F - sidewall				0.6	0.6 + s/c
G - roof				1.1	1.1 + s/c
G - sidewall				0.6	0.6 + s/c
H - roof				1.1	1.1 + s/c
H - sidewall				0.6	0.6 + s/c
I - roof	M20 smooth bar	2.2	0.41	0.58	0.99 + m&l
I - sidewall	M20 smooth bar	2.2	0.69	0.29	0.98 + m&l
J - roof	16 mm rebar	2.2	0.32	0.93	1.25 + m&l
J - sidewall	16 mm rebar	2.2	0.73	0.21	0.94 + m&l
K - roof	16 mm rebar	2.2	0.36	0.94	1.3 + m&l
K - sidewall	16 mm rebar	2.2	0.69	0.43	1.12 + m&l
L - roof	M20 smooth bar	2.0	0.37	0.92	1.29 + m&l
L - sidewall	M20 smooth bar	2.0	0.74	0.55	1.29 + m&l
M - roof	16 mm rebar	2.2	0.36	0.93	2.52 + m&l
	M20 rockstud	3.0	1.23		
M - sidewall	16 mm rebar	2.2	0.81	0.57	1.38 + m&l

The experimental tunnel was developed in argillaceous quartzite, with an average uniaxial compressive strength (UCS) of approximately 151 MPa. This quartzite rock mass includes bedding planes at approximately 0.4 m spacing, with a dip of 10°, parallel to the reef horizon. The intact rock has a modulus of 66 GPa and a Poisson's ratio of 0.21, as derived from laboratory testing. Virgin stress conditions in the near vicinity were determined from in situ Doorstopper strain gauge stress measurement cells and calculated to be

σ_1 = 67 MPa (30° off vertical in down dip direction)

σ_2 = 46 MPa (approximately orientated in the dip direction of the strata)

σ_3 = 31 MPa (approximately horizontal and oriented along strike)

The stress environment under which the tunnel was developed was subsequently estimated from numerical modelling based on elastic theory. The maximum principle stress is estimated to

range from 80 MPa to 100 MPa. Tunnel development under these conditions resulted in failure of the rock mass in the periphery of the tunnel as development proceeded.

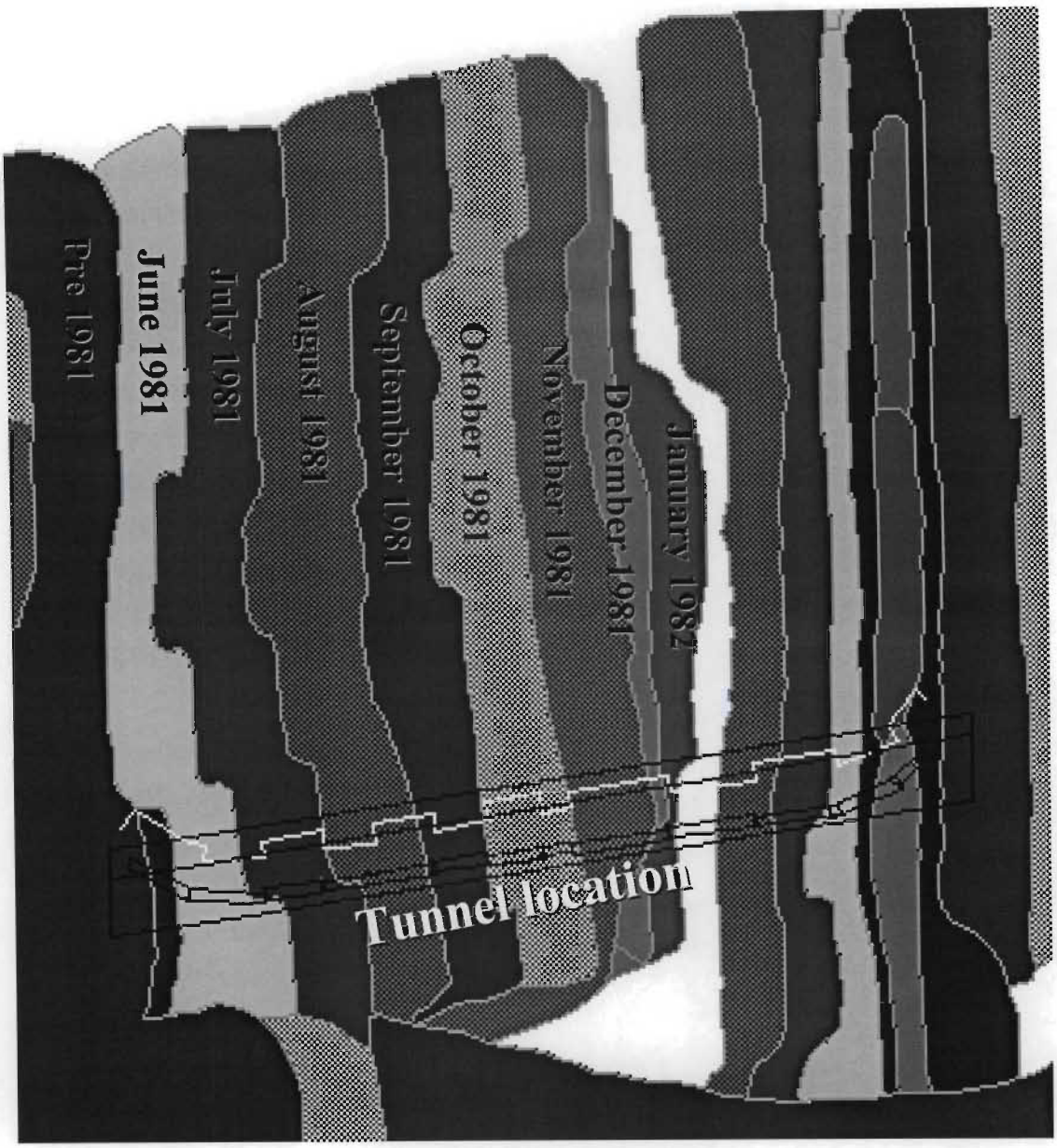

Figure 4-12. Details of mining sequence for experimental tunnel as modelled under the current investigation.

Hepworth's analysis was principally focused on a comparison of the deformation associated with the different support sections within the experimental tunnel. The following were general comments of the performance of the support sections as made by Hepworth (1984):

Up dip sidewall deformation - deformation in the majority of the support sections occurred between 2 m and 3 m into the sidewalls. The main exceptions were the shotcreted sections where the maximum deformation was between 0 m and 0.5 m and in the integrated split set sections where it was between 1 m and 2 m. The degree of sidewall deformation increased generally in relation to the maximum principal stress increase.

Down dip sidewall deformation - deformation again occurred at a depth of 2 m to 3 m for most of the support sections. The shotcreted sections again experienced maximum dilation at between 0 m and 0.5 m and the integrated split set support sections between 1 m and 2 m. In general the overall amount of dilation increases with the maximum principal stress increase.

Overall sidewall deformation of the up dip and down dip sidewalls indicated an overall increase of approximately 17 % in the dilation of the down dip sidewall, which was not considered to be of significance. However, a far larger number of support sections experienced maximum dilation between 0 m and 0.5 m in the down dip sidewall. An estimation of dilation greater than 3 m depth was made by subtracting the measured dilation within the rock mass, from the overall measured tunnel closure. This indicated that the amount of dilation deeper then 3 m generally increased in relation to the maximum principal stress increase plus was related to the support resistance.

Roof deformation - generally roof dilation occurred between 0 m and 2 m and again increased towards the central support sections of the tunnel. The maximum deformations were associated with the shotcrete and split set integrated support sections, where a significant amount of dilation occurred between 0 m and 1 m.

Footwall heave - footwall heave was experienced by some of the support sections. This resulted in a dip of the footwall parallel to the dip of the general stratigraphy.

In general, Hepworth considered that the amount of deformation of the tunnel could be related to the magnitude of increase in the maximum principle stress and that the stress decrease had no significant influence on the deformation. No correlation could be obtained between the duration of the peak stress level and the amount of deformation. No time dependency was associated with the fracture process.

The influence of the local stratigraphy was examined in regard to the differences in the dilation of the down dip and up dip sidewalls. It was observed that significant shearing occurred on bedding planes at the top of the down dip sidewall and bottom of the up dip sidewall. This mechanism was considered to be responsible for the observed footwall heave on the up dip side of the tunnel. In addition, it was considered by Hepworth that this strata geometry resulted in the confinement of the top section of the down dip sidewall. It was also noted that the down dip sidewall dilation responded more to the stress decrease than the up dip sidewall. This was considered to be a function of toppling of the sidewall parallel blocks.

Support performance - the need for yieldability in the support system was recognised. Hepworth considered that the increased yieldability of the tendon improves the confinement of the fracture zone within its depth of influence but generally results in lower confinement to the

deeper rock mass. The density of tendons within the sidewall of the tunnel sections was considered to directly influence the amount of dilation in the immediate skin of the tunnel but not greatly influence the overall amount of deformation. An evaluation of the influence of the fabric support indicated that the un-reinforced shotcrete was the least effective, and the shotcrete reinforced with mesh and lacing to be the most effective.

General conclusions made by Hepworth included:

- increased support yieldability and fabric "effectiveness" resulted in reduced overall deformation.
- no apparent benefit was derived from increasing the tendon length
- the influence of tendon density on overall deformation was inconclusive
- un-reinforced shotcrete was ineffective in controlling deformation and was considered to represent an additional hazard to worker safety.
- most deformation is associated with a stress increase.

4.3.2 Motivation for re-evaluation of Buffelsfontein experimental site

The purpose of further evaluation of this case study is to try to derive a more detailed understanding of the mechanisms of rock mass deformation around an excavation. The tunnel was subjected to a high initial and increasing vertical stress field, and a subsequent vertical stress reduction due to overstoping. The qualification of the deformation mechanisms was not considered by Hepworth, or in subsequent similar studies such as Laas (1995). In these investigations the performance of the support system was evaluated purely on the dilation or total deformation. An understanding of the deformation mechanisms under the conditions of the complex stress environment, associated with overstoping, is considered critical to the ability to assess the relative performance of the support systems in controlling the respective deformation processes.

In order to try and simplify the analysis process, and derive deformation mechanisms, the analysis is based on the stress magnitudes in the vertical (z) and two horizontal (x and y) axis's. These are orientated approximately parallel and perpendicular to the experimental tunnel axis. This also corresponded closely with the initial principal stress directions. The analysis of the relative magnitude of these stress components will also, simplistically capture the period of change in orientation of the maximum principal stress. The most significant change in principal stress was the change in orientation of the maximum principal stress. The orientation of which changed from sub-vertical to sub-horizontal in the plane of the tunnel axis. For this analysis it was considered that this change in principal stress direction would be adequately captured by analysis of the vertical and horizontal stress components in the plane of the tunnel axis.

4.3.3 Analysis of deformation mechanisms

In the analysis of the deformation mechanisms it is the relationship between the changing rock mass environment, principally as a function of the stress changes, and the associated excavation response, with regard to the location of dilation, which is considered to be of primary importance. This initial analysis is conducted for all the test sections, with limited regard to the support type at this point as this may be considered to only influence the relative magnitude of the response but not fundamentally influence the deformation mechanisms.

A rough estimation of the depth of major sidewall deformation in excess of 3 m, as a function of the maximum vertical stress, was conducted. This was done by comparison between the amount of total sidewall deformation for each section and a summation of the sidewall dilation of the first 3 m of rock mass. The difference is plotted against the peak principal stress level, as shown in Figure 4-13. This analysis indicates that major deformation of the rock mass at depths greater than 3 m, as a function of a peak stress level, occurs in excess of a vertical stress of approximately 110 MPa. This is further analysed on the basis of the estimated maximum tangential stress for an equivalent circular excavation normalised to the average UCS of the rock type (see section 4.2), shown in Figure 4-14. This shows that a ratio of the tangential stress / UCS of approximately 1.9 would define a depth of instability of 3 m.

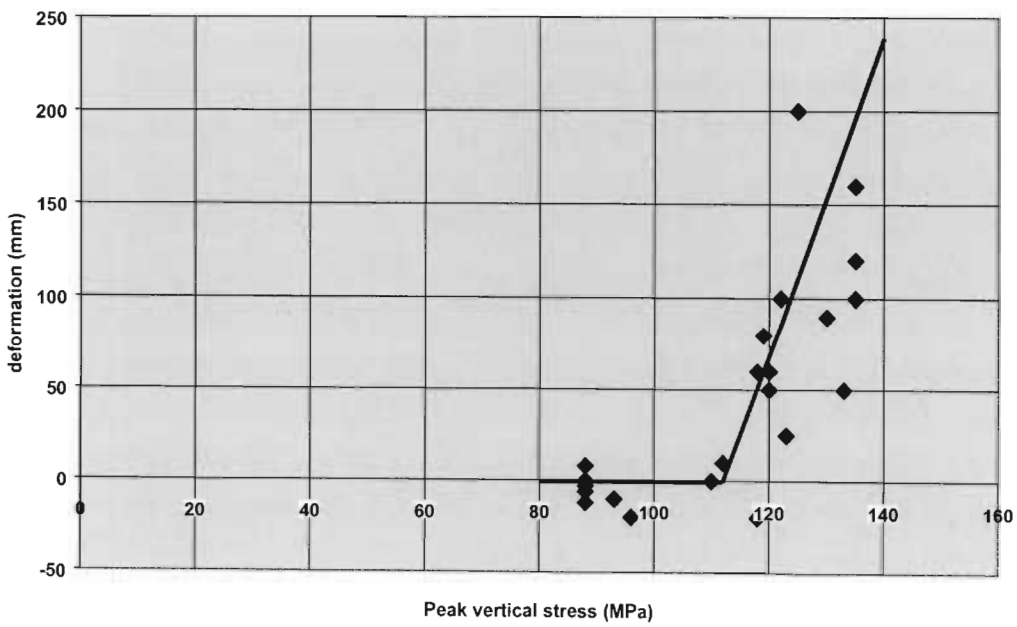

Figure 4-13. Relationship between peak vertical field stress and amount of deformation in excess of 3 m for Buffelsfontein experimental tunnel sections.

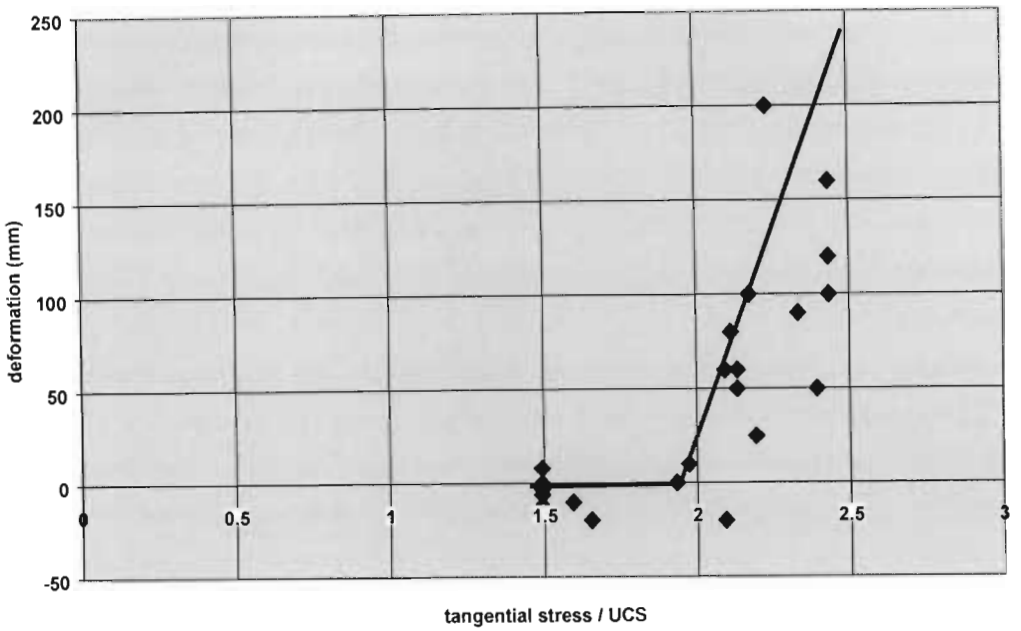

Figure 4-13. Relationship between ratio of peak tangential stress on sidewall of the excavation to the UCS of the rock, against deformation located in excess of 3 m depth for tunnel sections.

This relationship was compared with that proposed by Martin *et al* (1997), as shown in Figure 4-5. The stress levels to which the experimental tunnel was subjected, and those to which many tunnels on South African gold mines are subjected, greatly exceed the limit of Martin's data range, and thus his criterion. The linear fit of Martin's data would indicate that at a maximum tangential stress to UCS ratio of 1.9 an expected depth of instability, as a function of the excavation equivalent radius, would be approximately two times the equivalent radius, i.e. a depth of 5 m into the tunnel sidewall.

A depth of significant inelastic deformation, which is considered to be representative of the limit of instability, of 3 m, would equate to a radius of failure 2.1 times the equivalent excavation radius (equation 4-3). If this is compared to the envelope fitted to Martin's data, as shown in Figure 4-15, conducted in section 4.2 then a good correlation is obtained. In this analysis it has been assumed that the performance of the support system in the tunnel sections does not significantly influence the depth of unsupported rock instability.

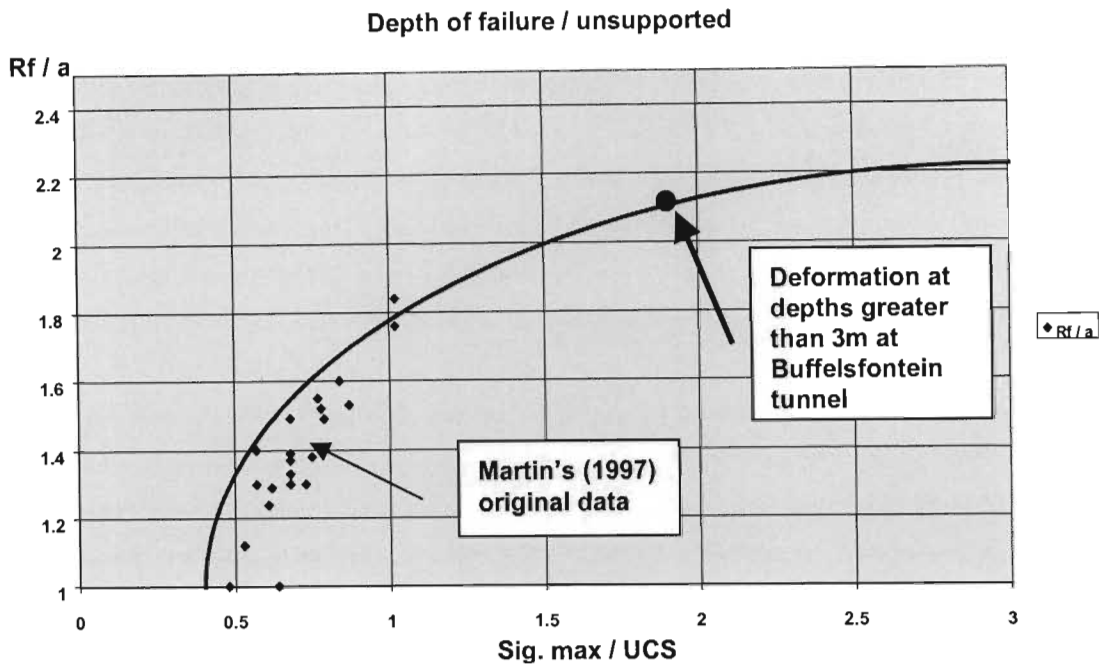

Figure 4-14. Extrapolation of Martin *et al* (1997) data for deformation at depths greater than 3 m for the Buffelsfontein experimental tunnel.

Hepworth's analysis and thus this evaluation of the deformation mechanisms are based on the prevailing rock mass structure and anticipated stress induced fracture orientations for this particular site. Therefore, the application of the proposed deformation mechanisms to other geotechnical sites must be considered with regard to its rock mass structure.

Analysis of the relationship between the vertical stress increase and deformation of the sidewall, for tunnel sections between A and I (Figure 4-11) indicated a linear correlation (Figure 4-17). The mechanism of this deformation is generally well understood, and considered to be a function of both the elastic and inelastic deformation of the rock mass into the excavation. Elastic deformation will be a function of compression of the sidewall rock mass and horizontal expansion due to Poisson's ratio into the excavation. This mechanism, however, represents only a small fraction of the typical displacements observed in deep level tunnels. In addition, and particularly in this environment where the tangential stress on the sidewall of the excavation is well in excess of the UCS, the development of a fracture zone in the tunnel sidewall, and associated dilation of the rock mass under failure, will account for most of the deformation. This second mechanism will dominate the behaviour of the sidewall in this stress environment and result in sidewall deformation proportional to the stress increase. The mechanism of increasing vertical stress is shown in Figure 4-16.

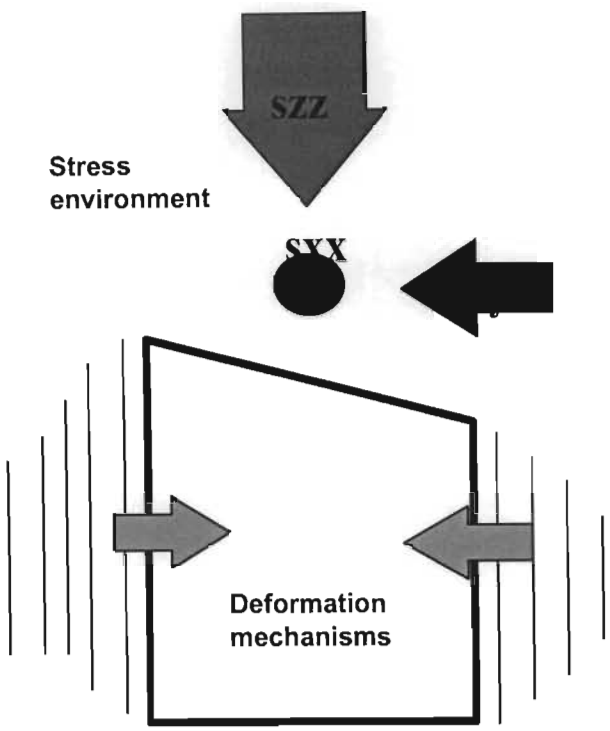

Figure 4-16. Tunnel sidewall deformation as a function of a high vertical stress component.

The analysis of the tunnel sections also indicated a relative increase in the vertical stress component compared to the horizontal stress components. This is also considered to marginally increase the degree of sidewall failure and deformation, and is supported by failure criteria as utilised to determine the extent of instability (equations 4-2 and 4-4).

In both of the criteria, the relative increase in the maximum principle stress (σ_1), which in this investigation corresponds closely to the vertical stress component, is dominant on the anticipated degree of instability. However, in some of the tunnel support sections, particularly at the peak stress level, where small absolute changes in the vertical and maximum principal stress magnitude are indicated, relatively large deformations occur (Figure 4-17). The analysis period of stress change, on a monthly basis, may also potentially miss the peak induced stress level as experienced in situ, and thus give a poor correlation of deformation over this period on this hypothesis, as illustrated in Figure4-17.

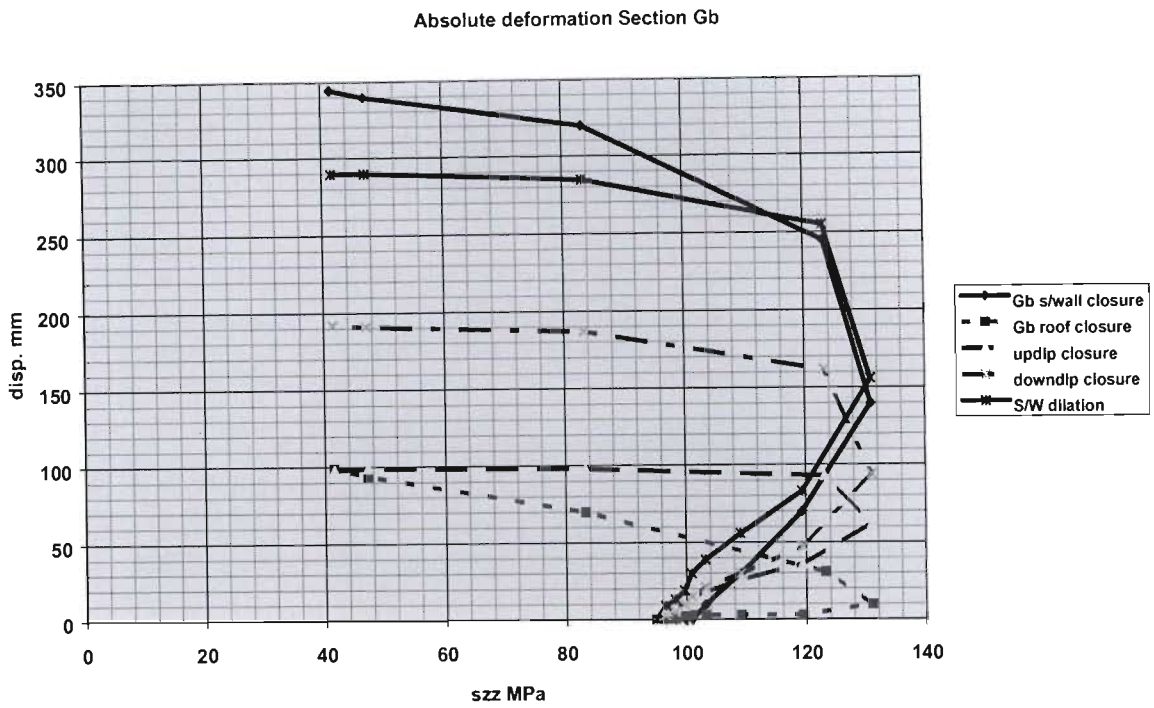

Figure 4-17. Example of poor correlation, based on current hypotheses, between sidewall closure and vertical stress over the period of the peak stress level.

A further explanation, which is explored later, may be that over this period there is a large relative increase in the vertical stress component compared to the horizontal stress components (sections E to I, Figure 4-11). This may be a function of a change in the orientation of the principal stress as expressed by the relative change between the vertical and horizontal stress components.

The location of deformation in the tunnel sidewall during this period of vertical stress increase is associated, to some extent, with all depths in the rock mass. In general it is anticipated that the development of the fracture zone at depth will also result in further dilation of the rock mass in the skin of the excavation expressed as differential deformation across the sidewall profile. It is generally considered that the primary deformation mechanism of the sidewall under this loading environment is dilational. However, the lateral loading of the rock mass at the skin of the excavation, due to the deeper failure process, may also result in relative shear of blocks within the immediate skin of the excavation.

In this stress environment and with the proposed sidewall deformation mechanism, hangingwall deformation would not be anticipated unless the tangential horizontal stress component perpendicular to the tunnel axis was of sufficient magnitude to induce failure or minor slip on bedding planes. In the analysis of the tunnel sections, particularly from A to I (Figure 4-11), there is very limited deformation associated with the tunnel hangingwall strata during the period of vertical stress increase.

However, in some sections, particularly sections J to M, hangingwall deformation is associated with periods of increasing, or stable, vertical stress fields. The proposed mechanism of hangingwall deformation for these sections, and also, but to a lesser extent in the other sections, is a relative increase in one of the horizontal stress components. This may be particularly relevant when considering the horizontal stress component perpendicular to the tunnel axis. This increase, absolute or relative, in the horizontal stress components is considered to result in localised deformation of the hangingwall strata, particularly due to shearing on existing discontinuities. This mechanism may be particularly prevalent within the induced vertical tensile zone in the immediate hangingwall of the excavation. Reference to the location of hangingwall deformation associated with these tunnel sections indicates most of the dilation to be in the immediate hangingwall rock mass (approximately 0.5m). This mechanism is illustrated in Figure 4-18 and an example of the relative stress histories and its correlation to hangingwall deformation is shown in Figure 4-19. The mechanism of changes in the horizontal stress components relative to a stable vertical stress, and maximum principle stress, may also result in minor deformations associated with the sidewalls of the excavation. These deformations were observed in sections L and M.

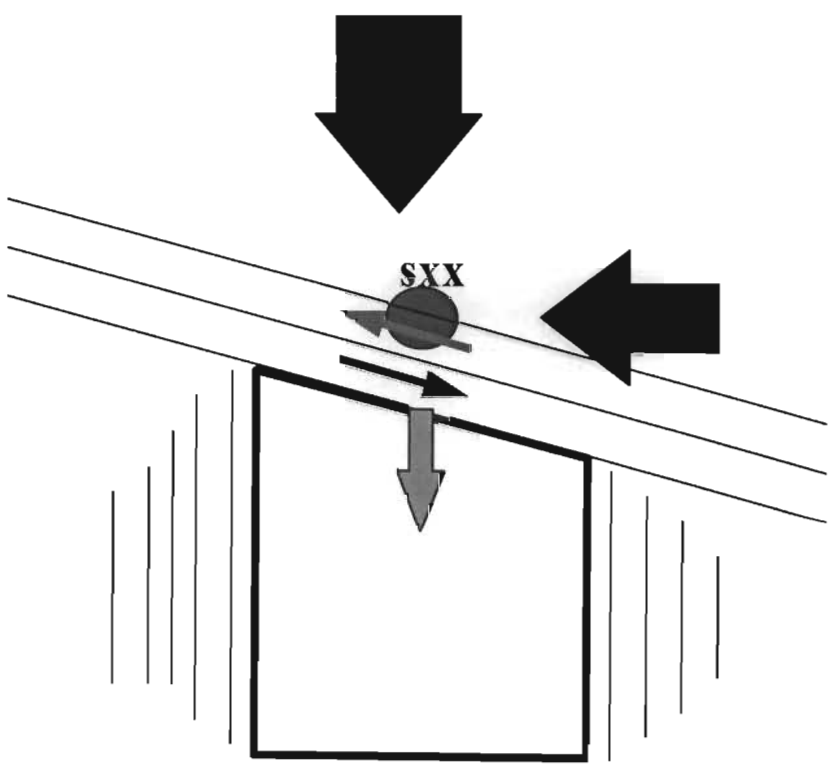

Figure 4-18. Proposed mechanism of minor hangingwall deformation with high vertical stress regime.

In the majority of the tunnel sections it is significant that the major component of hangingwall deformation occurs during vertical stress reduction. Analysis of the relationship between the

vertical stress reduction and hangingwall deformation generally shows a linear correlation, particularly for the initial periods. Numerical modelling of the relative changes in the magnitude of the field stress components shows that the drop in the vertical stress, due to overstoping, is not accompanied by a significant reduction in the horizontal stress. It is also noted that a significant amount of sidewall deformation may also be associated with this period.

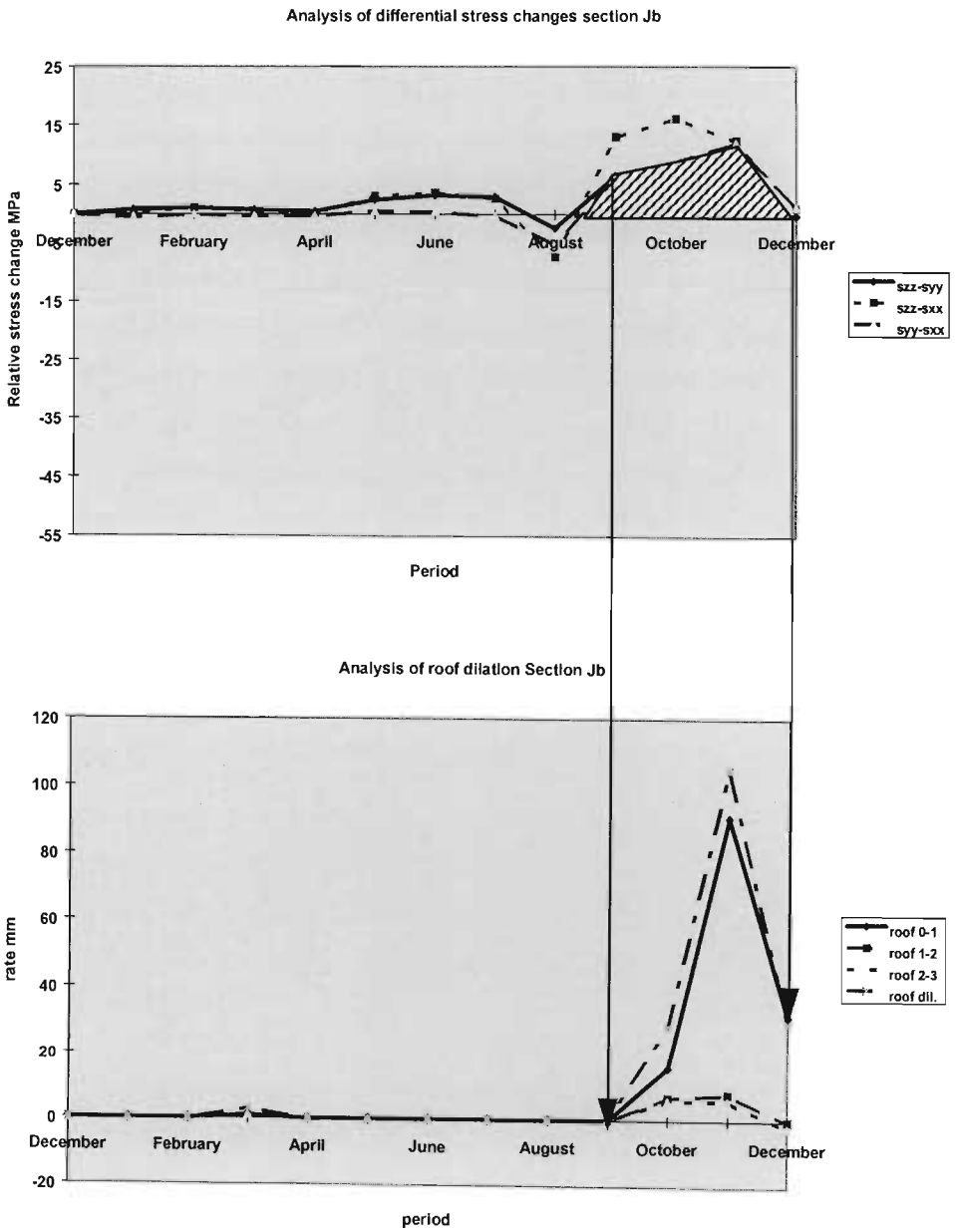

Figure 4-19. Correlation between relative change in horizontal stress components and hangingwall deformation section Jb.

As discussed above, hangingwall deformation is generally associated with a period of significant vertical stress reduction due to overstoping. The proposed mechanism of deformation is that the reduction in the clamping stresses on the bedding planes, or sub-horizontal discontinuities such

as hangingwall fracturing, results in freedom for shear movement due to the horizontal stress component, and thus dilation of the hangingwall. This dilation of the hangingwall rock mass may also occur over the relatively soft sidewall fracture zone, resulting in shear movement and wedging within the sidewall rock mass, particularly under lower lateral confinement. These deformation mechanisms are illustrated in Figure 4-20 and may also be attributed to footwall dilation. This will compound the sidewall deformation. The deformation mechanism may be restricted to the initial phase of vertical stress reduction only, due to build up of shear resistance within the rock mass as a function of support.

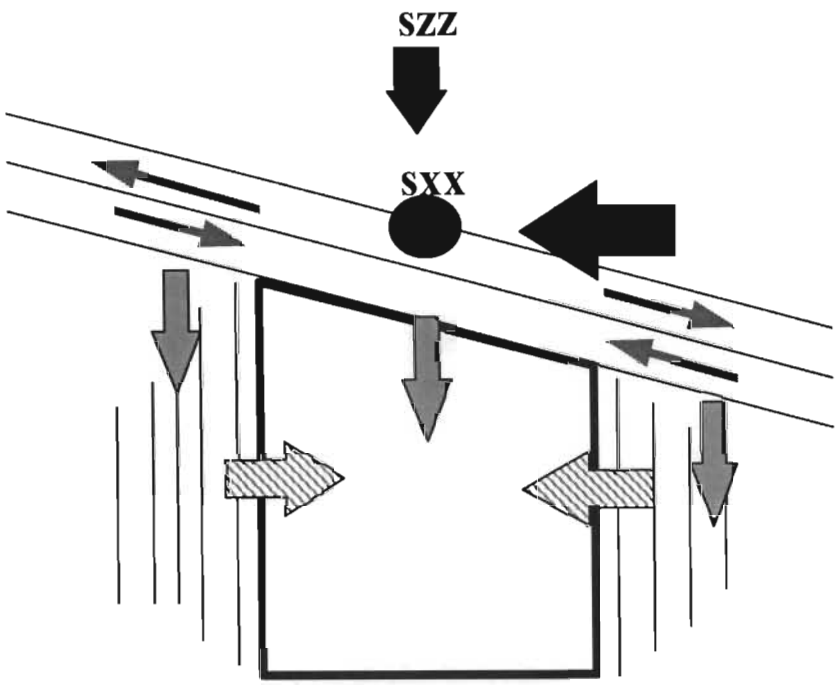

Figure 4-20. Proposed mechanism of hangingwall and sidewall deformation under vertical stress reduction.

In an excavation with a fairly marked lean-to profile, that is developed with an inclined parting plane representing the hangingwall contact, the up dip sidewall height is greater than the down dip. Thus for a given amount of hangingwall deformation, as proposed in Figure 4-20, over the fracture zone, the down dip sidewall will experience greater compressional strain than the up dip. This is envisaged to result in increased down dip sidewall deformation under these conditions. This increased deformation associated with the down dip sidewall was commented upon by Hepworth (1985) and Laas (1995), but was considered to be insignificant with regard to the accuracy of measurements. The relative importance of this mechanism may be a function of the geotechnical environment. Tunnel environments with relatively shallow dipping parting planes, which is the case with both of the above studies, may result in limited differences in the deformation of the two sidewalls. However, this factor may be of more significance in geotechnical environments where the dip of the strata is steeper, with a greater difference in height of the two sidewalls.

These proposed deformation mechanisms may be validated by numerical modelling.

4.3.3.1 Numerical modelling of deformation mechanisms

The proposed mechanisms of rock mass deformation in the vicinity of a square tunnel were investigated further by numerical modelling using the Universal Distinct Element Code (UDEC, Anon., 1996b). This is code allows for the failure of predefined planes of weakness within the medium (rock mass) and the formation of discrete blocks. This is considered suitable for the analysis of the deformation mechanisms, particularly those associated with the hangingwall of the excavation. The model was constructed to capture the formation of discrete blocks by failure of the intact rock and interaction of these 'fractures' with pre-existing bedding planes. The intact rock mass was represented by elastic blocks defined by planes of weakness orientated at 0°, 30°, 60°, 90°, 120°, 150° from the positive x axis. Properties of intact rock cohesion (29e6 Pa), tension (3e6 Pa), friction (45°) and dilation (25°) were attributed to these planes. The bedding planes, orientated at 30° from the positive x axis, represented additional planes of weakness within the elastic rock mass with much lower cohesion (1e6 Pa), Tension (0e6 Pa), friction (35°) and dilation (10°). As the mechanisms of deformation are the primary concern of this aspect of the investigation the modelling of support units was excluded.

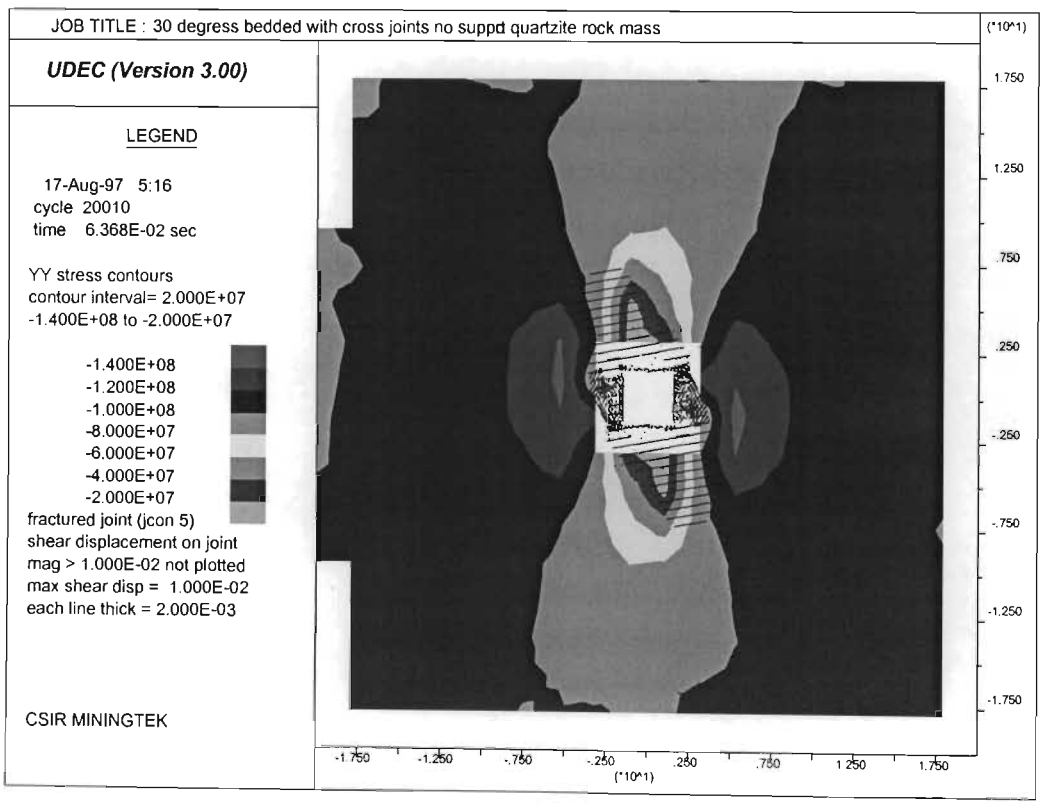

Figure 4-21. Numerical modelling plot of the vertical stress field and rock mass failure around a square tunnel in a stress field of 100 MPa vertical and 50 MPa horizontal.

Figure 4-21 shows the vertical stress field in the vicinity of the tunnel and the initial extent of rock mass failure (dark lines) around the excavation due to the initial stress field of 100 MPa vertical and 50 MPa horizontal. The development of the fracture zone in the sidewall of the tunnel and the corresponding dilation of the rock mass into the excavation are more clearly illustrated in Figure 4-22.

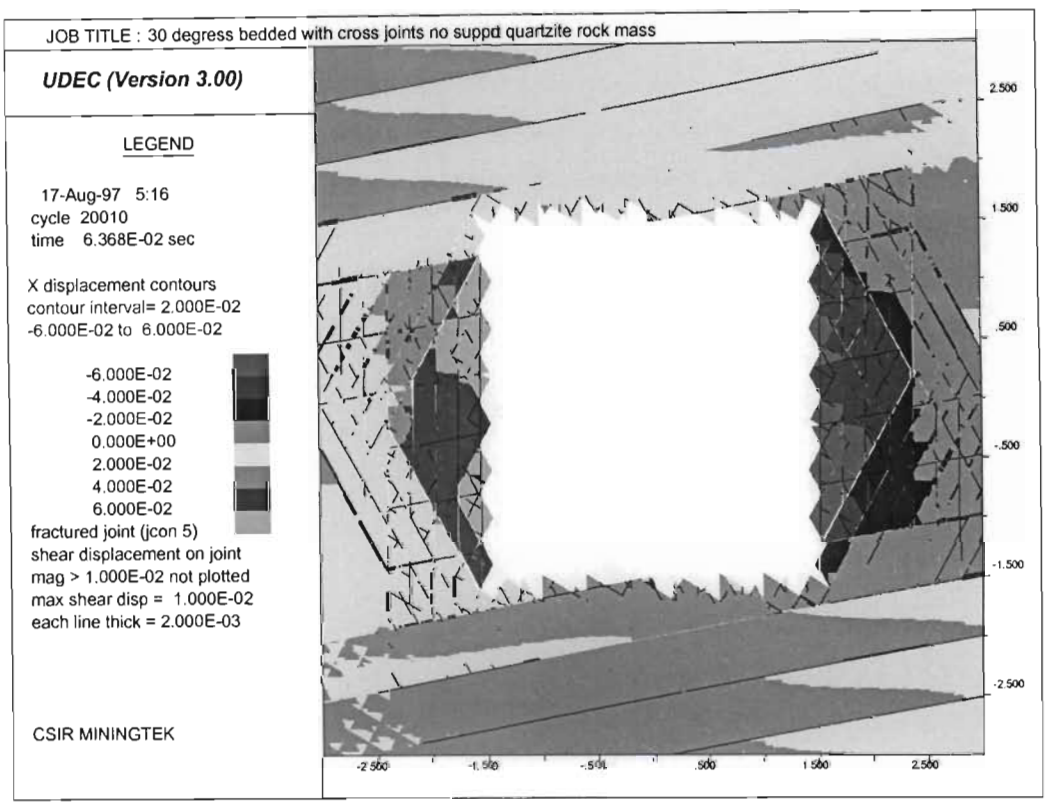

Figure 4-22. Numerical modelling plot of the failure of discontinuities in the rock mass medium and the associated x-direction displacement of the rock mass for the initial stress field.

Analysis of Figure 4-22 indicates, for the defined rock mass properties that the depth of failure within the sidewall, due to fracturing of the intact rock material is to a depth of approximately 2.5 m. This results in a maximum sidewall displacement (elastic and inelastic) of between 6 cm and 8 cm. It is noted that there is no indication of differential x-displacement indicative of shear in the hangingwall or footwall of the tunnel.

Figure 4-23 shows the y direction displacement around the tunnel excavation in relation to the illustrated failure within the rock mass structure. The vertical displacement contours within the hangingwall and footwall of the tunnel are indicative of principally elastic relaxation of the rock mass. Vertical displacement within the hanging- and footwall is of the order of 3 cm.

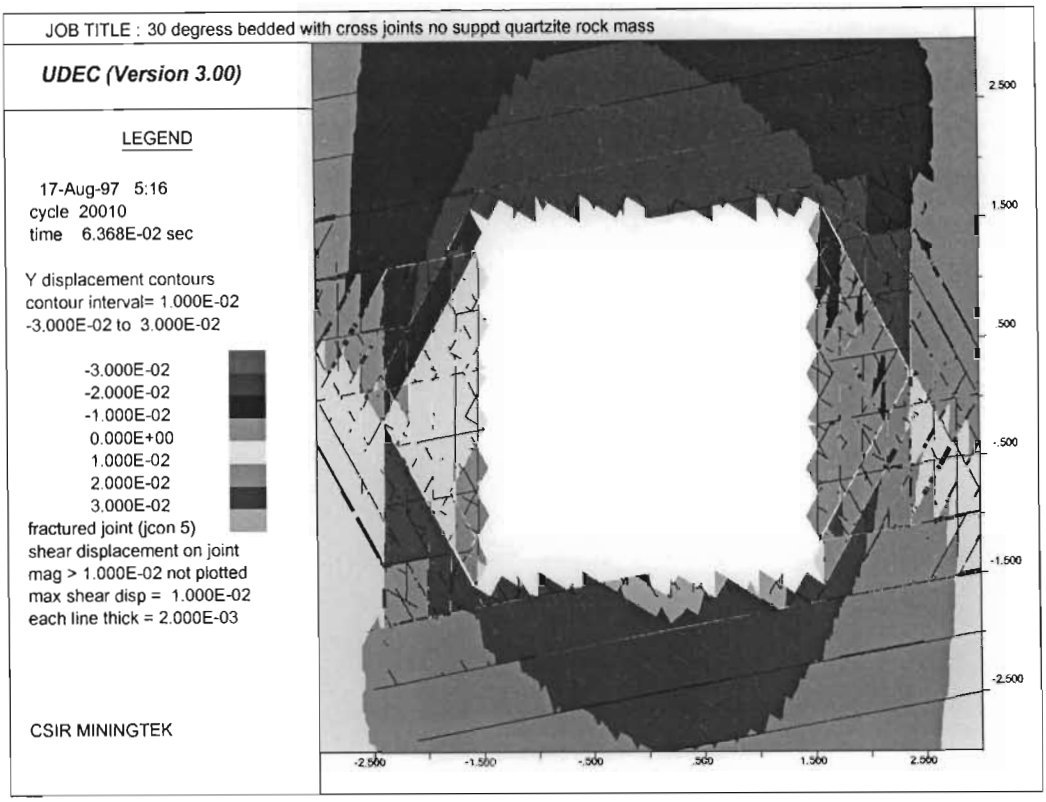

Figure 4-23. Numerical modelling plot of the failure of discontinuities in the rock mass medium and the associated y-direction displacement of the rock mass for the initial stress field.

In Figure 4-23 differential y-direction displacement is shown within the simulated fracture zone in the sidewalls of the tunnel. This may be indicative of shear deformation within the rock mass at this location.

The mechanisms illustrated by the numerical model would confirm the observations and analysis of the data from the in situ experiment. Of importance is the lack of deformation associated with the hangingwall of the tunnel under these conditions.

Subsequent to the stabilisation (numerical) of the model under the defined initial stress state the field (boundary) stresses were relaxed in the vertical and horizontal directions to simulate the overstoping of the tunnel, typical of that for the in situ experimental tunnel. The field stresses were thus relaxed to a state of 5 MPa vertical stress and 30 MPa horizontal stress. This stress state represents a large increase in the horizontal stress component relative to the vertical. The following Figures are used to illustrate the mechanisms of rock mass deformation associated with this change in the stress state.

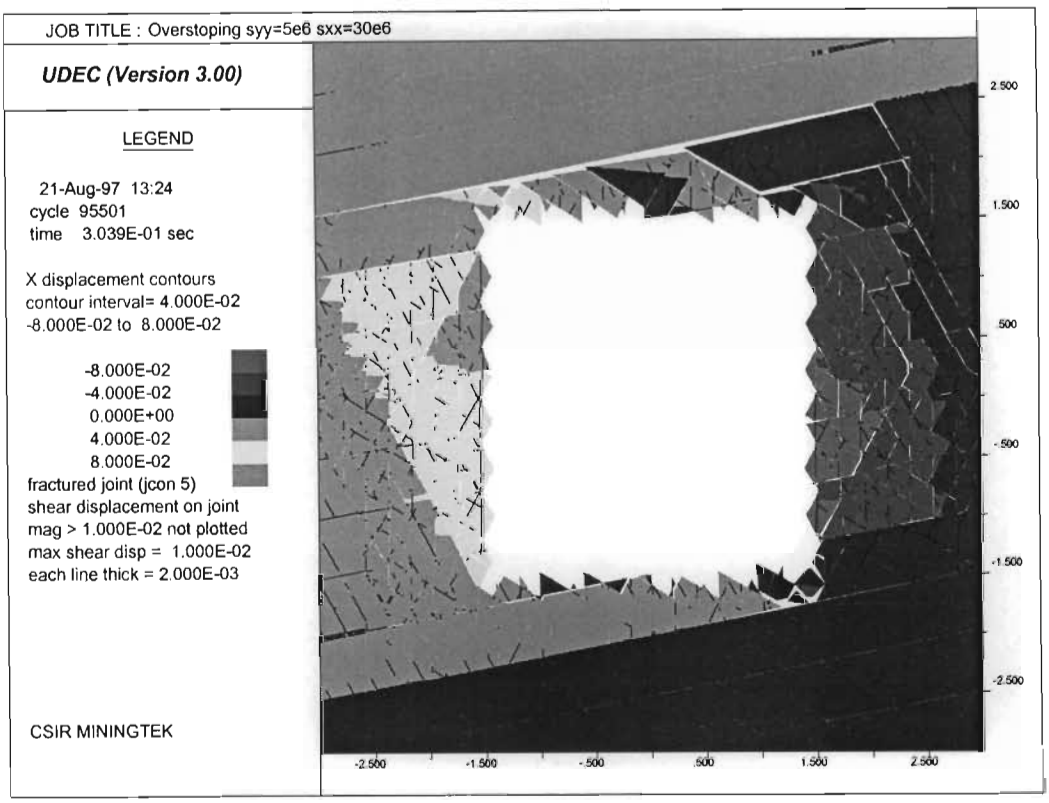

Figure 4-24. Numerical modelling plot of the failure of discontinuities in the rock mass medium and the associated x direction displacement of the rock mass for the overstoped stress state.

Figure 4-24 shows an increase in the general failure of the rock mass structure due to the stress reduction. Of significance, with regard to the analysis of the x-direction displacement, is the large differential deformation within the hangingwall of the tunnel. This is indicative of large shear deformations associated with the immediate hangingwall rock mass and confirmation of the proposed deformation mechanisms derived from the analysis of the in situ data. It is also illustrated in Figure 4-24 that increased deformation of the sidewall of the tunnel, of the order of approximately 2 cm is also associated with the vertical stress reduction.

Numerical analysis of the y-direction displacement shown in Figure 4-25 confirms the large scale deformation, and instability of the hangingwall of the tunnel. The separation of the immediate hangingwall blocks from the bulk of the rock mass is also illustrated in Figures 4-24 and 4-25, and ultimate collapse will result in the absence of support systems.

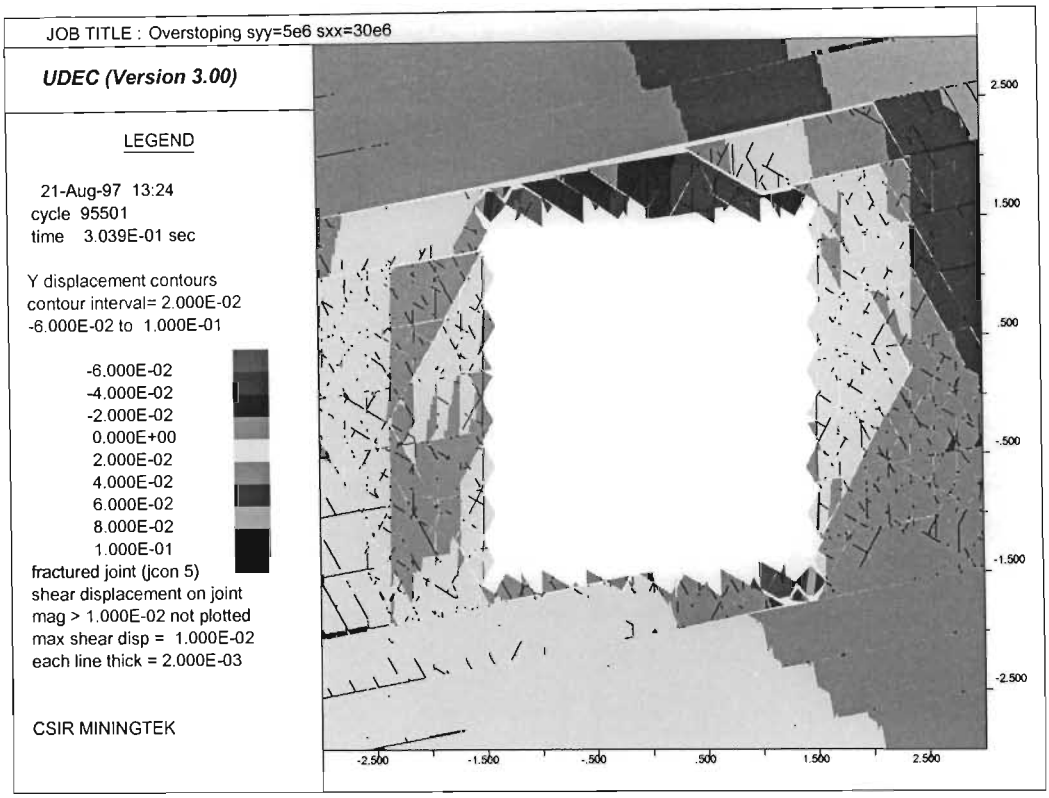

Figure 4-25. Numerical modelling plot of the failure of discontinuities in the rock mass medium and the associated y-direction displacement of the rock mass for the overstoped stress state.

It is considered that this numerical analysis confirms the general mechanisms of rock mass behaviour defined for the geotechnical environment, which is typical of the deep level South African gold mines. The understanding of the deformation mechanisms is an important consideration in the performance characteristics of the support systems that will be implemented to ensure the stability of the excavation. Chapter 5 of this document examines the performance of typical rock bolts under shear deformation. This aspect of design is not generally considered in the current design procedures but has been shown in this analysis to be an important mechanism of rock mass deformation, particularly under conditions of overstoping.

4.3.4 Analysis of support performance

An important component of the evaluation of support performance is the mechanisms of deformation. This will enable an assessment of the relative influence of the support systems on the modes of rock mass deformation. The above analysis (section 4.3.3), has indicated the importance of shear in the quasi static, and dynamic, deformation of a tunnel, particularly in overstoping conditions; this has not previously been considered, especially with regard to the design of support systems in the deep level gold mining environment.

As discussed previously the majority of the tunnel support sections analysed by Hepworth (1985) were located in a stress environment in which the extent of significant sidewall deformation, and thus potentially the extent of instability, were in excess of the support length. It is thus considered that the support stabilisation mechanism was not one of containment, as is the typical support design methodology on the South African gold mines, but rather of reinforcement of a discontinuous rock mass to create a stable structure. In the majority of the tunnel sections it is therefore not the direct characteristics of the support units that will influence the deformation of the excavation, but rather their interaction with the rock mass to create a reinforced rock mass structure. The characteristics of the reinforced rock mass structure will thus govern the degree of rock mass deformation and relative stability of the excavation.

The deformation rates with respect to the vertical stress component, derived from Hepworth's data as part of this investigation are given in Table 4-3.

Table 4-3. Summary of tunnel deformation rates with respect to the vertical stress component.

	H/W dil.		S/W up dip dil.		S/W dn dip dil.		S/W total dil.		S/W closure	
Sect.	(-MPa)	(+MPa)	(+MPa)	(-MPa)	(+MPa)	(-MPa)	(+MPa)	(-MPa)	(+MPa)	(-MPa)
Aa	0.3	0.3	6	0					8.3	0.35
Ab	0.1	0.64	2.5	0	8	0.25	10.5	0.25		
Ba	0.5	0.3	2.5	0.25	5	0.4	7.5	0.65	6.5	0.8
Bb	0.6	0.2	2.8	0	6.4	0.46	9.2	0.46		
Ca	0.54	0.3	3.3	0.16	5	0.06	8.3	0.22	10	0.9
Cb	0.3	0.3			1.8	0.07				
Da	0.3	0.39	2	0	2	0	4	0	4.4	0.44
Ea	0.22	0.25	1.2	0.08	0.67	0.04	1.87	0.12		
Eb	0.11	0.25	2	0	2	0	4	0	4	0.73
Fa	0.26	0.4	2.2	0.2	2.2	0.2	4.4	0.4		0.28
Fb	0.73	0.77	3.3	0.25	2.6	0	5.9	0.25	6.9	0.7
Ga	0.5	0.33	1.33	0	3.3	0	4.63	0		
Gb	1	0.29	1.76	0	2.8	0.4	4.56	0.4	4.7	1.25
Ha	1.2	0.59	2.8	0.33	1.6	0.33	4.4	0.66	4.4	1.7
Ia	1	1.25	1.5	0	0.88	0	2.38	0		
Ib			1.25	0.4	1.25	0.4	2.5	0.8	3.25	1.5
Ic	2.5	0.47	1.6	0.63	1.6	0.63	3.2	1.26		

Sections A and B, and J to M experienced minimal deformation in excess of a depth of 3 m in the sidewall of the excavation. Sections A and B were found to have abnormally high deformation rates, particularly associated with the down dip sidewall. In these sections Hepworth also commented that extremely poor ground conditions were experienced in the tunnel under development, and difficulty was experienced in the installation of instrumentation in these sections. In addition numerous failures of the Split Set support system were observed. It is considered that problems may have been experienced with these tunnel sections, and particularly the down dip sidewalls, due to the proximity of the original 29-55 cross cut (Figure 4-

11). The proximity of an adjacent tunnel would also apply to section M, but the lower general stress field would result in a lower level of induced stress and thus reduced damage potential. The use of these sections in further analysis was therefore generally excluded.

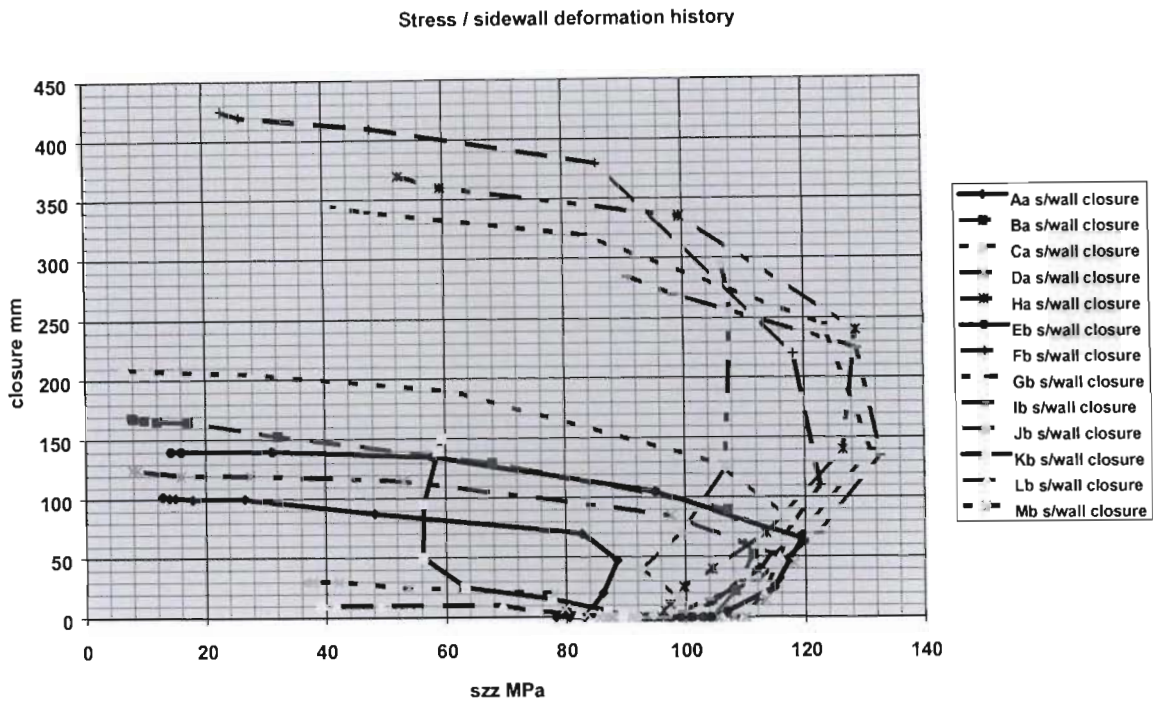

Figure 4-26. Summary of sidewall deformation with respect to the vertical stress component.

There is a marked difference in the deformation characteristics of the overall sidewall deformation rates with respect to the vertical stress component as shown in Figure 4-26. Figure 4-26 (and Figure 4-27) is a plot of the total deformation history of the sidewall (hangingwall) of the tunnel section with respect to the vertical stress at that time. From this data it is possible to subdivide the sections into two groups. The one group, which represents the lower stress environments, and comprises sections A to E and K to M, has a relatively linear relationship between the vertical stress changes and total deformation. The second group, comprising sections F to J, experiences generally higher stress environments, and also relatively large changes in the horizontal stress components and shows poor correlation with respect to vertical stress change only. The rate of overall deformation associated with vertical stress increase does not appear to be strongly influenced by the support system (Figure 4-26). This relatively large variability in the in situ measurements would however be anticipated for a highly variable, and complex, rock mass environment. It is also shown in Figure 4-26 that there is continued deformation of the sidewall during the period of vertical stress reduction. This appears to be approximately linear, but again is difficult to determine if there is significant influence of the support system on this deformation rate.

Analysis of hangingwall deformation with respect to the vertical stress component clearly shows that most of the deformation is associated with periods of vertical stress decrease (Figure 4-27). Again high deformation of the hangingwall is associated with sections F to K over the period of peak stress level, which is also associated with large changes in the horizontal stress components.

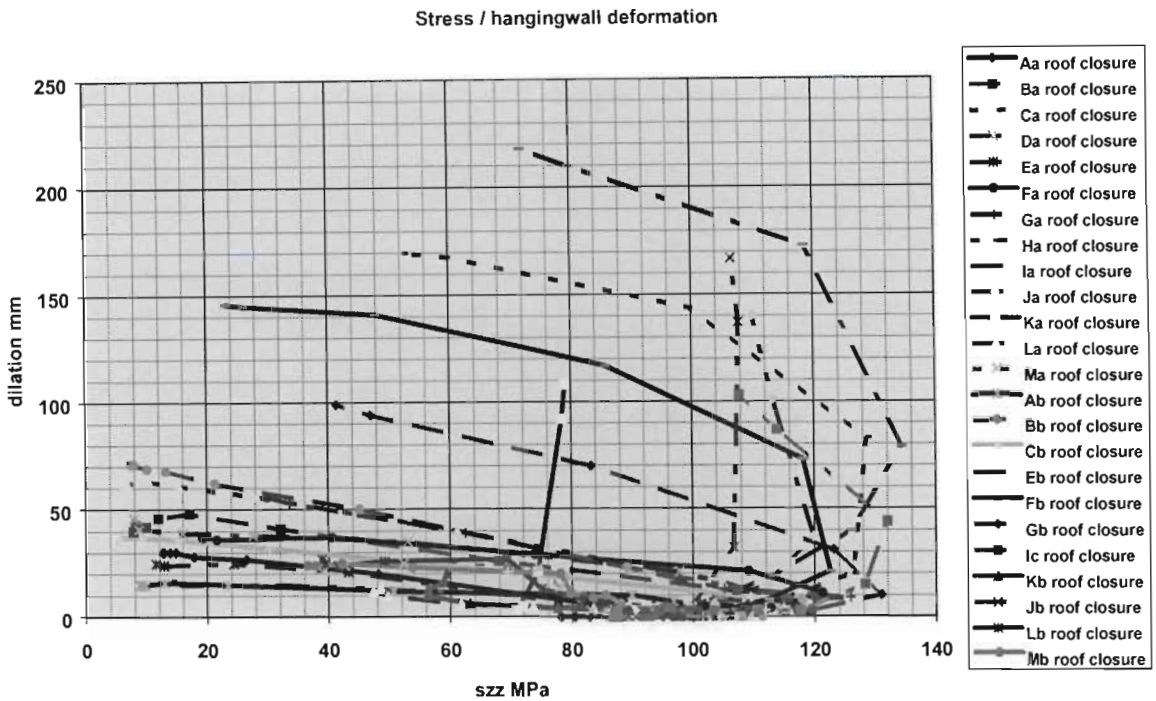

Figure 4-27. Summary of hangingwall deformation with respect to the vertical stress component

The overall rate of hangingwall deformation with respect to the vertical stress component appears to be influenced by the support system. However, section J and K indicate poor correlation between the hangingwall deformation and the vertical stress change associated with these sections. This is considered to be a function of significant changes in the horizontal stress components, relative to each other and the vertical stress, under a fairly constant vertical stress field, as discussed in section 4.3.3.

Using the above analysis the general influence of the characteristics of the individual support systems were evaluated. The determined support system characteristics, specifically with regard to the rock bolt reinforcement, are given in Table 4-4. The influence of the fabric support type has not been considered at this point, as its characteristics are currently not incorporated into the selected design parameters of support resistance, support density and shear stiffness.

Table 4-4. Characteristics for rock bolt reinforcement in tunnel sections.

Section	Suppt resis.		Suppt dens.		Support shear stiffness (N/m)				
	H/W	S/W	H/W	S/W	primary	secondary	tertiary	total H/W	total S/W
Aa	271	133	2.3	1.4	3.40E+06	4.20E+06	3.50E+06	8402000	5272000
Ab	271	133	2.3	1.4	3.40E+06	4.20E+06	3.50E+06	8402000	5272000
Ba	163	132	2	1.4	3.40E+06	4.20E+06	3.50E+06	7205000	5504000
Bb	163	132	2	1.4	3.40E+06	4.20E+06	3.50E+06	7205000	5504000
Ca	101	141	1.3	1.4	3.40E+06	5.80E+06		5372000	6454000
Cb	101	141	1.3	1.4	3.40E+06	5.80E+06		5372000	6454000
Da	100	127	1.4	1.3	3.40E+06	4.20E+06	shotcrete	5210000	5190000
Ea	100	127	1.4	1.3	3.40E+06	4.20E+06	shotcrete	5210000	5190000
Eb	100	127	1.4	1.3	3.40E+06	4.20E+06	shotcrete	5210000	5190000
Fa	55	30	1.1	0.6	3.40E+06		shotcrete	3740000	2040000
Fb	55	30	1.1	0.6	3.40E+06		shotcrete	3740000	2040000
Ga	55	30	1.1	0.6	3.40E+06		shotcrete	3740000	2040000
Gb	55	30	1.1	0.6	3.40E+06		shotcrete	3740000	2040000
Ha	55	30	1.1	0.6	3.40E+06		shotcrete	3740000	2040000
Ia	111	152	1	1	3.40E+06	3.50E+06		3407000	3401000
Ib	111	152	1	1	3.40E+06	3.50E+06		3407000	3401000
Ic	111	152	1	1	3.40E+06	3.50E+06		3407000	3401000

The support density is the average number of rock bolts per square metre of tunnel sidewall, or hangingwall, based on a regular rock bolt installation pattern. The support resistance of the support system is the product of the support density and the yield load of the reinforcement units expressed as kN/m^2. The shear stiffness of the support system is the product of the support density and the shear stiffness of an individual rock bolt installation (rock bolt and grout system) as determined from laboratory investigation (Chapter 5 and Roberts, 1995).

4.3.4.1 Analysis of hangingwall support performance

Analysis of the hangingwall deformation, based on vertical stress reduction rates, against support density as shown in Figure 4-28, shows a general reduction in deformation rate with increased rock bolt density. The analysis is normalised to the amount of deformation (mm) of the hangingwall per unit decrease in the vertical stress component (MPa). The proposed mechanism of hangingwall deformation (section 4.3.3), under the environment of a vertical stress reduction, is the potential for shear along sub-horizontal discontinuities within the hangingwall of the tunnel. The increase in the density of reinforcement perpendicular to the potential shear planes will result in a relative increase in shear resistance. This would be envisaged to result in a reduction in shear deformation and associated dilation into the excavation.

In this analysis, as with all the following analyses, only very general correlation can be made due to the highly variable nature of the in situ rock mass medium, loading environment and

installation quality of the support system, all of which are factors that can significantly influence the response of the reinforcement system.

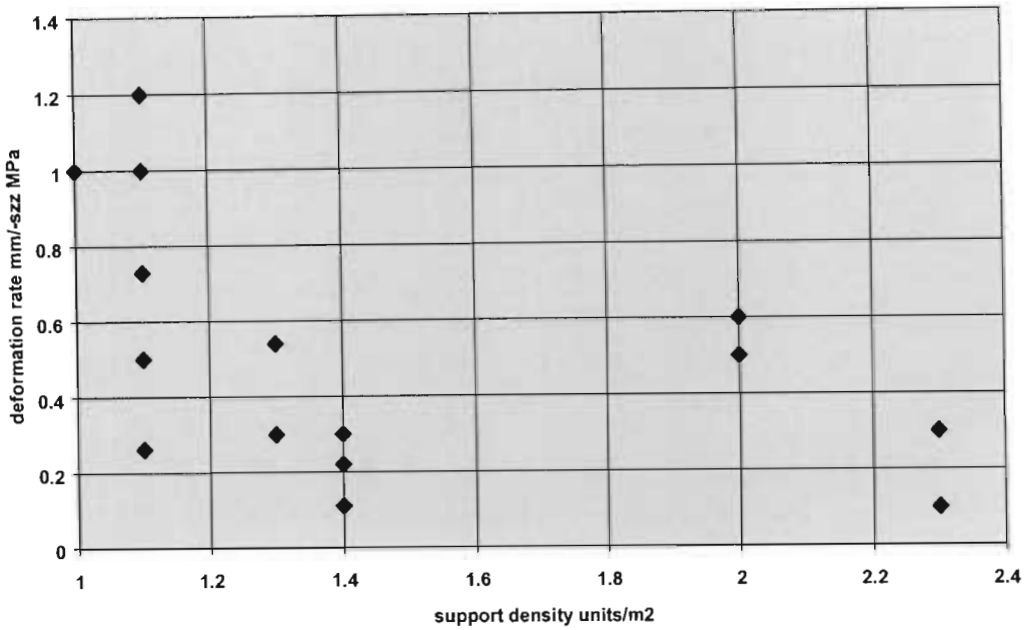

Figure 4-28. Analysis of hangingwall deformation against support density (sections A to I).

Examination of the distribution of data points within Figure 4-28 indicates a poor correlation between the support density and deformation rate. However, a trend of potentially higher rates of deformation for lower support densities may be implied.

The same data range was evaluated with regard to the calculated support resistance of the support systems in tunnel sections A to I, as shown in Figure 4-29. This indicates a similar correlation to that of the support density, as would be expected. However an improved correlation could be anticipated as the deformation mechanism would anticipate that an increased support resistance would limit potential rock mass dilation. This would result in an increase in the shear resistance of the discontinuities, due to the generation of increased normal forces on the shear planes. However, it is noted that the general correlation between the support resistance and deformation is poorer than that for support density. This may be a function of the calculated support resistance being a poor estimation of the actual in situ support resistance due to poor installation practice. Alternatively the application of tributary area considerations to support resistance is not a good reflection of the true degree of rock mass interaction in this case.

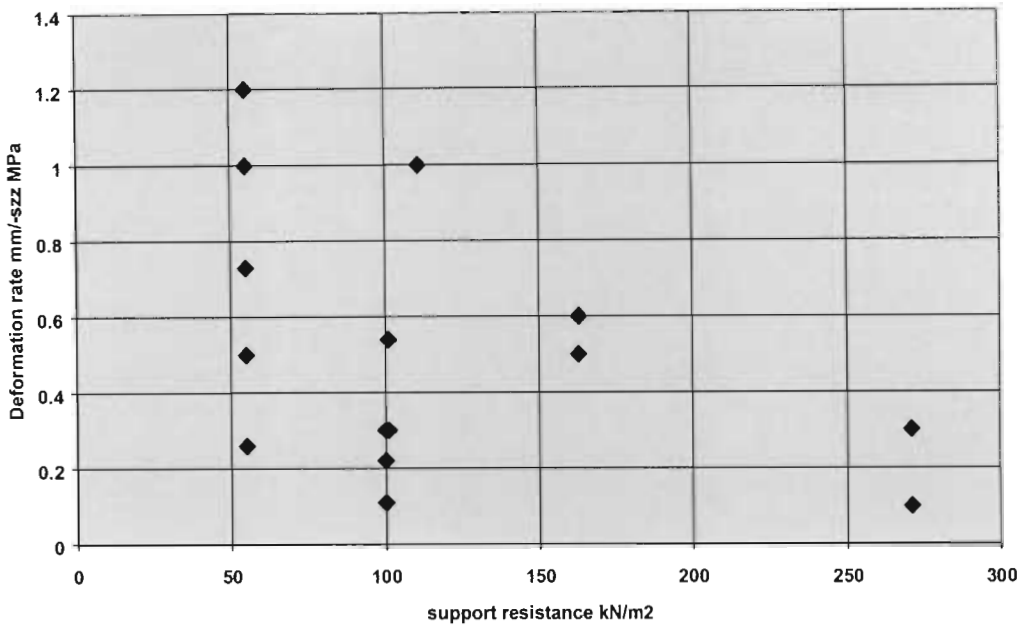

Figure 4-29. Analysis of hangingwall deformation against support resistance (sections A to I).

As the proposed mechanism of hangingwall dilation is based on shear deformation on sub-horizontal hangingwall discontinuities, the performance of the support system was evaluated with respect to an estimation of shear stiffness (Figure 4-30). Although it is proposed that the mechanism of hangingwall deformation, under an environment of vertical stress reduction, is due to shear movements in the hangingwall rock mass, the influence of shear stiffness, as determined in the laboratory, does not correlate well. This again may be a function of the poor correlation between the laboratory determined shear characteristic and the in situ performance.

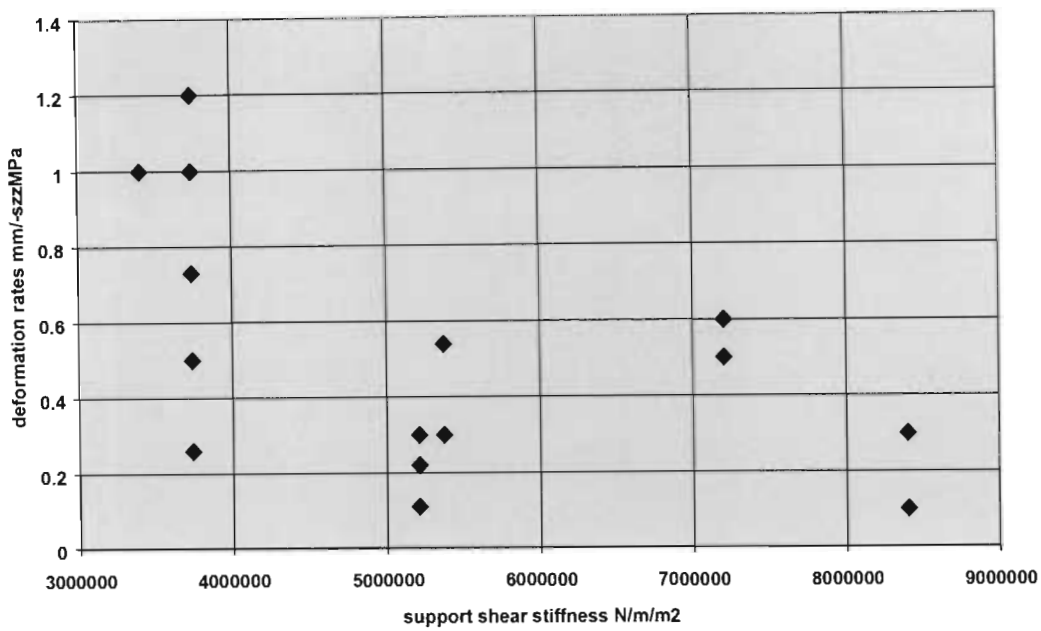

Figure 4-30. Analysis of influence of shear stiffness on hangingwall deformation with respect to vertical stress reduction.

Although most of the hangingwall deformation was associated with the period of vertical stress reduction, a comparison of the deformation rates for both positive and negative stress change indicates a similar magnitude of deformation rate for a given reinforcement density (Figure 4-31). The larger component of hangingwall deformation associated with the period of vertical stress reduction in situ is due to the larger magnitude of negative vertical stress change in the majority of sections. The similar deformation rates may be indicative of a similar deformation mechanism. The average rate of tunnel hangingwall deformation, over the range of support densities analysed, is approximately 0.4 mm/MPa, although there is a general tendency for increased deformation rates at low support densities.

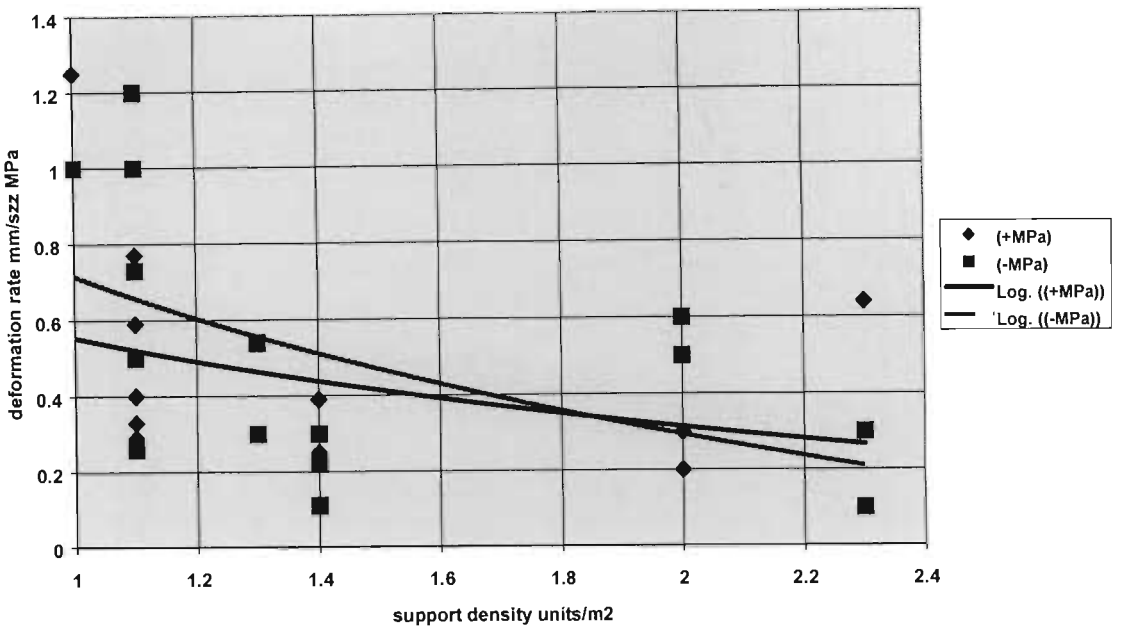

Figure 4-31. Analysis of the influence of support density on hangingwall deformation rates with respect to positive and negative vertical stress change.

It is proposed that for design considerations, although the correlation is extremely poor and the defined trends are only for indicative purposes, that figure 4-31 may be utilised to estimate the amount of total quasi static deformation that the tunnel hangingwall will experience due to the anticipated stress history.

Analysis of the distribution of hangingwall dilation (Figure 4-32) shows that most of deformation in the first 1 m of rock mass. In this rock mass environment it is thus considered that the action of the hangingwall rock bolts is the reinforcement and containment of the rock mass by anchorage in excess of the potentially unstable rock mass depth. Sections of the experimental tunnel that experienced large hangingwall deformations are generally associated with low support densities with large inter-bolt distances. Measuring points, although not specifically indicated by Hepworth, are considered to have been located approximately midway between anchors. It should therefore be considered that the hangingwall deformation may result in localised instabilities, which may result in collapse between the rock bolt reinforcement. This may be the case particularly with shotcrete fabric support, as significant deformation is likely to cause localised failure of the shotcrete skin.

High localised skin deformation associated with section Ia is likely to be due to the difference in hangingwall elevation between section H and I due to tunnel holing.

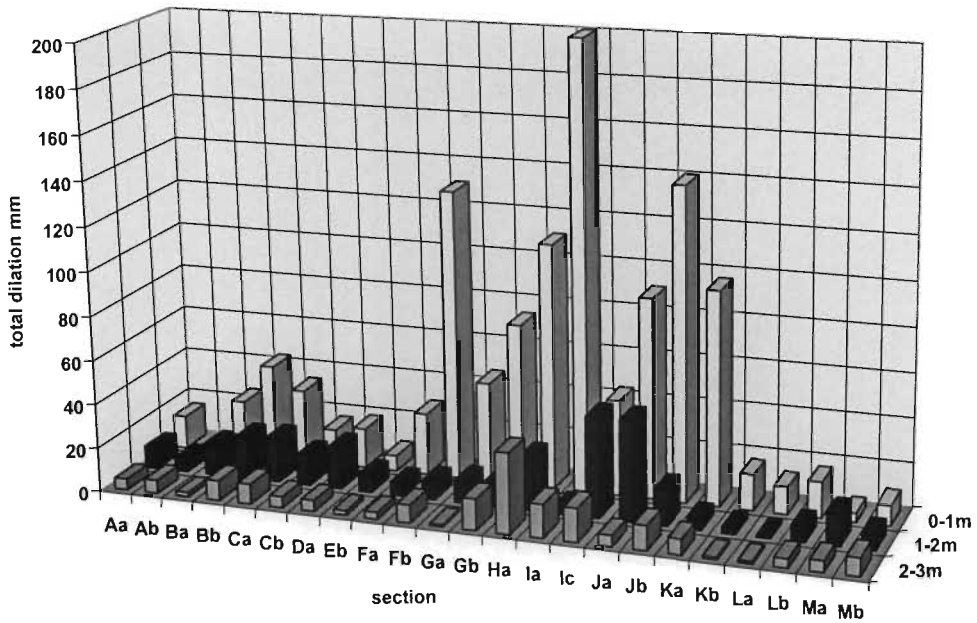

Figure 4-32. Analysis of distribution of dilation with the support sections of the tunnel hangingwall.

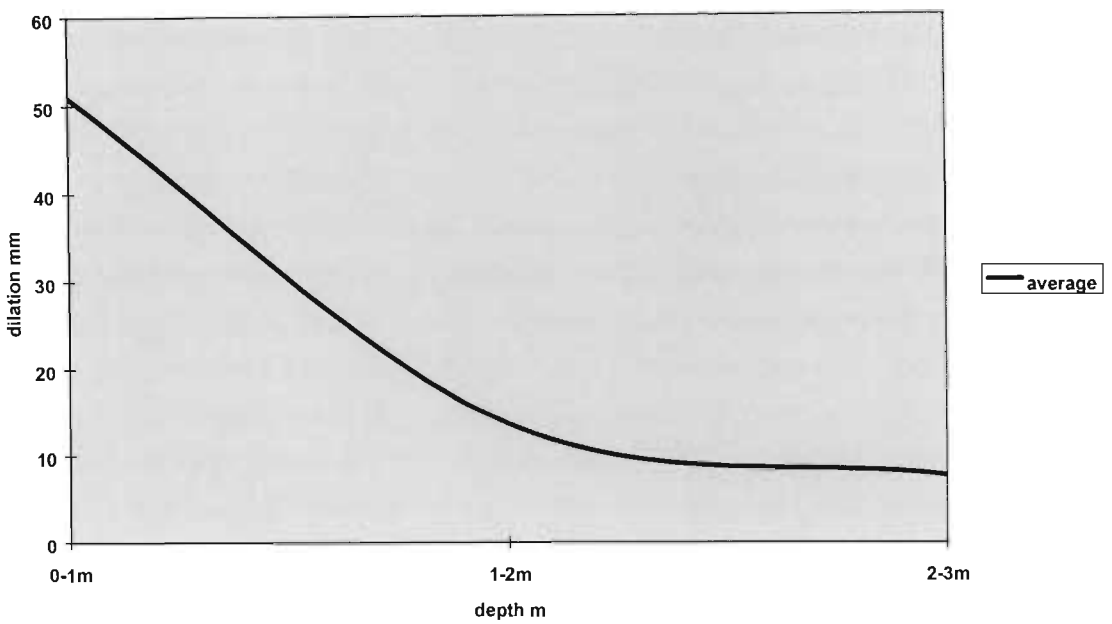

Figure 4-33. Analysis of average distribution of tunnel hangingwall dilation.

The concentration of deformation in the immediate hangingwall rock mass of the tunnel is also shown graphically in Figure 4-33. This clearly indicates the limited amount of deformation in excess of 1 m depth, and also the fairly uniform dilation in excess of this depth. This uniform dilation in excess of the first metre, for all types of support may be indicative of the limited

influence of the rock bolt reinforcement in excess of the depth of potential instability. An analysis of the rates of dilation associated with the different depths of hangingwall rock mass is shown in Figure 4-34. Although a poor correlation is shown, the indicated trends are included for clarity between the data sets and for general guidelines.

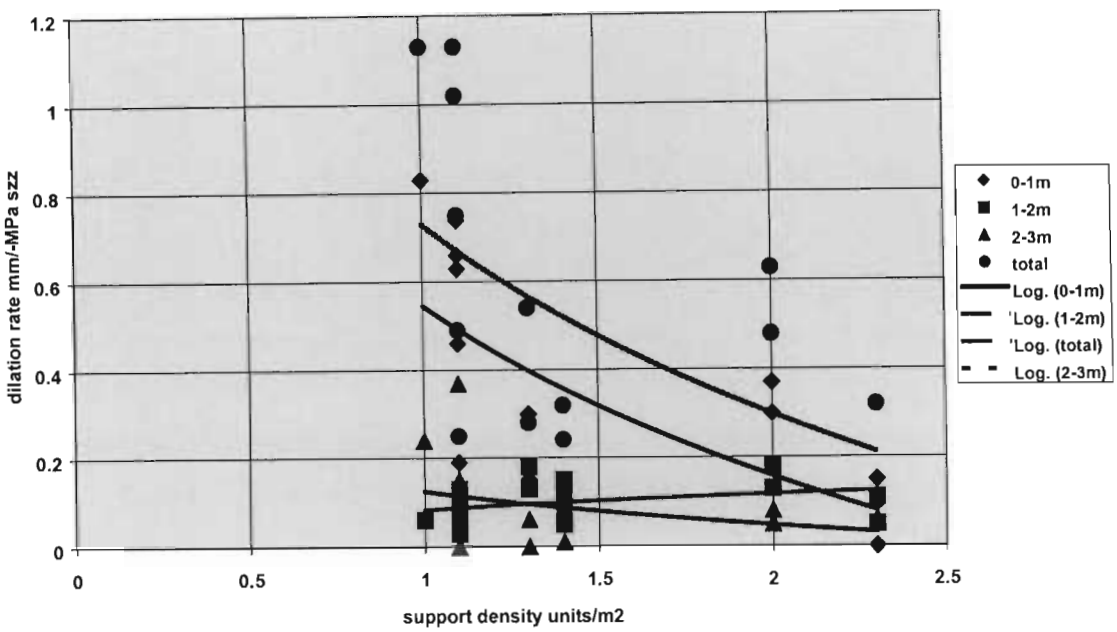

Figure 4-34. Analysis of hangingwall dilation rate with rock mass depth and support density.

Analysis of the dilation rates, per metre depth interval, as a function of reinforcement density, again indicates the large component of dilation associated with the first metre of tunnel hangingwall. This is particularly evident at low support densities. The average dilation rate of the rock mass in the immediate hangingwall is approximately 0.3 mm/-MPa. Analysis of the dilation rate associated with the deeper rock mass indicates a fairly constant rate for all support densities of approximately 0.1 mm/-MPa.

The relatively constant dilation rate at these greater depths is considered to be indicative of a relatively stable rock mass state, and thus limited influence of rock bolt reinforcement. Reinforcement anchorage within this area must however still have the capacity to accommodate this dilation over the envisaged stress history of the excavation. Dilation of the rock mass as measured between 0 m and 1 m may not be fully indicative of the anticipated interaction between the rock bolt reinforcement units and the rock mass. Particularly at low support densities this may be more a function of the effectiveness of the fabric support between the rock bolt units. At the higher support densities it is considered that greater reinforcement interaction occurs, and thus the design of the reinforcement system will have a greater influence on the immediate hangingwall rock mass dilation. It may thus be envisaged that the dilation rate

experienced by the rock bolt is lower than the indicated 0.3 mm/-MPa, particularly if this rock mass volume is highly discontinuous.

4.3.4.2 Analysis of sidewall support performance

Analysis of the sidewall deformation mechanisms (section 4.3.3) indicated a correlation between changes in the vertical stress component relative to the horizontal stress components. This relationship is considered to be the primary indicator for analysis of sidewall deformation, although it should be considered that changes in the relative magnitude of the horizontal stress components will also influence the sidewall deformation history under a constant vertical stress environment. This would also reflect the influence of the change in orientation of the maximum principal stress.

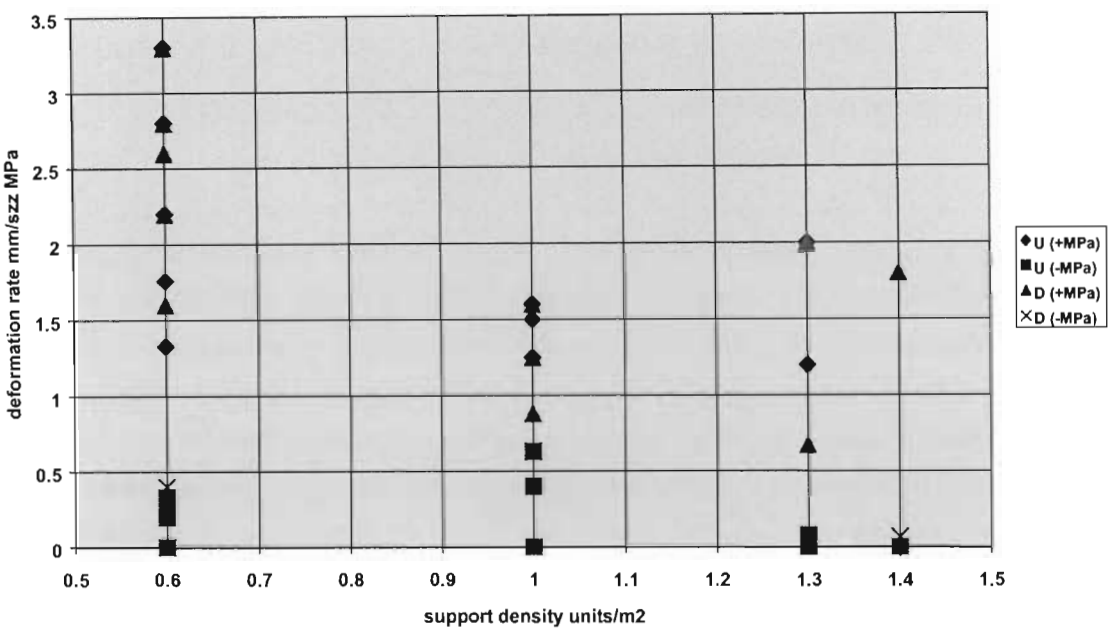

Figure 4-35. Influence of support density on sidewall rock mass deformation rates.

Analysis of the influence of support density, relative to the deformation rate associated with changes in the vertical stress component, indicates a poor correlation (Figure 4-35). This analysis does however indicate the difference in deformation between vertical stress increase and vertical stress reduction. For simplification, this analysis is restricted to the deformation of tunnel sections that are primarily influenced by vertical stress changes only. Figure 4-35 also shows the lack of differentiation between the deformation rates of the updip and downdip sidewalls.

Analysis of the influence of support resistance (kN/m^2) on deformation rates was also examined (Figure 4-36).

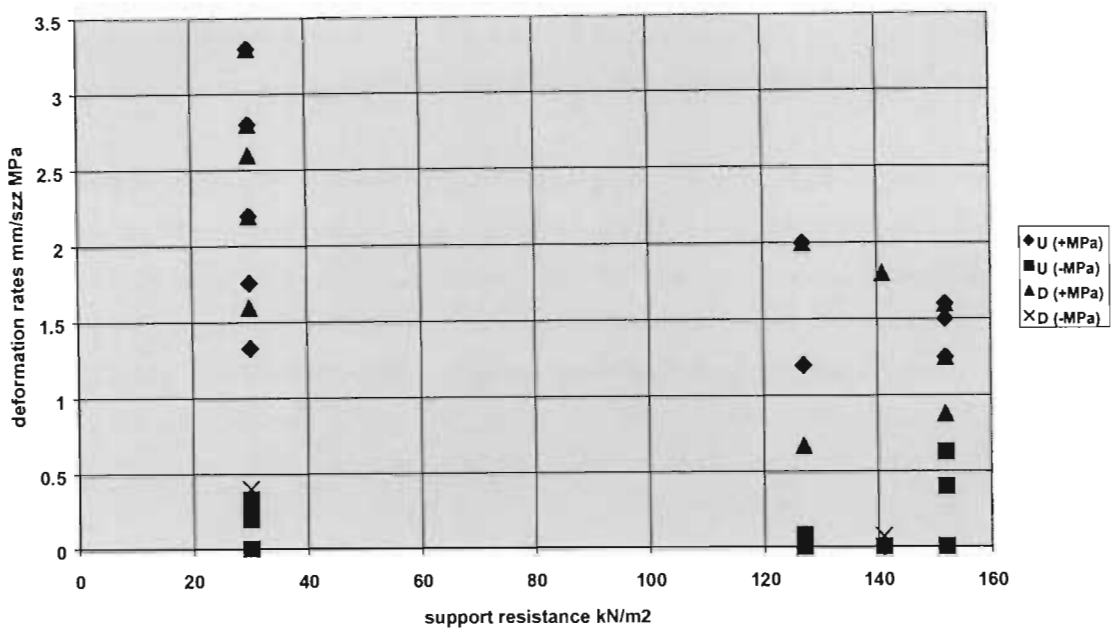

Figure 4-36. Influence of support resistance on deformation rates with respect to the vertical stress component.

A similar lack of correlation to that of support density is indicated for sidewall dilation under a vertical stress increase with respect to support resistance. This may be anticipated, as the in situ capacity of the support units utilised in the respective support sections may be strongly influenced by the installation quality. However there is implied to be a slightly improved correlation between support resistance and deformation rate for higher support resistances. It may be considered that the mechanism of confinement, as expressed in the support resistance, has a greater influence on the deformation mechanism than the density of rock bolts. Under vertical stress reduction there is a poor correlation between support resistance and deformation rates.

Analysis of the overall closure rates of the excavation with respect to support resistance on the closure indicates, although of poor correlation, a reduction in deformation rates with increased support resistance (Figure 4-37). This analysis differs from the previous in that it considers the total sidewall closure, as opposed to a summation of the dilation associated with the immediate first 3 m depth.

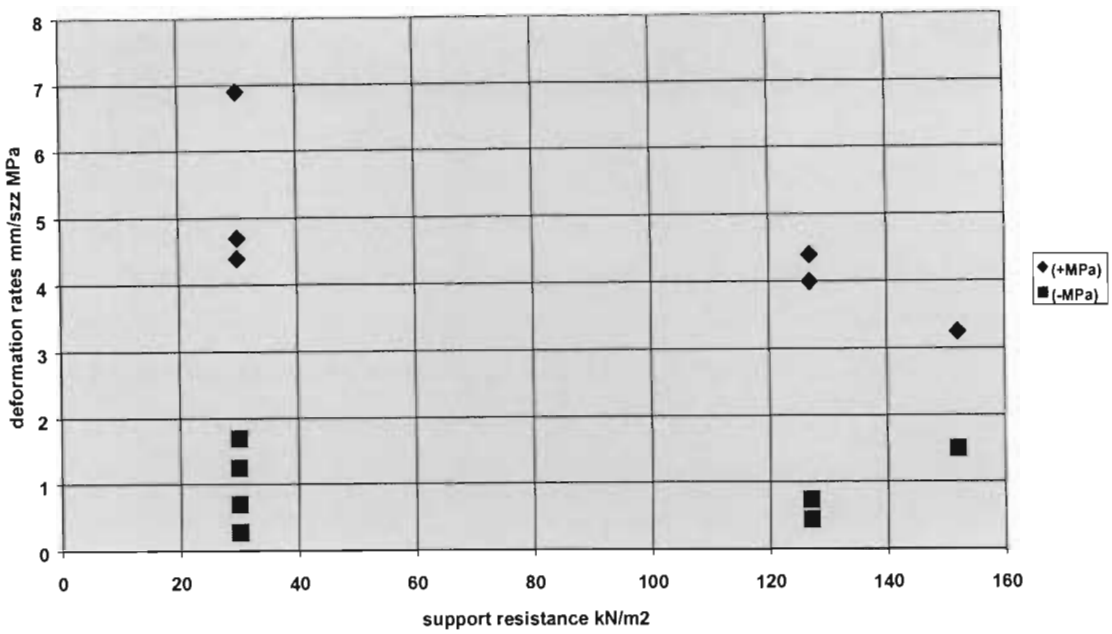

Figure 4-37. Influence of support resistance on overall sidewall closure rates with respect to the vertical stress component.

Fewer data points are available for this analysis and correlation between the parameters is still poor. However, if the overall trends are evaluated it, there is a reduced influence of support resistance and support density (Figure 4-38) on the deformation rates (illustrated by the flatter trend). This is a function of the larger component of deformation which is accounted for in excess of the depth which is directly confined by the reinforcement units (2 m or 3 m depth dependent on rock bolt length). Mechanistically, the degree of reinforcement of the skin of the excavation will influence the dilation rate of the deeper rock mass. This would, however, be a function of the effectiveness of the rock bolt reinforcement in creating a confining structure. Comparison of the relative influence between the low and high support resistance, and support densities, indicates more effective control of dilation within the reinforced rock mass (0 m to 3 m) than to that of the deeper rock mass. Within the immediate skin of the excavation the interaction of the reinforcement with the rock mass is direct, and thus more likely to be more effective in controlling deformation. The influence of the rock bolt reinforcement in controlling deformation in excess of its installed length will be a function of its effectiveness in creating a reinforced rock mass structure, and thus of indirect influence.

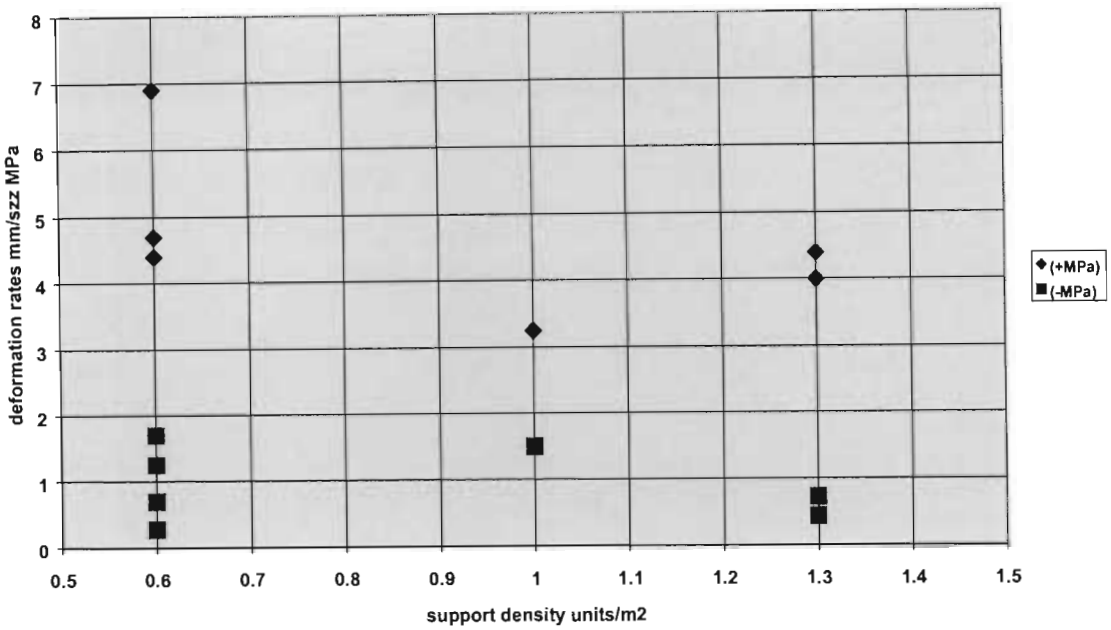

Figure 4-38. The influence of support density on overall tunnel closure rates with respect to the vertical stress change.

An analysis was also conducted on the potential influence of the shear stiffness of the rock bolt reinforcement units on the sidewall rock mass deformation rates. This was based on the proposed indirect sidewall shear mechanism under induced hangingwall deformation. The shear stiffness of the reinforcement system is derived from laboratory shear tests of the rock bolt reinforcement unit, grout and rock system characteristics, typical of those utilised in the South African mining industry (see Chapter 5).

Examination of the influence of the shear stiffness of the support system, as shown in Figures 4-39 and 4-40, indicates a poor correlation. There appears to be an overall trend that an increase in the shear stiffness density of the support system results in a reduction in the deformation rate but there can be very limited confidence in this due to the high scatter in data. Mechanistically it may be envisaged that increased shear resistance will result in the reinforcement of the blocky rock mass structure and restriction in block wedging in the sidewall.

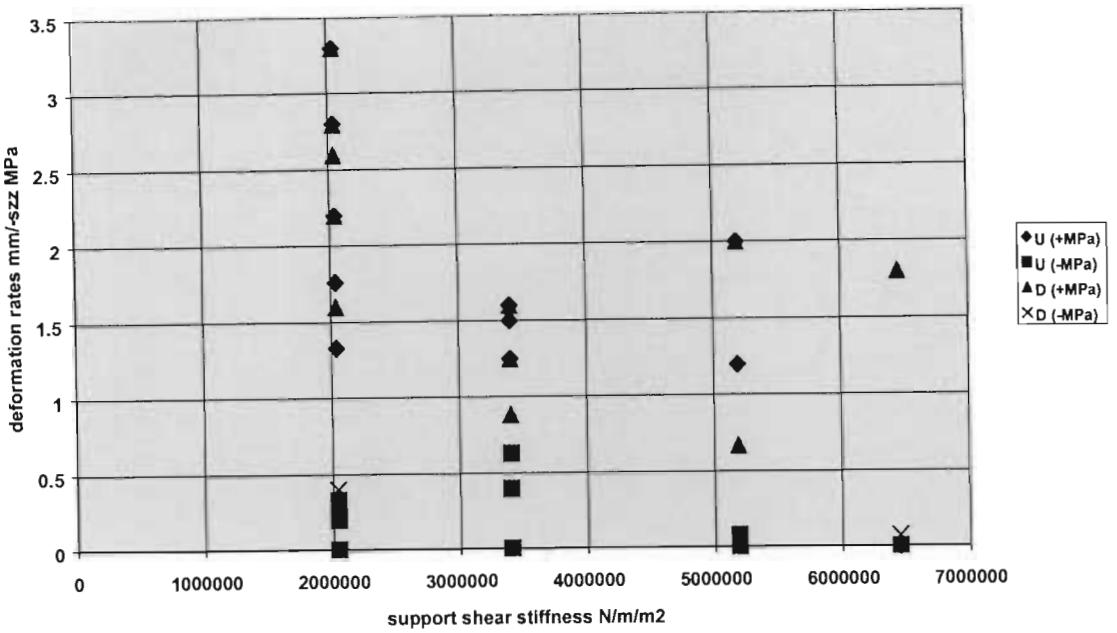

Figure 4-39. Influence of support system shear stiffness on deformation rate within reinforced rock mass with respect to the vertical stress change.

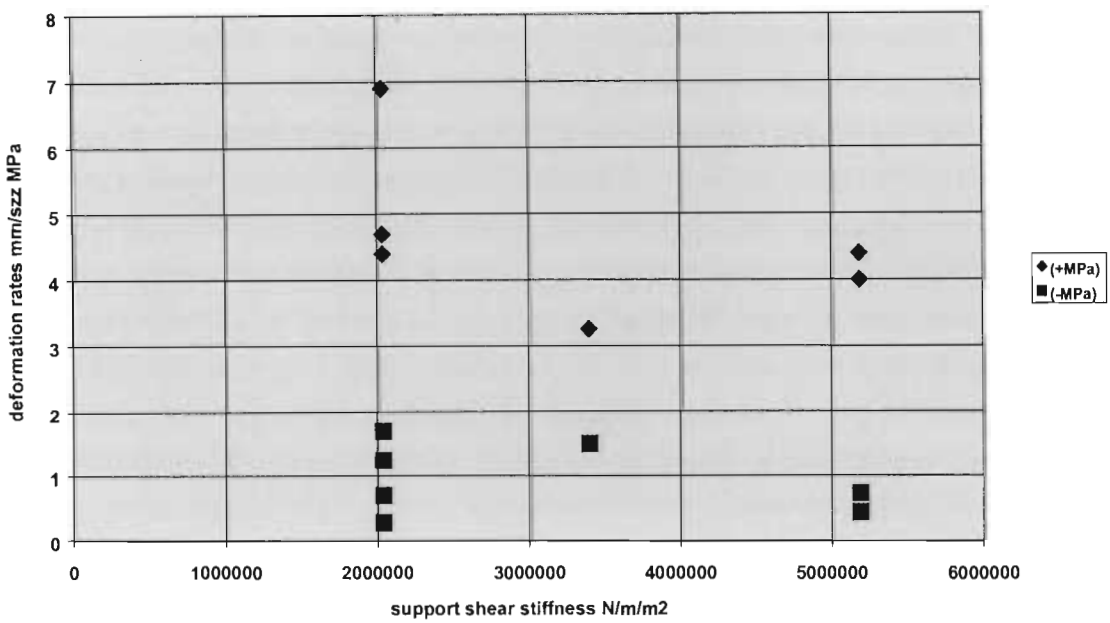

Figure 4-40. Influence of support system shear stiffness on overall tunnel closure rate with respect to the vertical stress change.

Due to the limited variation in the capacity (axial and shear load) of the reinforcement types and obvious inter-relationship of the parameters examined in the tunnel test sections, it is difficult to determine the relative influence of the individual reinforcement characteristics in excess of that

of the influence of the support density. The discussions above are based on limited data, with poor correlation and thus should be treated accordingly. Nevertheless the results do indicate a general trend of reduced rock mass deformation with increased support installation.

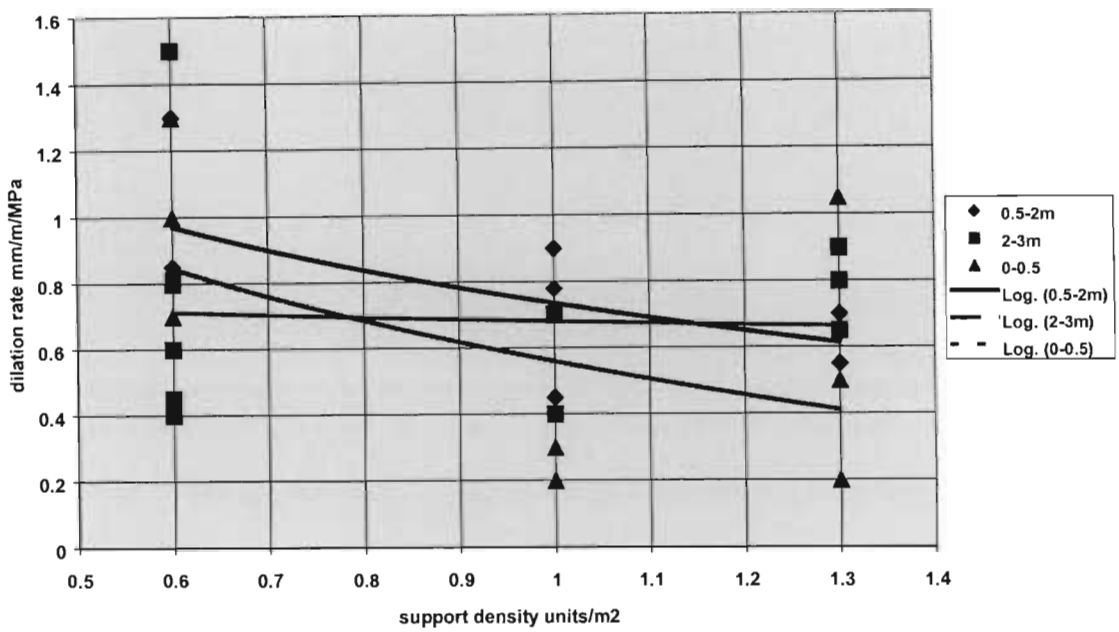

Figure 4-41. Influence of support density on rock mass dilation with depth.

The influence of the reinforcement system can also be evaluated with regard to the rate of dilation with depth within the reinforced rock mass (Figure 4-41). In Figure 4-41, although a poor correlation exists within the data set the trends give an indication of the rate of dilation per unit metre of depth within the tunnel sidewall, and the influence of the support density on this dilation rate. The majority of the tunnel test sections are reinforced with rock bolts of just over 2 m in length, and it is shown in Figure 4-41 that within this depth of sidewall the support density can influence the volumetric dilation rate. In excess of this depth there is little influence of the reinforcement system on the dilation rate with respect to the vertical stress change.

Mechanistically it may be envisaged that an increase in rock bolt reinforcement, and associated reduction in dilation of the reinforced rock mass, would result in a reduction in dilation of the deeper rock mass. However, this is not indicated by this data set. This may be due to the limited nature of the data set and the relatively small variation in support density. Alternatively, it may be indicative of low effective reinforcement interaction, thus allowing shear within the reinforced rock mass along weak bedding planes which will tend be sub-parallel to the rock bolt reinforcement axis. It is also noted that the general dilation rate of the immediate skin of the excavation, between 0 m and 0.5 m, is lower than that of the reinforced rock mass between 0.5 m and 2 m. This reduced dilation rate may be due to the increased interaction between the fabric support and the rock mass reinforcement. Alternatively, significant dilation of this rock

mass may have occurred in this rock mass volume during the development of the tunnel, and thus the dilation rate during the period of measurement will be lower by an unknown amount.

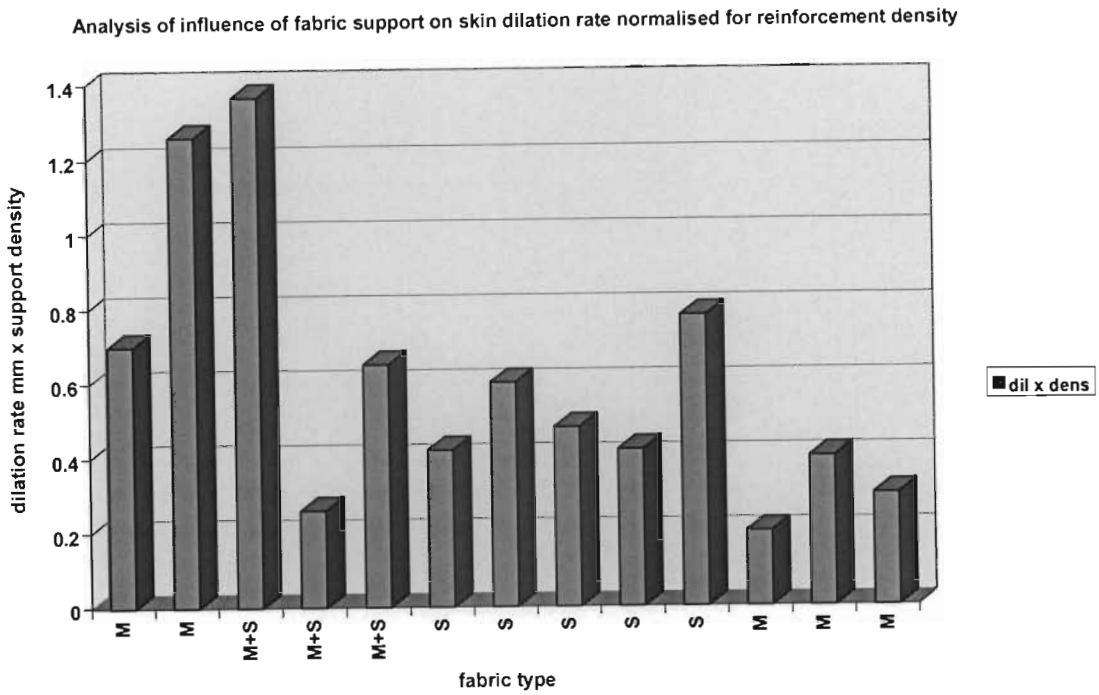

Figure 4-42. Analysis of the influence of fabric type on rock mass dilation between 0 m and 0.5 m.

An analysis of the influence of the fabric type on the dilation rate of this immediate skin rock mass was carried out (Figure 4-42) where M represents mesh only, S represents shotcrete and M+S is a combination of these fabric systems. This data has been normalised for the rock bolt reinforcement density to try to obtain a clearer indication of the fabric influence. However, the analysis of the data set does not give a good insight into the relative influence of the fabric type under these conditions, as indicated by the high degree of variability between similar fabric types.

A previous analysis (Chapter 3), has indicated that in an environment where the rock bolt reinforcement system is designed or results in the creation of a reinforced rock mass structure then significant differential deformation at the surface of the excavation is not envisaged. As the depth of significant deformation, and implied instability was in excess of the length of the rock bolts in most of the sections, this mechanism of deformation and reinforcement would thus be envisaged. Within this environment the utilisation of fabric support should not contribute significantly to the capacity of the reinforced rock mass structure, but is implemented to control the potential of unravelling of the immediate skin only. Control of the unravelling of the immediate skin is, however, important in maintaining effective interaction of the rock bolt reinforcement within the deeper rock mass.

4.4 Conclusions

The above analyses have evaluated the anticipated in situ rock mass behaviour around tunnel excavations sited in stress levels that result in failure of the rock mass around the excavation. The understanding gained from this evaluation has given important insight into the mechanisms of rock mass deformation and the influence of the interaction of the rock bolt reinforcement with the rock mass in controlling this deformation. Within the South African gold mining environment, where the virgin vertical field stress is approximately twice the horizontal stress and often represents the maximum principle stress, the analyses have focused on the relative influence of the vertical stress on these deformation mechanisms. The structure of the rock mass due to fracturing, and thus the deformation mechanisms, as discussed here will also be with respect to this stress environment. Thus South African design considerations in practice often focus on the vertical stress regime. In many of the discussions above, the deformation associated with a change in the stress state is evaluated with respect to the vertical stress component. This analysis and other empirical relationships have shown that this is relative to the horizontal stress components and thus changes in these must be considered in relation to the deformation mechanisms. Analysis in section 4.2 examined the influence of seismicity on excavation stability by means of an induced dynamic stress field. It should be considered that these transient dynamic stresses will also initiate the proposed deformation mechanisms. In other geotechnical environments due consideration should be given to the orientation of the stress field, and any changes, relative to the excavation boundaries to determine the anticipated deformation mechanisms and values.

Aspects of the work in this section, which are considered to have an important influence in support design considerations, are summarised in the following points:

- A revised criterion for the estimation of depth of instability of the rock mass may be used to determine either the length of rock bolt reinforcement or the mechanism of interaction with the rock mass and thus design methodology.

- It is indicated from South African case studies that for a given excavation dimension there is an upper limit of the extent of rock mass instability around an excavation due to fracturing.

- Mechanisms of deformation of the rock mass in the vicinity of an excavation have been proposed. Significantly this indicates the importance of shear deformation within the rock mass, particularly of the hangingwall, and under an environment of relative vertical stress reduction. Consideration should be given to the transient effects of induced dynamic stress with regard to the proposed mechanisms. From the rockburst investigations in Chapter 3 this would be particularly true for hangingwall shear deformation.

- The importance of all components of the quasi static and dynamic stress field, and the full stress history acting on the excavation, has been indicated by the analysis.

- Deformation rates of the hangingwall and sidewalls of an excavation have been associated with the magnitude of relative change in the vertical stress component to the horizontal stress components. The change in the vertical and horizontal stress components will also simplistically capture the change in magnitude and direction of the maximum principal stress. The influence of support on these deformation rates could only be evaluated in very general terms because of the poor correlation of the in situ data. These can however be used to make an estimation of the total deformation of the excavation for a given stress history. In addition, estimation may be made of the anticipated dilation of the rock mass along the length of the rock bolt and thus its required yield capacity. This is an important consideration in the selection of suitable rock bolt systems.

- The influence of the fabric support could not be effectively evaluated in this rock mass and support design environment.

Chapter 5

5. Evaluation of shear characteristics of rock bolt systems

5.1 Introduction

The case studies of rockburst investigations (Chapter 3) and the in situ evaluation of deformation mechanisms associated with the rock mass around tunnel excavations (Chapter 4) have both indicated the mechanism of shear deformation within the rock mass. The importance of the understanding of the shear characteristic of the rock bolt units for control, of rock mass behaviour is thus indicated. This aspect of support design, although previously recognised within the South African mining industry, is not typically considered by the design engineer. A reason for this lack of consideration may be the previously poor understanding of the mechanisms of shear within the rock mass and thus design applicability, and also a lack of understanding of the capabilities of the typical support systems to accommodate shear, particularly under dynamic loading conditions.

As part of the investigation into the performance of support systems as typically utilised in the South African mining industry (Haile, Jager and Wojno, 1995), a laboratory testing programme of the shear capacities of these rock bolt systems was initiated (Roberts, 1995) and is evaluated in this section. Work in this area has also focused on a numerical modelling simulation of the initial laboratory testing data in order to extrapolate these results to evaluate optimum installation procedures for rock bolts to control rock mass deformation. The results of the testing programme and numerical modelling analysis will thus be utilised in formulating design considerations for support systems under shear loading.

Typical rock bolt systems as utilised in the South African mining industry comprise a circular steel bar of between 12 mm and 20 mm diameter, often with surface protrusions, encapsulated in cementitious grout in a 30 mm to 40 mm diameter borehole drilled into the rock mass. Some units, such as Split Sets or Swellex, comprise a steel tube, forced or expanded into the borehole, and operate on the frictional resistance between the steel and the borehole surface. These rock bolt systems stabilise the rock mass, in the immediate periphery of an excavation, by providing reinforcement across the discontinuities in the rock mass.

The applicability of this aspect of the investigation to the overall development of a tunnel support design procedure for the South African mining industry is illustrated in Figure 5-1.

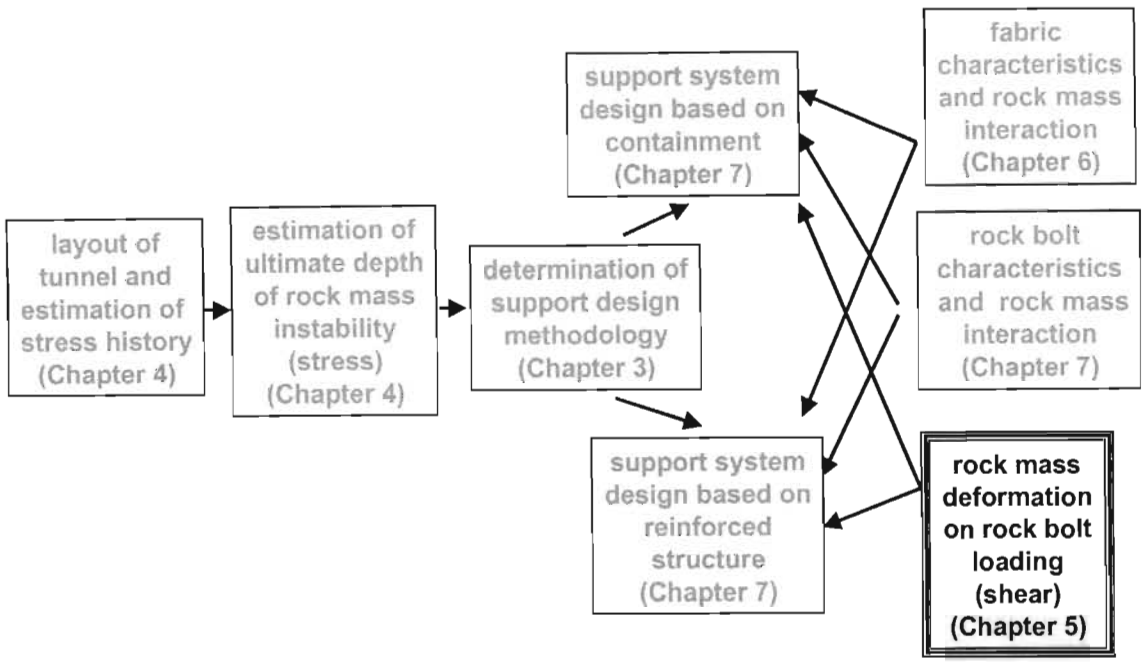

Figure 5-1. The relevance of research conducted under Chapter 5 on the overall tunnel support design methodology.

5.2 Laboratory testing programme

Testing was conducted initially using a double shear test rig as shown in Figure 5-2. This apparatus consisted of three blocks through which the rock bolt system (bolt/grout/rock annulus) was installed. The aim was to approximate the in situ characteristic of the rock bolt system installation. The test procedure involved the displacement of the central block relative to the outer blocks. The load – deformation history of the system was monitored up to failure. This testing procedure was conducted under quasi static and dynamic loading conditions.

Dynamic loading was applied via the Terratek press. This facility allows loading rates to be varied between zero and 3 m/s during the test procedure. Initially the test apparatus would be 'settled' under slow loading (15mm/min) and subsequently loaded at 3 m/s to determine its dynamic response. This loading rate is restricted by the current capability of the Terratek press, but is also typical of the loading rates used in current design analysis of support under dynamic loading conditions.

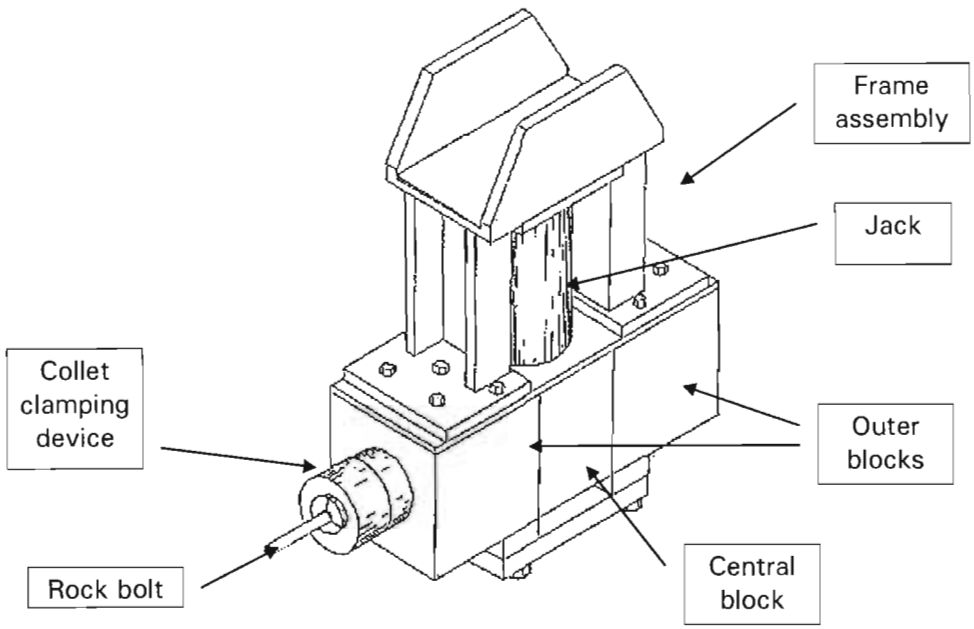

Figure 5-2. Double shear test rig.

However it was found that the failure of the rock bolt system at the two shear interfaces was complex, none simultaneous, and thus difficult to interpret. It was often noted that initial failure would occur on one plane and this would influence the subsequent loading of the rock bolt at the second shear plane resulting in none simultaneous failure. It was also found that the confinement to the outer blocks was insufficient to prevent separation of the blocks under loading. This would result in increased deformation of the rock bolt unit into the shear plane and the development of an exaggerated and uncontrollable crank handle configuration of the rock bolt bar.

Subsequent to these initial tests a single shear plane rig was designed and constructed in order to simplify the understanding of the mechanism of the test procedure and enable the simulation of guillotining as observed in the underground case studies. This test rig also allowed increased confinement to prevent the separation of the shear blocks, Figure 5-3. A significant consideration with the design of this test rig was the ability to maintain the shear plane parallel to the loading direction. This involved the design of a substantial bolting system in order to secure the fixed block to the test rig and prevent rotation of the apparatus.

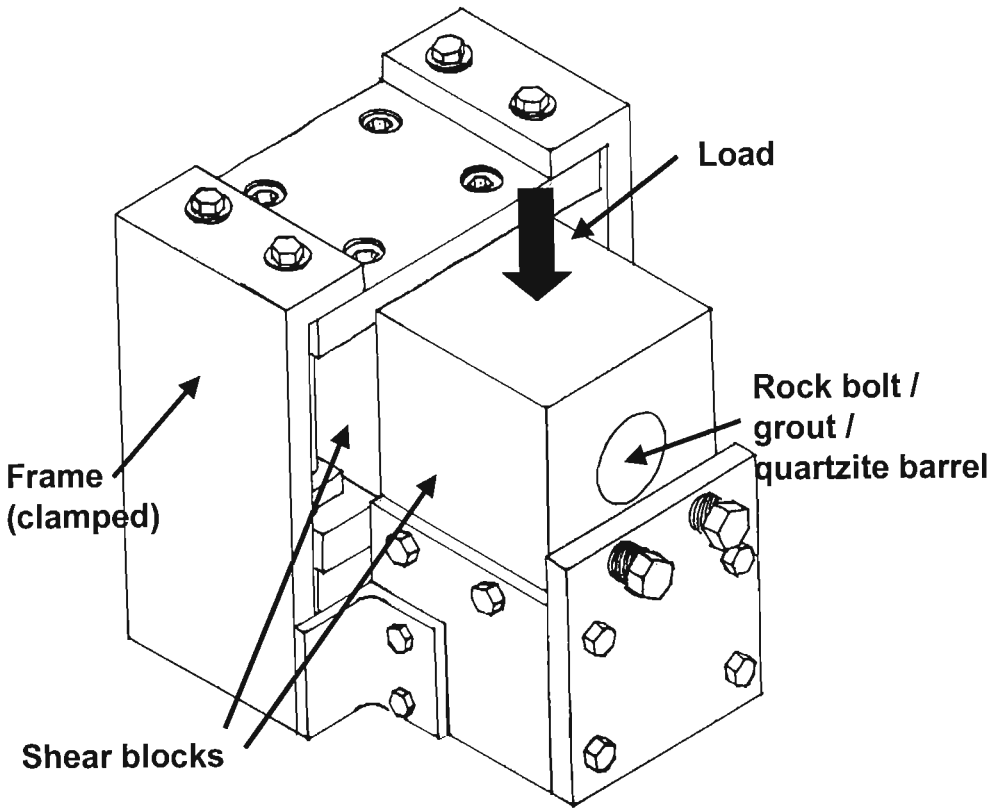

Figure 5-3. Single shear test rig

The results used in the evaluation of the rock bolt support systems were obtained using this single shear test rig.

Both test rigs incorporated 'rock rings' at the shear interface to represent the rock mass surrounding the support drill hole. The inner diameter of the ring was 40 mm, typical of boreholes drilled for support installation. The uniaxial compressive strength of the grout used in the test procedure was approximately 20 MPa, also equivalent to that used underground. Load displacement plots were derived for each of the rock bolt systems and a qualitative examination of the failure surface of the rock bolt and the rock / grout annulus condition was carried out.

5.2.1 Analysis of shear performance of rock bolt systems

The apparatus, as described above, was used to test a series of typical rock bolts. A summary of their load displacement performance is given in Table 5-1. This data represents an average of a series of tests and the critical performance characteristics of the load – deformation curves have been extracted. Failure characteristics are discussed for the individual support units in the subsequent sections.

Support systems as tested under this programme, and evaluated here with regard to their typical axial characteristics, include:

- 16 mm smooth bar. A grout based system with a smooth, 16 mm diameter, circular rock bolt unit. Anchorage within the rock mass is via the surface bonding between the bar and the grout, and the grout and the borehole rockwall.

- 16 mm rebar. A grout based system with a 16 mm outer diameter rock bolt unit having 2 mm herringbone ridges on the outer surface. Anchorage within the rock mass is via the surface bonding between the bar and the grout, and the grout and the borehole rockwall. Bonding between the grout and the rock bolt is far superior to the smooth bar due to the surface irregularities.

- 12 mm twist bar. A grout based system with a rock bolt unit that is a smooth, square profile bar that has been twisted along its length to give a helix type structure. Interaction with the rock mass is via surface bonding. The twisted nature of the rock bolt results in relatively stiff axial load characteristics on debonding.

- 16 mm V bar. A grout based system with a rock bolt unit that is based on a smooth bar but with regular "pinches" of the steel surface to create protrusions along the bar. This process results in a very stiff (work hardened) rock bolt with very brittle failure characteristics.

- 16 mm cone bolt. A grout based system with a rock bolt unit that is again based on a typical smooth bar profile. However, the surface of the shaft of the rock bolt is coated with a thin layer of wax that debonds the rock bolt from the encapsulating grout. A cone is forged at the end of the bolt and tension is developed within the rock bolt due to dilation of the rock mass between this cone and a faceplate on the surface of the excavation. Tension within the bolt results in compression within the surrounding rock mass. The cone is shaped such that at the designed yield capacity of the rock bolt system the cone is dragged through the grout, developing high frictional forces whilst compacting and crushing and yielding through the encapsulating grout medium.

- 12 mm, 14 mm and 16 mm steel rope. A grout based system with a reinforcement unit that is a steel cable strand made up of several steel wires of various configurations. The system thus has a coiled characteristic of a rope. Interaction with the rock mass is through surface bonding. These reinforcement cables are generally made from de-stranded hoist rope. The greased nature of this rope often results in poor direct bonding with the grout, but its coiled nature results in the generation of high support resistance and good yield characteristics.

- SS39 Split Set. A friction based system with a rock bolt unit that is a split tube of high tensile steel of outside diameter slightly greater than the installation borehole diameter. The installation procedure involves the forcing of the steel tube into the borehole. This results in radial compression of the tube and partial closure of the split. This in turn results in an equal and opposite radial force on the surface of the borehole. Interaction with the rock mass under axial loading is thus frictional resistance to sliding of the rock bolt within the borehole.

Table 5-1. Summary of shear test results.

Tendon	Tensile Strength [kN]	Static Shear Strength [kN]	Static Shear Strength [% of UTS]	Dynamic Shear Strength [kN]	Dynamic Shear Strength [% of UTS]	Dynamic Shear Strength [% of static]	Loss in Strength [%]	Static Disp. at Failure [mm]	Dynamic Disp. at Failure [mm]
Smooth bar (16 mm)	116	120	103.4	122	105.2	101.7	0.0	34	33
Rebar (16 mm)	156	140	89.7	124	79.5	88.6	11.4	33	32
Twist bar (12mm)	139	137	98.6	63	45.3	46.0	54.0	33	32
V-bar (16 mm) *	120	85	70.8	38	31.7	44.7	55.3	11-20	10-15
Cone bolt (16 mm)	116	190	163.8	120	103.4	63.2	36.8	68	33-65
Rope #1 (12 mm)	117	116	99.1	76	65.0	65.5	34.5	40	-
Rope #2 (12 mm)	135	142	105.2	73	54.1	51.4	48.6	42	23-30
Rope #3 * (14 mm)	243	242	99.6	179	73.7	74.0	26.0	37	33
Rope #4 (16 mm)	221	227	102.7	118	53.4	52.0	48.0	39	-
Split Set (SS39)	110	97.7	88.8	60	54.5	61.4	38.6	31	26-33

* Results are for double shear tests, where the ultimate capacity is halved

The shear characteristics of the typical rock bolt support systems, as tested, are shown in Figure 5-4. In general it is noted that all the grout based systems (16 mm smooth bar, 12 mm twist bar, 16 mm rebar, 16 mm cone bolt and 16 mm rope) show an initial period of relatively high stiffness, followed by a general softening in the system. The softening in the system is considered to be indicative of the initiation of the crushing of the grout within the rock annulus. This may also indicate the onset of bending and elongation of the rock bolt unit in conformance with the development of shear displacement. The final failure of the system is generally violent in nature. The fairly linear increase in load, with deformation, of the Split Set is considered to be a function of this system comprising only the steel tube of the rock bolt unit within the rock annulus. This results in a more elastic, linear response of the system.

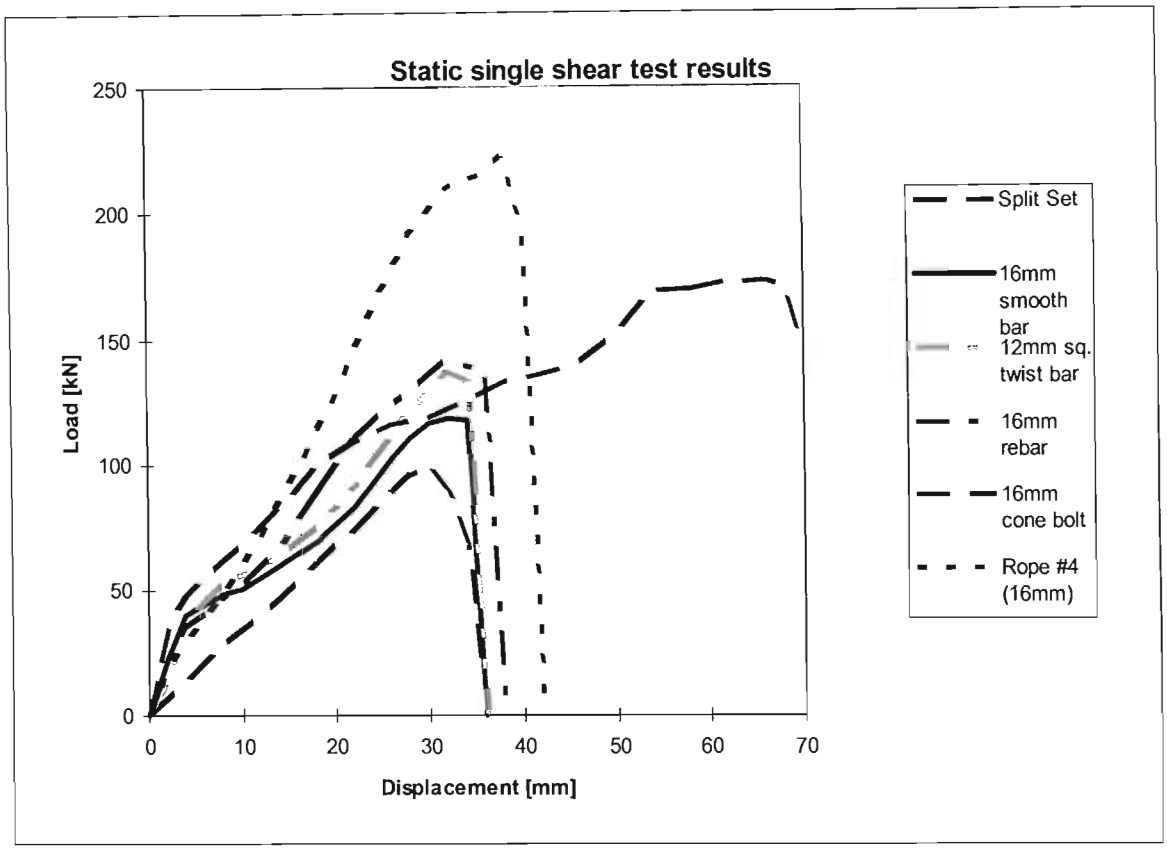

Figure 5-4. Single shear test results of support units

Comparison, and analysis of results, is conducted on the basis that the theoretical maximum shear strength of a steel bar is 50 per cent of the ultimate tensile strength of the material. This relationship is derived from analysis of the failure criterion as defined using Mohr's circle (section 5.3.2). In the laboratory tests this differs significantly from the ultimate shear strength of the rock bolt system comprising the rock bolt bar, grout and rock annulus.

In the majority of the tests, where failure is in excess of this value, the mode of failure can not be totally attributed to the shear strength of the rock bolt unit but is rather a characteristic of the system, which is analysed below.

16 mm Smooth Bar

Ultimate failure of the rock bolt unit occurred parallel to the shear plane. Prior to failure, significant plastic deformation adjacent to the shear plane had occurred. This plastic deformation had disintegrated the grout annulus around the rock bolt until it made contact with the rock ring. Loading of the rock ring had resulted in fracturing and some spalling prior to failure of the system at this point. Analysis of the failure surface indicated that the smooth bar rock bolt had failed in components of both shear and tension, but predominantly in shear. Debonding and bending of the rock bolt had occurred over an average length of 36 mm from the

shear plane for a lateral shear deformation of the order of 34 mm. Dynamic and quasi-static performance of the rock bolt system was found to be similar.

16 mm Rebar

Failure of the rebar support system was similar to that of the smooth bar, with plastic deformation of the rock bolt through the grout annulus prior to failure. Debonding and bending of the bar had occurred over a length of 30 mm each side of the shear plane. This reduced debonding, probably due to increased bond strength, may have resulted in the increased shear strength. Under dynamic testing this increased bond strength results in increased stiffness of the system with resultant brittle failure of the bar. Examination of the failure process under dynamic loading indicated an increased component of shear at failure.

12 mm Square Twist Bar

The mode of failure of the twist bar is again similar to that of the smooth bar and rebar rock bolt units. Debonding occurred over a length of 35 mm from the shear plane with a shear displacement of 37 mm. Under dynamic loading a far more brittle behaviour of the bar was observed. This resulted in a substantial drop in the shear resistance of the system. This behaviour is considered to be due to a combination of the high tensile strength (972 MPa.) of the material and the complex bonding resulting in a change of tensile strain distribution. The increased stiffness of the system under dynamic loading would result in a more direct shear loading of the twist bar and a limitation in the development of plastic bending within the shear plane.

16 mm Cone Bolt

The test set up for the cone bolt was altered in order to obtain symmetry of the bolt across the shear plane. This was necessitated by the unique mechanism of interaction between the cone bolt rock bolt system and the rock mass. The symmetrical behaviour of the cone bolt across the shear plane was achieved by creating a unit with cones on either end. This was considered necessary in order to obtain data that could be interpreted and understood. The cone bolt behaviour was fundamentally different to the previously tested rock bolt systems under shear deformation. Failure of the cone bolt shaft was observed to have occurred predominantly in tension, as evident from the pronounced necking fracture. This mode of failure was due to the relatively large shear displacement, 68 mm, compared to 33 mm that occurred prior to failure of the smooth bar. It was observed that displacement of the cones had occurred prior to failure, allowing the bar to bend along the displacement plane. This deformation resulted in the disintegration of the grout and the rock annulus. Figure 5-5 illustrates the degree of plastic bending that the cone bolt could tolerate prior to failure, thus changing the mechanism of failure of the bar from primarily shear to tension.

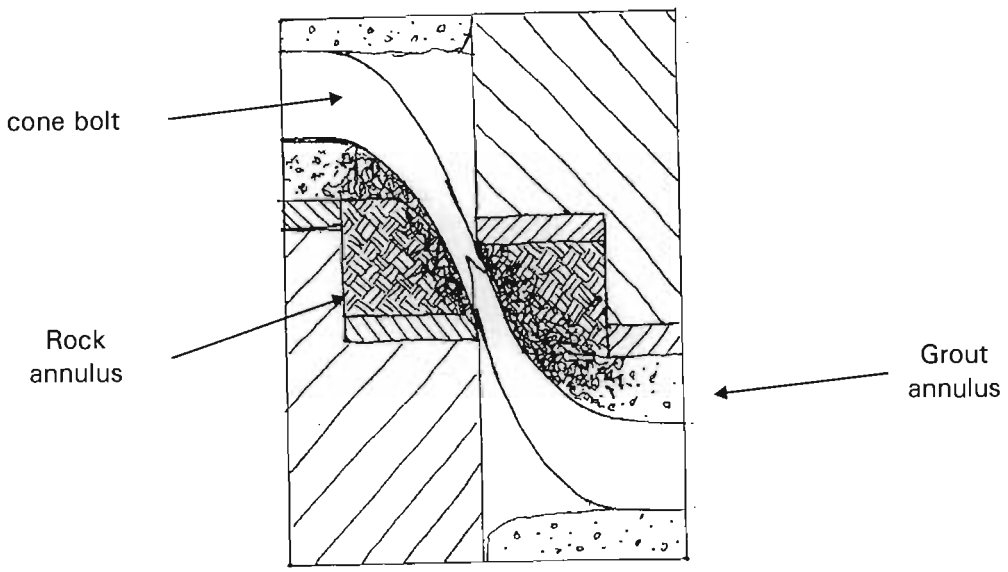

Figure 5-5. Shear deformation of 16mm cone bolt.

The evaluation of the performance of the cone bolt under dynamic loading considered the effect of the location of the cones, from the shear plane. Tests at cone to shear plane distances of 300 mm and 600 mm were conducted. In the 300 mm test, the performance of the cone bolt was similar to the quasi-static tests, in which the rock bolt system yielded with resultant cone displacement. In the 600 mm test dynamic shear failure of the cone bolt occurred, in a similar manner to that of the smooth bar, where shear failure was at a shear displacement of approximately 32 mm. It was noted that no displacement of the cones was evident under this test. It is thus considered that under dynamic loading the position of the cone relative to the shear plane will determine the ability of the system to yield at the cone allowing greater tolerance to shear in preference to a guillotining mechanism of failure.

Split Sets

The failure of the Split Sets was predominantly in shear with minimum plastic elongation. Observed plastic deformation of the rock bolt was restricted to the upper quadrant of the Split Set annulus. Some damage was observed to the rock annulus in the lower portion of the borehole. The shear movement of the blocks (approximately 21 mm) squashed the upper portion of the Split Set until it came into contact with the lower portion of the Split Set, at which point shear failure of the unit occurred. Similar modes of failure were observed under dynamic testing conditions, although of reduced ultimate shear capacity.

Grouted De-stranded Hoist Ropes

The failure of the hoist ropes, due to bending into the shear plane, was predominantly in tension. The failure mechanism was considered to be due to the flexible nature of the rope enabling bending with limited plastic deformation. The stress distribution within individual strands of the rope would be dependent on the position of the strand within the cable, the upper strands of the rope, at the shear plane, being exposed to the greatest tensile stress. Failure of the cable would thus not propagate violently, resulting in a gradual failure process from sequential failure of individual strands of the rope. This resulted in relatively high failure loads and deformations compared to equivalent diameter bars due to an increased tensile component of loading at failure. Shear deformations at failure were of the order of approximately 40 mm. The rock annulus surrounding the cable was often crushed adjacent to the shear plane. It was also observed that 'yielding' of the cable occurred as the inner wires of the rope were pulled through the outer lay, which was in contact with the grout annulus. Under dynamic loading conditions a significant drop (up to 50 %) in the shear strength of the cable was apparent for all tests, although some samples did not fail completely at the full shear displacement (65 mm).

16 mm V-bar

The construction of this support unit involves the 'pinching' of a smooth bar unit along its length to produce an exaggerated ripple effect. This cold working of the bar introduces brittleness into the support unit. The failure of the bar due to the shear displacement was brittle and predominantly of shear mode. This is indicated by the jagged failure surface, with minor plastic bending of the rock bolt bar. Failure was considered to have initiated at the site of a 'pinch' adjacent to the shear plane. The performance of the bar, with regard to shear load and displacement, varied greatly depending on the position and orientation of the pinches relative to the shear plane. If a pinch is located on the shear plane and positioned vertically, brittle failure will initiate at the shear plane with minimal shear displacement (11 mm). If the shear plane is located between the pinches, and they are positioned horizontally, brittle failure was observed to occur away from the shear plane. This thus allows increased shear displacement prior to loss of load (20 mm). These mechanisms are illustrated in Figure 5-6.

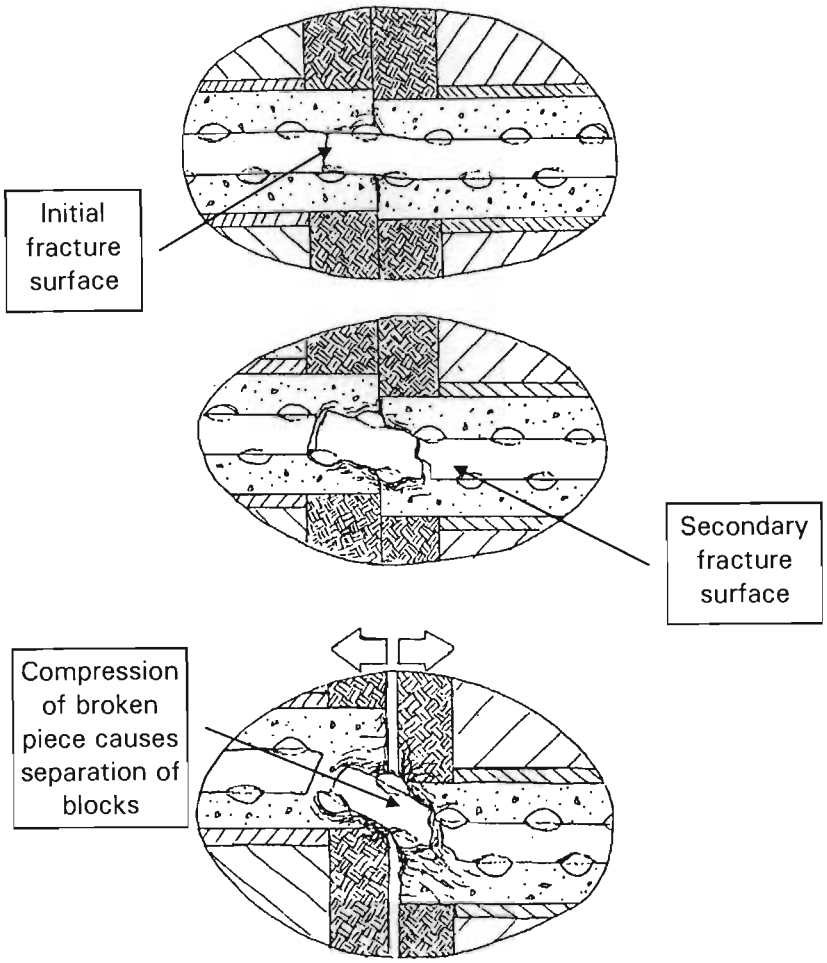

Figure 5-6. Failure mechanism of 16 mm V-bar

5.2.2 Evaluation of shear performance of rock bolt systems

It is noted that the support units with higher yield characteristics had failure loads in excess of the maximum theoretical tensile strength of the support unit. The reasoning for this is not entirely clear but several mechanisms have been considered. These include i) natural variations in the tensile strength of similar rock bolt units in the limited number of tests, ii) interference by the support unit and crushed material on the shear plane increasing its effective friction, iii) bending loads generated within the frame of the test equipment. Although the mechanism is not clear, this does not detract from the relative performance of the support units under shear as discussed above, and thus the design considerations for such support systems under shear conditions.

5.3 Numerical modelling analysis of the shear performance of rock bolt systems

In order to evaluate the influence of the parameters of a rock bolt system on its ultimate shear capacity a detailed numerical modelling investigation. This numerical modelling study, conducted under the supervision of the author in collaboration with Professor V Verijenko and his MSc student J Apsey, of the University of Natal, utilises two and three-dimensional finite element models to conduct back analysis of the laboratory investigation. This was based on the determination of the stress distribution within the rock bolt units under shear as the basis for predicting their ultimate shear deformation capacity. The large deformations necessitated the consideration of large strain and plastic deformation within the system. Non-linearity was observed to occur in the physical experimentation as plastic bending of the rock bolt unit, crushing of the grout and separation of the grout above the rock bolt. The separation of the grout from the rock bolt was most accurately modelled by the deletion of the contact grout elements once they attained a critical tensile stress level. This procedure is considered acceptable as only the stresses and deformations of the rock bolt are being considered in this analysis. In addition the contribution of the rock and grout under compression would have a far greater influence on the constraint of the rock bolt within the system.

5.3.1 Analysis of material behaviour characteristics for a rock bolt system

Various methods exist to incorporate the material constitutive models of the steel, grout and rock into a finite element computer program for the solution of problems that require non-linear stress analyses. The first step towards establishment of a model requires definition of the yield limit for the specific material. This is known as the "yield function" since it is a certain function of the stress components. A plastic material is called "perfectly plastic", "work-hardening" or "work-softening" according to the yield function, which can be fixed or variable in stress space as plastic strain develops.

Strain- or work-hardening plasticity theories describe the stress-strain behaviour of the materials under cyclic loading conditions. The fundamental difference between elastic and plastic models lies in the treatment of loading and unloading. In plastic models, upon load removal, unloading follows an entirely different path from that followed by loading. If an elastic model is used to describe material behaviour then unloading will follow the same path as loading.

An important aspect of deformation theory for work-hardening materials is that the state of strain determines the state of stress uniquely as long as deformation continues. Work-hardening materials may therefore be treated as perfectly plastic as long as unloading does not occur (as in the case of analysis of the rock bolt up to its peak load). Work-softening materials (grout and rock) may also be considered as perfectly plastic for this condition, but pose a greater concern due to the decrease in strength after yield. This important consideration has to be taken into account when the results of non-linear analysis are interpreted.

5.3.2 Deformation theories

The total deformations of a material can be decomposed into elastic and plastic components:

$$\{\varepsilon\} = \{\varepsilon\}_{elastic} + \{\varepsilon\}_{plastic} \tag{5-1}$$

The plastic strain is obtained by the following flow rule:

$$\{\varepsilon\}_{plastic} = \varphi \frac{\partial f}{\partial [\sigma]} \tag{5-2}$$

where, φ is a scalar function related to a uniaxial test curve, and f is a scalar function of the stress tensor $[\sigma]$ and plastic potential hardening parameters.

In the development of the stress increment-strain increment relationship, the strain increment is assumed to be the sum of the elastic strain increment and the plastic strain increment.

$$\{\Delta\varepsilon\} = \{\Delta\varepsilon\}_{elastic} + \{\Delta\varepsilon\}_{plastic}. \tag{5-3}$$

The elastic strain increment is assumed to be completely described by Hooke's law where the two parameters E and G are constant. To estimate the plastic strain increment, the following is required:

(i) The existence of a yield surface

(ii) A flow rule that specifies the general form of the relationship between the incremental stress and the incremental plastic strain.

It is then necessary to define the onset of plasticity, i.e. the point at which purely elastic relations cease to be valid.

It is impractical to test every material for every combination of σ_1, σ_2 and σ_3 stresses. A failure theory (yield criterion) is needed for making predictions on the basis of a material's performance on a simple tensile, compression or shear test. This is necessary to make an assessment of the strength of this material under any conditions of static loading. Classical failure theories are based on the assumption that whatever factor is responsible for the failure in the standard test will also be responsible for the failure under all other conditions of static loading. These failure theories are easily visualised using Mohr's circles. For the tensile test, $\sigma_2 = \sigma_3 = 0$ and there is only one Mohr's circle (Figure 5-7).

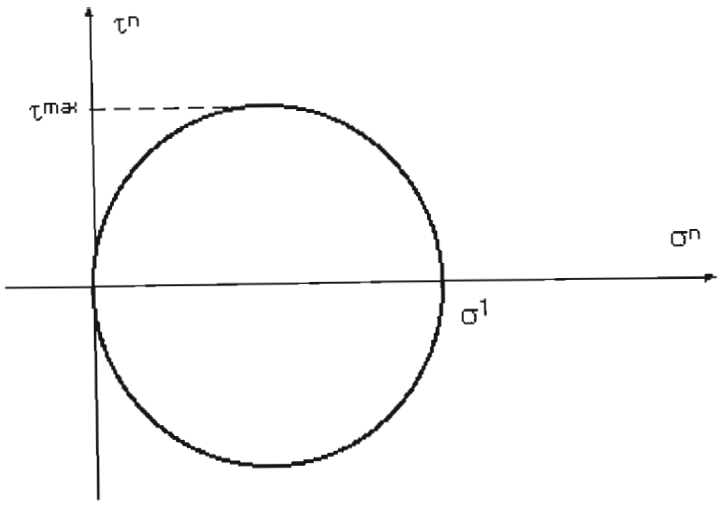

Figure 5-7. Mohr's circle for tensile test of a material. The positive x axis represents tensile stresses.

For example, "maximum-normal stress theory" only takes into account that the material fails in the static tensile test because it is unable to withstand a tensile stress above a certain value. The theory predicts that under any conditions of loading, the material will fail only if σ_1 exceeds this value, or if the largest compressive stress exceeds the uniaxial compressive strength. This theory has been found to correlate reasonably well with test data for brittle fractures, but is not suited for predicting ductile failures.

Suppose that it is postulated that failure during the tensile test occurred because the material is limited by its inherent capacity to resist shear stress. The maximum shear stress experienced by the material in the tensile test equals half the value of σ_1. The so-called "maximum-shear stress theory" predicts that under any conditions of loading, failure will only occur if the maximum shear stress exceeds the value of τ_{max} where:

$$\tau_{max} = \frac{1}{2}(\sigma_1 - \sigma_3). \qquad (5\text{-}4)$$

This theory is sometimes referred to as "Tresca" theory and correlates reasonably well with the yielding of ductile materials such as steel. However, the maximum distortion energy theory is found to correlate better with actual test data for ductile materials (such as the rock bolt unit) during yielding.

The maximum distortion energy yield criterion, also referred to as "maximum-octahedral-shear-stress theory", or more commonly as "von Mises's" theory, recognises that any elastically stressed material undergoes a slight change in shape, volume or both. The energy required to produce this change is stored as elastic energy. Metals in particular can withstand enormous

hydrostatic pressures (where $\sigma_1 = \sigma_2 = \sigma_3$) without damage. Therefore, the criterion suggests that a given material has a definite limited capacity to absorb energy of distortion (i.e. energy tending to change shape but not volume). Attempts to subject the material to greater amounts of distortion energy result in yielding. This is typical of rock bolt failure.

When using von Mises's theory, it is convenient to work with an equivalent stress, σ_E, defined as the value of uniaxial tensile stress that would produce the same level of distortion energy (hence, according to the theory, the same likelihood of failure) as the actual stresses involved. σ_E can also be defined as the value of uniaxial tensile stress which produces the same level of shear stress on the octahedral planes (again, according to the theory, the same likelihood of failure) as the applied tensile stress. In terms of the principal axes, the equation for equivalent stress is:

$$\sigma_E = \frac{\sqrt{2}}{2}\left[(\sigma_2 - \sigma_1)^2 + (\sigma_3 - \sigma_1)^2 + (\sigma_3 - \sigma_2)^2\right]. \qquad (5\text{-}5)$$

In the static tensile test, $\sigma_2 = \sigma_3 = 0$. Then the octahedral shear stress can be evaluated as:

$$\tau_{oct} = \frac{\sqrt{2}}{3}\sigma_1 . \qquad (5\text{-}6)$$

The equivalent stress σ_E has factored out the constant and equals σ_E in the tensile test.

$$\sigma_E = \frac{3}{\sqrt{2}}\tau_{oct} . \qquad (5\text{-}7)$$

If the direct stresses σ_X, σ_Y, σ_Z, σ_{XY}, σ_{YZ} and σ_{XZ} are more readily available, a convenient form of the equivalent stress equation is:

$$\sigma_E = \frac{1}{\sqrt{2}}\left[(\sigma_X - \sigma_Y)^2 + (\sigma_Y - \sigma_Z)^2 + (\sigma_Z - \sigma_X)^2 + 6\left(\tau_{XY}^2 + \tau_{YZ}^2 + \tau_{XZ}^2\right)\right]^{\frac{1}{2}} \qquad (5\text{-}8)$$

Once the equivalent stress is obtained, this is compared with the yield strength S_y from the standard tensile test. If σ_E exceeds S_y, yielding is predicted.

The Mohr-Coulomb Yield criterion has been proposed for geotechnical materials, and is the most widely known failure criterion in rock and soil mechanics (Desai and Christian, 1977). Failure is postulated to occur when the shear stress τ_n and the normal stress σ_n acting on a given failure plane satisfy the linear equation:

$$|\tau_n| + \sigma_n \tan(\phi) - c = 0. \qquad (5\text{-}9)$$

The values of c (the cohesion strength) and ϕ (the angle of internal friction) are found from the testing of multiple samples. Figure 5-8 shows the Mohr circles for a set of triaxial tests, the tangent of which gives the Mohr envelope, which is usually curved in practice.

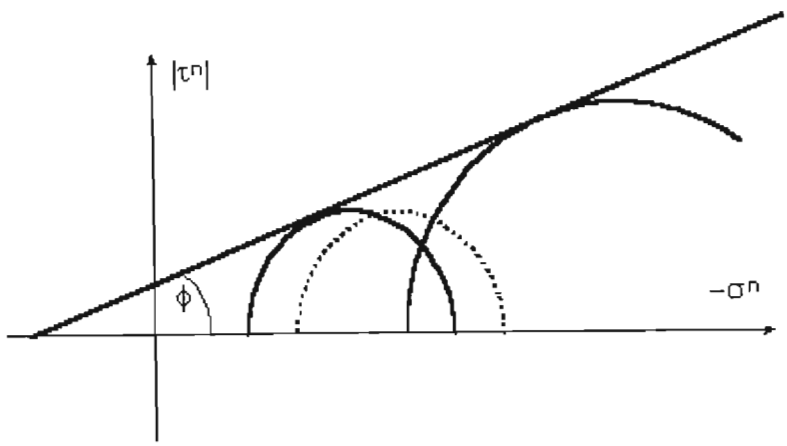

Figure 5-8. Mohr's circles for triaxial tests.

This Mohr envelope corresponds to Coulomb's Criterion. In terms of principal stresses this can be written as:

$$\frac{1}{2}(\sigma_1 - \sigma_3) = -\frac{1}{2}(\sigma_1 + \sigma_3)\sin(\phi) + c \cdot \cos(\phi). \qquad (5\text{-}10)$$

For the special case of frictionless materials (for which $\phi = 0$), this reduces to Tresca's maximum shear stress criterion, $|\tau_n = c|$, and the cohesion becomes equal to the yield stress in pure shear.

The Mohr-Coulomb surface exhibits corners (or singularities) in a three-dimensional principal stress space. The resulting general yield or failure function, with singularities can give rise to some difficulties in numerical analysis. Also, the criterion neglects the influence of the intermediate principal stress σ_2.

The Drucker-Prager yield criterion represents the first attempt to approximate the Coulomb criterion by a simple smooth function, and has the form:

$$\alpha(\sigma_1+\sigma_2+\sigma_3)+\left(\frac{1}{6}\left[(\sigma_1-\sigma_2)^2+(\sigma_2-\sigma_3)^2+(\sigma_3-\sigma_1)^2\right]+\sigma_{12}^2+\sigma_{23}^2+\sigma_{31}^2\right)^{\frac{1}{2}}=\beta \quad (5\text{-}10)$$

If α = 0, in this three-dimensional principal stress space, using graphical methods to match the Drucker-Prager criterion with a shear-stress apex of the Coulomb criterion, then:

$$\alpha=\frac{2\,sin(\phi)}{\sqrt{3}(3-sin(\phi))}, \quad (5\text{-}11)$$

$$\beta=\frac{6c\cdot cos(\phi)}{\sqrt{3}(3-sin(\phi))}. \quad (5\text{-}12)$$

The Drucker-Prager surface may be described as an extension of the von Mises's surface for pressure-dependent materials such as rock, soil and concrete (or grout) (Desai and Christian 1977).

A flow rule defines the relationship between an increment of plastic strain $\{\Delta\varepsilon\}_{plastic}$ and the present state of stress (σ) for a yielding element of material. Since the rock bolt undergoes continued and increasing deformation as slip occurs, it may be analysed as a plastic model. In this case, there is a unique value for $\{\Delta\varepsilon\}_{plastic}$ found from the material stress-strain curve, for each value of stress.

5.3.3 Application of theories to grout separation and quartzite fracture

As observed from the physical testing (section 5.2), the sides of the sections of the bolt adjacent to a shear slip plane in the test rig are displaced along plane AB (see Figure 5-9) through the relatively soft grout during shear deformation.

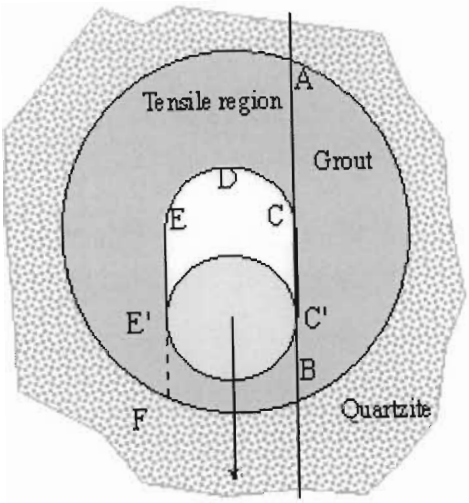

Figure 5-9. Representation of the displacement of the rock bolt through the grout.

When the grout in the tensile region reaches a certain critical stress, it separates from the rock bolt along CDE as slip increases and point C on the bolt is displaced to point C'. The region CBFE, initially occupied by grout, is compressed to region C'BFE' (neglecting lateral strains). In this finite element analysis, elements cannot separate from each other since the nodes defining the element boundaries are shared. The node at point C will therefore move to point C'. For this reason, different material properties must be specified for the separating grout to those of the rest of the grout.

One method of dealing with this problem is to delete applicable grout elements as slip develops. As the test is only concerned with the rock bolt behaviour this was found to be far too arduous a process unless applied to the single value of slip at bolt failure.

In the physical tests (section 5.2), the quartzite rock was prevented from fracturing through the blocks by a steel ring. It is therefore assumed that should the quartzite model exceed its yield point during slip, fracture through the continuum need not be considered. This may not be a valid assumption for actual behaviour, but is considered acceptable if comparisons of results are to be made with the physical model.

5.3.4 Techniques for non-linear finite element analysis

The analysis of the rock bolt system exhibits two types of non-linearity. Since the large strains associated with slip result in plastic deformation of the bolt, and in the crushing of the grout in highly compressed areas, the main mechanism of deformation is material non-linearity. The separation of the grout from the bolt in areas of high tensile stress is the other non-linearity. Material non-linearity's result from a non-linear stress-strain relationship at some point, or points, in a continuum. The stiffness of the system is affected by the large displacement, and

equilibrium must be established in the current configuration. At each equilibrium state along the equilibrium path, the resulting set of simultaneous equations [K](D) = {P}, where P is the applied load, is non-linear, since the stiffness matrix [K] is no longer constant. Note that (D) is identical to (Δ). Therefore, a direct solution is not possible and an iterative method is required. Non-linear behaviour is approximated as piecewise linear, and the linear laws are thus used for each piece. At the end of each iteration, a check is made by the relevant computer software to test whether the iteration converged within realistic tolerances, or if it is diverging (Zienkiewicz and Cheung, 1967).

For the step-iterative procedure, the applied load is broken down into several "time" steps (Figure 5-10).

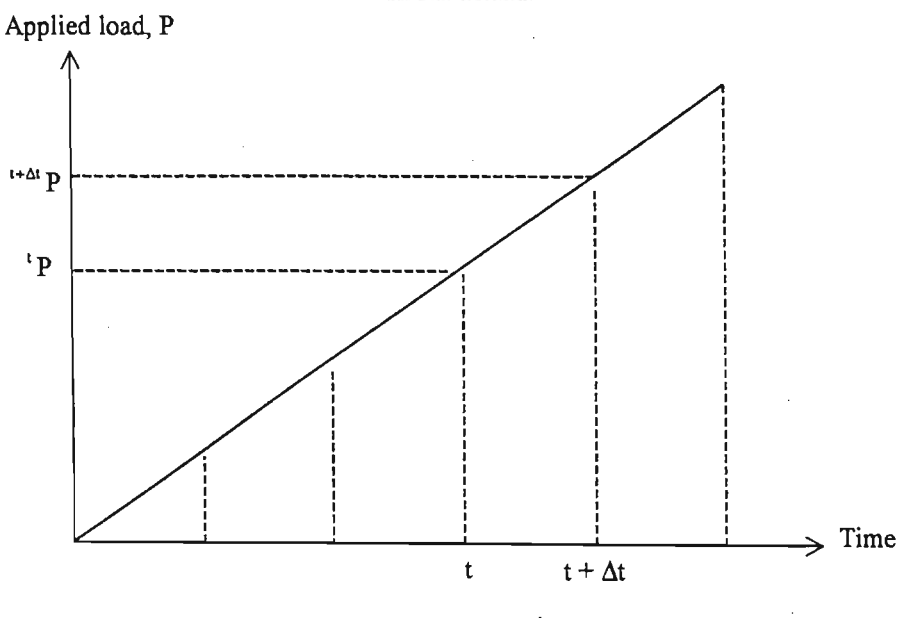

Figure 5-10. Graphical representation of applied load via time steps.

In non-linear static analysis the basic set of equations to be solved at any time step t + Δt is:

$$ {}^{t+\Delta t}\{P\} - {}^{t+\Delta t}\{R\} = 0 \qquad (5\text{-}13) $$

Where {P} is the vector of externally applied nodal loads and {R} is the vector of internally generated nodal reactions. Since the initial nodal forces ${}^{t+\Delta t}\{R\}$ depend on nodal displacements at time t + Δt, denoted here as ${}^{t+\Delta t}\{D\}$, an iterative method must be used.

Thus the aim is to find the displacement such that equation (5-13) is satisfied. In the Newton-Raphson procedure, the value of the stiffness matrix is established at time t + Δt by initially using the value at time t.

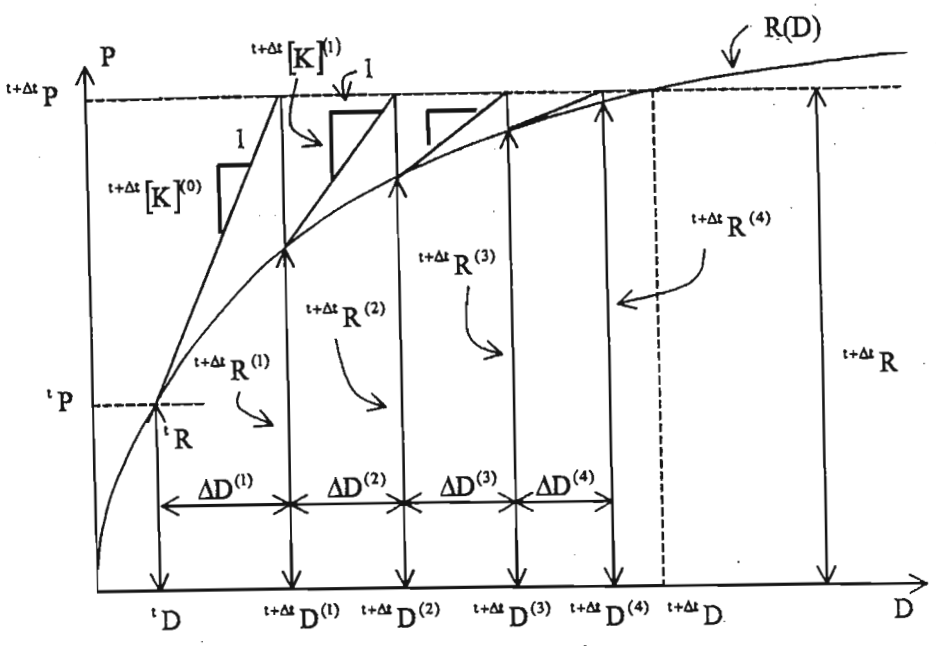

Figure 5-11. Newton-Raphson iterative method.

As shown in Figure 5-11, for iteration number (i-1):

$$\{\Delta P\}^{(i-1)} = {}^{t+\Delta t}\{P\} - {}^{t+\Delta t}\{R\}\ , \tag{5-14}$$

$${}^{t+\Delta t}[K]^{(i-1)} \cdot \{D\}^{i} = \{\Delta P\}^{i-1}\ . \tag{5-15}$$

Combining these two equations, we can write:

$${}^{t+\Delta t}[K]^{(i-1)} \cdot \{D\}^{(i)} = {}^{t+\Delta t}\{P\} - {}^{t+\Delta t}\{R\}^{(i-1)}. \tag{5-16}$$

Under the Newton-Raphson scheme, the matrix [K] is formed at each iteration and then decomposed using Gaussian elimination to evaluate $\{\Delta D\}^{(i)}$. This iteration scheme has a high convergence rate. However, because of the continual formation and decomposition of the stiffness matrix, the method can become prohibitively expensive for large systems (such as the three-dimensional rock bolt problem).

The value of the internal load {R}, after n increments, in any time step is calculated as:

$$ {}^{t+\Delta t}\{R\}^{(n)} = {}^{t+\Delta t}\{R\}^{(0)} + \sum_{i=1}^{n-1} {}^{t+\Delta t}\{R\}^{(i)} . \qquad (5\text{-}17) $$

In the so-called "modified Newton-Raphson scheme", the tangential stiffness matrix is formed and decomposed at the beginning of each time step (or at some other specified re-formation interval) and used throughout the iterations associated with that step. It has to be emphasised that the actual value of the stiffness matrix at time t + Δt is in itself not of any great importance, as long as equation (5-13) is satisfied.

For any incremental procedure based on iterative methods to be effective, a practical termination scheme must be implemented. At the end of each iteration a check is made by the software package to test if the iteration converged within a required tolerance (TOL), or if it is converging. Convergence occurs if equation (5-15) tends to zero.

The "displacement convergence" criterion is based on the displacement increments during iterations and is presented mathematically as:

$$ \left| \{\Delta D\}^{(i)} \right| \leq \mathrm{TOL}_d \left| {}^{t+\Delta t}\{\Delta D\}^{(i)} \right| , \qquad (5\text{-}18) $$

where $|\{..\}|$ denotes the Euclidean norm of {..}.

The "force convergence" criterion is based on the out-of-balance (residual) loads during iterations. It requires that the norm of the residual load vector be within a tolerance of the applied load increment, i.e.:

$$ \left| {}^{t+\Delta t}\{P\} - {}^{t+\Delta t}\{R\}^{(i)} \right| \leq \mathrm{TOL}_f \left| {}^{t+\Delta t}\{P\} - {}^{t}\{R\} \right| . \qquad (5\text{-}19) $$

In the "energy tolerance" criterion, the increment in the internal energy during each iteration, which is the work done by the residual forces through the incremental displacements, is compared with the initial energy increment. Convergence is assumed to be achieved when the following is satisfied:

$$ \left(\{\Delta D\}^{(i)} \right)^T \cdot \left({}^{t+\Delta t}\{P\} - {}^{t+\Delta t}\{R\}^{(i-1)} \right) \leq \mathrm{TOL}_e \cdot \left(\{\Delta D\}^{(1)} \right)^T \cdot \left({}^{t+\Delta t}\{P\} - {}^{t}\{R\} \right) . \qquad (5\text{-}20) $$

In addition, a number of schemes have been described as divergence criteria, and follow similar lines to the aforementioned criteria.

5.3.5 Establishment of finite element model

The three-dimensional geometry of the finite element computer model as used in the initial analysis is shown in Figure 5-12. All dimensions were taken from those of the laboratory test apparatus (section 5.2).

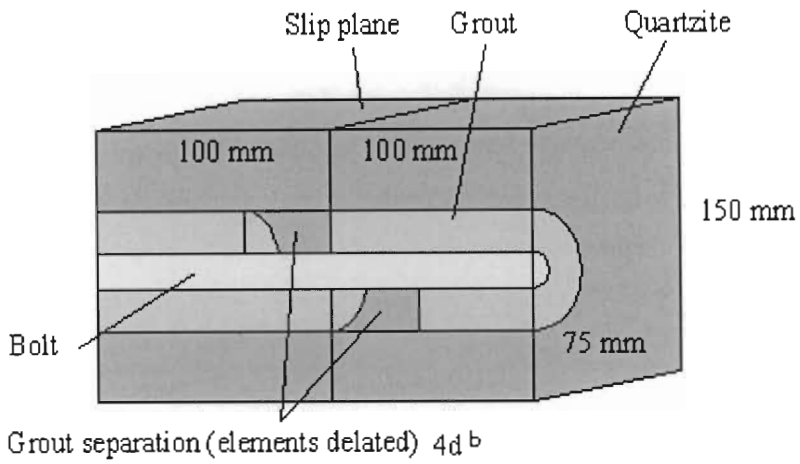

Figure 5-12. Geometry of finite element model to simulate laboratory shear testing.

Several assumptions, which were made for the construction of the model, were:

(i) The bolt and grout were given concentric circumferences (no eccentricities).

(ii) The grout was assumed to fill completely and uniformly the gap between the bolt and the rock.

(iii) A 1 mm gap was created between the two quartzite blocks.

The mesh of eight-node three –dimensional elements, which defined the model, is illustrated in Figure 5-13.

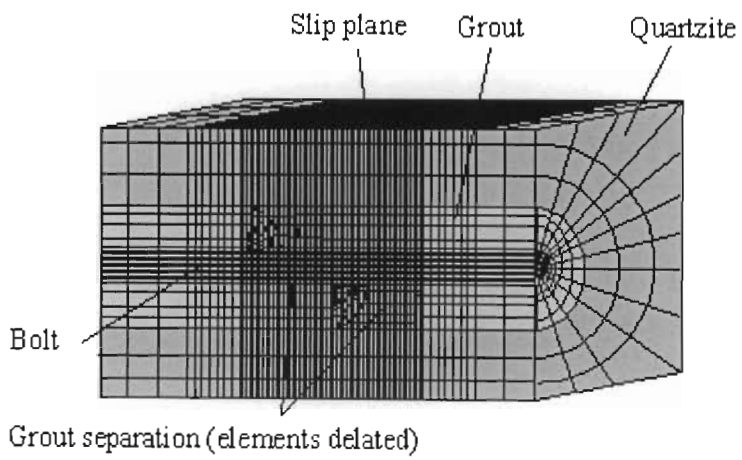

Figure 5-13. Mesh of finite element model of laboratory shear test.

The mesh is refined in the critical region adjacent to the slip plane to cater for the increased stress gradients. Because the intention of the analysis is to replicate conditions of rock bolt failure, grout elements were deleted in areas of tensile separation. However, it was found that including an additional iterative method to delete grout elements as they reached critical tension during slip was highly impractical, due to the amount of time involved.

By exploiting the symmetry within the model (Figures 5-12 and 5-13), both of the blocks were loaded in opposite directions. Forced displacements were applied to their exterior boundaries as shown in Figure 5-14. The relative displacement of the blocks was increased during the simulation.

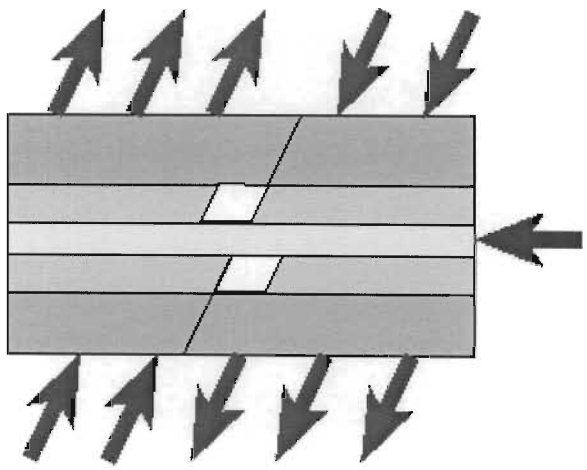

Figure 5-14. Generic loading of model (inclination of shear plane and loads varied according to model analysis).

The three-dimensional, non-linear solution was found to diverge at less than 1 mm of slip of the shear plane. To determine the reason for this, a simple two-dimensional plane stress model was created (Figure 5-15) and a linear static analysis performed.

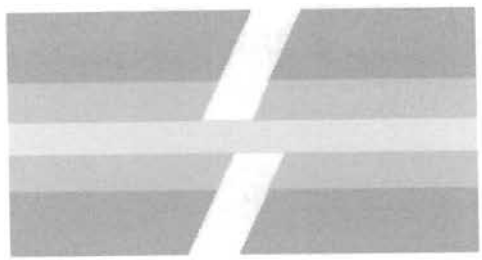

Figure 5-15. 2-dimensional plane stress model.

Figure 5-16 shows the example of the resulting deformation of the system.

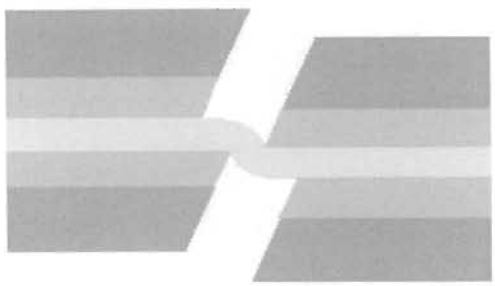

Figure 5-16. 2-dimensional linear static deformation

Overlap of the elements, and the bolt swelling at the slip plane, was noted under this analysis. It was determined that the bolt nodes are displaced "through" the grout elements at the slip plane, since they are not connected to these elements. Thus, slide lines are required to simulate the bolt-to-grout contact. This non-linear option was thus implemented in the finite element analysis. Because of this additional requirement, a three-dimensional analysis becomes far too complicated, and time-consuming, to perform on a regular basis. A two-dimensional analysis is thus more practical for further evaluation.

The generic two-dimensional model used for further analysis is illustrated in Figure 5-17.

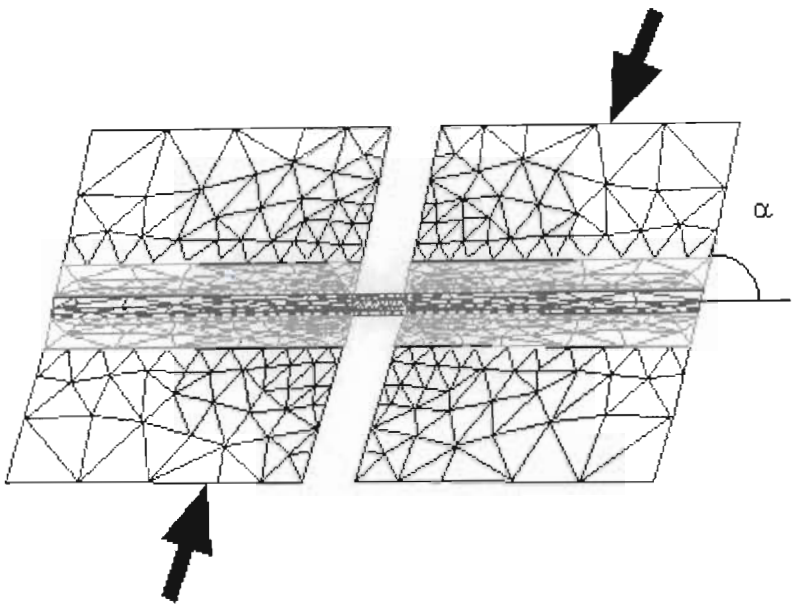

Figure 5-17. Generic two-dimensional finite element model with mesh.

A more refined mesh is implemented adjacent to the slip plane to improve model accuracy in this area. It was important that the grout elements in this area be sufficiently refined since grout deformation into the slip plane occurs as the grout is squashed between the bolt and the rock. A refined mesh is required to satisfactorily simulate the shape of the bulging grout so that the resulting effect on the bolt, via the slide lines, is realistic. Also, the bolt elements must be refined at the slip plane because, from the test results (section 5-2), maximum bolt deformation occurs here.

The gap between the two blocks was increased to 3.5 mm within the model, as the grout and quartzite are envisaged, from the physical tests, to fail and dilate near the bolt at the slip plane.

It is necessary to determine the optimum mode of analysis in the numerical model that best represents the physical model. An initial attempt to model the physical test (the bolt, grout and quartzite) was defined with plane-stress element properties. Although the deformed bolt had the correct shape, the largest stresses are seen to occur due to bending away from the slip plane (Figure 5-18).

Figure 5-18. Results of plane stress analysis.

Under plane strain analysis, using plane strain elements, the bolt is now seen to experience maximum stresses and deformation at the slip plane (Figure 5-19). This is considered to be more representative of the mode of failure of the laboratory test programme. However, the degree of deformation in this area is now greater than that encountered in the laboratory testing programme.

Figure 5-19. Results of plane strain analysis.

On the basis of the results discussed above, a decision was made on the choice of the final finite element model (FEM). The two-dimensional plane stress model was chosen for the numerical simulation of the rock bolt behaviour. The properties of the materials, as utilised within the model, are indicated below:

Rock bolt

Young's modulus = 206 GPa

Poisson's ratio = 0.33

Grout

Young's modulus = 10.4 GPa

Poisson's ratio = 0.12

Cohesion strength = 8.8 MPa

Angle of internal friction = 36.9°

Rock mass (quartzite)

Young's modulus = 73.2 GPa

Poisson's ratio = 0.13

Cohesion strength = 42 MPa

Angle of internal friction = 43°

The idealised stress-strain curve of the rock bolt material is shown in Fig. 5-20.

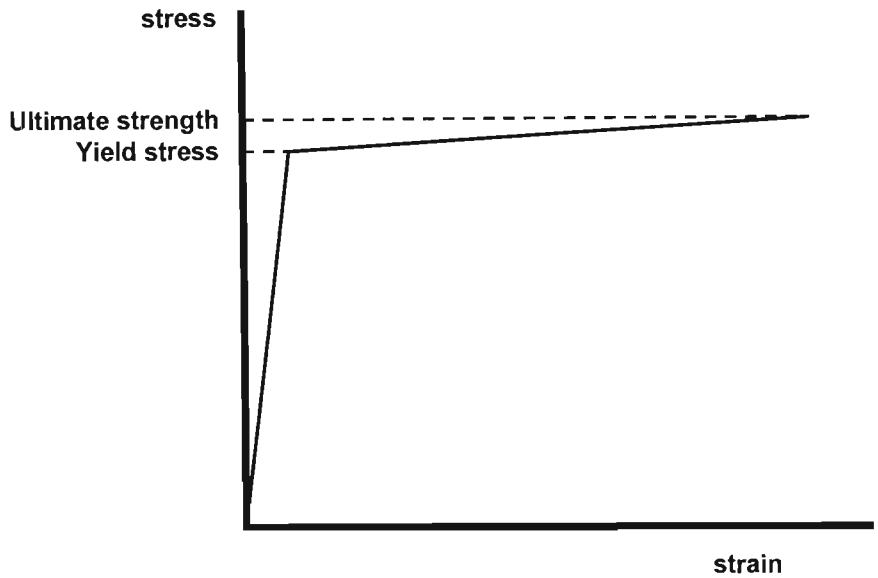

Figure 5-20. Stress-strain diagram of the rock bolt unit.

The rock bolt is connected to the rock mass by the grout. This material possesses brittle properties and its fracture stress is sufficiently less than the plasticity limit of the steel.

It is interpreted from the laboratory physical modelling that the deformability of the bolt depends on the diameter of the hole in the rock. Within the numerical analysis consideration is primarily given to the relationship $R_h/R_b = 2.5$, where R_h and R_b are the hole and the bolt radii, respectively. Calculations are also made for $R_h/R_b = 5.0$ and $R_h/R_b = 2.0$

It is assumed that the grout adjacent to the sliding plane becomes fractured almost simultaneously with the start of shear. Accordingly, two cuts are made in the initial mesh.

The ultimate stress for the steel rock bolt, for analysis based on von Mises's criterion, is 738.5 MPa. This rock bolt strength sustains a rock mass displacement of up to $4R_b$, and at this point failure of the rock bolt starts to occur. For a typical 16 mm diameter rock bolt this would equate to a displacement of the shear plane of approximately 32 mm. It is also seen that the maximal von Mises's stress occurs in the shear plane or its immediate vicinity. These preliminary results agree well with the physical laboratory experimental results (section 5.2).

5.3.6 Parametric study of the shear characteristics of rock bolt systems

In order to gain an understanding of the influence of the rock bolt systems on the response to shear of a discontinuity within a rock mass, a parametric study was conducted based on the numerical model calibrated against the physical laboratory model. The following parameters are varied in the numerical modelling:

- type of steel (relation between yield stress and ultimate failure strength)
- diameter of the rock bolt, in relation to the hole diameter
- direction of the rock mass displacement in relation to the axis of the rock bolt

5.3.6.1 Influence of steel type

The yield stresses and ultimate tensile strength are given in the Table 5-2.

Table 5-2 Mechanical properties of different types of steel.

Steel Grade	Yield stress (MPa)	Ultimate tensile strength (MPa)
BS 4360	250	350
WR 50 A	345	380
SABS 1431 300WA	300	450
SABS 1431 350WA	350	480
SABS 1431 450WA	450	555

The results of the numerical analysis are summarised in Figure 5-21. Figure 5-21 corresponds to a rock bolt diameter, d^b , equal to 16 mm, hole diameter, $d^h = 2d^b$, and direction of the displacement perpendicular to the axis of the rock bolt.

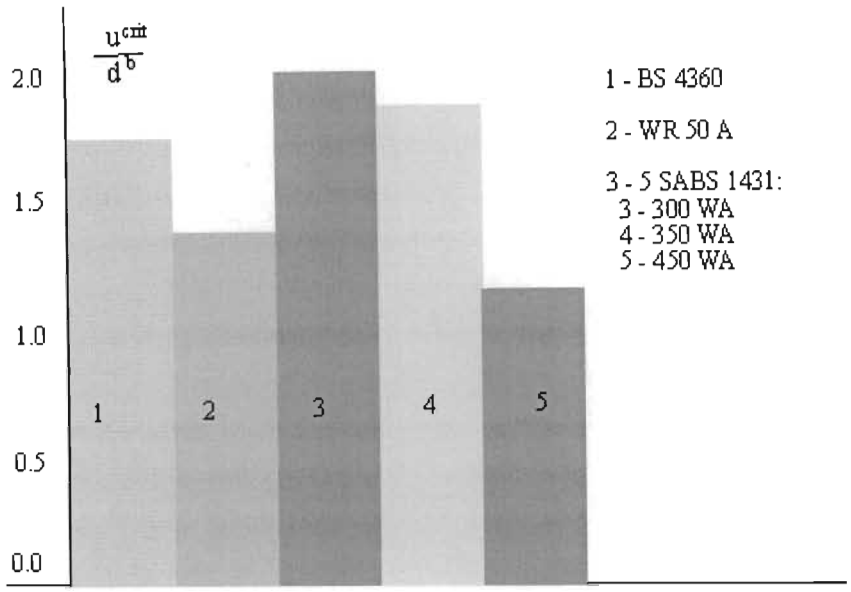

Figure 5-21.Dependence of critical displacement on the type of steel.

where, in figure 5-21: u^{crit} is the displacement at failure as a proportion of the initial rock bolt diameter.

This analysis clearly indicates the importance of the yield capacity within the rock bolt prior to ultimate failure.

5.3.6.2 Influence of rock bolt diameter

This analysis evaluated the relationship between shear deformation and the interaction of the rock bolt diameter in relation to the hole diameter. The evaluation considered rock bolt diameters of: 12 mm, 16 mm, and 20 mm and for different ratios d^b/ d^h : 0.1, 0.25, 0.4, 0.5, 0.6, 0.75, 0.9. The results are summarised in Figure 5-22.

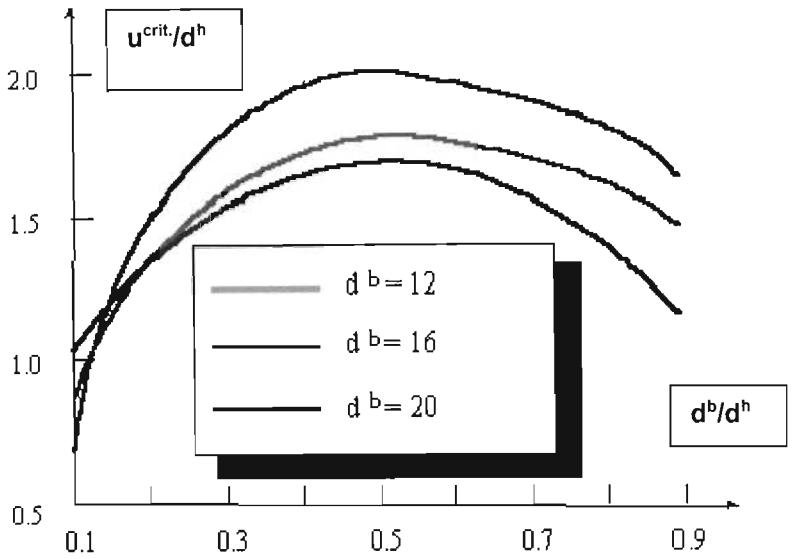

Figure 5-22. Results for analysis of different bolt and hole diameters.

Analysis of Figure 5-22 indicates that the optimum ratio of rock bolt diameter to hole diameter is 0.5. In excess of this ratio there is a tendency for premature guillotining of the rock bolt. It is also indicated in Figure 5-22 that, for a 16 mm rock bolt, typical of underground installations, the maximum shear displacement of rock mass is approximately equal to $2d^b$, i.e. 32 mm. This value correlates well with the displacements obtained experimentally for the 16 mm rock bolts which were indicated to be able to sustain approximately 33 mm displacement (Table 5-1). At small rock bolt diameters, in relation to a given hole diameter, the earlier failure of the system under conditions of very small deformation is due to the critical stress level being reached in the rock bolt unit at these relatively low displacements.

5.3.6.3 Influence of angle of shear plane

The orientation of the shear plane, relative to the rock bolt axis, will determine the mechanism of loading of the rock bolt unit. With reference to loading condition as defined in Figure 5-17, if the angle of the shear plane, relative to the rock bolt axis, is $\alpha < 90°$ (Figure 5-17), then the rock bolt will be placed in compression due to shear deformation. If the angle $\alpha > 90°$, then the rock bolt will be placed in immediate tension due to the shear deformation. The relationship between shear deformation and the angle of rock bolt orientation (α), based on a rock bolt diameter of 16 mm, and $d^h = 2d^b$, is shown in Figure 5-23.

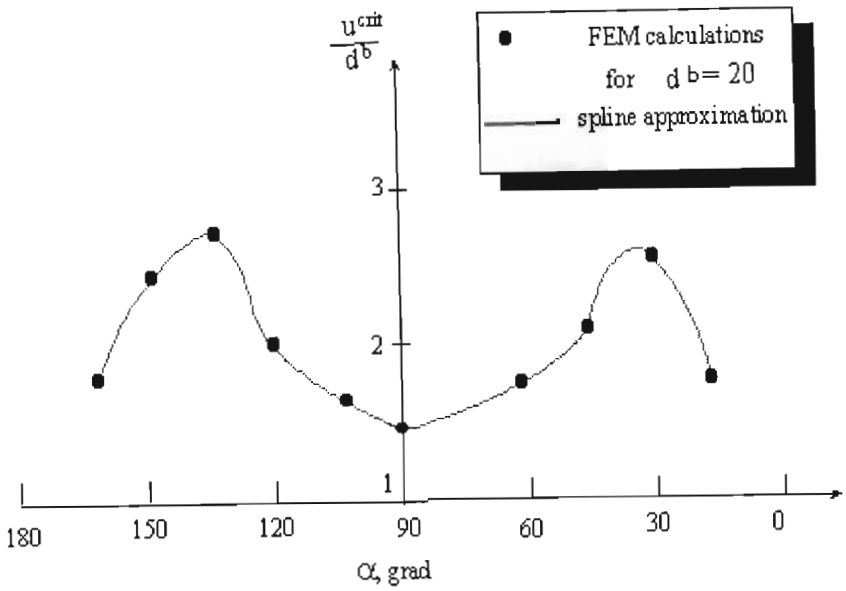

Figure 5-23. Influence of shear plane orientation and effective shear direction on rock bolt shear deformation.

It is indicated from this analysis that the rock bolt sustains the maximum shear deformation at an angle (α) of approximately $|50°|$ from the vertical (90°).

5.4 Design considerations of rock bolt systems under shear loading conditions

The physical and numerical experimental work is considered to give good insight into practical considerations for the design of rock bolt systems under conditions of shear loading. Indicated below are design considerations that may be applied to the design of tunnel support systems in the mining industry.

- Increase in the effective bond strength between the rock bolt unit and grout annulus results in reduced ability of the rock bolt system to accommodate shear displacement, particularly under dynamic loading conditions.

- Yielding type tendons are able to accommodate the greatest degree of shear displacement by yielding along the length of the grout annulus under quasi-static loading conditions and allowing increased bending of the bolt or cable at the shear plane. However under dynamic loading conditions the ability to translate the tensile strains along the rock bolt / cable unit, to enable sufficient yield, may be limited, resulting in premature failure of the rock bolt system.

- The relative brittleness of the rock bolt material in the direction of shear will also govern its ability to accommodate shear displacement. The more ductile the material in the plane of shear, the better the rock bolt is able to undergo plastic bending at the shear plane. This results in the bending of the rock bolt sub parallel to the direction of shear and thus

translating the mode of failure from shear to tensile. This results in an enhanced ability to resist shear forces and accommodate shear displacement. The theoretical shear strength of a rock bolt is half of its ultimate tensile strength. Generally under dynamic loading the support unit offers reduced shear resistance and deformation due to the reduced toughness of the rock bolt shaft. Numerical modelling has also indicated the relative importance of the selection of steel type on shear deformation capacity.

- The higher the tensile strength of the rock bolt unit the greater its theoretical shear resistance, with due regard of the above mentioned failure mechanisms. However, it is also shown by numerical modelling that as the "diameter" (two-dimensional analysis) of the rock bolt is increased in relation to the borehole "diameter", to increase its tensile strength, its ability to deform plastically may be reduced and the overall increased shear performance not realised. Numerical modelling has indicated an optimum ratio of rock bolt diameter to hole diameter of 0.5 for maximum shear deformation.

- The orientation of a rock bolt system to potential planes of shear will influence its capacity to accommodate shear deformation. Although it is generally not practical to achieve a desired, optimum installation orientation, consideration can be given to the influence of the orientation, and direction of loading, on maximum shear deformation capacity.

Previous investigations (Chapters 3 and 4) have indicated the importance of consideration of shear within the rock mass in the performance of the support system and thus stability of the excavation. The above analysis has allowed the derivation of practical design considerations for rock bolt reinforcement systems where shear deformation within the rock mass may be envisaged.

Chapter 6

6. Analysis of load deformation characteristics of fabric support systems

6.1 Introduction

Fabric support constitutes the component of the support system that spans the exposed, and potentially unstable, rock mass between the rock bolt reinforcement units. Fabric support systems typically comprise various types of shotcrete, mesh and lacing systems, or the more recent developments of flexible membranes. They may interact directly with the rock mass through adhesive properties, or provide containment in response to dilation of the rock mass between anchor points. The relative response of the fabric support element to the rock mass dilation may greatly influence the distribution of load within support system. This in turn will influence the required design capacity of the components of the support system.

Fabric support systems have been recognised to provide an essential support role, especially in highly fractured or discontinuous rock mass structures, where the reinforcement of the rock mass by rock bolts alone is practically and economically limited. Within the South African mining industry, this is particularly experienced under high stress and dynamic loading conditions. Although the importance of fabric support elements within the support system has been recognised, the evaluation of the capacity of these support systems and their interaction with the rock mass has been very limited. The design of such systems has primarily been based on empirical design guidelines, which are thus applicable only in their appropriate environments, and as such may be problematic with regard to design under other rock mass conditions. This aspect of the research evaluates the capacity of typical fabric support systems for evaluation against the estimated demand on such systems as derived from the proposed design procedure (Figure 6-1).

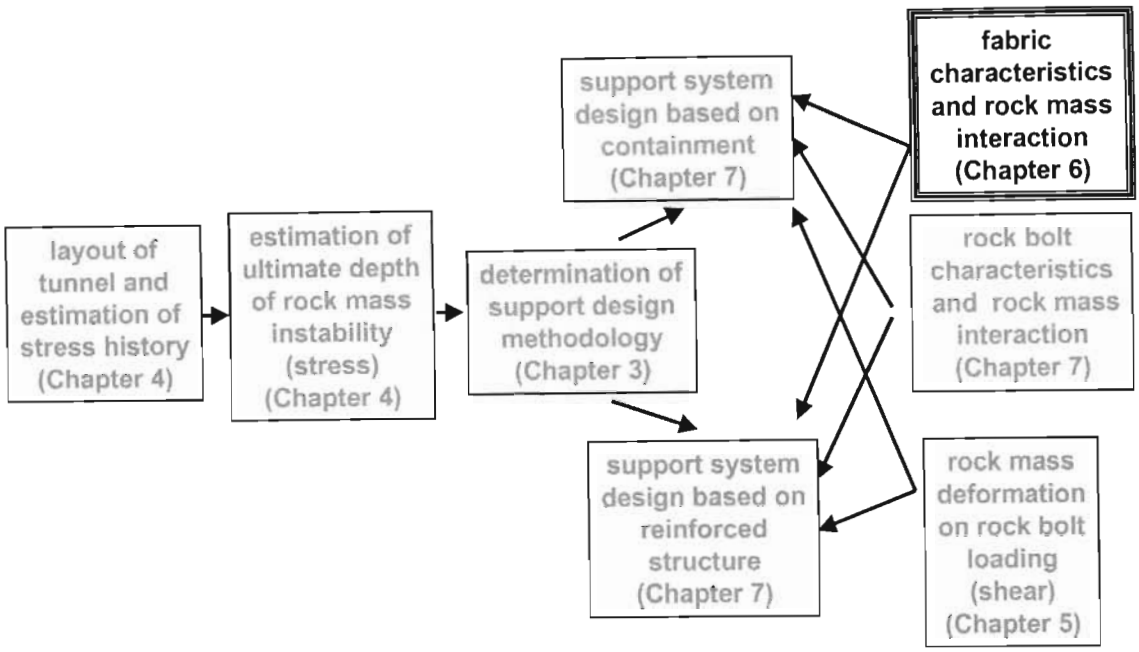

Figure 6-1. The relevance of the research conducted in Chapter 6 within the overall proposed tunnel support design procedure.

The most widely used fabric support system is that of steel wire mesh with rope lacing. The steel wire mesh may be either diamond mesh or weld mesh, and the lacing component of the system is often made from de-stranded hoist rope of approximately 10 mm to 20 mm diameter. The mesh panels afford a flexible, high-areal-coverage fabric capable of preventing the unravelling of a highly discontinuous rock mass structure. The lacing component of this system provides the higher capacity to the system to control the larger rock mass deformation or the instability of large isolated blocks.

Ortlepp (1983) has conducted previous work on the laboratory load deformation characteristics of mesh and lace systems and the in situ characteristics of shotcrete. These tests are comparable to the current set of investigations as discussed in the following section.

6.2 Laboratory and in situ testing procedure of mesh and lace support

Laboratory testing of typical mesh and lacing support components was conducted in order to evaluate the relative capacity and deformation characteristics of these fabric type supports (Roberts 1995). The testing apparatus was constructed to enable testing of representative samples of the fabric and also to be compatible with the available testing equipment. The mesh and lace testing frame, as shown in Figure 6-2, allows central loading of a mesh panel of dimensions approximately 800 mm square, with fixed boundary conditions.

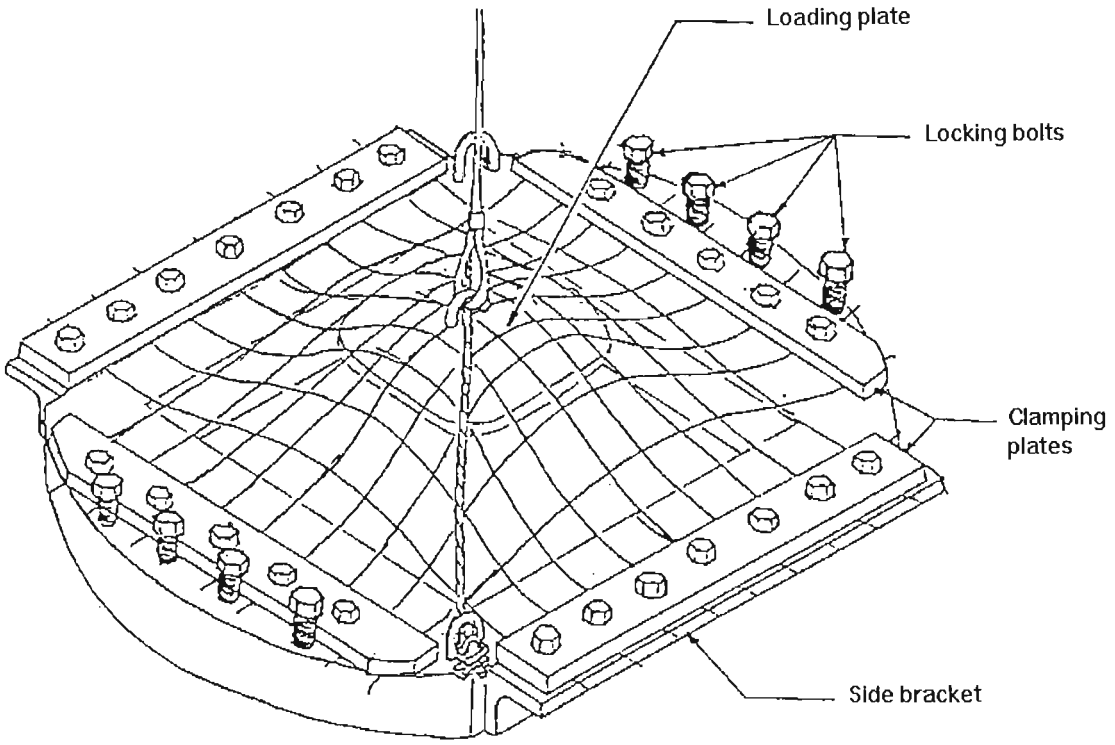

Figure 6-2. Mesh and lacing laboratory testing frame.

The loading plate, which is attached to the testing machine via a rope sling, had chamfered edges to prevent premature cutting of the mesh wire strands with increased deflection. The clamping plates, which impose the boundary conditions, were originally considered to enable varying clamping forces representative of in situ boundary conditions. However, initial testing revealed that the laboratory imposed boundary conditions could not simulate those typical of in situ, and thus for comparative purposes the plates were subsequently rigidly clamped. The testing frame also allowed for the inclusion of lacing rope diagonally spanning the mesh panel. The lacing rope is clamped on the edge of the frame. Again it was difficult to obtain tension in the lacing rope representative of the in situ conditions, which are typically tensioned to approximately 3 – 5 tonnes.

The laboratory testing programme comprised both static and dynamic loading of typical mesh and lacing support components. Loading was applied perpendicular to the mesh panel via the loading plate that was attached to the hydraulic ram within the Terratek test rig. This test equipment allows loads to be applied at rates up to 3 m/s, which are currently considered typical of underground loading rates under dynamic (rockburst) conditions.

Due to the difficulties of the representation of mesh and lacing systems under laboratory conditions, it was considered necessary to also conduct an in situ evaluation. The equipment for this test series comprised a loading plate attached to a hydraulic ram, which was inserted between the fabric and the rock wall as illustrated in Figure 6-3.

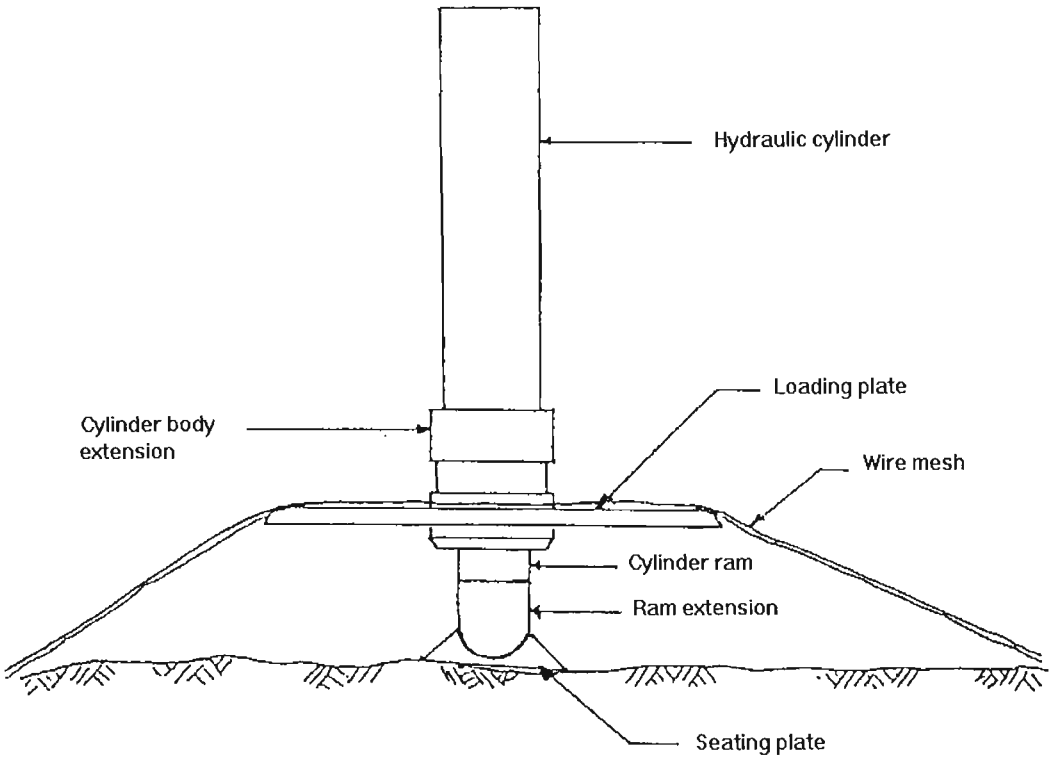

Figure 6-3. In situ mesh and lacing testing equipment

This equipment had the major advantage of being reasonably light and portable, and thus enabling a comprehensive testing programme to be conducted in underground conditions. The load - deflection characteristic of the mesh and lace fabric in situ was determined under static loading conditions only. To obtain an estimate of the overall stiffness of the fabric support system, three measurements (A to C, Figure 6-4) were obtained for each mesh type and lacing configuration.

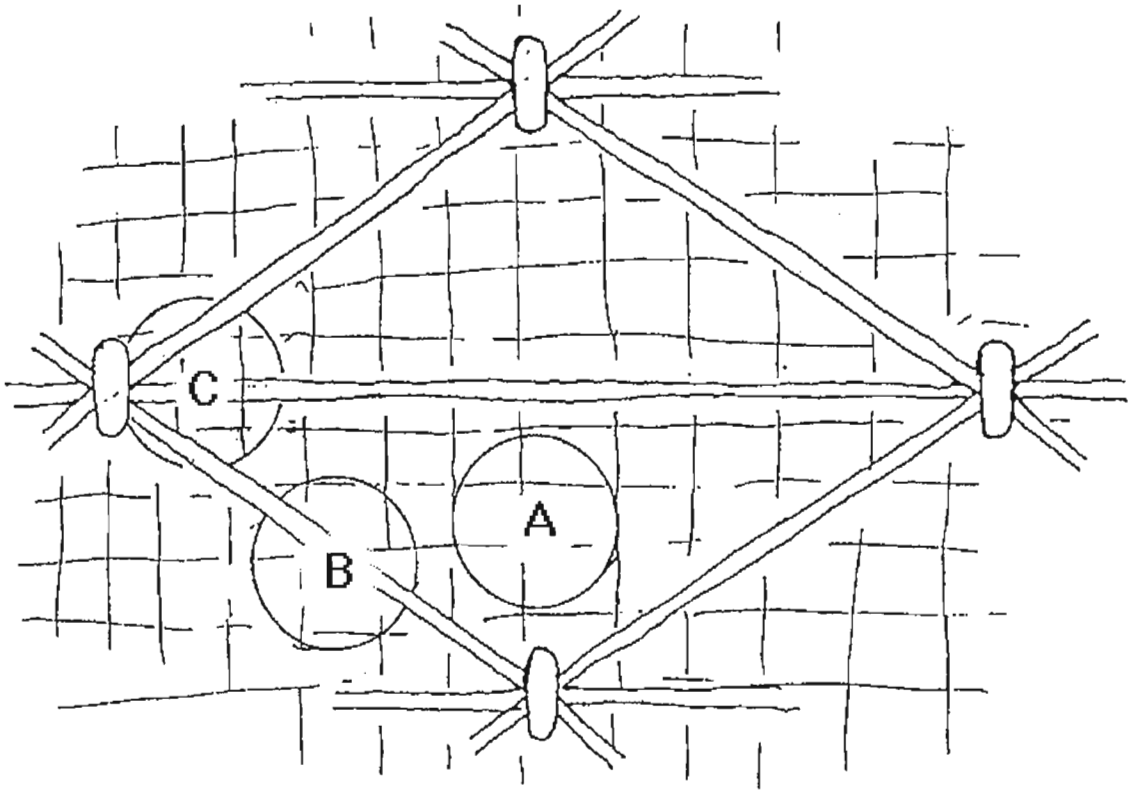

Figure 6-4. Mesh and lace support system load - deflection measuring points.

The in situ testing programme evaluated six lacing configurations and four mesh types typical of those used within the industry; these are specified in detail under the analysis of results (section 6.3). A standard lacing rope diameter of 16 mm was utilised in all the test sections. Anchorage of the mesh and lacing to the rock mass was by means of shepherd crook, rebar rock bolts on the designated pattern. These rock bolts would provide a rigid point of anchorage of the fabric support system relative to the rock wall.

6.3 Laboratory evaluation of mesh and lacing systems

6.3.1 Results of laboratory testing program

The initial evaluation programme of the mesh and lacing support systems was conducted within the laboratory (Roberts 1995). As discussed previously, it was difficult to obtain boundary conditions on the testing frame that were considered to be comparable with those in situ. Thus the test programme concentrated primarily on the relative evaluation of the different mesh types typical of underground use. Examples of the typical quasi static results for weld mesh and diamond mesh respectively are illustrated in Figures 6-5 and 6-6.

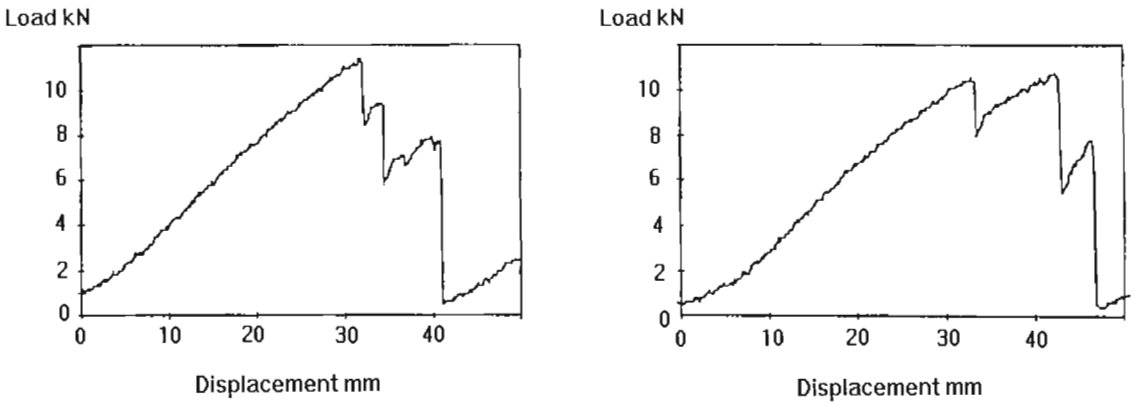

Figure 6-5. Load - deformation results under quasi static loading for 75 mm weld mesh

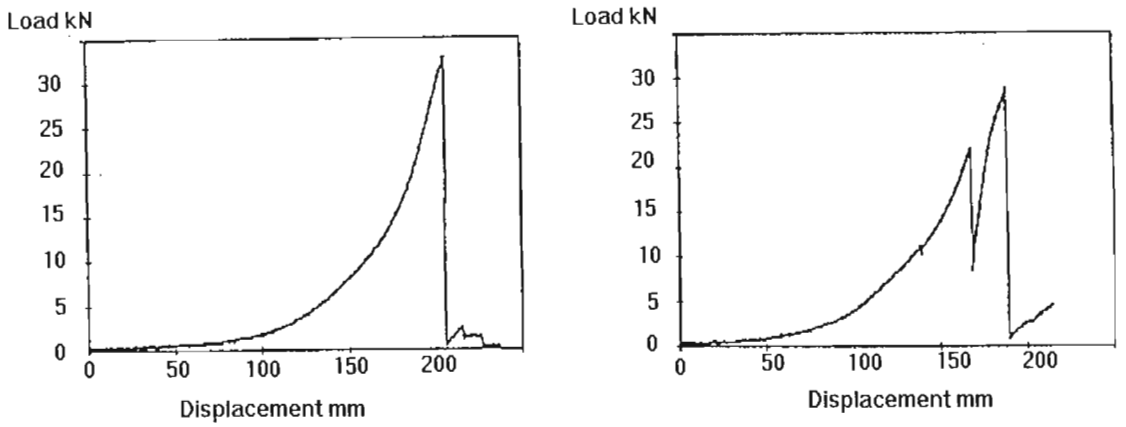

Figure 6-6. Load - deformation results under quasi static loading for 75 mm diamond mesh.

Analysis of the relative load deformation characteristics of the weld mesh compared to the diamond mesh indicates a far greater initial stiffness, but lower ultimate load and displacement. The periodic drops in the load bearing capacity during the tests were observed to correspond to the periodic failure of individual wire strands within the mesh fabric. This would continue until total loss of integrity of the mesh usually in the vicinity of the loading plate would result in termination of the test.

A summary of the results for the laboratory test programme is given in Table 6-1 for static and dynamic loading conditions.

Table 6-1. Summary of average peak laboratory load - deformation characteristics for typical mesh panels.

Description	Static (average)				Dynamic (average)			
	Load kN	Disp mm	kN/m m	Energy J	Load kN	Disp mm	kN/m m	Energy J
75 mm weld mesh	11.3	40	0.28	226	15.3	59	0.26	451
100 mm weld mesh	7.8	68	0.11	265	13.4	59	0.23	395
75 mm dia. mesh	31	198	0.16	3069	13.4	151	0.09	1011
100 mm dia. mesh	26.7	176	0.15	2350	29	144	0.2	2088
50 mm dia. mesh	39	196	0.2	3822	37	184	0.2	3404
75 wld msh + lace	20	270	0.07	2700				

The results above generally indicate the superior performance of the diamond mesh panels with regard to peak load, deformation and energy absorption capability. In addition, there appears to be little difference in the overall stiffness between the two mesh types. However, it is considered important to evaluate the initial stiffness of the mesh fabric, as this is considered to significantly influence its ability to contribute to maintaining the inherent rock mass strength. A comparison of weld mesh and diamond mesh is made in Figure 6-7. This clearly illustrates the superior initial stiffness of the weld mesh in comparison to diamond mesh. This high initial stiffness was also considered to be the reason for the relatively early failure of the weld mesh in comparison to the diamond mesh. The increased stiffness would result in the development of higher shear loads within the mesh at the points of contact with the loading and clamping plates. The theoretical shear strength of the mesh is approximately half that of its tensile strength, and thus the development of higher shear loads was considered to contribute to the early failure. An evaluation of the angle to the horizontal of the mesh fabric, at the load of failure of the weld mesh (11 kN), would indicate the weld mesh to have an angle of 8° compared to 32° for the diamond mesh. This would result in a higher component of tensile strength being developed within the diamond mesh compared to the weld mesh.

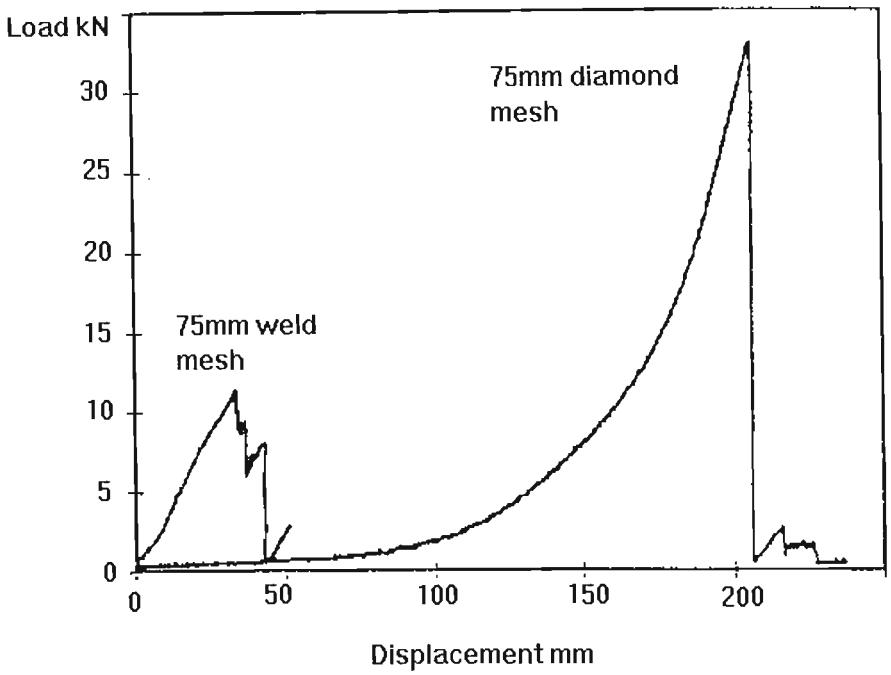

Figure 6-7. Comparison of 75 mm weld mesh and diamond mesh under quasi static loading.

Experimental evidence, however, did not indicate the failure of the weld mesh fabric to be a function of shear. Examination of the failed strands showed necking, characteristic of tensile failure.

A further evaluation of the failure mode of the weld mesh in comparison to the diamond mesh considered the coherent structure of the mesh panel (Figure 6-8), due to the welded contacts, to result in a more complex distribution of stresses. This would cause the development of stress concentrations within the overall mesh structure. Failures were generally localised, and in close proximity to the plate edges, and associated with bending of the mesh structure. The much softer structure of the diamond mesh, due to the frictional linkage between the interwoven mesh strands (Figure 6-9), results in limited development of stress concentrations within the mesh structure. Under these conditions failure is also predominantly associated with significant bending at the plate edges.

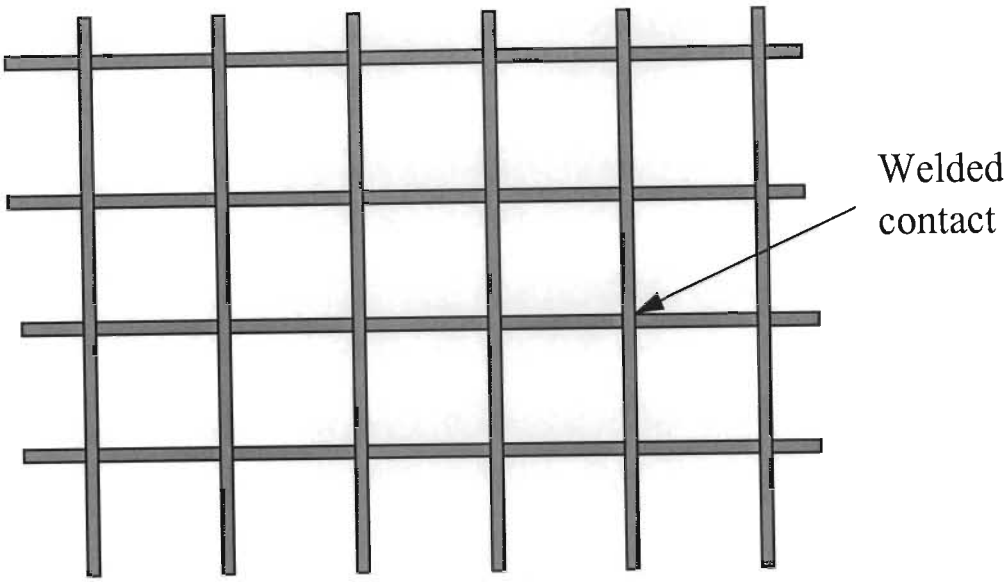

Figure 6-8. Schematic of weld mesh construction.

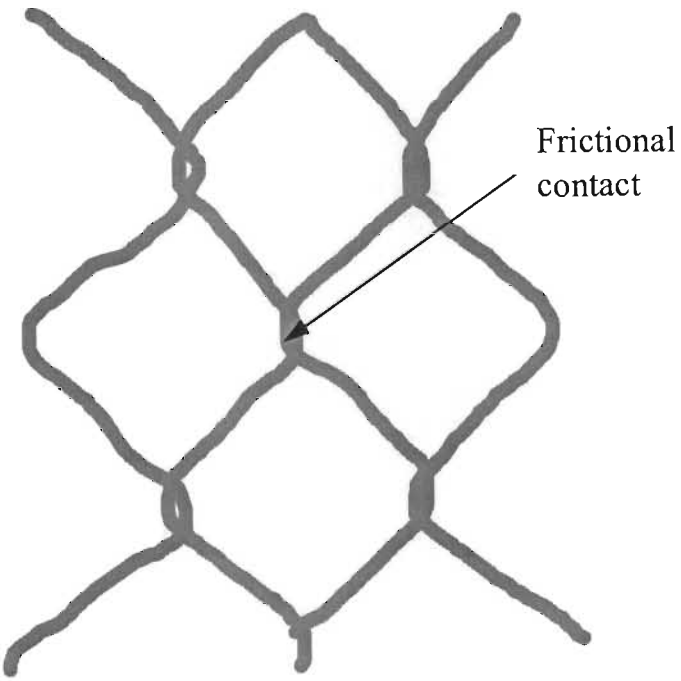

Figure 6-9. Schematic of diamond mesh construction.

This would tend to imply that the weld mesh fabric has limited deformation capacity. However, in situ observations do not support this laboratory finding, and weld mesh may accommodate relatively large deformations. The difference between the laboratory and in situ performance is in the rigid boundary and loading conditions of the laboratory tests. In situ the boundary conditions of a mesh panel are imposed by the lacing structure. These provide much softer confinement perpendicular to the rock wall, and also offer only frictional resistance to lateral deformation of the mesh beneath the lacing. The loading condition in situ is also much softer, as the general fractured nature of the rock mass results in more evenly distributed load across the mesh panel. This is compared to the stiff loading plate of the laboratory evaluation. In situ

loading will thus tend not to develop significant localised bending within the mesh fabric with associated stress concentrations within the mesh structure.

Simple analytical evaluations may be conducted in order to assess the relative influence of the boundary conditions on the performance of a mesh fabric.

Initially a single strand is considered, clamped over a span (L) and displaced through a vertical distance (y) by a loading plate of diameter (Lp) with a force (F), as illustrated in Figure 6-10,

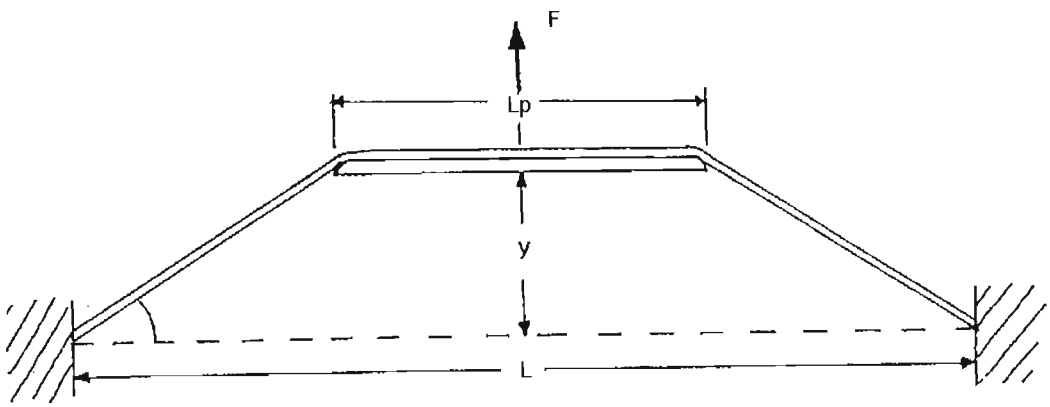

Figure 6-10. Diagrammatic representation of clamped mesh panel under vertical loading.

the strain in the strand ε_y, for a displacement y, is given by:

$$\varepsilon_y = (\sqrt{(4y^2 + a^2)} - a) / L \qquad (6\text{-}1)$$

where $a = L - Lp.$ (6-2)

Substitution of a typical value of y=50mm would yield strain in the strand of 1.13×10^{-2}. An increase in the span of the mesh panel by a factor of 4 would reduce the strain in the strand by 21 times, thus illustrating the importance of the span of the mesh panel on the system performance. In addition, if the effective length of the strand was increased, such as in the diamond mesh configuration, where the effective strand length over a span of L is estimated to be $\sqrt{2}L$, then it may be anticipated that, for a given strain at failure, significantly greater deformation (y) would be necessary. However, consideration should be given to the development of localised stress concentrations at the points of contact between the interwoven wire strands.

The following analytical model, as illustrated in Figure 6-11, may give an improved representation of the boundary conditions in situ.

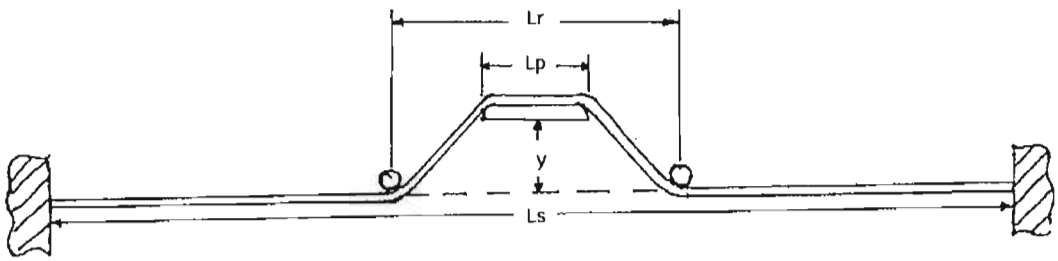

Figure 6-11. Diagrammatic representation of mesh panel with roller defined span.

$$\varepsilon_y = (\sqrt{(4y^2 + a^2)} - a) / Ls \quad (6\text{-}3)$$

where $a = Lr - Lp$. (6-4)

A comparative analysis with Lr=800 mm and Ls=3.2 m, which is representative of a complete mesh panel span, for a deformation (y) of 50 mm would give a strain within a wire strand of 2.82×10^{-3}. This is approximately four times less than the edge clamped strand over the equivalent inner mesh panel span as defined by equation (6-1).

6.3.2 Evaluation of laboratory testing programme

Comparison of the overall laboratory results, under quasi static loading, show a general reduction in peak load and stiffness of the mesh fabric with a reduction in the number of wire strands per unit area. Thus, within a mesh type the strand density will influence the relative capacity of the mesh fabric.

Under dynamic loading conditions (3 m/s) there is a small, but general increase in the peak load and system stiffness. In comparison to quasi static loading, where failure of the mesh panel may be gradual and localised on individual strands or areas of the mesh panel, under dynamic loading it is considered that the mesh panel is loaded more uniformly. This results in a greater number of wire strands contributing to the load - deformation characteristic of the system. Under such conditions it may be anticipated that the system will exhibit greater strength and stiffness. However, the laboratory testing programme does indicate that the relative performance of the in situ mesh panels under quasi static loading should be comparable to their performance under dynamic loading.

Only one test was conducted with a lacing strand, due to difficulties experienced with the setting up of the test and its applicability to in situ evaluation. Analysis of the load - deformation characteristic of this system indicates that the initial performance is governed by the mesh panel, due to the inability to sufficiently tension the lacing against the mesh, up to a deformation of approximately 200 mm. This deformation is, however, far in excess of that for a 75 mm weld

mesh panel alone. It was observed that where localised failure of the mesh occurred, the lacing prevented the loading plate from additionally loading other areas of the mesh panel. Thus the failure of the mesh occurred in a far more gradual process until significant load was transferred to the lacing rope. It was the characteristic of the lacing rope that subsequently determined the remainder of the system deformation characteristic.

6.4 In situ evaluation of mesh and lacing systems

6.4.1 Results of in situ testing programme

An in situ testing programme was conducted using the previously described hydraulic jack for loading of the mesh and lacing system (Figure 6-3). A series of typical mining industry mesh and lacing configurations were evaluated as illustrated in Figures 6-12 to 6-17. The evaluation involved the determination of the load deformation characteristic of the mesh and lacing configuration at three loading points (Figure 6-4).

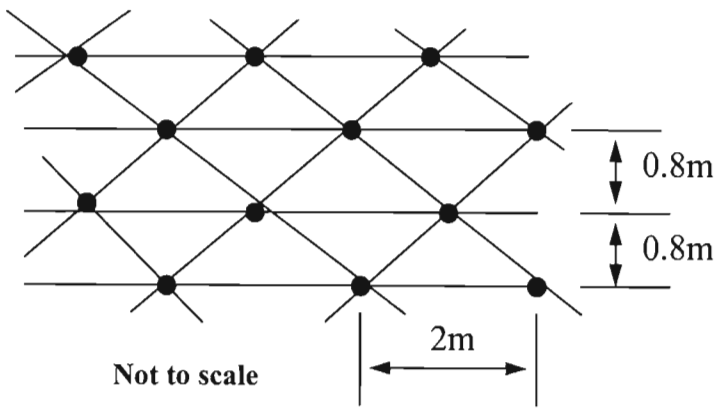

Figure 6-12. Lacing array 1 and 4.

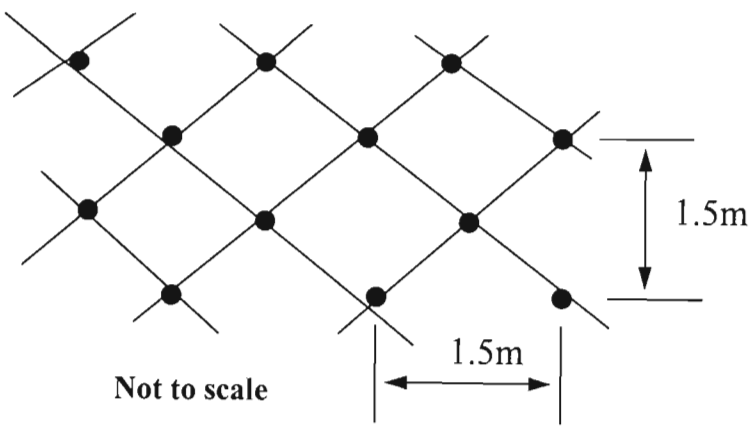

Figure 6-13. Lacing array 2

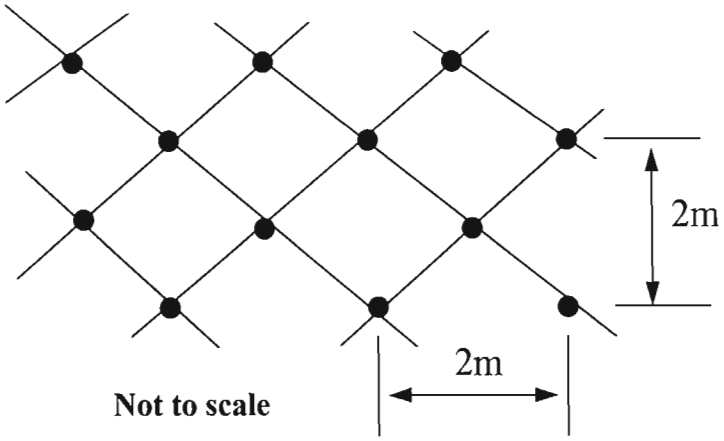

Figure 6-14. Lacing array 3

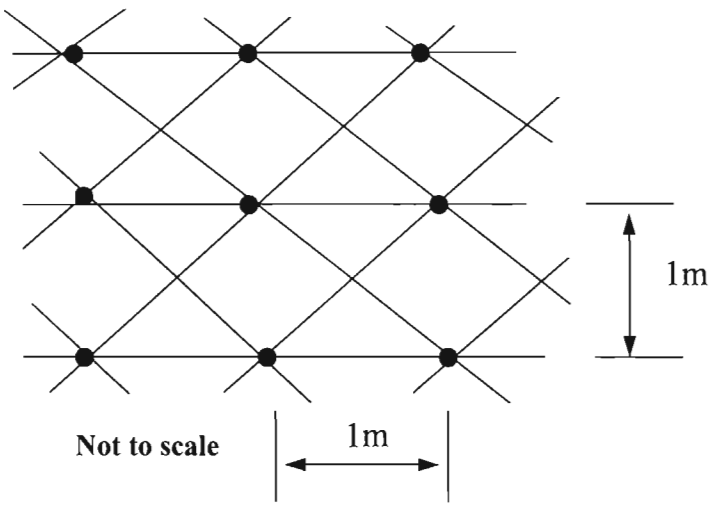

Figure 6-15. Lacing array 5.

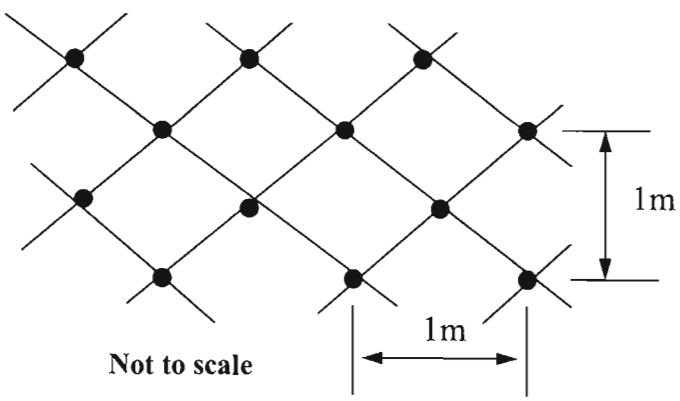

Figure 6-16. Lacing array 6.

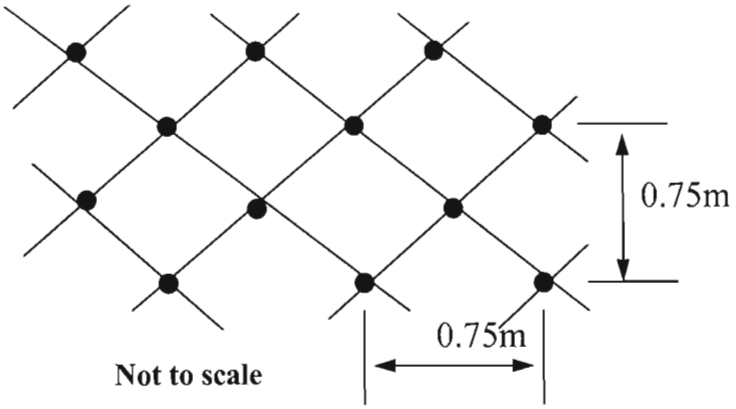

Figure 6-17. Lacing array 7.

Due to the nature of the in situ installation, significant variations in the initial load - deformation characteristic of the mesh and lace fabric were evident. The initial load-deformation characteristic would be indicated, from the laboratory system test, to be more representative of the mesh type than the characteristic of the mesh and lace system. The determination of the performance of the array was thus based on the final stiffness of the system and not the initial load deformation characteristic.

Array 1 is a typical lacing configuration for standard tunnels at depth that will be subjected to average stress induced fracturing and limited dynamic loading. The load-deformation characteristics of array 1 are shown in Figure 6-18.

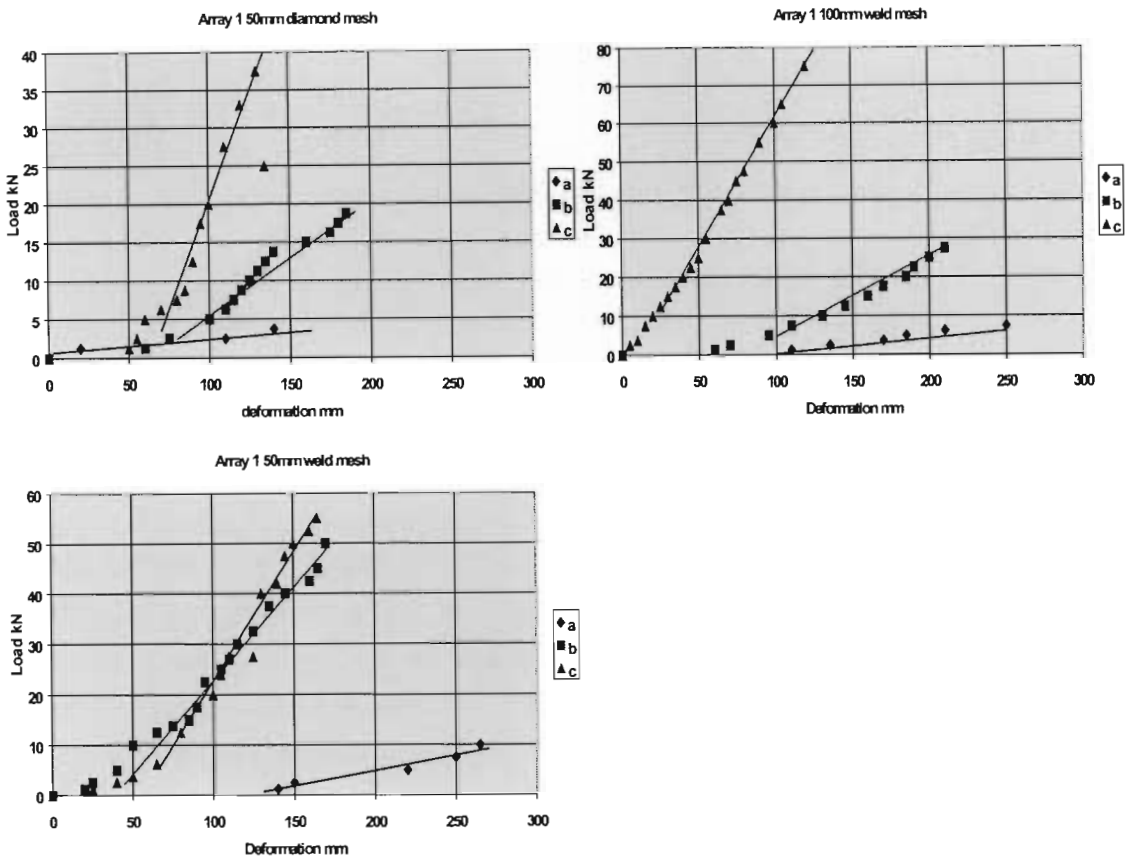

Figure 6-18. Load - deformation characteristics for lacing array 1.

The solid trend lines indicate the estimated stiffness of the point of analysis of the mesh and lace system. It may be noted that, particularly for the analysis of measuring points B and C, the initial stiffness of the system is much lower. This is considered to represent the amount of initial "slackness" in the system due to the installation process. Where substantial "slackness" is present, the initial stiffness may be comparable to that of the mesh panel as given by the load - deformation characteristic of point A. The estimated stiffness of the system, for the indicated sections of the curves as defined by the trend lines, is given in Table 6-2.

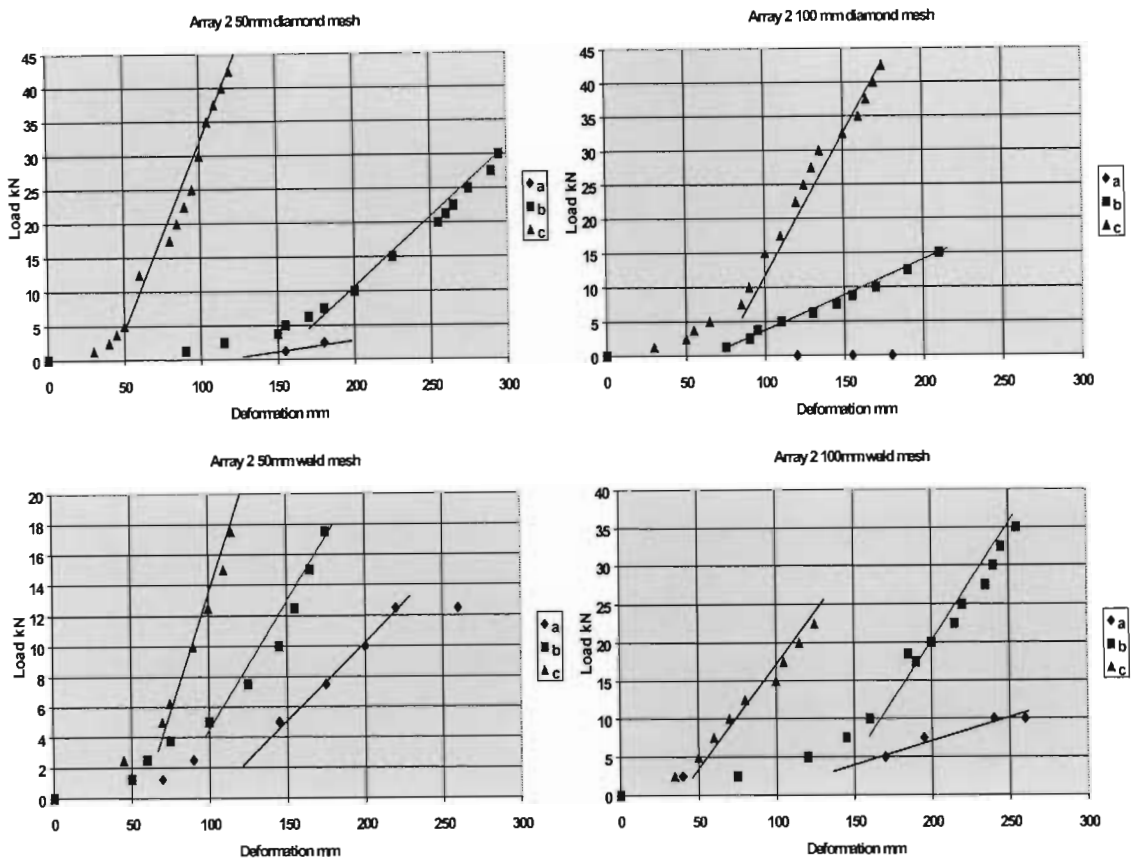

Figure 6-19. Load - deformation characteristics for lacing array 2.

The load - deformation characteristics of array 2 are shown in Figure 6-19. This lacing configuration is a simple diamond pattern on a staggered 1.5 m rock bolt pattern. The initial slackness in the system and lower stiffness of the mesh panel, in comparison to array 1, are reflections of the lower density of lacing per unit area of support. This is due to the absence of "straights" within the lacing pattern. The "straight" lacing is the constant horizontal lacing within the pattern as shown for array 1 in Figure 6-12. The "straight" lacing also allows for more effective tensioning in comparison to the diagonal lacing, and this may also contribute to the increased initial, relatively low stiffness deformation. The absence of data for position A of the 100 mm diamond mesh panel is a reflection of the very low stiffness of this fabric over the maximum stroke of the hydraulic ram.

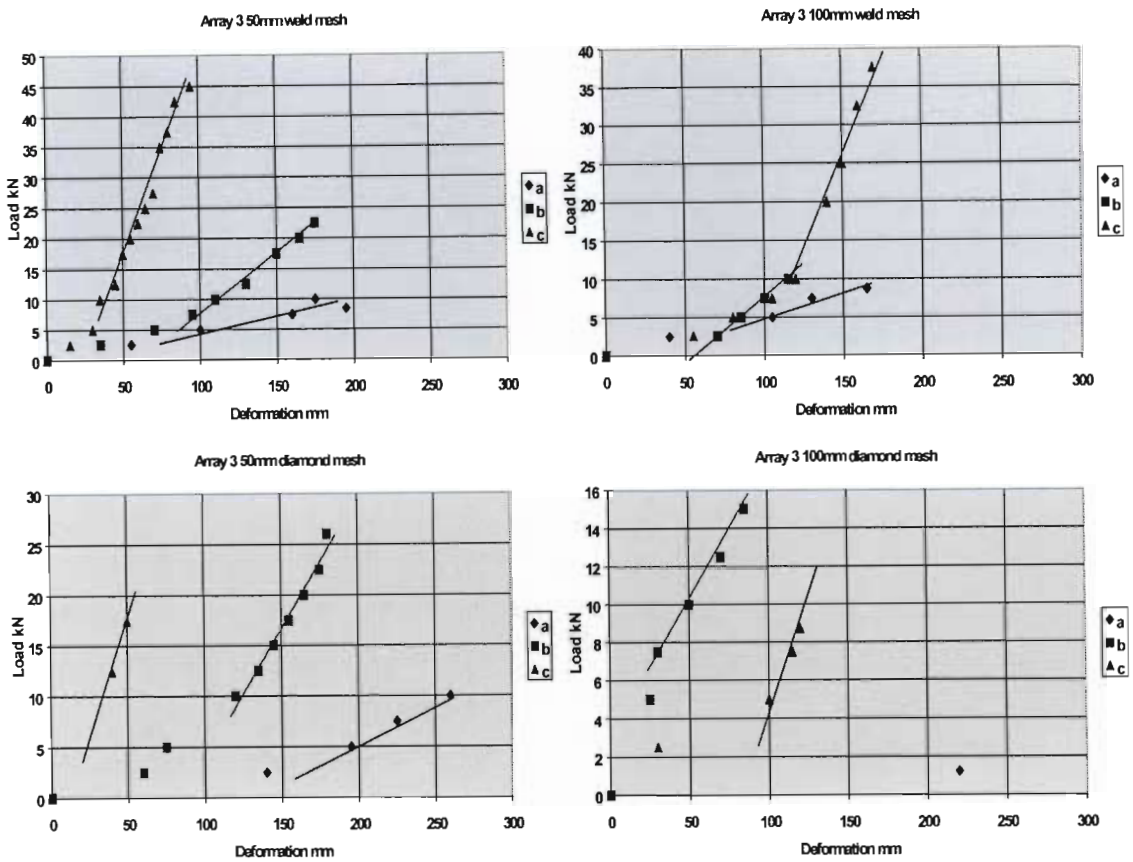

Figure 6-20. Load - deformation characteristics for lacing array 3.

Array 3 represents a similar lacing configuration to array 2, but on a wider rock bolt (anchorage) spacing. It may thus be anticipated to have a softer load - deformation characteristic, particularly for loading points A and B. Analysis of the calculated stiffness, as shown in Table 6-2, indicates a minimal difference between the two arrays in practice. This may be a function of the high degree of variability of the quality of rock bolt, mesh and lacing installation in situ, being in excess of the relative difference in the support system performance.

Array 4, as shown in Figure 6-12, represents the sidewall configuration of a mesh and lacing system identical to the system in array 1. The original difference between array 1 and array 4 was the higher rock bolt and lacing installation density within the hangingwall of the excavation. Comparison of the load - deformation characteristics and the estimated stiffness of the systems, as shown in Table 6-2, indicates some variation, but in general overall comparability. The general trends of an initial "slackness" in the system, and jumps in the load - deformation characteristic, are also evident for array 4 as shown in Figure 6-21.

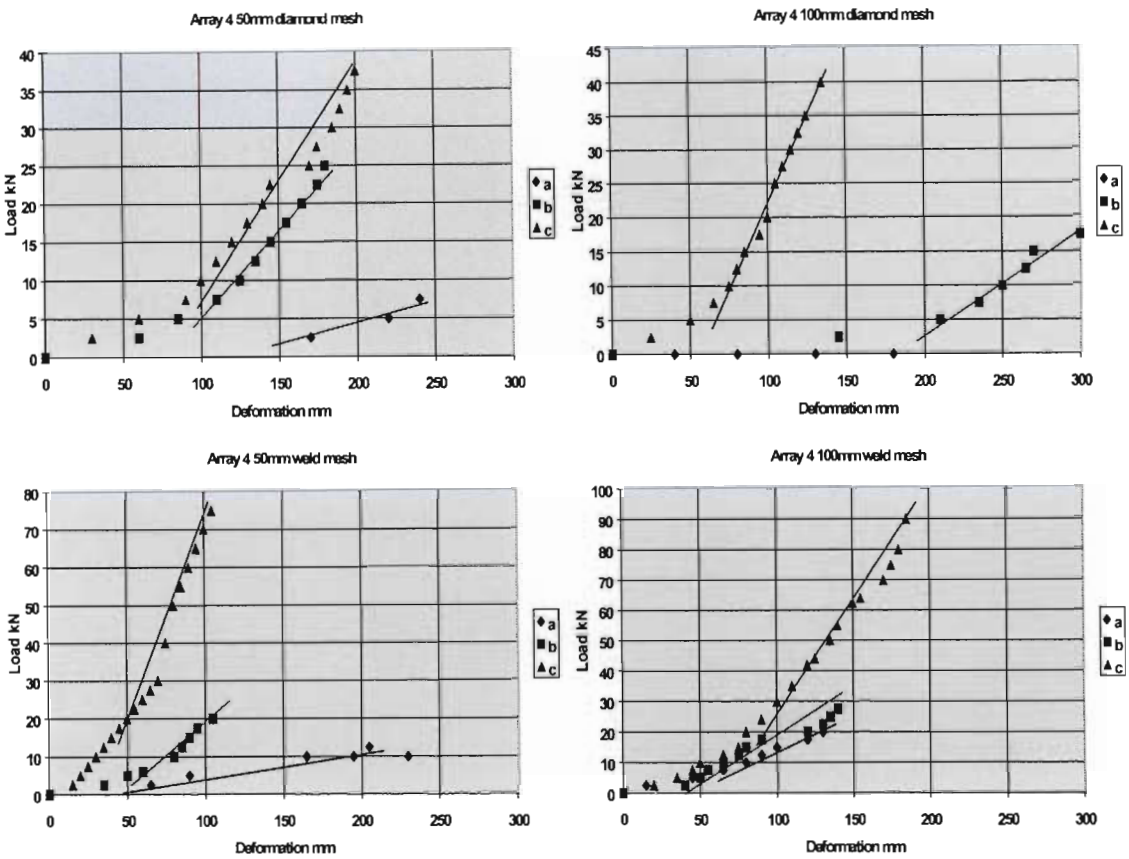

Figure 6-21. Load - deformation characteristics for lacing array 4.

Array 5, as shown in Figure 6-15, represents the lacing configuration for a "square" pattern of rock bolt installation. All other lacing configurations analysed are based on a "diamond" rock bolt configuration more typical for gold mines of the West Rand gold field in South Africa. The difference in the square pattern is the resultant formation of an unconstrained lacing "cross over" at the centre of the square rock bolt pattern. All other configurations tested had rock bolt anchorage at the points of lacing "cross over" and thus restraint at this point. In this regard position C of the load - deformation characteristic is based on the unconstrained lacing "cross over" in this array. This may be indicative of the abnormal (in comparison to the other arrays) amount of initial deformation at the loading position C prior to the significant development of load at this position (Figure 6-22).

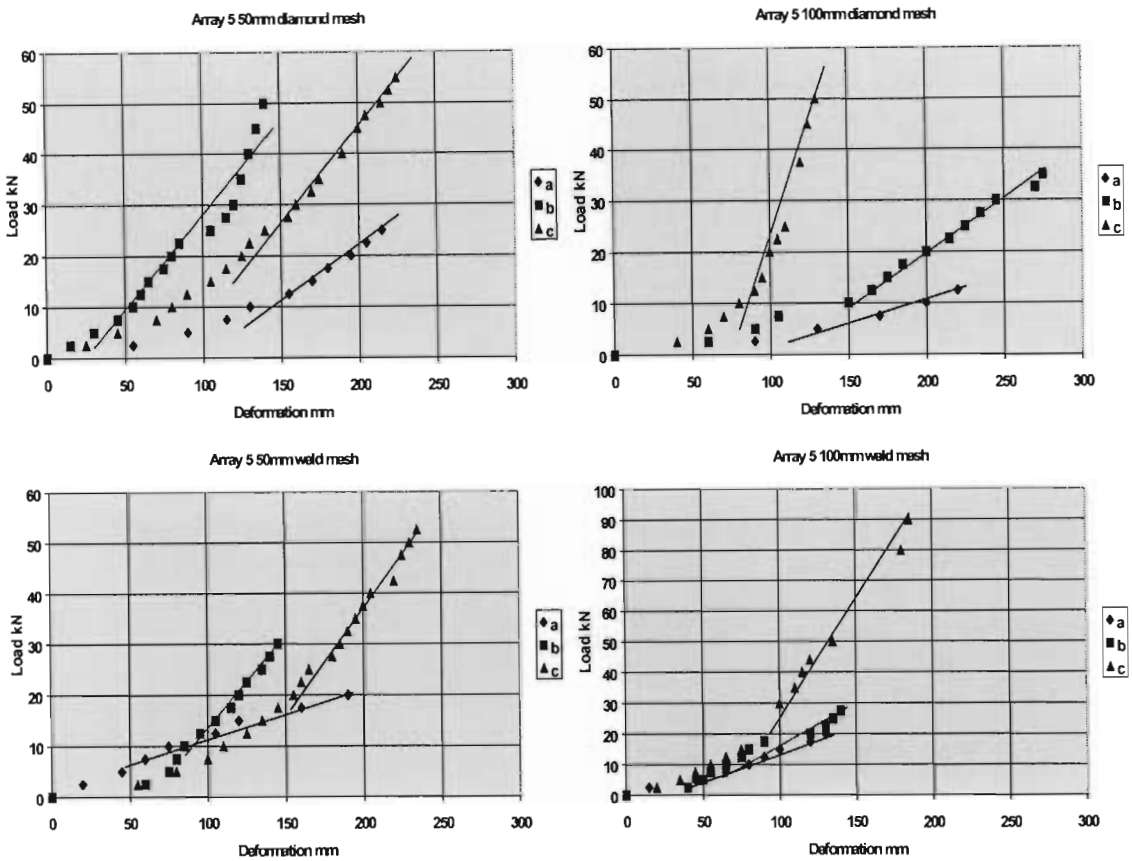

Figure 6-22. Load - deformation characteristics for lacing array 5.

The extent to which the initial slackness in the lacing system must be accommodated, for loading position C, is illustrated by the position of the analysed system stiffness trend for position C relative to position B (Figure 6-22). Under the conditions as analysed previously, it would be anticipated that the development of load, with displacement, would be more rapid for position C than B. In this case, due to the testing configuration, this is often reversed. Once the initial slackness has been taken up in the system, the lacing configuration stiffness is comparable to the other configurations.

Array 6 represents a 1 m diamond pattern lacing configuration, which is based on a relatively high rock bolt density. Analysis of the load - deformation characteristics, as shown in Figure 6-23, indicates a system with a relatively limited phase of low initial stiffness, and a subsequent dramatic increase in system stiffness. Again within this array there appears to be a relatively larger deformation of low initial stiffness at loading position C relative to B, although the position of loading point C corresponds to the position of the constraining rock bolt in this array.

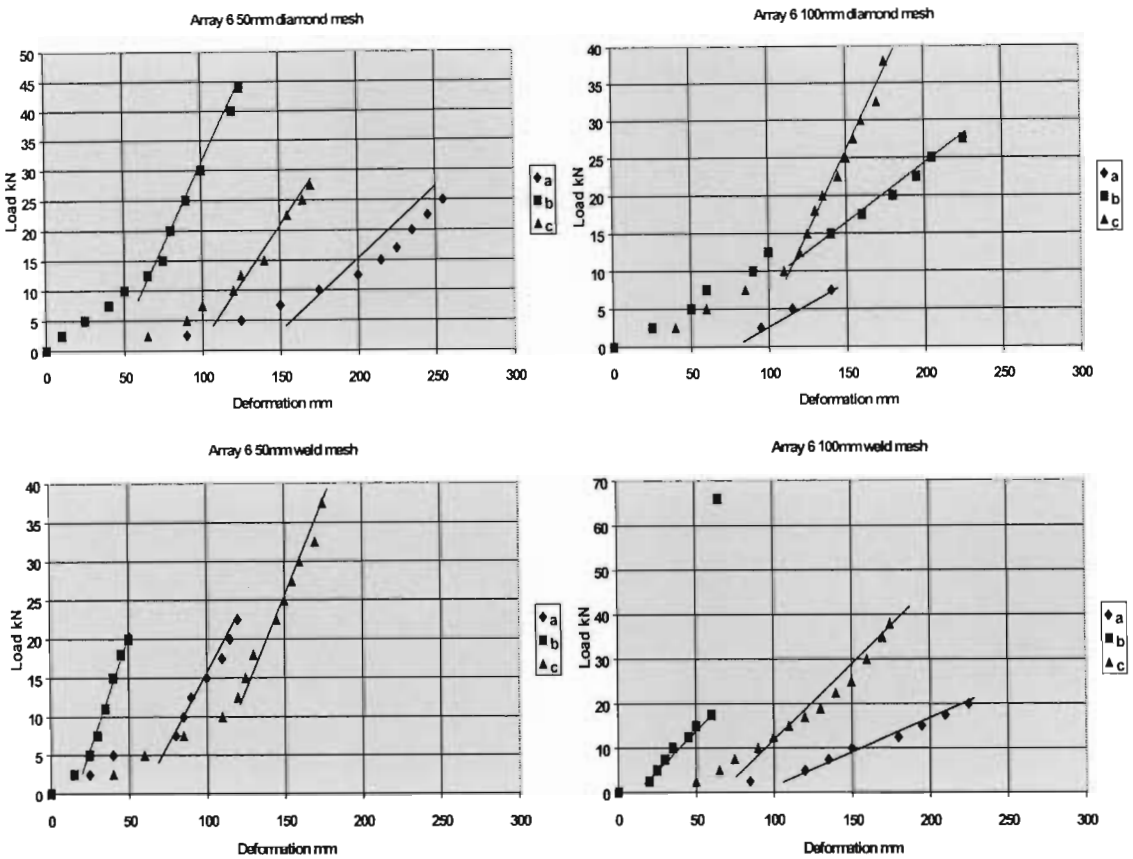

Figure 6-23. Load - deformation characteristics for lacing array 6.

The significance of the higher density of the rock bolts and lacing configuration within array 6 is clearly shown by the relative stiffness of the mesh panels (loading point A), particularly for the 50 mm mesh, compared to the previous arrays.

Array 7 is a similar rock bolt and lacing configuration to array 6, but on a 0.75 m diamond pattern as opposed to a 1 m diamond pattern. Figure 6-24 shows the load - deformation characteristics of array 7, indicating the very limited extent of low initial stiffness and high overall system stiffness. Again the relatively high stiffness of the 50 mm mesh panels illustrates the general constraint imposed on the mesh by the higher density of the lacing configuration.

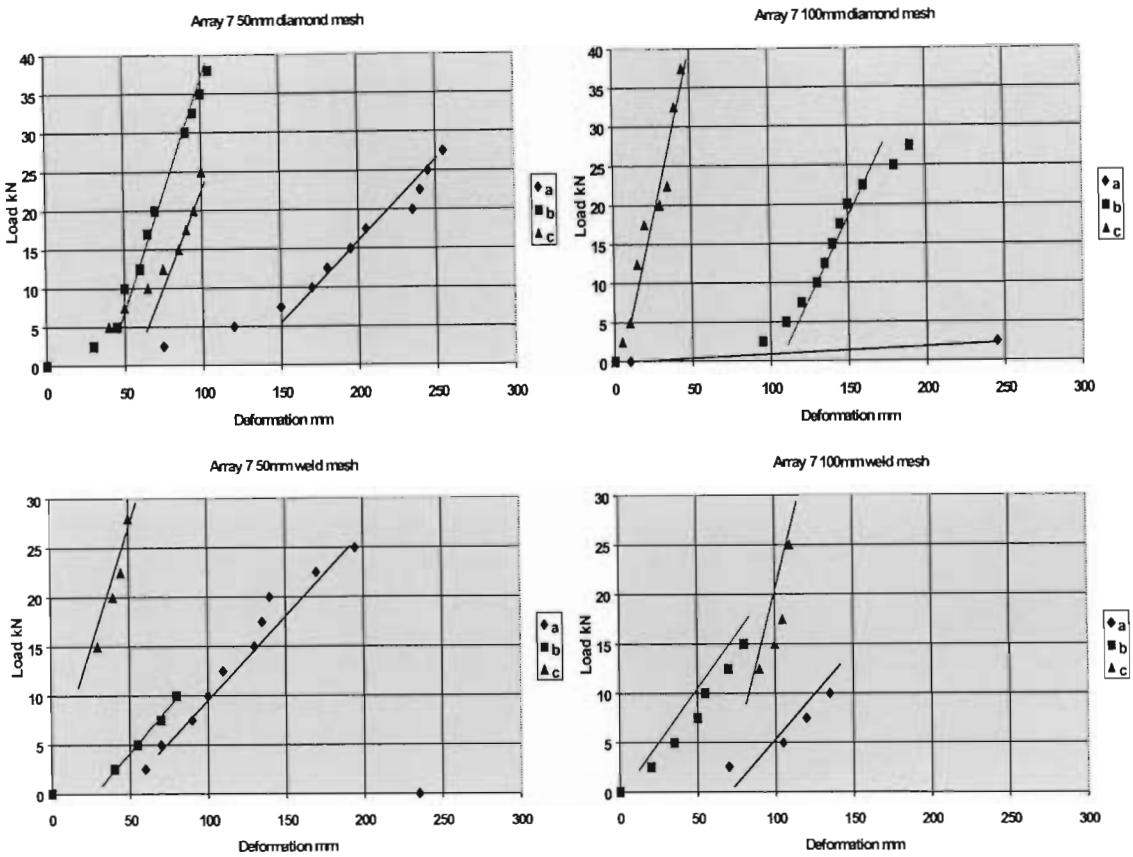

Figure 6-24. Load - deformation characteristics for lacing array 7.

Within many of the above load - deformation characteristics, significant "steps" are indicated, particularly after the period of low initial stiffness. These represent periodic adjustments within the lacing system to the applied load, due to the relatively stiff nature of the lacing strands and the natural coiling of the cable. Individual lacing strands may be up to 30 m in length and thus interact with numerous rock bolt anchoring positions, dependent on the pattern, which may represent points of localised lock up of the tension in the lacing. At a given load these points of lock up may be prone to sudden release, and thus loss of tension which is associated with a jump in the deformation characteristic.

A summary of the estimated system stiffness at the defined points of loading for the lacing arrays and mesh type combinations is shown in Table 6-2.

In order to compare the relative influence of the different lacing arrays, it is necessary to define their geometries by suitable physical characteristics. The most suitable parameters for purposes of analysis of their load – deformation characteristics are considered to be the area of unconfined mesh, for analysis of loading points A and C, and the diagonal lacing length between fixed points (rock bolts) for loading point B, as defined in Figure 6-25. The characteristics of the lacing array configurations are shown in Figure 6-26.

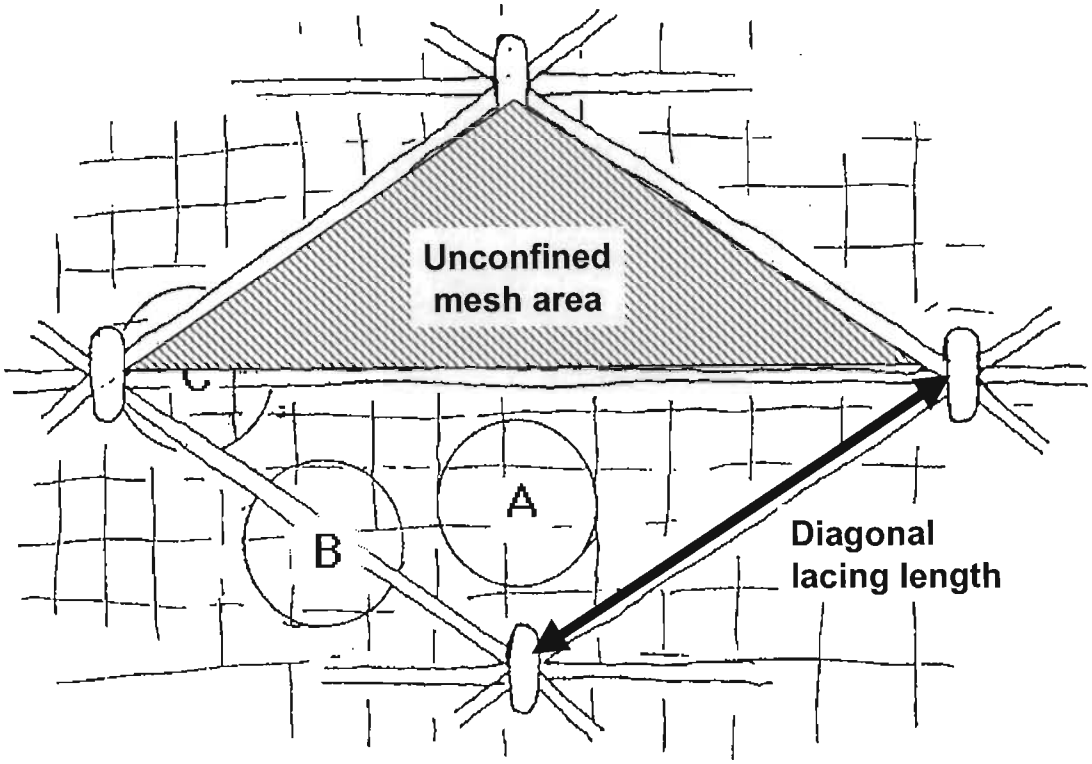

Figure 6-25. Definition of characteristics of lacing array.

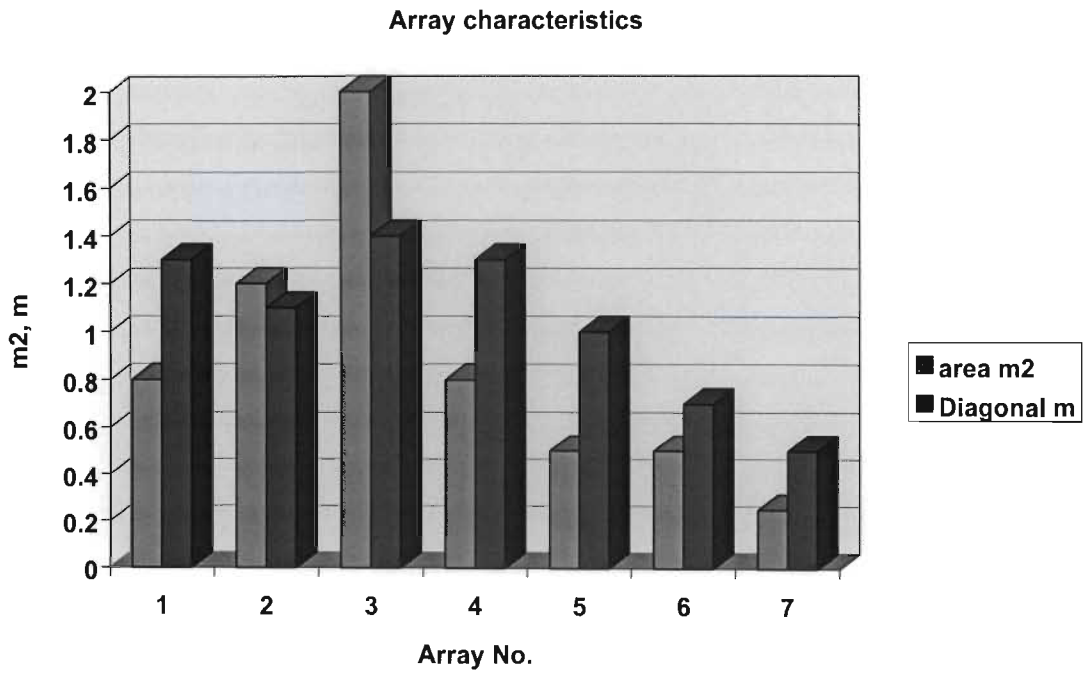

Figure 6-26. Lacing array geometrical characteristics.

Table 6-2. Stiffness (kN/m) of mesh and lacing configurations, after initial slackness, as indicated in Figures 6-12 to 6-17.

Array	area	Diag.	50 mm dia	50 mm dia	50 mm dia	100 mm dia	100 mm dia	100 mm dia	50 mm weld	50 mm weld	50 mm weld	100 mm weld	100 mm weld	100 mm weld
	m^2	m	a	b	c	a	b	c	a	b	c	a	b	c
1	0.8	1.3	38	233	625				50	340	500	50	210	700
2	1.2	1.1	15	400	540	0	110	400	80	120	240	30	220	260
3	2	1.4	70	120	560	10	120	200	40	180	580	60	170	540
4	0.8	1.3	40	220	300	0	160	420	60	240	600	160	260	540
5	0.5	1	180	300	380	60	220	680	80	400	500	180	300	700
6	0.5	0.7	200	400	320	100	140	380	280	500	420	130	320	340
7	0.25	0.5	220	480	600	27	200	900	160	200	640	120	200	340

As would be expected, there is often a close relationship between the diagonal lacing length (as tested) and the area of unconfined mesh. As such the diagonal lacing length is utilised as the primary characteristic for the assessment of the mesh and lacing configurations.

Analysis of the stiffness of the lacing arrays with respect to the 50 mm-diamond mesh is shown in Figure 6-27.

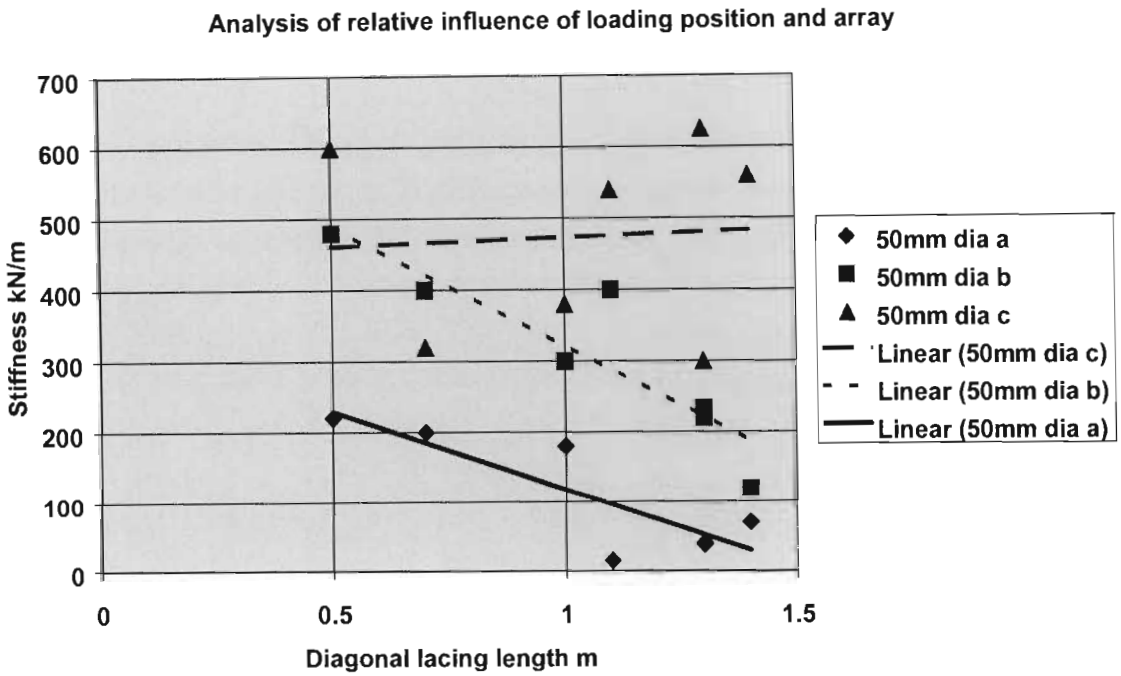

Figure 6-27. Stiffness of 50 mm diamond mesh with respect to diagonal lacing length.

It is immediately clear that a high degree of variability exists in the system stiffness, and, thus, a high degree of variability in the resistance of the mesh and lacing system to rock mass deformation. As may be anticipated an increase in the diagonal lacing length generally results in an overall reduction in stiffness of the system, as is shown by examination of loading points A and B. The stiffness of loading point C does not show good correlation with the density of the

lacing system, as reflected by the analysis of the diagonal lacing length. The response of loading point C is considered to be more a function of its proximity to the rock bolt anchorage, than the relative distance between points of anchorage. This would lead to a characteristic that loading point C is influenced only marginally by the lacing configuration. It may, however, be anticipated that as the density of lacing increased, so the stiffness of loading point C might also increase as a function of the number of lacing strands at the point of anchorage.

A similar relationship to the above is indicated for the 100 mm diamond mesh, as shown in Figure 6- 28. The absolute stiffness of the mesh and lacing system is lower than for the 50 mm diamond mesh as would be anticipated. There is a trend between the stiffness of loading point C and the lacing configuration as defined by the diagonal lacing length. However, within the limited number of tests, and the potential high degree of variability that would be anticipated for this part of the lacing system, this relationship should not be realised in situ.

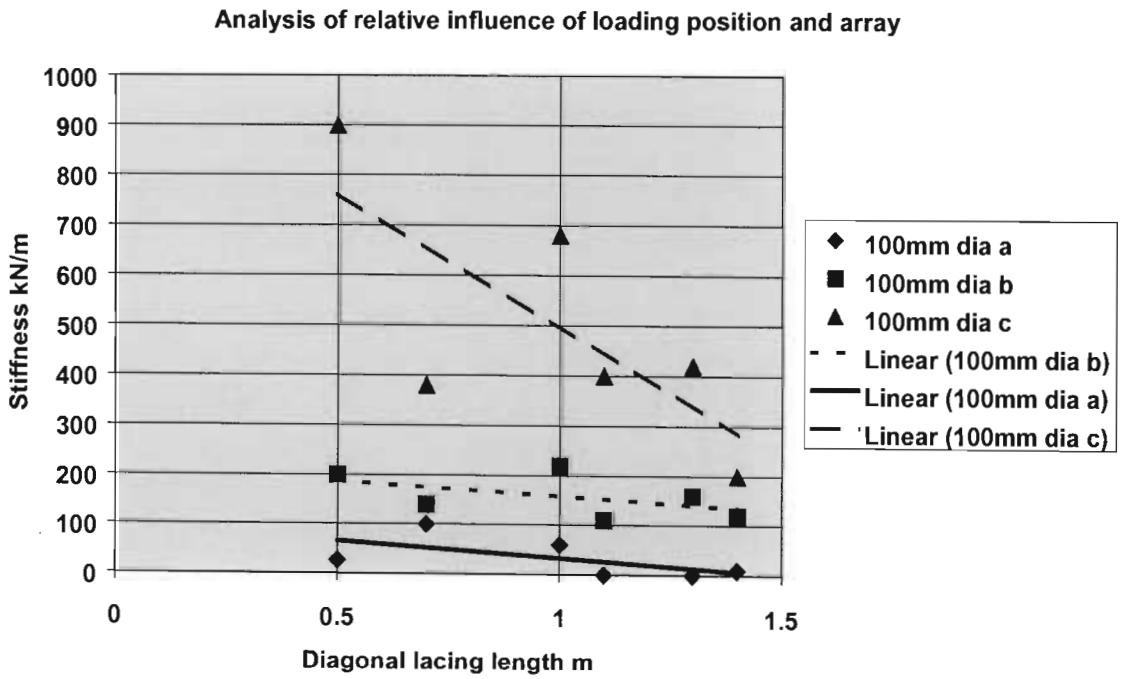

Figure 6-28. Stiffness of 100 mm diamond mesh with respect to diagonal lacing length.

Analysis of the 50 mm weld mesh, as shown in Figure 6-29, indicates a general reduction in the mesh and lacing system stiffness with increasing diagonal lacing length. The absolute stiffness of the system is similar to that of the 50 mm diamond mesh. It would, however, have been anticipated that the system stiffness, particularly that of loading point A, would be substantially higher. Again this potential discrepancy may be a function of the inherent variability in the in situ testing programme compared to laboratory evaluation, and the differences in the boundary condition of the mesh panel. Analysis of Figure 6-29 also indicates the limited influence of the lacing configuration for loading point C on the system stiffness, as previously discussed.

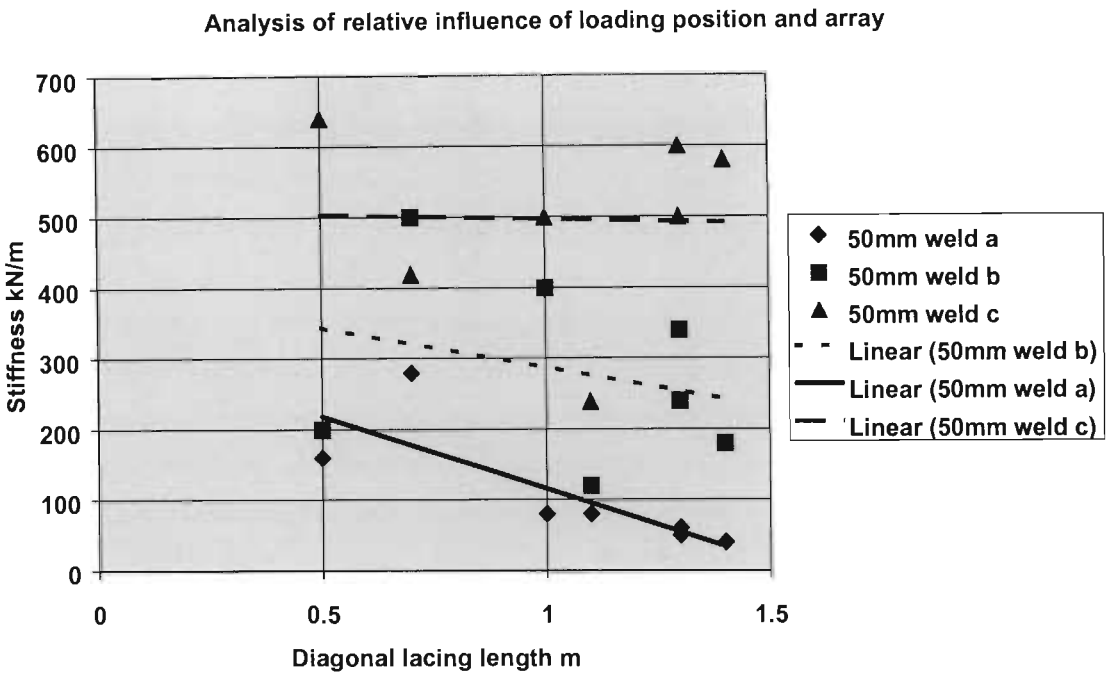

Figure 6-29. Stiffness of 50 mm weld mesh with respect to diagonal lacing length.

Analysis of the stiffness of the loading points, and lacing arrays for the 100 mm weld mesh panels, as shown in Figure 6-30, indicates the general trend of a reduction in system stiffness with larger lacing spans, and lower rock bolt density, as reflected by the increasing diagonal lacing length. The erratic nature of the in situ testing configuration is illustrated by the anomalous indication of increased stiffness of loading point C with increased diagonal lacing length. This would be against the general trend shown with the other mesh types, and against the anticipated relationship as previously discussed.

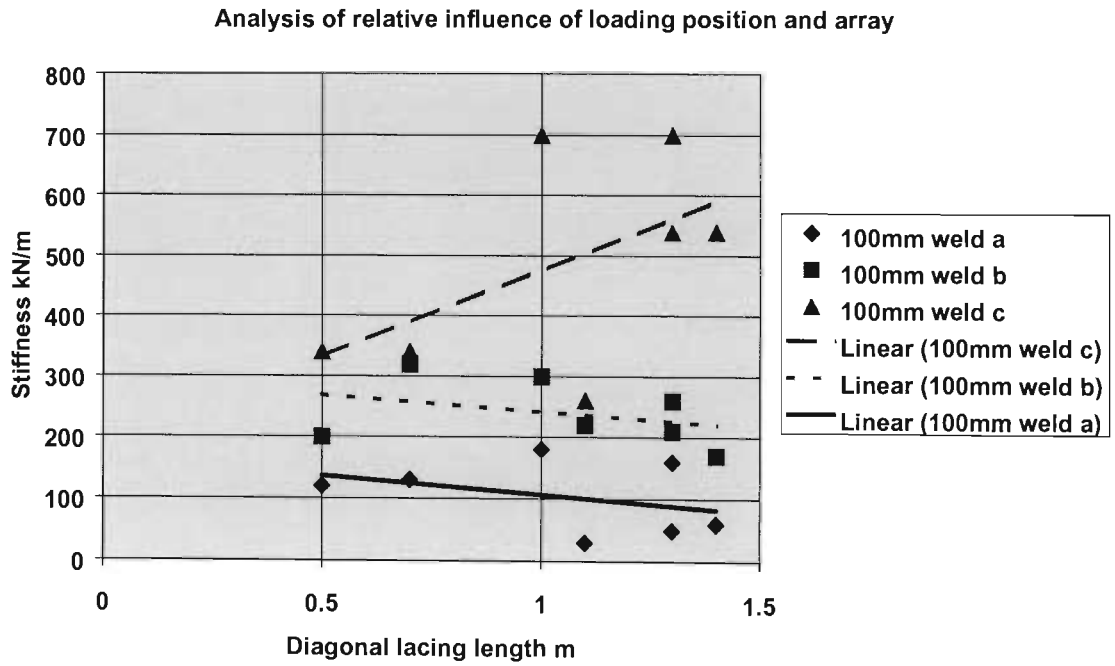

Figure 6-30. Stiffness of 100 mm weld mesh with respect to diagonal lacing length.

Analysis of loading point A, with respect to the unconfined mesh area, for the different lacing configurations, is shown in Figure 6-31. Of significance with regard to the system design, and the selection of mesh types, is the limited difference in the performance of the 50 mm diamond mesh, 50 mm weld mesh and 100 mm weld mesh, particularly under higher density lacing configurations. This consideration may have important operational and financial implications. A reduction in the relative density of the lacing configuration also results in an increased differentiation between the lower stiffness diamond mesh panels and the high stiffness weld mesh panels. However, within the limits of conventional lacing configurations, this differentiation may be insignificant.

Of significance is the very low stiffness of the 100 mm diamond mesh, where in several cases it was not possible to register load within the limits of deformation of the test equipment (300 mm).

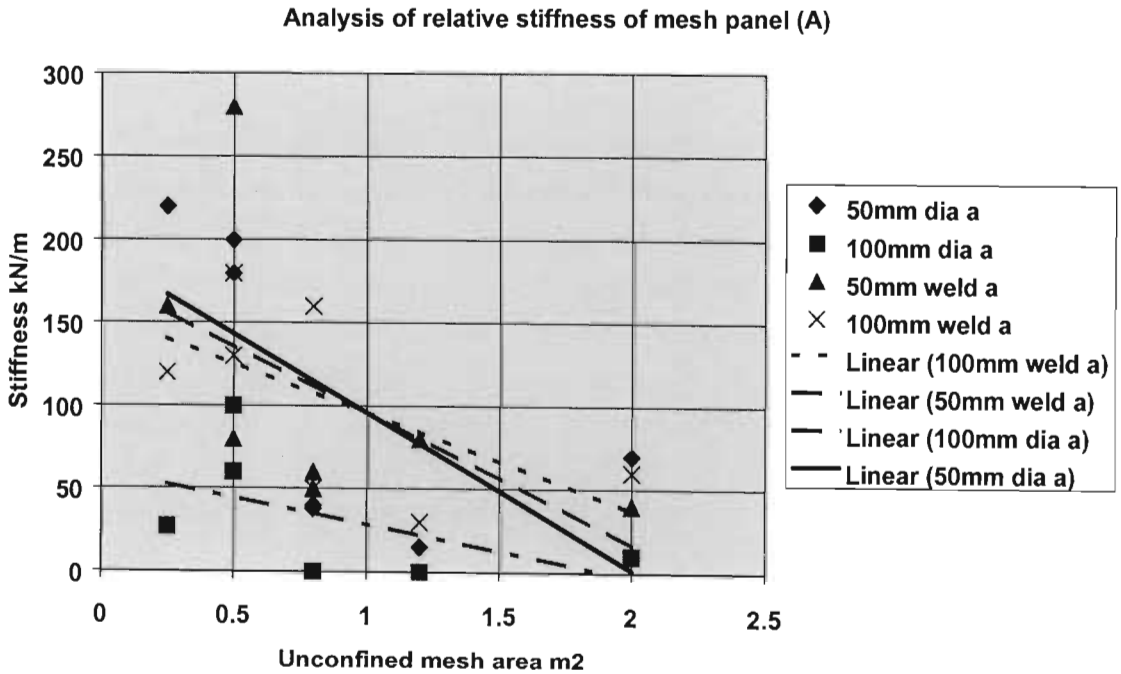

Figure 6-31. Stiffness of mesh panels (point A) within mesh and lacing arrays.

A comparison of the stiffness characteristic of the in situ lacing arrays, with respect to the diagonal lacing strand length, is shown in Figure 6-32.

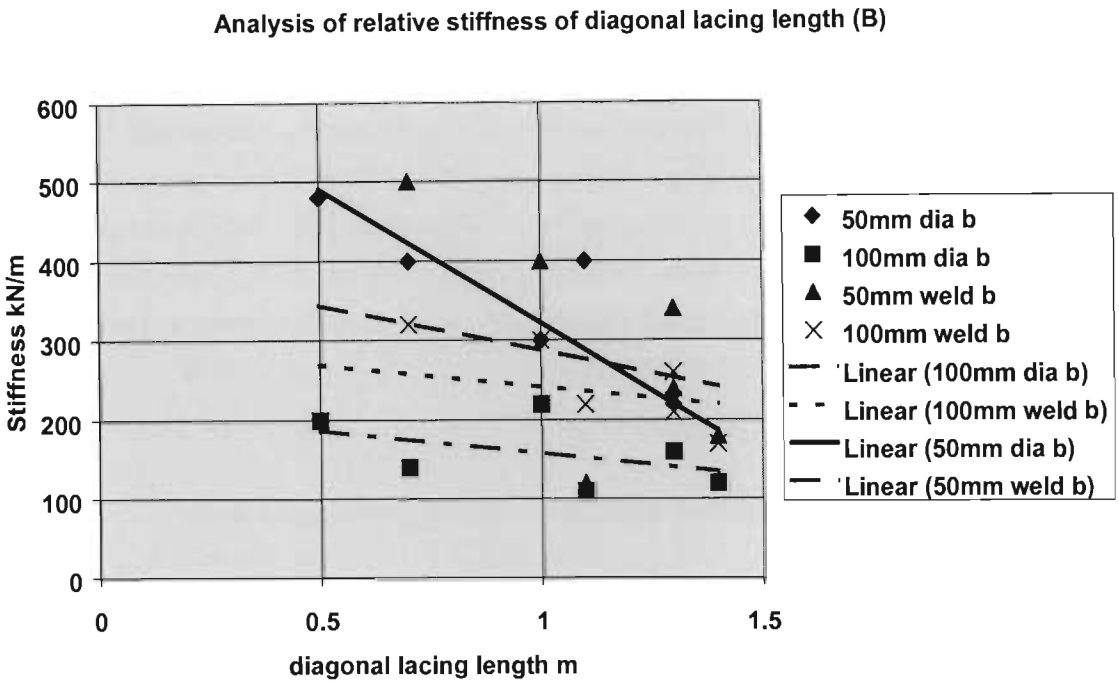

Figure 6-32. Stiffness of diagonal lacing (point B) within mesh and lacing arrays.

This indicates the general reduction, although of poor correlation, in system stiffness with reduced lacing density; however, it also indicates the importance of mesh type on the stiffness of the system at this loading point (B). Generally an increase in the stiffness of the mesh panel, as evaluated within the laboratory, results in a significant increase in the stiffness of the mesh and lacing system as loaded under the diagonal lacing strand. The 100 mm-diamond mesh represents the lowest stiffness system for a given lacing configuration. The 50 mm-diamond mesh indicates, what is considered to be an anomalous high stiffness at high lacing densities, but at lower lacing densities is similar to the 50 mm- and 100 mm-weld mesh. Comparison between the 50 mm- and 100 mm-weld mesh indicates the anticipated higher relative stiffness of the 50 mm-weld mesh lacing systems.

An analysis of the stiffness of the mesh and lacing configurations at the point of lacing cross over is given in Figure 6-33, with respect to the unconfined mesh panel area.

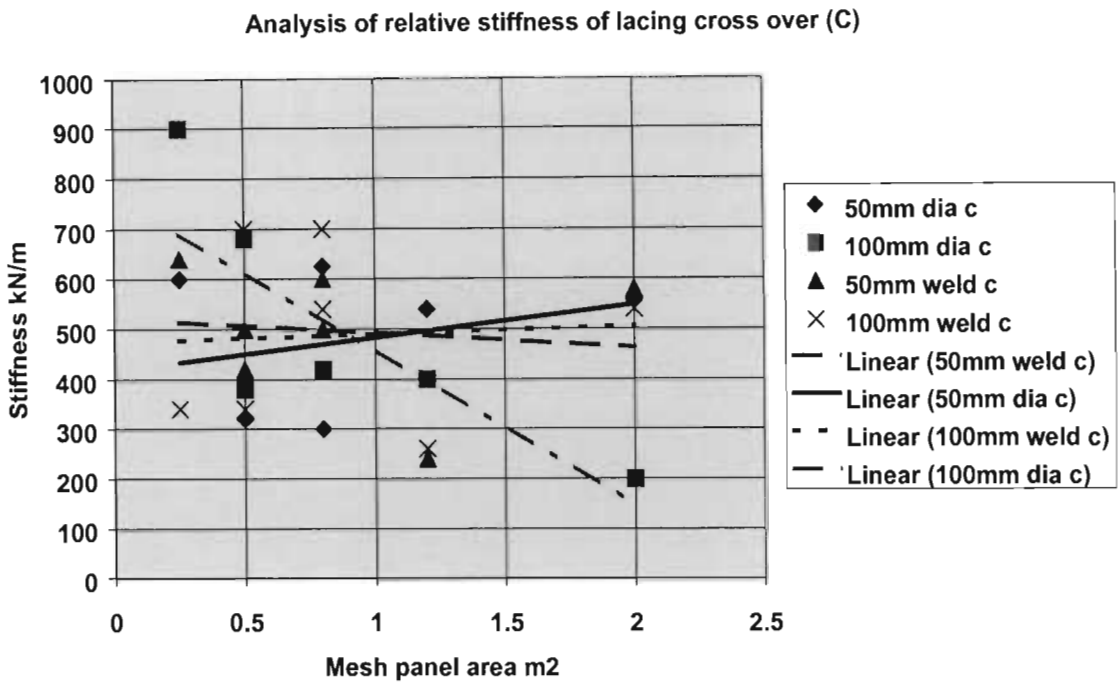

Figure 6-33. Stiffness of lacing "cross over" (Point C) within mesh and lacing arrays.

In general it is indicated that the mesh and lacing configuration has limited influence on the stiffness of the mesh and lacing system at the point of lacing cross over, given the poor correlation of the data. It would appear from the general results that the proximity of this position to the point of anchorage dominates the characteristic of the fabric system at this point. The data was also evaluated with regard to the number of lacing strands at the point of cross over; however, this is also indicated to have little influence on the stiffness characteristic of this area.

6.4.2 Evaluation of in situ testing programme

In general it is apparent that improved system stiffness is principally due to a reduction in the fabric anchorage spacing and a corresponding increase in the density of the lacing per unit area of rock wall. In addition, the characteristics of the mesh may also influence the stiffness of the system, particularly that of the unconfined mesh panel area. This is the area that represents the lowest component of system stiffness and potentially lowest load bearing capacity. From a design point of view this, however, has significant influence in maintaining the inherent rock mass strength between the rock bolt reinforcement. The relative influence of the fabric type on the overall system stiffness is small in comparison to the influence of the lacing configuration. The importance of the mesh characteristic is more pronounced within fabric support systems with low lacing density. The requirement for mesh within the fabric system is still important to prevent unravelling of smaller blocks from the rock mass and thus maintain the overall rock mass integrity. Due to the large differences in the stiffness of mesh and lace fabric over its area of application, the conservative design evaluation of the fabric support system should be based on the stiffness of the point furthest from the rock bolt anchorage. In most cases this will be represented by the stiffness of the mesh panel (loading point A) or, to a lesser extent, a lacing strand (loading point B).

Thus for practical design purposes it is considered that mesh with the lowest installed cost (material and installation cost) should be combined with a lacing configuration of the highest density for the given rock bolt anchorage pattern. The capacity of the lacing configuration should be based on a defined minimum stiffness requirement of a mesh and lace fabric support system for tolerable rock mass deformation limits.

6.5 Evaluation of interaction between the rock mass and fabric support

Recent work has been conducted (Stacey and Ortlepp, 1997) on the dynamic behaviour of mesh and lace systems with simulated rock mass structures under laboratory testing conditions. These tests comprised mesh panels suspended on a 1 m square rock bolt pattern without lacing, and additional tests with lacing similar to the configuration in array 5 (Figure 6-15). In addition, tests were also conducted on reinforced and un-reinforced shotcrete panels. The simulated rock mass comprised of bricks stacked within the defined rock bolt pattern in the geometry of a pyramid. The system was loaded dynamically by means of a drop weight from which the kinetic energy imparted to the system could be defined. The fabric support systems were evaluated on the basis of the deformation associated with an impact of known kinetic energy, and the maximum kinetic energy that the system could sustain prior to substantial loss of fabric integrity.

An adapted summary of the results, to indicate possible trend lines, is shown in Figure 6-34.

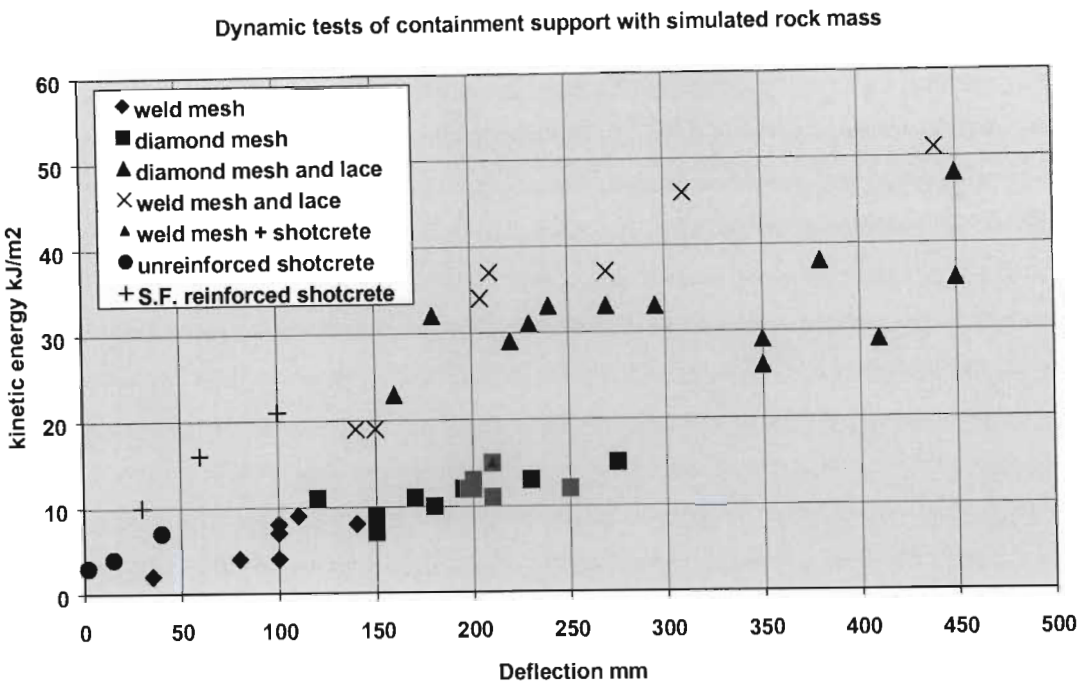

Figure 6-34. Dynamic tests conducted on fabric support systems with simulated rock mass (Stacey and Ortlepp, 1997)

Within a laboratory testing scenario let it be assumed that there is minimal initial slackness in the fabric system and the load deformation characteristic of the fabric may be approximated to be linear. A comparison between the laboratory and in situ static load deformation tests, as conducted under this evaluation, can then be made against the dynamic tests on the basis that the energy absorption capability of the fabric support system may be given by:

$$\text{Energy} = {}^{1}/_{2}.F.d. \qquad (6\text{-}5)$$

where F = resistance load generated within the fabric at deformation d
d = deformation of centre of fabric panel

Thus, from Table 6-1. the dynamic stiffness of a 100 mm weld mesh panel, 800 mm x 800 mm (typical of underground installation), with rigid boundary conditions (conservative) would be 0.23 kN/mm. For a deflection of 100 mm the anticipated resistance would be approximately 23 kN and the energy absorption 1.15 kJ, from equation 6-5. This would compare to an energy absorption capability of approximately 7 kJ/m^2, or 4.5 kJ adjusted for an 800 mm x 800 mm panel as estimated from Figure 6-34. Of importance is the relatively large discrepancy between the energy absorption based on the load - deformation characteristic as directly derived under static loading and that absorbed by weld mesh via a simulated rock mass. A comparable analysis conducted with 50 mm diamond mesh would indicate an energy absorption of 6.25 kJ derived from direct static loading tests compared to 9.6 kJ based on dynamic simulated rock

mass tests. As indicated previously (section 6.3), there is a minimal difference in the load – deformation characteristic of the mesh panels tested under quasi static and dynamic conditions.

A second example would be the more direct comparison of the in situ mesh and lacing configuration as given by array 5 (Figure 6-15). Here both the in situ static loading tests and the dynamic simulated rock mass tests are based on a 1 m square rock bolt pattern and comparable lacing configuration. The performance of the in situ mesh and lacing configuration is again based on the behaviour subsequent to the take up of the low stiffness portion of the load - deformation characteristic. For the 100 mm weld mesh, the in situ load at the centre of the rock bolt array (loading point C in this case), for 200 mm deflection is 100 kN (Figure 6-22), thus giving an energy absorption of 10 kJ (equation 6-5). This would compare to the dynamic test results of 28 kJ for weld mesh plus lace (Figure 6-34).

It may be difficult to make comparisons between the testing systems due to differences in the boundary conditions, but, given these limitations, it is still considered that relatively large differences in the evaluated performance of the systems exist. These differences are considered to be a function of the difference between the direct loading (static), and indirect loading (dynamic), techniques employed. Under the laboratory testing conditions of the mesh panels, as conducted under this evaluation, it is again stressed that there were relatively small differences between the static and dynamic load - deformation characteristics, and thus this is not considered to significantly contribute to differences between the in situ and dynamic (simulated rock mass) tests.

It is considered that the differences in the energy absorption capability of the systems, under dynamic indirect loading via the simulated rock mass, may reflect a large component of energy absorbed within the simulated rock mass structure. This would be due to block movement and damage, and the associated frictional energy losses. The comparison between the simulated rock mass and the in situ tests for weld mesh and lacing is illustrated in Figure 6-35.

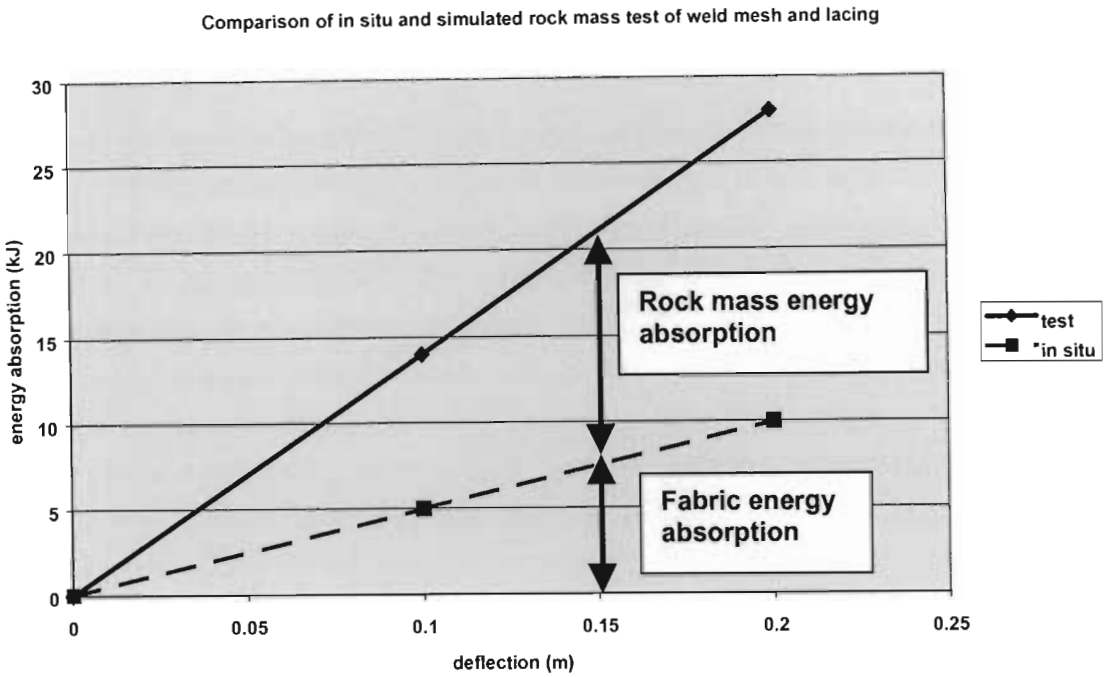

Figure 6-35. Estimation of relative energy absorption of mesh and lace fabric and contained rock mass.

For the simulated rock mass structure, comprising of interlocking concrete bricks, it is estimated, based on the rock mass volume used in the tests conducted by Stacey and Ortlepp, that the energy absorption capacity with deformation of the discontinuous rock mass is 160 kJ/m^3/m.

A similar comparison for a weld mesh panel of 1 m^2 in situ and for the simulated rock mass tests is shown in Figure 6-36. For the defined rock mass structure it is estimated, based on the rock mass volume, that the energy absorption capacity with deformation of the discontinuous rock mass is 100 kJ/m^3/m.

This would indicate that the energy absorption capability of the contained rock mass system is a function of the relative stiffness of the containing fabric support. For a typical mesh and lacing configuration over a 1 m^2 pattern, this would be approximately 200 kN/m, and for a weld mesh panel approximately 100 kN/m (Figures 6-32 and 6-31 respectively).

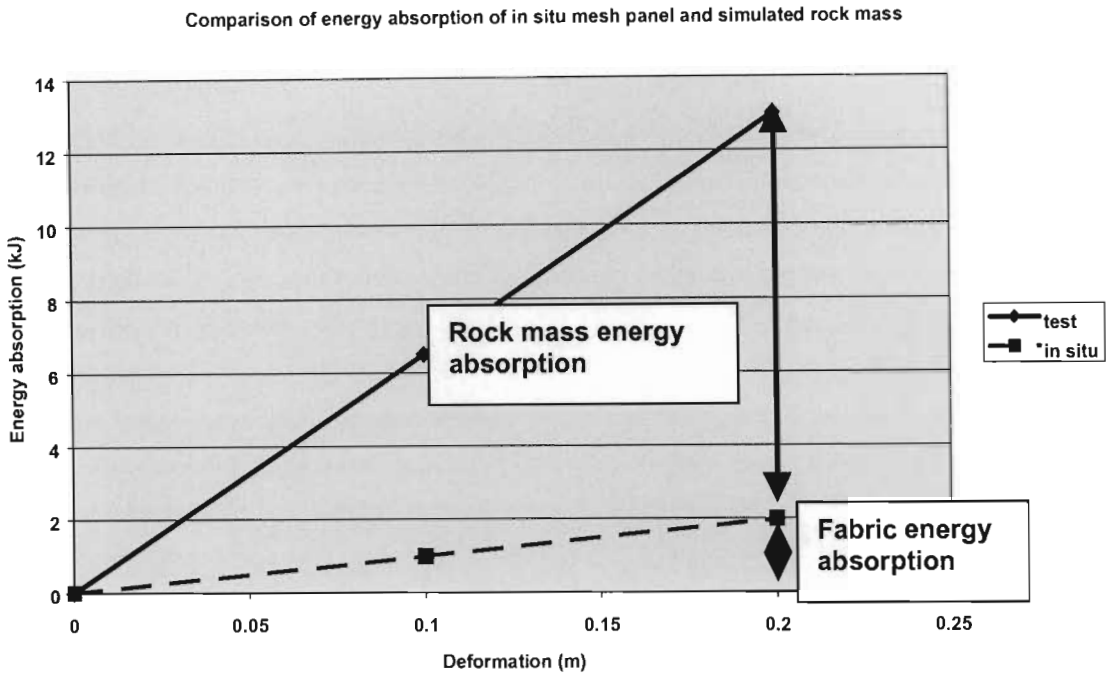

Figure 6-36. Estimation of relative energy absorption of weld mesh fabric and contained rock mass system.

The relationship between the fabric stiffness and the energy absorption of the discontinuous rock mass system, based on this simple laboratory simulated rock mass structure, is shown in Figure 6-37. This analysis is based on a very limited data set in very specific laboratory conditions and would thus require far more detailed investigation.

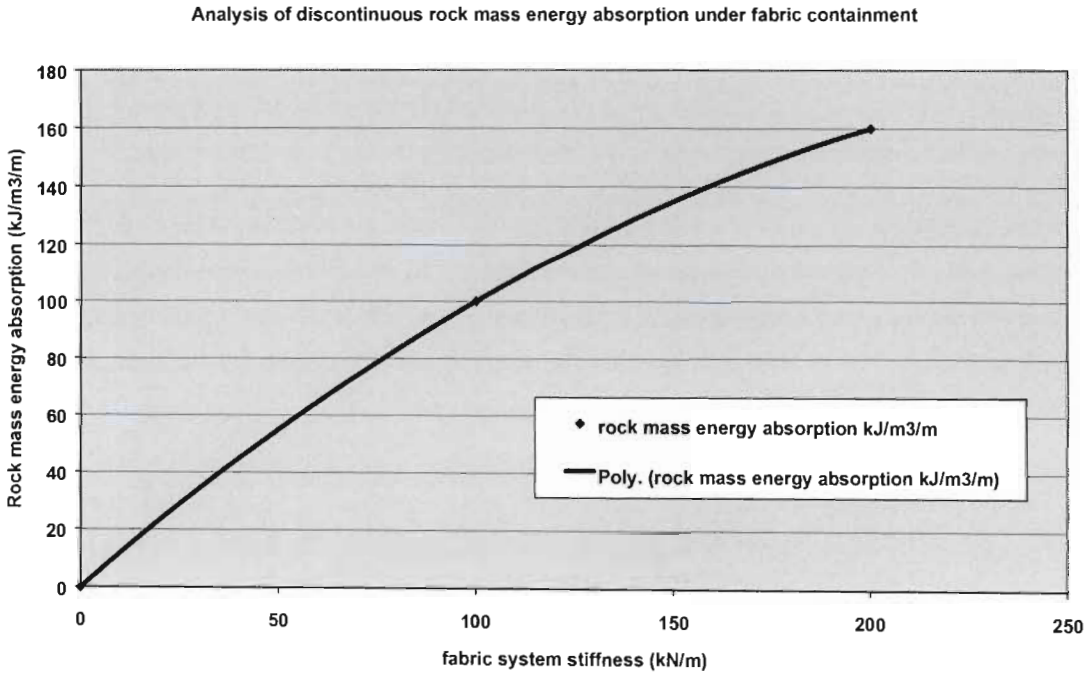

Figure 6-37. Estimation of discontinuous rock mass energy absorption due to fabric containment.

In addition, differences in the energy absorption between the simulated rock mass tests and the fabric only test may be attributed to the static loading tests being based on point loading of the fabric that results in a conical deformation (Figure 6-2). This should be compared to a more uniform loading of the mesh and lacing panel under the simulated rock mass conditions. The later loading characteristic will thus be influenced by all components of stiffness of the fabric support (loading points A, B and C) which may result in a larger energy absorption capability for a given deformation of the central point (point of dynamic, simulated rock mass, measurement).

However, it is still considered that the major component of additional energy absorption is attributable to movements within the simulated fractured rock mass. In comparison to the current design assumptions of tributary area, and homogeneous loading of the support system, this would indicate that the contained rock mass, between the rock bolt reinforcement, has a relatively large capacity to absorb energy, if its structural integrity is maintained by a suitable fabric support system. This conclusion, based on a comparison of the static and dynamic testing methods, is considered to be important in the understanding of the capability of support systems to survive relatively large energy inputs from seismic events in comparison to their assumed designed capacity.

The direct application of the energy absorption capacities of the systems as tested under the conditions of a simulated rock mass (interlocking concrete brick structure) must consider the applicability of the characteristics of the simulated rock mass to in situ geotechnical environments. The analysis does however allow comparative evaluation of the performance of support systems in an improved simulation of the in situ loading conditions.

6.6 Conclusions

The laboratory and in situ testing programmes as evaluated in this section of the thesis have enabled insight into the relative effectiveness of typical mesh and lace fabric support systems t control rock mass deformation. The following are points of significance with regard to desi considerations for the application of mesh and lacing areal coverage support systems that h been derived from this investigation:

- The overall performance of the mesh and lacing system is primarily controlled by th configuration. As such the selection of the mesh, although an important compone system, should be based more on operational considerations. The characteris mesh, however, will influence the stability of the rock mass between th reinforcement and lacing strands, and is thus of increasing importance in low c configurations.

- The load – deformation characteristics, and thus energy absorption capacity, of the mesh and lacing configurations has been quantified and thus can be utilised to make improved judgements in the use of mesh and lace as fabric support components within a support system design.

- The relative stiffness of a mesh and lacing system is variable dependent on the distance from the point of attachment to the rock bolt anchorage.

- An evaluation of the stiffness of the fabric support system is considered important in maintaining the integrity and inherent strength of the rock mass between the rock bolt reinforcement units.

- The energy absorption capability of a contained fractured rock mass between the rock bolt reinforcement units of a support system has been estimated, and for the conditions evaluated is greater than that estimated by the mesh and lace alone.

Chapter 7

7 Numerical modelling analysis of rock bolt interaction with the rock mass

7.1 Introduction

A critical component of the design of support and stabilisation of an underground excavation is the understanding of the interaction between the rock bolt reinforcement and the rock mass (Figure 7-1). This is particularly relevant in highly discontinuous rock mass structures such as are associated with the fracturing around tunnels in deep level mines. Initial evaluations of the interaction between the support system and the rock mass were based on observations of rockburst case studies (Chapter 3) and the evaluation of in situ monitoring (Chapter 4). To complement these previous studies, and gain a detailed understanding of the mechanistic interaction between a rock bolt and a discontinuous rock mass, numerical modelling tools have been used.

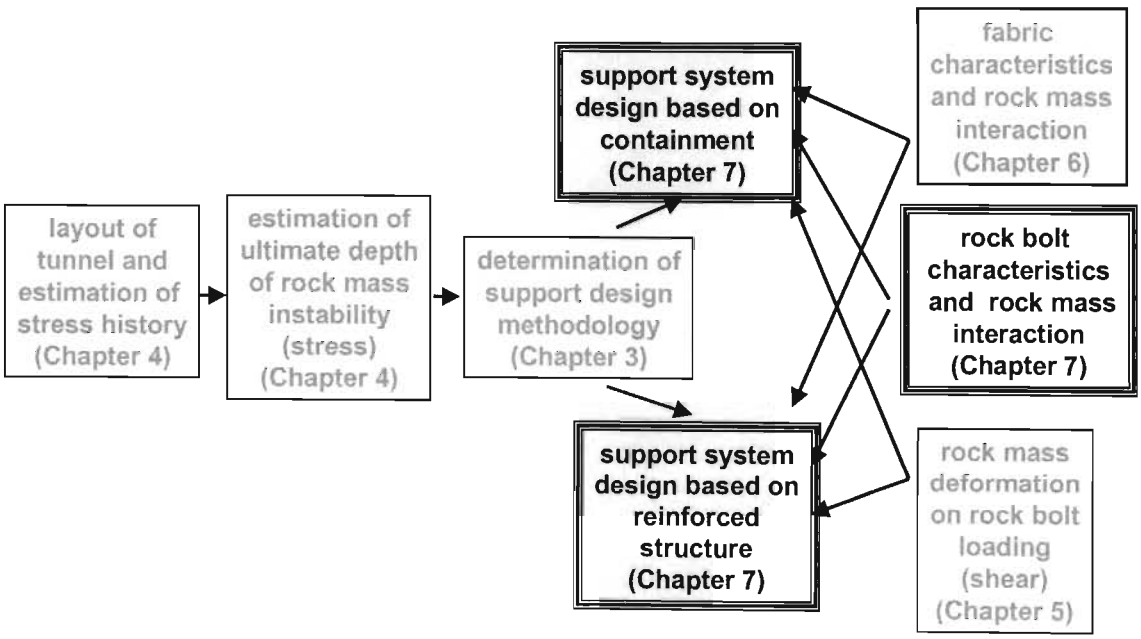

Figure 7-1. The relevance of the research conducted in Chapter 7 within the overall proposed tunnel support design methodology.

The application of numerical modelling to the analysis of this concept was considered to be the most effective means of elucidating the potential mechanisms of interaction of rock bolt units within the rock mass. The selection of a suitable code was based on the requirements of modelling a discontinuous medium, to represent the rock mass structure, and of having the ability to evaluate the influence of reinforcement within this medium. The findings of the

numerical analysis, and the derivation of conceptual design relationships between the rock mass and support characteristics, can then be tested against the case studies of support performance (Chapters 3 and 4).

7.2 Evaluation of rock bolt interaction based on reinforcement

The numerical analysis examines the interaction of rock bolts within an interlocking rock mass structure. In this analysis the depth of instability of the rock mass due to the excavation is assumed to be known (Chapter 4) and the support system is evaluated on the basis of rock mass containment by stable anchorage, or reinforcement of the unstable rock mass to create a reinforced rock mass structure. The deformation of the rock mass under the defined loading conditions results in the development of confining forces in the rock bolt reinforcement units. This is typical of the vast majority of rock bolt systems used in the South African gold mining industry.

7.2.1 Numerical code selection and model development

Due to the nature of the evaluation, to simulate the reinforcement of a discontinuous rock mass structure the Universal Distinct Element Code (UDEC, Anon., 1996b) was utilised. UDEC is a two dimensional modelling program based on the distinct element method of discontinuum modelling, with plane strain assumptions for the out of plane direction. The model is defined by an assemblage of discrete blocks to represent a discontinuous medium, which responds to the loads (static or dynamic) applied to the model. The behaviour of the model is controlled by the relative movement of the blocks as governed by an applied linear or non-linear force - displacement relationship of the joints defining the blocks. The user, to represent the rock mass structure, defines the joint orientation. The joints are assumed to be planar or piecewise "planer" in plane and continuous in the out of plane direction. The blocks themselves can be rigid or deformable, with the application of linear or non-linear stress / strain laws to define the deformable material behaviour. The loading conditions are applied within the model, or to the boundary of the model, and the progressive reaction of the model to the applied loads is examined.

This code was selected for the analyses because it was considered to adequately address the relationships between the rock bolt reinforcement and the rock mass, while maintaining a relative simplicity of analysis. However consideration must be given to the influence of the structure of the rock mass in the out of plane direction as the rock mass is a fully three-dimensional medium. In the following analysis it is assumed that the influence of a rock bolt reinforcement unit within the rock mass can be evaluated by analysis of two orthogonal planes, perpendicular to the rock bolt axis, within the rock mass (Figure 7-2).

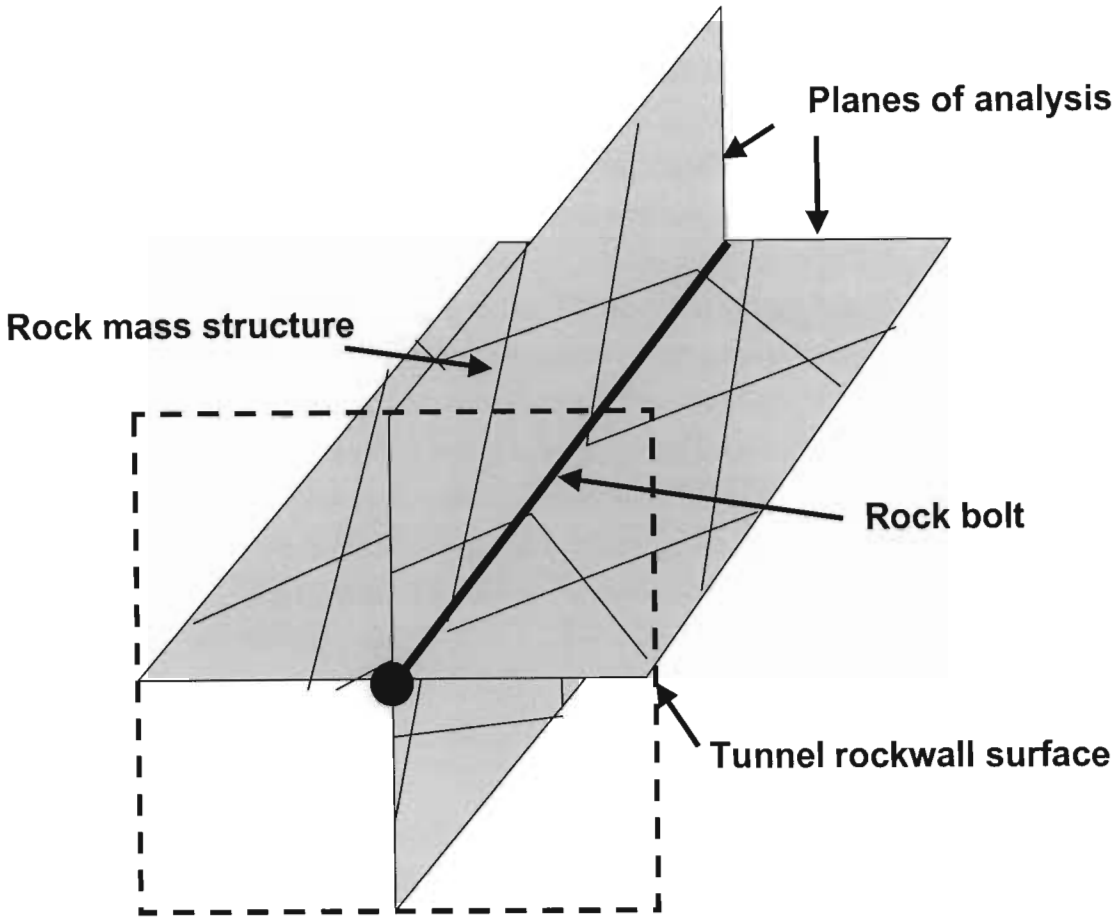

Figure 7-2. Illustration of two-dimensional planes of analysis relative to a rock bolt reinforcement within the tunnel rockwall.

The considerations of two-dimensional modelling verses three-dimensional modelling were further examined. An initial evaluation, using the Fast Lagrangian Analysis of Continua (FLAC, Anon., 1993), considered the extent of influence of a point load applied to the surface of a homogeneous material. The plane strain analysis is shown in Figure 7-3 and is to be compared to an axi-symmetrical (three-dimensional) analysis shown in Figure 7-4 for the same loading conditions and model properties. A comparison of these models illustrates that the ultimate extent of influence of an actively applied confinement is comparable in the two-dimensional analysis to that of the three-dimensional analysis. However, a significant reduction in higher confinements is shown.

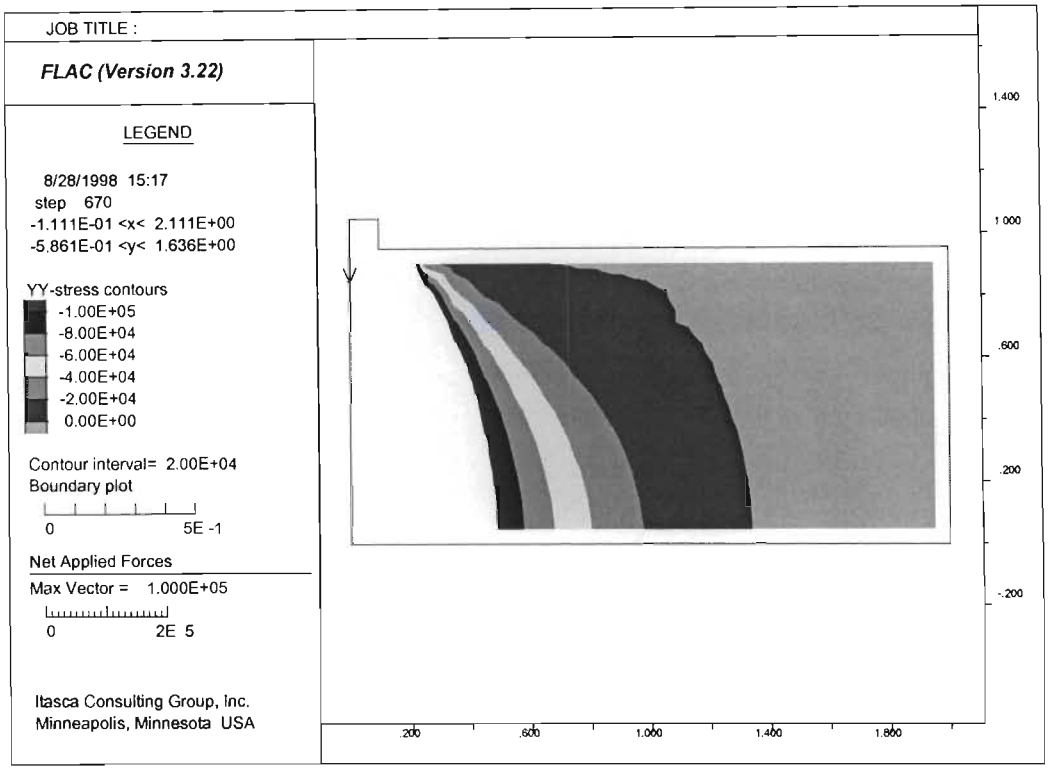

Figure 7-3. Plane strain (two-dimensional) analysis of a point load applied to the surface of a homogeneous material.

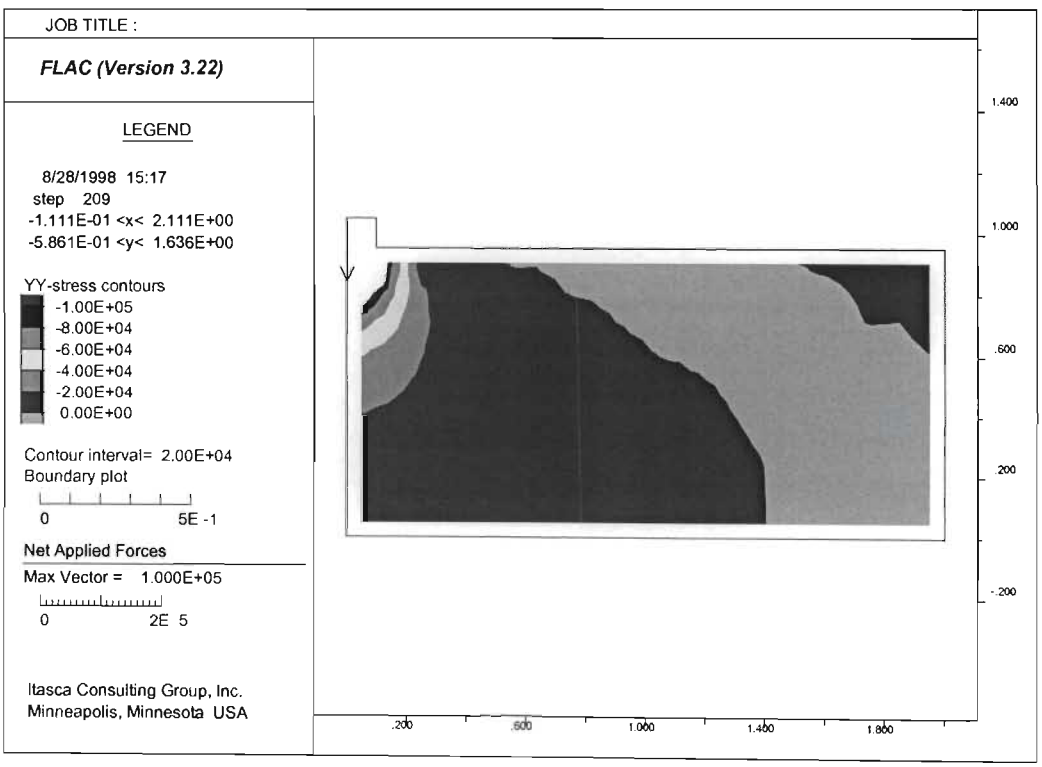

Figure 7-4. Axi-symmetrical (three-dimensional) analysis of a point load applied to the surface of a homogeneous material of equivalent properties to that illustrated in Figure 7-3.

This analysis clearly illustrates the discrepancy between two-dimensional analysis and three-dimensional analysis under conditions of directly applied load to the medium under evaluation. However, with regard to the current analysis, the stability of the system is evaluated by the potential for displacement and detachment of discrete blocks from the simulated rock mass medium due to (gravitational) loading. The action of the reinforcement unit in the model is the limitation of deformation (axial and rotational) of the blocks in its immediate contact and thus restriction to blocks further from the reinforcement unit due to the interlocking structure of the blocks. Under these conditions the mechanism of stabilisation of the model by a simulated rock bolt reinforcement unit is not directly a function of its load capacity but of the potential of the assemblage of blocks, representing the rock mass structure, to unravel. It is considered that for a defined plane of analysis and associated defined rock mass structure, that this potential for unravelling is not significantly influenced by the structure of the rock mass out of the plane of analysis. This does not imply that in situ, unravelling of the rock mass out of the plane of analysis will not occur, but that this unravelling will have only a relatively minor influence on the current plane of analysis. The total volume of unravelling of the rock mass can then be estimated by subsequent evaluation of the rock mass structure in the out of plane, orthogonal direction.

Examples of the coding as implemented in an evaluation of the stability of the rock mass, between stable anchored rock bolt reinforcement, is given in Appendix 1. For purposes of the evaluation of the concepts of rock mass reinforcement, certain assumptions were made with regard to the development of the models:

- Two-dimensional plane strain analysis

- Simple rock mass structure consisting of either intersecting sub-horizontal discontinuities (+-10°) of different spacing, or blocky "brick wall" structure of different block aspect ratio and area.

- Evaluated block geometries are representative of a rock mass structure with major discontinuities sub-parallel to the excavation rockwall, and thus sub-perpendicular to the axis of rock bolt reinforcement. This is considered to be representative of an excavation in a high stress environment where the principle discontinuities are due to induced fracturing of the rock mass.

- Symmetry, as applied in the evaluation of containment, is implemented at the defined reinforcement spacing with fixed x boundary condition and cable unit to control y dilation.

- Discontinuity normal and shear stiffness is based on mechanistic compatibility with in situ observations of rock mass unravelling. This was kept constant throughout the evaluation of

stable reinforcement and containment, and reinforced beam structural analysis, in order to evaluate the relative merits of the different support design methodologies.

- Program termination logic was implemented for displacement of the reinforced rock mass beam structure at a mid-point displacement in excess of 0.25 m, for optimisation of running time. This is also considered to be a reasonable practical limit of rock mass deformation associated with an excavation rockwall.

- Evaluation of reinforced beam structure assumed end conditions, which were allowed to slide in the x-direction, but fixed in the y direction.

- Loading within the containment models is a function of gravitational, or dynamic, acceleration in the negative y direction. Loading within the reinforced beam analysis was by incremental stress increase on the upper boundary.

- The blocks defined by the discontinuities (joints) within the model are elastic, with a Young's modulus of 70 GPa.

Examples of the numerical models as used in this analysis are shown in Figures 7-5 to 7-7. These illustrations clearly indicate the unravelling mechanism of rock mass instability under the simulated rock mass acceleration (gravitational).

Block stability, under these conditions, will be a function of the rock mass structure and the characteristics of the discontinuities. It is assumed that because the discontinuous nature of the rock mass is due predominantly to fracturing sub-parallel to the excavation boundary there is no cohesion, or tension, between the blocks. If some cohesion exists then this design assumption will be conservative. In addition the discontinuities are considered to have frictional and dilational properties of 35° and 10° respectively.

The left and right hand side boundaries of the models illustrated in Figures 7-5 to 7-7 represent the location of rock bolt reinforcement units. The conditions at these boundaries are that the rock mass structure is fixed in the x-direction, thus limiting rotation of blocks at this point, and in the y-direction reinforcement units are explicitly modelled to simulate the bonding and deformation properties typical of grouted steel rock bolt. These cable reinforcing units are anchored to the block at the top of the model. This y-direction boundary condition allows potential separation of blocks along the reinforcement unit and thus increased rotational deformation of adjacent blocks within the rock mass model.

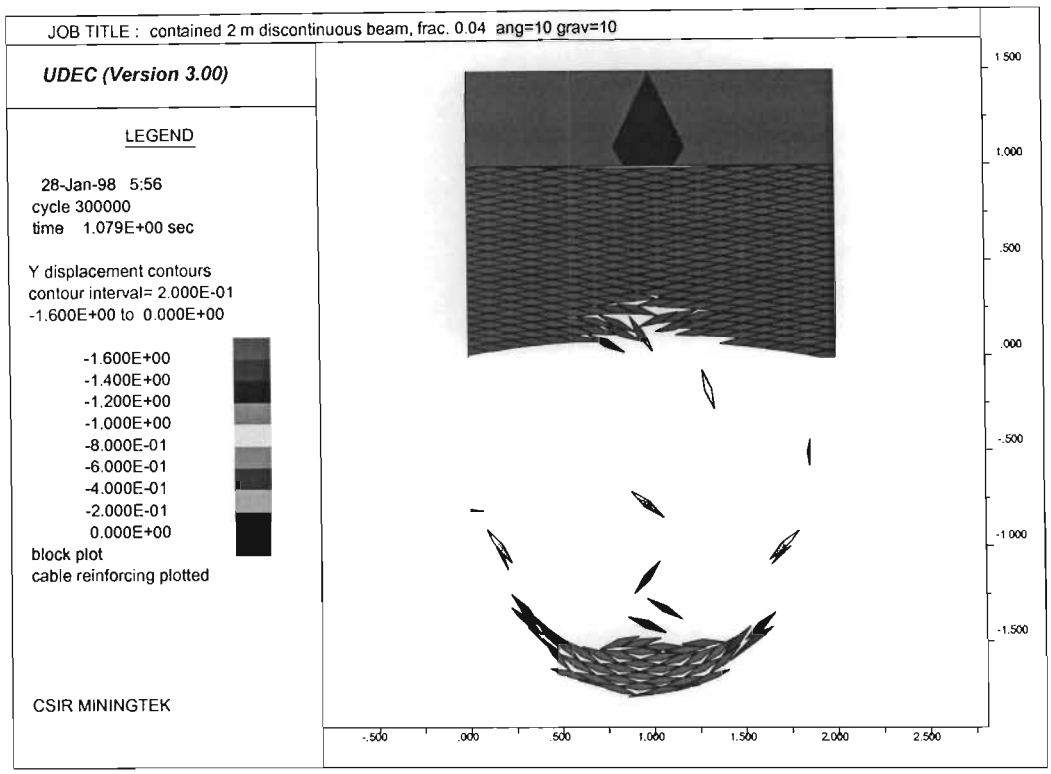

Figure 7-5. Example of rock bolt reinforcement evaluation based on a rock mass structure of low angle intersecting discontinuities.

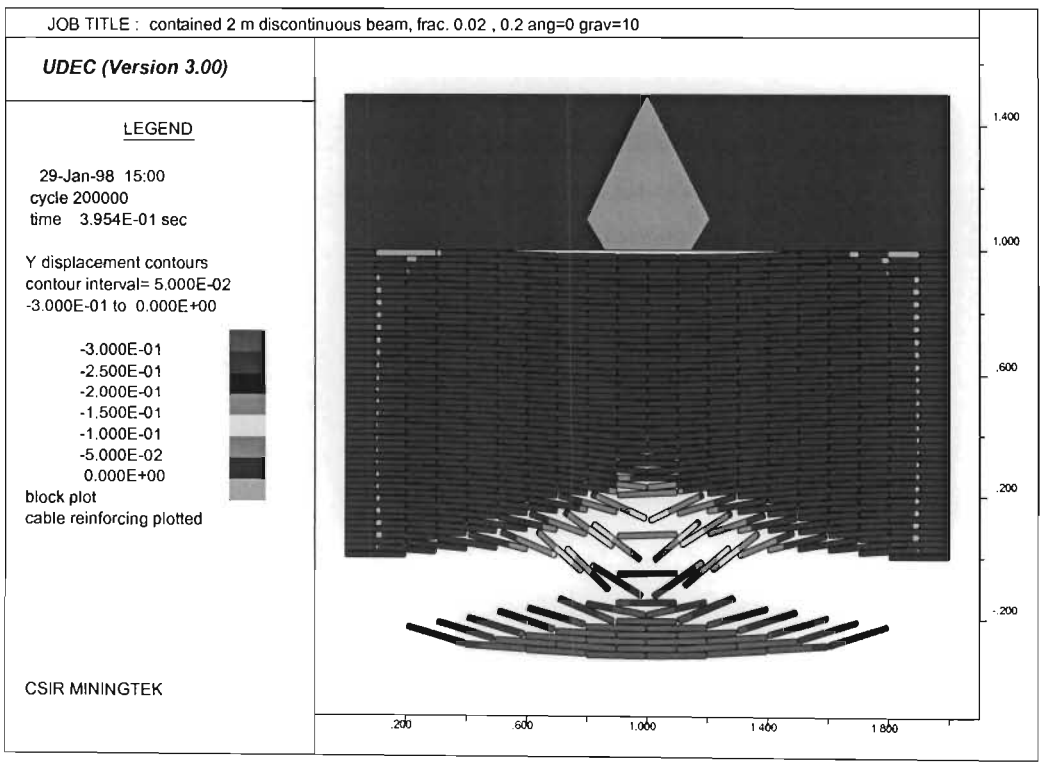

Figure 7-6. Example of rock bolt reinforcement evaluation based on a blocky "brick wall" rock mass structure.

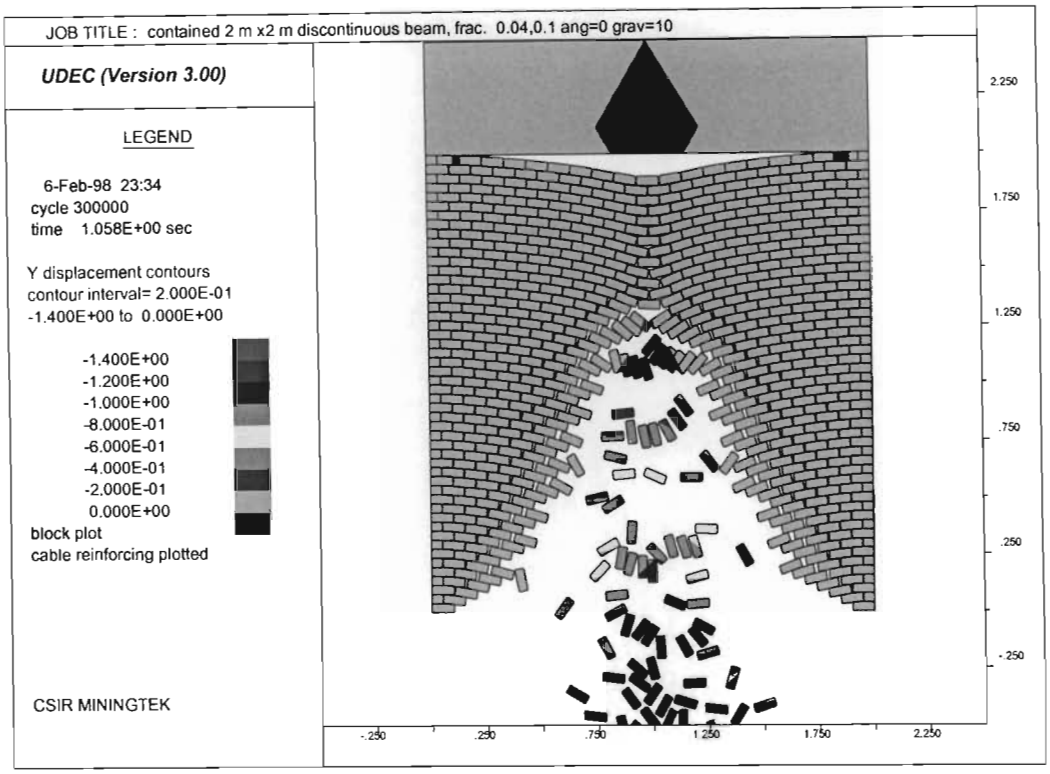

Figure 7-7. Example of rock mass unravelling instability due to block rotation between rock bolt reinforcement at 2 m spacing.

7.2.2 Analysis of numerical modelling of containment reinforcement

Evaluation of the numerical modelling study, into this aspect of support design, has enabled an estimation of relationships between the simplified rock mass structure and the extent of rock bolt reinforcement interaction. This also enables a direct estimation of the extent of instability between the rock bolt reinforcement units, and, thus, the potential demand on, or necessity for, the fabric support systems.

The evaluation of the support systems, as modelled, is thus primarily based on the depth of instability between the rock bolt reinforcement. Based on the rock mass structure, the shape of the zone of instability is defined, and, thus, the volume of unstable rock mass, per unit depth out of the plane of analysis, can be estimated. This estimate can be improved by modelling the interaction in planes of different orientation to the original.

Initial analysis of the influence of the rock mass structure on the depth of instability was conducted for the low angle, intersecting discontinuities (Figure 7-5). In this analysis the angle of the discontinuities is kept constant (10° from positive and negative x-axis), and variation in the rock mass structure is represented by the spacing of the discontinuities (Figure 7-8). This can be likened to the frequency of fracturing within an otherwise relatively homogeneous rock mass.

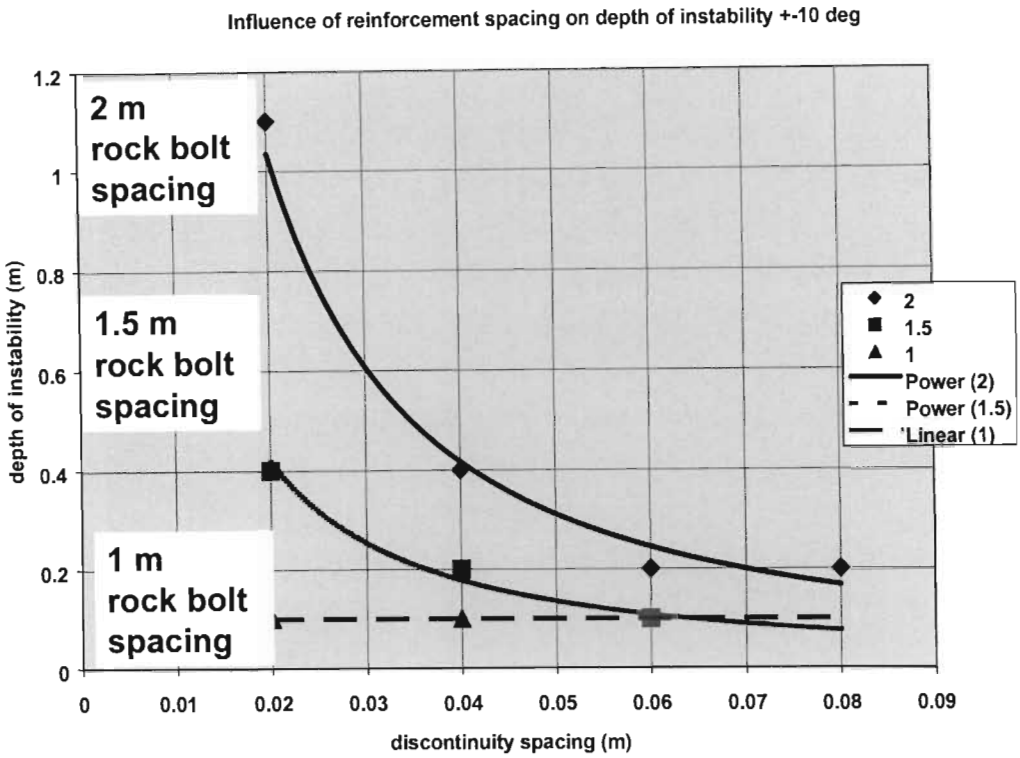

Figure 7-8. Analysis of the influence of fracture frequency on the interaction of rock bolt reinforcement and thus depth of instability between reinforcement units.

It is shown in Figure 7-8 that as the structure of the rock mass becomes more discontinuous, and the spacing of the rock bolt reinforcement increases, so the extent (depth) of instability between the rock bolt reinforcement increases. Conversely, the extent of direct interaction of the rock bolt reinforcement units reduces with increased discontinuity of the rock mass. At high discontinuity spacing the mechanism of instability of the rock mass is controlled only by geometrically unstable key block structures. Thus, in this environment, the depth of instability between the rock bolt reinforcement is only a function of the geometry of the key blocks and not a function of an unravelling mechanism. The trend of the fitted curves indicates the concept that within highly discontinuous rock mass structures, total unravelling of the rock mass, between the rock bolt reinforcement units, may occur. This will be associated with the total loss of direct loading onto the rock bolt component of the support system. In this environment tributary area loading of the rock bolt reinforcement does not occur. Tributary area should thus not be used in the design of support for these conditions, unless the spacing of the rock bolts and stiffness of the fabric support is such that they ensure total transfer of the forces resulting from the deformation of the rock mass to the rock bolts. With current empirical and mechanistic design methods the strength of rock bolts is thus often over designed, the spacing under designed and the capacity of the fabric support is inadequate to ensure rockwall stability, particularly under dynamic loading.

A similar analysis is shown in Figure 7-9. In this graph the influence of the rock bolt reinforcement spacing, with respect to the discontinuity spacing, is evaluated against the potential depth of inter-bolt instability.

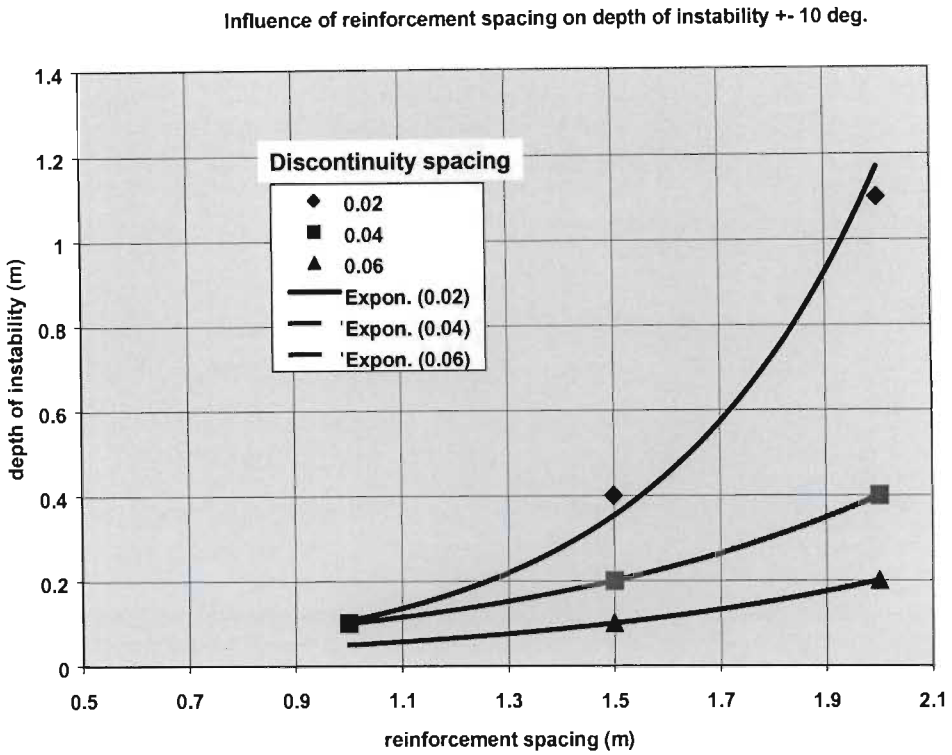

Figure 7-9. Analysis of reinforcement spacing on depth of instability between rock bolt reinforcement for low angle, intersecting discontinuities for different spacing of discontinuities.

In Figure 7-9 the relatively rapid increase in inter-bolt instability is shown with increased rock bolt reinforcement spacing.

A similar analysis was conducted for a blocky, interlocking rock mass structure (Figure 7-6). Comparison of this analysis with that for the low angle, intersecting rock mass structure gives some indication of the influence of the geometry (shape) of the blocks on the potential depth of instability.

The analysis, shown in Figure 7-10, is based on a block length of 0.1 m, and the thickness of the block, perpendicular to the free surface, is varied to reflect changes in the rock mass structure. This effectively changes the area and aspect ratio of the blocks that make up the rock mass structure.

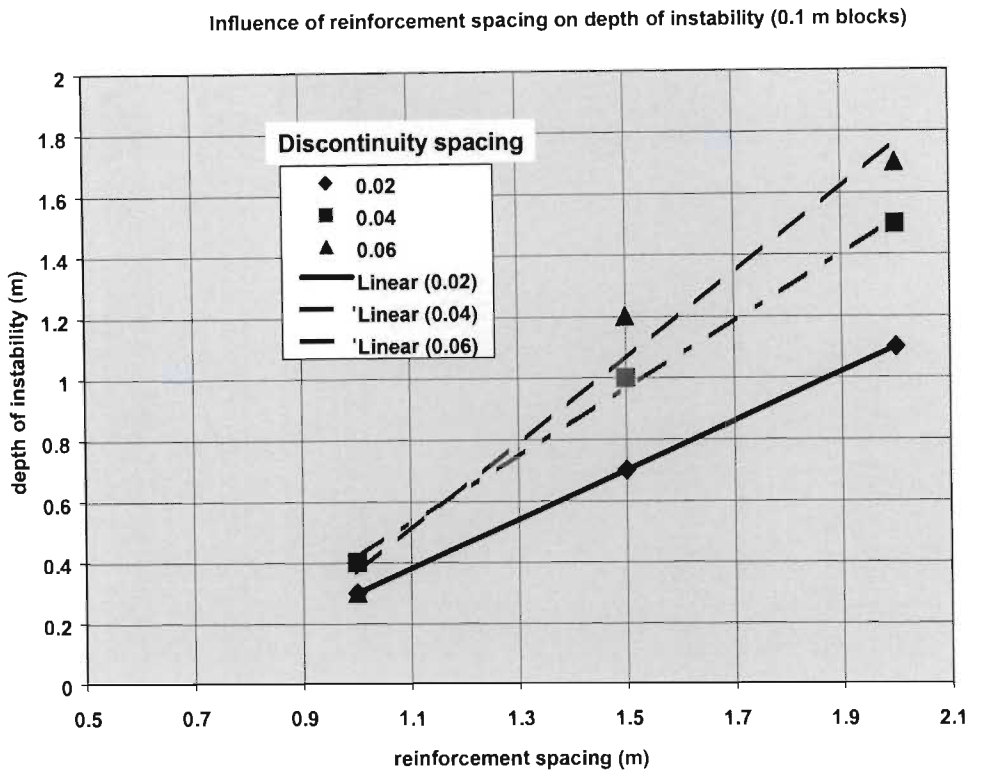

Figure 7-10. Analysis of influence of rock bolt reinforcement spacing and rock mass structure on the depth of inter-bolt instability.

The trend lines in Figure 7-10 again indicate the rapid increase in instability with increased rock bolt reinforcement spacing. This trend of instability, is similar to that indicated in Figure 7-9, but the magnitude of instability is greater for the blocky rock mass structure (Figure 7-10). This is considered to be indicative of the importance of the shape of the blocks that make up the rock mass structure in influencing the depth of instability. The greater elongation of the blocks defined by the intersecting low angle discontinuities as shown in Figure 7-5 and the stability of which is reflected in Figure 7-9, results in increased rock mass stability relative to the more blocky rock mass structure as shown in Figure 7-7.

Further analysis of the influence of the rock mass structure on the depth of instability between rock bolt reinforcement is shown in Figure 7-11. This clearly illustrates the good correlation between the block length and width, and the depth of instability for a fixed rock bolt reinforcement spacing (2 m).

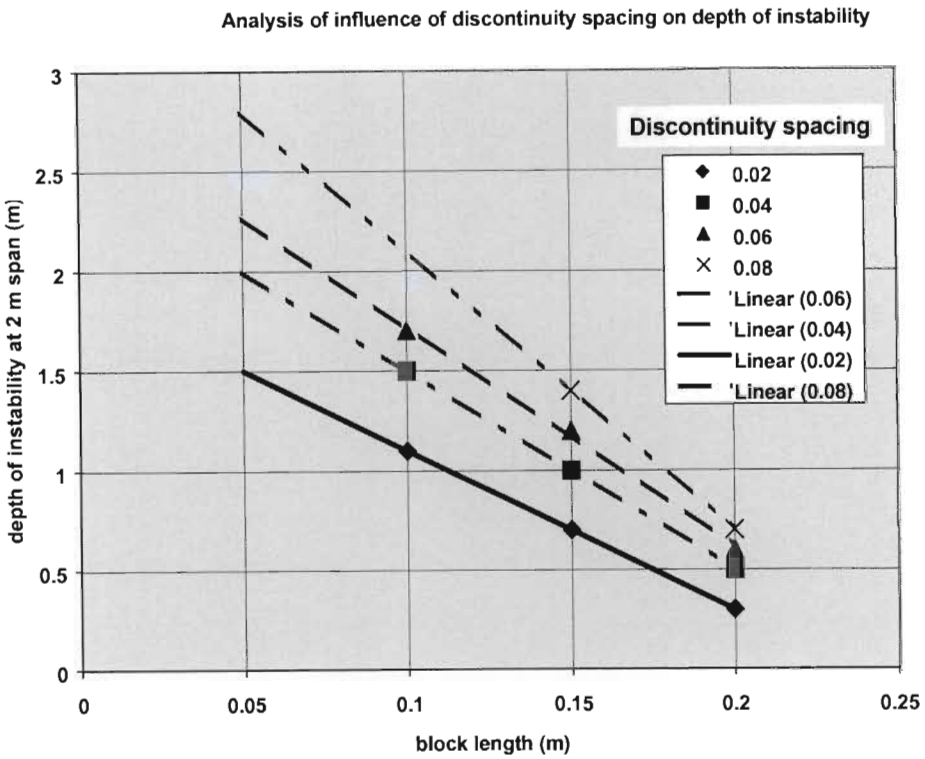

Figure 7-11. Analysis of the influence of the rock mass structure, expressed as a ratio of block length to width, on the depth of rock mass instability.

7.2.2.1 Derivation of design relationships

Analysis of the relationships indicated in Figures 7-8 to 7-11 enabled the derivation of a simple rock mass classification system based on the block geometry and the potential for unravelling instability between rock bolt reinforcement. This relationship is illustrated in Figure 7-12 and caters for the relative stability of both the intersecting low angle discontinuities and the blocky rock mass structures. The critical rock mass geometrical parameters were determined to be the aspect ratio of the blocks perpendicular to the axis of rock bolt installation and the volume (area with unit depth of block in the out of plane direction) of the blocks. These two parameters were found to satisfactorily represent the variations in size and geometry of the blocks that make up the modelled rock mass structures, and reflect their relative stability. This correlation is best expressed in the form of a log-log plot, where linear divisions between the rock mass classes, which are based on the relative stability with regard to rock mass unravelling, can be made (Figure 7-30).

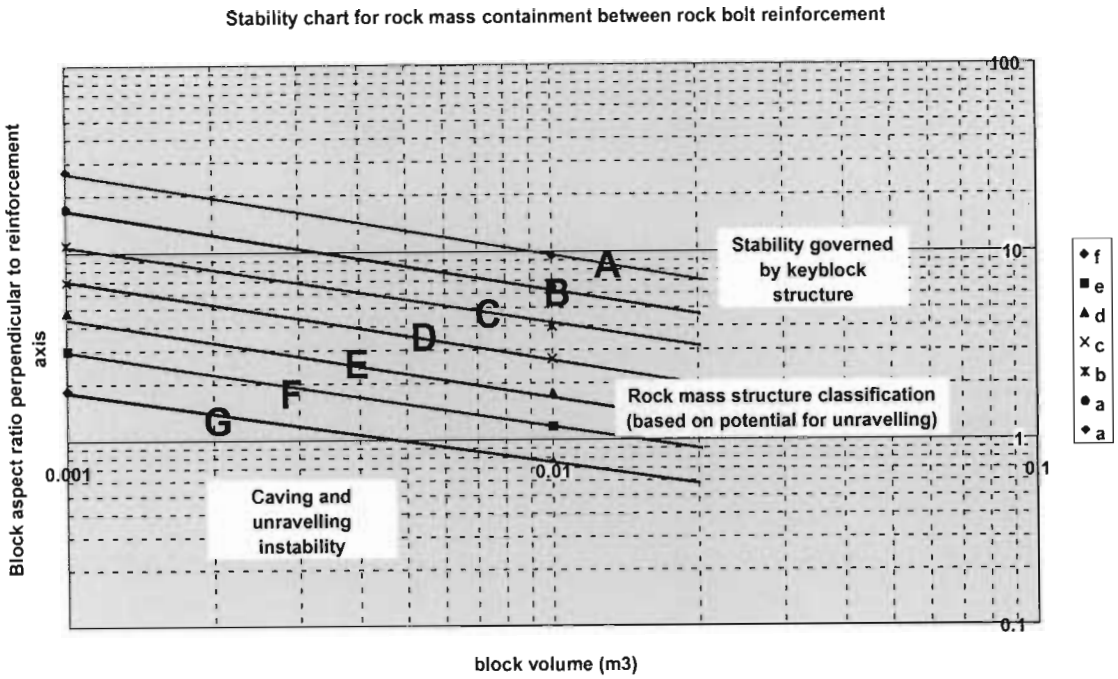

Figure 7-12. Classification of a rock mass on the basis of the volume of blocks and the aspect ratio perpendicular to the rock bolt axis.

The gradient of the lines defining the rock mass classes in Figure 7-12 show that the interlocking nature of the rock mass is strongly controlled by the geometry of the blocks which make up the rock mass structure. This is expressed as the aspect ratio of the block perpendicular to the rock bolt axis. The rock mass classes A to G represent the potential of the rock mass structure for unravelling. This division into 7 classes was considered to adequately represent the likely design divisions between a rock mass instability based on fall out of isolated blocks to the granular behaviour of a highly discontinuous block assemblage.

In practice, rock mass structure may be determined by an assessment of the natural discontinuities within the rock mass, and an understanding of the fabric of fracturing within the rock mass. This will allow the design engineer to make initial estimations of the overall structure of the rock mass relative to the rockwall and support installation. However, where the understanding of the rock fracture process does not allow estimations of rock mass fragmentation to be accurately predicted, determination of the rock mass structure should be established from site investigations in comparable geotechnical environments. These comparable geotechnical environments should take consideration of the rock mass characteristics, excavation geometry, and both the quasi static and dynamic loading conditions.

Once the rock mass classification is established, the impact of the rock bolt reinforcement pattern on the relative stability of the rock mass needs to be determined. This relationship, as derived from the numerical modelling, is illustrated in Figure 7-13.

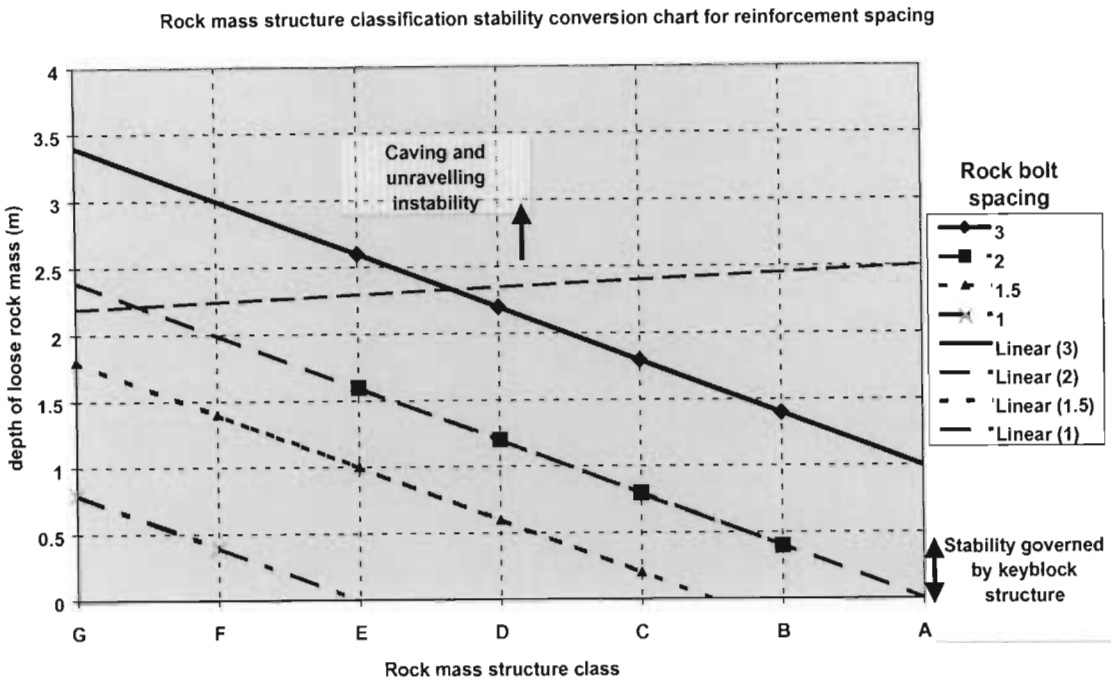

Figure 7-13. Influence of rock bolt reinforcement spacing on depth of rock mass instability between rock bolts.

This analysis is based on the spacing of the rock bolt reinforcement. The containment / retainment method of rock mass stabilisation assumes suitable anchorage within the zone of natural rock mass stability, and, thus, the length of the rock bolt is defined by this depth. Figure 7-13 illustrates the increased reinforcement of the rock mass, as indicated by the reduction in depth of instability (y-axis) between the rock bolt units, by the reduction in the spacing of rock bolts. Limits of characteristic failure modes are also estimated in Figure 7-13. The lower area defines the mechanism of failure due predominantly to potentially unstable key blocks, where failure is not dependent on the rock bolt spacing. The upper limit reflects a transition to total unravelling of the rock mass between the rock bolt units in excess of the analysed length of rock bolt reinforcement. At this level of instability there is no direct interaction between rock bolt reinforcement units and thus the stability of the rock mass is purely a function of the ability of the fabric support to withstand the full rock mass loading. Currently behaviour in excess of this limit is not clearly defined under the current investigation.

Due to the blocky nature of the rock mass, there will be a theoretical natural depth of structural instability as a function of the block aspect ratio. An evaluation of this (Figures 7-14 and 7-15) indicates, for the simulated conditions of rock bolt spacing and block volume, that with the more competent rock mass structures (class A, B and C) the instability is controlled structurally.

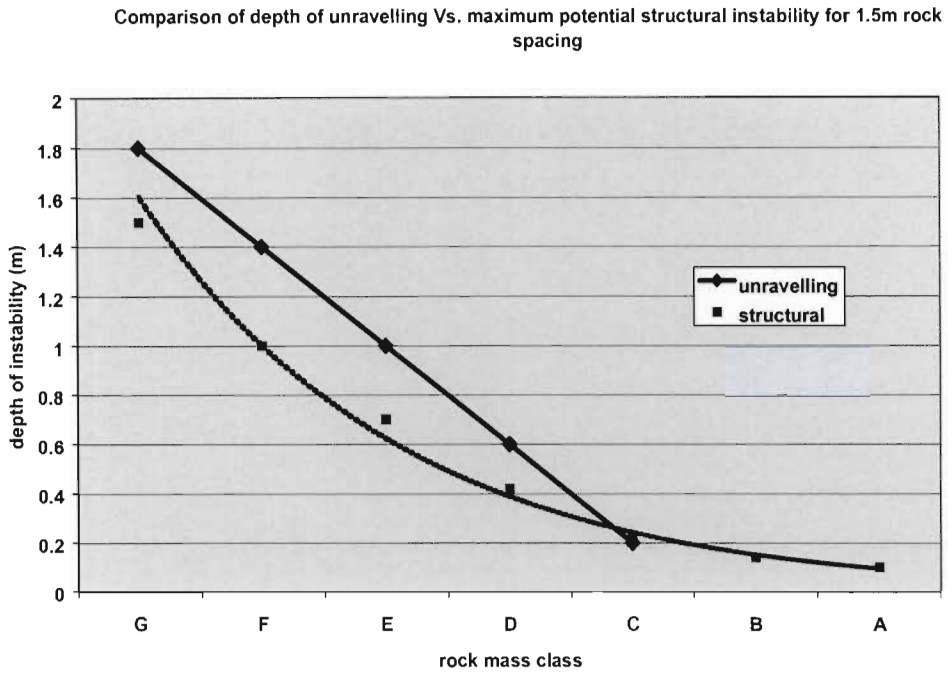

Figure 7-14. Comparison of depth of unravelling instability against potential maximum structural instability for 1.5 m rock bolt reinforcement spacing for constant block volume.

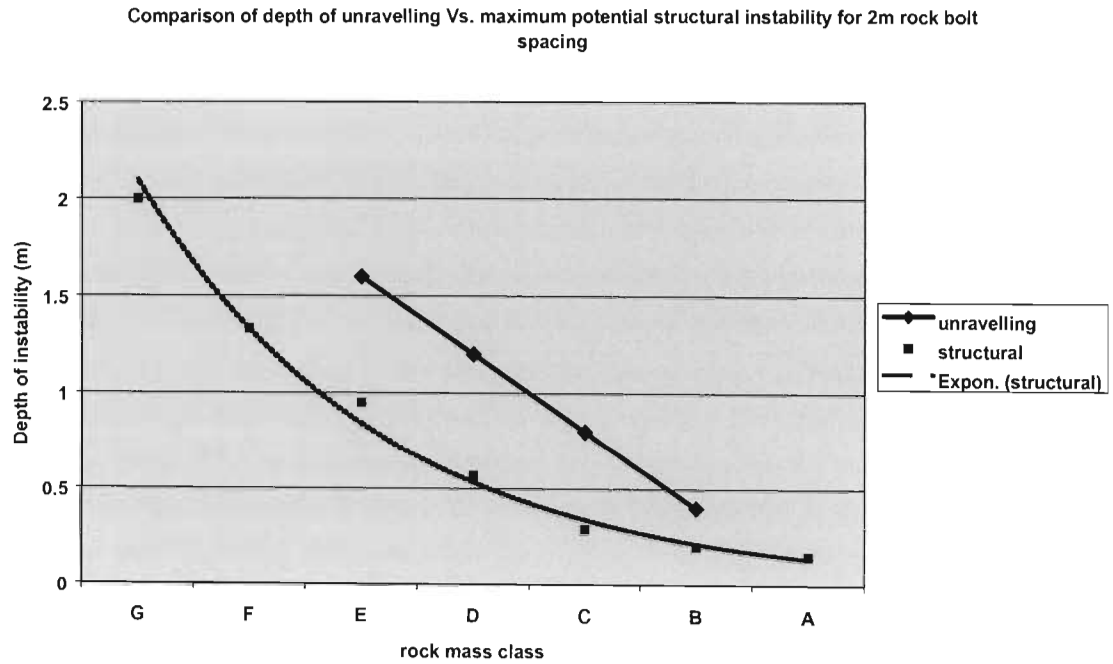

Figure 7-15. Comparison of depth of unravelling instability against potential maximum structural instability for 2 m rock bolt reinforcement spacing, for constant block volume.

Comparison of Figures 7-14 and 7-15 shows the increased susceptibility of the rock mass to unravel under increasing rock bolt reinforcement spacing. The trends of structural instability, for a fixed block volume, suggest that a reduced aspect ratio (class G), relative to the rock bolt axis,

results in increased depth of structural instability. However, in reality, and in the numerical model, the effects of the discontinuity dilation will inhibit the tendency for structural instability. Thus, the difference between the depth of unravelling instability and structural instability will be greater than is indicated in Figures 7-14 and 7-15.

The previous analysis of the relative stability of the rock mass between the rock bolt reinforcement was evaluated on the basis of gravitational loading. In many of the environments in which this analysis is applicable, tunnels will be subjected to dynamic loading. The evaluation of in situ case studies has indicated the increased potential for unravelling of the rock mass between the rock bolt units under dynamic loading caused by major seismic events (Chapter 3). This was seen to be particularly true where the rock mass was more highly discontinuous and failure or significant bagging of the fabric is seen in preference to failure of the rock bolt units. An example of the increased unravelling of the rock mass and the associated deformation history (within the remaining stable rock mass) is illustrated in Figures 7-16 and 7-17.

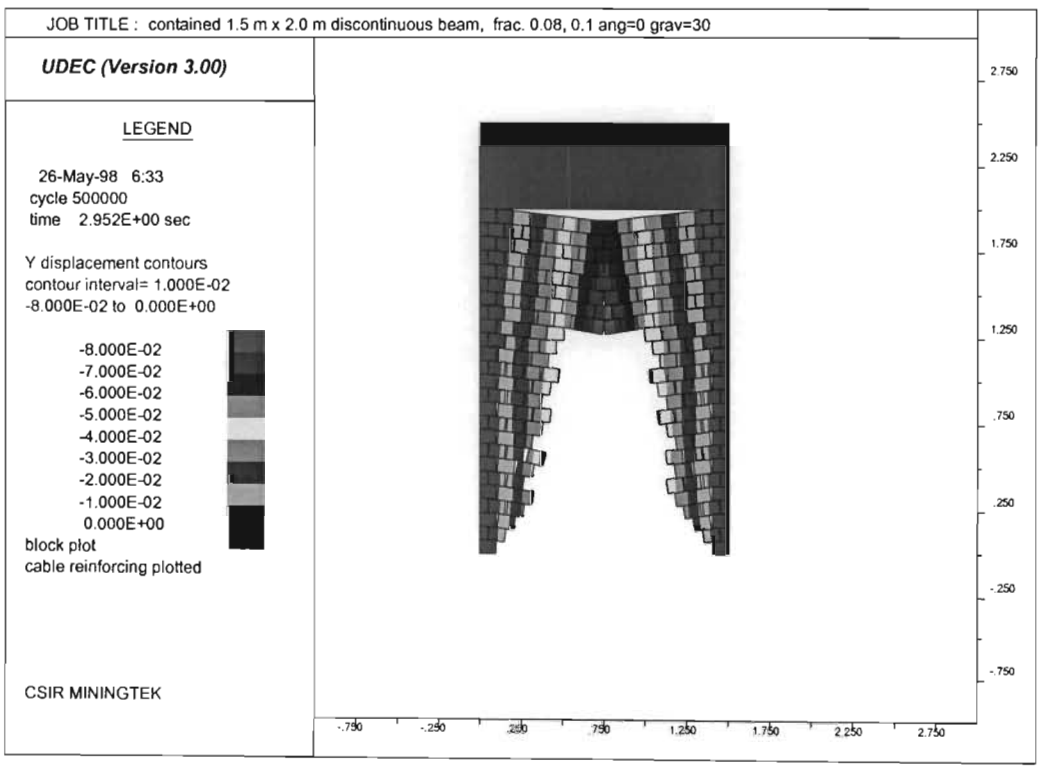

Figure 7-16. Example of increased unravelling and deformation of the rock mass between stable rock bolt reinforcement due to dynamic loading.

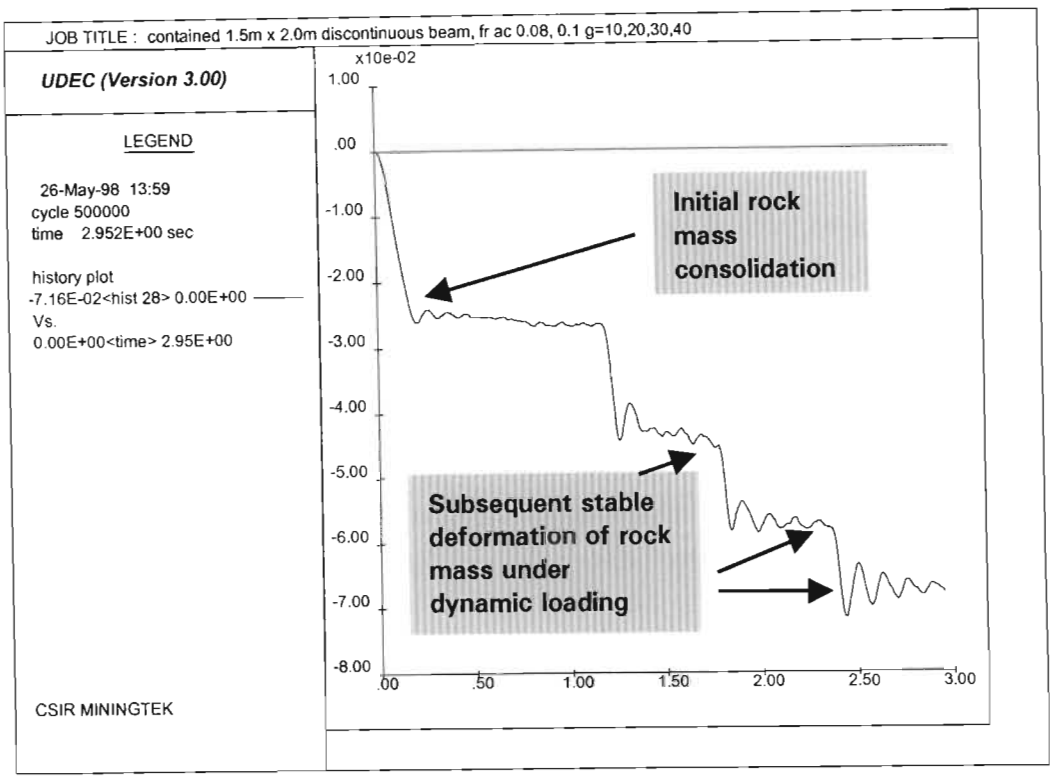

Figure 7-17. Example of deformation history within rock mass for simulated increased gravitational loading.

The results of this evaluation are summarised in Figure 7-18.

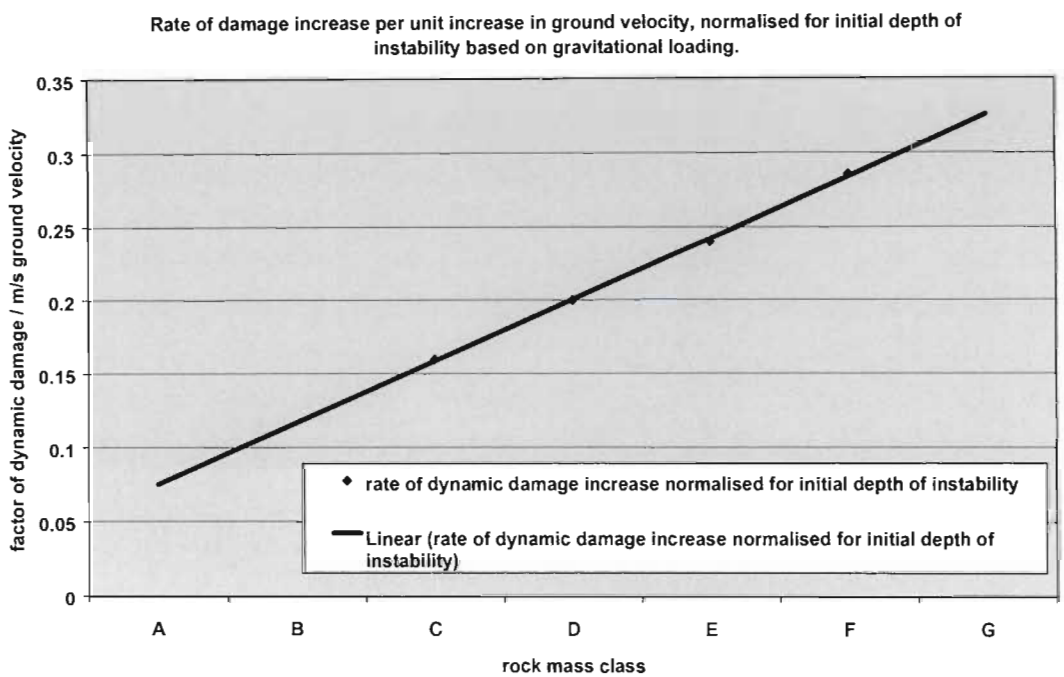

Figure 7-18. Rate of increase in depth of unravelling, normalised to initial depth of instability, due to increase in dynamic ground velocity (m/s), for a defined rock mass class.

This analysis (Figure 7-18) estimates the increase in the depth of unravelling between the rock bolt reinforcement due to an increase in ground motion, due in turn to a seismic event. The relationship is shown to be linear. The analysis was based on the influence of an incremental increase in gravitational loading on the stable deformation of the rock mass, and the respective increased extent of instability (Figure 7-19).

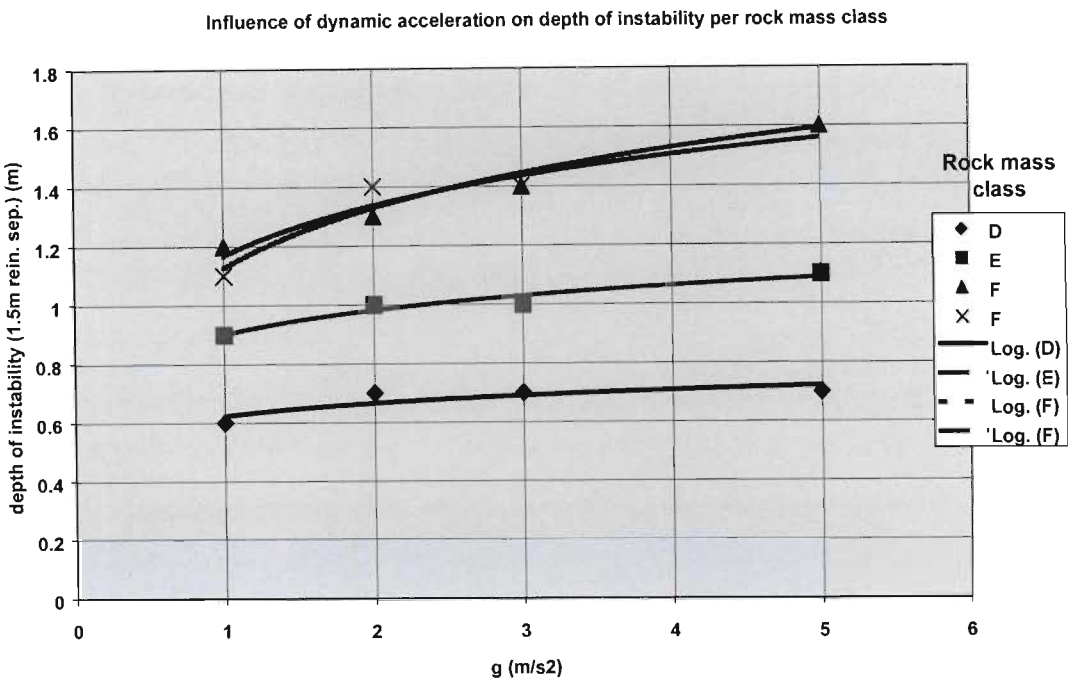

Figure 7-19. Example of increased depth of rock mass unravelling within different rock mass classes due to increased gravitational acceleration of the rock mass.

The increased gravitational acceleration may be equated to increased loading of the rock mass with a resultant stable deformation. The increased loading per unit volume of rock mass, and the associated displacement, may be equated to an energy change in the system. This energy change can be compared to the equivalent kinetic energy, associated with a seismic event, and thus derive an equivalent ground motion velocity to produce the same stable rock mass deformation. This stable deformation of the deeper rock mass is also associated with an increase in the extent of unravelling of the rock mass between the rock bolt reinforcement at the free surface of the model. This increased depth of unravelling corresponds to a reduction in the extent of lateral influence of the rock bolt reinforcement within the defined rock mass structure.

In order to determine the demand on the fabric support system due to the potential instability of the rock mass between the rock bolt reinforcement units, it is necessary to estimate of the volume of instability from the derived depth of instability. Due to the highly variable nature of the rock mass, and thus the limited degree of confidence that can be placed on the estimation of the depth of instability, a simple geometric relationship is considered suitable (Figure 7-20).

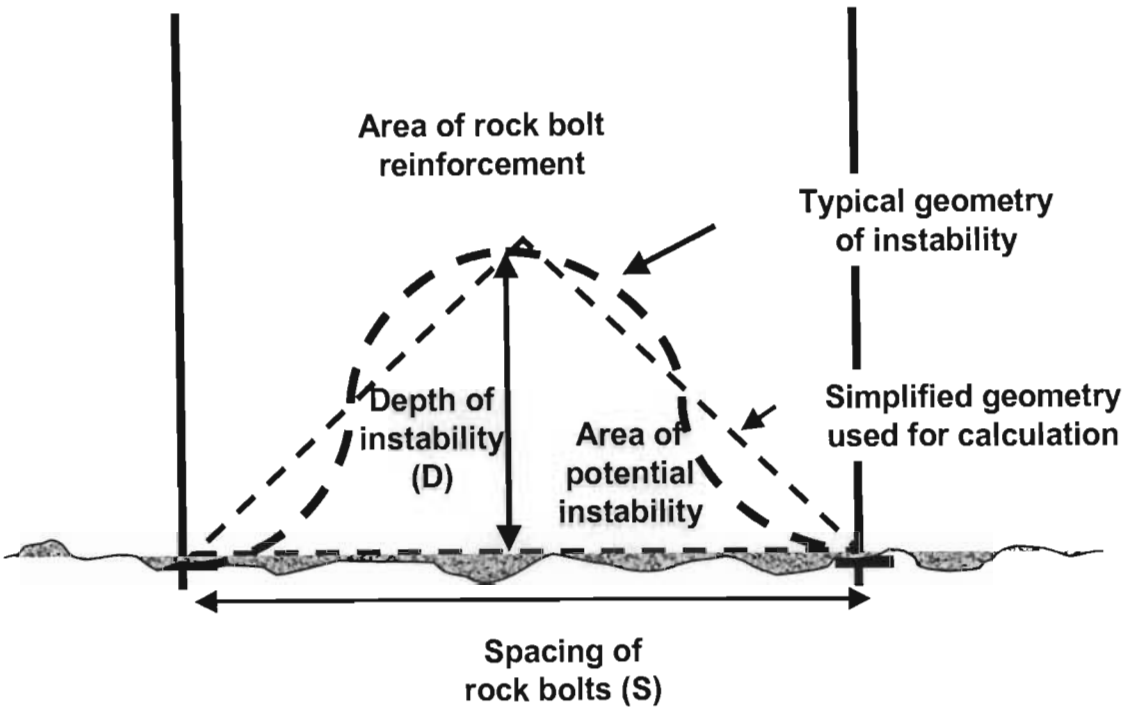

Figure 7-20. Representation of depth of potential instability and definition of area (volume) of instability.

For the design of the fabric support systems the volume of instability between the rock bolt reinforcement is required. It will thus be necessary to estimate the potential instability in at least the two orthogonal planes that typically define the spacing of the rock bolt reinforcement within the support pattern. The nature of the rock mass structure in the periphery of the excavation, relative to the spacing of the support units in a pre-defined pattern, will result in a different depths of instability. Again the interaction of these potential zones of instability is analysed in a relatively simplistic geometrical manner. This aspect of the design process is discussed in Chapter 8 as part of the overall design process.

This analysis only considered the instability of the rock mass to freely unravel between the rock bolt reinforcement. Further analysis examines the influence of the interaction of a fabric support on the behaviour of the system.

The influence of a fabric support was evaluated by monitoring, within the numerical model, the stable deformation of the rock mass for a given areal-coverage support resistance on the surface of the excavation. This is similar to the approach adopted for analysis of support reaction based on the ground reaction curve (Hoek and Brown, 1980). However, here we do not examine the elastic / plastic response of the rock mass due to initial excavation, but the inelastic, unravelling response of an already discontinuous rock mass structure.

This analysis considers the deformation of the rock mass, both at the surface and internally, for a given areal-coverage support resistance. Analysis of the example "ground reaction curves" in Figures 7-21 and 7-22 shows the limit of stable deformation for the defined rock mass class, at the defined reinforcement spacing, and the minimum areal support capacity requirement. The relationship between the fabric support resistance and the deformation of the rock mass will define the minimum stiffness requirement of the fabric support system.

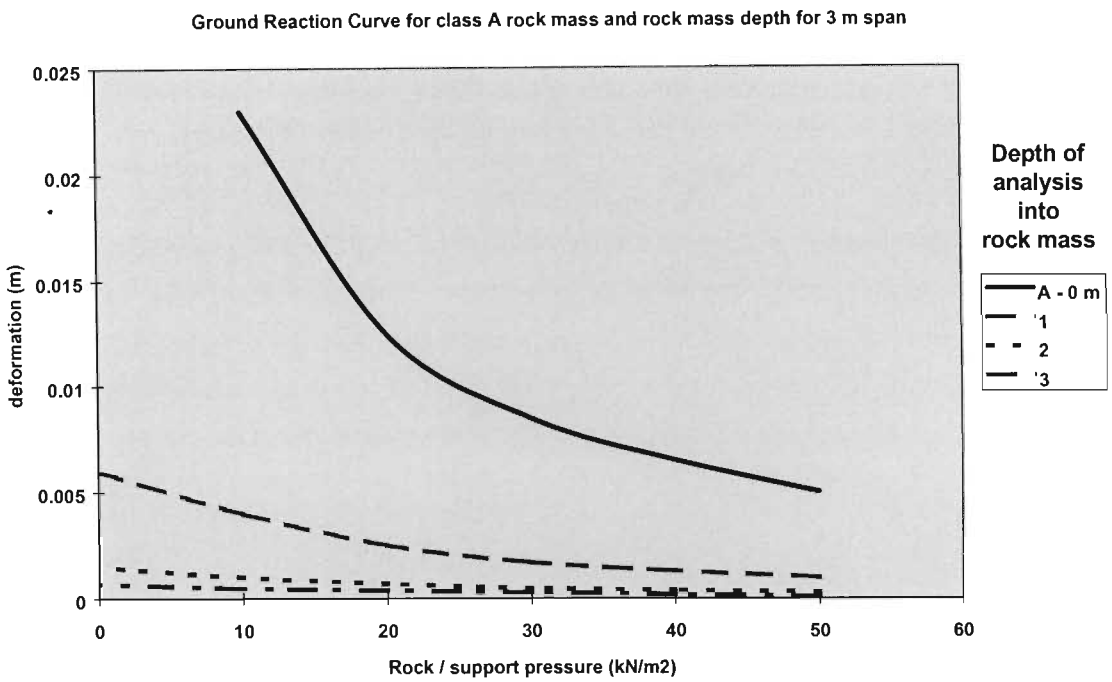

Figure 7-21. "Ground reaction curve" for class A rock mass over 3 m rock bolt span indicating rock mass deformation for different depths within the rockwall and minimum fabric support pressure to ensure stable deformation.

Figures 7-21 and 7-22 were derived from a series of numerical runs in which a support pressure was applied to the lower, free surface of the simulated rock mass between the rock bolt reinforcement boundaries. For each applied support pressure the displacement at the surface and at points of 1 m, 2 m and 3 m into the rock mass structure were recorded at the mid span between the rock bolt units. Where termination of the support pressure / deformation relationship is shown in Figure 7-21 and 7-22 then instability of the rock mass occurred in excess of this deformation and below this critical support pressure for the defined rock mass depth.

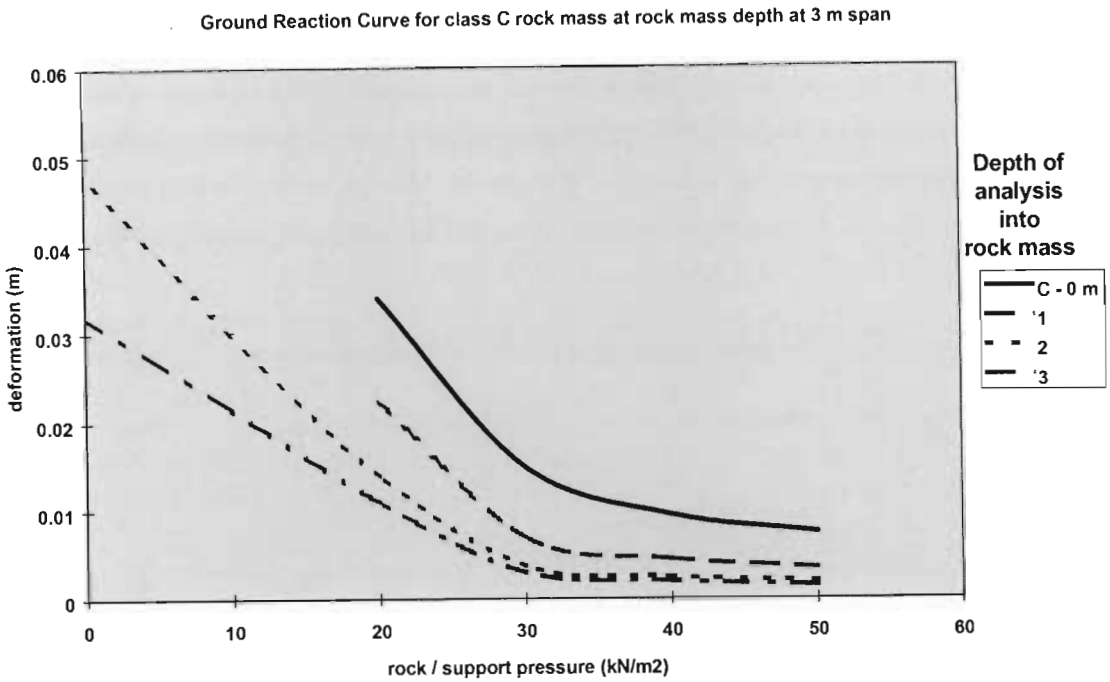

Figure 7-22. "Ground reaction curve" for class C rock mass over 3 m rock bolt span indicating rock mass deformation for different depths within the rockwall and minimum fabric support pressure to ensure stable deformation.

Figure 7-21 indicates that the natural depth of instability is between 0 and 1 m from the excavation boundary under gravitational loading. This is indicated by the stable deformation of the rock mass, at 1 m depth, with no surface constraint. The minimum support resistance, or support pressure, to maintain stability of the peripheral rock mass is 10 kN/m^2, at a maximum displacement of approximately 0.025 m. The deformation of 0.025 m thus represents the maximum tolerable differential deformation between the point of anchorage of the rock bolt reinforcement and the mid span of the fabric support to maintain the inherent rock mass strength. The minimum fabric support stiffness is thus 400 kN/m^2/m.

A similar analysis may be conducted for Figure 7-22. In this case the increased degree of rock mass discontinuity, or reduced block aspect ratio, results in an increased depth of instability associated with an increased deformation of the stable rock mass. The depth of instability due to the defined rock bolt reinforcement spacing is, in this case, between 1 to 2 m. The minimum fabric support resistance is 20 kN/m^2, at a maximum deformation of approximately 0.04 m, to maintain structural interaction of the rock mass. If unravelling of the rock mass at the skin of the excavation is allowed to commence, then instability will occur up to the depth defined by zero support pressure. However, this analysis does not consider the potential for bulking of this unstable rock mass volume, and thus the limitation of further instability due to the constraint eventually generated by the fabric support. . The minimum fabric support stiffness is thus 500 kN/m^2/m.

The application of the above in the design considerations for support systems in highly fractured rock mass conditions is further evaluated in Chapter 8.

7.2.3 Analysis of numerical modelling of a reinforced rock mass beam structure

Consideration is also given to the interaction of rock bolt reinforcement in creating a reinforced rock mass structure. This design consideration is based on the rock bolt reinforcement length being less than the natural depth of instability of the rock mass. For comparative purposes, the rock mass parameters and modelling philosophy are the same as the previous analysis (section 7.2.2). The rock bolt reinforcement, within the numerical model, is represented by reinforcement units across the discontinuities, as defined in the UDEC code (Anon., 1996b), with properties typical of grout encapsulated 16 mm steel (untensioned) rock bolt systems. These reinforcement units capture both the axial and shear characteristics of the rock bolt reinforcement system typical of those defined by laboratory testing (Chapter 5).

Examples of the output of the numerical modelling programme are given in Figures 7-23 to 7-26.

The beam structure is loaded via a uniform stress on the upper boundary. The relationship between this load (per unit area) and the resultant deformation is monitored by subroutines within the UDEC code to determine if the structure remains stable under the defined load. If the structure is stable at this point then the load is incrementally increased and monitored until it either becomes unstable or exceeds a deformation of 0.25 m. This deformation limit was imposed on the analysis as it is considered a practical limit of rock mass deformation within an excavation, and also to optimise available analysis time. The history of load - deformation characteristics is captured by defined "history" functions within the numerical code. The end conditions on the beam are a restriction in the vertical (y-axis) displacement over a lateral (x-axis) distance of 0.5 m from either end of the beam (not included in the definition of the beam length) with free horizontal (x-axis) displacement.

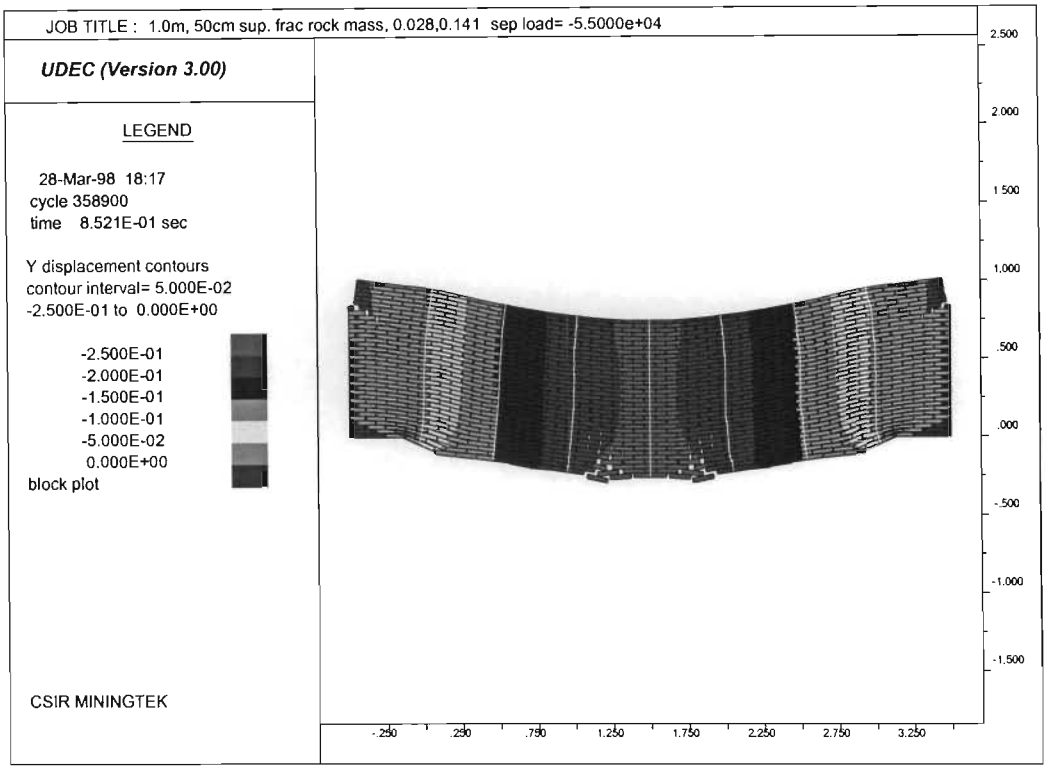

Figure 7-23. Example of 1 m x 3 m reinforced rock mass beam indicating vertical displacement and reinforcement location. Note shear of reinforcement units.

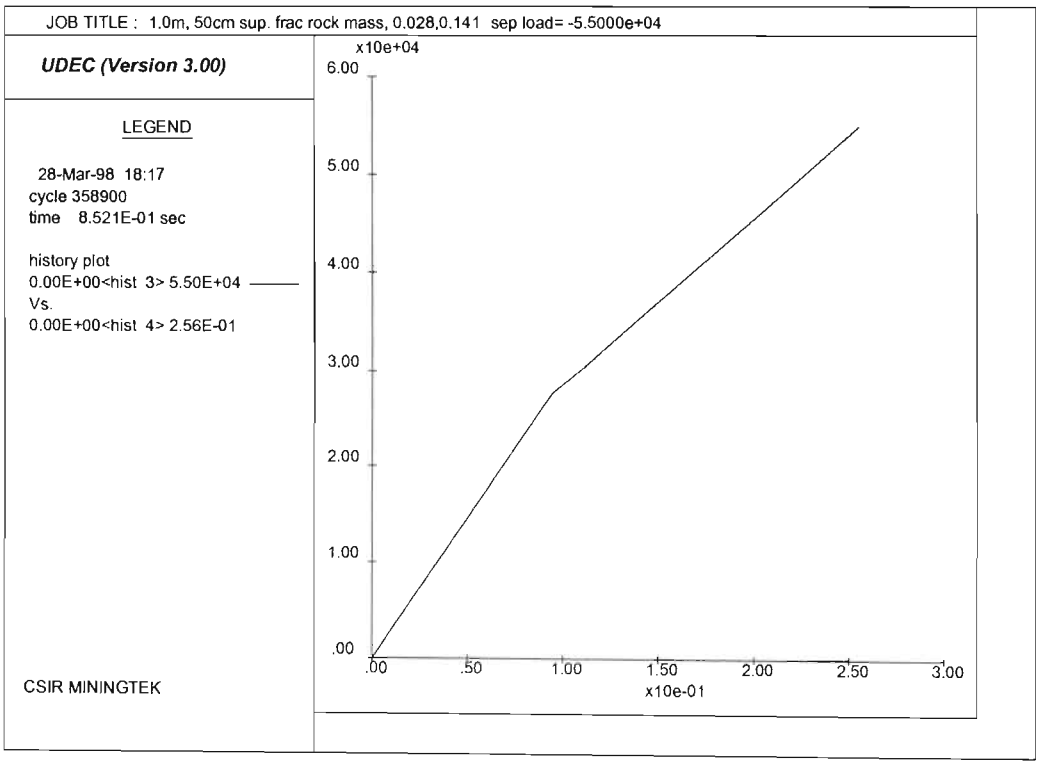

Figure 7-24. Example of load – deformation characteristic of reinforced rock mass beam as illustrated in Figure 7-23.

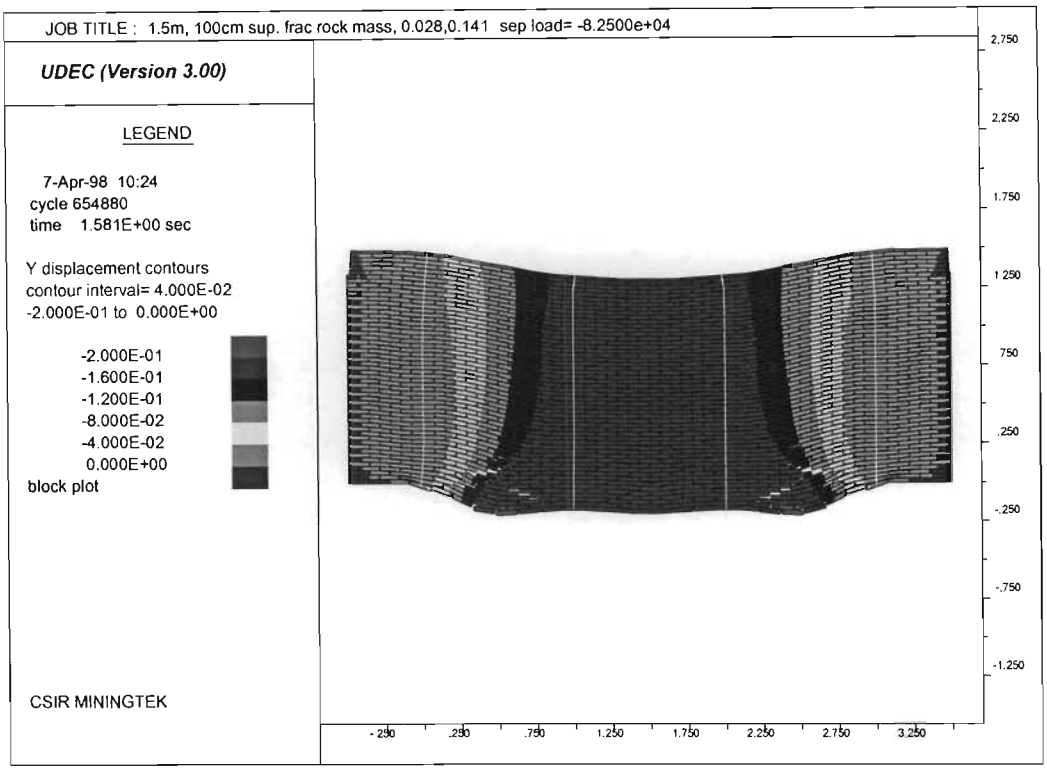

Figure 7-25. Example of 1.5 m x 3 m reinforced rock mass beam indicating vertical displacement and reinforcement location.

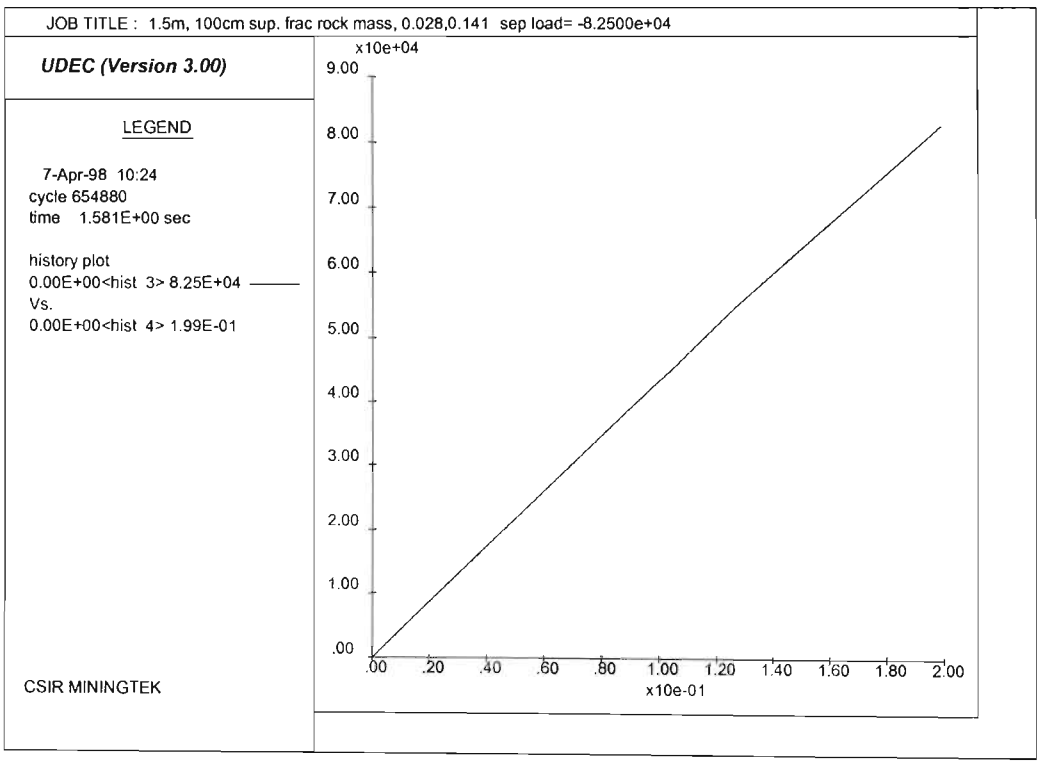

Figure 7-26. Example of load – deformation characteristic of reinforced rock mass beam as illustrated in Figure 7-25.

Evaluation of the performance of the reinforced rock mass structure was based on the load - deformation characteristic of the system (Figures 7-24 and 7-26) at the midpoint of the beam. Comparisons between the different reinforced rock mass systems, as defined by the rock mass structure beam geometry and reinforcement density, is based on the energy absorption capacity (per unit area) at the midpoint of the structure. This was calculated from the area under the load – deformation curve of the upper surface (loading area) of the beam, up to either failure of the system or a deformation of 0.25 m. Consideration of the midpoint deflection generally represents the point of initiation of failure of the system (Figure 7-27). Within the high vertical stress environments of deep level mines, this midpoint position will also represent the maximum depth of sidewall instability, and, thus, potentially the maximum position of loading (quasi static and dynamic).

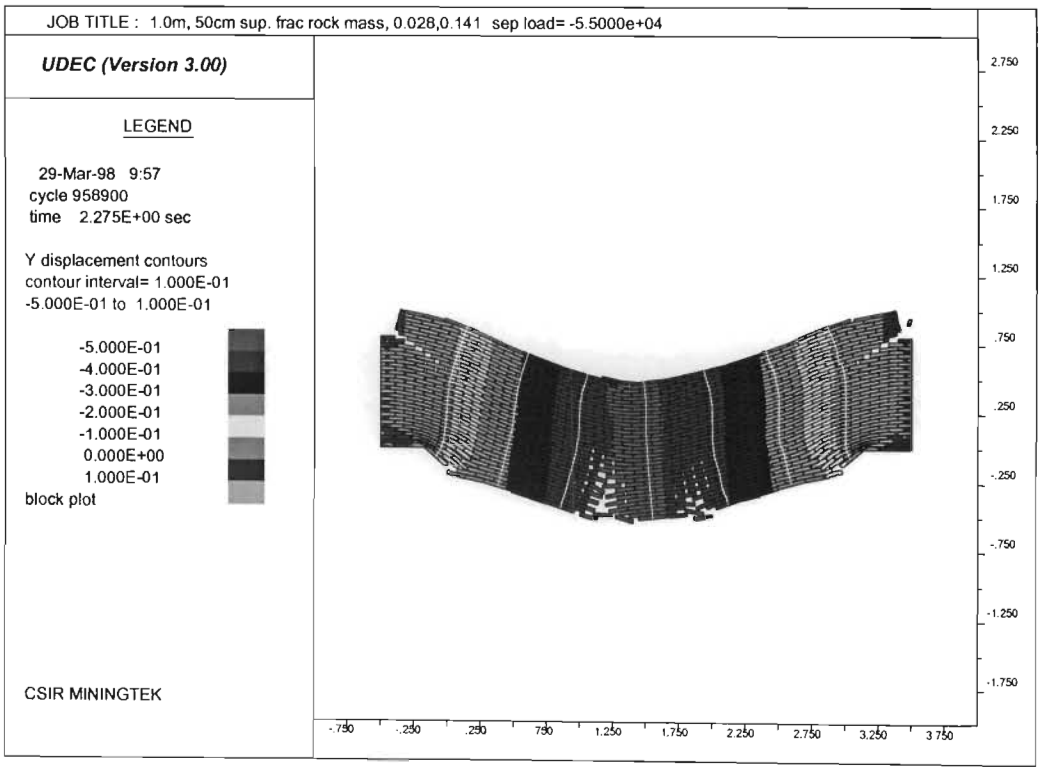

Figure 7-27. Failure of reinforced rock mass beam structure.

Analysis of the aspect ratio of the beam, that is the ratio of the beam length to thickness, is representative of the length of rock bolt reinforcement within the rock mass in relation to the size of the excavation. Thus a beam aspect ratio of three would be equivalent to the support of the unstable rockwall of a 3 m square excavation by 1 m rock bolt reinforcement. The influence of the aspect ratio of the reinforced beam, within different rock mass classes, is illustrated in Figure 7-28.

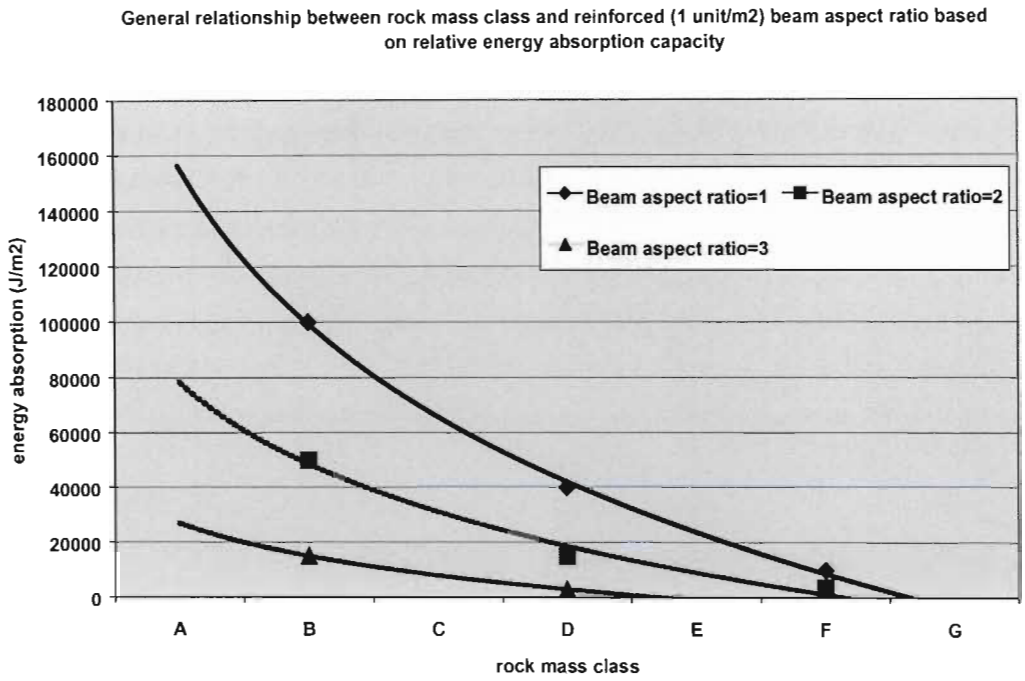

Figure 7-28. Relationship between beam aspect ratio and energy absorption capacity (per unit area) for different rock mass class (reinforcement density 1 unit/m^2).

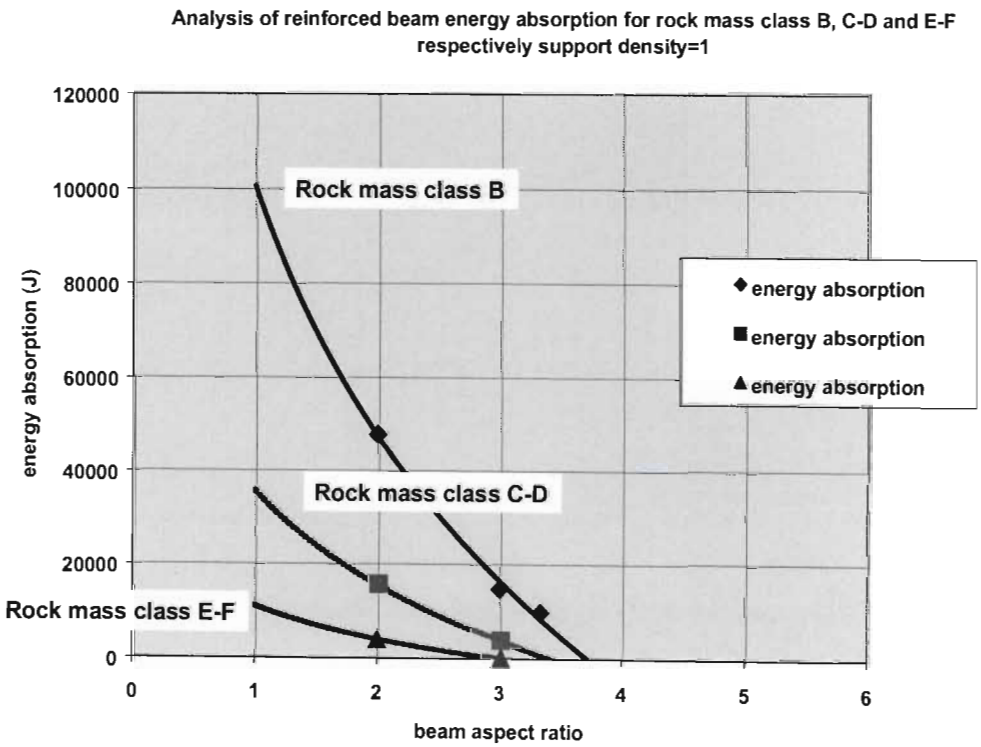

Figure 7-47. Relationship between beam aspect ratio, rock mass class and energy absorption capability for a support density of 1 unit/m^2.

It is clearly shown in Figure 7-28 that the reduced aspect ratio of the beam results in a far more competent structure as defined by the energy absorption capability.

This is similarly expressed with respect to rock mass class and beam aspect ratio in Figure 7-29.

Again it is evident from Figure 7-29 that the beam aspect ratio and the rock mass structure, for the defined support density, greatly influence the load – deformation capability of the structure. Most of the increased energy absorption capability is due to the increased stiffness of the rock mass structure, rather than a difference in the amount of allowable deformation (Figure 7-30).

The reinforced rock mass structures evaluated indicate that there was limited capacity, either due to failure of the structure or excessive deformation, at a beam aspect ratio greater than three. However, an increase in rock bolt reinforcement density results in increased beam capacity and also the ability to sustain load, within the deformation limitations, for beam aspect ratio's in excess of three (Figure 7-31). Beam aspect ratios in the mines are typically 1.7.

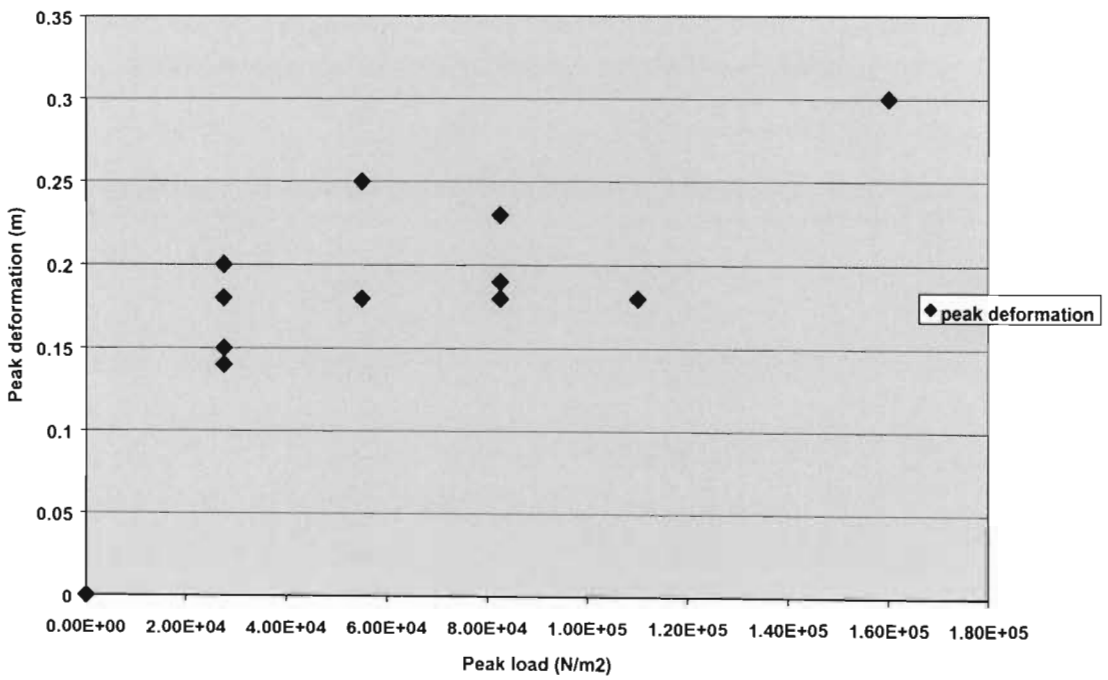

Figure 7-30. Evaluation of relative contribution of peak deformation and peak load to differences in energy absorption capability.

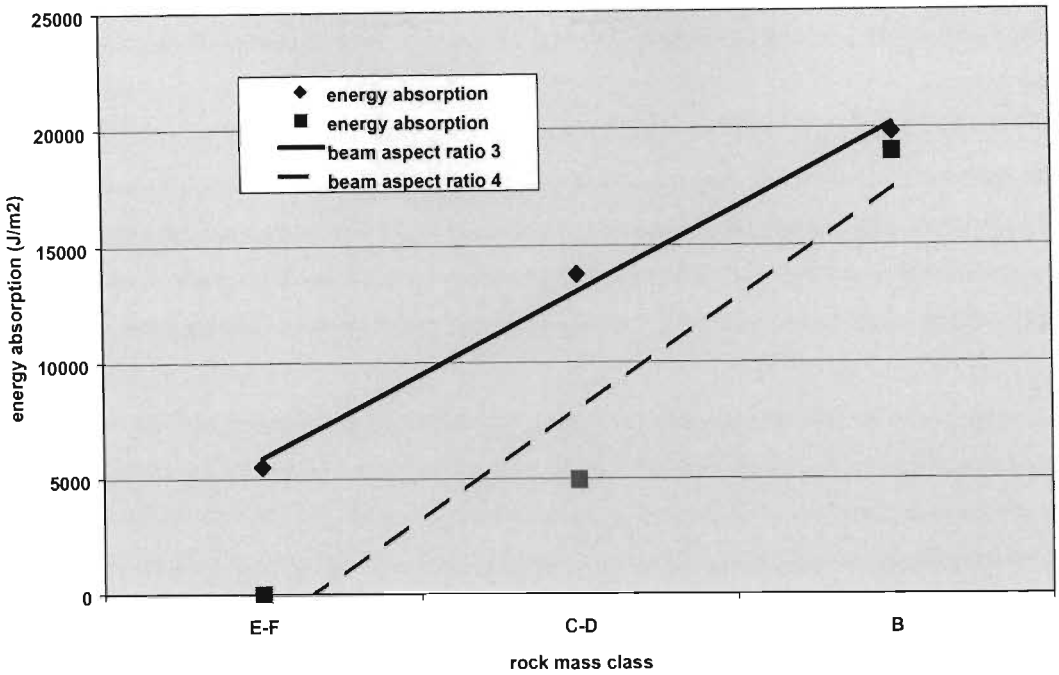

Figure 7-31. Relative capacity of beam aspect ratio at high reinforcement density (2 units/m^2) for different rock mass classes.

The relative influence of reinforcement density on the capacity of the reinforced rock mass structure is also shown in Figure 7-32. Here a comparison is made between reinforcement density for the defined rock mass classes. The density of reinforcement within the rock mass structure has a relatively large influence on the capacity of the structure. Mechanistically the reinforcement restricts the ability of the rock mass to shear and unravel between the locations of rock bolt installation. Of note is the relative reduction in influence of the reinforcement within the more competent rock mass structures (A). In this case the inherent strength of the rock mass overshadows the influence of the reinforcement unit.

However, even this more competent rock mass structure is not stable over the typical dimensions of underground tunnel excavations, and, thus, still requires the use of reinforcement to ensure stability. An assessment of the relative influence of the reinforcement density, and the critical density below which instability of the structure occurs, is shown in Figure 7-33 for rock mass class B. Even for this relatively competent rock mass structure, there is a rapid reduction in the beam capacity below a reinforcement density of 1 unit/m^2. In addition it is indicated that a reinforcement density above this level has a proportionally less significant effect (Figure 7-32).

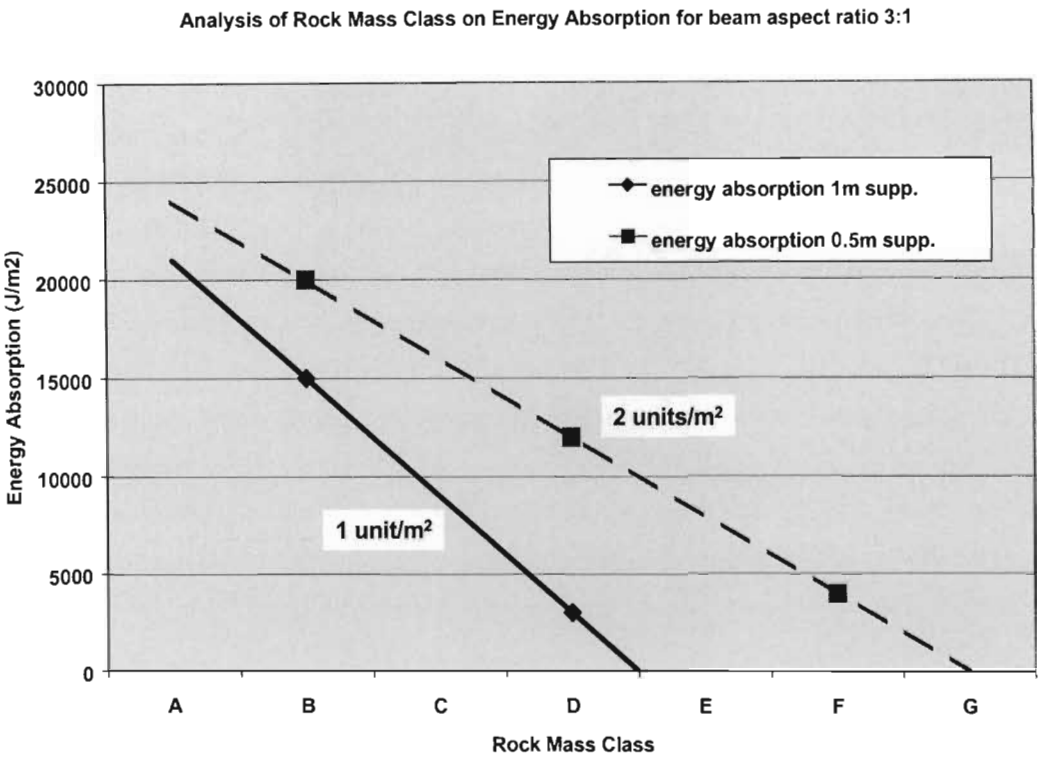

Figure 7-32. Relative influence of reinforcement density on reinforced rock mass structure capacity for a beam aspect ratio of 3.

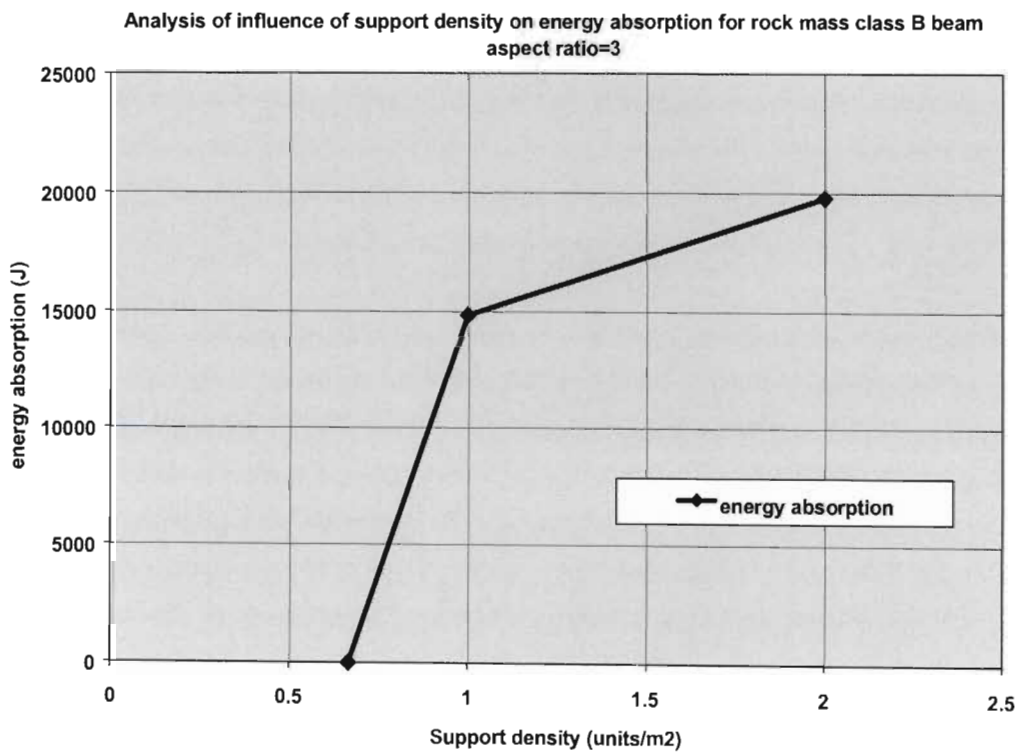

Figure 7-33. Evaluation of influence, and criticality, of rock bolt reinforcement density on reinforced beam competency.

With reference to the above charts, a comparison may be conducted as to the relative merits of a design based on the creation of a reinforced rock mass structure to that based on rock mass containment. An example of this evaluation is given in Chapter 8.

7.3 Evaluation of numerical modelling for analysis of rock mass reinforcement.

Numerical modelling is utilised to obtain an improved understanding of the mechanistic interaction of rock bolt reinforcement units within an unstable rock mass structure. This evaluation is based on the relative sensitivity of the system performance to characteristics of the rock bolt reinforcement system and the rock mass. The applicability of the numerical model is based on their ability to capture mechanisms as evaluated from in situ observations (Chapter 3).

In general it is considered that this analysis has given important new insight into the interaction between the rock bolt reinforcement and the rock mass. Due to the complexity of the rock mass environment in situ, it is considered inappropriate to try to explicitly model this environment with the current limited understanding. Thus the validity of this exercise should rather be compared to the current basis of the industries design considerations of the interaction between a rock bolt and the rock mass. Thus, compared to the currently assumed tributary area loading, this work provides simple tools to make improved estimations of the behaviour of rock mass reinforcement systems within the highly discontinuous and dynamic rock mass environments of deep level mines.

Considerations of the relative applicability of this analysis to the understanding of rock mass reinforcement mechanisms are as follows:

- In a highly discontinuous rock mass structure interaction between rock bolt reinforcement is restricted resulting in large volumes of potentially unstable rock mass between these units.

- The critical rock mass parameters are the structure of the rock mass (block shape) relative to the axis of rock bolt reinforcement installation, and the intensity of discontinuity (block volume) within the rock mass.

- The critical reinforcement system parameters are the spacing and length of the rock bolt units within the support system for a defined rock mass structure and depth of instability.

- The degree of confinement provided to the rock mass, by the rock bolt unit and the system spacing, may influences the degree of deformation of the rock mass between the reinforcement units and thus the potential for unravelling.

- The increased frequency and persistence of discontinuities, sub-parallel to the axis of the rock bolt reinforcement, results in an increased restriction of the rock bolt reinforcement interaction.

- Increased loading of the rock mass (quasi static or dynamic) results in further reduction in rock bolt reinforcement interaction and thus increased unravelling of the rock mass.

- Reinforcement of the rock mass, to depths less than the overall depth of instability of a potentially unstable rock mass volume, can create a competent reinforced rock mass structure.

Assumptions in the analysis of containment and structural stability by rock mass reinforcement and thus applicability are:

- The structure of the rock mass is dominated by highly persistent stress fracture discontinuities sub-parallel to the boundary of the excavation and thus sub-perpendicular to the axis of the rock bolt reinforcement.

- The properties of the rock bolt reinforcement, within the reinforced rock mass structure analysis are based on typical 16mm steel rock bolt grouted systems.

- The structure of the rock mass is uniform over the defined depth of instability.

- Rock mass properties are uniform within the area of analysis.

- Loading is uniform within the rock mass over the area of analysis

Analysis of these factors, using the applicable charts as discussed in this section, may allow an improved estimation of loading within a support system based on this mechanistic evaluation of rock bolt reinforcement interaction. This consideration will allow improved tunnel support design under the conditions of a highly discontinuous rock mass structure.

Chapter 8

8 The mechanistic design of support systems in deep level mining environments, conclusions and recommendations

8.1 Introduction

The influence of rock mass structure on the extent of interaction of rock bolt reinforcement, with anchorage within, or external to, an unstable rock mass, has been examined in Chapter 7. Design tools have been derived to enable an assessment of the degree and extent of interaction between a reinforcement unit and the adjacent rock mass for specific geotechnical environments and support characteristics. This previous analysis may be used to design a support system based on a mechanistic understanding of the interaction of the rock bolt units within a highly discontinuous rock mass structure

8.2 Application of design methodology

8.2.1 Evaluation of rock mass environment

The mechanism of rock mass stabilisation is dependent on the relationship between the depth of instability of the rock mass in the vicinity of an excavation and the length of the rock bolt reinforcement. Thus, for the application of the design methodologies, the length of the rock bolt reinforcement unit must be established in relation to the extent of the unstable rock mass, under the anticipated geotechnical environment and loading conditions. This may currently be determined by analysis of fall of ground and rockburst ejection thickness for the applicable geotechnical area. For the purpose of anticipated rockburst ejection, a cumulative percentage graph of recorded thickness data may be used (Figure 8-1), as an example for all gold mines.

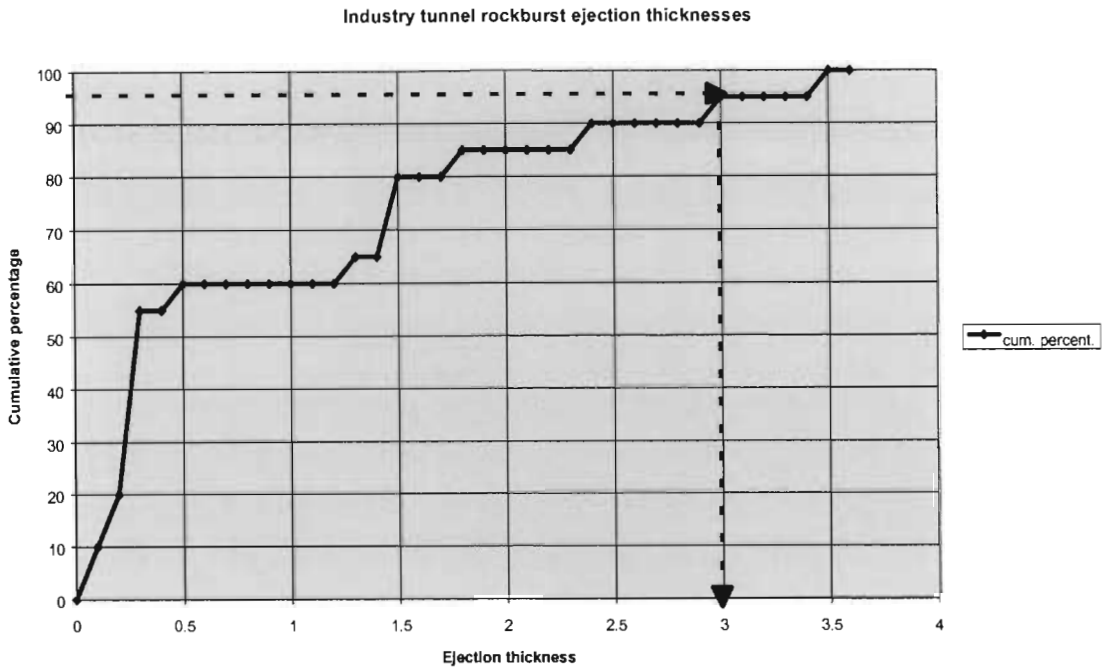

Figure 8-1. Graph of cumulative percentage of gold mine tunnel (< 4 mx4 m) rockburst ejection thickness' indicating 95 % design level.

A suitable level of design confidence is selected (95 per cent) in order to determine the design thickness of the potentially unstable rock mass. Thus the length of the reinforcement unit should be this thickness plus sufficient length to provide a secure anchorage in the stable ground beyond the defined unstable design thickness.

Alternatively, and more fundamentally, the thickness of a potentially unstable rock mass may be determined from failure criteria, instrumentation, or empirical design guidelines. It is important that these methods fully reflect the design geotechnical environment and extent of rock mass instability. It is suggested that in the environment typical of deep level mines that the natural depth of instability around an excavation be determined from the application of the chart as shown in Figure 8-2. What follows is an example of the application of the methodology.

If we assume that the excavation under consideration is a tunnel with typical square profile of dimensions 3.5 m x 3.5 m (h), and is sited in a quartzite rock mass with a uniaxial compressive strength of 200 MPa. Virgin stress conditions are estimated at approximately 60 MPa vertical and 30 MPa horizontal and the tunnel is initially isolated from the influence of stoping operations. Over the life of the excavation the mining of a stoping abutment, which results in a maximum vertical stress level of 90 MPa and a subsequent reduction to 20 MPa, will influence the tunnel. In addition, it is anticipated that the tunnel will subsequently be subject to dynamic loading due to seismicity associated with the stoping abutment. The influence of seismicity may be determined from either the maximum anticipated magnitude of seismic events and proximity to the tunnel, or directly from the maximum anticipated dynamic ground velocity. At this stage let it

be assumed that the maximum anticipated seismic event is magnitude M=3.0 at a distance of approximately 50 m from the tunnel.

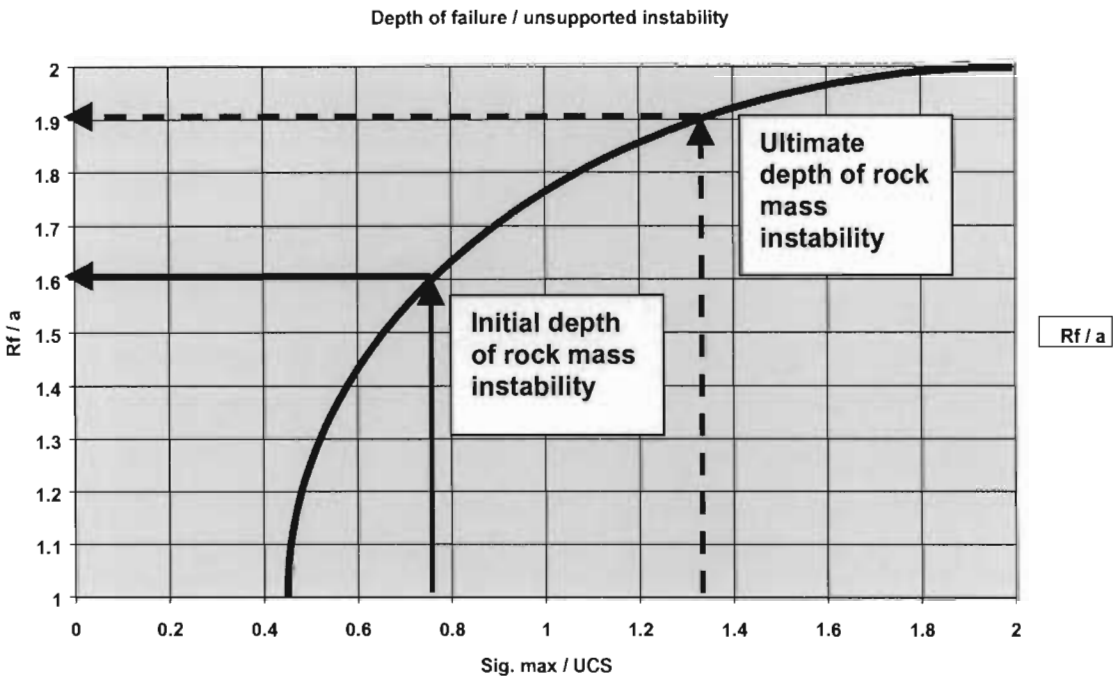

Figure 8-2. Chart to determine depth of instability due to stress induced fracturing.

The following methodology indicates the application of the charts in the determination of the rock mass characteristics in the vicinity of the tunnel.

The equivalent dimension (a) for the square tunnel is given by equation 8-1

$$a = h / \sqrt{2} = 3.5 / \sqrt{2} = 2.5 \text{ m} \qquad (8\text{-}1)$$

The initial induced stress on the sidewall of the tunnel (parallel to the maximum stress vector) is given by equation 8-2.

$$\sigma_{max} = 3\sigma_1 - \sigma_3 = 3 \times 60 - 30 = 150 \text{ MPa} \qquad (8\text{-}2)$$

Thus sig.max (σ_{max}) / UCS in figure 8-2 is given by equation 8-3.

$$\text{sig. max/UCS} = 150 / 200 = 0.75 \qquad (8\text{-}3)$$

From Figure 8-2 the initial depth of instability relative to the excavation size is given by $R_f / a = 1.6$. The natural depth of instability of the rock mass in the sidewall of the tunnel is given by equation 8-4 for (a) as derived from equation 8-1.

$$R_f - h/2 = 1.6 \times a - 3.5 / 2 = 1.6 \times 2.5 - 1.75 = 2.25 \text{ m} \qquad (8\text{-}4)$$

It is now necessary to evaluate the increased depth of instability due to the influence of the higher induced stress levels and seismicity associated with the stoping abutment. From Figure 8-3 an estimate of the dynamic stress associated with seismicity can be made. This is a function of the maximum anticipated seismic event magnitude and the proximity of the seismic event to the excavation. From the description of the excavation environment as defined previously, the maximum induced dynamic stress, as estimated from Figure 8-3, is approximately 30 MPa.

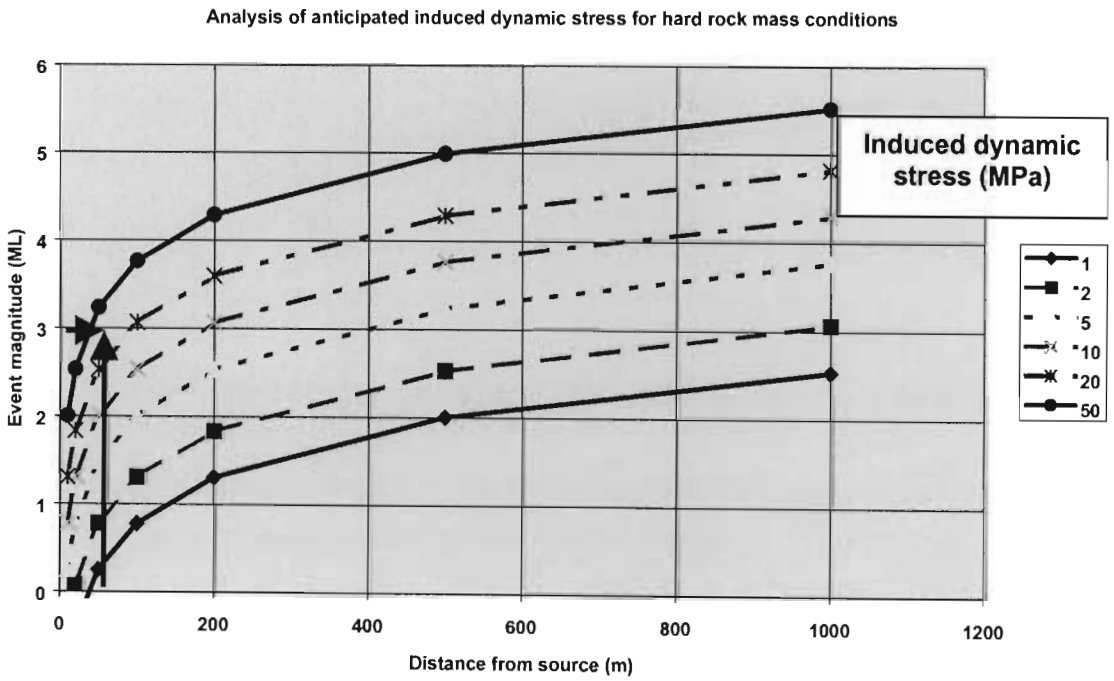

Figure 8-3. Estimation of maximum dynamic induced stress.

This dynamic stress is additive to the higher induced stress level due to the proximity of the stoping abutment. The maximum induced stress is thus given by equation 8-5.

$$\sigma_{max} = 3\sigma_1 - \sigma_3 + \sigma_d = 3 \times 90 - 30 + 30 = 270 \text{ MPa} \qquad (8\text{-}5)$$

Following the procedure as indicated above in equations 8-1 to 8-4, the ratio of sig.max / UCS is 1.35, thus R_f / a is approximately 1.9 as derived from Figure 8-2. The natural depth of instability due to stress induced fracturing under the future static and dynamic stresses will be approximately 3.0 m.

The tunnel is subsequently subjected to a significant stress reduction, and although this is currently considered not to result in the further extent of natural instability, it does result in significant further dilation of the rock mass around the tunnel excavation. An estimation of the

dilation history of the rock mass in relation to the rock bolt characteristics is important in order to determine the capacity of the rock bolt system at any point during the life of the excavation. The dilation of the fracture zone around the excavation, as a function of stress change, both positive and negative, may be estimated from the charts indicated in Figures 8-4 to 8-7 as derived in Chapter 4. Let it be estimated that the initial support density is 1 unit/m^2. From the example case study, the tunnel is subjected to a vertical stress increase of 30 MPa, from its initial state of 60 MPa, to 90 MPa, and a subsequent stress reduction of 70 MPa to an overstoped stress state of 20 MPa.

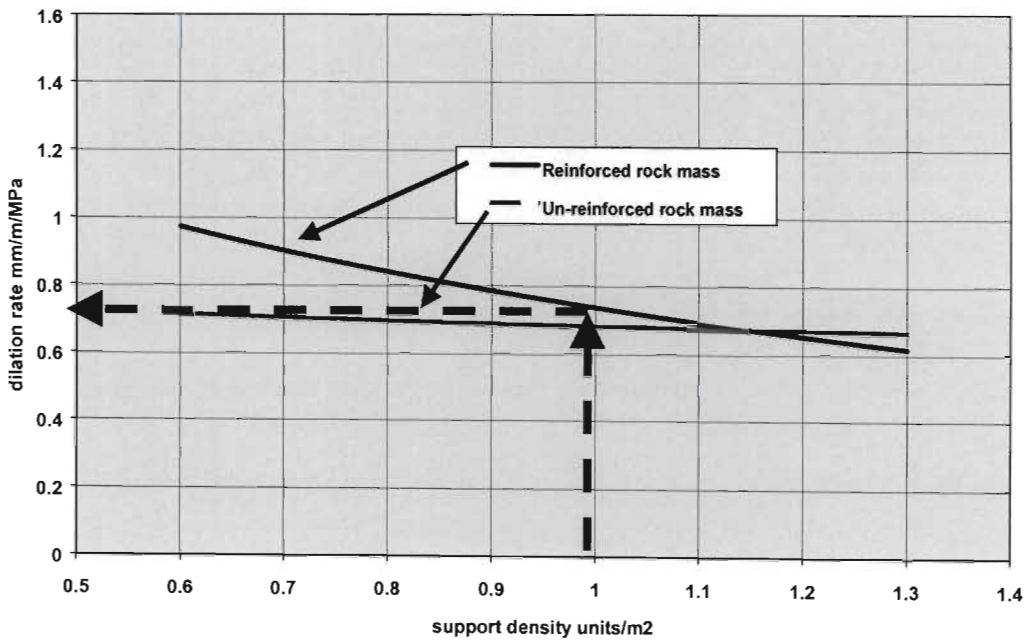

Figure 8-4. Estimation of sidewall dilation rates per metre per unit increase in vertical stress field.

Analysis for the sidewall of the excavation indicates that the estimated dilation rate per unit increase (MPa) in vertical stress is approximately 0.75 mm per metre depth of fractured rock mass. Thus over the vertical stress increase of 30 MPa it is anticipated that the rock bolt reinforcement would be subjected to a strain of:

$$0.00075 \times 30 = 0.023 \text{ or } 2.3\% \text{ elongation.}$$

Over the maximum depth of natural instability (3 m) this would equate to a yield demand of approximately 69 mm.

Using Figure 8-5 the rate of dilation of the sidewall of the excavation during the period of vertical stress reduction is estimated. This is derived as a factor between the difference in the rate of deformation due to vertical stress increase to that of vertical stress decrease. It is assumed that

the deformation mechanism is mechanistically similar and thus dilation per unit volume of rock mass will be comparable, however, the rate is substantially lower by a factor of:

$$0.2 / 1.7 = 0.12$$

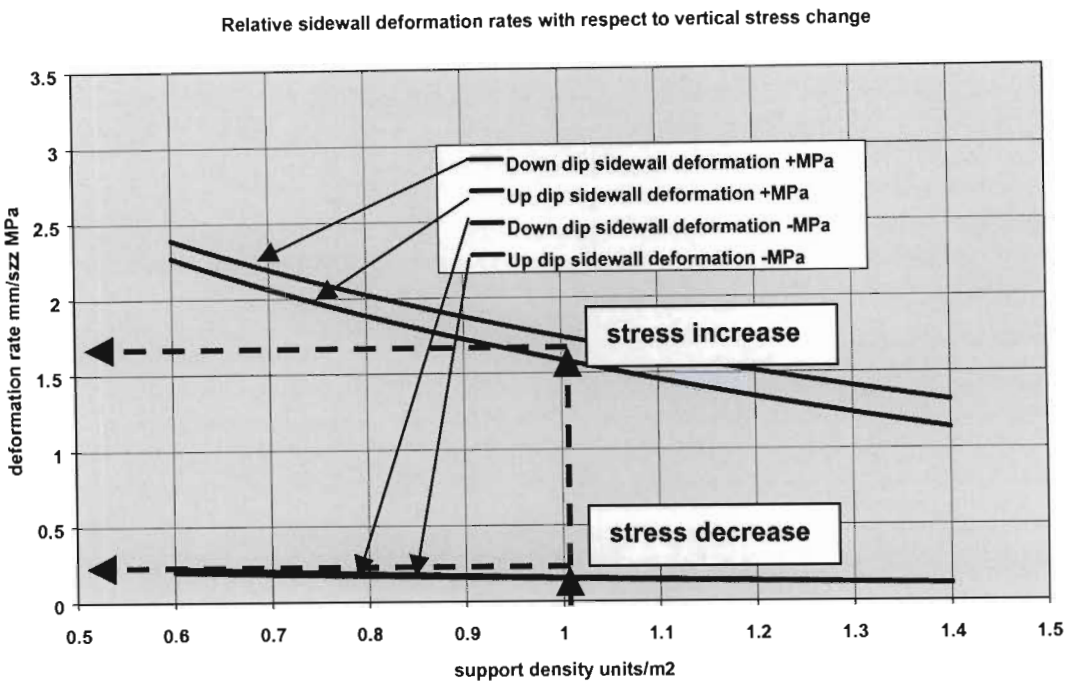

Figure 8-5. Estimation of relative sidewall dilation rates for vertical stress increase and decrease.

Therefore during the period of vertical stress decrease (70 MPa), it is estimated that the rock bolt reinforcement system will be subjected to a further elongation during this period of stress change of:

$$0.00075 \times 0.12 \times 70 = 0.0063 \text{ or } 0.63\% \text{ elongation}$$

Thus over the maximum depth of natural instability (3 m) this would equate to a further yield demand of approximately 20 mm.

Analysis of the hangingwall of the excavation in this stress environment indicates limited potential for stress induced fracturing, although structural instability, or damage due to blasting practice may be envisaged. An estimation of the extent of potential natural instability may be made from the difference between the actual excavation size and the effective excavation dimension (Kaiser *et al* 1996) as given by equation 8-6.

$$a - h/2 = 2.5 - 3.5 / 2 = 0.75\text{m} \qquad (8\text{-}6)$$

The depth of natural instability as defined by equation 8-6 is similar to that defined in the in situ analysis conducted in Chapter 4.

An estimation of the dilation associated with the unstable hangingwall rock mass may be made from Figures 8-6 and 8-7.

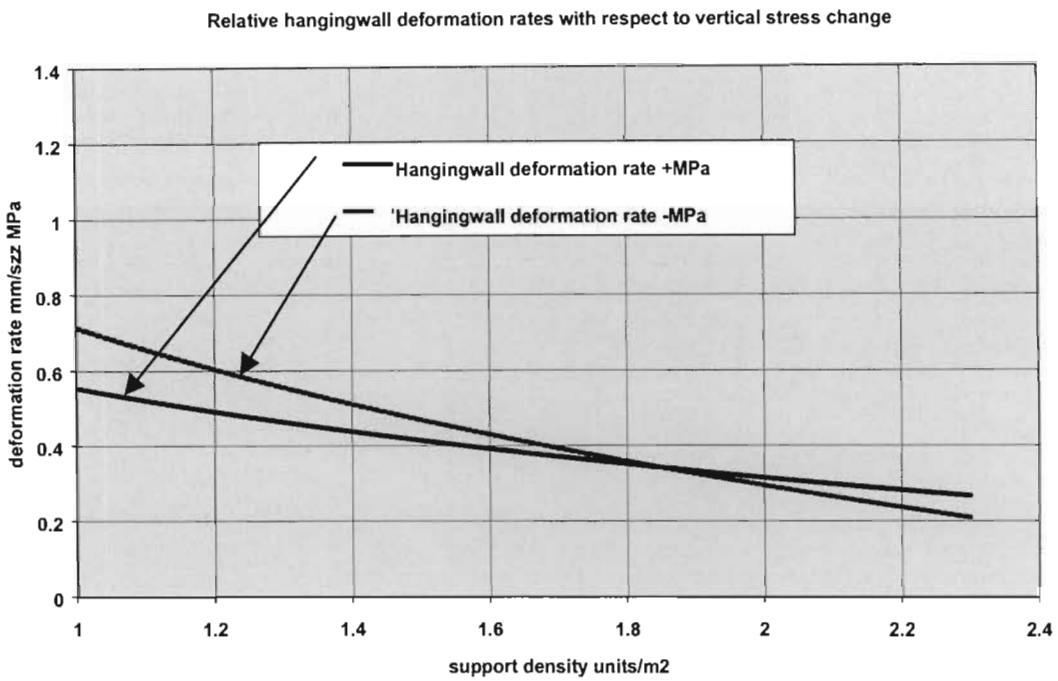

Figure 8-6. Estimation of relative hangingwall dilation rates for vertical stress increase and decrease.

The overall deformation rates as shown in Figure 8-6 indicate limited difference between vertical stress increase and vertical stress reduction. The influence of the reinforcement density on the dilation rate within the reinforced rock mass is shown in Figure 8-7.

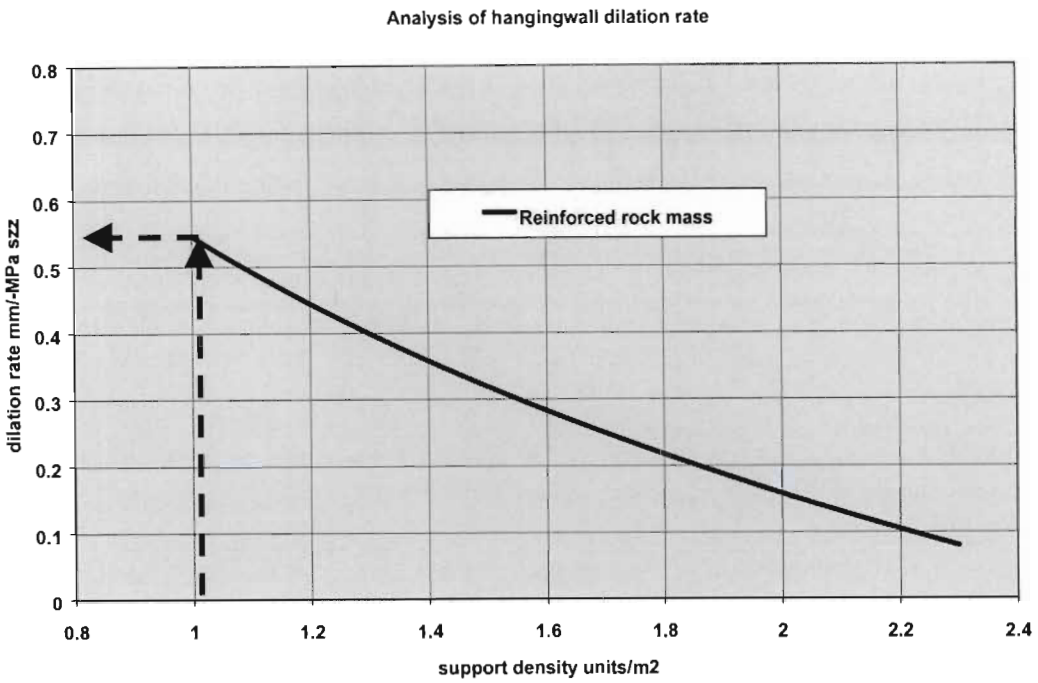

Figure 8.7. Estimation of hangingwall dilation rates per metre per unit decrease in vertical stress field (MPa).

Thus in this analysis, with a vertical stress increase of 30 MPa, the anticipated dilation of the hangingwall rock mass is estimated to be 17 mm per metre reinforcement, and for the period of vertical stress reduction of 70 MPa it is estimated to be 39 mm per metre reinforcement. Elongation over the unstable hangingwall height of 0.75 m is thus estimated at 5.6 %.

The above procedure may alternatively be expressed graphically by representation of the deformation of the rock mass in relation to the rock bolt reinforcement load-deformation characteristics. The loading, or confinement, of the rock mass, is currently assumed to be a function of the rock bolt reinforcement characteristics, and, thus, it is assumed that the deformation characteristics of the directly reinforced or contained rock mass are similar to that of the reinforcement unit (Figure 8-8).

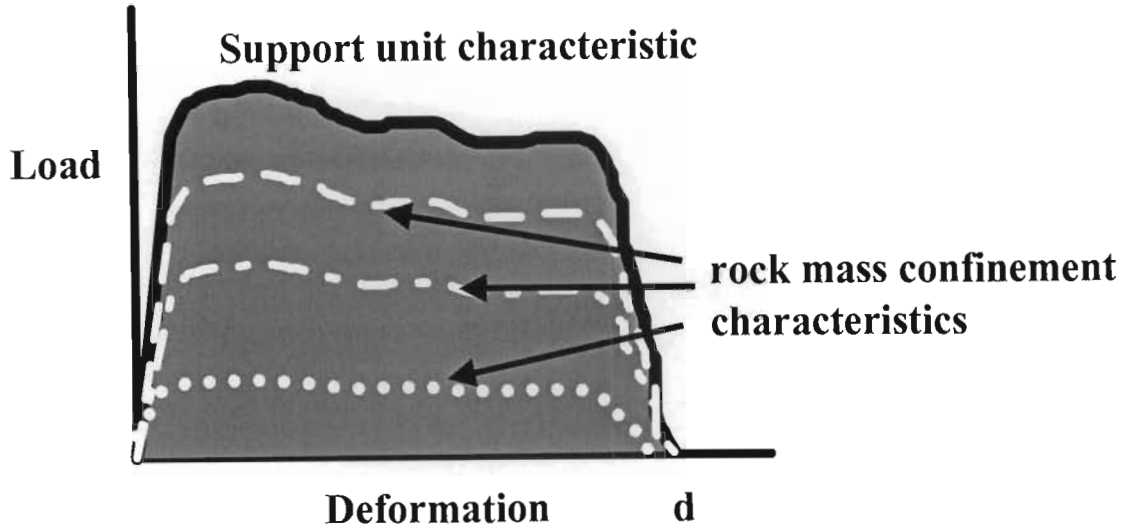

Figure 8-8. Conceptual illustration of reinforcement and rock mass confinement characteristics

The energy absorption capability of the rock bolt unit and the associated relative levels of rock mass confinement are given by the area under the indicated load-deformation curves. Analysis in Chapter 7 has indicated that under external loading conditions the volume of rock mass that is directly reinforced by the rock bolt unit is reduced. In Figure 8-8 the potential for increased instability in the rock mass is illustrated by the rock mass confinement characteristics. The lower this confinement characteristic with distance from the rock bolt axis, the greater the potential of rock mass unravelling.

The rate of progressive rock mass dilation with stress change is estimated from Figures 8-4 to 8-7 for the typical geotechnical environment of a deep level gold mine. It is assumed that the closure of the excavation may be attributed to deformation between the point of natural instability and the skin of the excavation. The deformation will thus limit the degree of remaining energy absorption capability within the reinforcement support system, principally as a function of the reduced deformation capability.

The incorporation of the defined rock mass deformation characteristics for the excavation sidewall or hangingwall, on the negative Y axis of the rock bolt load-deformation characteristic curve, will allow a graphical estimation of the remaining deformation capability, and thus energy absorption capability, of the rock bolt reinforcement system at any time in the life of the excavation life (Figure 8-9).

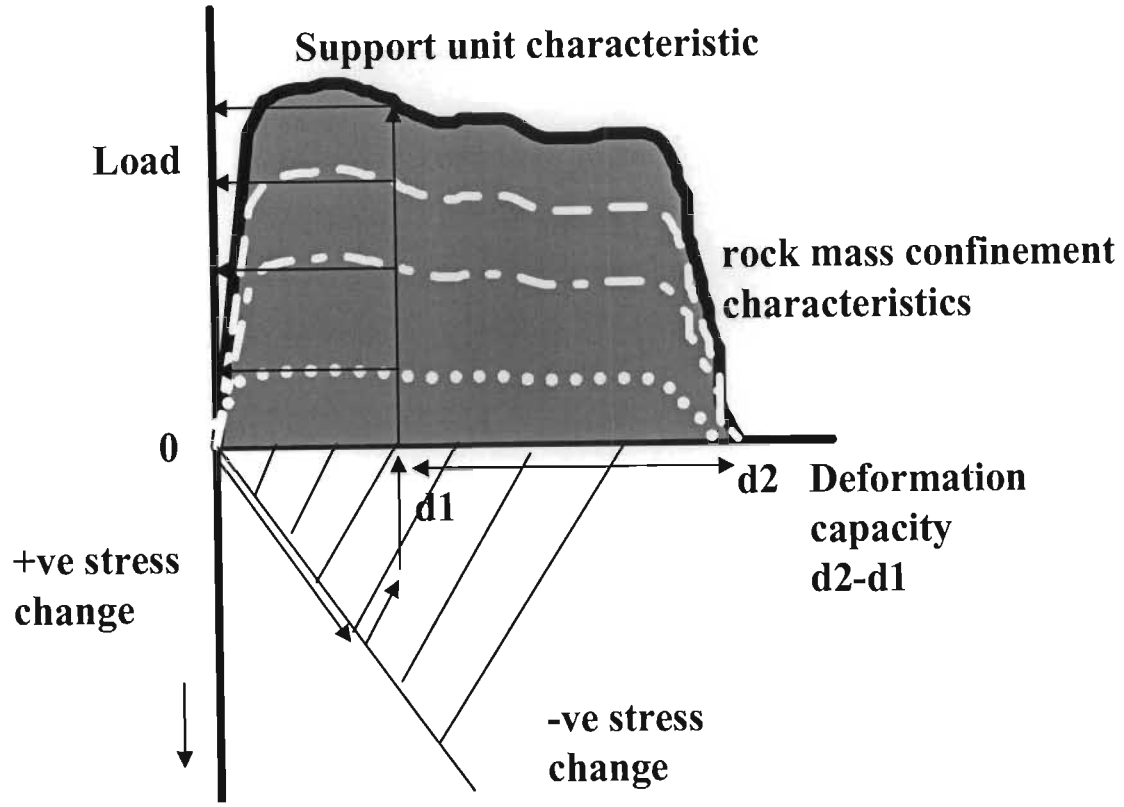

Figure 8-9. Estimation of remaining deformation and energy absorption capacity of rock bolt reinforcement system due to stress change.

For the above case the energy absorption for the zone of rock bolt confinement may be expressed as:

$$E = F.d \qquad (8\text{-}7)$$

where E = energy absorption capability
F = average ultimate force over the deformation range
d = deformation capacity (remaining deformation capacity)

Once the overall characteristic of the rock mass behaviour has been defined for the excavation, over its anticipated life, the next stage of the design methodology is to determine the interaction of the components of the support system within the unstable rock mass volume.

8.2.2 Design based on rock mass reinforcement

Application of the design concepts and charts as derived in section 7.2 are applicable to a blocky (fractured), interlocking rock mass where the major discontinuity within the rock mass is sub-parallel to the boundary of the excavation. In this analysis both rock mass containment / retainment and rock mass structural reinforcement are evaluated. The initial steps of the

analysis are based on the determination of the natural extent of instability around the excavation and the anticipated quasi static deformation due to the stress history over the life of the excavation as derived in section 8.2.1.

8.2.2.1 Application of design procedure for rock mass containment / retainment

Using this design consideration, the length of the rock bolt reinforcement is sufficient to ensure adequate anchorage in excess of the depth of natural rock mass instability around the excavation. This is not necessarily the total thickness of stress fractured rock. Classification of the rock mass is based on the geometry of the blocks within the rock mass structure relative to the rock bolt installation. Classification is based on the chart as shown in Figure 8-10.

Also indicated on this chart are equivalent RQD (Rock Quality Designation) values as derived from the work of Palmstrøm (1996). He developed a rock mass classification system (Rock Mass Index -RMi) which gives consideration to the block volume and a correlation to RQD.

An example of a typical blocky rock mass structure due to stress induced fracturing and dynamic loading is shown in Photograph 8-1. The dimensions of the blocks that comprise the rock mass structure are approximately 30 cm in length (L) (horizontal) and 15 cm width (W) (vertical) with a thickness (T) of approximately 5 cm (fracture intensity within the rockwall). This would give an average estimated block volume of 0.002 m^3 and an average aspect ratio in the horizontal direction of six and in the vertical direction of three. The difference in the aspect ratio of the blocks relative to the rock bolt reinforcement will result in different levels of rock mass instability in the orthogonal directions. If a regular rock bolt pattern is to be analysed then an average aspect ratio (4.5) may be used for simplified analysis.

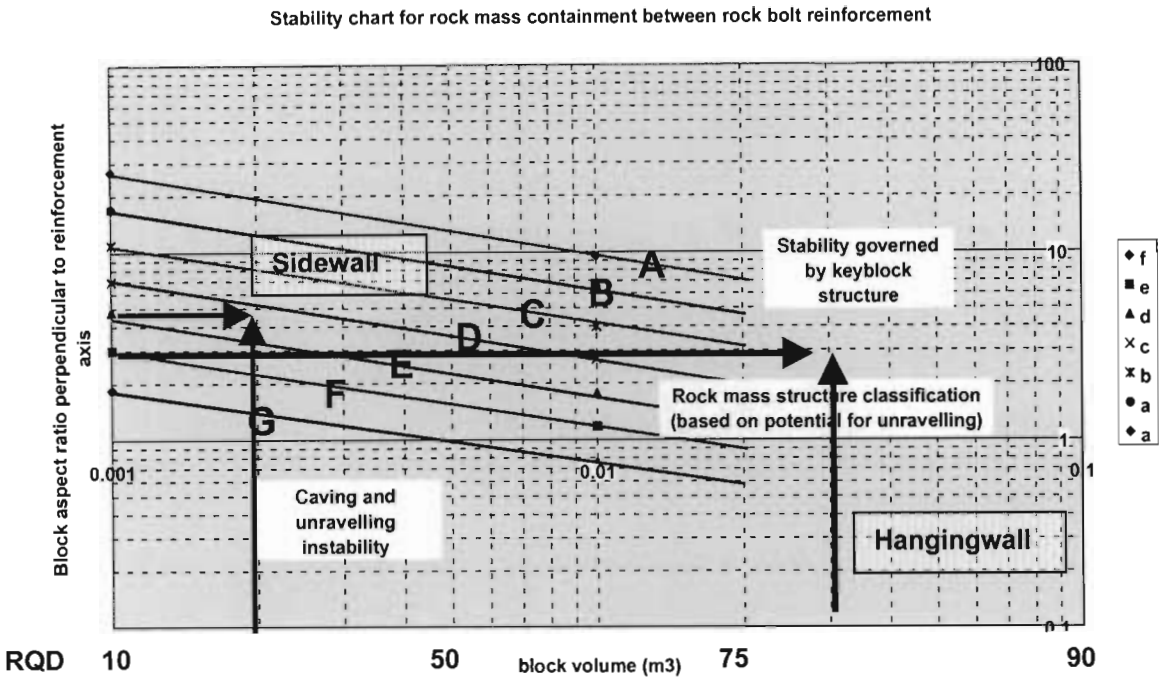

Figure 8-10. Classification of rock mass based on block volume and aspect ratio relative to the rock bolt reinforcement with equivalent RQD values after Palmstrøm (1996).

Based on a required assessment of only the average depth of instability between the rock bolt reinforcement, a rock mass class of D/E would be used for further analysis, based on evaluation of the rock mass structure in Photograph 8-1.

Estimation of the rock mass structure in the hangingwall of the excavation is based on an assumed block dimension of approximately 0.1 m thickness and 0.3 m width. This would give an average volume of 0.03 m^3 and a block aspect ratio three. From Figure 8-10 this would define approximately a class B/C rock mass.

Classification of the rock mass now allows an estimation of the volume of rock mass instability between the rock bolt reinforcement for the specified, or initial design estimation, rock bolt reinforcement spacing (Figure 8-11.)

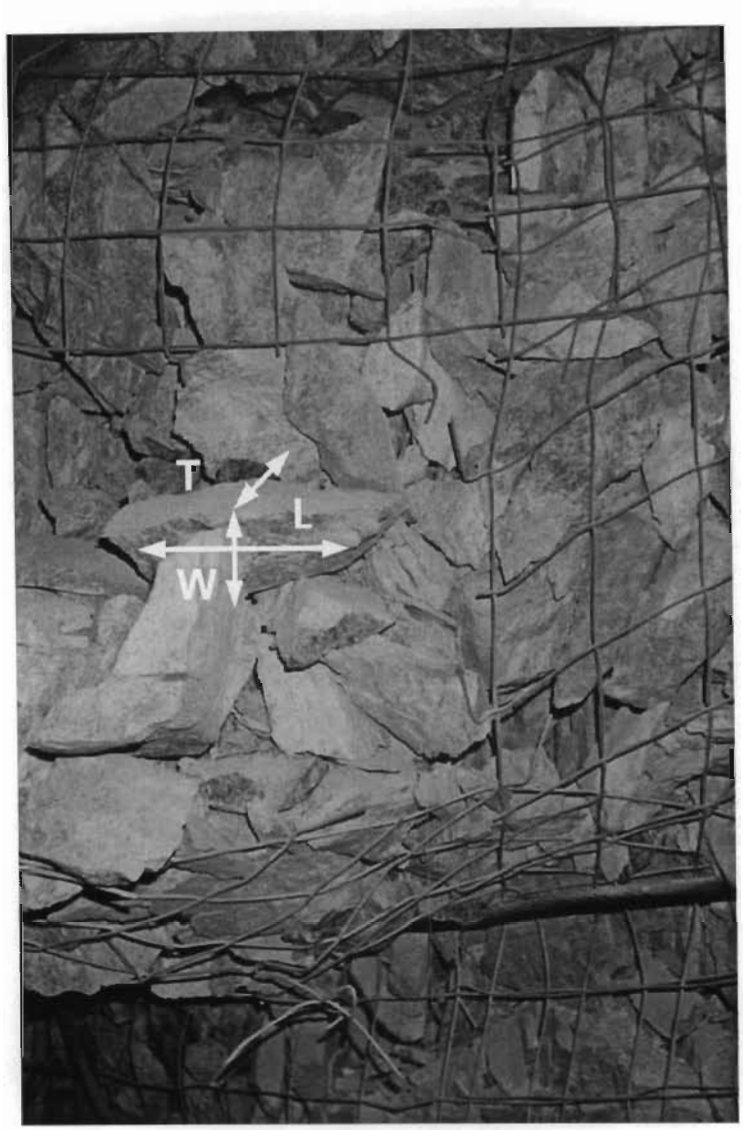

Photograph 8-1. Example of typical fracturing and resultant blocky nature of rock mass within a deep level gold mine in quartzite rock mass.

In Figure 8-11 the defined depth of instability is due to gravitational loading of the rock mass structure. This would be applicable to reinforcement within the hangingwall of an excavation but would be an initial over estimation of instability within the sidewall of the excavation, which would be controlled more by structural instability than unravelling under gravitational loading.

For design purposes it is necessary to assume that the depth of instability for equivalent gravitational loading in the sidewall of the excavation, for a rock mass class defined as D/E, and a rock bolt reinforcement spacing of 1.5 m (square pattern) would be estimated at 0.75 m (D_G). An analysis conducted in section 7.2.2 showed that the stable deformation within the rock mass structure due to gravitational loading would be equivalent to a ground motion velocity of approximately 0.7 m/s.

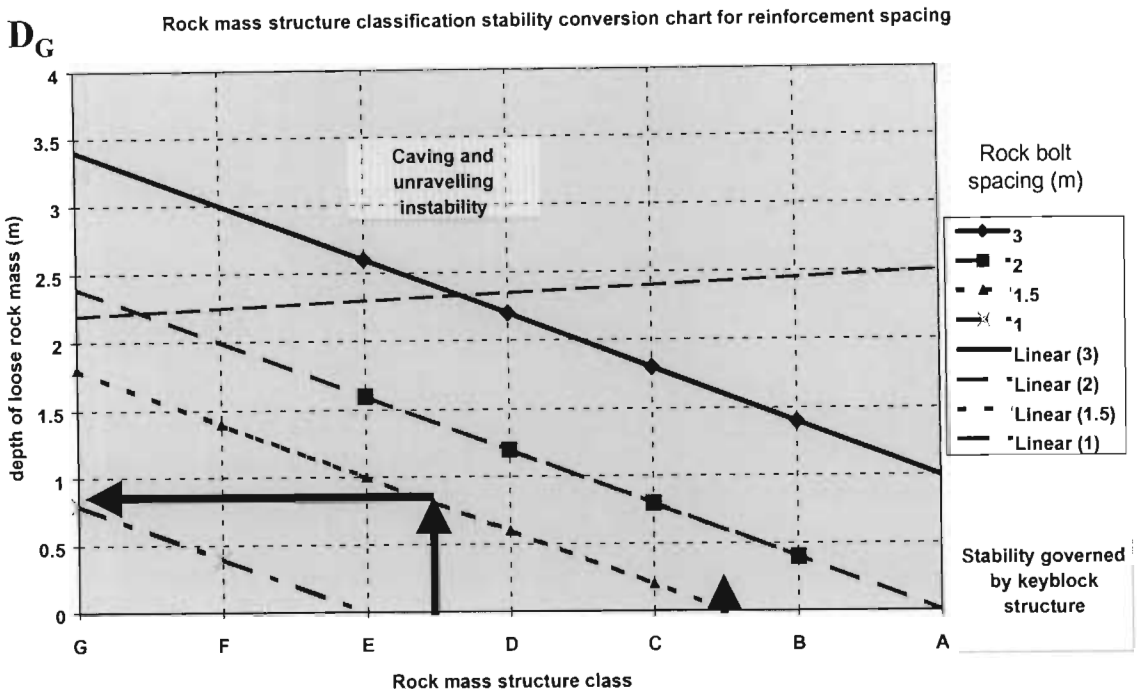

Figure 8-11. Determination of depth of instability due to unravelling of the rock mass under gravitational loading.

In the hangingwall of the excavation only structural instability would be anticipated (estimate 0.25 m).

For the example rock mass environment, it is also anticipated that the excavation will be subjected to dynamic loading due to the close proximity of a seismic event. An estimation of the increased potential for unravelling of the rock mass under these conditions is thus necessary. This is based on the anticipated ground velocity that the excavation peripheral rock mass will be subjected to under the conditions of dynamic loading (Figure 8-12). This chart is based on the relative increase in the depth of unravelling as a function of that under gravitational loading. For analysis of the sidewall of the excavation, the equivalent ground velocity that will result in instability equivalent to that due to gravitational loading should be considered first. This must then be subtracted from that of the anticipated maximum ground velocity in order to estimate the ultimate depth of rock mass instability between the rock bolt reinforcement.

In this example (Figure 8-12), for a rock mass class D/E, the factor of increased unravelling due to dynamic loading in excess of gravitational instability is approximately 0.22 times the initial depth of instability per unit increase in dynamic ground velocity (m/s) (F_D). The maximum depth of unravelling between the defined rock bolt reinforcement spacing is estimated from equation 8-8.

$$D_{max} = D_G (1 + F_D.V_{max}) \qquad (8\text{-}8)$$

where D_{max} is the maximum anticipated depth of instability and V_{max} is the maximum anticipated dynamic ground velocity (in excess of gravitational loading). For the sidewall it is assumed that the maximum dynamic ground velocity (estimated to be 2 m/s), in excess of the equivalent gravitational loading of 0.7 m/s, is 1.3 m/s, then the maximum depth of unravelling between the rock bolt reinforcement will be approximately 1.0 m (equation 8-8).

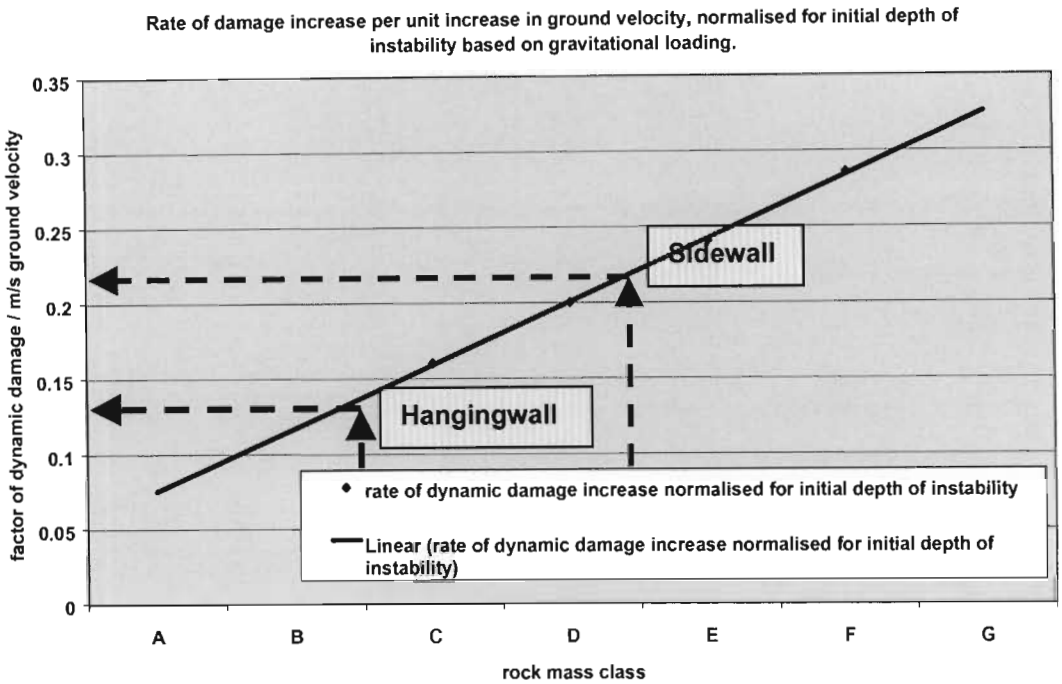

Figure 8-12. Rate of increased unravelling instability due to dynamic loading.

A similar evaluation for the hangingwall rock mass would consider the full dynamic loading of 2 m/s, in addition to gravitational loading. This gives an anticipated maximum depth of unravelling between the hangingwall reinforcement of 0.31 m.

The above analysis can be conducted for orthogonal planes within the support system, and, thus, enable determination of the potential for unravelling of the rock mass in three dimensions. Based on a simplified geometry (Figure 7-20), the area of potential unravelling between the rock bolt reinforcement may be estimated. The generalised solution for this is given in equation 8-9.

$$Vol_I = {}^1/_2.D_{max}.S_{max}.S_{min} + {}^2/_6.S_{min}.(D_{min})^2.\tan(90\text{-}\tan^{-1}(D_{max}/({}^1/_2.S_{max}))) \qquad (8\text{-}9)$$

where Vol_I is the volume of rock mass unravelling per unit spacing of the rock bolt reinforcement, D_{max} and D_{min} are the depth of unravelling in the two orthogonal directions, D_{max} being the larger of the two. S_{max} and S_{min} are the respective spacing of the rock bolt reinforcements.

If however D_{max}, is indicated to be in excess of the natural depth of instability, and if D_{min} is in excess of the natural depth of instability then include the function contained in brackets [], then let

$$\alpha = D_{min}.\tan(90\text{-}\tan^{-1}(D_{max}/{}^{1}/_{2}S_{max}) \qquad (8\text{-}10)$$

then

$$Vol_I' = {}^{1}/_{2}.((D_{max}\text{-}D_N)^2.S_{max}/D_{max}).S_{min} + [2({}^{1}/_{2}.((D_{min}\text{-}D_N)^3.S_{min}/D_{min}{}^{2}).S_{min}.\alpha + {}^{\alpha}/_{3}.({}^{1}/_{2}.((D_{min}\text{-}D_N)^2.S_{min}/D_{min}).(1\text{-}(D_{min}\text{-}D_N)/D_{min}))] \qquad (8\text{-}11)$$

where D_N is the natural depth of instability in the absence of rock bolt reinforcement, as derived in section 8.2.1. The volume of rock mass instability between the rock bolt reinforcement is then given as.

$$Vol_U = Vol_I - Vol_I' \qquad (8\text{-}12)$$

In the example application, the depth of unravelling in the sidewall of the excavation, based on a regular rock bolt pattern is given by (8-8)

$$Vol_U = 0.5 \times 1 \times 1.5 \times 1.5 + {}^{2}/_{6} \times 1.5 \times 1^2 \times \tan(90 - \tan^{-1}(1 / (0.5 \times 1.5)))$$
$$= 1.5\ m^3$$

For the hangingwall of the excavation the anticipated volume of unravelling would be estimated at 0.47 m^3.

Alternatively, this analysis may be utilised to define a spacing of the rock bolt reinforcement that will prevent complete unravelling of the rock mass between the rock bolts by comparison of the depth of unravelling instability (D_{max}) with the natural depth of instability (D_N).

The volume of the rock mass that is directly reinforced by the rock bolt units (Vol_R) is calculated as the difference between the tributary area volume (Vol_T) and the volume of unravelling (Vol_U).

$$Vol_R = Vol_T - Vol_U \qquad (8\text{-}13)$$

For the example application for the sidewall and hangingwall of the excavation, the volume of direct loading on the rock bolt unit, for the maximum developed depth of instability is estimated to be 5.25 m^3 and 1.78 m^3 respectively.

The direct loading on the rock bolt reinforcement and the fabric support may now be estimated based on the analysis as conducted in section 8.2.3.

8.2.2.2 Application of design procedure for rock mass structural reinforcement

The relative effectiveness of excavation stabilisation based purely on rock mass structural reinforcement is also examined. With this design, the length of the rock bolt reinforcement is less than the depth of natural rock mass instability around the excavation.

Classification of the rock mass is based on the same system as discussed in section 8.2.2.1 and shown in Figure 8-10.

The analysis of the effectiveness of the rock bolt reinforcement within the defined rock mass structure is based on the performance of the overall system as evaluated by its energy absorption capability at the mid-point of the structure, express as kJ/m^2. Additional analysis can however also be conducted to determine the requirement for, or capacity of, fabric support within the support system.

The total unstable volume and the defined loading condition (static or dynamic) define the loading of the structure. Generally in the environment of the deep level gold mines, the mechanism of structural reinforcement is only applicable to the sidewalls of the excavation (Chapter 3), due to the increased depth of instability in this area in comparison to the hangingwall. Thus loading of the structure is a function of either progressive dilation of the rock mass (section 8.2.1) or dynamic loading. Under conditions of dynamic loading the energy demand on the structure is assumed to be given by the kinetic energy of the unstable rock mass volume for the maximum anticipated ground velocity.

$$\text{Kinetic energy} = {}^{1}/_{2}.\ \rho.D_N.v^2 \qquad (8\text{-}14)$$

For a depth of instability in the sidewall of the typical 3.5 m x 3.5 m excavation of 3 m (D_N), under dynamic loading with a maximum anticipated ground velocity of 2 m/s (v) and a rock mass density of 2750 kg/m^3 (ρ) then the energy demand will be approximately 16.5 kJ/m^2. If we assume a comparable rock mass structure as shown in Photograph 8-1, then a support system can be defined from Figure 8-13 for the defined energy absorption requirement.

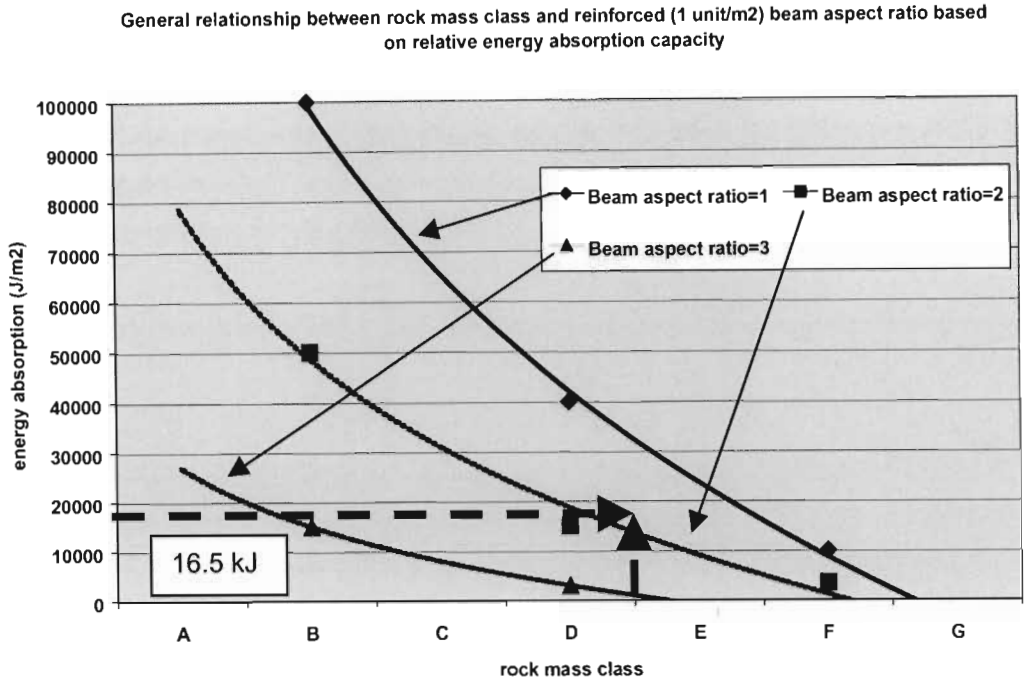

Figure 8-13. Reinforced rock mass structure for defined rock mass class and energy demand.

Thus at a reinforcement density of 1 unit/m^2, a beam aspect ratio of approximately 2:1 is required. For a typical 3.5 m x 3.5 m tunnel this would indicate a rock bolt reinforcement length of 1.75 m. At a rock bolt reinforcement spacing of 1 m the extent of instability between the rock bolts would only be due to structural instability (Figure 8-11). This therefore will only necessitate the use of light mesh and a low density lacing pattern to maintain the stability of the surface rock mass.

At a beam aspect ratio of 3:1, an increased reinforcement density to the level of 2 units/m^2 is still indicated to be insufficient to maintain structural integrity of the reinforced rock mass (Figure 8-14).

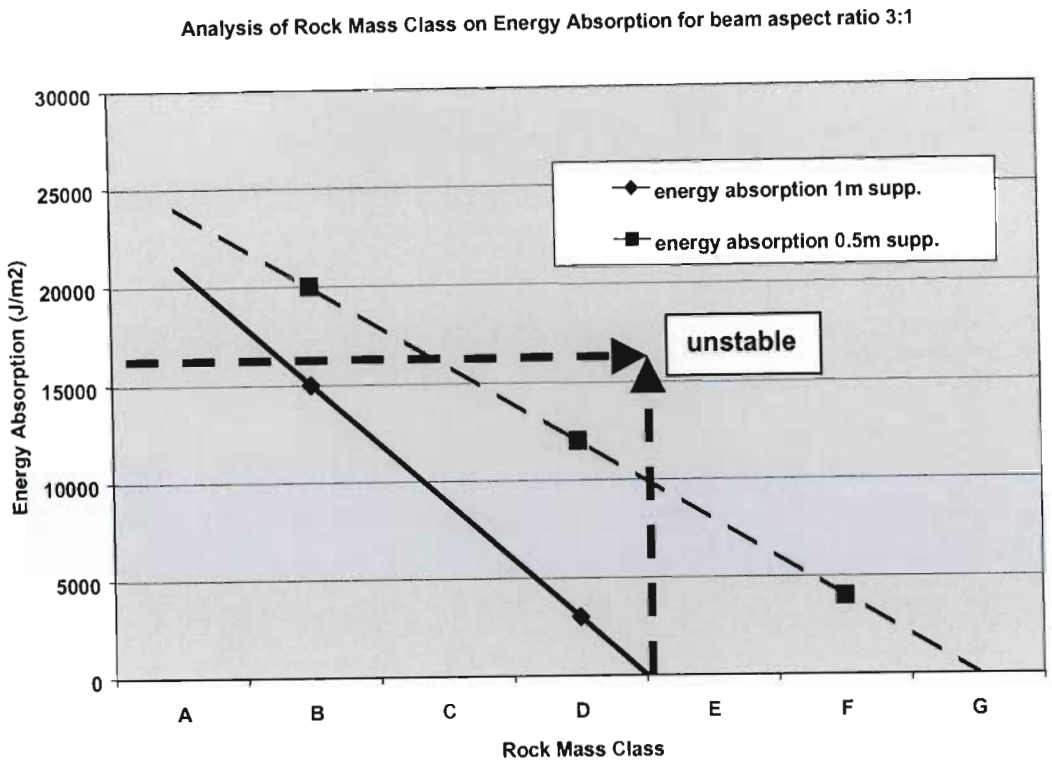

Figure 8-14. Analysis of stability of reinforced 3:1 aspect ratio beam for defined rock mass class and energy demand.

This simple analysis thus allows a comparison of the relative merits of the support design philosophy based on the mechanistic interaction of the rock bolt reinforcement units within the rock mass structure.

8.2.3 Fabric demand and support system interaction

This section examines the envisaged loading of the components of the support system in relation to their load deformation characteristics, and, thus, the ability to evaluate, or design, the support system based on the proposed mechanistic approach. This process is examined again by means of an example.

The quasi static loading environment due to the progressive stress changes over the life of the excavation has been considered in section 8.2.1. In this evaluation it is assumed that the dilation of the rock mass acts across the whole support system and does not result in differential deformation across the support system. Consideration could be given to this differential deformation by evaluation of the extent of interaction of the components of the support system at the initial stress state and at any point during the stress history. This analysis, and a detailed understanding of the influence of the support resistance on the degree of dilation of the rock mass, may allow an estimation of differential bulking factors which will result in differential dilation over the rockwall of the excavation. However, for the purposes of this analysis, let it be

assumed that the rockwall undergoes uniform deformation as a function of the quasi static stress history. This therefore results in limited initial loading of the fabric of the support system but may result in significant deformation of the rock bolt reinforcement. The ability of the rock bolt reinforcement to absorb additional dynamic energy, at any time in its history, will be a function of its initial load and deformation capacity minus the deformation utilised in controlling the quasi static dilation of the rock mass. More detailed analysis may also consider the influence of prior seismic loading, during the excavation history, on the current status of the support system. This could be captured by site specific analysis that encompasses the average dynamic dilation rates within the general dilation characteristic. The specific consideration of the rate and influence of prior seismicity is not considered in this analysis.

Based on the example rock mass environment, previous evaluations have considered a tunnel in an initial vertical quasi static stress environment which increases from 60 MPa to 90 MPa due to the advance of a mining abutment. This is anticipated to result in seismic events of maximum magnitude M=3.0 at a source distance of approximately 50 m, which is anticipated to result in a maximum ground velocity on the skin of the excavation of approximately 2 m/s. The excavation will then be subjected to a vertical stress reduction of approximately 70 MPa due to the over mining of the stoping abutment. For purposes of illustration of the design methodology, consider the extent of interaction of the components of the support system as derived under section 8.2.2.1 for untensioned rock bolt reinforcement.

From the characterisation of the unstable rock mass around the tunnel excavation based on the above environment, and a 1.5 m x 1.5 m rock bolt pattern, it was defined that the rock bolt reinforcement, under dynamic loading of the sidewall of the excavation, would contain approximately 5.25 m^3. This would thus result in approximately 1.5 m^3 being unstable between the rock bolt reinforcement, which would cause loading of the fabric support. The ultimate depth of natural instability in the sidewall of the excavation is estimated to ultimately be approximately 3 m. A similar analysis of the hangingwall of the excavation indicated the unstable volume between the rock bolt reinforcement to be approximately 0.47 m^3 and the volume directly reinforced by the rock bolt units to be 1.78 m^3 over an unstable depth of approximately 1 m.

In a dynamic environment the criterion for evaluating, and designing, tunnel support systems is based on the energy absorption capacity of the components of the support system. This is evaluated in relation to the anticipated energy demand due to the kinetic energy associated with the unstable rock mass volume, under the dynamic loading conditions.

The initial step in the methodology for evaluation of the loading of the components of the support system is to estimate the anticipated demand on the fabric support system between the defined rock bolt reinforcement pattern. Consider first the anticipated demand on the hangingwall area of the tunnel. The energy demand due to the unstable rock mass volume between the rock bolt reinforcement is given by:

$$E = m\,g\,d + {}^{1}/_{2}\,m\,v^{2} \qquad 8\text{-}15)$$

Where: E = energy demand on components of the support system (J)

g = constant gravitational demand on rock mass

m = mass of unstable rock loading the components of the support system (ρ x vol.) (kg)

d = deformation capability of support component (m)

v = anticipated peak ground velocity perpendicular to excavation boundary (m/s)

$$E = 2750 \times 0.47 \times 9.81 \times d + 0.5 \times 2750 \times 0.47 \times 2^{2}$$

$$E = 13000d + 2600 \text{ (J)}$$

The energy demand on the fabric support is evaluated against the capacity of the fabric contained rock mass. The energy absorption capacity of a typical weld mesh and lace fabric containment system has been examined in Chapter 6 of this document. Traditionally the consideration for support system design has been that the dynamic tributary area loading of the support element and therefore is a function of the load – deformation characteristic of the support units. However, the analysis in Chapter 6 (Figure 6-35) examined the concept that a large proportion of the energy absorption associated with the deformation and containment of an unstable rock mass volume may be associated with the deformation processes which occur in a discontinuous rock mass medium. This was estimated to be of the order of 160 kJ/m^3/m for the specific rock mass structure contained by a typical weld mesh and lacing support (Figure 8-15). The energy absorption capacity of the system under evaluation, based on typical load deformation characteristics of fabric support systems (Chapter 6), may be expressed as:

$$E = {}^{1}/_{2}.F\,d + E_{RM}\,vol_{U}\,d \qquad (8\text{-}16)$$

Where: E = energy absorption capacity of contained rock mass system (kJ)

F = normal force on fabric support system (kN)

d = deformation of fabric support system (m)

E_{RM} = estimated energy absorption capacity of the specific discontinuous rock mass (160 kJ/m^3/m)

Vol_U = volume of unstable rock mass under analysis

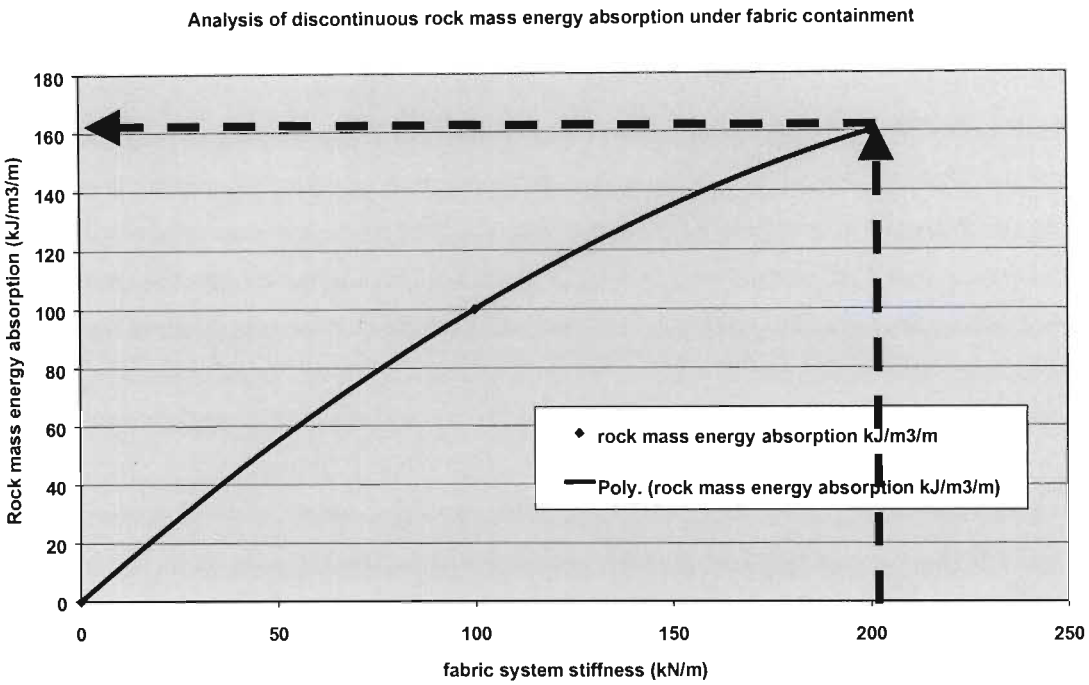

Figure 8-15. Estimation of energy absorption capacity of contained discontinuous rock mass based on a typical mesh and lace fabric support stiffness of 200 kN/m.

It is estimated that the stiffness of a typical weld mesh and lacing system at the defined rock bolt reinforcement spacing of 1.5m is approximately 200 kN/m based on analysis of the lacing strand (Figure 8-16). It is assumed that this approximately represents the overall stiffness of the analysed mesh and lacing system. Thus, by substitution in equation 8-16 the energy capacity of the fabric support system is expressed as:

$$E = 0.5 \times 200 \times d^2 + 160 \times 0.47 \times d$$
$$= 100d^2 + 75d \text{ (kJ)}$$

Balancing of the energy demand and energy capacity from equations 8-15 and 8-16 gives:

$$13d + 2.6 = 100d^2 + 75d$$

therefore

$$d \cong 0.04 \text{ m}$$

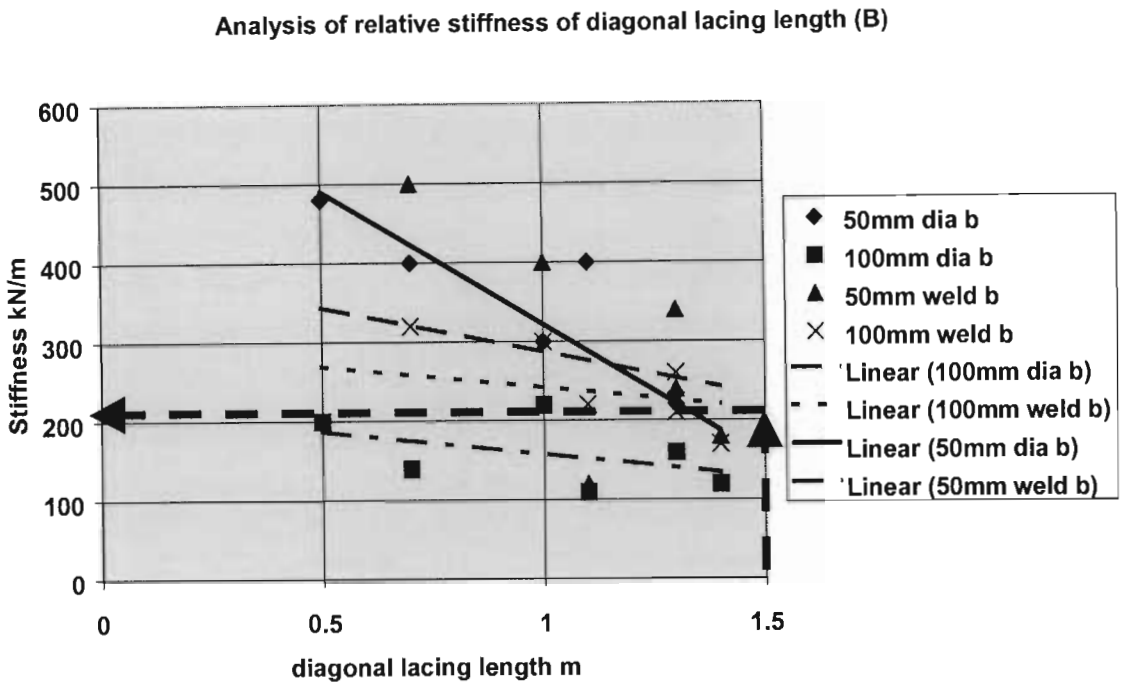

Figure 8-16. Estimation of weld mesh and lace fabric system stiffness for rock bolt spacing of 1.5 m.

It is therefore anticipated that the fabric support will deflect approximately 40 mm under the defined loading condition. Substitution back into the normal stiffness, representative of the mesh and lacing system, would thus indicate an additional normal force of approximately 8 kN due to dynamic loading. This dynamic loading will be additional to any gravitational loading of the fabric and also result in additional loading on the rock bolt reinforcement. The original gravitational loading of the fabric for the example rock mass structure of the hangingwall is estimated to be approximately 9 kN due to structural instability (Vol_U = 0.32 m^3). The peak normal loading in the fabric under conditions of dynamic loading is thus approximately 17 kN. The additional dynamic deformation of the fabric may be partially recovered after the seismic event, but this will be a function of the fabric and rock mass characteristics and is not considered in this investigation.

A similar process is applied to the rock mass directly reinforced by the rock bolt units. It is assumed that the rock bolts have a yield characteristic similar to that illustrated in Figure 8-17. Thus over the majority of the deformation range the energy absorption capacity can be expressed as the average yield force, say 140 kN, multiplied by the deformation.

$$E_R = F\ d \qquad (8\text{-}17)$$

Where: E_R = energy absorption of the rock bolt over the defined deformation (kJ)
F = average yield force (140 kN)

d = deformation, or elongation, of the rock bolt (m)

Due to the reinforcing mechanism of the rock bolt on the rock mass, the energy absorption capability of the discontinuous rock mass volume is not considered in this analysis. The reinforcement of the rock mass by the rock bolt unit is considered to limit the normal and shear deformation within the rock mass and thus the energy absorption capacity of this component of the system. The laboratory test work conducted by Ortlepp and Stacey (1997) only incorporated the energy absorption of a fabric contained rock mass structure. With regard to the rock bolt reinforced rock mass system the omission of this capability may result in a conservative design consideration.

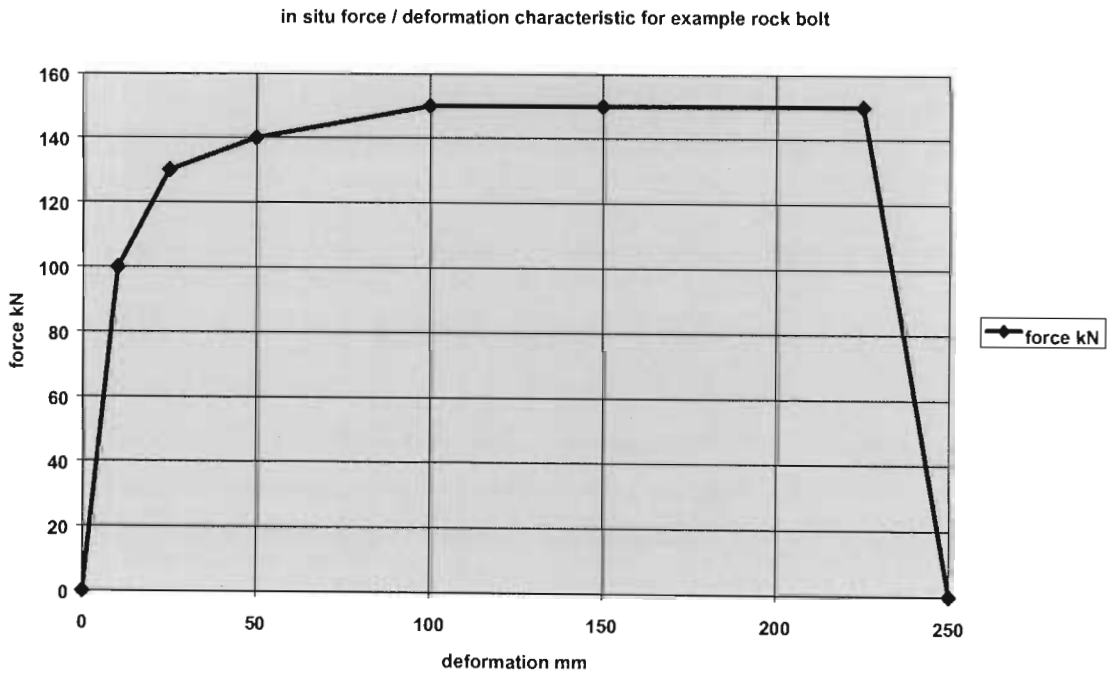

Figure 8-17. Example rock bolt load – deformation characteristic

The energy demand on the rock bolt unit due to the 1.78 m^3 of unstable rock mass volume is given by equation 8-18.

$$E = {}^1/_2 (F_I + F_E) d + m g d + {}^1/_2 m v^2 \qquad (8\text{-}18)$$

where F_I and F_E are the initial and final additional forces (kJ) transferred to the rock bolt due to the fabric support system during the period of dynamic loading. For the defined loading environment and support system the energy demand on the rock bolt is:

$$E = 0.5 \times (9 + 17) d + 2.75 \times 1.78 \times 9.81 d + 0.5 \times 2.75 \times 1.78 \times 2^2$$
$$E = 61 d + 10$$

Therefore balancing the energy demand and the capacity from equations 8-17 and 8-18, the deformation of the rock bolt system is:

$$140\ d = 61\ d + 10$$

$$d = 0.13\ m$$

As discussed above it is considered that this deformation may be conservative (over estimation) due to the omission of the consideration of any energy absorbing potential of the discontinuous rock mass volume directly reinforced by the rock bolt unit.

From the analysis in section 8.2.1 it is estimated that the hangingwall of the excavation will undergo progressive deformation of approximately 17 mm due to the vertical stress increase from 60 MPa to 90 MPa. With consideration purely of this quasi static deformation and the deformation associated with the analysed seismic event, the total deformation of the rock bolt system will be 147 mm. The deformation and energy absorption distribution due to the analysed seismic event is illustrated in Figure 8-18.

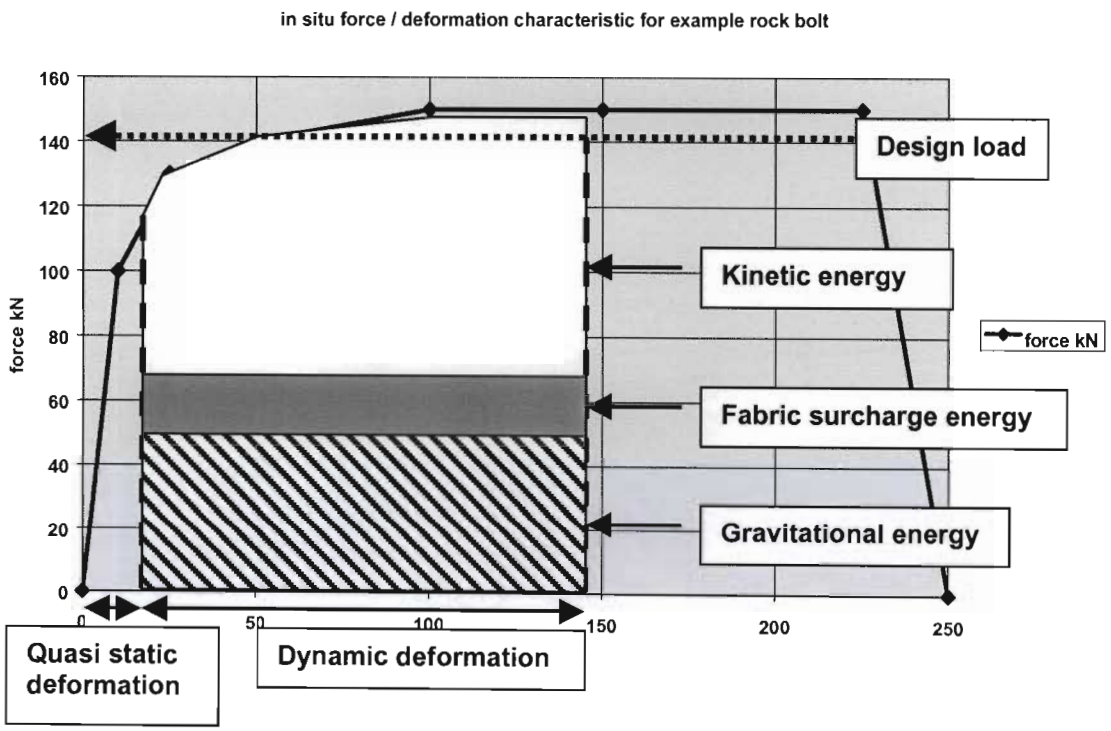

Figure 8-18. Distribution of deformation and dynamic energy demand / absorption.

For the hangingwall of the excavation it is thus estimated that, for the defined rock mass environment and support system, the rock bolt reinforcement will deform to approximately 130 mm, and the mesh and lace fabric will deform a further 40 mm relative to the rock bolt anchorage.

The deformation of the mesh and lace fabric is well within its capacity. However, it may be anticipated that the deformation of the mesh panels (1.1 m^2) defined by the lacing pattern will deform more due to lower stiffness (Figure 6-31). For the defined rock bolt pattern and typical lacing configuration as illustrated in Figure 8-19, the relative stiffness of the mesh panel is approximately 40 per cent that of the diagonal lacing strand. For purposes of determining the load transfer to the rock bolt reinforcement it is considered more suitable to base the fabric deformation analysis on the mesh and lace system derived from the lacing stiffness.

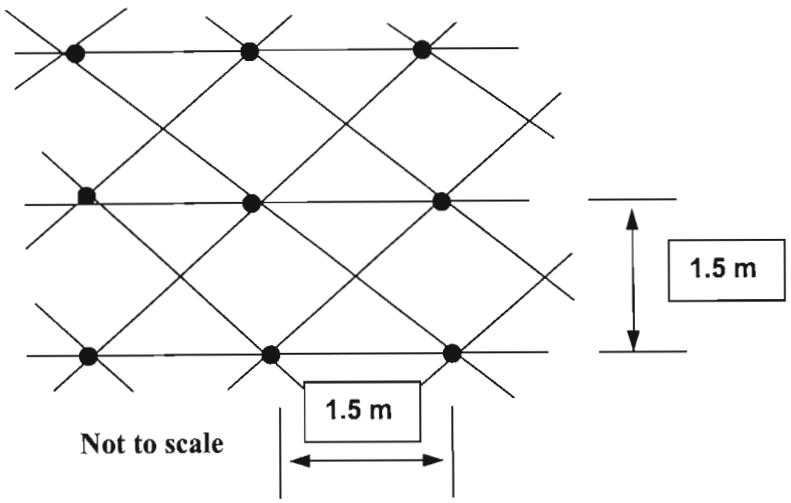

Figure 8-19. Typical lacing configuration for square rock bolt reinforcement pattern.

Based on the reduced volume acting on an individual mesh panel and the reduced confined rock mass energy absorption capability as estimated from Figure 8-15, for a mesh panel stiffness of 80 kN/m, it is estimated that the deformation of an isolated mesh panel would be approximately 85 mm. This deformation is within the capacity of a mesh panel; thus failure would not be anticipated.

This analysis has indicated that for the hangingwall of the excavation, the rock bolt reinforcement at a spacing of 1.5 m, and of a length to ensure stable anchorage in excess of an unstable depth of 1 m, must have a yield capability of at least 0.15 m.

The stability of the sidewall of the excavation is now evaluated. In this evaluation gravitational loading of the rock mass is not considered as the analysis of dynamic expulsion is based on expulsion perpendicular to the vertical rockwall. Thus the loading consideration, in excess of the quasi static deformation of the rock mass, is purely due to the dynamic loading.

In the sidewall of the excavation the volume of unstable rock mass between the rock bolt reinforcement has been estimated to be approximately 1.5 m^3. The energy absorption demand on the fabric, for the defined dynamic loading environment is given as:

$$E = {}^1/_2 \, m \, v^2 \qquad (8\text{-}19)$$

thus

$$E = 0.5 \times 2.75 \times 1.5 \times 2^2 = 8 \text{ kJ}$$

The energy absorption capacity of the mesh and lace contained rock mass system, as determined from equation 8-16 is:

$$E = 100\, d^2 + 240\, d$$

Balancing of the energy demand and energy capacity indicates an anticipated deformation of the mesh and lace system, relative to the rock bolt anchorage of approximately 35 mm. Based on a mesh and lace system stiffness of 200 kN/m, this would give a peak dynamic loading force on the rock bolt attachment of approximately 7 kN.

The demand on the rock bolt reinforcement in the sidewall of the excavation is given by:

$$E = {}^1/_2 (F_I + F_E)\, d + {}^1/_2\, m\, v^2 \qquad (8\text{-}20)$$

Thus

$$E = 0.5 \times (0 + 7)\, d + 0.5 \times 2.75 \times 5.25 \times 2^2$$

$$E = 3.5\, d + 29 \text{ (kJ)}$$

The load deformation characteristics of the rock bolts in the sidewall of the excavation are assumed to be similar to that represented in Figure 8-17. Balancing the energy demand and capacity of the rock bolt system based on equations 8-19 and 8-20, the anticipated deformation of the rock bolt system is estimated to be approximately 210 mm. The quasi static deformation associated with the sidewall of the tunnel, as derived in section 8.2.1 is estimated at 70 mm. This would indicate a total deformation of 280 mm, which is in excess of the deformation capacity of the defined rock bolt system, Figure 8-20

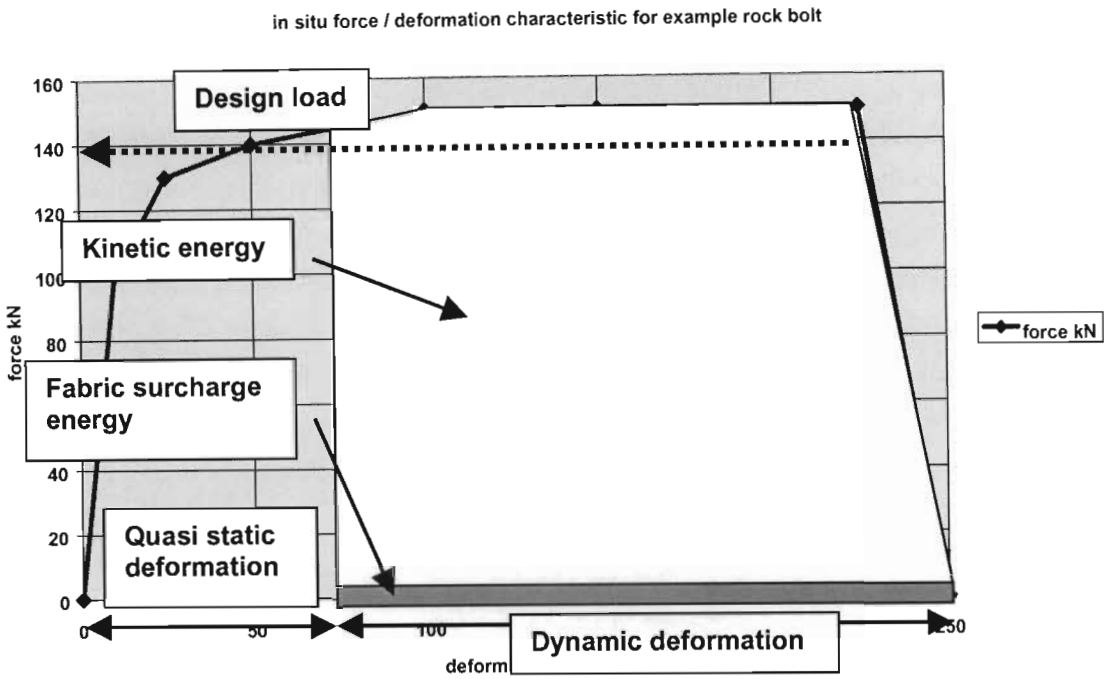

Figure 8-20. Distribution of deformation and dynamic energy demand / absorption.

It would thus be necessary to re-evaluate the sidewall rock bolt reinforcement by increasing the density of similar rock bolt reinforcement, or increasing the capacity of the rock bolt reinforcement for the defined support pattern.

For a sidewall rock bolt reinforcement pattern based on a spacing of 1.5 m and a length to ensure stable anchorage in excess of the unstable rock mass depth of 3 m, a yield capability of greater than 0.28 m, or a yield load capacity greater than approximately 150 kN is required. Alternatively a more closely spaced rock bolt pattern should be evaluated.

Due to the increased depth of instability associated with the sidewall of the excavation, a comparison can be made between the above design analysis based on unstable rock mass containment and that based on the creation of a reinforced rock mass structure, as conducted in section 8.2.2.2. This analysis indicates that for the defined rock mass environment, and a comparable deformation, a rock bolt reinforcement system based on 1.75 m long, 120 kN grouted rock bolts, at a spacing of 1 unit/m^2, would result in a similar energy absorption capability. In this instance only mesh with a low density lacing pattern would be required as a fabric support. The cost effectiveness of the support systems may be evaluated to determine the optimum support design philosophy.

In the above analysis it has been assumed that the defined volume of unstable rock mass between the rock bolt reinforcement is able to detach fully from the bulk rock mass and load the fabric in isolation. Evaluation may also be conducted as to the effectiveness of the fabric support system to maintain the inherent strength of the rock mass. This is based on the ability

of the fabric support system to prevent differential deformation of the rock mass between the rock bolt reinforcement, to the extent that detachment and unravelling of the rock mass between the rock bolts does not occur. This may be evaluated for a specific rock mass classification based on its ground reaction curve, for the defined reinforcement spacing as discussed in section 7.2.2. An estimation of the ground reaction curve allows an evaluation of the minimum fabric stiffness to maintain rock mass integrity (Figure 8-21).

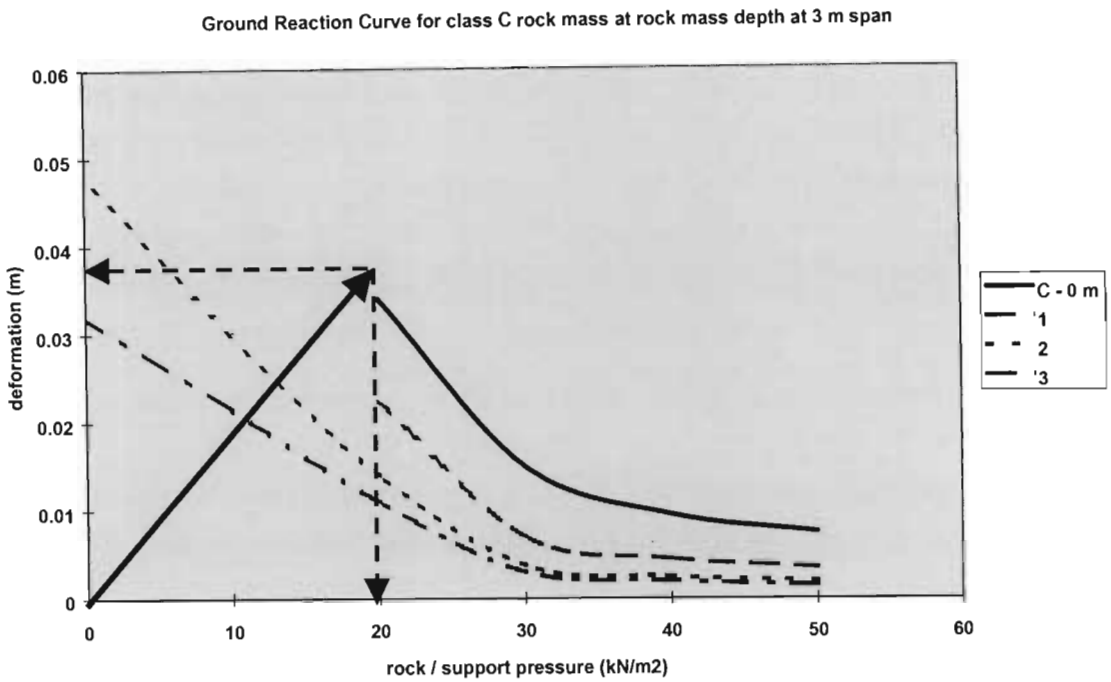

Figure 8-21. Example of ground reaction curve for estimation of stiffness of fabric support to maintain the inherent rock mass strength.

For the example illustrated in Figure 8-21 the minimum fabric stiffness to prevent unravelling of the surface rock mass, for a class C rock mass and a reinforcement spacing of 3 m, is estimated at 500 kN/m^2/m. This is based on the assumption that at the point of installation of the fabric support system unravelling of the rock mass had not initiated.

If this requirement is compared with typical mesh and lacing systems, even ignoring the initial slackness of the order of 70 mm, the required stiffness is far in excess of that generated by mesh and lacing systems. However comparison against typical shotcrete panel tests (Ortlepp and Stacey 1998) indicates stiffnesses of an order of magnitude greater (20 MN/m, over 1 m^2 panels). This is an important design consideration, as it implies that if the inherent rock mass strength is maintained between the rock bolt reinforcement by the use of stiff fabric, then it may be envisaged that the rock bolts will be subjected to increased direct loading under dynamic conditions. Where historically mesh and lacing systems were attached to rock bolt units with limited yield capability, and these systems have been observed to survive dynamic loading, it may now be anticipated that a change to shotcrete systems will result in the failure of these rock

bolts. This illustrates the importance of the consideration of the interaction between the rock mass and all components of the support system.

8.3 Conclusions, design recommendations and further work

The work contained in this thesis and formulated into a design procedure has attempted to elucidate our understanding of the complex interaction between rock bolt reinforcement and a highly discontinuous rock mass structure. This understanding is based on a mechanistic evaluation of in situ observations and measurements, and detailed numerical analysis.

Due to the highly complex, and erratic nature of the highly fractured and discontinuous rock mass around deep level tunnel excavations, particularly under dynamic loading due to seismic events, much of the mechanistic understanding has been based on observations made at underground sites of severe rockburst damage. These conditions would be extremely difficult to simulate physically, but it is considered that a mechanistic understanding was gained from suitable numerical modelling. There are many components to the analysis and design of tunnel support systems, and, where applicable, the work of other authors and researchers has been incorporated into the design process to try to formulate a coherent design methodology.

Empirical design guidelines for the selection of support systems cater well in the environments for which they have been calibrated and for the technology on which they are based. However, as the rock mass environment changes, these systems generally indicate a step wise change in the support system. That is, within a rock mass classification system a slight change in the rock mass condition may result in the definition of a different rock mass class and thus a significantly different support recommendation. A more fundamental understanding of the interaction of rock bolts and fabric support systems with the rock mass allows a continual adjustment and optimisation of a support system based on available support units. This leads to greater flexibility in the design process, particularly in highly variable rock mass environments, and thus improved utilisation of available resources. Particularly in the deep level South African gold mining environment, a more fundamental, mechanistic, understanding of the design of a support system should lead to improved design considerations with regard to ensuring the stability of excavations and optimum economic support installation. The significant aspects of the proposed design process and areas of investigation are reviewed in the following section.

Within the South African deep level gold mining environment, the principal design mechanism is rock mass retainment based on tributary area loading of the rock bolts, and the depth of instability derived from historical data. No consideration is given to the demand on the often required use of mesh and lace fabric support. Often large differential deformations occur within this discontinuous rock mass structure, which result in dilation and significant bagging, or ultimately failure, of the typical mesh and lace fabric between the rock bolt reinforcement. In this environment the survival of rock bolt units, with very limited yield capability, is often observed

under severe dynamic loading conditions. Again, on the basis of the current design considerations, this would not be anticipated. This phenomenon has been shown to be a reflection of the very limited direct interaction between the rock bolt reinforcement and the unstable rock mass volume. In areas of abnormally high stresses, due to major mining abutments, or in areas of generally weaker rock, the mechanism of structural reinforcement may be observed, although this is often not considered in the design process. The stability of this reinforced rock mass structure is also very dependent on the interaction of the rock bolt reinforcement units with the rock mass and thus an understanding of the critical rock mass parameters is required. Additional observations of support system behaviour under conditions of dynamic loading indicated the susceptibility of the rock bolt reinforcement, particularly in the hangingwall of the excavation, to shear failure. This is not directly addressed in the methodology but is an important design consideration in these rock mass environments.

The need for a more mechanistic understanding of the interaction of the components of a support system with the unstable rock mass volume, and thus the derivation of a rational design methodology, was established. Investigation of the behaviour of the components of this complex system was thus conducted in the thesis.

In order to establish support design methodologies, an understanding of the anticipated extent, and volume of instability around an excavation is required. This determines whether a rock bolt reinforcement system should retain the unstable rock mass volume by anchorage beyond this limit of natural instability, or reinforce the boundary of the excavation to form a stable structure which also provides sufficient constraint to the deeper unstable rock mass. A simple design philosophy and support system selection table to this effect has been proposed (Chapter 3). The work of Martin (1997) and Kaiser *et al.* (1996) in defining the depth of instability due to stress fracturing is considered very suitable for this purpose in the deep level mining environment. However it was found that the linear empirical data range established by these authors did not cater for the higher stress conditions which are sometimes experienced in the South African mining environment. On a very limited number of available case studies it was attempted to extrapolate this data for higher field stress levels. This work indicated that there is a tendency for the increasing extent of natural instability, with increasing stress level to flatten off. Mechanistically, for a given size of excavation and typical stress fractured rock mass characteristics, this would indicate a finite depth of instability beyond which it is increasingly improbable for instability to occur. The observation of the tendency for deep level excavations to break out to an elliptical profile, with the short axis parallel to the maximum stress trajectory, supports this hypothesis. The use of the derived criterion to estimate the natural depth of instability (in the absence of reinforcement and support), in this particular environment, is considered to be superior to the current use of historical databases of fallout thickness. The use of these databases will inherently encompass may other factors of excavation instability, including the performance of the support systems and the relative stability of past rock mass environments. In rock mass environments where instability is due to the natural discontinuity

within the rock mass then this criterion is not applicable and it is recommended that the effect of local geological features be incorporated into the evaluation of the depth of instability.

In a mining environment the tunnel excavations are often subjected to large stress changes over their operational life. These stress changes cause large progressive deformations of the rock mass around the tunnel. Of significance from this investigation is the large component of hangingwall deformation associated with a reduction in the vertical stress environment. Mechanistically it is proposed that this is due to shear deformation on the sub-horizontal bedding within the typical rock mass of the South African gold mining environment, caused by the vertical stress relaxation. An understanding of the deformation associated with quasi static stress changes is important for the determination of the required yield capacity and characteristics of the rock bolt reinforcement to ensure excavation stability, and to design the support system to limit deformation so as to maintain the excavation in operational condition.

Analyses carried out as part of this investigation have shown that there is a better correlation, although poorly defined, between the rate of dilation within the reinforced rock mass and the density of the rock bolt reinforcement. In the past, support resistance has been used as the primary means of evaluation. Although support resistance does encompass the rock bolt density, it does not differentiate between the actual in situ support resistance or loading and the design value. Also the support resistance does not give consideration to the effective zone of interaction of a rock bolt unit, in as much as that a single 200 kN rock bolt unit would be given the same weighting as two 100 kN units over the same area, whereas the increased density of the reinforcement within the rock mass volume has been shown to have a significant beneficial effect on the overall rock mass stability.

The current work on tunnel support design has also evaluated the analysis technique to derive dilation rates which may be used in applicable geotechnical environments, and evaluated the mechanisms of rock mass deformation due to changes in the stress environment. This is applicable to a typical South African gold mine rock mass environment, which consists mainly of bedded quartzites subjected to stress induced fracturing, and caution should be observed in the application of these deformation rates and mechanisms in other rock mass environments.

The installation of rock bolt reinforcement is generally the primary method of maintaining the stability of the excavation. It has been shown that within these highly discontinuous rock mass environments the interaction between the rock bolt reinforcement and the rock mass is critical to the mechanisms of quasi static and dynamic rock mass deformation. In an attempt to understand this interaction, relatively simple numerical models were established. The construction of these models gave consideration to the practical limitations of the ability to classify a highly complex rock mass structure in a relatively simple manner. Thus, simple, planar, and regular discontinuities, with discontinuity properties generally applicable to the South African gold mining environment were used to represent the rock mass structure.

The analysis scheme used evaluates the interaction between untensioned rock bolt reinforcement and a stress fractured interlocking blocky rock mass structure. The rock mass structure in the analysis is dominated by discontinuities perpendicular to the rock bolt axis and is broken into interlocking blocks by intermittent discontinuities. The stability of the system is assessed directly by the extent of rock mass unravelling under the defined loading conditions and reinforcement spacing. The mechanism of stabilisation between the rock bolt reinforcement and the rock mass is based on the restriction of block deformation and rotation within the unstable rock mass volume. This analysis is applicable to the South African gold mines where untensioned, fully grouted rock bolts are used for excavation stabilisation. The purpose of the analysis is to estimate the extent of direct reinforcement of the rock bolt units and thus the volume of unstable rock mass that will load the fabric support system. Further evaluation examined the interaction of rock bolt reinforcement to create a reinforced rock mass structure that is loaded by the deeper unstable rock mass volume. This analysis is used to compare the relative merits of the two support design philosophies.

An important design parameter, which can now be derived from this analysis, is the stiffness requirement of the fabric support under both static and dynamic loading conditions. If the fabric support has a relatively soft load deformation characteristic, such as the analysed mesh and lacing systems, then significant loading of the fabric will result as illustrated in Figure 8-22.

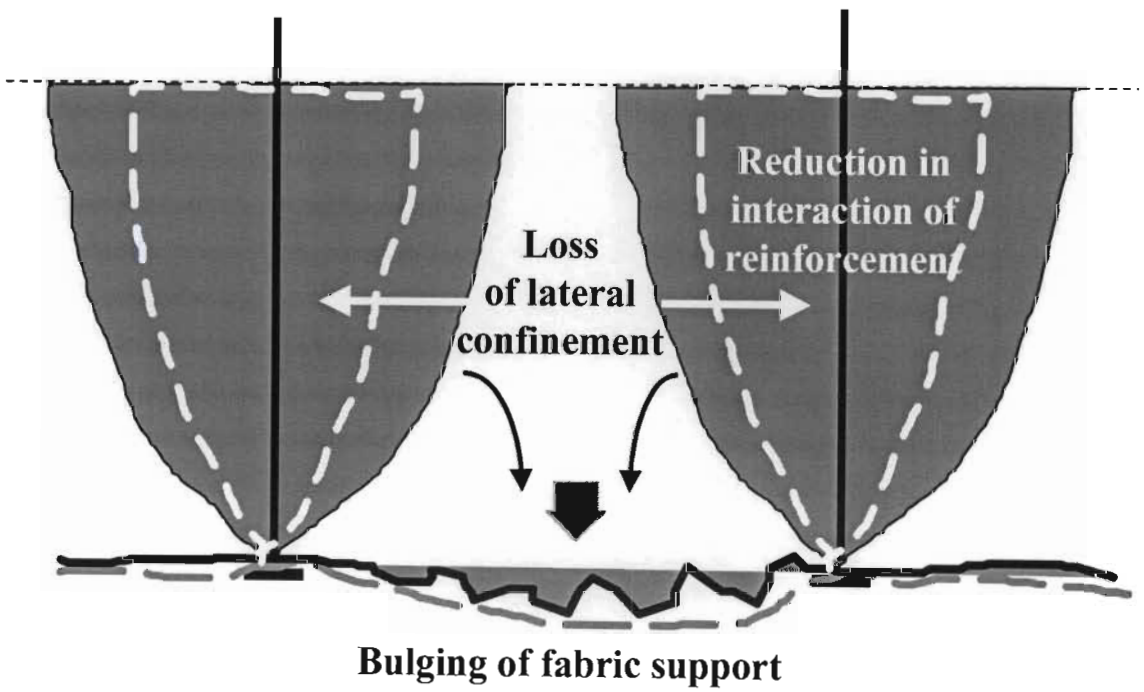

Figure 8-22. Conceptual representation of the influence of relative reinforcement and fabric support stiffness on rock mass unravelling.

The mechanism illustrated in Figure 8-22 has been observed to result in either significant bagging or failure of the fabric (mesh and lacing), with the consequence that the relatively stiff rebar rock bolt reinforcement, which is considered to be unsuitable under dynamic loading conditions, has survived. It is now clear that this is due to the loss of interaction of the intervening rock causing limited load being transferred directly onto the rock bolt reinforcement units. The load no longer carried by the rock bolts must therefore result in higher loading of the fabric.

Of significance to the recent trend in the use of shotcrete in the deep level mining environment is that the limitation of the deformation of the rock mass between the rock bolt reinforcement is likely to result in increased direct loading of the rock bolt units. This must be considered in relation to the previous observation of the survival of stiff rock bolt units under severe dynamic loading due to low direct rock mass interaction. Thus, a change in the fabric component of a support system must be evaluated in relation to the impact on the loading distribution within the system and the capacity of the other components, particularly their yieldability.

The assessment of the influence of seismicity on excavation stability is based on the energy absorption capability of the confined rock mass normal to the excavation boundary and parallel to the reinforcement confinement. Dynamic ground motions may also result in shear movement within the rock mass and/or transient induced tensile tangential stresses. These may result in a further reduction in the extent of reinforcement confinement and thus an increase in fabric support demand.

Finally the demand on the components of the support system may be estimated based on the defined rock mass and loading environment. For the design of a suitable support system this must be compared with the capacity of the components of the system. The axial capacity of rock bolt units has historically been investigated and is relatively well understood, and thus these performance characteristics have been accepted for this analysis. However, the shear capacity of the rock bolt system has previously received limited consideration, particularly within the South African mining environment. This has been shown to be an important consideration of rock mass deformation under quasi static stress changes, and particularly under dynamic loading. Of significance is the importance of yield capability and the relationship between the diameter of the rock bolt and the grout annulus in the estimation of the shear capacity of the system. The anticipated shear demand on the system is still not understood, but in situ observations have indicated the necessity for improved shear capacity under the specified rock mass environments.

The other major component of tunnel support systems in the South African mining environment is the mesh and lacing fabric support. Analysis of this component of the support system under quasi static and dynamic loading conditions indicates the high initial slackness in the system, which is detrimental to maintaining the inherent strength of the potentially unstable rock mass

volume between the rock bolt reinforcement. However, its load deformation characteristic allows for large deformations under dynamic loading, and, thus, the associated capability to absorb kinetic energy of the unstable rock mass. Of significance to the evaluation of these fabric support systems is the proposed consideration of the energy absorbing capability of the contained discontinuous rock mass system, which may be significantly greater than that implied by analysis of the load-deformation characteristic of the fabric in isolation. This important aspect of the interaction between the support system and the rock mass requires far greater investigation.

It is considered that the analyses as reviewed above enable a mechanistic approach to support system design based on an understanding of the interaction between the components of the support system and the rock mass. Estimations of the loading of the components of the support system under rock mass environments as defined by the design engineer can be made. However, consideration must be given to the inherent assumptions of this analysis in relation to the extremely complex rock mass environment. The design process does, however, capture the behavioural characteristics of the rock mass and the support systems as observed in situ, and thus, compared to the current design process, gives greatly improved understanding into the design of support systems in this environment.

The following recommendations are made with regard to the design of tunnel support systems under the defined rock mass environment:

1) The extent of natural rock mass stability, under conditions of quasi static and dynamic stress fracturing, can be estimated from the proposed design analysis. This will form the basis of the selection of a suitable tunnel support design philosophy for the prevailing rock mass environment. This analysis captures the increased extent of instability due to the dynamic loading of the rock mass as a result of seismic events.

2) The dilation rates for the reinforced and unreinforced rock mass, as a function of the anticipated stress change over the life of the excavation can be estimated. These will define the minimum deformation requirements of the rock bolt reinforcement in order to ensure excavation stability due to stress induced rock mass deformation. It has been shown that the density of the rock bolt reinforcement may better predict the influence on dilation of the rock mass than the in situ support resistance. Analysis of the deformation mechanisms has indicated the importance of the consideration of shear deformation within the rock mass, particularly under conditions of a vertical stress reduction.

3) The extent of interaction of the rock bolts within the defined rock mass structure and loading environment can be estimated from the application of charts based on rock mass reinforcement. The charts indicate the importance of variations in the structure of the rock mass, which defines the geometry of the rock mass blocks relative to the axis of the rock

bolt installation. The dominance of discontinuities orientated sub-parallel to the rock bolt reinforcement result in a significant reduction in the interaction of the rock bolt reinforcement. This will limit the extent of direct loading on the rock bolt unit and thus define the extent of potential instability between the rock bolt reinforcement dependent on the designed reinforcement spacing.

4) The extent of the potentially unstable rock mass volume between the rock bolt reinforcement can be estimated. This will allow the determination of either the necessity for, or the demand on, the fabric support system. The design process captures the increased unravelling of the rock mass between the rock bolt reinforcement under conditions of dynamic loading, and thus the increased loading and deformation of the fabric support system under these conditions.

5) The load-deformation characteristic of the fabric support system also influences the extent of interaction of the rock mass with the rock bolt reinforcement units. Mesh and lacing fabric support systems as used in South African gold mines allow relatively large deformations of the rock mass between the rock bolt reinforcement. Analysis of these mesh and lacing configurations has shown that all the systems had an average initial slackness of approximately 70 mm prior to any appreciable load generation. This may increase the potential for rock mass unravelling, and, thus, reduced direct loading on the rock bolt units. However, the containment of this unstable rock mass volume by the fabric support systems results in significantly greater energy absorption than analysis of the fabric in isolation would indicate. The implementation of relatively stiff fabric support systems, such as shotcrete, is likely to result in a significant reduction in initial rock mass unravelling, and, thus, significantly increased direct loading on the rock bolt reinforcement. Consideration of this interaction between the fabric support system and the rock bolt units is therefore an important aspect of the support system design that ensures compatibility of the characteristics of the components of the support system.

6) Under conditions of dynamic loading and large vertical stress reductions, rock bolt reinforcement with high shear capacity is indicated, particularly in the hangingwall of the excavation. Where grouted rock bolt systems are used, the optimum hole diameter is approximately twice the bolt diameter.

Many of the concepts explored in this analysis are simple estimations of an extremely complex environment and system behaviour, and as such there is much scope for further work. But this should not detract from the insight gained, and the design procedures developed, in relation to the current understanding of tunnel support system design in the high stress, highly discontinuous, dynamic rock mass environment of deep level mines. Current investigations, beyond the scope of this document, are being conducted into the in situ verification of the

interaction between rock bolt reinforcement and the rock mass, under quasi static and dynamic deformation. However, some other important areas of further work are highlighted below.

1) Additional case studies of the extent of natural instability of the rock mass should be obtained and analysed to verify the method used to determine the extent of instability under highly stressed conditions.

2) Deformation mechanisms and dilation rates should be evaluated for different rock mass structural and loading environments.

3) The in situ shear demand on rock bolt reinforcement should be investigated to quantify the required shear capacity of a rock bolt system.

4) The energy absorption capability of a reinforced and contained rock mass system should be further investigated. This is the implied ability of a contained rock mass system to absorb significantly greater energy than would be indicated by analysis of the fabric, or rock bolt reinforcement in isolation. This will have important implications for the understanding of the energy absorption capacity of the stabilised rock mass system.

5) The three dimensional interaction of the support system within a defined rock mass structure should be evaluated.

6) An empirical evaluation of the applicability of the rock mass classification systems and support design process, as proposed in this analysis, with regard to the successful and failed performance of current support systems should be carried out.

7) This investigation has assumed that rock mass instability under conditions of dynamic loading is due to expulsion normal to the excavation boundary, or simple increased acceleration loading within the rock mass. There is evidence of diagonal and longitudinal dynamic loading and deformation of tunnels. It is therefore necessary that the mechanism of interaction of dynamic waves impinging on tunnel excavations from different directions, and thus, the deformation and stability of the rock mass under these conditions would require far more detailed analysis.

8) An evaluation of the interaction of shotcrete with a potentially unstable rock mass volume has only been implied in this analysis and thus would require further investigation. It is considered that the interaction of shotcrete, and other membrane type support systems, will be fundamentally different due to their direct adhesion to the rock mass and potential significantly greater system stiffness. However their limited ability to tolerate large deformations, or their ability combined with the implied greater effectiveness of the

reinforcing bolts to control the large potential deformations needs to be thoroughly investigated before application of these systems can be fully endorsed.

References

Anon., (1988), *An industry guide to methods of ameliorating the hazards of rockfalls and rockbursts*, Chamber of Mines Research Organization, Johannesburg, South Africa.

Anon., (1993), Fast Lagrangian Analysis of Continua, Version 3.2, *Users Manual*, Itasca, Minnesota, U.S.A.

Anon., (1996a), *Guideline for the compilation of a mandatory code of practice to combat rockfall and rockburst accidents in metalliferous mines and mines other than coal*, Department of Minerals and Energy Ref. GME 7/4/118-AB2, South Africa.

Anon., (1996b), Universal Distinct Element Code, Version 3.0, *Users Manual*, Itasca, Minnesota, U.S.A.

Barrow, K, (1966), "Development of Rock Failure Around a Single Haulage Way", *Rock Mechanics Division Report*, National Mechanical Engineering Research Institute, Council for Scientific and Industrial Research.

Barton, N, Lien, R & Lunde, J, (1974), "Engineering classification of jointed rock masses for the design of tunnel support", *Rock Mech.* 6, p.189-236.

Barton, N, (1997), *Workshop on rock mass characterisation* (course notes), Rustenburg, South Africa.

Bieniawski, ZT, (1973), "Engineering classification of rock masses", *Trans. S. African Institute Civil Eng.* 15, p.335-344.

Bieniawski, ZT, (1979), "The Geomechanics Classification in rock engineering applications", *Proceedings 4th congress ISRM*, Montreux.

Choquet, P & Charette, F, (1988) "The applicability of rock mass classifications in the design of rock support in mines", *Proceedings 15th Canadian Symposium on Rock Mechanics*, Toronto, p. 39 - 48.

Choquet, P & Hadjigeorgiou, J, (1993), "The design of support for underground excavations", *Comprehensive Rock Engineering*, Volume 4, p 313 - 348, Ed. Hudson, J.A.

Desai, CS, & Chritian, JT, (1977), *Numerical methods in geotechnical engineering*. McGraw Hill Inc.

Douglas, TH & Arthur, LJ, (1983*), A guide to the use of rock reinforcement in underground excavations*, CIRIA Report 101, London.

Durrheim, RJ, Kullmann, DH, Stewart, RD & Cichowicz, A, (1996), "Seismic excitation of the rock mass surrounding an excavation in highly stressed ground", *2nd North American Rock Mechanics Symposium on Rock Mechanics tools and techniques*, Montreal, Quebec, Canada, p. 389-393.

Fairhurst, C & Cook, MGW, (1965), "The phenomenon of rock splitting parallel to a surface under a compressive stress", *Chamber Of Mines report*, Project No. 105 / 65, Johannesburg, South Africa.

Farmer, IW & Shelton, PD, (1980), "Factors that effect underground rock bolt reinforcement systems design", *Transactions Institution of Mining and Metallurgy*, 89, A68 - A83, London.

Haile, AT, Jager, AJ & Wojno, L, (1995), "Strata control in tunnels and an evaluation of support units and systems currently used with a view to improving the effectiveness of support, stability and safety of tunnels", *Final Report GAP026*, Safety in Mines Research Advisory Committee, Johannesburg, South Africa.

Hepworth, N, (1985), "Correlation between deformation observations and support performance in a tunnel in a high stress, hard rock, mining environment" *MSc thesis*, University of Witwatersrand, Johannesburg, South Africa.

Hoek, E & Brown, ET, (1982), *Underground Excavations in Rock*, Institution of Mining and Metallurgy, London.

Jager, AJ & Wojno, LZ, (1991), "Damage to tunnels in gold mines – are there cost effective solutions?", *Proceedings SANGORM Symposium, Impact of Rock Engineering on Mining and Tunnelling Economics*, Welkom, South Africa, p. 55-60.

Jager, AJ, Wojno, LZ & Henderson, NB, (1990), "New Developments in the Design and Support of Tunnels Under High Stress Conditions", *Proceedings SAIMM Symposium, Technical Challenges in Deep Level Mining*, Johannesburg, South Africa, p. 1155-1171.

Kaiser, PK, McCreath, DR & Tannant, DD, (1996), *Canadian Rockburst Support Handbook*, Geomechanics Research Centre, Laurentian University, Sudbury, Ontario, Canada.

Kersten, R, Piper, P & Greef, H, (1983), "Assessment of Support Requirements for a Large Excavation at Depth". *Rock Mechanics in the design of tunnels*, SANGORM symposium, Johannesburg, South Africa, p. 41-46.

Laas, JJ, (1995), "Evaluation of the support contribution of long tendons in a tunnel subjected to varying field stress in a deep level, hard rock mine", *MSc thesis*, University of the Witwatersrand, Johannesburg.

Lang, TA & Bischoff, JA, (1982), "Stabilisation of rock excavations using rock reinforcement" *Proceedings 23rd U.S. Symposium on Rock Mechanics*, Berkeley, California (Edited by RE Goodman and FE Heuze), AIME, New York, p. 935 - 944.

Laubscher, DH & Taylor, HW, (1976), "The importance of geomechanics classification of jointed rock masses in mining operations", *Proceedings of Symposium on Exploration for Rock Engineering*, Vol. 1, Johannesburg, South Africa.

Martin, CD, (1993), "The strength of Lac du Bonnet granite around underground openings", *PhD Thesis*, University of Manitoba, Winnipeg, Canada.

Martin, CD, McCreath, DR & Stochmal, M, (1997), "Estimating Support Demand-Loads Caused by Stress Induced Failure Around Tunnels", *Rock Support – Applied solutions for underground structures*, June 22-25, 1997, Lillehammer, Norway, p. 235-248.

More O"Ferral, RC & Brinch, GH, (1983), "An Approach to the Design of Tunnels for Ultra Deep Mining in the Klerksdorp District", *Rock Mechanics in the Design of tunnels*, SANGORM symposium, Johannesburg, South Africa.

Ortlepp, WD, (1983a), "The Design of Support for Rockburst Prone Tunnels", *Rock Mechanics in the Design of Tunnels*, SANGORM symposium, Johannesburg, South Africa.

Ortlepp, WD, (1983b), "Considerations in the design of support for deep, hard rock tunnels", *Fifth International Congress of I.S.R.M.*, Melbourne, Australia.

Ortlepp, WD & Gay, NC, (1984), "Performance of an Experimental Tunnel Subjected to Stresses Ranging from 50 MPa to 230 MPa", *Design and Performance of Underground Excavations*, ISRM symposium, Cambridge, U.K.

Ortlepp, WD, Stacey, TR, (1998), "Performance of tunnel support under large deformation static and dynamic loadings", *Tunnelling and Underground Space Technology*, Volume 13, No.1, Pergamon Press.

Palmstrøm, A, (1996), "Characterising rock masses by the RMi for use in practical rock engineering Part 1: The development of the Rock Mass Index (RMi)", *Tunnelling and Underground Space Technology*, Volume 11, No.2, Pergamon Press.

Piper, PS, (1983), "The Effect of Rock Mass Characteristics on Fracturing Around Large Excavations at Depth", *Design and construction of large underground openings*, SANCOT seminar, Pretoria, South Africa, p. 7-16.

Piper, PS, (1985), "The Application and Evaluation of Rock Mass Classification Methods for the Design and Support of Underground Excavations at Depth", *Rock mass characterisation symposium*, SANGORM, Randburg, South Africa, p. 45-54.

Roberts, DP, (1995), "Testing of mining tunnel support elements and systems for hard rock mines", *MSc thesis*, University of Natal, Durban, South Africa.

Schach, R, Garschol, K & Heltzen, AM, (1979), *Rock bolting: A practical handbook*, Pergamon, Oxford.

Stacey, TR, Ortlepp, WD, (1997), "Testing of tunnel support: Dynamic load testing of rock support containment systems (e.g. wire mesh)", *Final Project Report GAP221*, Safety in Mines Research Advisory Committee, Johannesburg, South Africa.

Stillborg, B, (1986), *Professional users handbook for rock bolting*, Series on Rock and Soil Mechanics, Vol. 15., Trans Tech Publications.

Stimpson, BA, (1989), "A simplified conceptual model for estimating roof bolting requirements", *International Journal Mining and Geolotechnical Engineering*, 7, p. 147 - 162.

Wagner, H, Wiseman, N, (1979), "The Significance of Fracturing in the Design and Support of Mine Excavations", *Fracture '79*, Johannesburg, South Africa, p. 381-389.

Wagner, H, (1983), "Some Considerations Concerning the Support of Tunnels in Deep Mines", *Rock Mechanics in the design of tunnels*, SANGORM symposium, Johannesburg, South Africa, p. 51-59.

Wiseman, N, (1979), "Factors Effecting the Design and Condition of Mine Tunnels", *Chamber of Mines Research Organization report*, project No. G01G10, Johannesburg, South Africa.

Wojno, L, Jager, AJ, (1987), "Rock Reinforcement in Tunnels Under High Stress Conditions in South African Gold Mines", *6th International conference on ground control in mining*, Morgantown, Virginia, USA.

Wojno, L, Jager, AJ & Roberts, MKC, (1987), "Recommended Performance Requirements for Yielding Rock Tendons", *Design of rock reinforcing, Components and systems symposium*, Johannesburg, South Africa, p. 71-74.

Zienkiewicz, OC, Cheung, YK, (1967), *The Finite Element Method in Structural and Continuum Mechanics*, McGraw Hill Inc.